The Combustion of Low Grade Fuels in Fluidised Bed Combustors

Stephen Lewis Chilton

Submitted in accordance with the requirements for the degree of Doctor of Philosophy
as part of the integrated PhD with MSc in Low Carbon Technologies

May 2017

Doctoral Training Centre in Low Carbon Technologies
School of Chemical and Process Engineering, University of Leeds

Dedication

I would like to dedicate this thesis to my grandmother, Audrey Chilton who sadly passed away before I completed my PhD. She was a bubbly charismatic character who always saw the best in people. My grandmother was an inspiring woman who played so many roles in her local and wider community. A testament to her successes was the sheer number of people who came to show their respects at her funeral. You may not have understood the topic of my thesis, but you always knew what to say and I miss you dearly. I wish you were still here so I could see your proud smile one more time.

Declaration of Authorship

The candidate confirms that the work submitted is his own, except where work which has formed part of jointly-authored publications has been included. The contribution of the candidate and the other authors to this work has been explicitly indicated below. The candidate confirms that appropriate credit has been given within the thesis where reference has been made to the work of other.

The following papers include information from the investigations in this thesis and include a description to the authors input and use:

1) Chilton. S, Daood. S, Nimmo. W, Rehman.S & Williams.G. (2017). *The effects of low grade coals in pilot scale fluidised bed combustion with respect to agglomeration and fuel upgrading.*

I am the lead author of this paper. I shared the experimental work with Mr Rehman but conducted all the characterisation, analysis etc. myself. The results of this paper are taken from Chapter 5 and are a condensed version of the agglomeration and operational findings within the results.

2) Asad Naeem Shah, Nasir Hayat, Fiaz Hussain Shah, Muhammad Javed, Muhammad Akram, Stephen Chilton, William Nimmo. (2016) *Optimization of fluidized bed combustion (FBC) to control emissions with emphasis on desulfurization of high sulphur coals during combustion using limestone and biomass*. Fuel Processing Technology.

I am a co-author in this paper and the experimental work and results what part of shared experimental workload presented in Chapter 5. The previous papers uses data from the same series of investigations but this paper investigates emissions and fuel improvement instead of bed and physical phenomena.

3) Chilton. S, Daood. S, Nimmo. W, Rehman.S & Williamss.G. (2016/7) *Prediction of agglomeration from the Combustion of biomass in a 350kW Pilot Scale Bubbling Fluidised Bed Combustion (BFBC) Unit.*

I am the lead author of this paper. I shared the experimental work with Mr Rehman and Dr Daood. I conducted all the characterisation, analysis etc. myself. The results of this paper are taken from Chapter 6 and are a condensed version of the agglomeration and operational findings within the results.

4) Xing, P., Mason, P. E., Chilton, S., Lloyd, S., Jones, J. M., Williams, A. & Pourkashanian, M. (2016). *A comparative assessment of biomass ash preparation methods using X-ray fluorescence and wet chemical analysis*. Fuel, 182, 161-165.

I contributed data, methodology and reviews to this paper. I was part of a team including Xing, P., Mason, P. E., Chilton, S. and L. Lloyd who studied the use of biomass and its bi products in XRF applications. The work included in this Chapter and separate investigations to this paper are included in Chapter 4.

5) Rehman S, Shah AN, Mughal HU, Javed MT, Akram M, Chilton S & Nimmo W (2016) *Geology and combustion perspectives of Pakistani coals from Salt Range and Trans Indus Range.* International Journal of Coal Geology, 168, 202-213.

I shared experimental work load with Rehman S for this paper and supplied fuel characterisation data included. Fuel characterisation data of the coals was taken from this paper and included in Chapters 4 and 5.

6) Belhadj E, Chilton S, Nimmo W, Roth H & Pourkashanian M (2016) *Numerical simulation and experimental validation of the hydrodynamics in a 350 kW bubbling fluidized bed combustor.* International Journal of Energy and Environmental Engineering.

I supplied experimental data and results for the validation of Belhadj E CFD model and as such aided in the validation of results used in the paper. The data that was supplied for validation is included in Chapters 5 and 6.

7) Ullah, A., Hong, K., Chilton, S., & Nimmo, W. (2015). *Bubble-based EMMS mixture model applied to turbulent fluidization*. Powder Technology, 281, 129-137.

Experimental data was used for validation of the CFD model and was taken from Chapter 6 and 7.

Acknowledgments

Throughout the course of my PhD I have received support from countless friends, families and supervisors who have guided and aided me to my thesis submission. To all of you I say thank you.

I would like to thank my supervisors for the ongoing guidance and support I have received. This includes: Dr William Nimmo and Professor Derek Ingham at the University of Sheffield and Professor William Gale at the University of Leeds. My supervisor's circumstances changed throughout my PhD but I always felt as though I had support and I appreciate the friendship and mutual respect for each other that has come from working together.

I would like to thank my partner Laura Sellers, who has been by my side throughout both our PhD's. Even though we were at times stressed, over worked and burning the candle from all angles, she still managed to cheer me up and keep me motivated. I feel as though the challenges the PhD's have presented has only bought us closer together.

A thank you to all my friends, including those back in Grimsby who pretend to understand what I'm on about but smile never the less. To my friends in Leeds and on the DTC who have been there to share a pint. You all bring your own identities and personalities and each one of you has helped me in some way to enjoy my time as a PhD student.

To the Chilton's and Sellers' alike, whilst many of you still don't understand what my PhD is about or why people do a PhD, I say thank you for humouring me. Your ongoing support be that financial, moral, emotional or simply keeping a level of sanity in my life that I can rely on has proven priceless to my motivation. Each of you has contributed in your own way and I appreciate all of it.

I have received a wide range of training from different technical and academic personnel at Leeds and Sheffield University and to all of you thank you. A special thanks to: Simon Lloyd, Robert Harris and Adrian Cunliffe of Leeds University for showing me the ropes in the laboratory and demonstrating the patience of saints. A big thanks to all the staff at The Low Carbon Combustion Centre (LCCC) and to Sheraz Daood for aiding my ongoing education with pilot scale facilities.

I must express my gratitude to the Engineering and Physical research council (ESPRC) and the Low Carbon Technologies doctoral training centre (DTC) for funding and managing me throughout the PhD. The research council and DTC has given me the

opportunity of a life time and allowed me to undertake something I never imagined possible.

My PhD has included both international and national involvement. I'd like to acknowledge EON and Uniper (Paul James, Colin Davis and others), CRIEPI (central research institute of electric power industry Japan), KEP British council/Pakistan research grant collaboration and the UK carbon capture and storage research centre (UKCCSRC). Thank you to Michitaka Ikeda, Shafiq Rehman, Emberak Belhadj, Atta Ullah and Paul Vonesdunk, Toby LockWood and Karen Mcfinney.

Abstract

Global energy consumption is projected to increase the world over from 546 EJ in 2010 to an estimated 879 EJ in 2050 (Frei et al., 2013). Several factors contribute to this projected increase including growing global population, better quality of life globally, and continued electrification of services and products. Three serious issues arise from the increase in consumption and production, that is, fuel supply, and availability and increased anthropogenic emissions. To meet demand, developing countries, such as Pakistan, are investing in power generation research and technologies. Whilst a number of technologies are available, fluidised bed combustion (FBC) is an attractive technological option because of its ability to handle fuels with variable calorific content, moisture content, mineral content and high alkaline content. FBC offers reliable thermal output because of the large thermal mass (fluidised bed) associated with the method. This thesis set out to explore the possibility of using low grade fuels in FBC and investigate the impact the fuels have on agglomerate formation rates and combustion efficiencies.

To explore the potential of FBC in the first experimental investigation presented in this thesis, a 350KW pilot scale FBC rig was used to perform a series of combustion experiments on ten Pakistani coal blends from the Northern Punjab salt rage coal seams. The coals had high sulphur and alkaline content and presented challenges in both combustion and emissions control. Operational variables including bed temperature, bed additives (limestone), sulphur: calcium fuel ratio, additive particle size and co-firing with wood biomass were employed to evaluate the effect of fuel blending, combustion and emissions optimisation. This thesis argues high SO_2 emissions resulting from the combustion of high sulphur coals can be reduced in emission concentration when optimising operational variables. The high alkaline content, because of pyrite (FeS) concentrations in the fuel caused bed agglomeration and slagging in the beds. The investigation analyses the agglomerates and defines the mechanisms involved. This research allows for remedies and implementation choices when considering the coals application in full scale systems.

It is not only coal which can be utilised. Further work investigated the effects of five different biomass fuels in FBC. Biomass can be classified as a CO_2 neutral fuel as the CO_2 released during combustion is relatively equal to the CO_2 absorbed in the growth of the original plant. However, biomass is known to contain high concentrations of alkaline species such as potassium (K) and sodium (Na) which were shown in the literature to cause agglomeration. The biomasses were combusted in the FBC rig to evaluate the

combustion, emissions, agglomerates, temperatures and pressure outputs associated with each fuel. Following tests the air distribution plate was modified to simulate both a uniform air distribution system and a non-uniform air distribution system. This allowed for comparisons of the fuels in a system with uniform air flows and non-uniform airflows/distribution which would be experienced in damaged systems. Thus, this thesis argues biomass is significant and relevant to industrial application and allowed for identification of significant chemical components in the agglomeration mechanisms of each fuel as well as establishing the performance of each fuel in variable systems.

In order to understand the fundamental chemical and physiological makeup of the low-grade fuels it was necessary to conduct an extensive series of fuel characterisation. The fuel characterisation research undertaken yielded information as to the fuels energy content, chemical makeup, combustion characteristic and identify key components such as alkaline species associated with the negative mechanisms seen in pilot scale testing. In order to analyse the fuels x-ray fluorescence (XRF) was used. This technique identifies major and minor oxides in coal samples. However, as demonstrated in the fuel characterisation work, there were limitations, inaccuracies and repeatability issues when analysing low grade fuels with XRF. Thus, a significant effort was made to improve the sampling, ashing, XRF medium and normalisation process. The results of this research led to a more reliable XRF method for analysing low grade fuels and their bi-product of combustion which is applicable for any industry utilising these types of fuels and techniques.

The final part of the investigations focused on the prediction of agglomeration and slagging tendencies of the fuels. This was done by applying the results seen in the pilot scale tests and the results of the fuel characterisation work with slagging indices and the application of a thermodynamic model (FACTSAGE). FACTSAGE can be used to predict slagging tendencies of the fuels by modelling chemical species released over temperature ranges. The results showed correlation between the theoretical results and the experimental results

Together this research demonstrates the implications of using low-grade fuels in small scale FBC. This thesis explores how this research can then be used in full scale FBC operations. This thesis not only highlights the problems with using low grade fuels in FBC but suggests remedies and potential solutions to the problems based on the results from experimental data and FACTSAGE modelling. It also presents suggestions on how to continue development of the technology to reduce or avoid some of the difficulties in combusting low grade fuels.

Contents

List of figures

List of Tables

Reactions

Nomenclature

ΔP = pressure drop (N/m^2)
λ= friction factor
L= distance (m)
D= Tube diameter (m)
v= velocity of gas (m/s)
ρ_f=fluid gas density (kg/m^3)
U_{mf}= minimum fluidisation velocity (m/s)
V_{mf},Q =volumetric flow rate (m^3/s)
A=cross sectional area (m^2)
Dp=particle diameter (mm)
ρ_s=solid density (kg/m^3)
ρ_g= gas density (kg/m^3)
g and g_c = gravity (9.81 m/s^2)
D_p=average particle size (mm^2)
d_{sph}=diameter of sphere (m)
d_{eff}=effective particle diameter (m^2)
Δp_{fr}=frictional pressure drop (Pa)
L_m=height of bed (m)
ε_m, ε=void fraction
μ=viscosity of gas (kg/ms^{-1})
μ_o=superficial gas velocity (m/s)
φ_s=Spherity of a particle
$\bar{u}$=interstitial velocity (m/s)
u= carrier gas
j=pressure gradient factor
ρ_p=particle density including pores (kg/m^3)
V_b=bed volume (m^3)
P_b=bulk density (kg/m^3)
m_b= mass of bed (kg)
v_P= volume of the particle (m^3)
v_b=bed volume (m^3)
H= Bed height (m)
H_{mf}= minimum fluidisation bed height (m)
δ_b=pressure change across bed (kPa)
ε_{mf}= volume of void fraction at minimum fluidisation (mm^3)
u_t=terminal velocity (m/s)
D_b=bubble diameter (m)
D_t= bed diameter (m)
u_{br}= bubble rise velocity (m/s)
N= number of holes
d_h=grid hole diameter (m)
Cd= discharge coefficient
N_j= hole density (m^2)
N_d= number of holes' density (holes/m^2)

Abbreviations

AFBC-Atmospheric Fludised bed combustion

CFBC- Circulating fluidised bed combustion

PFBC-Pressurised Fludised bed combustion

FBC-Fludised bed combustion

OECD-Organisation for Economic Co-operation and Development

PF-Pulverised fuel

Mtoe-Million tonnes of oil equivalent

Xrf-X-ray fluorescence

SEM-EDX-Scanning Electron Microscopy with Energy Dispersive X-Ray Analysis

1 Introduction

In the UK ,power generation companies are shifting from large centralised facilities such as those brought online up to the early 1980's, plants such as; Ratcliffe (2GW), Ferrybridge (1GW), Eggbrough (2GW) and Drax (4.4GW), to medium and small scale localised facilities(Breeze, 2014).

Centralised power generation facilities were chosen as a result of political, social and environmental climates at the time. Coal was cheaper and secure with national and international fuel stocks plentiful and accessible. However, global politics, public opinions, anthropogenic emission impacts, fuel security, developing countries and advances in technology have moved the UK from larger facilities to small-medium scale more localised facilities fuelled by alternative fuels.

Power generation industry has continued to evolve and adapt to the changes in production choices. Figure 1-1 show how the fuel types for generation has changed since 1980. As the figure shows, coal use has reduced since 1985 with discoveries in the North Sea leading to large construction of gas plants across the UK, and then drive to implement sustainable fuel sources.

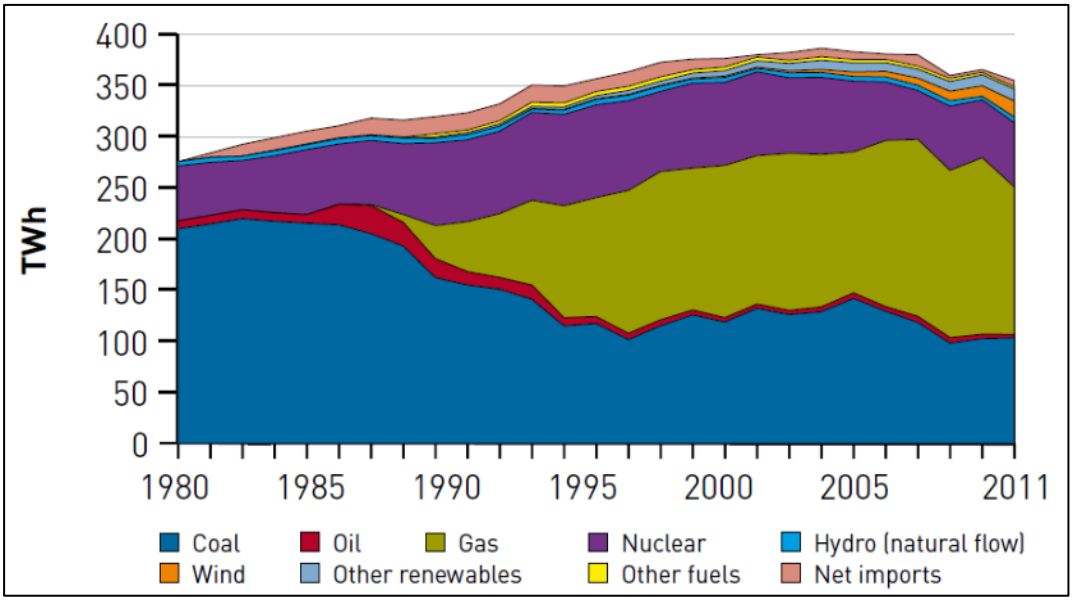

Figure 1-1 Electricity generation by fuels 1980-2011 (DECC, 2012)

The UK government is a member of directives such as; directive 2009/28/EC, 2001/77/EC and 2003/30/EC (Renewable Energy Directive 2009) which promotes the use of renewables in the power generation sector to achieve a target of 15% of the UK's power fuelled by renewables by 2020 (Glachant, 2001). Legislation and directives such as these

are a response to the growing concern over emissions from anthropogenic sources and the potential consequences forecasted to impact the atmosphere and environment in the future (Hassan, 2014).

The power sector has responded to the need for renewable power by constructing wind farms, solar arrays, installing biomass fired facilities and modifying coal fired units. This is demonstrated by the changes seen in Figure 1-2 which shows the overall increase in renewable generation.

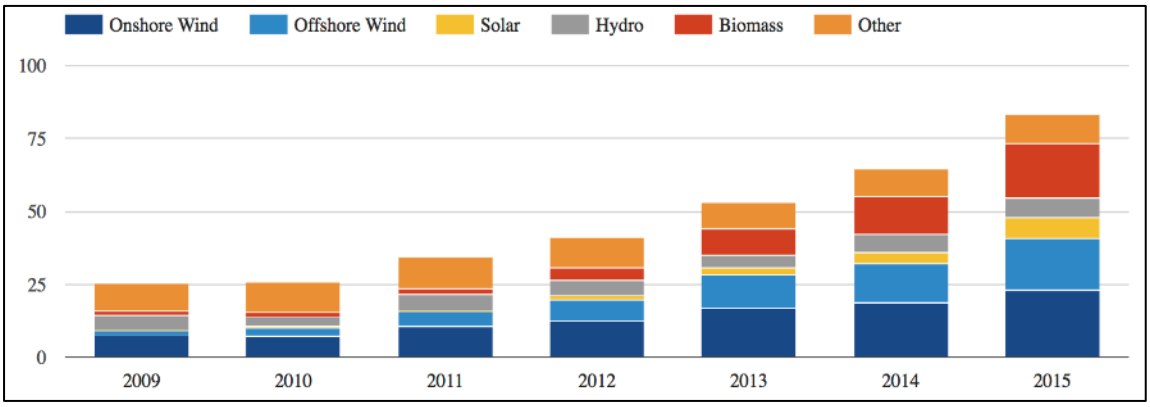

Figure 1-2 UK renewable electricity generation, 2009-2015 (Evans, 2016)

Examples of the increase in biomass use include Drax power station which has converted from pulverised fuel (PF) (coal units) to biomass fired units, the construction of Steven's Croft virgin wood fluidised bed, Blackburn Meadows recycled wood fluidised bed, Wilton 10 virgin/recycled wood fluidised bed and Aberthaw virgin wood PF units (Breeze, 2014).

With the renewable power sector commissioning, more and more biomass fired stations across the UK, the focus of this thesis will be towards the application of low grade fuels such as biomass in full scale technologies. As fluidised bed combustion is being utilised to combust low grade and renewable fuels, this thesis will investigate problems with their use in fluidised bed combustion and propose remedies based in critical evaluation of the results.

1.1 Global Energy

Power generation technologies vary from country to country and between local requirements. Many factors dictate the choice of power generation including technology type, economics, power requirement and most significantly fuel sources.

Energy sources can be divided into two categories, namely non-renewable and renewable sources. Non-renewable sources are made up primarily of fossil fuels. These are the remnants of ancient plants and animals which have been exposed to pressure and heat over millennia e.g. coal, natural gas and crude oil. Non-renewable fuels also include nuclear because of its depleting finite fuel source. Renewable energy sources include solar, onshore/offshore wind, tidal and biomass. Renewable energy utilisation has increased as a result of global emissions and public awareness towards the environmental impacts of conventional power generation methods. Whilst the work in this thesis will evaluate the potential for environmental impact of using both renewable and non-renewable fuels, the focus is drawn to engineering problems and limitations of utilising low grade fuels and thus how to remedy the issues.

1.1.1 Global Energy Consumption

Global energy consumption is projected to continue increase over the next century. In projections modelled by the world energy council it was suggested that world energy consumption will increase from 546 EJ in 2010 to 879 EJ by 2050 (Frei et al., 2013). In another independent study the international energy agency projects that by 2050, the world energy consumption will have reached 22 Gtoe (gigatons of oil equivalent) compared to the current 10 Gtoe a year (EIA, 2016).

There are a number of key global factors which will cause an increase in the global energy consumption increase to 2050 and beyond:

- Global population is predicted to increase to between 9 and 12.1 billion people before 2100. There is a large margin of error associated with this type of study because of global economies, social dynamics, and technological innovation. However, the population is expected to peak and then reduce to a balanced value of approximately 9 billion people as we approach the year 2100 (Lutz et al., 2001; Cohen, 2003). The global cap is estimated by taking into account global resource availability and free space, without consequence to environmental damage. The distribution of the global population will increase in continents such as Asia and significantly in Africa. A decrease is expected in developed countries such as Europe (Cohen, 2001). Each of the 9 billion people will create an increasing demand on energy production as individual demand on electrically driven appliances and lifestyles increase. This is until the efficiencies of power rise in the devices is optimised along with technological innovation.

- Quality of life can be correlated with the units of energy per capita head a person consumes annually. In countries with sufficient energy reserves/production, there is an ability to provide services and products which improve the quality of life; medical and health facilities for instance (Hoogwijk, 2004). Studies have indicated that when the energy consumption per capita head for a state reaches 2.6 Gtoe/yr, there is no further improvement without industrialisation Growing globalisation and economic growth is most prevalent in developing countries creating a deficit in energy production as the populations of those states come to expect the same amenities as citizens in developed countries. This brings with it a significant increase in energy demand and consumption.
- Other factors are predicted to increase the global energy consumption such as increasing wealth in emerging markets e.g. China and industrialisation in these markets accompanied with globalisation. However, these factors will fluctuate whereas population growth and the demand of each individual is highly probable.

1.1.2 Global Energy Production

In order to meet the demand for electrical production it will be necessary to create more efficient systems whilst producing more power generation facilities, of a larger energy producing capacity, using the available energy resources available in the future. The type of energy resource is expected to also change in the future as fuel reserves are depleted and discovered, as different technologies become more efficient and as individual states alter their policies and address national pressures such as producing less CO_2 intensive electricity.

1.1.3 Energy in the Future

When considering the potential sources of energy in the future there are two leading factors which affect the decision process; land availability/required for that fuel source and the respective yield achievable. This is especially true when considering renewables; solar, PV, wind turbines, wave, hydro and biomass. An example being a study by Berndes et al. (2003), who reviewed 17 studies on the potential for biomass power generation for future global energy deficit. The conclusions of this studies illustrated that depending on the land availability and yield achieved by that land, the energy produced by the biomass could vary between 100 and 400 EJ/yr by 2050 (Sieminski, 2014). This type of difference is shared with global energy associations such as IEA which predicted a 56% global energy consumption increase from 2010 to 2040 equating to an increase from 524 quadrillion btu to 820 quadrillion btu (Birol, 2010).

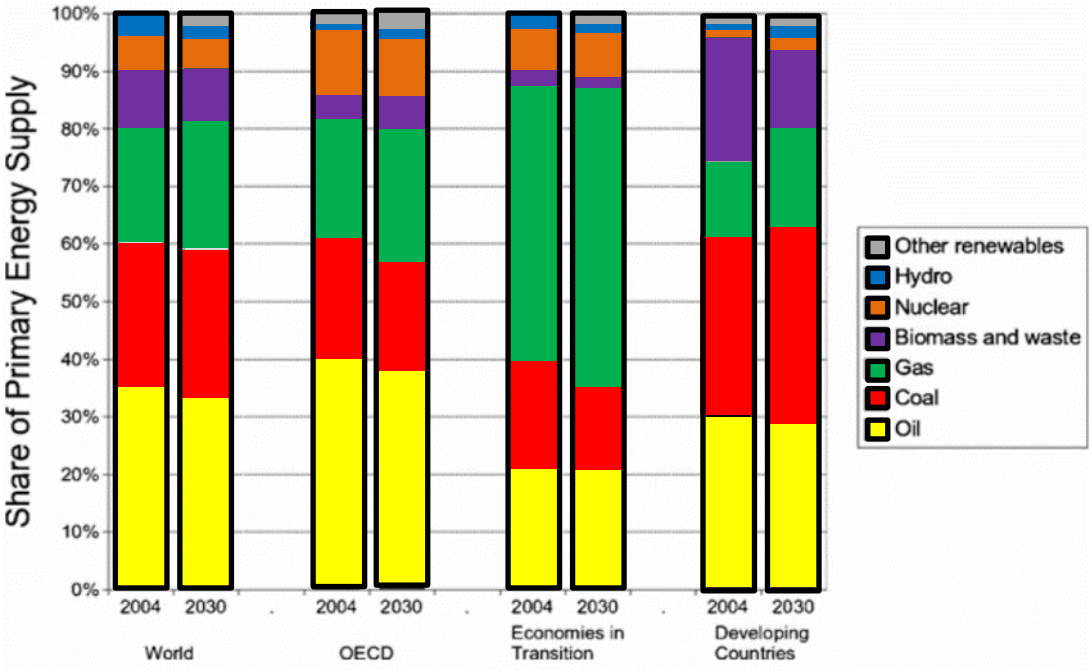

Figure 1-3 Primary energy use profiles for countries within different forums (Kaygusuz, 2012)

As Figure 1-3 shows developing countries will be a large proportion of future increased power demand. These types of country will initially utilise their indigenous fuel stocks and import cheap alternatives. In order to address energy consumption, these countries will change and utilise the most economic option available to them. Figure 1-3 illustrates how the trend of energy sources is likely to alter by 2030. Note should be taken to the dependence of fossil fuels such as coal in the developing countries. So, the question is to what fuel stocks are to be utilised and thus what technologies, for future energy use will likely to be adopted.

1.1.4 Fuel Stocks

In the past, fuel availability and stockpiles have been governed by two key factors; political ramification and economic feasibility. Political ramifications have been drastically steered by global political peer pressure and local social trends for climate change and the effect energy producers are having on anthropogenic environmental issues (Verrastro and Ladislaw, 2007). This is then combined with the cost of fuels as technologies fall in and out of fashion, nuclear energy disasters such as Chernobyl being a key example, means that energy generation has changed over the last 50 years (Van der Pligt, 1992). As a direct result, the need for the energy sector to continue sourcing new fuel reserves to match these trends and pressures alongside the continuing depletion has an effect on fuel prices which influences energy producers decisions with regards to fuel choice for generation (Perlack et al., 2005; Rogner, 1997).

1.1.4.1 Low Grade Coal

Coal is a combination of carbon, hydrogen, oxygen, nitrogen, sulphur and low concentrations of mineral/inorganic impurities. The high carbon content makes this fuel ideal for combustion and power generation. Different ranks of coals exists due to the variance in the content of carbon, moisture, mineral matter, ash and inherent impurities (Volborth, 1987).

The price of higher ranks coal such as anthracite ($80-$90/tonne) and bituminous coal ($57-$60/tonne) is more than three times the cost of sub bituminous coals ($12-$14/tonne) and lignite's ($19-$20/tonne) (EIA, 2013)(Hecking, 2016). This has fluctuated more recently with North America investing in indigenous fracking and tar sands thus resulting in an excess in coal production and exports. For developing countries, the variability of the cost is forcing governments such as Pakistan, India, and China etc. to look at utilising indigenous fuel stocks.

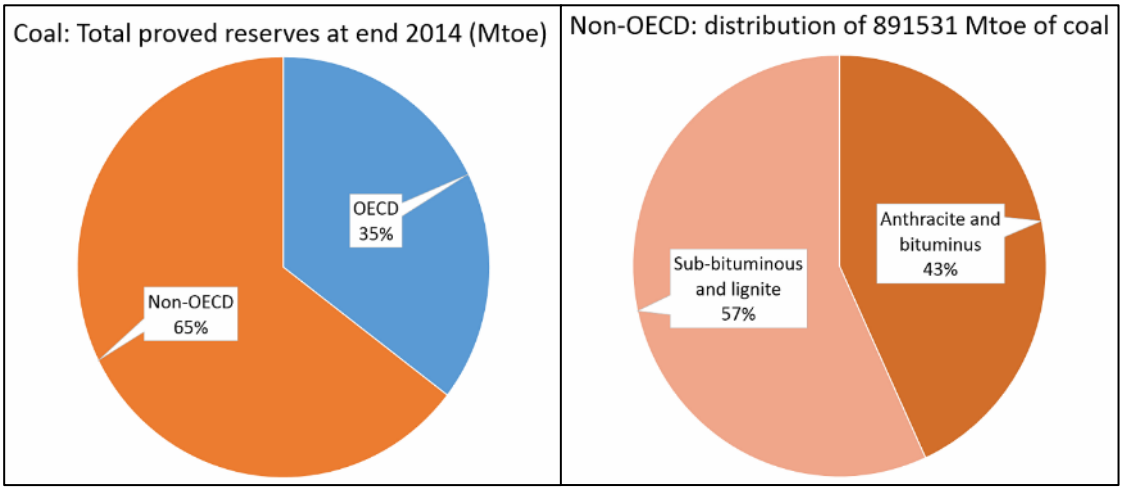

Figure 1-4 Distribution of coal reserves globally and the trend for developing countries (Petroleum, 2015)

Figure 1-4 shows how the proven world coal reserves are found more in developing, non OECD countries (Petroleum, 2015). Within non-OECD countries there is currently a proven total proven reserve of 891531 Mtoe of coal. However, more than half, 57%, of these reserves are sub bituminous or lignite ranks(Ishiguro and Akiyama, 1995; Husain, 2010).

The available data illustrates a trend for developing countries to utilise their indigenous low grade coals in the future. Alternative fuels in developing countries include biomasses (wastes, virgin materials and recycling) which have the added potential for CO_2 emissions reductions.

1.1.4.2 Biomass

Biomass is organic materials such as wood, farming residues, municipal solid wastes (MSW) etc. which contain high concentrations of hydrocarbons and thus have high calorific potential.

The potential for biomass fuels to meet power production globally is dependent on land availability and the yield achieved. Studies suggest that biomass could supply between 100 and 600 EJ of electricity depending on growth variables and the local strategies adopted in producing the power (Slade et al., 2011). It is difficult to quantify the actual global availability of biomass for generation when there are so many different types and applications.

The International Renewable energy agency, IRENA (2012), quantified the investment cost required to utilise biomass in different technologies, as shown in Table 1-1. This indicates that technologies such as stoker boilers and fluidised beds could potentially produce the cheapest electricity using biomass; 1880-4260 $/kW and 2170-4500 $/kW respectively.

Table 1-1 Typical capital costs and the levelised cost of electricity using different biomass power generation technologies (IRENA, 2012)

	Investment costs USD/kW	LCOE range USD/kWh
Stoker boiler	1 880 - 4 260	0.06 - 0.21
Bubbling and circulating fluidised boilers	2 170 - 4 500	0.07 - 0.21
Fixed and fluidised bed gasifiers	2 140 - 5 700	0.07 - 0 24
Stoker CHP	3 550 - 6 820	0.07 - 0.29
Gasifier CHP	5 570 - 6 545	0.11 - 0.28
Landfill gas	1 917 - 2 436	0.09 - 0.12
Digesters	2 574 - 6 104	0.06 - 0.15

1.2 Fluidised Bed Combustion (FBC)

Cheaper initial capital investment and high potential electrical output means fluidised bed combustion (FBC) adopted heavily in non-OECD countries. Malaysia uses FBC for agricultural and forestry residues (Shafie et al., 2012), Brazil for high moisture sugar cane residues and MSW (Hoffmann et al., 2012), China for MSW also for power (Cheng and Hu, 2010) and Thailand to combust residues from the fruit farming industry (Nagle et al., 2011).

Fluidised beds are also being used to combust the lower ranked coals (previously described), examples including; Pakistan (Shah et al., 1994), Australia (Vuthaluru et al., 2000), Greece (Koukouzas et al., 2009) and Africa (Papo, 2015).

FBC is different from conventional combustion methods such as PF combustion. In FBC a continuous stream of air is used to lift and suspend a bed of inert bed material, such as silica sand. Within the turbulent bed, solid fuel enters and combusts, resulting in rapid heat transfer and high combustion efficiencies. FBC is particularly useful for the combustion of biomass and low ranks coals. The use of a bed results in a high thermal reservoir/mass. Therefore, any fluctuation in fuel quality (calorific value, moisture content etc.) is absorbed whilst a constant thermal and hence electrical output can be achieved. Additionally, FBC is capable of handling high ash, high mineral impurities, high alkali concentration by having constant bottom and fly ash removal techniques (Wu, 2003a).

1.2.1 Fluidised Bed Combustion Problems

As with any combustion technology, there are bi-products this includes the residues in the form of bottom ash, fly ash and fine particulate matter and ashes from the complete combustion of the fuels. Depending on the type of fuel and its relative quality/ranking, the fuel can contain elevated concentrations of inorganic elements, heavy metals and other chemical impurities resulting from the fuels chemical and physical structure (Khan et al., 2009).

Low rank coals and biomass contain elevated concentrations of inorganic elements such as alkali species; sodium (Na) and potassium (K). These species have melting temperatures (≥764°C for Na and ≥790°C for K) (Bartels et al., 2008g) lower than the temperature of the combustion environment (800-900°C) (Kunii et al., 2013). The alkali species and ash enter a liquid melt/gas phase which coats the bed material creating a sticky surface. Collisions of these particles results in adhesion and growth to larger particles. The agglomerates grow in size and structural rigidity. The presence of agglomerates within the bed interferes with the hydrodynamics of the bed and turbulence. Hence combustion efficiency and system performance reduces. If agglomeration is not addressed upon detection of a system change, a bed can eventually defluidise which will result in a furnace outage (Öhman et al., 2000; Elled et al., 2013b; Duan et al., 2015).

1.3 Synopsis of Research

The rationale of the research for this thesis was to undertake an investigation in the use of low rank coals and biomass fuels in pilot scale FBC and evaluate the application to full scale. This was to be done by completing a literature review to encompass all necessary theory and current research, extensive experimental testing of fuels in a pilot scale test rig and by conducting thorough analytical analysis of results. The literature review allowed for the identification and outlining of gaps in the current available research. Experiments and methodology were proposed and designed in order to address the outlined research gaps. By consulting the literature and evident theory, it was possible to approach the research in such a way as to evaluate the effect that the fuels had upon the fluidised bed system. Further work was conducted in order to assess the impact of operational changes such as the use of additives, bed temperatures, particle size etc. on the fluidised.

Further analysis and characterisation of the fuels was necessary to understand the underpinning fundamentals and thus the effect the fuels had upon the technology. Further gaps in analytical techniques, such as XRF, for measuring elemental content of ashes were identified to develop the technique to improve accuracy and reliability in results.

The research also involved the use of theoretical thermodynamic modelling for the use of predicting agglomeration and slag based mechanisms in FBC. The results will be used to validate the results of experimental data. The result of this work included validation of the software package itself and use of the technique in predicting FBC agglomeration likelihood when using the fuels included in the investigations of later Chapters

1.4 Aims and Objectives

The key aims which defined the core research objectives are as the following points indicate:

- Investigate the effect that combusting industrially relevant biomasses and economically viable sub-bituminous coals have on the formation of agglomerates within the bed of an FBC. The aim of this is to quantify the mechanism of the agglomerate formation and to compare the fuels applicability in the technology.
- Evaluate the affect operational variables have on the formation of agglomerates, emissions, combustion performances, temperature distribution and system pressures. By varying operational parameters conclusions will be drawn as to the flexibility and applicability of the fuels in FBC systems.

- Using the information of the previous objectives, a series of engineering remedies will be presented including operational parameter choice/optimisation and the alternative methods that the results indicate could be beneficial in FBC.
- Investigate the application of indices, fuel characterisation and thermodynamic modelling in the prediction of slag and agglomeration formation in FBC. In doing so conclude on the use of different techniques and the use for predicting FBC issues.
- Investigate the effect of damaged air distribution systems in FBC. Evaluate the impact on agglomeration, air distribution etc. and conclude as to the impact on industrial scale systems.
- The overall objective is to define the applicability of the fuels in these investigations, the effect of operational variables, use of modelling and remedies for full scale power generation FBC facilities.

Each Chapter addresses different aspects of low grade fuels for FBC. However, the focus is to evaluate the implications that the low-grade fuel would have if employed on full scale FBC technology. The following sections describe the aims of the Chapter and their significance.

The is a comprehensive literature review which overviews important theory and previously undertaken research. This is fundamental for an understanding in the techniques and technology used throughout the investigations. The research is used to identify areas which haven't previously considered or a need for further investigation or more rigorous validation is needed. Throughout this Chapter the aim is to identify gaps in the research and explain where the research in the subsequent investigations fit in the bigger picture.

Chapter 3 is a detailed description into the methodology applied and experimental choices made in order to rigorously and accurately test the applicability of the fuels in FBC systems. Developments of the testing equipment, plans of tests and validation of operational choices for investigation are explained. By doing so this Chapter aims to indicate the logical and systematic approach taken to thoroughly test key operational parameters within the research in order to achieve representative and reliable results to be used to compare the fuels, techniques and scale of operation.

Chapter 4 is aimed towards producing an understanding of the fundamental physical and chemical make-up of the fuels. The objective of this is to produce a series of data sets that will be used to draw links to the agglomerates and combustion mechanisms seen in later Chapters. This Chapter also aims to develop XRF as a more accurate and applicable

technique for measuring low grade fuel ashes and combustion bi-products. This data will also be critical for identifying key components within the combustion mechanisms and devising conclusions as to their importance to the research.

Chapter 5 applies theoretical approaches including indices, predictions based on the fuel characterisation studies and a thermodynamic model (FACTSAGE) for the determination of slagging and agglomeration issues with low grade fuels in FBC. The aim is to evaluate the accuracy and applicability of these techniques for predicting bed issues by validating the results in experimental chapters. The overall objective is to identify the strengths and weaknesses of the methods and to suggest how the techniques could be used to predict bed issues in full scale operations.

Chapter 6 aims to investigate the effect sub-bituminous coals have on a FBC bed and the impact the fuel has on agglomerates. The objective of this Chapter is to evaluate the opportunity to improve the fuel with the addition of bed additives and operational changes. By doing so, the work allows for conclusions to be drawn between operational variables whilst linking phenomena seen in the bed to the fuel characterisation work of Chapter 4. The overall aim of the Chapter is to conclude as to the applicability of the fuels in full scale operations and to offer methods for improving the fuels as a result of the data gathered during experimental testing.

Chapter 7 aims to evaluate the effect combusting different biomass fuels in FBC has on the rates of agglomeration and the impact of operational variables on the ability to achieve stable combustion. The air distribution plate will be modified in order to understand the effect poor air flow and restriction has on the bed and combustion. The overall aim of this Chapter is to evaluate the biomasses and to evaluate the application of the fuels in full scale operations and recommend techniques that should be employed in order to mitigate the engineering challenges highlighted by the experimental results.

1.5 Outline of Thesis

This thesis contains 8 Chapters. Chapter 1 introduces the problem and rationale for the research undertaken in the following document. Chapter 2 develops an understanding of the theory and explains research in the literature. In doing so highlighting the gaps in the available research and the need for the research. Chapter 3 describes the experimental methodology, equipment and testing plan designed to vigorously the theories and variables defined. Chapter 4 is focused on fuel and material characterisation and the lab analysis techniques/methodologies development. Chapter 5 through 7 are results Chapters

specifically looking at areas in which the literature review has highlighted. Chapter 6 investigates low rank Pakistani coals in FBC, Chapter 7 investigates the impact of biomass in FBC and the effect of a damaged air distribution system on agglomeration, and Chapter 5 demonstrates work conducted in the modelling package "FACTSAGE". Chapter 8 outlines the conclusions and the future work required to further develop ideas and theories founded in this thesis. The research shows how the fuels can be employed in full scale utilities and the remedies which should be considered on their application.

2 Literature Review

2.1 Introduction

An ongoing area of research is the application of biomass fuels and sub bituminous coals due to the economic and technological implication in the power generation industry. In order to understand what research has been undertaken beforehand and identify where the research gaps are a thorough literature review was conducted. The following Chapter is a comprehensive cross section of technical, chemical and physical areas which needed consideration when addressing potential operational issues for the combustion of low grade fuels in FBC technologies.

2.2 Coal Utilisation

Coal in its many variations, can be found in a number of geologically significant locations around the world, especially in large quantities in countries such as North America, Russia, Australia, South Africa, Columbia and China (Speight, 2012). Coal is the result of dead plant life from the carboniferous period (300 million years ago) which has been subjected to great pressure and heat. The first formations of coal come in the form of soft peats, but with longer periods of heat and pressure, give rise to bituminous and less abundant anthracites (Stone, 2004). Due to the plant life origins of the coal, the elemental make up of coal consists mainly of carbon, hydrogen, oxygen, nitrogen and sulphur. Coal also contains small amounts of a number of major and minor groups varying from alkaline species such as sodium and potassium to heavy metals such as cadmium and mercury. These components would normally be found in small concentrations in plant life but due to the compaction process and leaching from local land formations, high concentrations of these elemental groups can build up in the coal (Wiser, 1999).

The price of Coal has continued to increase overall since the 1950's with economic changes and increasing consumption globally, as indicated by Figure 2-1. An example of change would altering coal utilisation is the collapse of the world market in the mid 2000's followed by record coal production in the USA in 2006-2008 resulting in a fluctuation in global coal prices from $97.68 per short tonne exported to $39.31 per short tonne exported respectively (Freme, 2009). This then led to increased use of coal for power generation, domestic heating etc. in developing countries such as China which increased its

consumption to 2580 Mt in 2008 which was 41% of the global consumption (Lin and Liu, 2010). However, with the re-stabilisation of world markets by 2010. The increase in coal prices has left countries such as Japan unable to fund coal power generation after their nuclear power plant fleet was shut down amid fears post Fukushima tsunami nuclear disaster, 2011 (Kim et al., 2013). It is for reasons such as these that research and investments are being made towards the exploitation of abundant lower grade coal sources.

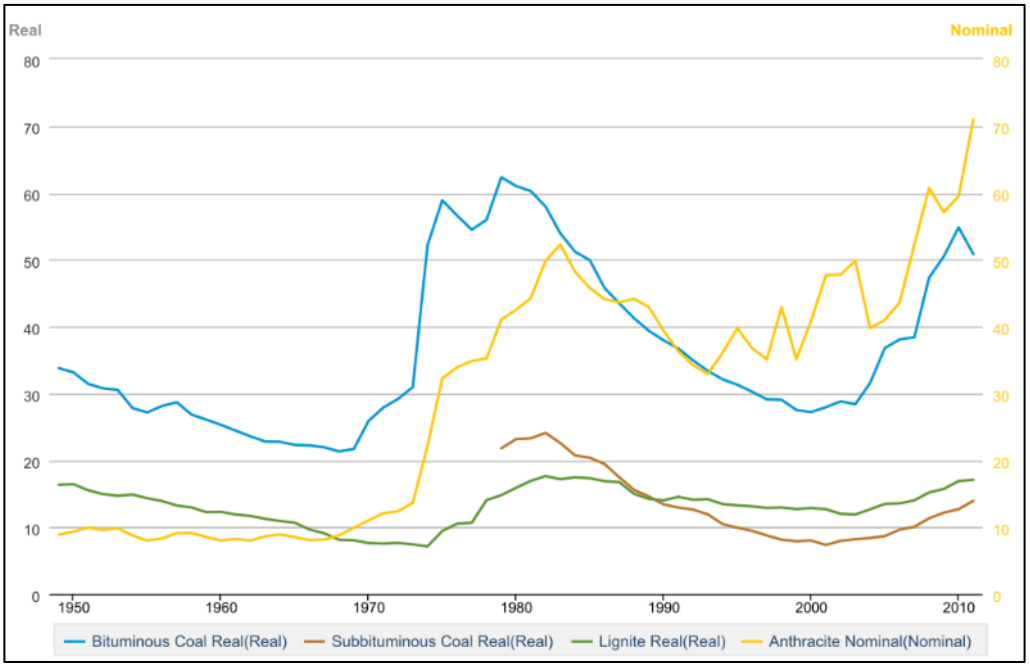

Figure 2-1 Estimated coal market prices, 1949-2011 (Dollars per short Ton) (Paduano, 2016)

Barnes (2015) defines low grade fuels as followed:

"materials that have an energy content that may be recovered by direct (e.g. combustion) or indirect (e.g. gasification) processes, but where that energy content is significantly lower than the range expressed in normal fossil fuels (oil, gas and coal)".

The lower energy content in low grade fuels can be due to higher mineral matter and moisture content, thus diluting the hydrocarbon content and also negatively effecting the combustion properties of the fuel (Barnes, 2015).

A review of the available literature finds significant investigative works in numerous research institutes for low grade fuel-electrical power utilisation globally. Li (2004) reviewed research and exploratory work in Australia aimed towards the liberation and application of Victorian brown coals and lignite's. There are numerous reserves of low grade coals including Murray Basin Mt, 19600, Gippsland Basin, 395000 Mt and Otway Basin, 15500 Mt. The conclusions of fuel availability, ease of extraction and its critical

role in the future of Australia's energy production and economic exports indicate the vast potential and need for technological applications. Numerous other studies including; (Ward and Christie, 1994; Dunne and Agnew, 1992; Karthikeyan et al., 2009; Barton et al., 1993) have been conducted on Australian coals because of their fuel supply potential. This is an example of the growing desire to use these types of fuels and thus the effect and application in combustion systems needs evaluation.

2.3 Biomass

Biomass is defined by the international energy association as:

"Organic, i.e. decomposable, matter derived from plants or animals available on a renewable basis. Biomass includes wood and agricultural crops, herbaceous and woody energy crops, municipal organic wastes as well as manure (D'Apote, 1998)"

Whilst the utilisation of low grade coals could potentially alleviate some of the growing global electrical demand resulting from the projected population growth of 18.6% (8.5 billion by 2030) (Davis et al., 2014), concerns towards anthropogenic climate change has refocused research and development to less CO_2 intensive methods of electrical generation. CO_2 measurements over the last 60 years have seen average atmospheric concentrations increase from measurements over the last 60 years have seen average atmospheric CO_2 concentrations increase from 316 ppm to 400 ppm (Davis et al., 2014). One method to reduce this is to replace CO_2 intensive fossil fuels with biomass fuels such as those previously described as these types of fuels have potential to be carbon neutral or negative if combined with carbon capture method (Mathews, 2008).

In order to utilise biomass, it is impotent to understand the difference biomass has to coal both chemically and physically. Biomass, like coal, contains mainly carbon, hydrogen, nitrogen and oxygen. Biomass contains very little sulphur and is of a varied concentration to the impurities such as alkaline earth groups (Quaak et al., 1999). The difference in biomass composition poses challenges in its application; from harvesting and logistical issues (McKendry, 2002; De Wit and Faaij, 2010; Thorsell et al., 2004; Sokhansanj et al., 2009; Ekşioğlu et al., 2009; Lewandowski and Heinz, 2003; Spinelli et al., 2005), processing of the fuel damaging traditional grinders and cutting equipment (Nunes et al., 2016; CHEN et al., 2005; Xutao and Bailiang, 2008; SUI et al., 2012; Yonglong and HouShulin, 2013), to physical and chemical reactions causing abrasion, agglomeration, corrosion, slagging and fouling in furnaces (Qing-tao, 2009; Wang et al., 2009; Bartels et al., 2008a; Basu and Sarka, 1983; Chaivatamaset et al., 2013).

As part of this study, biomass will be assessed in its application in FBC. This is a technology suited to low grade fuels such as biomass and the following sections will elaborate.

2.4 Fluidised Bed Combustion (FBC)

In order to combust biomass and other low grade fuels it is necessary to utilise a technology which has combustion flexibility that can adapt to the variable mineral, calorific and moisture content alongside other varying impurities. Fluidisation refers to the flow of gases through a bed of solid particles suspended on a bed of gas, usually air. When gases (air) with sufficient velocity enters under a bed via a distribution method, the bed expands and lifts as the voids between particles increase. Once combustion takes place in the bed either through solid fuel combustion or, usually oil or gas, pre-heat system. With increased air flow and heat the bed material flows and reacts more like a fluid and thus "fluidisation" has begun (Cotton et al., 2013). Figure 2-2 illustrates different stages of fluidisation a bed will undergo with increased airflow. As the airflow is increased the bed void increase as they are filled with the fluidisation medium. The bed will begin to bubble, with bubbles erupting on the surface.

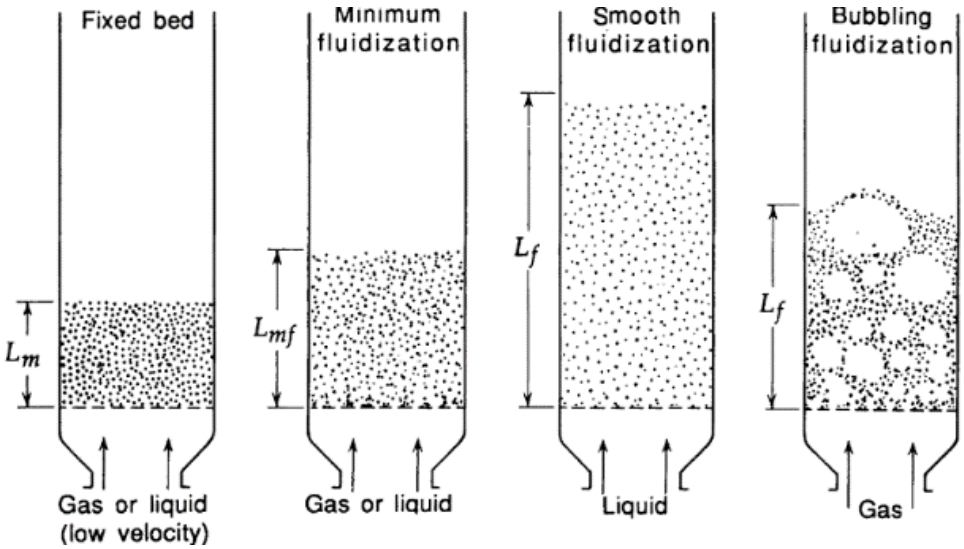

Figure 2-2 Different fluidisation modes a bed can experience depending on air flow, fluidisation medium and bed material choice.(Kunii et al., 2013)

The following sections describe technological considerations and design choices for FBC systems which will be applied in later Chapters and experimental design. The reviewed literature has been used to devise the method for investigations and the need for research in specific areas of FBC utilisation for low grade fuels.

2.5 Fluidisation Theory and Fundamentals

Operating and monitoring a FBC requires understanding and application of fundamental rules and mechanisms including; minimum fluidisation velocity, combustion optimisation, pressure drop and bed hydrodynamics. As such it is necessary to review the literature on the effect operational variables have on them to better understand and operate the experimental rig during testing and conception of tests.

2.5.1 Minimum & Maximum Fluidisation Velocity

Possibly the most important factor affecting the operation of a fluidised bed is the fluidisation velocity. That is, the velocity of the gas or liquid flowing through a packed bed in order to commence fluidisation. The following sections describe the fundamental properties and theory required for both understanding how a bed fluidises and how to modify and operate a bed successfully. The following sections are of particular importance to the air distribution, efficiencies and state of turbulence underpinning the rates and type of agglomeration that can occur in a bed. The theory described are a justification for picking operational variables to tests in later investigations including, use of additive, modification of air flows, particle sizes, combustion temperatures and co-firing of different fuel ratios.

The variables affecting minimum fluidisation are summarised by Figure 2-3, and indicate how fluidisation cannot occur until the forces acting down upon the bed are counteracted by the forces being applied to the bed from the inlet air etc.

$$\begin{pmatrix}\text{pressure drop}\\ \text{across bed}\end{pmatrix}+\begin{pmatrix}\text{cross section}\\ \text{area of}\\ \text{combustion}\\ \text{chamber}\end{pmatrix}=\begin{pmatrix}\text{volume}\\ \text{of bed}\end{pmatrix}+\begin{pmatrix}\text{fraction}\\ \text{consisting}\\ \text{of solids}\end{pmatrix}+\begin{pmatrix}\text{specific weight}\\ \text{of solids}\end{pmatrix}$$

Figure 2-3 (Kunii and Levenspiel, 1991)

When air is introduced to the system the bed will undergo a number of stages as fluidisation occurs; 1) initially the bed will be packed; 2) the initial development of fluidisation and raising of the whole bed; 3) bubbling bed starts and intensifies; 4) slugging of the bed occurs 5) entrainment of the bed. Initially low air velocities present no change in the bed due to the frictional forces between particles etc. overcoming the opposing forces against the bed. However, there is a pressure drop across the bed which is a result of a loss of mechanical energy caused by the beds particle friction (ΔP). The pressure drop across the bed which is influenced by the properties of the particles is calculated using Equation 2-1(Anthony, 2003).

$$\Delta P = \lambda \times \frac{L}{D} \times \frac{v^2}{2} \rho_f$$ Equation 2-1 (Anthony, 2003)

Where ΔP is pressure drop, λ is friction factor, L is distance across the bed, v is velocity of the gas and ρ_f is the fluid/gas density.

Whilst Equation 2-1 calculates the pressure drop across a bed with a good level of accuracy with particles above 150μm in diameter, Equation 2-1 requires modification to retain accuracy when considering different particle sizes. With larger bed particles, the bed voidage between irregular shaped particles will also increase thus influencing the displacement properties of the fluidising air. The increase in voidage also has an effect on the particle wall effect of the particles. Therefore, taking these parameters into consideration Equation 2-2 develops Equation 2-1 (Kunii and Levenspiel, 1991; Anthony, 2003).

$$\frac{\Delta p_{fr}}{L_m} g_c = 150 \frac{(1-\varepsilon_m)^2}{\varepsilon_m^3} \times \frac{\mu u_o}{(\varphi_s d_p)^2} + 1.75 \times \frac{1-\varepsilon_m}{\varepsilon_m^3} \times \frac{\rho_g u_o^2}{\varphi_s d_p}$$ Equation 2-2 (Anthony, 2003)

Where Δp_{fr} is frictional pressure drop, L_m is the height of the bed, g_c gravity constant, ε_m is the void fraction, μ is the viscosity of the gas, u_o is the superficial gas velocity, d_p particle diameter, ρ_g is gas density and φ_s is the spherity of a particle.

With an increase of fluidisation air the fluidisation of the bed will begin. The initial incipient fluidisation of the bed can be calculated and is referred to as the minimum fluidisation velocity (U_{mf}). Equation 2-3 illustrates the relationship with the minimum fluidisation to inlet velocity air and the cross-sectional area of the bed. The flow rate of inlet air is in reality greater than that of the calculated minimum fluidisation air value. This is due to frictional forces in the inlet pipes, the irregularity of bed materials such as sand which will not be perfectly spherical, the variable weight of the individual particles and the physical dimensions which will contribute to aerodynamic factors and buoyancy influence (Howard, 1989). Equation 2-4 develops on Equation 2-3 and gives a more realistic minimum fluidisation value when the average bed particles are less than 40μm whilst Equation 2-5 is more applicable for bed particles averaging > 1000μm. Whilst there are variations of these equations between authors, Equation 2-3, Equation 2-4 and Equation 2-5 are widely accepted for materials such as silica sand for bed materials (Howard, 1989; Kunii and Levenspiel, 1991) and will be applied during air distributor and experimental rig design.

$U_{mf} = \frac{V_{mf}}{A}$	Equation 2-3	(Howard, 1989)
$U_{mf} = \frac{d_p^2(\rho_s - \rho_g)g}{150\mu} \times \frac{\varepsilon_{mf}^3 \varphi_s^2}{1-\varepsilon_{mf}}$ Rep, mf<40	Equation 2-4	(Kunii and Levenspiel, 1991)
$U_{mf}^2 = \frac{d_p\,(\rho_s - \rho_g)g}{1.75\rho_g} \times \varepsilon_{mf}^3 \varphi_s$ Rep, mf>1000	Equation 2-5	

Where U_{mf} is the minimum fluidisation velocity, V_{mf} is the volumetric flow rate, A is the cross-sectional area of the bed, d_p is the particle diameter, ρ_s is the solid density, ρ_g is the gas density, μ viscosity of the gas, ε_{mf} is the volume of void fraction at minimum fluidisation, g is gravity constant and φ_s is the spherity of the bed particles.

With the onset of incipient fluidisation, the pressure drop across the bed will remain stationary, however, the particles in the bed will increase in voidage until a state of equilibrium has been achieved. At this point bubbles, will form and collapse throughout the bed. The bed will sustain its level of buoyancy as long as no other variables are introduced or altered (Anthony, 2003).

With further increases in the fluidisation inlet velocity the bed will move to a third stage and the bubbling will intensify. At this point the fuel particles and temperature will distribute within the bed resulting in a near homogenous bed with continued mixing. The bubbles at this point will be small and irregular and variant. As the fluidisation velocity continues to increase the bed enters stage 4 resulting in slugging of the bed. At this stage, smaller particles become entrained within the bed i.e. they are no longer mixing but become trapped within the bed which is stage 5. The entrainment of particles will result in changes of pressure drop across the bed. If these are too great the bed risks slumping or inefficient mixing throughout the bed (Howard, 1989; Kunii and Levenspiel, 1991; Anthony, 2003). These factors need consideration when analysing shape and spread formation of agglomerates in the bed to understand fuel distribution and the effect of operational parameters influencing bed turbulence.

2.5.2 Pressure Drop vs. Velocity

Pressure drop and the inlet fluidisation velocity is a common method for monitoring a bed condition because of its more simplistic representation of the bed air movement and particle mixing.

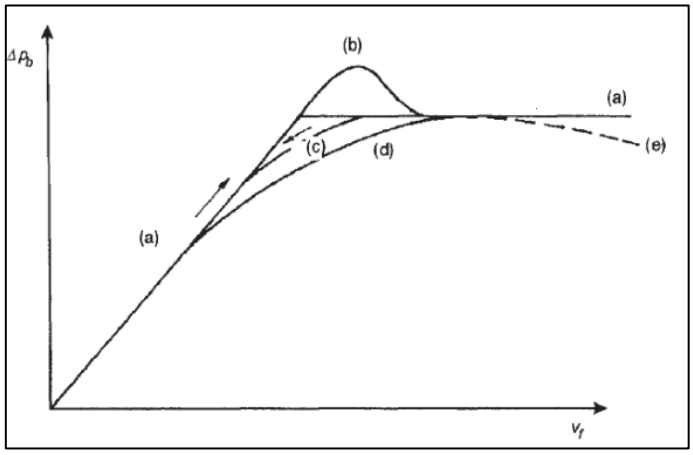

Figure 2-4 Characteristic curves of bed pressure drop and its dependence on fluidisation velocity (Anthony, 2003)

As the pressure drop remains constant post fluidisation of the bed, the increasing inlet fluidisation velocity causes some fundamental changes as shown in Figure 2-4. These can be used to determine the status of a FBC in operation. The changes of increasing inlet velocity are as follows; (a) the increasing inlet air is approaching fluidisation. When the onset of fluidisation occurs the hump as shown by (b) will present followed by a stabilisation (this stable line is an average value as the values will oscillate around this value with the bubbling occurring within the bed) (Anthony, 2003). (Kunii and Levenspiel, 1991).

The region shown as (c) above the line represented as (d) is a buffer zone which can occur with smaller average particle diameters. The smaller particles are effected by buoyancy forces differently to that of larger particles and as a result of when minimum fluidisation occurs the pressure drop diminishes until a further increase in fluidisation velocity re-establishes fluidisation. The line at which (e) occurs indicates the entrainment of material with the bed resulting in a decrease in pressure drop across the bed (Howard, 1989).

Overall the theory covered will be used to evaluate the bed conditions, operational choices and start-up procedure.

2.5.3 Theoretical Properties of Fluidising Particles

Different particles interact with the bed in different ways and based on their particle classification this can be used to predict the particles interactions with the bed. Another purpose for a particle classification is that not all particles can be fluidised and therefore, it is important that proper classification gives an operator the information needed to run an FBC correctly.

The literature shows different approaches used to try and classify the interactions of the particles within a FBC bed, the mode of fluidisation and the criteria for transition from one mode to another. Initially Wilhelm and Kwauk (1948) proposed a criteria system based on inter particle forces between bubbles using the Froude number. This was then developed by Romero (1962) which included dimensionless groups such as Reynolds number and Froude number. Additional approaches and takes on the classification were attempted and developed however, it was Geldart (1973) who approached the issue in terms of particle characteristics and the way they fluidise as illustrated in Figure 2-5.

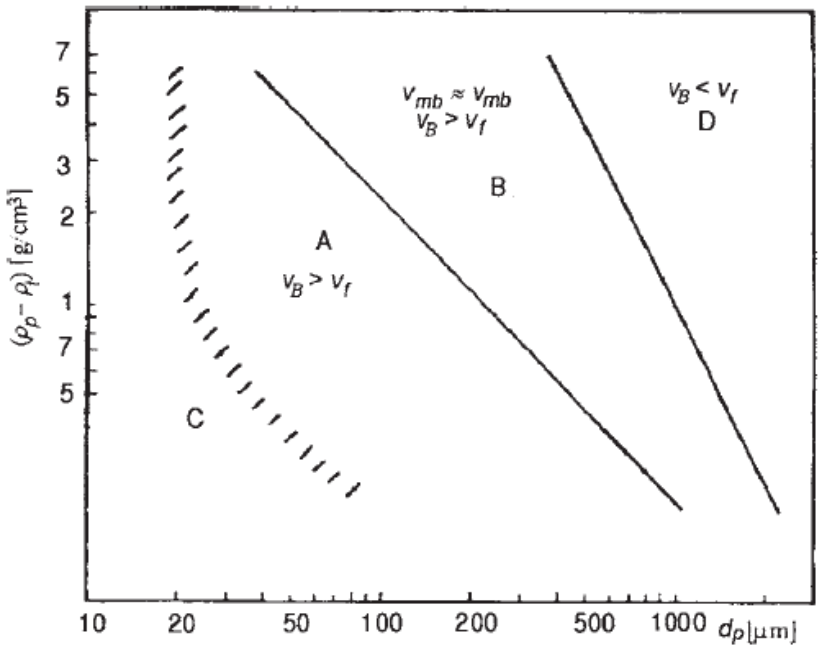

Figure 2-5 Geldarts approach to particle classification in fluidisation (Geldart, 1973)

The Geldart diagram compromises of four categories and are as follows:

- Group A-consists of particles which have a small mean size and low bulk density (ρ_ρ<1400kg/m^3). These particles can be fluidised easily with smooth fluidisation being observed at low inlet velocities. Due to the large buoyancy effect on the small particles, the fluidisation of these materials results in large bed expansions and a homogeneous fluidisation. The bubble rising velocity will exceed the interstitial gas velocity during the emulsion phase resulting in a maximum bubble size achievable (Geldart, 1973; Kunii and Levenspiel, 1991). The interstitial gas velocity is defined as the velocity of the gases moving in an opposing direction to a particle in the bed and is summarised by Equation 2-6 (where $\bar{u}$.is interstitial velocity, u is the carrier gas and j is a pressure gradient factor).

$$\bar{u} = uj$$ Equation 2-6 (Subramanian, 2004)

- Group B-particles are of a medium size (40μm<Dp<500μm) and medium density (1400<ρ_s<4000kg/m^3) and therefore, covers a large variety of different materials (Kunii and Levenspiel, 1991). Most particles of this group are described as "sand" like and bubbles occur immediately after minimum fluidisation has been achieved. There is no maximum bubble size associated with this group which allows slugging etc. of beds made of this particle category (Anthony, 2003). This is a visual indicator for poor fluidisation brought on by operational changes.
- Group C-is made up of fine particles (Dp<30μm) with extremely low density which can be described as cohesive. The fluidisation of these particles is difficult due to the inter particle forces being very strong. The velocity of the inlet gases required are too large for fluidisation but instead blow away bed material. These types of particles form channels and irregular slug patterns and thus the pressure drop seen in fluidised beds is not achieved. For this reason, the bed will remain fairly static hence poor mixing and no fluidisation is achieved (Geldart, 1973; Kunii and Levenspiel, 1991; Anthony, 2003; Jones and Williams, 2008).
- Group D-is made up of larger (Dp>600μm) and more dense particles which commonly have coarse shapes which will influence fluidisation greatly. Because of the larger physical weight etc. of the particles, deeper beds are difficult to fluidise. However, once fluidisation has been achieved bubbles will rise slowly through the bed, specifically slower than the interstitial gas velocity. The slow bubble formation develops explosive bubbles on the surface of a bed and can lead to channelling or spouting through the bed (Howard, 1989; Kunii and Levenspiel, 1991).

The Geldart diagram will be referred to in later results to correlate average bed particle size change to agglomeration formation and fluidisation.

2.6 Physical Properties of Fluidising Particles

There are a number of physical properties which affect the hydrodynamics of bed particles and hence the ability to fluidise that bed. The different physical properties such as particle size, density, size distribution, particle voidage, physical shape and how coarse the particles are etc. will contribute to the particles classification in the Geldart diagram and therefore, the requirements for fluidisation. Understanding these values is important for operators to determine what mechanisms are taking place in the bed and why.

The following sections and theory are fundamental for the understanding of bed interactions that occur between gases, gas-solids and solids. The bulk density for instance will influence how the bed will fluidise, how the gases will move throughout the bed, bubble formation and consequently this impacts in the physical mechanisms associated with agglomeration. Furthermore, these physical properties will alter the impact that test variables can pose on the outcome of agglomerate formation, defluidisation times and the resulting flame from bed/above bed combustion.

2.6.1 Spherity

Each particle will interact differently within a bed due to its shape and size and therefore, influence the fluidisation and voidage of a packed bed. Average particle sizes are used to encompass variance in size and shape of particles within a bed and the large number of individual particles present. The term d_{eff} is the effective diameter of each particle within the bed. Whilst particles over $1mm^2$ can be measured manually by either sieve or callipers, particles $\leq 1mm^2$ are calculated from available data. The first method is to average particles by giving an equivalent spherical diameter for volume, thus mitigating the shape of each individual particle and is defined as Equation 2-7 (Kunii and Levenspiel, 1991).

$$d_{sph} = \begin{pmatrix} diameter\ of\ a\ sphere\ with\ the\ volume \\ of\ the\ average\ partivcle\ volume \end{pmatrix} \quad \text{Equation 2-7} \quad \text{(Kunii and Levenspiel, 1991)}$$

Due to the irregularity in particle shape, voidage, non-spherical nature and the non-uniform particles it is more common for the Spherity to be calculated using the method in Equation 2-8.

$$\varphi_s = \frac{surface\ area\ of\ a\ sphere}{surface\ area\ of\ a\ particle} \quad \text{Equation 2-8} \quad \text{(Kunii and Levenspiel, 1991)}$$

$\varphi_s=1$ is the definition for a spherical particle, therefore, for irregularly shaped particles the value will be ≤ 1 (Kunii and Levenspiel, 1991). During combustion and the fluidisation of a bed, the particles will move against each other creating abrasion and erosion. This results in the coarser particles becoming more spherical and smooth therefore, increasing the φ_s value. A standard value for a granular particle such as that found in silica sand based beds is 0.6 (Howard, 1989).

The d_{eff} can represent a bed of non-spherical particles in terms of spherical particles by using the developed Equation 2-9 which takes two theoretical beds of the same particles including the same total surface area and the total voidage fraction.

$$d_{eff} = \varphi_s d_{sph} \qquad \text{Equation 2-9} \qquad \text{(Kunii and Levenspiel, 1991)}$$

The spherity of particles is significant when introducing fuels such as biomass which has large irregularity and variance thus altering the flow through a bed and thus potentially effecting mixing of the bed.

2.6.2 Terminal Velocity

Terminal velocity is the velocity of particle falling through a gas with external forces acting upon the particle whilst the particle achieves a maximum falling speed which will max at 9.8m/s (gravity). Figure 2-6 illustrates a particle which is falling within a gas stream. The forces exerted on the particle include gravity, drag and buoyancy.

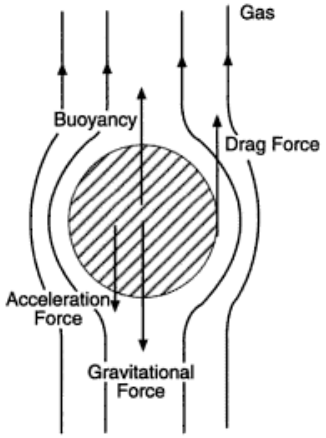

Figure 2-6 Forces exerted on a particle moving upward in a gas stream. The net forces acting on the particle come to equilibrium as terminal velocity is achieved. (Basu, 2006)

When the forces acting upon the particle come to equilibrium i.e. the particle is moving towards the earth at the same magnitude as the particle is accelerating away from it, then the particle is at terminal velocity (Gupta and Sathiyamoorthy, 1998).

When the force generated by velocity exceeds free fall forces of the particle it will travel in the gas stream. This would be an indication that the fluidisation inlet air velocity is to excessive. The terminal velocity of a particle can be calculated using Equation 2-10 and Equation 2-11 (Basu, 2006).

$$u_t = \frac{\rho_p d_p^2 g}{18\mu} \ (Re < 0.4)$$ Equation 2-10

$$u_t = \left(\frac{1.78 \times 10^{-2} \times {\rho_p}^2}{\rho_g \mu}\right)^{\frac{1}{3}} \times d_p \ (0.4 < Re < 500)$$ Equation 2-11

(Davidson and Harrison, 1987a)

Where u_t is the terminal velocity, ρ_p is gas density, μ viscocity of gas, g is the gravity constant, $\rho_g$is gas density and $d_p$is particle diameter.

The terminal velocity should be calculated for the smallest particle in the bed as a velocity in excess to this value will result in the eluration of particles as they become entrained in the gases potentially forcing particles to exit with flue gases (Gupta and Sathiyamoorthy, 1998). Because of the loss of material from a bed, cyclones and recycle circuits are built in to capture and replace bed materials.

2.6.3 Bulk Density

The bulk density of the bed refers to the mass of particulates per unit within the bed volume. This value is calculated using Equation 2-12 which will give a smaller value than the true density of the particles as the bulk/bed density includes the voidage between each particle. The bulk density is determined by the size and shape of the particles which in turns alters the voidage between particles (Howard, 1989).

$$P_b = \frac{m_b}{V_b} = \rho_p(1 - \varepsilon)$$ Equation 2-12 (Howard, 1989)

Where P_b is bulk density, m_b is mass of bed and V_b is bed volume.

The bulk density is an often overlooked value when considering the interactions occurring within a fluidised bed. The bulk density is a function of the voidage which directly alters the pressure drop across the fluidised bed and hence the interactions between solids and gases within an FBC system (Ergun and Orning, 1949).

Therefore, in a batch bed system such as that in the experiments chapters, the constant input of fuel and lack of removal indicates there will be a change in bulk density. Therefore, a consideration will be needed for material build up in terms of fuel ash and mineral content in fluidisation.

2.6.4 Bed Voidage

As previously described, the bed voidage is the space which occurs between particles within a bed. The size of the voids will change with particle shape, air ingress and size.

Irregular particles produce more voids compared to regular particles as they fit together better resulting in smaller void space. On average a fixed bed will have a voidage value between 0.4-0.45 (Howard, 1989). The bed voidage is calculated using Equation 2-13.

$$\varepsilon = \frac{V_b - \Sigma V_p}{V_p} = 1 - \frac{\rho_b}{\rho_p} \qquad \text{Equation 2-13} \qquad \text{(Howard, 1989)}$$

Where ε is void fraction, V_p volume of particle, V_b is bed volume, ρ_b bed density and $\rho_p$particle density.

The voidage is a fundamental property when considering fluidised bed combustion as the combustion can be directly influenced by bed voidage in terms of both mixing solids and gases as well as the development of combusting fuel particles. It has been shown in studies such as Kuo et al. (1997), that larger void fractions in a bed can lead to lower bed temperatures. This is due to the distribution of oxygen and combustion gases throughout the bed and depletion of oxygen resulting in inefficient fuel burnout. An increase in voidage has also been shown to decrease the average combustion rate, once again due to the reduced mixing regime within the bed. Other possible reasons stem from the formation of slugging when the larger voids join adjacent bubbles.

2.6.5 Bed Height

Bed height is a parameter which describes a macroscopic behaviour of a fluidised bed and the consequent bubbling regime. Whilst the surface of a bed will constantly vary with the rising and collapsing of bubbles, there is a clear relationship with bed height and the fluidisation velocity. However, based on the "Davidson two phase model" then the bed particles are outside rising bubbles and therefore, in a state of minimum fluidisation (Davidson and Harrison, 1987c). When the fluidisation velocity is increased beyond minimum fluidisation, the voids voidage and porosity of the bed will increase resulting in an increased bed height. Hence the critical value is the void space which is occupied by bubbles throughout the bed (Hetsroni, 1982; Davidson and Harrison, 1987a; Yang, 2003). The relationship for bed height, particle voidage and space occupied by bubbles has not been validated in the literature but can be summarised by Equation 2-14. Constants are required for subsequent calculations which are unique to each fluidised scenario and system variables.

$$\frac{H}{H_{mf}} = \frac{1}{1 - \delta_b} = \frac{1 - \varepsilon_{mf}}{1 - \varepsilon} \qquad \text{Equation 2-14} \qquad \text{(Hetsroni, 1982)}$$

Where H is bed height, H_{mf} is minimum fluidisation bed height, δ_b is pressure change across the bed, ε is void fraction and ε_{mf} is volume of void fraction at minimum fluidisation.

Whilst increasing the fluidisation air velocity increases the bed height, there is a limit to the bed height. For each specific fluidised bed and operational conditions to the maximum bed height will be a result of the free fall velocity of fuel particles inlet gas velocity. This is termed as the transport disengagement height (TDH) and can be summarised using the Geldart equation in Equation 2-15 (Hetsroni, 1982).

$$TDH = 1200 \times H_{mf} \times Re_p^{1.55} \times A_r^{-1.1} \qquad \text{Equation 2-15} \qquad \text{(Hetsroni, 1982)}$$

However, instead of determining a bed by its initial height a more suitable parameter to incorporate is the bed weight. Whilst an increasing bed height can be influenced directly by the fluidisation air velocity, the beds weight remains constant (excluding transport and loss of bed material). An increase in bed weight will require a higher minimum fluidisation velocity but will also decrease the voidage between particles as bubbles will be smaller and occupying less space (Yang, 2003). Therefore, varying bed weight for a constant fluidisation velocity will directly impact the hydrodynamic performance of the bed and rising bubbles and hence an effect macroscopic interactions which influence agglomeration and combustion.

Bed height has been studied throughout the literature looking at the influence of fluidisation velocities on bed height utilising different materials for the bed. Zhong et al. (2008) investigated the effect of bed height with a number of biomass fuels and the influence of different bed materials. As the different fuels were introduced to the bed it was found that the density of the bed would alter resulting in a change in the minimum fluidisation velocity. The different beds and fuels also directly influenced the height of the bed by varying inlet air velocity.

Further studies have been conducted on the influence of bed height with different mediums, bed shapes, height, fuel inlets etc. in (Escudero and Heindel, 2011; Sau et al., 2007; Ramos Caicedo et al., 2002; Geldart, 1968; Cranfield and Geldart, 1974; Zhong et al., 2006). These studies highlight the potential variance which is to be expected when operating a FBC. When conducting tests with varying bed weights/height it is prudent to consider the alteration the different fuels will have upon the bed.

2.7 Fluidised Bed Combustion (FBC)

In order to combust biomass and other low grade fuels it is necessary to utilise a technology which has combustion flexibility that can adapt to the variable mineral, calorific and moisture content alongside other varying impurities. Fluidisation refers to the flow of gases through a bed of solid particles suspended on a bed of gas, usually air. When gases (air) with sufficient velocity enters under a bed via a distribution method, the bed expands and lifts as the voids between particles increase. Once combustion takes place in the bed either through solid fuel combustion or, usually oil or gas, pre-heat system. With increased air flow and heat the bed material flows and reacts more like a fluid and thus "fluidisation" has begun (Cotton et al., 2013). Figure 2-7 illustrates different stages of fluidisation a bed will undergo with increased airflow. As the airflow is increased the bed void increase as they are filled with the fluidisation medium. The bed will begin to bubble, with bubbles erupting on the surface.

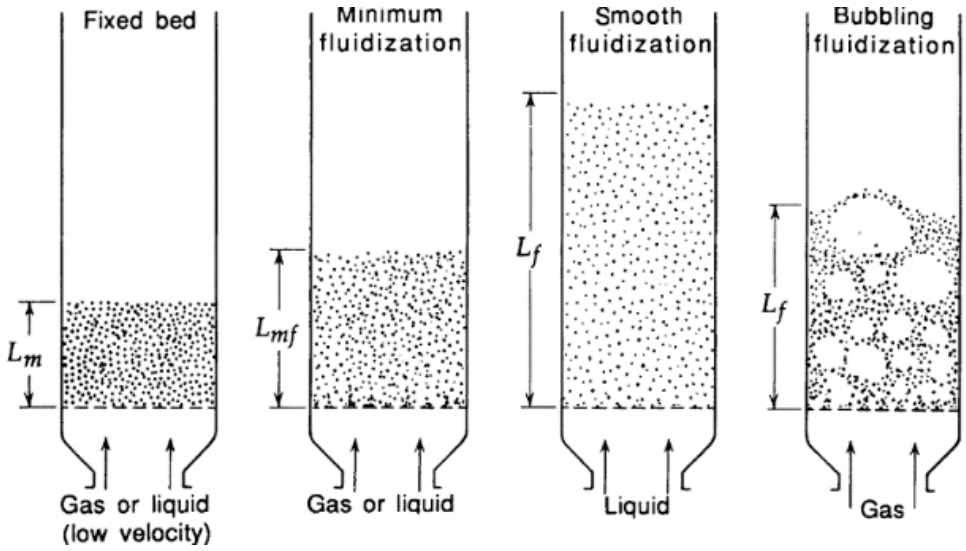

Figure 2-7 Different fluidisation modes a bed can experience depending on air flow, fluidisation medium and bed material choice.(Kunii et al., 2013)

The following sections describe technological considerations and design choices for FBC systems which will be applied in later Chapters and experimental design. The reviewed literature has been used to devise the method for investigations and the need for research in specific areas of FBC utilisation for low grade fuels.

2.8 FBC Technologies

FBC units are commonly made up of a number of key components. The bed is placed on a distributor plate which contains holes, caps, flanges etc. The primary air is fed beneath

the bed and through this plate with the initial ignition system (gas/oil burners) which lifts/fluidises the bed whilst heating it. Above the bed is normally a secondary air input area as well as a fuel feeder system in which fuels are fed into the combustion chamber and bed. The fuel will become mixed within the bed material as the turbulent bed moves like a liquid. Fuel will combust above the bed as well as the collapsing air bubbles entering fuel particles to combust within the body of the bed. This form of combustion is very thermally efficient as fuel particles move against other particles and gases, maximising thermal transmission and accomplishing complete utilisation of combustible material. Post combustion flue gases move through a freeboard space above the bed that is tall enough for entrained particles to disengage. This combined with flue gas clean up systems such as bag filters or electrostatic precipitators remove particulates and degraded bed material before emitting gases through an exit flue stack (Kunii and Levenspiel, 1991; Wu, 2003a).

When considering which method of FBC is most advantageous for a given application there are a number of pros and cons that need be considered for each method. This includes electrical or thermal output, the ability to combust specific fuels, scale of operation intended or economic limitations (Ltd and Ltd) (Koornneef et al., 2007).

2.8.1 Atmospheric Fluidised Bed Combustion (AFBC)

Figure 2-8 is a schematic of a typical AFBC system. In this design the bed material is fluidised from primary air which is fed from below the bed. The air flow is enough to fluidise the bed but not significant enough to carry over the material through the freeboard and into the downstream ducting. In AFBC the fuel is fed from above, and gravity drops the fuel onto the top of the bed. The turbulent mixing entrains the fuel and in doing so heating the fuel and causing it to combust. The bed and fuel will then move around the submerged tubes within the bed and in doing so create a high rate of heat transfer to the pipes and fluids. Alternatively the hot gases and radiant heat can be captured using super heater tubes above the bed and downstream economiser (Merrick, 1984). This is more common in medium to large scale operations.

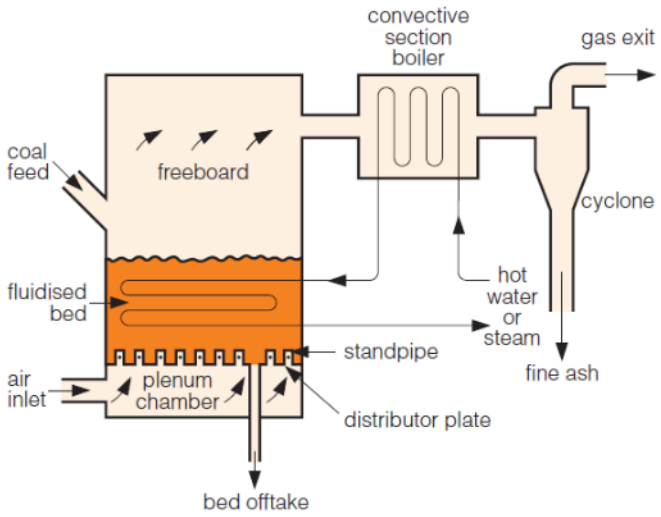

Figure 2-8 Atmospheric bubbling fluidised bed combustor design (Merrick, 1984)

AFBC systems are designed to operate at lower combustion temperatures of 800-950°C. This is achieved by having a uniform distribution of primary and excess air across the bed combined with secondary over bed air which results in a cooler flame (Wu, 2003a). The use of secondary over bed air in the freeboard ensures complete combustion and conversion of volatiles or gaseous species. This is especially important for biomass fuels which have high volatile matter which can be released above the bed, requiring modification of the flame location to ensure complete combustion (Quaak et al., 1999).

The advantages of AFBC compared to conventional or similar technologies is the lower flame temperatures which will decrease NO formation, decrease higher temperatures alkaline species in slag formation, good heat transfer rates, high thermal retention within the bed for more efficient fuel conversion and easily applied emissions control technologies such as SO_2 capture options. AFBC suffers primarily in two ways; firstly, the bed accumulates combustion bi products such as bottom ash, degraded bed materials and agglomerates which require an identification/removal and secondly, these types of systems have scale up limitations to 100-150 $MW_{electrical}$ (Anthony et al., 2003; McIlveen-Wright et al., 1999). Scale up is limited due to economic balance i.e. the cost of generating further under-bed air to suspend an increasing bed size vs. the energy output of such a system.

2.8.2 Circulating Fluidised Bed Combustion (CFBC)

CFBC systems share similarities with AFBC systems. CFBC systems operate at much higher fluidising air velocities and with a slightly lower range of combustion temperatures

(800-900°C). This is due to the increased system air flow rate. Figure 2-9 illustrates a schematic for an CFBC system (Kunii and Levenspiel, 1991).

In a CFBC the high primary air velocities entrain the bed particles which results in them being transported through the freeboard with flue gases. For this reason a heavy duty cyclone is employed to remove bed particles from the flue stream and return them to the main combustion chamber (Gayan et al., 2004). In more efficient CFBC setups a secondary combustion chamber/bed (number 8 on Figure 2-9) can be implemented. This is charged with low velocity secondary air producing a second, smaller fluidise bed for combustion of residual materials which is then employed to preheat the input airs of the primary furnace and thus improve net energy efficiency (Wu, 2003a; Van de Velden et al., 2008).

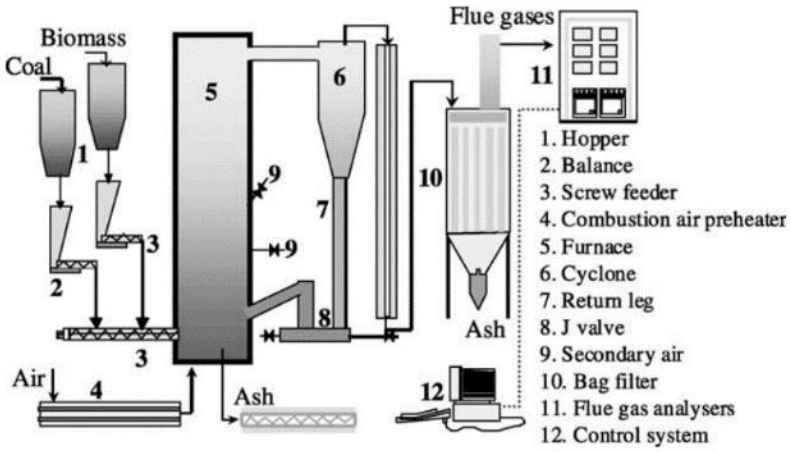

Figure 2-9 Circulating fluidised bed combustor design (Gayan et al., 2004; Kunii and Levenspiel, 1991)

In CFBC the main chamber is host to the majority of combustion and heat transfer to water tubes. Heat recovery occurs downstream, commonly after the heavy-duty cyclone in an economiser. The CFBC systems have a number of advantages over the conventional AFBC systems; higher SO_2 capture potential due to particle interactions and high turbulence resulting in better solid gas mixing, smaller bed area required, fewer fuel injection points required with high turbulence, erosion and corrosion propensity is much less as all tubes are submerged in material and the heat transfer coefficients are potentially the highest for all conventional combustion power generation techniques (Davidson, 2000; Kunii and Levenspiel, 1991). However, these advantages can be offset by the requirements for larger more powerful fans for the higher air flow demand of the system. Higher pressure drop is generated across a less resistant/less densely packed bed requiring further fan air demand. The high particle recycle rates require very efficient flue gas clean

up to capture large quantities of coarse and fine particles, which will become subject to erosion with high flow velocities and high particle loading (Chen et al., 2004; Wu, 2003a).

2.8.3 Pressurised Fluidised Bed Combustion (PFBC)

A PFBC unit is in essence an AFBC unit within a pressurised vessel. Typically, these pressures range between 1-1.5MPa. The unit operates under these pressures at combustion temperatures between 800-900°C (K.Gounder, 1995).

Figure 2-10 illustrates a typical design for a PFBC unit and illustrates how the combustion zone is encapsulated within a pressurised vessel. The pressurised system results in a more, even and frequent production of bubbles throughout the bed (Bonn and Richter, 1990). The increase in particle distribution results in a higher overall thermal and combustion efficiency from the unit.

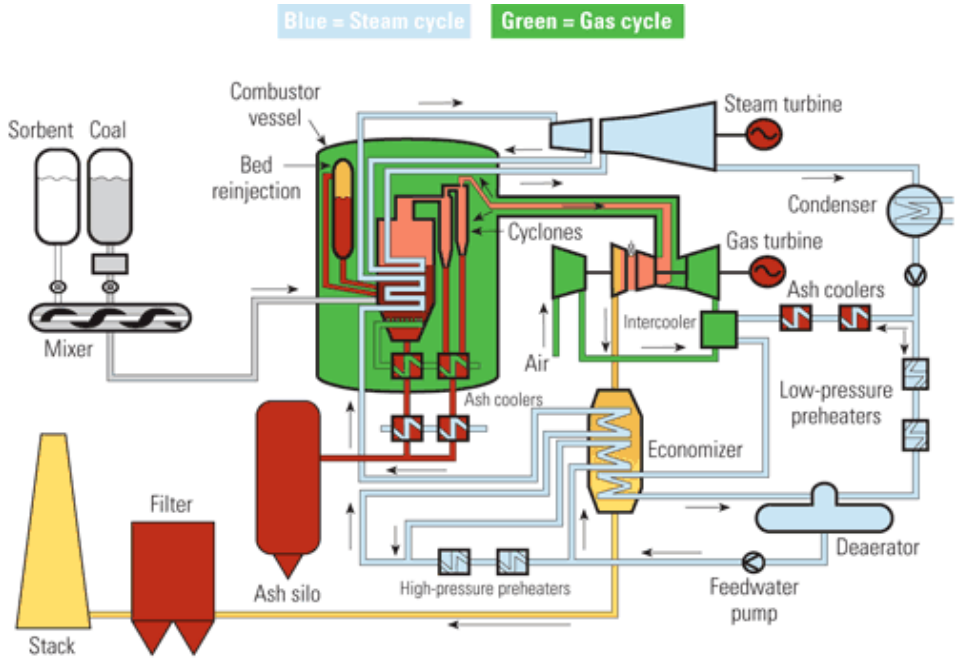

Figure 2-10 Pressurised bubbling fluidised bed combustor design (Makansi, 2005)

The fuel feed, bed replacement and ash removal systems are difficult to manage in order to maintain system pressure. Each of these sub systems will have to be opened to atmosphere and thus requiring a charging and sealing stage to bring them to system pressure. If pressure is lost in any of the feeders etc. the gases and material could potentially leak. As they would be at operating temperatures this poses a serious safety and fire risk (Wu, 2003a; Cuenca and Anthony, 2012). The primary method for limiting this is to incorporate “lock hoppers”. These are devises which use pneumatic transport lines to transport and contain fuel in batch feed flows in to the main combustion chamber.

This would also be adapted to add bed material, sorbents, additives and to remove ashes (Cuenca and Anthony, 2012).

If the system is pressurised sufficiently, then the flue gases can be used as part of a combined cycle system by physically driving a turbine thus generating higher overall efficiencies which is an advantage over other fluidised bed technologies.

The disadvantages of this technology however, the high level of erosion to which equipment experiences and higher particulate content in the flue gases. This requires expensive materials to coat and protect the blades and surfaces etc. The energy required to maintain a pressurised system will be parasitic on the units energy production as well as the safety implications of operating a pressurised system rather than atmospheric (Bonn and Richter, 1990).

2.8.4 Oxyfuel Fluidised Bed Combustion

Oxyfuel combustion uses O_2 instead of air as oxidant. By using O_2 instead of air combustion produces a flue gas which is high in CO_2 concertation and reduced NO_x etc. Combining Oxyfuel combustion with scrubbing systems and CO_2 capture/sequestration technologies it is theoretically possible to mitigate the release of greenhouse gases and thus reduce the anthropogenic impact of power generation from hydrocarbon fuels.

In order to introduce O_2, the fuel line would be doped with high concentration O_2 and fed into the primary air. A disadvantage of using O_2 instead of air as an oxidant is the higher flame temperatures that result from O_2 combustion. Higher temperatures can impact material costs and integrity, emission impacts such as the formation of NO_x from organically bound nitrogen and high temperature corrosion mechanisms. To control this the O_2 inlet has additional recirculated CO_2 from the flue to dilute the O_2 and allow reductions in flame temperature and size which will reduce equipment damage (Czakiert et al., 2010). This type of technology is still in early development stages and no large scale industrial data has been published on the technology (Seddighi K et al., 2013). Laboratory scale tests shave controlled flame temperatures from 900-1200°C to 950-1000°C by doping the O_2 feed with flue gases and inert gases such as N_2 (García-Labiano et al., 2011; de Diego, 2013). Oxyfuel systems could theoretically achieve high combustion efficiencies as it combines technologies previously explained as well as offering a carbon neutral end use for the offset of CO_2 related climate change. However, the key limitation thus far is the technology has yet to be proved at full industrial scale (Bolea et al., 2014).

Whilst there are a number of technological differences between fluidised beds variations, for the purpose of the work conducted in the following investigations a BFBC will be used for experimental work. This type of design offers the simplest mode of operation whilst giving flexibility to operators to alter operational variables.

2.9 Combustion Mechanism of Coal & Biomass

In order to understand the formation of agglomerates it is necessary to review the fundamental mechanisms of combustion that fuel particles will undergo once introduced into the heated bed. Moreover, coal and biomass are fundamentally different in their chemical and physical makeup and thus the mechanism of combustion will vary.

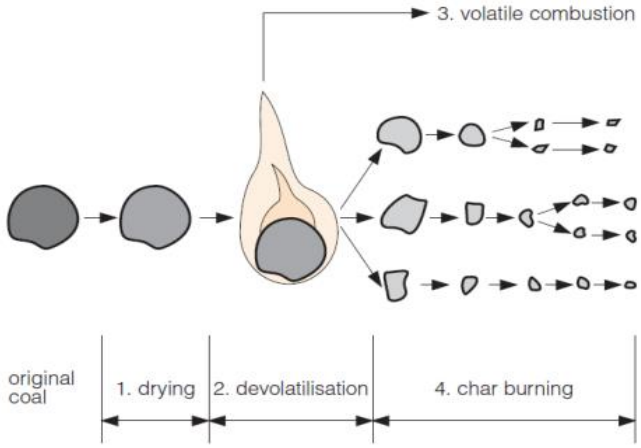

Figure 2-11 Coal combustion process (Wu, 2003a)

When coal particles are fed into a FBC it undergoes a number of stages before complete combustion has occurred. Figure 2-11 illustrates these stages; the initial drying of the particle and moisture driven from the coal, devolitisation of the coal particle which can occur with or without fragmentation of the particle, combustion of the gaseous volatile matter and then the combustion of the coal char particle which will reduce the char to its final ash content (Wu, 2003a). The biomass drying mechanism is slightly different, a biomass particle will undergo drying, devolitisation, gasification and then complete combustion of the char. These stages are similar to the stages coal undergoes but the significance of the differences will be discussed in the following sections.

2.9.1 Drying

The first stage for coal combustion is the initial drying as the coal particles enter the fluidised bed. Moisture is driven off from the particle causing inflammation for high moisture coals. Coal can contain a wide range of moistures from 2-70% in extreme

circumstances (Baxter, 1993). The moisture content will alter the time of drying and subsequent steps, therefore, alter combustion efficiency and particle resident times within the bed. This is an important factor when considering the use of low rank coals which can contain 40%+ moisture (Wu, 2003a). The water content which evaporates from the coal particle is reported to play little if any part in reactions for the following combustion mechanisms (Agarwal and La Nauze, 1989).

In biomass combustion, the drying stage is similar to low grade coal because of its moisture content. Moisture is driven off at low temperatures ≤100°C however, higher moisture contents lowers the system temperature which slows the combustion process. It should be noted also that evaporation is an endothermic process and thus requires energy (latent heat loss) (Koppejan and van Loo, 2012).

2.9.2 Devolitisation Mechanism in Fluidised Bed

As the heat exerted upon the fuel particles continues to increases the particle begins to devolatise. When the coal particles land on/in the bed, a plume shaped flame will form around the particle, as the bed will be at a temperature in excess to the requirements of ignition for the gases being released from the particle. Significant devolitisation will begin to occur at ≥300°C (Wu, 2003a). At lower temperatures, weaker chemical bonds break down resulting in an initial softening of the coal particle and the formation of a metaplastic. As well as the initial moisture lost from the coal particles, there will also be the onset of gas release as lighter components such as methane (Borah et al., 2011). Figure 2-12 illustrates the change particles undergo during the devolitisation stage with increasing temperature. The next stage of devolitisation takes place at approx. 400°C and results in the stronger aromatic, carboxyl, aliphatic and hydroxyl group bonds breaking, leading to the formation of heavy tars and liquids. The larger volatiles produced with increased temperature will also decompose into secondary volatile components (Wu, 2003a; Strezov et al., 2000). At >600°C, condensation of the aromatics to char takes place. At this point the char is primarily a carbon-based char (typically ≥98% Carbon). The release of volatiles has an expansion effect of the fuel particle depending on the rank of the fuel (referred to as the swelling index). The expansion is stated in the literature (Urkan and Arikol, 1994; Oka, 2003) to be around 3 times the original particle volume but authors such as Anthony and Preto (1995e) have noted for a more bituminous coal this expansion factor can be of a magnitude of 5 due to different distributions of tar and liquid components in this particular type of coal. For biomass, the mechanisms described and in Figure 2-12 applies but with different rates of emission and combustion. Biomass has

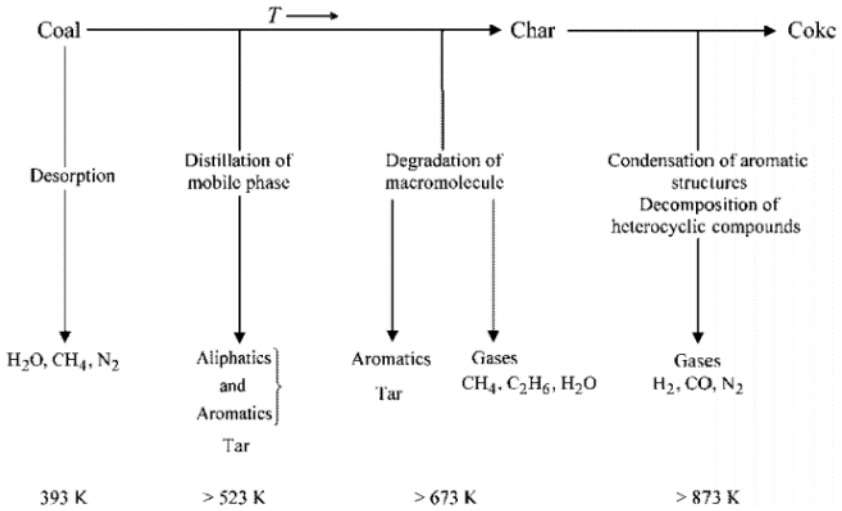

Figure 2-12 The primary reaction mechanisms for the pyrolysis and devolitisation of coal as proposed by the Van Heek and Hodek team (van Heek and Hodek, 1994)

higher volatile content than coal and as a result a larger percentage of the energy produced from the combustion of biomass comes from volatile combustion rather than char combustion. This also moves the flame from the bed to above the bed as gases moving away from the fuel ignite rather than combusting in the bed where the majority of char loading is found (Biagini et al., 2002).

The available heat, size of particles, chemical makeup of the fuel, localised diffusion gradient, oxygen concentrations, type of fuel and moisture content will affect the rate, extent and time of devolitisation of any coal. This is due to three main mechanisms; chemical reactions kinetics, heat transfer to and within the coal particle and physical mass transfer of a coal particle being directly affected. All of these factors will affect the extent the devolitisation step plays in a combustion system and therefore, effect the following steps and overall combustion of any coal particle (Borghi et al., 1985; Agarwal et al., 1986).

2.9.3 Combustion of Volatiles

Coals and biomasses are made up primarily of C, H, N, O and S. During combustion the volatile components containing these elements evaporate and oxidise (Koppejan and van Loo, 2012). There are a number of reactions which take place during the combustion of coal volatile species in a fluidised bed. The reactions in Table 2-1 lists significant reactions for volatile combustion. As most of the reactions involve hydrocarbon combustion, the significant reactions are summarised by Reaction 2-1 to Reaction 2-15. Oxygen is assumed to be available in each reaction as fluidised bed combustion usually

operates with high excess air. Reactions concerning emissions such as the formation of SO_2, NO_x etc. are defined and explained in the later emission sections.

Table 2-1 Fundamental volatile combustion reactions for FBC			
Description	Reaction	Label	Source
Partial oxidation	$C + \frac{1}{2}O_2 \rightleftarrows CO$	Reaction 2-1	(Merrick, 1984; Wu, 2003ae)
Boudouard reaction	$C + CO_2 \rightleftarrows 2CO$	Reaction 2-2	(Merrick, 1984; Wu, 2003ae)
Hydro-gasification	$C + 2H_2 \rightleftarrows CH_4$	Reaction 2-3	(Merrick, 1984; Wu, 2003ae)
Carbon monoxide combustion	$CO + \frac{1}{2}O_2 \rightarrow CO_2$	Reaction 2-4	(Wu, 2003a; Kulasekaran et al., 1999; Howard and Elliott, 1983)
Hydrogen combustion	$2H_2 + O_2 \rightarrow 2H_2O$	Reaction 2-5	(Wu, 2003a; Kulasekaran et al., 1999)
Methane combustion	$CH_4 + \frac{3}{2}O_2 \rightarrow CO + H_2O$	Reaction 2-6	(Wu, 2003a; Kulasekaran et al., 1999; Eslami et al., 2012)
Ethane combustion	$C_2H_6 + \frac{5}{2}O_2 \rightarrow 2CO + 3H_2O$	Reaction 2-7	(Eslami et al., 2012; Kulasekaran et al., 1999; Wu, 2003a)
Propane combustion (stepwise oxidation)	$C_3H_8 \rightarrow \frac{3}{2}C_2H_4 + H_2$ $C_2H_4 + O_2 \rightarrow 2CO + 2H_2$ $CO + \frac{1}{2}O_2 \rightarrow 2CO_2$ $H_2 + \frac{1}{2}O_2 \rightarrow H_2O$	Reaction 2-8 Reaction 2-9 Reaction 2-10 Reaction 2-11	(Solomon and Colket, 1979; Kabe, 2004; Howard, 1987; Kulasekaran et al., 1999; Wu, 2003a; Eslami et al., 2012)
Devolitisation of Carboxyl group	$z - COOH \rightarrow z - H + CO_2$ $z - OH + z - H \rightarrow z - z + H_2O$ $z - OH + z - OH \rightarrow z - O - z + H_2O$	Reaction 2-12 Reaction 2-13 Reaction 2-14	(Solomon and Colket, 1979; Wilson, 1972)
Hydrocarbon combustion equation	$C_nH_m + \frac{1}{2}nO_2 \rightarrow nCO_2 + \frac{1}{2}mH_2O$	Reaction 2-15	(Fu et al., 1989; Solomon and Colket, 1979; Kabe, 2004; Baxter et al., 1995)

The way in which volatiles combust has been reviewed in Srinivasan et al. (1998) and found that at low bed temperatures of 700-750°C the volatiles can instead of burning in the bed move into the freeboard; at mid-range bed temperatures of 830-900°C the

volatiles are only likely to combust within bubble formations within the bed; and at high bed temperatures >900°C combustion will occur within bubbles and between the particles. These mechanisms are subject to particle size and combustion regimes but fundamentally describe the internal modes of the combustion process. The fraction of volatiles burning in, on and above the bed are determined by the available oxygen and volatile content in the fuel (Zhou et al., 2011). Table 2-1 shows the fundamental reactions which occur during the combustion of volatile species. Whilst Reaction 2-1 to Reaction 2-15 can be found in combustion of coal or biomass fuels, Reaction 2-12 to Reaction 2-15 are biomass focused. This is because of the species in Reaction 2-12 etc. containing oxygen rich species associated with plant life etc.

The mechanisms for volatile combustion is significant when combusting different fuels or co-firing fuels such as coal and biomass as the flame temperature and placement will change. Different biomass and coals will release localised gases with slight variations in pressure and intensity which will fundamentally influence localised combustion, and the entrainment of volatile gases into the freeboard. This will affect the overall combustion process and thus influence the location of a flame in and above the bed, distribution of gaseous alkali species and therefore, the formation of agglomerates and slags.

As the fuel particle combusts, there is a volatile gas release which contains high concentrations of inorganic alkali species Thus, the gas emitted around the particle contains high concentrations of components fundamental to agglomerate and slag formation as described in later sections. The rate of release of the volatiles, volume and location in the FBC i.e. higher in the freeboard for biomass than coal, will alter the location of combustion zones and the severity of impact that temperature and chemical composition has on the formation of slags and agglomerates.

As the fuel particle undergoes pyrolysis there are a release of volatile gases from the surface of the particles. The release of gaseous volatiles directly impacts the fluid mechanics around the particle. Furthermore, the release of gaseous and partially melted inorganics will impact the formation of eutectics, agglomerates and slagging mechanisms. The release of volatile species will also impact the localised combustion both in the bed and within the freeboard. Considering the previous section, the difference in volatile flame and volatile release seen between coal and biomass particles could significantly influence agglomerate formation and must be considered in later Chapters along with other such mechanisms experienced with the flame and combustion.

2.9.4 Char Combustion

Char combustion is the burning of the remaining material which is left once volatiles have been lost from the fuel particle. The combustion of the char particle produces a slower burning flame which emits less heat energy than that found in volatile flame.

Once volatile species have been driven off the fuel particle, the solid char will undergo a depolymerisation, re-polymerisation, pore opening/closing and gaseous transport throughout the particle. The resulting char produced is relatively consistent for the same sample under different mechanisms. Different coal and biomass types will however, produce different char weights compared to the initial sample weight (Borah et al., 2011; Ross et al., 2000; Strezov et al., 2000).

Char is of significance more so for the combustion of coal as the bed can contain between 1% and 5% char depending on the particle sizes of the coal. Whereas, for biomass the char content can be <1 wt. % as a result of the low fixed carbon and high rate of carbon oxidation during combustion. Biomass fuels will result in less combustion occurring in the bed via char combustion and therefore, the primary energy is in the volatile flame above the bed and in the freeboard (Wu, 2003ae).

Char is made up of ash, nitrogen, sulphur, fixed carbon and any mineral impurities in the fuel. At temperatures ≥750°C oxygen reacts on the surface as well as penetrating the surface of the char particle, producing gaseous species such as CO, CO_2, and NO. The reaction mechanisms can be seen in Figure 2-13.

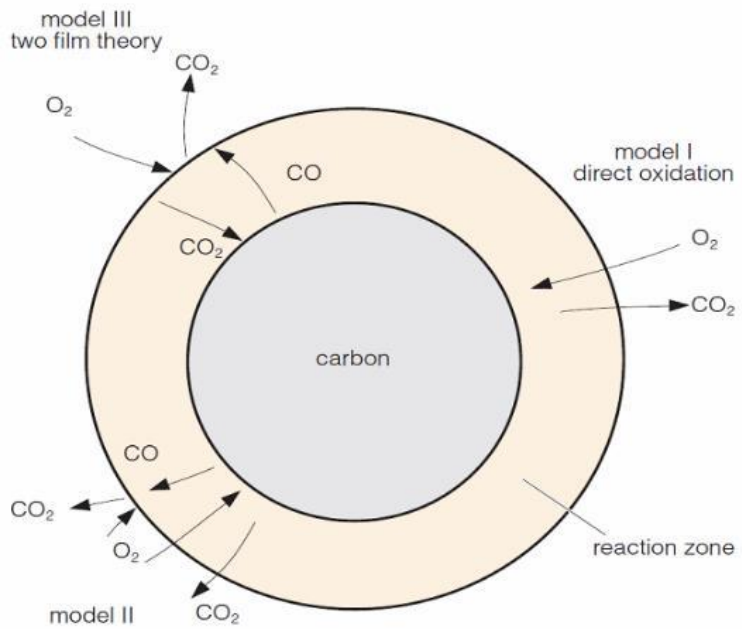

Figure 2-13 Char combustion mechanisms (Wu, 2003)

The main reactions in forming gaseous species from char are shown in Reaction 2-1, Reaction 2-2 and Reaction 2-3.

There are three mechanism suggested in the literature for char burnout (Wu, 2003ae; Desroches-Ducarne et al., 1998; Basu, 1999; Kulasekaran et al., 1999), these models shown in Figure 2-13 and express the findings of the authors in terms of available oxygen penetration in the fuel particle.

The char combustion is of significant importance for the combustion process as well as the formation of agglomerates. The localised combustion of char particles will influence temperature gradients within the proximity of the bed in which alkali specie availability will form agglomerates.

2.10 Agglomeration

Any combustion technology will suffer deposition, corrosion, fouling, slagging or agglomeration as a direct result of changes in operational variables, mechanical design, oxidation conditions and inorganic chemical presence from the fuel and other materials found in combustor units.

In particular, FBC, because of its bed and applications with low grade fuels suffers from agglomeration. Agglomeration is the clumping and adhesion of particles in the bed, molten ash coats the particles with a sticky layer, as a result of alkaline species melting. If these clustered particles are allowed to propagate in size, then the hydrodynamics of the bed and the fluidisation can be negatively affected. Thus, if allowed to build up, eventually defluidisation of the bed can occur and the furnace will be forced offline. This is both costly in terms of shutdown time and boiler damage (Thy et al., 2010a).

The following sections will discuss the mechanisms of agglomeration and the influence that using low-grade, high inorganic content fuels has upon the rates of agglomerate formation and counter measures to the issue.

2.10.1 Mechanisms of Agglomeration

In a FBC system the gas moving between solids creates a turbulent mixing movement. In doing so particles will interact with neighbouring particles through physical contact/collisions and attractive forces between interacting particles (Kunii and Levenspiel, 2013).

FBC, in particular atmospheric FBC’s suffer from the process of agglomeration. Agglomeration is the result of bed material becoming coated and sticky as a result of

alkaline species present. Coated refers to particles becoming coated in alkali slag melt phase (such as K and Na) from the fuel. The chemical matrix of the sticky coating will be directly affected by operational variables such as bed temperature due to the influence on melt temperatures for individual alkali groups; 764°C for Na rich melt phases compared to 790-874°C for K rich melts (Tangsathitkulchai and Tangsathitkulchai, 2001). Attractiveness of particles to one another refers to inter-particle forces such as electrostatic and van der Waals (Bartels et al., 2008a). The formation of the initial sticky particles leads to a build-up of adhering particles which can lead to other mechanisms associated with agglomeration such as sintering.

A significant focus of research in the field of agglomeration is the effect of alkali groups and the effect they have on forming eutectics within FBC. Low grade fuels in particular have a large literature base because of the variance in ash content; sub-bituminous coals 3-12 wt.% (Pahari and Chauhan, 2006) and biomasses 1-5 wt.% (Koppejan and van Loo, 2012). When such melt phases occur in the bed, they coat the bed material, usually silica sand, forming low melting temperature eutectics, which are a complex of the more reactive species. Typically, agglomerates will be found to contain complexes containing lower melting phase species such as K, P, Si and Na as these will be the first to coat the particles. Further heating caused by poor mixing, the formation of hot spots and localised combustion lead to higher temperature melting groups being liberated into the gas phase thus propagating the agglomerates(Natarajan et al., 1998).

2.10.2 Physical Agglomeration Mechanisms

Agglomeration mechanisms are still being researched as the difference in fuels creates unique complexes and eutectics forming mechanisms. Bartels et al. (2008a) discusses by means of experimental validation, that agglomeration should be categorised to hydrodynamics, chemical reactions, particle interactions and molecular cramming. However, this doesn't consider the overlapping effect of one mechanism to another or the impact. A better approach is defined by Visser et al. (2008) for melt induced and coating induced agglomeration mechanisms. This approach allows consideration on how the movement of particles (hydrodynamics) directly influences the bridging of coated particles for instance, as higher velocities will decrease agglomeration formation.

Figure 2-14 illustrates these two mechanisms; 1) the coating mechanism is a result of ash melts, condensation or alkalis in gas phase from alkali compounds in the fuel, reacting with the surface of bed particles, 2) the melting mechanism is the result of molten ash

from alkali compounds, creating sticky areas on bed particles. This then creates a “bridge” as particles move over each other (Visser et al., 2008).

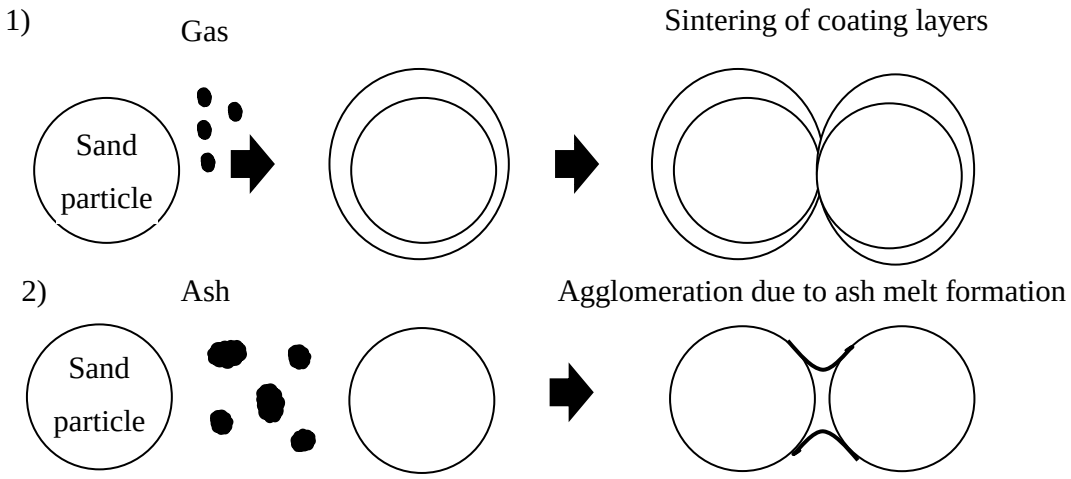

Figure 2-14 Agglomeration mechanism of bed material; 1) coating induced, 2) melt formation with ash components (Visser et al., 2008)

The two mechanisms illustrated by Figure 2-14 underpin the mechanism by which agglomeration occurs. Agglomeration growth and the process in formation are broken down into three routes (Pietsch, 2008a; Skrifvars et al., 1994):-

1) Tumble or growth agglomeration is the process in which bed particles with adhere to one another depending on volume related separation and the adhesive forces of each particle surface. In order for the formation of agglomerates to occur by this process and to adhere permanently, the sum of all the forces acting against the adhesion must be overcome i.e. gravity, momentum, drag etc. This type of process is commonly experienced in FBC agglomerate formation but complements other processes which contribute together to cause agglomeration.
2) Pressure agglomeration or molecular cramming, whilst less common in FBC systems is a physical mechanism for agglomeration in a bed. It can occur if there are barriers, baffles, areas in which particles are squashed together, and in doing so reduce friability and break up of agglomerates. This can occur within tumble agglomeration when agglomerated material obstructs particle movement and thus, localised pressure between particles accelerates agglomerate propagation.
3) Sintering is common and occurs at elevated temperatures seen with the onset of agglomerates and when inorganics are allowed to build up in the bed. Sintering is the interface between particles changes as surface matter diffuses between the particles to form bridges. These solidify on cooling but also promote liquid phase movement between particles with localised heat elevation, thus causing further structural

stability in the localised matrix. This leads to further propagation of the agglomerate structure and compliments tumble agglomeration and in doing so agglomerates develop, in three dimensions, usually to the detriment of the fluidity of the bed and combustion operations.

Whilst the mechanisms and processes for agglomeration have been described, with respect to low grade fuels and biomasses in FBC, tumble growth is the most significant agglomeration method. At elevated temperatures, however, sintering becomes more significant as sticky alkali groups from the fuel, create a liquid/gas phases creating the sticky surface on bed particles, causing agglomeration. Further to this, sintering with more elevated temperatures leads to localised defluidisation and hotspot formation. Consequently, the rate and strength of the agglomerates in these areas increases leading to the onset of more severe localised or complete defluidisation (Skrifvars et al., 1992; Knutsson et al., 2014; Tangsathitkulchai and Tangsathitkulchai, 2001; Skrifvars et al., 1994). Once the agglomerates have become significant enough in volume and/or mass the bed will defluidise. This is a consequence of the hydrodynamics of the bed material being altered and the distribution of fluidisation air throughout the bed becoming non-uniform. Defluidisation will result in less than favourable operating conditions i.e. temperature spikes and poor combustion thus leading to furnace down time.

2.10.3 Operational Variables Effects on Agglomeration

Operational variables and their effect on agglomerates have been researched and can be found in abundance in the literature as the following passages will demonstrate; Öhman et al. (2000) outlined the possible effects of 300 fuels in which the fuels were rated in terms of their inorganic concentration and the links that this presented to agglomeration and other negative combustion effects. The study demonstrated the significance of particular species such as K and Si by linking them to agglomeration and how common they are in biomass fuels. As later sections will describe, these chemicals species play a major role in the formation of slags and agglomerates and how there is a commonality between the fuels and how the biomasses will generally present challenges in combustion. Within this review styled investigation, Öhman et al. (2000) showed the significance in the concentration of specific alkali components such as K_2O and Na_2O and their relationship to agglomeration.

This type of work laid foundation for authors such as Brus et al. (2005) and Duan et al. (2015) who investigated additives and operational variables respectively. However, because of the high potassium concentrations in fuels they used (straw and grasses), both

sets of authors concluding remarks were dominated by potassium melt phase and coating mechanisms. Duan et al. (2015) went on to described the significance of the low melting (≤955°C), eutectic formation and offered a series of reactions; Reaction 2-16 to Reaction 2-18.

$$K_2O \cdot nSiO_2 + Fe_2O_3 \rightarrow K_2O \cdot Fe_2O_3 \cdot nSiO_2$$ Reaction 2-16

$$K_2O \cdot nSiO_2 + Al_2O_3 \rightarrow K_2O \cdot Al_2O_3 \cdot nSiO_2$$ Reaction 2-17

$$K_2O \cdot nSiO_2 + Al_2O_3 \rightarrow K_2O \cdot Al_2O_3 \cdot (n-1)SiO_2 + SiO_2$$ Reaction 2-18

(Duan et al., 2015)

These investigations highlight the impact of multiple factors effecting the formation of eutectics high in alkali concentrations. Other authors such as Latva-Somppi (1998); Grubor et al. (1995) both conducted extensive experimental work with focus on the alkali content of biomasses and the direct influence excessive bed temperatures etc. have on the movement of alkali liquid phases. Seville and Clift (1984) showed experimentally, that a small amount of volatile alkali liquid when added to a fluidised bed will increase the inter-particle adhesion forces significantly between particles in the bed. The presence of increased alkali liquid melt phases was seen to correlate with increased localised bed temperatures and incomplete combustion. These studies showed that a small disruption in the bed through agglomeration formation when burning low grade fuels could quickly escalate to defluidisation. Therefore, based on this type of evidence it can be theorised that a damaged air distribution system could quickly lead to bed agglomerations.

Numerous authors have evaluated different aspects of low grade coals (Basu and Sarka, 1983; Siegell, 1984a; Skrifvars et al., 1994; Lin and Dam-Johansen, 1999) and biomasses (Brus et al., 2005; Chirone et al., 2006; Bartels et al., 2008g; Lin et al., 2003; Olofsson et al., 2002; Öhman et al., 2000; Scala and Chirone, 2006; Thy et al., 2010b) in respect to operational conditions and the subsequent effect the fuels have on agglomerate formation due to alkali content. Whilst each investigation critiques the effect on agglomeration and in many cases, specify chemical reactions and eutectic formation mechanisms, little is stated to a system that is less than isothermal or ideal. There is little, if any consideration to the effect caused by a damaged air distribution system or to physical aspects of the bed. What is the consequence of a broken bubble cap? How does this affect fluidisation? Is there a remedy that doesn't involve taking the furnace offline? What effect does this have on agglomerate formation? What are the implications of using these fuels in a full-scale operation.

Oka (2003) explains theoretically that if a system were to suffer an issue with the air distribution system, then the thermal diffusivity within the bed would decrease. Air pressure would play a key role in the change in air velocity experienced across the bed. A broken bubble cap for instance will have a larger opening than that of an intact bubble cap and thus, the hydrodynamics of the bed would alter. Regions of high and low turbulence would occur with the redistribution of air throughout the air distributor. Consequently, the decrease in thermal distribution and increase of localised hotspot would be expected to increase the formation of agglomerates.

Kuo et al. (1997) investigated the effect of different air distribution options and the association of varying combustion operations by altering inlet air velocity. The work presented has the most relevance to this investigation in respect to a non-uniform air distribution system. The results presented and critique of flame distribution and combustion rates, and the effect on emissions. The author found changing the air distributor didn't necessarily impact the combustion as predicted however, more significantly limited the spreading of the flame. This coupled with varying air flows created cooler regions. Therefore, it could be theoretically possible that in a system in which the air distribution plate is damaged the combination of high/low flows could create heating/cooling zones that could influence the rate of agglomerate formation. More so this type of system would encounter a variety of agglomeration mechanisms in which higher temperature sintering could be taking place alongside lower temperature eutectic formation. Lin et al. (2011) found that if there was an extreme increase in inlet air velocity, regardless of fuel alkaline content, there was a decrease in the formation of agglomerates. The increasingly turbulent bed acted to break up agglomerates. Instead a larger overall particle size of the bed occurred eventually leading to defluidisation as displayed in Figure 2-5, but this took longer than in a more typical fluidisation regime. Hence there could be a benefit of a highly turbulent region within the bed to break apart freshly formed and still fragile agglomerates within the bed. The question persists, to what extent the positive effects outweigh if at all the negative effects. This is a factor that none of the available literature has elaborated on but should still be considered.

2.10.4 Agglomeration Summary

From the work presented in the literature it is possible to draw some conclusions on the effect of non-ideal air distribution and operation variables on the combustion of low grade fuels:

- Low grade fuels have been shown/found to contain higher concentrations of agglomeration causing alkali inorganic species such as K, Fe and Na. The eutectic matrices these species form lead to the onset of agglomerates by coating and bonding to ash particles and bed materials. This leads to the propagation of rigid structures resulting from sticky particles colliding and forming bridges between the formed materials. Particularly it was seen that the lower melting temperature species such as K and Na would react with compounds such as Si and Fe resulting in lowered temperature melts in silicates. The silicates are much stronger and rigid which lead to the growth of more structurally formidable agglomerates in fluidised beds.
- Air distribution is a fundamental factor in the turbulence, distribution and fluidity of bed material and entrainment of fuel particles. If the air flow is disrupted by the onset of agglomerates, localised poor mixing and combustion will lead to the formation of higher melt eutectics. Therefore, a lower melting temperature eutectic causing initial agglomeration can lead to the onset of alternative mechanisms involving higher melt species resulting in more structurally hardened complexes.
- Further to the previous point, if the air distribution technique employed to fluidise the bed is damaged or obstructed in any way, then there is the potential to increase the onset of agglomeration, reduce efficient combustion and reduce the performance of the bed. A damaged air distributor could see increased agglomeration rates as areas of poor mixing and turbulence allow for adhesion and cooling of molten ashes and slags which aren't being agitated through the bed.
- The literature reviewed indicates numerous mechanisms associated with the high inorganic content fuels such as biomass and agglomeration. The literature also shows how air flow could theoretically impact the rates of these formations. Therefore, the literature shows that these areas could radically impact the application of low grade fuels in full scale operations and present a series of engineering problems in altering operational variables. Thus, further research is needed for the larger scale applications.

In summary, the introduction of a damaged air distributor could potentially agglomerate the bed faster and in a specific manner. However, it is not known what factor on time this has and to what extent the bed and agglomerate morphology will alter. This will be investigated further in later Chapter of this thesis.

2.11 Agglomeration Prediction

There are a variety of ash behaviour prediction techniques described in standards and literature. On reviewing the available information, it is clear that the focus of the literature was to predict fouling and slagging of more conventional PF coal firing technology. This raises two issues; 1) Do the techniques apply for low grade fuels of a different chemical and physical type compared to the coals used to construct the standards in the literature (anthracite) and, 2) do these methods translate well for the mechanisms of agglomeration in FBC. The way in which alkali groups etc. will react are very different for a fouling mechanism to agglomeration.

2.11.1 Experimental Methods

Experimental methods approach the problem by assessing the fuels capacity to produce a melt phase or slag phase. This utilises fuel characterisation techniques such as thermos gravimetric analysis (TGA), ash X-ray fluorescence (XRF), thermal mechanical analysis (TMA) or ash fusion testing. The most widely adopted method is ash fusion testing, in which a sized particle of ash/fuel is heated and observed both visually and with a mass spectrometer. This method has ASTM accreditation and has been used to evaluate many fuels (Bartels et al., 2008a; Stallmann and Neavel, 1980; Skrifvars et al., 1999; Paulrud et al., 2001; Öhman et al., 2004). However, whist these techniques give reliably accurate results, they do not simulate the turbulent mixing of a FBC. For this reason studies such as Paulrud et al. (2001) have found that the melting temperature within a test bed is lower than that in a fusion furnace, usually as a result of localised heating or forced chemical mixing by the turbulent bed.

The only conclusive method of testing a fuel is to tests it under lab or pilot scale or ideally full scale operation. This isn't always feasible as this could both be costly and damaging to a test operation. However, Visser et al. (2008) noted on how during comparative work in scale up operation to lab scale tests; the agglomeration mechanisms shifted from a melting mechanism as shown in Figure 2-14 for industrial operation to coating mechanisms of agglomeration for lab scale tests. The conclusion of these findings indicates tendencies and trends, but variance between setups and there is no definitive answer.

2.11.2 Theoretical Methods (FACTSAGE)

An alternative approach is to use computational predictions and modelling software to predict outcomes of a system based on its thermodynamic and chemical properties. This

could be used alongside experimental data to construct a more informed picture for better decision making.

An example of such software is “FACTSAGE”. FACTSAGE uses Gibbs energy minimisation algorithm and thermochemical functions to calculate the outcome of systems described by a user. This includes reactant details and system variables to produce two-dimensional single phase mappings with phase transition and multicomponent mixtures.

Li et al. (2010) used various modules of the FACTSAGE software to determine slag phase melting, viscosity properties of slags and to analyse the effect of blending multi-fuel ashes together in a FBC. The results helped to approximate trends of the fuels and their relative potential influence on adhesive particle build up in the bed. However, criticisms of this approach included data gaps, misalignment of data between modules and the variance on results with small changes in system inputs. The same experience has been found by authors using this type of software for fouling and slag based deposition work (Van Dyk et al., 2009; Elled et al., 2013a; Fryda et al., 2008).

2.11.3 Indices

An alternative method for predicting agglomeration tendencies is through agglomeration indices. These are equations that have been derived from fuel composition data and process results for validation. The equations include critical reaction groups and mathematically equate them against other groups which have been seen in experimental work to cause a counter effect which has a measurable value tied to it.

Gatternig (2015) summarised key agglomeration indices Table 2-2. These have been developed with data for coals, however, in later Chapters the application to biomass was evaluated. The conclusions drawn addressed the limited application of the indices for biomass or co fired fuelled systems. These will reflect the work done by Barroso et al. (2006), who systematically compared the rates of deposition and agglomeration from fuels against the expected outcomes drawn from the indices. It was found that for biomass etc. that there was very little correlation, bringing to question the validity of these types of indices for predicting biomass fuelled systems.

Predictive method should be taken as an indication of how a system might react but the work in the literature shows there are limitations to each method. It is better to use a combination of approaches to form more informed conclusions before proceeding in application of a fuel or operational choice.

Table 2-2 Indices for the description of ash behaviour.(Gatternig, 2015)			
Index name	Definition	Agglomeration/ fouling risk	
Coal			
Silica ratio	$SR = \frac{SiO_2}{SiO_2 + Fe_2O_3 + CaO + MgO}$	0.8-0.72 low 0.72-0.65 medium 0.65-0.5 high	Equation 2-16
Base-to-acid ratio	$R_{b/a} = \frac{Fe_2O_3 + CaO + MgO + Na_2O + K_2O}{SiO_2 + Al_2O_3 + TiO_2} \left[\frac{mol}{mol}\right]$	<0.2 low 0.2-0.4 medium 0.4-0.55 high	Equation 2-17
Slagging number	$RS = R_{b/a} \cdot S \left[\frac{mol}{mol}\right]$	RS<0.6 low 0.6-2.0 medium 2.0-2.6 high >2.6 severe	Equation 2-18
Iron-to-calcium ratio	$\frac{Fe}{Ca} = \frac{Fe_2O_3}{CaO}$	<0.3 and >3	Equation 2-19
Fouling factor	$F_u = R_{b/a} \cdot (Na_2O + K_2O) \left[\frac{mol}{mol}\right]$	F_u<0.6 low 0.6-40 medium >40 high	Equation 2-20
Silica-to-alumina ratio	$\frac{Si}{Al} = \frac{SiO_2}{Al_2O_3}$	<1.4 low 1.4-2.8 medium >2.8 high	Equation 2-21
CCSEM index	$\sum \left[CaO + Fe_2O_3 \left(\frac{Fe_2O_3}{Fe_2O_{3+}Al_2O_3 + SiO_2}\right)\right]$	<15.3 low 15.3-30.6 medium >30.6 high	Equation 2-22
Biomass			
Alkali index	$AI = \frac{\alpha \cdot (K_2O + Na_2O)}{H_N}$	Al>0.34 fouling probable 0.17<Al<0.34 fouling possible	Equation 2-23
Bed agglomeration index	$BAI = \frac{Fe_2O_3}{K_2O + Na_2O}$	Higher value = increased risk	Equation 2-24
Agglomeration index 1	$I1 = \frac{Na + K}{2S + Cl}$	$I1$>1 fouling $I1$>1 agglomeration	Equation 2-25
Agglomeration index 2	$I2 = \frac{Na + K + Si}{Ca + P + Mg}$	$I2$<1	Equation 2-26
Note: Ash components are entered as wt. %; S is Sulphur as fuel ash (wt. %) if not stated as molar.			

2.11.4 Agglomeration Monitoring

Agglomeration is one of the most important problems which a FBC can experience during normal operational conditions. For this reason, early warning and detection of agglomeration and the mechanisms contributing to the formation of agglomerates is paramount. If a monitoring system is unable to accurately and reliably identify potential agglomerate formations, then the bed can degrade to the point of defluidisation. Monitoring methods used in industrial scale plants include; pressure, electrostatic, temperature, radiation and optical measurements to detect agglomeration. The ideal monitoring system should be sensitive enough to detect changes in a bed and detect

agglomerate sources before defluidisation has occurred, rather than simply identifying when the bed is defluidised (Wang et al., 2009).

Different approaches to agglomeration detection have limitations and specific applications. The following points consider systems currently used in agglomeration detection for FBC plants and the limitations experienced

2.11.4.1 Pressure Drop

The most common type of monitoring system used for FBC agglomerate detection is pressure drop. This is done by having a probe in/below the bed and one above the bed. The pressure difference generated gives the overall pressure drop (ΔP) across the bed. Linear and non-linear recognition algorithms are used to analyse any fluctuations and are compared against a baseline case value. Pressure readings give the operators information on bed hydrodynamics and averaged pressure drop gives real time feedback in terms of bed density and height (Bartels et al., 2008a; Wang et al., 2009). However, pressure drop monitoring is inhibited by probe blockages and its limited accuracy to identify local bed changes and only view the bed as a single entity. This means the formation of hotspots and sintering material can be averaged into the overall system rather than specific localised changes. Research in this field is focused towards the application of statistical analysis and various algorithmic approaches to better differentiate between pressure changes (Bartels et al., 2008g). Kai and Furusaki (1987) used standard deviance and variance in pressure, Davies and Fenton (1997) used windowed standard deviation and Chirone et al. (2006) used variance in high frequency pressure fluctuations. Each author investigated alternative approaches to the same problem and concluded on how to better the monitoring system under specific conditions. However, each bed has to be considered individually based on their operational variables. Pressure drop is the simplest method in terms of implementation and use and for this reason is the most commonly used technique. It is for this reason that the experimental methodology of this study will adopt pressure drop for agglomeration and defluidisation detection.

2.11.4.2 Electrostatic Measurements

Electrostatic forces and gas-solid interactions have been noted to influence hydrodynamics and agglomeration due to their impact on electrostatic forces. Electrostatic forces form as a result of the bed particles moving over the wall of the furnace and against each other. This charge then attracts particle to the wall creating less turbulent mixing and increasing the potential for agglomerate formation in these charged zones as sheets. The weight of the sheets will eventually overcome the electrostatic forces

of attraction and potential “sticky” particles which then fall into the bed leading to other agglomeration mechanisms (Yang et al., 2016; van Ommen et al., 2000; Hendrickson, 2006).

A number of authors have looked into mitigating static charge with different approaches to dispel electrostatic charge (Mehrani et al., 2005; Liu et al., 2010; Sowinski et al., 2010). The same probes used to discharge the walls can be used to monitor agglomeration build up and develop detection methods. By measuring the distribution of charge across a bed with a metal probe for instance, it is possible to measure charge and compare this against accumulation data seen at the point of agglomeration in the bed and walls of the furnace (Fang et al., 2008; Fujino et al., 1985; Gajewski, 1985). However, this type of detection method is still in development and has yet to be proven for different agglomeration mechanisms.

2.11.4.3 Temperature

Most mechanisms for agglomeration are the results of alkali species melting when a specific range of temperature is achieved. If there are enough points of measurements around the bed, theoretically it is possible to detect temperature change and give warning to agglomerates. This is especially true in dead zones where hotspots can form and lead to sintering and the formation of larger solids are monitored (Wang et al., 2009). The problem with temperature approaches is that whilst there may be a temperature spike in a small region due to the formation of agglomerates, differentiating the spike to the global temperature of the bed is difficult. Therefore, whilst some points of concern may be identified by the system, there is a large probability of missing agglomerates, thus rendering the monitor unreliable (Werther, 1999). Many authors have investigated numerous methods for reliably measuring localised temperature spikes; Khan and Turton (1992) used a network of thermocouples and temperature coefficients taken from immersed tubes to calculate temperature variations around a bed, whereas Basu (1990) took a more mathematical approach using wall measurements and statistical analysis to differentiate temperature variance against a normal operations case.

Thermocouples will be distributed throughout the test rig used in later experiments and the data collected in terms of temperature distribution through the bed will be used to detect and predict agglomeration. However, combining pressure and temperature monitoring, a better means for detecting agglomeration can be achieved compared to using a single approach.

2.11.4.4 Other Methods

Other methods are being developed for monitoring the bed in a FBC but are still in their early stages. Such development includes novel approaches towards optical systems using fibre optics immersed in the bed to measure bubble and hydrodynamic data. This method so far has been found to be limited to lab scale systems because of the size and shape of agglomerates in full scale operations (Ishida and Tanaka, 1982; Razzak et al., 2009; Link et al., 2004; Schweitzer et al., 2001). Other novel approaches include acoustic emissions, that is the measurement of inter particle and particle wall collisions as a signal. Work by authors such as Wang et al. (2009) show that potentially, with enough data, mathematical manipulation and case study information on agglomerate formation can give positive measurements of the bed. Sheahan and Briens (2015); Weiguo et al. (2015) and Jiang et al. (2014) have further researched the technique to positively identify specific agglomerate's and particles by improving statistical and mathematical analysis in real time test. However, further development of these types of technique are needed to hone them for reliable application in industrial type operations.

2.12 Hydrodynamics

The hydrodynamics of a fluidised bed combustor describes the physical interactions of solids and gases within the fluidising bed. The way in which the air entering the bed is distributed, the type of distributor, number of distributors etc. will affect the distribution of gases throughout the bed. The particles, air velocities, voidage and a number of other variables will influence how bubble develop throughout the bed. This directly affects mixing, fluidisation and overall combustion efficiencies (Gogolek and Grace, 1995). This section will describe the air enters the bed of a FBC unit and how that air then mixes and bubbles develop throughout the bed.

Hydrodynamics are fundamental to the fluidisation of FBC technology as it describes the gas particle interactions and variables that impact on flow. In order to analyse the effect of altering variables such as air distribution, volatile gas release and agglomerate formation it is necessary to review literature. The following section underlines the key fundamentals which could impact the tests described in Chapter 3.

2.12.1 Air Inlet and Distribution

Depending on the purpose of the fluidised bed and the materials within that bed, the way in which air is introduced is important for the even distribution of air across the bed. Different air inlet systems and techniques will affect the beds performance in different ways and alter the development of bubbles and mixing throughout the area of the bed. Figure 2-15 illustrates the different types of air distribution technologies that can be applied in fluidised bed technologies.

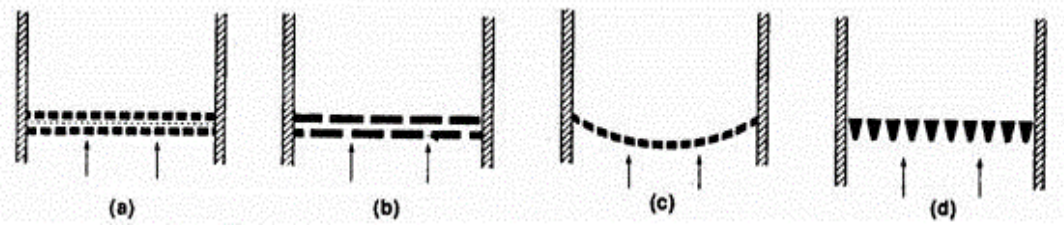

Figure 2-15 Plate and grate type distributors (a) sandwiching perforated plates (b) staggered perforated plate (c) dished perforated plate (d) grate bars (Kunii and Levenspiel, 1991)

It is common practice to use sintered or ceramic porous plate distributors for smaller scale rigs because this design gives good flow resistance with good bed distribution. However, these types of distributors wouldn't be considered for large scale operations because of high pressure drops resulting in higher pump power requirements, low physical strength, high design costs and eventual fine particle blockages (Kunii and Levenspiel, 1991). Bubble caps will be used in the pilot scale rig as they are used in full industrial scale boilers and will give the most representative data.

2.12.2 Gas-Solid Mixing

Within a fluidised bed there can be numerous mixtures of materials varying from coal, biomass, ashes, inorganic materials, alkali metals, sands, limestone etc. however, the way in which these materials act upon each other within a bed, based on their individual physical and chemical characteristics, will determine the overall movement and interactions within the bed.

2.12.3 Bubbles in Gas-Solid Flows

Sections 2.5 though to section 2.7 discussed fundamental physical and mechanical properties of a FBC bed which directly influence the fluidisation etc. However, to truly understand the way in which gas-particles interact and heat-mass transfer occurs in a bed the formation of bubbles must be understood.

Bubbles will form throughout the bed from the orifice to the surface of the bed immediately after minimum fluidisation and change in shape, velocity, pressure and size as bubble to bubble interactions take place. The formation of bubbles is completely random but generally after fluidisation the number of bubbles will decrease as they approach the surface of a bed. This is due to the small bubbles merging (coalescence) forming larger bubbles. The large bubbles will then either burst on the surface or break up into smaller bubbles in the bed due to bed turbulence and mixing (Howard, 1989). Figure 2-16 demonstrates how the different air distribution technologies will initially produce smaller bubbles that merge to larger bubbles.

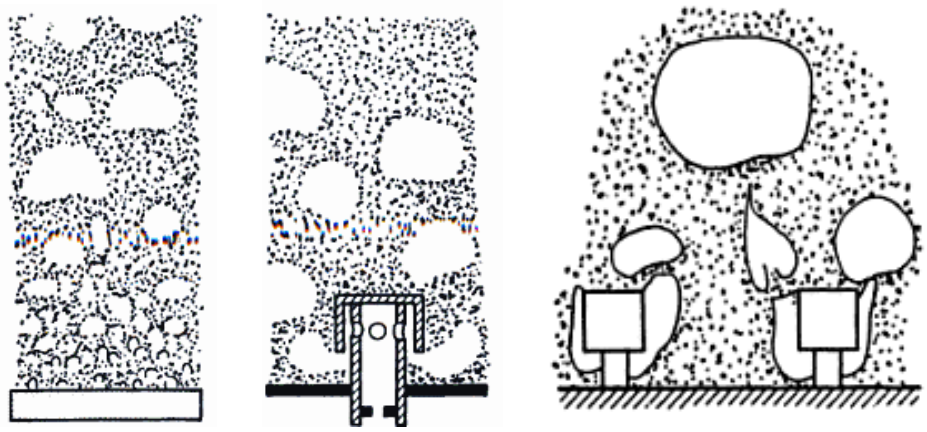

(a (b) (c)

Figure 2-16 the resulting behaviour of bubble formation from different distributor techniques (a) porous plate (b) bubble cap (c) resulting bubble formation (Sano et al., 1983; Kunii and Levenspiel, 1991)

2.12.4 Bubble Geometry

When the gas (air) leaves the air distributors, it will displace the sand around the cap creating a pressurised void. The gas will then begin to accelerate away from the cap and rise as a bubble would in water. The bubble will then form either into a spherical shape or into a spherical cap with an indentation in its rear (the wake).

2.12.4.1 Spherical Bubbles

Spherical bubbles will rise due to a change in pressure throughout the bubble. The pressure in the lower part of the bubble is lower than that of the surrounding bed. This allows gases from an emulsion phase to enter the bubble. This exchange of gases gives rise to the upward movement of the bubble. Around this type of bubble there is a lower density of particles due to the interactions with the gases and solids. As the bubble rises, mixing will take place throughout the surrounding and internal material. Most of the particles will be displaced around the bubble while a small fraction will “rain” down

through the bubble including large particles such as combustion products and fuel (Kunii and Levenspiel, 1991; Fueyo and Dopazo, 1995).

The rise velocity of a bubble can be calculated based on the exchange of pressure within the bubble and the materials. Therefore, the rise velocity of a bubble can be calculated on the interactions as shown in Equation 2-27. Spherically capped bubbles

$$u_{br} = [0.711 \times (gD_b)^{\frac{1}{2}}] \times 1.2 \exp\left(-1.49 \frac{D_b}{D_t}\right)$$ Equation 2-27 (Fueyo and Dopazo, 1995)

Where u_{br} is bubble rise velocity, g is gravity constant, D_b is bubble diameter and D_t is bed diameter.

Spherically capped bubbles are the more common bubble shape that is postulated to occur in a gas-solid bed. Figure 2-17 illustrates the shape of an ideal spherically capped bubble with the indentation or wake following in the bottom of the bubble. Whilst the exchange of gases is similar to that of a spherical bubble, due to the indentation, the interactions with particles differ. Critically the indentation is filled with particles which will follow the bubble as it rises. This will result in greater mixing throughout the bed as material can

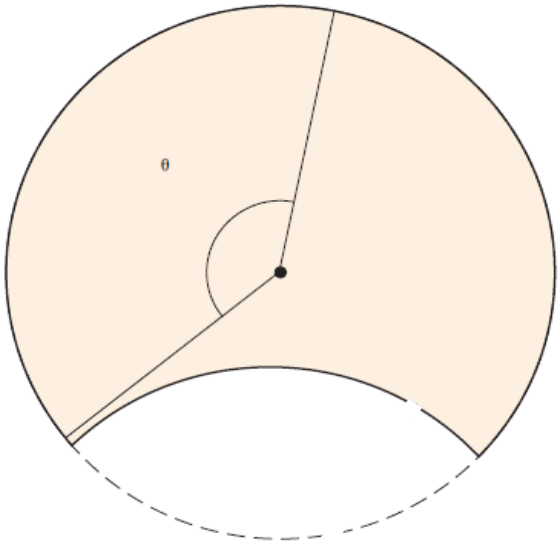

Figure 2-17 The bubble formation of a spherical capped gas bubble moving through solid particles producing a wake/indentation (Fueyo and Dopazo, 1995)

potentially travel from the bottom of the bed directly to the surface (Wu, 2003a).

Bubble caps were used in calculations for air distribution and offered the best distribution for air throughout the bed of the test rig.

The rising velocity of this type of bubble is as stated in Equation 2-28. Smaller bubbles have lower velocities whereas larger bubbles have larger bubbles have larger velocities

due to the buoyancy and pressure build up associated with varying bubble size (Fueyo and Dopazo, 1995).

$$u_{br} = 0.71 \times (g \times D_b)^{0.5} \qquad \text{Equation 2-28} \qquad \text{(Fueyo and Dopazo, 1995)}$$

2.12.5 Solid Mixing

Primary mixing throughout the bed occurs because of the movement of the bubbles. Air bubbles rising through the bed carry material upwards and material moves downward in areas which there are no bubbles. This is a balanced mechanism thus the more material is successfully moving upwards with bubbles, the more material will move downward to fill the displaced material (Wu, 2003a).

Secondary mixing occurs when a bubble reaches the surface of the bed and pops. This small explosion is relative to the size and pressure of the bubble. The resulting explosion will expel both hot gasses and particles above the bed. At the same point fuel and surface particles will fall into the temporary void mixing material into the bed. This is a significant part of fluidisation as transfers fuel and heat into the bed and in doing so sustains combustion (Howard, 1989).

Horizontal mixing occurs on the surface through turbulence created by the emergence of bubbles and around the distributor caps where turbulence is large enough to move the material (Stein et al., 2000).

Stein et al. (2000) studied the effects of deep beds on the mixing within FB's. It was found that with deeper beds the material rises through the centre of the bed because this is where there was a larger collection of bubbles. The material falling down occurred near the walls of the fluidised bed creating a circulating effect. Guenther et al. (2002) found that for shallow beds the upward movement of bubble in the bed induced the downward movement of material through the central area of the bed. Therefore, with alterations to the bed height there will be clear differences in the mixing and interactions of a FBC and potential with reactions occurring between those mixing particles including agglomerates.

The bubble geometry and solid-solid/solid-gas mixing will directly impact the rate of agglomerate formation. The rate is likely to increase further if an obstruction or negative modification were to be made to the air distribution system. Experimental testing in Chapter 5 and 7 will illustrate these hypotheses and elaborate on the literature described here by comparing an ideal and no ideal air distributor system while combusting high alkali content biomass fuels. Based on the understanding developed by previous sections,

it is expected that the rate of agglomerate formation will alter between the plates as well as the agglomerate structure forming.

2.13 Emissions

The process of combustion oxidises fuel, in the presence of heat, to products including flue gases. In this Chapter the mechanisms and chemistry for the formations of these emissions and the way in which they are controlled will be discussed including; carbon monoxide (CO), carbon dioxide (CO_2), sulphur dioxide (SO_2), Nitrogen oxides and nitrous oxides (NO/N_2O).

2.13.1 Carbon Monoxide (CO)

CO is the product of incomplete combustion of carbonaceous materials. CO is formed when the concentration of oxygen is below the required level to convert all free carbon molecules to CO_2. This is usually caused by poor mixing in the area of combustion or in a particularly fuel rich system i.e. where the ratio of fuel to excess air is fuel biased (Harrison, 2001).

The chemical formation of CO is illustrated in Reaction 2-19 and Reaction 2-20 as described by (Tsuji et al., 2002).

$$C + 0.5O_2 \longrightarrow CO\ \Delta G° = -137.168KJ \qquad \text{Reaction 2-19}$$

$$2C(s) + O_2(g) \longrightarrow 2CO(g)\ \Delta H_f^{\circ} = -110.5KJ/mol \qquad \text{Reaction 2-20}$$

In FBC the concentrations of CO is generally kept below 100ppm as a result of the relatively good mixing experienced in a fluidised bed (Minchener.A.J, 2000). Secondly the high air flow rate required to bring the bed of a FBC unit to minimum fluidisation increases the excess air beyond that found in alternative conventional combustion system such as PF regimes (Podolski et al., 1995). CFB systems and other fluidised bed systems with increased mixing have less CO emissions due to their increased mixing of fuel and available (excess) air.

The CO emissions produced by a combustion systems such as FBC will be directly influenced by the fuel type, bed temperature, fluidisation inlet air velocity, excess air and any secondary/tertiary air introduced in other areas of the furnace (Wu, 2003a).

2.13.2 Coal

The key parameter for CO production between fuel types is the reactivity of the fuel. Different coals have different reactivity. Studies such as (Armesto et al., 2003a; Chern

and Hayhurst, 2012; Cliffe and Patumsawad, 2001) have looked into the effect which fuel type has on the CO emissions produced, measured at the flue. Armesto et al. (2003a) has previously found that there is a difference between anthracite and lignite coal in terms of CO emissions. The anthracite was found to produce higher CO levels when in an FBC system compared to lignite. This was correlated to lower freeboard temperatures and above bed temperatures which could be linked to the lower reactivity and combustibility of the anthracite.

2.13.3 Biomass

Biomass has a larger volatile matter percentage than that of coal. Mechanisms described in section 2.9.3 describes how volatiles are released and combusted near the top of the fluidised bed and above this area closer to the freeboard section. As a result, the temperatures above bed and in freeboard are much higher when burning biomass in an FBC. This higher reactivity of biomass therefore, results in lower CO emissions. Ghani et al. (2009) studied the difference in CO emissions from coal, coal/biomass blends and dedicated biomass burning in FBC and found that coal produced the most CO emissions, the blends produced less with increasing biomass ratios and lowest CO when dedicated biomass burning occurs.

2.13.3.1 Bed Temperature

Bed temperature will alter the rate of combustion of fuel in the bed. Bed temperature will impact CO formation by influencing the energy available to carbonaceous molecules and react to CO_2. The temperature range in which CO is reduced depending on the FBC type being used and the relative flame temperature.

Leckner and Lyngfelt (2002) used various biomasses as “high volatile” fuels with increasing bed temperature to show that with increasing bed temperature from 740°C to 850°C, within a CFBC, the CO emissions could be reduced from 85ppm to almost zero. This was compared to a coal which was the “low volatile” fuel in comparison. It was found that there was a different correlation to bed temperature and coal rank. This was linked to the char content and volatile content difference in the fuels being opposing between fuels and thus shifting bulk of energy release to different parts of the flame. The data suggests that the correlation between bed temperature and CO emissions is still applicable but possibly with less significance in coal.

It has been found in Armesto et al. (2002) that the bed temperature increasing in temperature brought on the increase of CO emissions initially and then followed a significant decrease. This study was in a FBC unit. The difference in mixing and regime

of inlet air flow rate influences the CO reaction rate with bed temperature. The study showed the overall decrease in CO with increased bed temperature as the CO reacts completely to CO_2.

2.13.3.2 Inlet Air Velocity

The inlet/fluidisation air will directly affect the concentration and formation of CO in any FBC system. An increase in the inlet air velocity will result in a decrease in the CO residence time within the combustion chamber. This results in a decrease in the reaction of CO to CO_2 within the flame which increases the CO emissions. The study on rice husk utilisation in FBC units by Armesto et al. (2002) indicated a CO emission increase from 1085 mg/m^3 to 1688mg/m^3 with the increased inlet air velocity of 1 to 1.2m/s (Wu, 2003a). Apart from the CO residence time and dilution affect the physical cooling to the system influences this outcome by reducing the conversion efficiency of the CO to CO_2.

2.13.3.3 Excess Air

Excess air will influence the CO emissions through dilution, altering combustion characteristics and flame temperatures (Arromdee et al., 2010).

Abelha et al. (2003) investigated the effect of poultry litter in FBC with varying excess air levels. It was found that excess air could vary the CO emissions when varied between 10% and 40%. When 10% excess air resulted in the smallest CO concentration, however, as the excess air was increased to 25% the CO concentration range increased very slightly compared to 40% which resulted in high CO emissions. The most effective excess air was 25% and can attributed to better mixing within the bed whilst maintaining reasonable residence times for CO conversion and maintained combustion temperatures. In a similar investigation Annamalai et al. (1987) found that when burning manure the optimum emissions levels for CO and others was at 650°C and 10% excess air. It was also concluded in this investigation that the CO emissions could not be brought below 0.05vol% without manipulating other parameters other than excess air.

In other studies Ghani et al. (2009) found that there were variances in CO ranges between dedicated coal combustion, co firing and dedicated biomass burning. Across all fuel combinations the CO level and combustion efficiency found a peak and then decreased with increasing excess air. There is a point at which excess air can be applied for combustion optimisation which, based on the literature, is up to 25-30% for biomass and up to 40-45% for coal. The difference is based on the volatile content and char content difference between the fuels which require different excess air levels to complete combustion.

2.13.3.4 Secondary Air Regimes

The introduction of secondary air into a furnace results in CO concentrations decreasing. This is due to further conversion of CO to CO_2 within the freeboard where residual combustion heat will be present (Arromdee et al., 2010). The introduction of staged air or secondary air will also increase the mixing and turbulence above bed and throughout the freeboard further increasing the reaction rate to CO_2 before leaving the furnace (Wu, 2003a).

There have been a number of investigations into the effects of air staging especially over the last 10-15 years as a result of EU emissions limits. Work has been conducted to minimise all emissions as well as CO. Topal et al. (2003) investigated the combustion efficiency of olive cake on a CFB combustor unit with the aim of optimising emissions and combustion efficiency. It was found that with the secondary air staging the combustion efficiency could be improved from 82% to 98% (mitigating heat loss), which results in the CO emissions being decreased to less than 10ppm. Youssef et al. (2009) investigated air staging effects on four different biomasses; wheat straw, sawdust wood, cottonseed buds and corncobs. It was found in this study there was a difference of CO emissions of 3000mg/Nm^3 for sawdust to 250mg/m^3 for cottonseed. With control of air to the system combustion efficiency and CO emissions were reduced to below 100ppm. Further to this Abelha et al. (2003) found in a study of rice husks and air staging that during normal operation a FBC could produce between 1500-1600ppm CO but with a minimal air staging ratio to fluidisation inlet air of 1.4 the CO range could be reduced to 160-540ppm (Wu, 2003). Thus, by introducing air staging to a system it is suggested that combustion efficiency can be optimised and thus CO emissions can be decreased to reasonable or exceptional levels by cooling the flame or oxidising CO to CO_2.

2.13.4 Carbon Dioxide (CO_2)

CO_2 is a significant combustion emission component. As with CO the carbon comes from the carbonaceous material in the fuel which can vary in coals between 60-75% for sub-bituminous to 91-92% in anthracite and averaging around 45% for biomass (Beér, 1977; Suyadal, 2006; Gulyurtlu et al., 2013). During combustion, the carbon in the fuel oxidises and thus produces CO_2 in the flue gas.

There are a number of side and secondary reactions which can result in the production of CO_2 depending on the available oxygen within the chemical system and whether it is a reducing or oxidising reaction. Reaction 2-1 to Reaction 2-3 describe the overall formation of CO_2 in an ideal combustion system.

The net emission of CO_2 for coal is theoretically more than that of any biomass material because of the potential for the biomass to emit as much CO_2 as it requires to grow. This is due to the biomass absorbing CO_2 in the growth stage of the fuel and been deemed "carbon negative" at emission. If waste food, recycled timber, tree bark etc. is used as a fuel it will still have absorbed CO_2 during growth and therefore, the CO_2 emitted during combustion is equal to that absorbed during growth (Koppejan and van Loo, 2012). In reality however, biomass isn't carbon negative as other factors are overlooked including transport, crop fertilisation, crop prioritisation, processing and technique for best utilising the material downstream (Zanchi et al., 2012). CO_2 emitted from combustion such as FBC technology is a contributor to climate change globally but FBC allows fuel flexibility especially if in the future carbon capture and storage techniques can be applied to make biomass carbon negative (Abanades et al., 2005).

The literature has shown that operational variables and fuel composition will impact the emission of CO_2 and CO through temperature and redox dominated reactions. Therefore, it is assumed that during experimental testing these parameters will be varied and will evaluated against the impact of the fuels in FBC.

2.13.5 Sulphur Dioxide (SO_2)

SO_2 is formed when the organic sulphur contained within the fuel is combusted. In the combustion process, most of the Sulphur is oxidised to its stable gaseous form, SO_2. The higher the content of Sulphur in the fuel the more SO_2 will be produced and thus emitted as a flue gas component as the reaction of sulphur to SO_2 is a 1:1 reaction. (Wu, 2003a). Any sulphur which isn't oxidised is retained as ash. This retention can be between 5-60% for different coal and varying operational changes (Eggleston H.S., 2006) and as salts form in slags and fouling such as K_2SO_4 and H_2S found in downstream heat transfer surfaces where the lower temperatures condense the species out of the flue gases (Koppejan and van Loo, 2012).

2.13.5.1 Coal

The content of Sulphur in Coal is higher than that of other fuels such as biomass, natural gas and municipal solid wastes. Table 2-3 illustrates the variation in sulphur content between fuels.

The sulphur content of coals is commonly used as an indicator by power generators for blending coals. By blending two coals, one with a high sulphur content and one with a low sulphur content, it is possible to control and moderate the SO_2 emitted as a pollutant at the flue stack by simply limiting the available S in the fuel source (Cheng et al., 2003).

Table 2-3 Sample and default sulphur content values for different fuels (Harrison, 2001)

SAMPLE AND DEFAULT VALUES OF SULPHUR CONTENT (S) IN FUEL			
Fuel (IPCC grouping)		**Default value (wt%)**	**CORINAIR 90 range (wt%)**
Coal	- low S	0.5	≥ 0.001
	- medium S	1.5	-
	- high S	3.0	≤ 16.1
Heavy fuel oil	- low S	1.0	≥ 0.001
	- medium S	3.0	-
	- high S	4.0	≤ 4.0
Light fuel oil/diesel	- low S	0.3	≥ 0.14
	- high S	1.0	≤ 1.0
Diesel (road)		0.3	0.1-1.0
Gasoline (road)		0.1	0.012 - 0.15
Jet kerosene		0.05	0.0001-0.3
Oil shale		1.5(1.3-1.7)	NAV
Natural gas		negligible	NAV
Municipal waste		0.003	0.003
Industrial waste		0.2	0.200 - 1.000
Black liquor		1.5	0.004 - 8.09
Fuelwood		0.2	0.001-0.06
Other biomass		< 0.03	0.001 - 0.800

2.13.5.2 Biomass & Co-firing

Biomass combustion produces less SO_2 for a number of reasons; firstly, the organic sulphur content is much less than that of a fuel such as coal (as illustrated in Table 2-3) and secondly, biomass can contain a varying concentration of alkali metals and alkali earth compounds (Ca and Mg) which react with the sulphur resulting in a higher retention of the sulphur in the ash (Sloss, 2010a; Fernando, 2012b; Fernando et al., 2007).

The amount of sulphur in biomass is less than that of coal, however, waste derived fuels and sewage sludge can contain a varied source material resulting in higher sulphur

content. The sulphur level can range from that of biomass to something resembling a coal (Fernando et al., 2007).

One method of reducing the SO_2 emissions from the combustion of coal is co-firing coal with different ratios and blends of biomass. Apart from the overall sulphur component in the fuel, the alkali metals and alkali earth compounds can lead to advantageous reactions which retain a greater proportion of the sulphur as ash (Fernando, 2012b). Khan et al. (2009), found that it was possible using coal biomass blends, to increase the sulphur retention in ash from 10% to 50%. This is due to the amount of Ca within the biomass which acts as a reactant which forms a stable calcium sulphate compound. Whilst biomasses can reduce the amount of sulphur which is emitted as SO_2 either by reducing the amount of sulphur present or increasing retention, sewage sludge has been found to increase the SO_2 emitted during co-firing even though it typically has a high Ca content. It has been suggested that the higher combustion temperatures achieved during combustion of this blend results in a reduction in CaO reactions hence resulting in increased SO_2 emissions (Sloss, 2010a).

2.13.5.3 Sulphur Oxide Removal

SO_2 has been recognised as a serious pollutant and the problems associated with it since the early 1980's. In main land Europe, the emissions were found to lead to acid rain which resulted in mass deforestation and land/water pollution destroying local eco systems. As such the power generation sites across Europe including the UK had to incorporate desulphurisation techniques for flue gas desulphurisation (Harrison, 2001).

There are a number of methods for reducing the sulphur in a combustion system; firstly, using low sulphur content fuels such as biomass or the Co-firing of fuels can lead to a SO_2 reduction by reducing the total volume of sulphur entering the combustion zone, secondly, the construction of large desulphurisation units which spray liquid/atomised calcium compounds through absorber units which the flue gases pass through thus capturing the SO_2 as calcium sulphates and ,thirdly, using additives in the combustion zone to retain sulphur in ashes which leave through the bottom/fly ash systems (Álvarez-Ayuso et al., 2006). Operational parameters can be optimised to retain the maximum volume of sulphur in ashes or limit emission mechanisms whilst additive based desulphurisation is used for both in furnace retention and downstream cleaning techniques. Downstream additive based techniques are preferred for minimum changes to a combustion system whilst achieving high levels of efficient sulphur capture.

For a FBC system the most effective method (apart from utilising co-firing biomass) is to dope the bed with a limestone and/or dolomite mineral. This is fed in with the fuel/sand during operation and then removes the sulphur through a number of reactions shown in the following section. The product of these reactions are then emptied out with the bottom ash (Khan and Gibbs, 2000).

2.13.6 Sulphation Mechanisms

FBC systems using coal as a fuel require limestone, dolomite or chemically impregnated doping agents in the bed to retain the SO_2 compounds. The main reactants considered for the purpose of desulphurisation are chosen fundamentally because of their high CaO and/or CaO•MgO content (Wu, 2003a).

Podolski et al. (1995) and Wang et al. (2007) describe the overall reactions which take place in atmospheric desulphurisation system as shown in Reaction 2-21 to Reaction 2-24:

Limestone-

$CaCO_3 \rightarrow CaO + CO_2$	Reaction 2-21	(Podolski et al., 1995; Wang et al., 2007)
$2CaO + 2SO_2 + O_2 \rightarrow 2CaSO_4$	Reaction 2-22	(Podolski et al., 1995; Wang et al., 2007)

Dolomite-

$CaCO_3 \cdot MgCO_3 \rightarrow CaO \cdot MgO + 2CO_2$	Reaction 2-23	(Podolski et al., 1995; Wang et al., 2007)
$2CaO \cdot MgO + 2SO_2 + O_2 \rightarrow 2CaSO_4 \cdot MgO$	Reaction 2-24	(Podolski et al., 1995; Wang et al., 2007)

The effectiveness of the sorbents being used can be altered by physically altering the amount of sorbent in the combustion system. The volume of sorbent used ranges between 30-50% which is dictated by the efficiency of SO_2 removal by the technique and the offset cost of transport, material cost, disposal etc. (Basu, 1999).

2.13.7 Operational Variables

To control the amount of SO_2 emitted from a combustion system a user can manipulate the operational variables of the FBC system. Whilst excess air levels and pressure have effects on the formation of other pollutants and emissions, the retention of sulphur is affected very negligibly, instead the following variables are most significant (de Diego, 2013).

2.13.7.1 Bed Temperature

The optimum sulphur retention temperature range has been established for atmospheric combustion systems as 800-950°C (García-Labiano et al., 2011). Sulphur retention efficiency will vary with temperature as a result of the calcination reactions being temperature dependant, thus insufficient or excess heat can impeded the calcination mechanisms required for sulphur reactions. Podolski et al. (1995) found that when dolomite was used in a PFBC system an increase in bed temperature up to 950°C gave rise to increased sulphur retention.

The reasoning for bed temperature effecting sulphur retention is due to reverse Sulphation reactions occurring at the higher temperature range, as well as the position of equilibrium in the system changing the formation of SO_3 to instead promote the formation of SO_2 and the calcination reactions of the sorbents. The higher temperatures also induce sintering on the surface of the bed sorbent resulting in less effective sulphur uptake (Hlincik and Buryan, 2013; Zheng et al., 1982).

2.13.7.2 Fluidisation Air Velocity

As with the CO, an increase in the fluidisation air velocity results in a decreased residence time for molecules and particles contact in the bed. This reduces the contact time for the SO_2 with the bed sorbent, thus reducing the effective reaction time and therefore, the effectiveness of the sorbent (Lyngfelt and Leckner, 1992).

2.13.7.3 Sorbent Particle Size

Surface area affects the availability of effective sorbent reaction surface zones. With decreased particle size there is an increase in surface area and hence an increase in the sulphur retention. Podolski et al. (1995) found that the sulphur retention increased from 50-90% when the mean particle size was decreased from 0.99mm to 0.23mm. However, different systems have been found to show varying results.

2.13.7.4 Calcium to Sulphur Ratio

This Ca:S ratio is the most significant variable in terms of process engineering control. The reaction of SO_2 uptake to Ca availability is a 1:1 ratio. Therefore, the method to reduce an excess of SO_2 emissions is to simply increase the amount of sorbent available in the bed. Sulphur retention has been shown to be up to 90-95% in FBC by increasing the Ca/S ratio between 1-2 (Wang et al., 2007). For this reason, adding an excess of sorbent (which is a relatively cheap commodity) is the most common way of reducing SO_2 emissions in an industrial scale power generation system.

The high sulphur content of the Pakistani coals used in the experimental work of this study indicates that SO_2 will be an important parameter for judging the applicability of the coals in full scale systems. SO_2 emissions and the effect operational variables have on sulphur retention will be a key parameter to gauge each fuels application in FBC.

2.13.8 Nitrogen Oxides (NO and NO_2)

Nitrogen enters any combustion in two forms, organically bound to the fuel and in the atmospheric air used in combustion. The high temperatures and oxidising atmospheres in which combustion takes place react the nitrogen into NO_x. (Sloss, 2010c). Most of the nitrogen will, via a series of reactions, form NO_x compounds, this includes NO and NO_2 (Fernando, 2012a).

In FBC the combustion temperatures (750-900°C) are less than PF which can achieve ≥1400°C for pulverised coal (Barnes, 2010). The lower flame temperature results in a much lower yield of NO_x from thermal emission reactions. It is assumed that most nitrogen will be released in the form of NO and N_2O in FBC combustion. This means that nitrogen concentrations from fuel characterisation data can be used to approximate the concentrations of NO in the flue gases from FBC operations (Wu, 2003a).

2.13.8.1 NO and NO_2 Formation

The following discussion and description of reactions refers to the pathways shown in Figure 2-18.

The formation of NO and N_2O results from a series of complex reactions taking place during combustion which includes, devolitisation of the fuel particle(s), volatile species oxidation, char oxidation and partial reduction to N_2.

Initially the nitrogen organically bound in the fuel devolatilises and is portioned into volatile nitrogen and char nitrogen. The conversion of fuel bound nitrogen to oxides group can vary from less than 5% to 40% (Anthony and Preto, 1995a). The proportions of this split are dependent on process variables such as temperature, pressure and catalytic activity of the bed materials and subsequent process impurities such as ash. Armesto et al. (2003c) found that combusting lignite's and low grade sub-bituminous coals resulted in fuel bound nitrogen being converted to NO rather than N_2O. Whereas Boavida et al. (1997) found that by using African coals of a similar type but with varying bed temperatures yielded greater N_2O concentrations, thus emphasising the effects of devolitisation temperature and coal type.

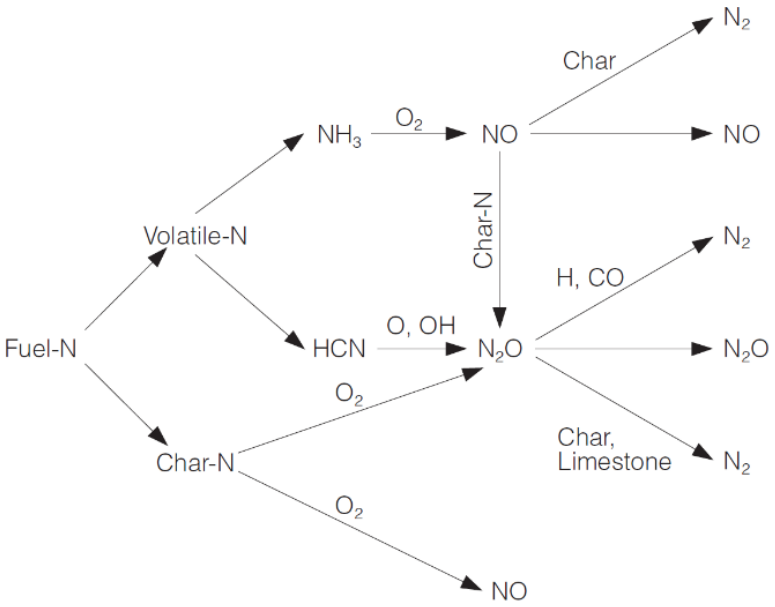

Figure 2-18 NO_x reactions; formation and reduction pathways (Anthony and Preto, 1995)

Volatile nitrogen undergoes a series of oxidation reactions via homogenous gas phase reactions or heterogeneous catalytic reactions over char or bed materials (sand, limestone, ash etc.). A number of authors; (Löffler et al., 2001; Johnsson, 1994; Okumura et al., 2002) have investigated nitrogen bound in fuel and its partition to HCN and NH_3 groups with varying results. Conclusions can be summarised to coal rank dramatically affecting portioning due to devolitisation temperature, effect of local particle gas pressure and impurities in the fuel. Thus, the quality of the coal is expected to influence NO formation and concentration in later experiments.

Nitrogen in char can oxidise to NO, N_2O and NO_2 via a number of intermediary stages when HCN and NH_3 are present. The NO and N_2O undergo partial reduction forming NO_2. NO can also be partially reduced in the presence of NH_3 whilst in its homogeneous phase. In the third instance, N_2O can be decomposed if there is sufficient heat energy to cause the "high temperature" effect. The forth pathway is that NO and N_2O are reduced in the presence of a CO with a catalyst. This catalyst includes char, bed material, sand and limestone.

The rate of formation for nitrogen oxides greatly varies due to the operational variables and the activity of available catalysts in the bed. For instance, calcined limestone which may have been introduced into the bed as a SO_2 reduction method has high catalytic activity when compared to silica sand. Lower grade coals have been found to have high nitrogen activity because of high ash content, but adversely the limestone in such tests

were found to have much less activity due to high Sulphation of the limestones active sites (Johnsson, 1994).

The addition of additives based on the literature presented previously suggests that the addition of an additive and alteration of operational variable is likely to influence NO emissions.

2.13.8.2 Operational Variables and NO Formation

The NO formation and concentration is of importance for any industrial scale FBC operation. Wu (2003a) reviewed the literature to evaluate the effect of operational variables on the formation of nitrogen oxides during FBC and the results are summarised in Table 2-4 The variables are described as follows:

Table 2-4 effect of operational variables on NO and N2O formation (Anthony.et.al.1995)

Increasing parameter	NO	N2O
Fuel nitrogen content	Increase	Increase
Fuel volatile content	Increase	Decrease
Temperature	Increase	Decrease
Excess air	Increase	Increase
Air staging	Decrease	Decrease
Gas velocity	-	Increase
Limestone addition	Increase	Decrease

1) Fuel nitrogen content- The greater the nitrogen content in the fuel, generally, the more nitrogen oxides released during combustion. Biomass has less organically bound nitrogen than coal thus it should yield less nitrogen oxides (Anthony and Preto, 1995a).
2) Fuel volatile content-Increased volatile content results in greater NO and reduced N_2O emissions. This is attributed to increased NH_3 production which has a bias for oxidation to NO (Basu, 1999).
3) Combustion temperature- Increased combustion temperature increases combustion rates and the concentration of nitrogen radicals. This further increases the oxidation of nitrogen radicals. Increased combustion temperature also results in reduced char and CO thus promoting reactions to form NO and reducing reduction reactions to N_2 (Lan et al., 2001).
4) Excess air-Increased excess air results in increased combustion rates leading to enhanced homogeneous oxidation reactions of HCN and NH_3. This has adverse effect on heterogeneous reduction reactions but overall increases the concentration of nitrogen oxides (Lan et al., 2001).

5) Air staging-Air staging in the freeboard reduces the formation of nitrogen oxides. This is attributed to an enhanced reducing atmosphere as well as cooling the localised flame (Leckner and Lyngfelt, 2002).
6) Gas velocity- N_2O has been reported to increase with superficial gas velocity as a result of decreasing residence time (Armesto et al., 2002).

The operational variables noted previously and the effects on the formation of NO have been described as the experiments in later Chapters will alter the operational variables and thus result in changing NO flue concentration.

2.14 Summary

The literature review is the result of a comprehensive investigation and evaluation of the available literature and understanding of fluidised bed technology. The review has focused on operational effects when combusting low grade fuels and the effect on system efficiencies, emissions and agglomerates.

As such, it has been found that there is an understanding of agglomeration with biomasses and low grade coals in FBC. However, the fuels in this investigation represent a range of fuels applicable to the current power generation industry. As such, the results of later investigation will offer the greatest comparison to full scale application in industrial utilities. This Chapter has focused the work in the following Chapters and emphasised the need for research in low grade fuels in fluidised bed with regards to operational variations for combustion optimisation and the application to industrial scale systems.

The information disseminated previously has indicated that co-firing coals and biomass, addition of bed sorbents, sorbent particle size, bed temperatures, sorbent fuel ratios and air distribution methodology require further research and development. This is due to their influence on agglomeration and slagging mechanisms, the resulting emissions and effectiveness for improving the fuels and the resulting combustion.

The information covered in the literature review is necessary for the understanding and validation of the work conducted in the investigations of the following Chapters and will be referred to and compared against. This will allow for the comparison and verification of the results and allow both internal and external validation possible. This will improve any accuracies and validity in the results achieved.

3 Experimental Fluidised Bed Combustion (FBC) Rig

Throughout this Chapter, details on the pilot scale rig which was used for combusting the low-grade fuels will be described. Initially the rig had to undergo a lengthy commissioning phase to bring it to a level of good operation. Significant commissioning work has been described as it was such a lengthy part of the testing process. After a series of test phases the rig was then taken offline and underwent heavy re-designing. The re-design phase is also included here and explains the reasons and necessity of the changes and to what end those changes achieved.

3.1 Pilot Scale Rig Description

The following is detailed descriptions of the test rig which was inherited from the Central Electricity Generation Board (CGB) and moved from a test facility located in Mitcheldean to its current location at the Low Carbon Combustion Centre (LCCC) in Beighton, Sheffield in 2010.

The rig is made up of a series of sub systems, (hoppers, feeders, gas burners, cyclones, heat exchangers, bag filter house, monitoring equipment, fans, etc.) which interact with the main body of the rig (approx. 1m x 1m x 5m) where the bed and combustion zones are located. The rig can be seen in the images shown in Figure 3-1, schematic is shown in Figure 3-2 layout of thermocouples shown in Figure 3-3 and arrangement of pressure transducers shown in Figure 3-4.

3.1.1 System Start-Up

The thermal rating of the rig is 350$kW_{thermal}$. In order to achieve this thermal output all systems need to be running in correct working order and brought into action through a series of steps to ensure safe and reliable operations. This series of steps is described in the “start-up procedure” document which was written based on the experiences of using the rig. The start-up procedure involves operators bringing each subsystem online, starting the pre-heat systems and sequence, the cross over to solid fuel and continuous operations and finally how to shut down the unit whilst maintaining safety of personnel and the equipment. The following sections describe each of the subsystems utilised to run the rig in normal operations.

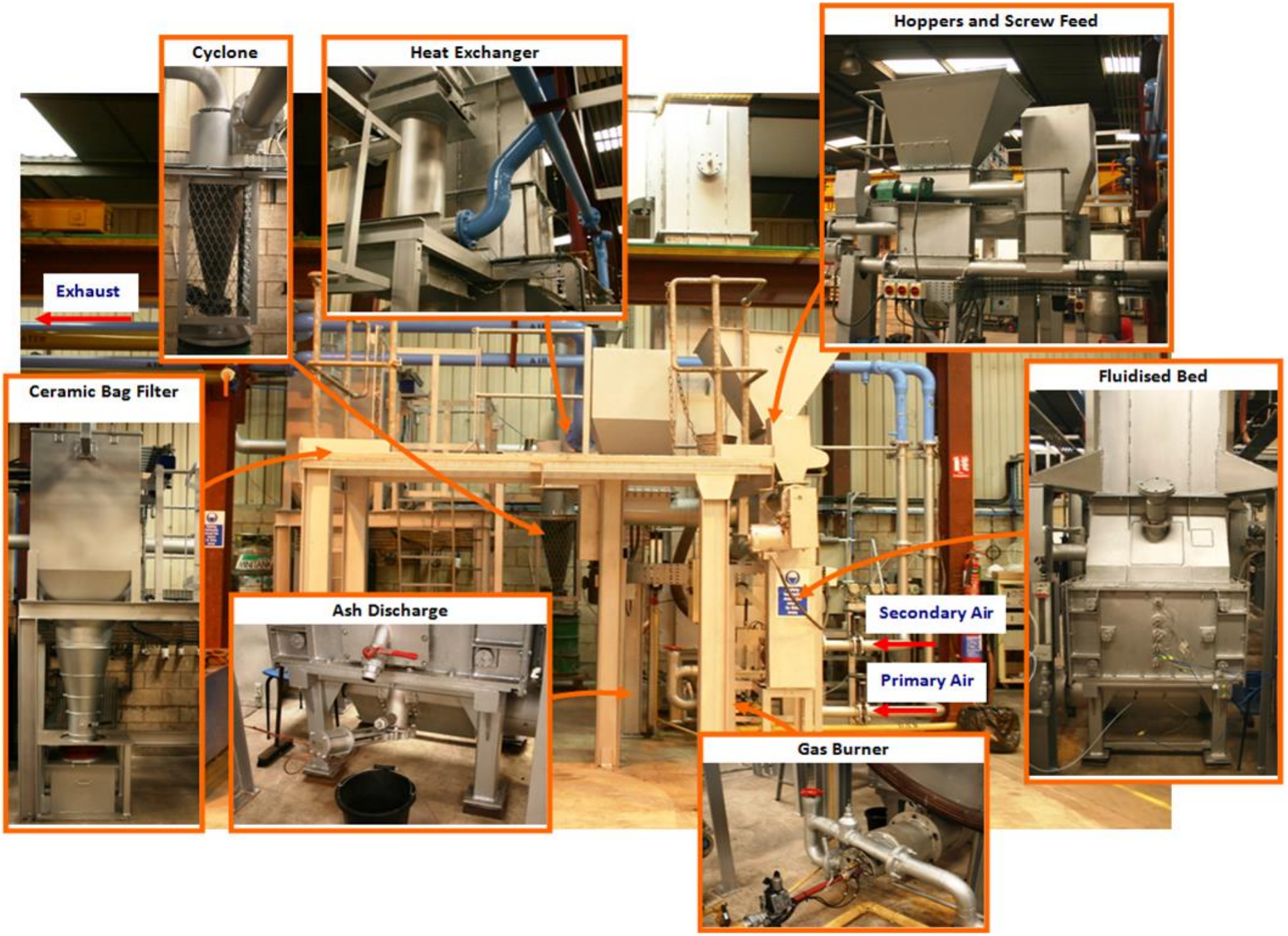

Figure 3-1 Images of the pilot scale FBC rig

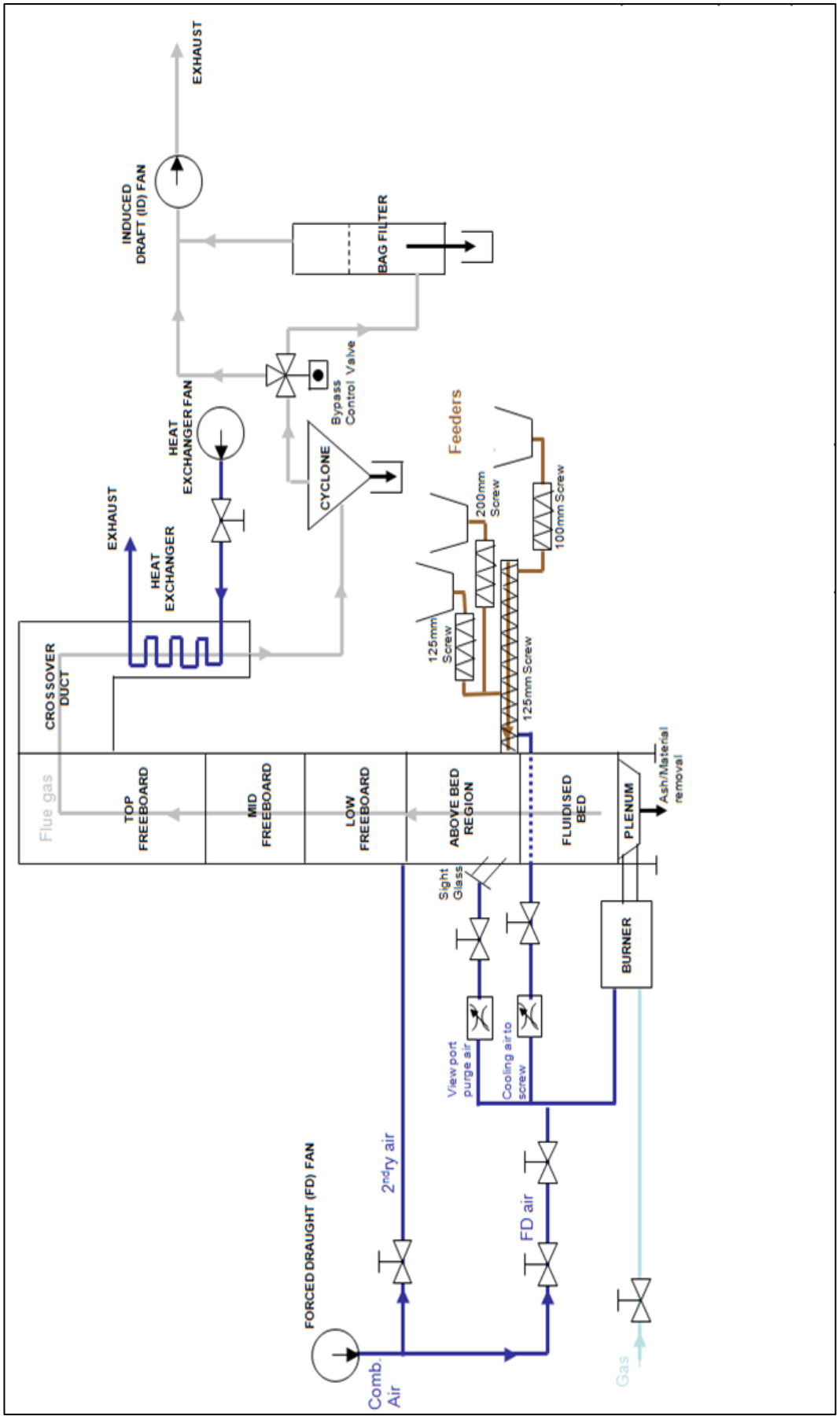

Figure 3-2 Schematic of FBC rig

Thermocouple	description
1	Primary air temp
2	Under bed burner temp
3	Secondary air temp
4	Sight glass air temp
5	Sight glass temp
6	Plenum temp
7	Bed A temp
8	Bed B temp
9	Bed C temp
10	Bed D temp
11	Bed E temp
12	Above bed temp
13	Mid freeboard temp
14	Top freeboard temp
15	Exit flue gas temp
16	Cyclone temp
17	Bag filter temp
18	Exhaust fan temp
19	Stack temp

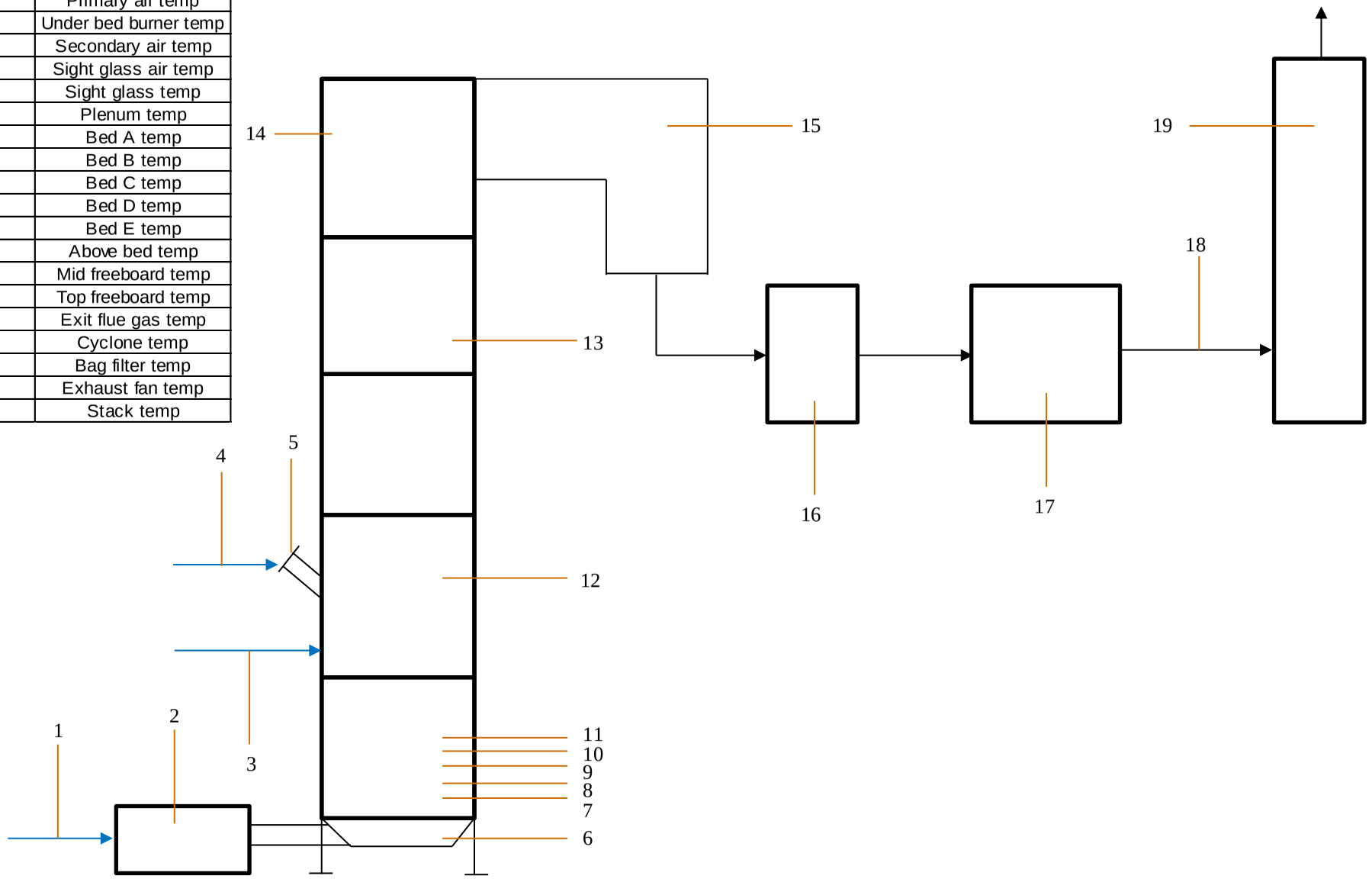

Figure 3-3 Thermocouples locations around the experimental rig and description

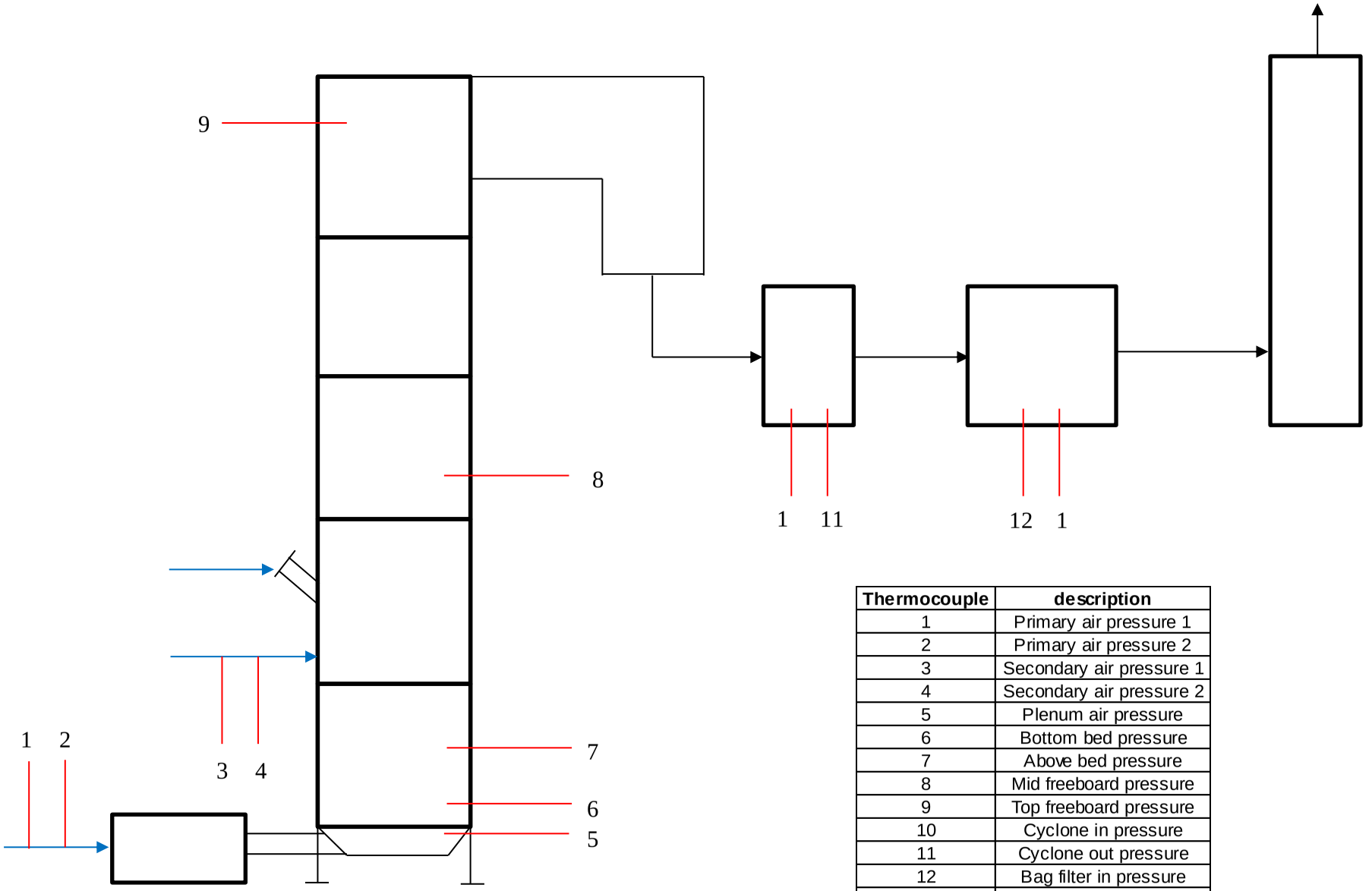

Thermocouple	description
1	Primary air pressure 1
2	Primary air pressure 2
3	Secondary air pressure 1
4	Secondary air pressure 2
5	Plenum air pressure
6	Bottom bed pressure
7	Above bed pressure
8	Mid freeboard pressure
9	Top freeboard pressure
10	Cyclone in pressure
11	Cyclone out pressure
12	Bag filter in pressure
13	Bag filter out pressure

Figure 3-4 Pressure transducers locations around the experimental rig and description of locations

3.1.1.1 Pre-Heat Systems

The rig has an under-bed gas burner rated at 60-80$kW_{Thermal}$ capacity. Once the operators are in a state of readiness, the gas burner is ignited. This drives high velocity hot gases through the plenum section, through the distribution plate and into the bed. The pre-heat time is approx. 2 hours depending on bed mass, ambient temperature and gas mains pressure available. The gas burner is capable of achieving temperature ranges of 650-800°C throughout the bed/freeboard regions. The gas burner is only operated during pre-heat. Solid fuel takes over combustion and the source of heat when desirable bed temperatures are reached.

3.1.1.2 Hoppers and Feeders

There are 3 hoppers which have independent screw feeders and controls. This allows individual control of different fuel streams and thus blending of fuels. The hoppers are equal in capacity; however, the screw diameters are different. There is a 200mm, 125mm and 100mm screw. This allows different types of fuel to be drawn through the fuel feeder system ranging from biomass pellets to coal fragments or to a more extreme options of sewage sludge and chicken litter. All hoppers and screws feed a main screw which directly feeds its contents into the combustion area. The fuel falls via gravity into the bed from an opening approximately 1m above the bed area.

3.1.1.3 Fluidised Bed and Freeboard

The combustion chamber is the main body of the rig. Whilst the dimensions of this section are approx. 1m x 1m x 5m, the internal bed area is approx. 0.5m^2. Combustion takes place within and above the bed in the bed and lower freeboard regions. The combustion gases then travel up through the freeboard and leave through the top of the unit into the gas clean up systems induced by an induction fan.

3.1.1.4 Air distribution

Primary air is fed through a perforated plate which is made up of a series of stand pipes. There is a total of 18 stand pipes in the bubble cap design shown in Figure 3-5. There is a large area occupying the space of 2 stand pipes in the centre of the pipe formation. This is for the removal of bed material post combustion.

The air leaves the stand pipes and filters through the bed material. This results in lifting and expansion of the bed as air fills voids between bed particles. This results in bed fluidisation.

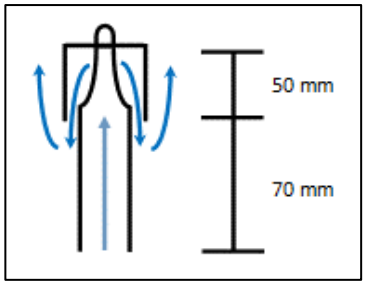

Figure 3-5 Bubble cap design

3.1.1.5 Bed

The bed is made up of silica sand. This is an inert material mainly consisting of particles ranging between 0.5-0.85 mm in diameter (Table 3-1), made up of 97% SiO_2. (Table 3-2). The average bulk density of the sand is 1461 kg/m^3 which is typical of most silica sand.

Table 3-1 Particle size distribution data

Apeture	Typical cumulative passing	Typical cumulative retained	typical retained each sieve	Typical retained	category
Microns	%	%	%	%	
1400	100.0	0.0	0.0	3.0	Very coarse sand
1180	100.0	0.0	0.0		
1000	97.0	3.0	3.0		
850	83.6	16.4	13.4	95.8	coarse sand
710	60.0	40.0	23.6		
600	11.7	88.3	48.3		
500	1.2	98.8	10.5		
425	0.3	99.7	0.9	1.2	medium sand
355	0.1	99.9	0.2		
<355	-	100.0	0.1		

Table 3-2 sand data of bed material	
Element	Average content (%)
SiO_2	97.15
Fe_2O_3	1.96
Al_2O_3	0.28
TiO_2	0.01
K_2O	0.05
Na_2O	0.05

The internal dimensions of the bed in 0.42m x 0.38m. During testing the beds depth can be varied between 0.22 and 0.3m. Depth variation is dependent on mass of the bed vs air fluidisation potential which was found to be limited to approx. 80 kg i.e. 0.3 m depth.

3.1.2 Post Combustion Systems

Combustion gases generated by the process move through the freeboard and exit into the heat exchanger. The flue gases are cooled by approx. 300°C. The cooled flue gases then

pass through a cyclone and bag filter which removes fly ash and particulate matter. The remaining gases are then expelled into the atmosphere via a flue stack.

3.1.2.1 Auxiliaries

There are a large number of auxiliary systems feeding to the rig and sub systems which are necessary to operate the rig properly.

There are 3 fans used to produce primary air, heat exchanger cooling air and an exhaust fan which is required to generate a slightly negative pressure in the combustion zone and draw exhaust gases to the flue stack.

A number of the valves and self-cleaning processes require pressurised air in order to operate, this is supplied via a site compressor.

There is a main control tower which is the hub for any electronic controls, allowing a centralised area to make adjustments to the rigs operations.

Each system relies on the other sub systems in order for combustion to be sustained in a safe way within the rig.

3.1.2.2 Monitoring and Analysis Systems

In order to control and monitor the rig during operation, there are a series of thermocouples and pressure transducers taking measurements across the rig. The placement of these devices is strategically located to measure important areas of combustion and to ensure that the correct combustion environment is being achieved.

A sampling line takes online gas samples from the flue gas, post cyclone. The sample is received by a chain of condensers to remove excess moisture in the gas line before entering two gas analysers. These measure the SO_2, NO_x, CO, CO_2 and O_2 concentrations in the flue gas.

All the measurements are taken in real time and are recorded, via national instrument signal clean up instrumentation, on the main computer. The computer is not part of the control system for the rig, this is a separate control tower. The labview program presents important data in a graphical format and saves the data in a way selected by the operator. The computer/labview set up allows operators to understand the internal workings of the process better and make faster and more informed decisions with regards to the operations of the rig. The design of the labview program was modified based on the information sourced for the control and monitoring described in the literature review.

3.2 Commissioning

When the rig was handed over for the use and operations it was found that there were significant issues with the rig operation both in terms of technical understanding by the previous operators and poor design choices with the rig itself. It was therefore, necessary for a 12 month commissioning phase which tested individual parts of the rig before operating it in extended runs. If any part of the rigid not meet the targeted requirement, then it was either replaced or alternative design options were looked into.

3.2.1 Rig Modifications

As the work, which was conducted was extensive it is not prudent to include every piece of work which was done on the rig but instead examples of significant changes will be presented in the following sections

At every stage of commissioning it was necessary to run a number of tests to ensure that equipment and installations were operating as expected. The following descriptions include examples of the modifications but are only a small sample of the work scope completed.

3.2.1.1 Cold Commissioning

The cold commissioning phase consists of a series of tests designed to evaluate individual parts/components of the rig without the need to bring any combustion processes online. The following samples show the type of work conducted.

3.2.1.2 Fans

New fans were installed to replace the previous primary air and exhaust fans which had become either damaged through age and poor maintenance or were insufficient in their location/loading capacity. Initial cold tests found that the old fans were incapable of achieving required flow rates and/or simply did not function correctly. New fans were sourced, purchased, installed and all relevant duct work and electrics were attached. Figure 3-6, shows the fans which have been installed in and around the rig to provide required air flows. As can be seen in Figure 3-6 the fans have been insulated to handle the high temperatures flue gas, also the fans had inverters attached to give better control of the fans speed which also allowed the instillation of emergency off switches for better

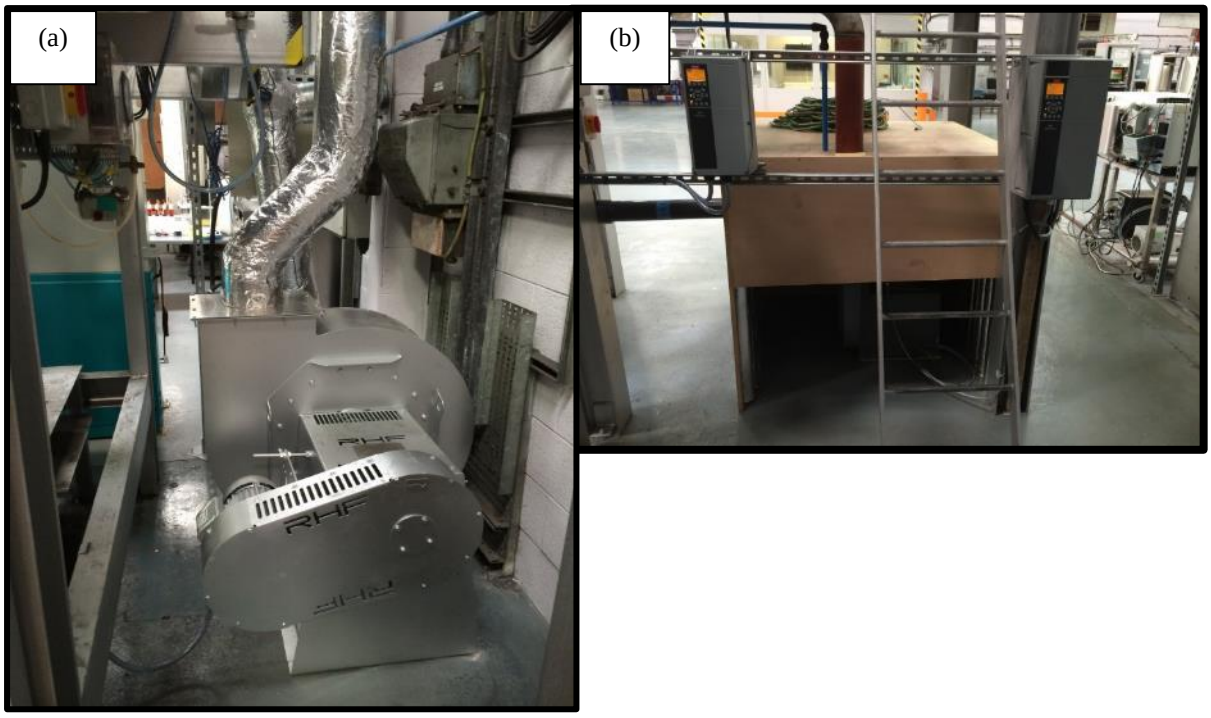

Figure 3-6 installation and sound proofing of new primary and exhaust fans

safety and operation procedure incorporation. Sound proofing can be seen which reduces and redirects the sound of the fan when in operation making the working environment safer and for better communications between operators.

Once the fans were fully installed the process of loading the bed into the test rigs operating at different fan flow rates was conducted. Fan settings and flow outputs were changed in order to define the best flows for operating the bed in different modes of operation. The limits in which rig operation could occur were a priority so operators knew what could be added in test design. It was also at this stage that other issues such as minimum negative pressures in the combustion chamber were discovered which lead to further work needed on and around the rig to reduce leakage.

3.2.1.3 Logging Program

The data logging program was designed and built in the software "labview". Labview is a commonly used platform for designing a range of interfaces for users both recording and displaying data simultaneously. Figure 3-7 shows the main page of the labview software in its most up to date view. As can be seen there are multiple readings being taken in real time and important values displayed in graphical format for operator's visual ease. There are also a number of other pages which include calculations done in order to inform operators of what values the rig is operating at.

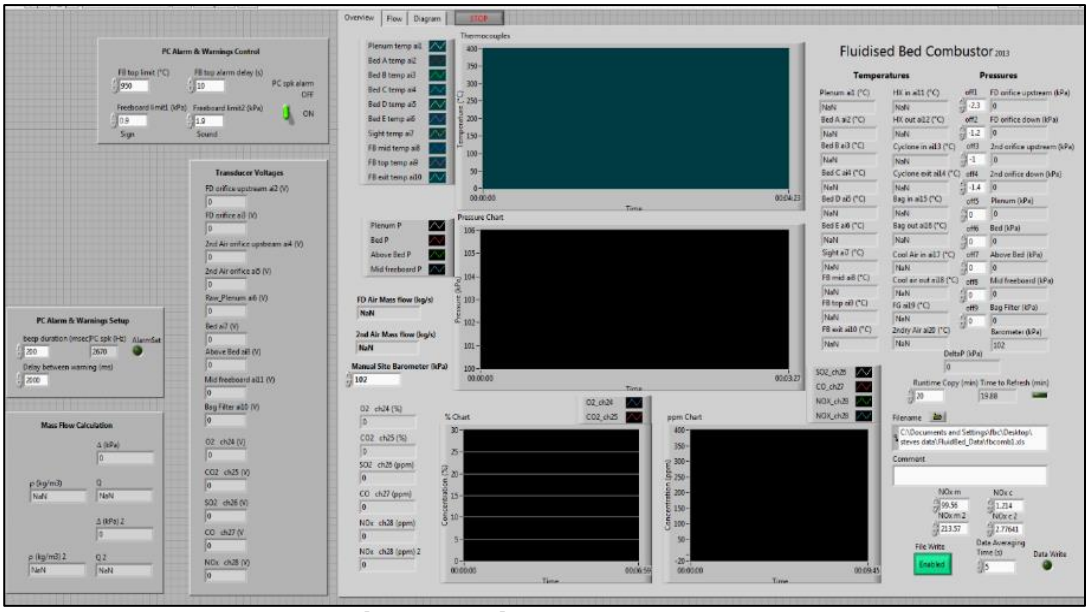

Figure 3-7 Labview_5_alarm program on its main screen

Testing the software was meticulous as each sensor had to be checked for a correct response and any bugs dealt with. The software and hardware was tested in every cold commissioning test possible to thoroughly test the set up before a full test was undertaken and data recorded.

3.2.1.4 Feeders

A number of different test phases were conducted on the feeders systems. This included operating the feeders both empty and were filled with different fuels, varying their

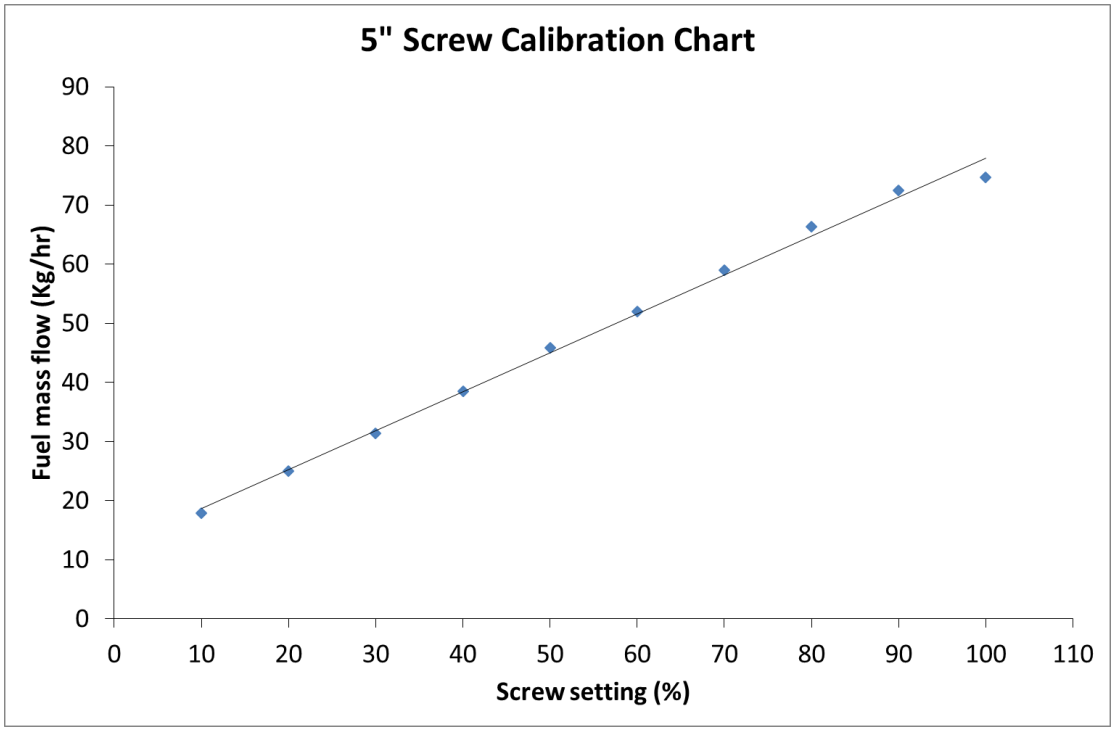

Figure 3-8 125mm screw feeder calibration chart

rotation/flow rates and calibrating the feeders for different types, sizes and weights of fuel.

Initial empty testing proved simple enough and gave good reliability in varying the feeders in series with other feeders. However, when the feeders were loaded with fuel it was found that different feeders had varying electrical loads which limited rotation and fuel loading. Electrical work was conducted on the systems to modify the existing system and ensure a good range of operation.

Calibration of the fully functional feeder systems was carried out giving data such as that shown in Figure 3-8.

3.3 Hot Commissioning

Once all systems had been tested using cold commissioning techniques and all operators were happy with the level of safety in operating the rig it was necessary to run a series of hot commissioning tests.

The tests consisted of brining different systems online in a slow systematic approach. This allowed the operators to evaluate the systems as changes occurred and make the changes needed to operate at a stable level.

Whilst the rig had been installed and previously shown to work, the documentation instructing on operational parameters, start-up and shut down procedure, health and safety etc. were all rendered void with the modifications and change in auxiliary equipment i.e.

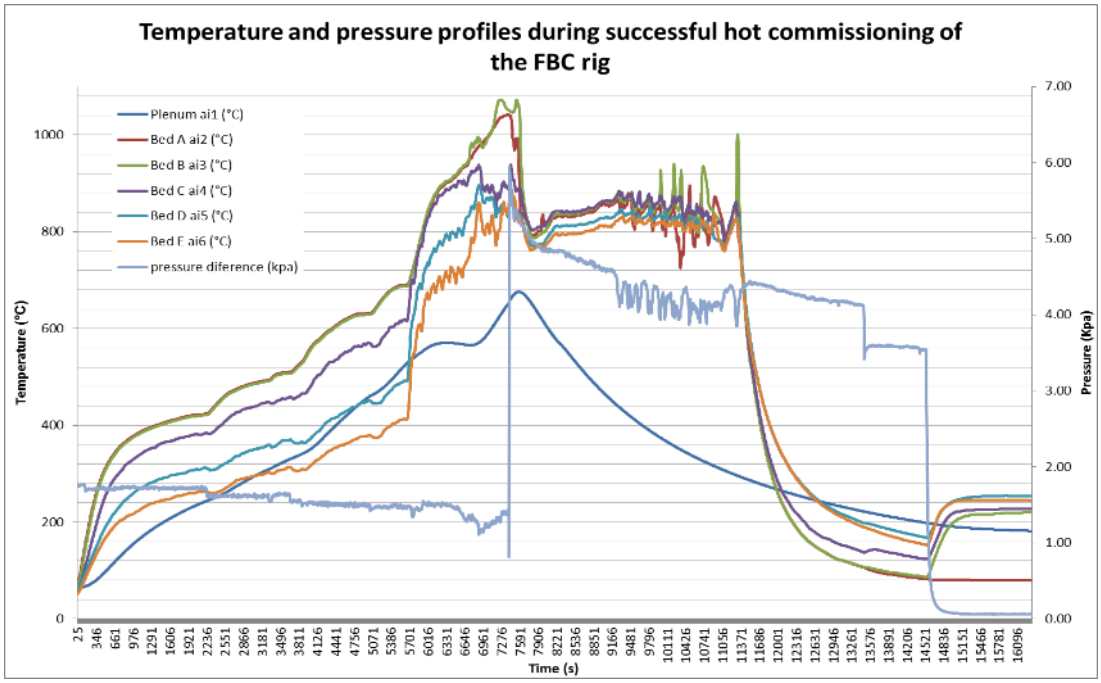

Figure 3-9 Operational data from the pilot scale rig under different fluidising regimes

the fans, bed materials etc. Therefore, the hot commissioning program had to include tests in order to check the modifications.

Once these tests were completed a final run was conducted, the data recorded shown in Figure 3-9. This test included full flow of fuel under varying air flow conditions and proved the operators could control the system when different aspects of the rig were altered, similar to the expected changes in planned tests.

This marked the finalisation of the commissioning phase and put the operators in a state ready for experimental testing.

3.4 Coal & Operational Variable(s) Test Methodology

3.4.1 Rig Specifications

The experimental rig is a 250-350kW bubbling fluidised bed combustion unit. The rig is made of a number of different key components; a feeder system, a combustion section, an air-cooled heat exchanger for flue gas temperature control, a cyclone and bag filter flue gas clean up system and the analysis and computer monitoring system.

The dimensions of the main body of the rig are 1m x 1m x 5m in which different stages of the combustion chamber are housed. These sections consist of the combustion fluidised bed section, the mid freeboard and extended freeboard section. The rig is mainly constructed from mild steel and any sections such as the combustion chamber which are exposed to temperature are refractory lined.

3.4.2 Main Rig Systems

The following sections briefly describe the different systems which contribute to successful combustion in the FBC unit.

3.4.3 Air Supply & Extraction

The primary air fan supplies air for the fluidisation of the bed. The air is controlled using inverters on the fan and through manual changes made to control valves embedded within the pipe network. The air is distributed throughout the base of the combustion chamber via 18 evenly arranged bubble baps. The fan can supply up to 6000L/min (at 20°C, pressure 101.3kPa air pressure) but normally runs at half speed producing between 2500-2700 L/min. The primary fan feeds both the under-bed air flow and secondary air flow.

The exhaust air fan draws the flue gases from the rig, via the air-cooled heat exchanger, and expels the gases out of the main flue stack. The stack has a small electric fan which

creates a draw on the system of 13 mmH_2O however, the exhaust fan can create a negative pressure of more than 130 mmH_2O when running at 100% load (equivalent to 12000L/min [at 20°C, pressure 101.3kPa air pressure]). Whist at ambient conditions the exhaust fan only need run at half load, when the rig is in operation the temperature of the flue gases reduces the density of the air thus increasing the volume of flue gases in the removal process. Temperatures normally reach 200-300°C at the exhaust fan and require the fan to run at 90-95% of maximum load to maintain a minimum negative pressure above the bed.

3.4.4 Fuel Feeders

Figure 3-10 shows the way in which the three different feeders can be used to feed the primary input screw. The primary input screw is 125mm in diameter and runs at a constant high rate to ensure fuel transport is maintained whilst minimising potential clogging within the pipe. The other three screws can be controlled from the main control tower to vary their rotation speed and thus vary the fuel input rate (based on calibration before combustion tests).

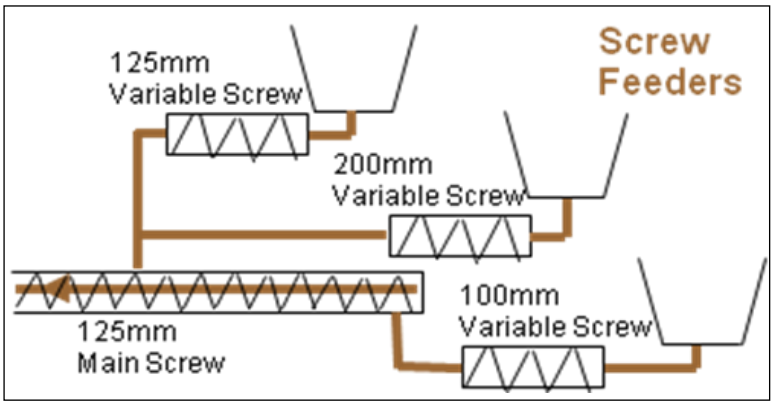

Figure 3-10 screw feeder layout

The smallest screw, 100mm, is designed to operate at up to 100% rotational speed whilst handling high calorific valued fuels such as coal and/or biomass pellets. The medium sized screw, 125mm, is designed to operate at 100% load when transporting medium density fuels such as china clay or building waste. The third screw is designed to operate up to 70% when moving lower density fuels such as paper and municipal solid waste (MSW).

3.4.5 Fluidised Bed

The combustion chamber of the rig is 4.7m in height with and internal dimensions of 0.76m x 0.56m. The bed area of the unit has an internal dimension of 0.42m x 0.38m due to extra refractory material.

The bed height has been found to operate well at 9” in depth for biomass and low grade coals. However, 3” of this is the dead zone where the air from the bubble caps cannot penetrate downwards. Beds with a depth of 12” and above have been successfully operated in commissioning tests. However, the preheat sequence time increases with bed height and total bed material. With a bed height of 9” it has been found that a fuel flow of 30-35kg/hr maintains a bed temperature of 800-850°C with an energy output of 250-280 MJ/kg for biomass. Low grade coals with similar GCV to biomass required 28-31kg/hr fuel flow to maintain bed temperatures due to differences in the fuel combustion characteristics of coal to biomass.

3.4.5.1 Bed Material

The material used in the bed is Sibelco Leighton Buzzard (16/30) which is sourced from mainland Europe because of its durability and chemical makeup. The sand has a density of 1471 kg/m^3 and a range in bulk particle size of 0.50-1.00mm. When a 9” bed is in operation the bed material (excluding fuel) weighs approximately 50kg.

Every test that was performed on the rig with or without fuel used a new load of bed material each time. This ensured a minimum cross contamination of ashes, chemistry etc. between samples from each test.

3.4.5.2 Flue Gas Clean Up

The flue gas exits through the top of the combustion chamber vie the extended freeboard. The gases then pass through a shell and tube heat exchanger made up of 19-25mm tubes which can remove between 200-300°C from the flue gas depending on furnace air flow. The gases then pass through a cyclone which removes fly ash and coarse particles within the exhaust stream.

The exhaust gases then leave via the exhaust fan and out through the main stack.

3.4.6 Auxiliary Rig Systems

The rig has a number of auxiliary systems which all contribute to the functionality.

3.4.6.1 Gas Burner

There is an 80kW gas burner attached to the plenum (bottom section) of the rig. This is used for the pre-heat sequence before solid fuel is introduced to the bed. The gas burner is located in the plenum to preheat the bed which is the biggest sink of heat and to heat the plenum to preheat air entering the rig from the primary air fan.

3.4.6.2 Compressed Air System

Dry compressed air is supplied from a central site compressor to pneumatic components around the rig. A number of lines can be charged with air which enables pneumatic valves to be opened and closed around the rig. The two most important uses of the compressed air are to supply a valve to empty the bed and another to fulfil the blow back cleaning function in the bag filter house.

3.4.6.3 Sampling Equipment

The sampling equipment is a permeant heat proof line which extracts an online sample from the flue gas stream after the heat exchanger and cyclone section of the rig. A series of pumps, dreschell bottles, a condensing unit and filters clean up the sample before it enters the analysis equipment.

The gas analysis equipment compromises of an ABB Magnos and Uras unit which are fixed into the advanced optima chasse. This allows the analysis of CO, CO_2, SO_2 and O_2. There is a paralleled signal analyser which measures the NO concentration in the flue gas stream.

All of these values are relayed to the main computer as well as giving a readout on the analyser for visual conformation as previously described.

3.4.6.4 Shutdown procedure

It should be noted that in order to preserve the formation of structures and agglomerates of varying bond integrity air flows at the end of every test were reduced. The airflows under-bed were reduced to 1000L/min for 24 hours to cool the bed and the surrounding thermal mass but to ensure that any flow of gases and particles were limited. The over bed airs and over bed burner air is also increased to cool the top of the bed and the upper furnace regions. A slow cool ensured the integrity and distribution of the bed materials and any agglomerate samples which may have formed during the experiment.

3.5 Coal Tests Overview

The specifications of the coals with regards to their chemical and physical make up are described in detail in section 4.4.

3.5.1 Baseline Tests

Each test had a set preheat and start up sequence using the gas burner unit (in accordance to the start-up manual), followed by a period in which solid fuel was introduced into the

rig. There was then a conversion stage in which the solid fuel provided the thermal input to the bed at which time the gas burner would be extinguished. It was then necessary to run the rig on solid fuel for at least 20-30 minutes whilst monitoring bed temperatures and rig pressures to ensure stable operations.

This stage was important as the cooling plenum from the extinguished gas burner results in a cooling of the primary air used to fluidise the bed. Therefore, it was necessary to monitor and alter fuel flow rates, to maintain the intended thermal output.

Once a stable period had been achieved, the baseline tests were performed. This was a 20-30 minute period in which nothing was changed in the operation of the rigs. Measurements were taken throughout the whole test but this period gave the baseline emissions produced form the fuel at those conditions as well as giving temperatures and pressures to work from when altering the operation variables of the test later on.

3.5.2 Pulse Tests

The first three tests and baseline tests, were entitled "Pulse tests" because of the method used to deliver the mediums and fuel into the bed.

3.5.2.1 Test 1

A generic UK coal was used to get a baseline value. This was done at a fuel flow rate of 45% in the 4" screw resulting in bed temperatures of 800-900°C. This was continued for 20-25 minutes until the coal in the hopper was depleted. The Pakistani "hybrid" coal was then put into the hopper to follow on from the British coal. This sequence was needed for a comparison and to allow for changes as a result of the fuels to be measured.

In the first test the operators were concerned that the high sulphur values shown in proximate analysis of the Pakistani coals would result in SO_2 values that would exceed the analyser's measurement range. It was decided to take 3kg of each Pakistani coal and mixed them together to create a coal representing an average coal from the Trans region, reducing the fluctuations in sulphur, minerology etc.

A baseline value was recorded for this hybrid coal as with any other fuel put into the rig. The hybrid fuel was entered at a rate of 30kg/hr (45% of the 4" screw feeder's power) resulting in bed temperatures of >900°C as well as peaks of SO_2 values of 4490 ppm and 4590ppm.

Once the initial baseline data had been operated with coal only, the feed was then run with limestone in measured/mixed batches. This was done by pulsing a secondary screw feeder for 2 minutes every 10 minutes. This would achieve 6kg/hr of limestone for every

20kg/hr of coal being put into the bed thus resulting in limestone present being at 30% of the total fuel input.

Once limestone had been introduced and pulsed into the bed the test was ended and data evaluated to look at the influence on further tests.

3.5.2.2 Test 2

Once the preheat sequence had been completed, the hopper was loaded with coal F and baseline data was gathered for 20-25 minutes. Fuel flow at 37% of 4" screw feeder power (18kg/hr) maintained a bed temperature of 900-950°C. The SO_2 values were at the maximum range of the analysers during this period.

Limestone was then introduced into the bed based on a minute to minute basis. The previous test used values for desulphurisation over an hour however, this resulted in little change because bulk limestone material simply resulted in a sharp drop in SO_2 followed by an immediate rise back to baseline levels of SO_2 without proving anything other than limestone can reduce SO_2 in the flue, but to an unknown extent.

The limestone, based on a minute by minute basis, was added to the bed for a total of 25-30 minutes achieving a sulphur ratio of 1:3.

The sulphur ratio was then altered to 1:2 and the test was repeated as before.

3.5.2.3 Test 3 & 4

Coal G was used during this as it contained less Sulphur, and it was hoped that this would produce SO_2 values which would remain within the 0-4500ppm range of the analyser.

Initially baseline data was collected for the coal in accordance to the previous tests and found that coal G operated at an optimum bed temperature at a fuel flow rate of 19kg/hr (39% power of 4" screw).

The first batch introduced limestone in a similar pulsed fashion to test 2 to achieve a Calcium: Sulphur (Ca:S) ratio of 1:3. This was performed for 20 minutes. The second batch was a repeat of the first batch.

The third batch introduced limestone at 40% that of coal for 20 minutes, which was then repeated in batch four.

The fifth batch was the same as batch one and two to test the response of the bed, however the weight of the material of the bed at this point had overcome the primary air and thus the test had to end.

3.5.3 Premixed Tests

After running the previous methods of test, where the introduction of limestone was maintained by manually turning a screw feeder on and off for set amounts of time, it was decided that an alternative method was needed. The previous tests while offering insights to desulphurisation of the coals and breakthrough curves was not accurate enough for evaluating the desulphurisation propensity of limestone with the Pakistani coals.

When running the tests the screw feeder would be turned on thus allowing limestone to enter the bed with the fuel. However, the Ca:S ratio was constantly changing and therefore, a constant and unknown variable. Initially the Ca:S would increase until the screw feeder with limestone was stopped as the bed was loaded. The ratio of Ca:S would not remain constant as the coal was still entering the bed therefore, the Sulphur value was changing and hence the Ca:S ratio was changing.

As a result, it was decided that the tests following the initial work should use fuel which had limestone blended into it. The time the test went on for each batch would be controlled by simply weighing out the fuel beforehand and the ratio would also be controlled by changing the total mass of limestone in the fuel mix.

3.5.3.1 Test 5

In this test coal G was pre-weighed into 25kg batches with different weights of limestone. Batches of coal and limestone were mixed beforehand at (S:Ca molar) ratios 1:0, 1:2, 1:3.5 and 1:4. These ratios were chosen to look at the effect of using conventional industry used ratios and testing beyond industry practiced limits.

Throughout this test the fuel flow rate was modified between batches in order to maintain the thermal input of the bed as limestone required heat energy to react fully as well as maintaining good combustion within the bed. As the ratio of Ca:S increased, the fuel flow rate needed increasing as the total fuel input decreased with increasing limestone content.

3.5.3.2 Test 6

This test repeated the work done in test 5 however, coal A was used to evaluate the differences between the different coals at the same premixed Ca:S ratios.

The same ratios were used and the same method of entering the batches were adopted i.e. pre-weighing out the material, blending and then feeding the batches in premixed whilst altering operational parameters to continue good combustion etc.

3.5.4 Temperature Range Tests (Test 7 & 8)

Whilst during other tests the temperatures of the bed alter over time and required alterations in fuel input, the change in emissions could not be specifically attributed to bed temperature. Therefore, in these tests bed temperatures were altered through changing fuel flows in order to evaluate the desulphurisation effect of the limestone with varied bed temperature.

Coal I was used during this test; therefore, the initial baseline work was completed in accordance with the previous tests.

The coal was premixed with limestone and then introduced at a Ca:S ratio of 1:3. The fuel flow was altered in order to hold the bed temperature at different ranges i.e. 750-800°C, 800-850°C, 850-900°C and 900-950°C.

Test 8 was a repeat of test 7.

3.5.5 Particle Size Tests (Test 9 & 10)

When 1kg samples of the limestone were sieved to find particle distribution it was found that 19% of the limestone on average had a particle size between 0-2.00mm, on average 81% had a particle size between 2.00-2.8mm and on average 4.1% had a particle size between 2.8-5.6mm. The limestone was sieved to separate these ranges to ensure there were several kg of each available for the planned tests.

Coal I was used for the particle size tests. Coal I had a particle size range of 10-20mm and was mixed into the three limestone particle ranges.

For these tests a batch containing a mix of coal and limestone whish had not been sifted i.e. standard limestone as used in all other tests was combined to produce a batch with a Ca:S ratio of 1:3.

Following this batch were three others made up to a Ca:S ratio of 1:3 as well but using the different fractions of limestone named in the particle distribution work previously. The bed temperature was maintained and no other variable was changed, one batch followed another and the effect on the SO_2 emissions were measured as the particle range altered.

3.5.6 Biomass Co-firing Tests

To evaluate the effect biomass has upon the desulphurisation propensity of sub-bituminous coals, different ratios of coal to biomass were tested using different coals and ratios whilst monitoring the SO_2 emissions in the flue.

Wood pellets were used as the biomass of choice for co-firing with coal J, B and D. Firstly, wood was shown in the XRF analysis performed in the fuel characterisation to contain the highest concentration of Ca and Mg in the ash. These are alkali species associated with sulphur retention as previously described and therefore, wood pellets offer the greatest reaction potential to retain sulphur within the bed and thus desulphurise the flue gas output. Secondly, white wood had a similar calorific value to the coals used. As Figure 3-11 shows, the theoretical thermal output was calculated of wood pellets and the array of coals over varying blends. The average thermal output of these was 200-204 kW which was the target output. This made operating the flows and maintaining bed temperature easier to control with ratio changes and thus limiting the impact of fuel changing and focus the study on ash reaction as the retention mechanism for desulphurisation.

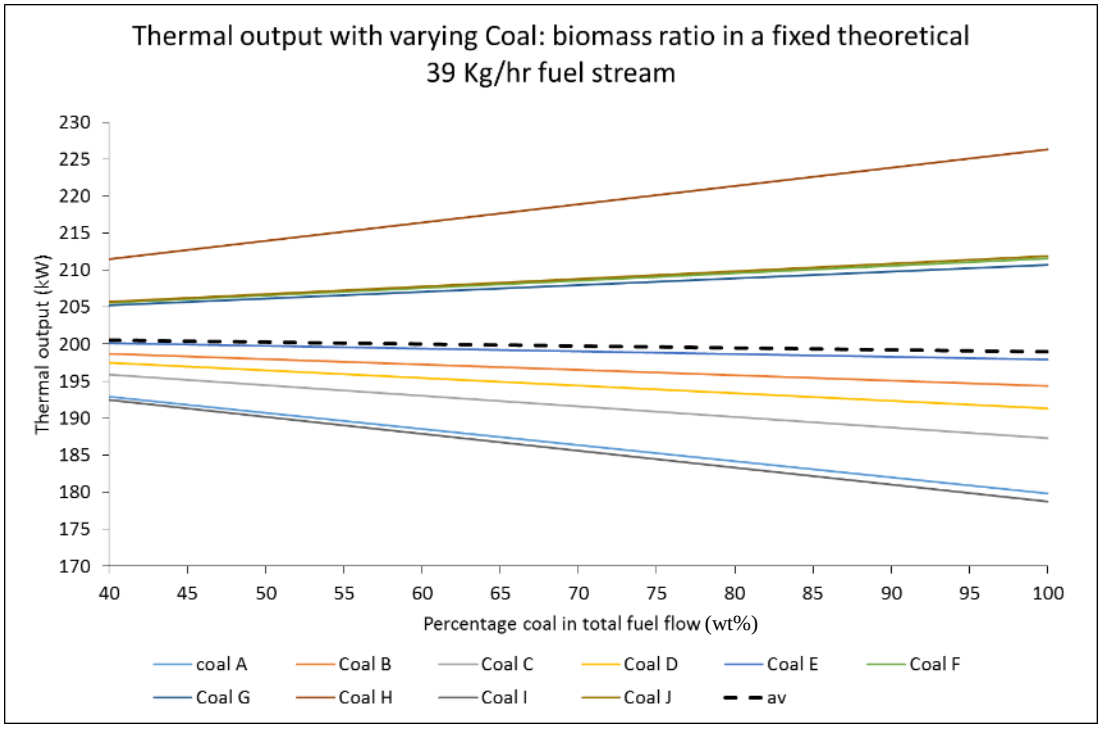

Figure 3-11 Thermal output with varying biomass: coal blends

3.5.6.1 Test 11

Coal J was used in this test and the baseline test was performed in accordance with previous tests.

Following the baseline test, batches of premixed coal and biomass (white wood pellet) were weighed out to produce batches with coal to biomass ratios of 7:3, 1:1, 3:2, 2:3 and 4:1. These were fed into the bed and the bed temperature was maintained by slightly altering the fuel flow rate.

3.5.6.2 Test 12

Coal B was used in this test and therefore, the baseline test was performed in accordance with previous tests.

Following the baseline test, batches of premixed coal and biomass (white wood pellet) were weighed out to produce batches with coal to biomass ratios of 7:3, 1:1, 3:2, 2:3 and 4:1. These were fed into the bed and the bed temperature was maintained by slightly altering the fuel flow rate.

3.5.6.3 Test 13

Coal D was used in this test and therefore, the baseline test was performed in accordance with previous tests.

Following the baseline test, batches of premixed coal and biomass (white wood pellet) were weighed out to produce batches with coal to biomass ratios of 7:3, 1:1, 3:2, 2:3 and 4:1. These were fed into the bed and the bed temperature was maintained by slightly altering the fuel flow rate.

3.6 Modification/Re-design Phase

During the first series of testing it was decided that an investigation into disrupted air via a modified distribution would be undertaken. In order to do this a section of the air distribution plate was allowed to leak a proportion of the primary air under the bed and created a non-uniform airflow to the bed altering fluidisation with non-uniform sir distribution could be potentially encountered in any industrial scale FBC.

However, after the testing was finished and the rig was taken offline for more extensive servicing it was found that the previous 40+ years of operations had degraded some parts of the rig beyond repair. Specifically, the combustion chamber of the rig had degraded. This included the air distribution plate, the refractory lining and the casing/insulation around areas which had not been previously refractory lined.

3.6.1 Rig Modifications

3.6.1.1 Air Distribution Plate

The previous air distribution plate was designed to allow leakage of air through alternative openings which diverted air away from the bubble caps. This resulted in an uneven air distribution and thus looked at the effects of the air distribution within a series of tests.

The new air distribution plate was designed to supply an even in flux of air underneath the sand bed. The design of the plate and its bubble caps was fundamental to the fluidisation of the bed material and for investigating the differences in FBC agglomeration potentials.

In order to make design choices based on the expected air flows, total bed mass, area of bed, number of nozzles etc. it was necessary to complete the following steps and calculation:

3.6.1.2 Pressure Drop Criteria (Bed and Plate)

The bed pressure drop for these series of calculation is shown in Equation 3-1:

$$\Delta P_{bed} = g \times \rho_b \times L_b \qquad \text{Equation 3-1} \qquad \text{(Yang, 2003)}$$

Where g is gravity (9.81 m/s), ρ_b is the density of bed material (kg/m^3) and L_b is depth of the bed (m).

Experimental data shown by Yang (2003), found that whilst investigating the effect of pressure drop across an air distributor (ΔP_{grid}) and air nozzle design the criteria in Equation 3-2 and Equation 3-3 are applicable for differently orientated flows through a plate. Equation 3-4's rule applies for full scale operations, as the pressure difference should not be less than 2500 Pa in order to design a stable system.

For an upwardly and laterally directed flow

$$\Delta P_{grid} \geq 0.3\Delta P_{bed} \qquad \text{Equation 3-2}$$

For a downwardly directed flow

$$\Delta P_{grid} \geq 0.1\Delta P_{grid} \qquad \text{Equation 3-3}$$

(Yang, 2003)

$$\Delta P_{grid} \geq 2500Pa \qquad \text{Equation 3-4}$$

The gas velocity of primary air (U_h) is calculated using the pressure drop across the air distributor grid and thus taking into account the effect of restricting flow. This value underpins further calculation and gives the foundation value required to make choices such as number plate holes and nozzle exit size.

$$U_h = C_d \sqrt{\frac{2\Delta P_{grid}}{\rho_g, h}} \qquad \text{Equation 3-5} \qquad \text{(Yang, 2003)}$$

Where U_h is gas velocity through the grid (m/s), $\rho_{g,h}$ is the density of air entering via an air box at a specific temperatures to each scenario (kg/m^3) and C_d is the discharge coefficient. A reasonable range for this coefficient is between 0.4-0.77 (Yang, 2003; Geldart and Rhodes, 1986).

In order to calculate the number of holes needed in the distribution plate it is also necessary to calculate the volumetric gas flow rate under the plate in the plenum/wind box section. This was done using the equation in Equation 3-6:

$$Q = U_{sup} \times \frac{\pi D^2}{4} \qquad \text{Equation 3-6} \qquad \text{(Yang, 2003)}$$

Where U_{sup} is the superficial gas velocity (U_s=Q/A) (m/s), D^2 is the bed diameter (m) and Q is the volumetric flow rate (m^3/s).

The number of holes in the air distribution plate was then calculated by the equation in Equation 3-7:

$$N = \left(\frac{Q}{U_h}\right) \times \left(\frac{1}{\left(\frac{\pi \times d_h^2}{4}\right)}\right) \qquad \text{Equation 3-7} \qquad \text{(Yang, 2003)}$$

Where d_h is the grid hole diameter (m) and N is number of holes. The hole diameters were taken as a minimum of 7 times larger than the average bed particle size (Graham, 2016)

The density of holes required in an area (m2) was then determined using the equation in Equation 3-8:

$$N_j = \frac{N}{\left(\frac{\pi}{4}\right) \times D^2} \qquad \text{Equation 3-8} \qquad \text{(Yang, 2003)}$$

Where N_j is hole density per m^2.

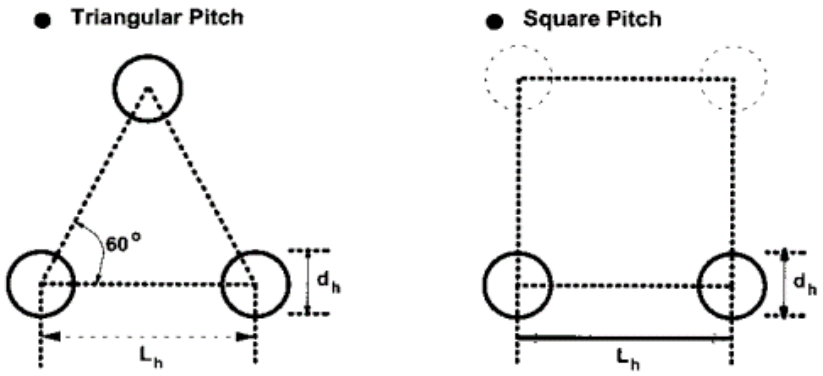

Figure 3-12 Shape choice for hole pitch (Yang, 2003)

There are an almost infinite number of design variations which could potentially be applied to the air distributors in order to achieve better outcomes depending on what the system is designed to achieve. One significant design choice is how to place the bubble caps/stand pipes next to one another on the plate. Figure 3-12 shows two options for

$$L_h = \frac{1}{\sqrt{N_d sin60^\circ}}$$ Equation 3-9

(Yang, 2003)

$$L_h = \frac{1}{\sqrt{N_d}}$$ Equation 3-10

equidistant pitches. The different pitches are used based on the design circumstance of the boiler and hole density per m^2. The triangular pitch offers less opportunity for "dead zones" between holes by achieving higher hole density. However, the square pitch is more suitable for a lot of boiler design as well as reducing dead zone opportunities at the wall of the boiler. The hole pitch for a square and a triangular pitch can be, and was determined using the equations in Equation 3-9 and Equation 3-10. The different aspects of the distribution plate were calculated based on data recorded from previous tests as well as referring to professional advice. The square pitch design was implemented into the air distribution plates based on the advice and advantages of the square pitch design above with a total of 30 bubble caps.

Where L_h is grid hole pitch and N_d number of holes' density (holes/m^2).

A design was assembled using the "Solidworks" CAD package as seen in Figure 3-13. This allowed for the visual checking and communication of ideas between the clients and the contractors. The air distribution arrangement shown in Figure 3-13 is the finalised version before manufacturing commenced and was the result of numerous modifications and changes to the plate as a consequence of other modifications being fitted to the rig. The objective of all modifications, including the air distribution plate, was to improve operational performance and allow for a more robust system in which future test plans could be successfully enacted.

Once the new plate, new burners etc. were installed the system rig in its entirety was checked by H&S representative with the assistance of the operators before initial recommissioning work could take place.

Other modifications to the experimental rig include the addition of a $50kW_{Thermal}$ over bed gas burner. This was placed 0.5m above the bed at a 45°angle in order to heat the top of the bed and freeboard region during pre-heat. By having this burner in place the pre-heat time for each test was reduced as well as ensuring the upper regions of the furnace were heated sufficiently for expansion and a uniform temperature throughout the furnace.

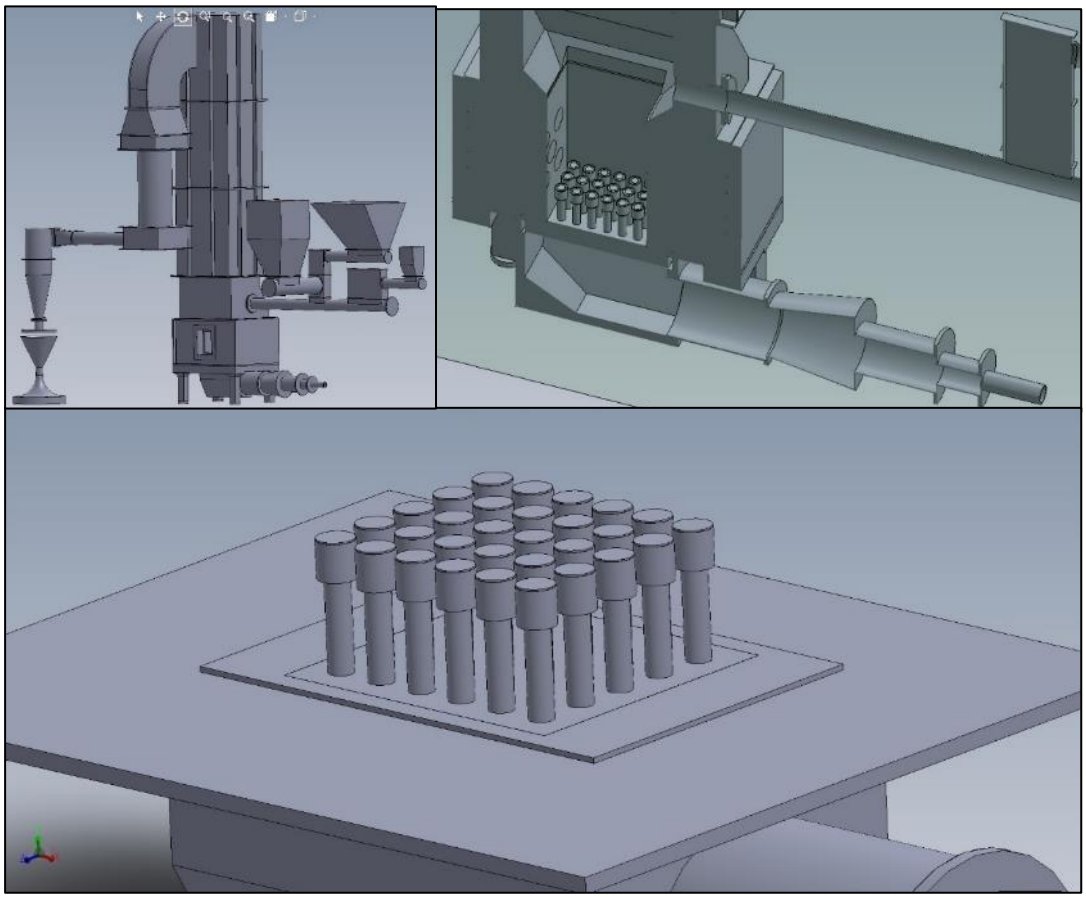

Figure 3-13 Solidworks imagery of the fluidised bed (top left), cut away of the main body of the rig (top right) and an expanded image of the purposed distribution plate layout (bottom)

A new under-bed gas burner (85kW) was installed which gave greater control on air flows and ramp rates. The burner was an off the shelf unit with high gas velocity capability better suited to penetrating the cold sand bed.

As part of the over bed burner installation the refractory lining around the bed and lower freeboard regions was relined. This was to create a more even area i.e. $0.5m^3$ in which the new plate design would create less dead zone around the outer edge of the distribution plate. The new refractory also ensured better insulation which in turn meant that the fuel flow required to heat the bed to 850°C and sustain stable combustion was less. The new refractory created a larger thermal mass to ensure all fuel particles combusted in and above the bed.

All the work previously described was necessary to produce a system that was robust and capable of operating under the conditions required for the later investigations.

3.6.2 Cold Re-Commissioning

As a result of the redesign and implementation of new equipment and parts across the rig, it was necessary to familiarise, calibrate and recommission the entire rig and its system. This included;

- Construction, testing, calibration and validation of the new analyser setup and equipment.
- Testing and safety checking of the new electrical power system to ensure the use and operation of electrical aspects of the rig were both safe to use and functioned as intended e.g. operation of screw feeders with variable fuel flow rates.
- Calibration and operational stress test of the motors and screw feeder assembly on all function screw feeder/fuel inlet systems.
- Operating, familiarising, and successfully operating the rig using newly installed burners and burner control modules.
- Familiarising and testing the air systems e.g. operating under "normal" conditions using new pipe network with existing fans in order to achieve a successfully fluidised bed.
- A number of smaller changes were added throughout the down period of the rig and as a result the operators took a systematic approach when commissioning the rig to evaluate the effect of these changes and to adapt to the new features.
- Testing of the new burners and optimising the system.

3.6.3 Hot Commissioning

Once the cold commissioning stage had been completed and post evaluation of the results reinforced the operator's justification to proceed, the hot commissioning stage could commence.

Initially the burners were operated without the presence of the bed in order to evaluate heating potential of the rig, with focus on the over bed burner and top of the freeboard temperatures. Figure 3-14 shows the temperature data recorded at points of interest during the test. Whilst testing the capabilities of the new burners was a priority, a secondary objective was to heat the new refractory lining. The operators had been advised to heat the system to 200-300°C, then 500-600°C and finally ≥800°C and hold at each stage to cure the new rig lining. This presented an opportunity to analyse the accuracy and ability to change the heat generated by the burners and demonstrate the ease in control.

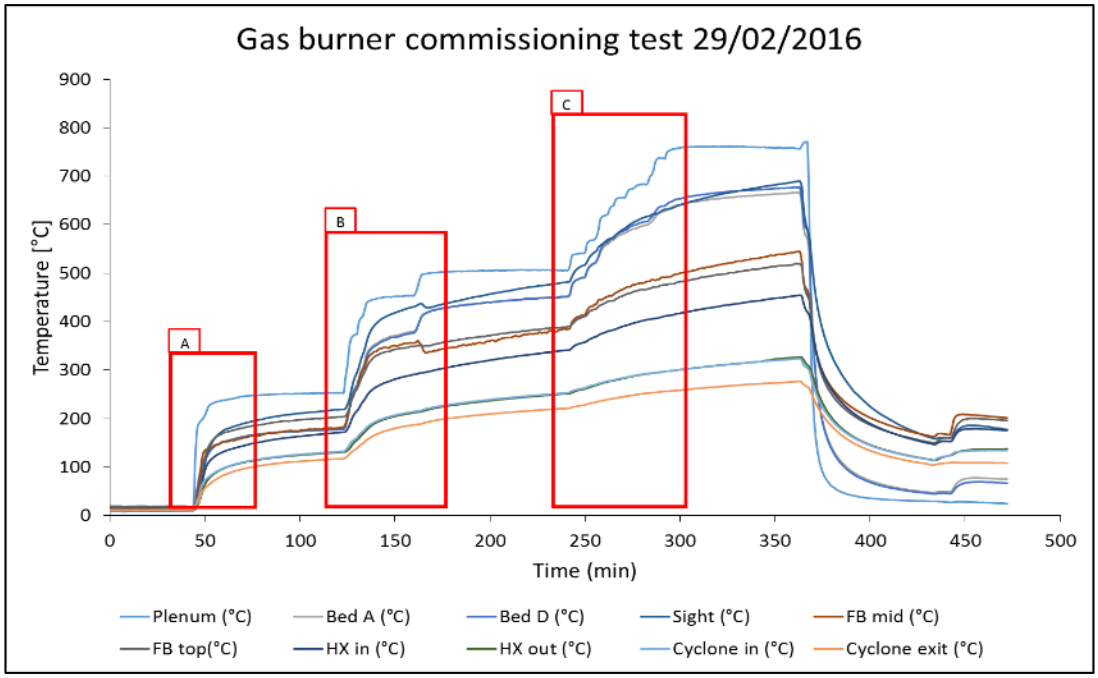

Figure 3-14 Hot commissioning test of new gas burner(s) temperature profiles

In Figure 3-14, there are three marked regions; A, B and C. These represent the end of waiting periods in which the heating was left to balance across the rig to cure the refractory lining. However, more significantly, in each of the marked zones, C for instance, there are a number of incremental increasing steps in the temperature values. These are a direct result of opening the control valves to each burner by half a turn, (this equates to a flow value but is not equal in value for each turn). The work shown here allowed operators to demonstrate the safe operation of the burners as well as giving a reference to what flows would allow for a successful heating process of the rig and bed. Additionally, the data showed that the top of the rig (FB mid and FB top) could be heated to a desirable temperature range in a much shorter time frame when compared to the previous rig/burner set up.

Following this initial test, it was then possible to run the rig with a bed and in a manner, that would be expected during a test using solid fuels. However, before full testing was conducted it was necessary to run the rig as a hot commissioning test but with solid fuel to evaluate performance of the rig and give indicators as to how a typical solid fuel test will operate and the values associated with good fluidisation and combustion.

Figure 3-15 shows the resulting temperature and differential bed pressure values recorded during testing. The period in section A of Figure 3-15 demonstrates the pre-heating of the combustion chamber. As the plenum temperature illustrates, the temperature fluctuated over time. This was a result of alterations made to primary air under the bed and to the under-bed burner. Operational variables were made to the exhaust fan to evaluate the

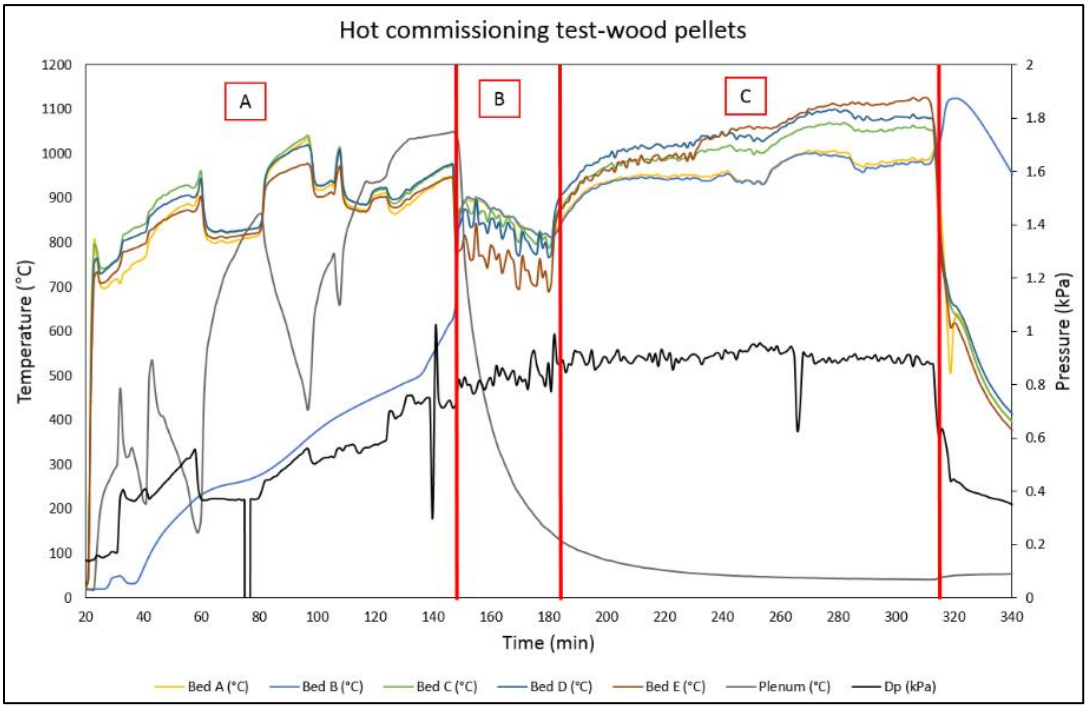

Figure 3-15 Hot commissioning test with solid fuel (white wood pellets)

impact on negative pressure in the freeboard section and burner blow outs. These changes were to find the best operating parameters during normal testing

Section B illustrates a period in which the under-bed air flows were altered and whilst the gas burners were extinguished. In this period air flows were altered as air was no longer directed through the gas burners, instead the air was directed through a single entrance under the bed as "primary air". The screw feeders were started in this period and the system was allowed to stabilise with the new air flow and the progressive introduction of wood pellets.

Section C is a period in which the solid fuel was the primary source of energy in the system and stable operation was sustained as demonstrated by the bed differential pressure. This was the key indicator for good combustion alongside the bed and above bed temperatures. Throughout this time fuel flows were altered and operating parameters were once again finely tuned to achieve the best operating conditions. Then the system was pushed beyond normal conditions to ensure the new air distribution plate and refractory lining could handle excess heat and abnormal air flows likely to occur during agglomeration within the bed.

All cold and hot commissioning proved to the operators the capabilities and limitations of the rig and how best to run the tests.

3.7 Biomass & Non-Uniform Air Distributor Test Methodology

3.7.1 Uniform Air Test Schedule

As described in the commissioning and recommissioning previously, the rig has undergone changes in design in order to facilitate the requirements for biomass testing with varied air distribution design. The rig operational changes and process choices will be described in the following sections. However, the overall thermal rating of the rig was decreased from 350kW to 200-220 KW. As part of the maintenance and redesign work, the refractory within the bed area was replaced. Additionally, the walls and structure around the bed was modified brining new materials to the rig. No alteration was made to the internal dimensions of the bed however, a greater thermal mass and more uniform air distributor resulted in greater bed temperatures at lower fuel flows (20kg/hr new flow compared to 35kg/hr for old system). The operation of fluidising and maintaining the bed remained the same and bed temperatures of 800-950 °C were maintained.

3.7.1.1 Operational Changes

With the new uniform air distribution plate a higher air flow of 9000 L/min is required to fluidise the bed completely. This was evenly distributed through the 30 bubble caps.

The bed depth in the new setup was 7.5 to 8 inches. The new air distributor plate used slightly shorter more effective bubble caps resulting in greater penetration of air downwards towards the base plate. This resulted in a greater volume of bed material being agitated and fluidised. With a fuel flow of 20-22 kg/hr, the combustion of biomass has been found to maintain an average temperature of ≥850 °C.

Throughout the tests period the analysers were modified and added to. The previous system yielded good measurements of a reliable and accurate nature, however, with sight to future work new gas analysers were installed. The first (ZKJ model chemiluminescence) measured NO (0-5000 ppm), SO_2 (0-5000 vol. %), CO (0-2000 ppm) and CO_2 (0-100 vol. %). The second, ZRE NDIR type infrared gas analyser, analysed NO (0-2000 ppm), SO_2 (0-2000 ppm), CO_2 (0-20 vol. %) CO (0-1000 ppm) and O_2 (0-25 vol. %).

The analysers were replaced or upgraded to ensure the ranges were appropriate for the flue gases being emitted during combustion. The SO_2 emissions produced from biomass combustion was within the range of the initial analysers, however, the upgrade increased the range necessary for the high sulphur coals. Furthermore, the new analysers used

alternative technology. This included the new chemiluminescence in the NO devices which gave much better readings with a more suitable measuring range.

Modifications were made to transducers and thermocouples around the rig and thus the calculations etc. had to be updated and improved. New pressure transducers allowed for more measurements and a more accurate real-time calculation of the bed pressure differential. Values such as these were displayed through a series of graphs and tabs and allowed the operators to better perform tests by replicating variables more reliably and allowing for quicker reactions to system/bed changes.

3.7.2 Biomass Test Schedule

3.7.2.1 Uniform Air Distributor

Every test followed a pre-heat sequence which was in accordance with the instructions laid out in the start-up operations (SOP) document. The pre-heating of the rig included the use of both under-bed and over bed burners. Pre-heat was accomplished when both the average bed temperature had reached ≥650 °C and more importantly when a pressure difference had been measured across the bed. This signified that the bed had begun and then fully fluidised and was in a state in which solid fuel could be fed. Figure 3-16 shows results from a commissioning test in which the system was pre-heated on gas and solid fuel was fed into the bed to achieve typical operational data. The area highlighted as A, is the point in which the onset of fluidisation occurs in the bed. The average bed

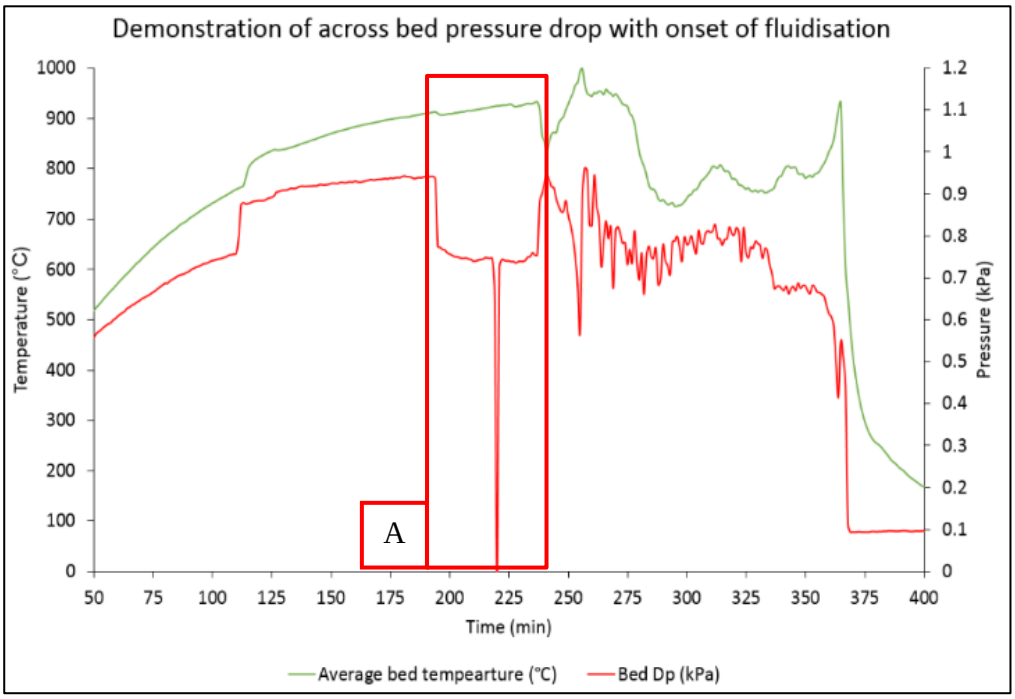

Figure 3-16 Average bed temperature and across bed pressure with increasing temperature during pre-heat and subsequent commissioning test

temperature reaches approx. 850 °C (note that the bed was not uniformly 850 °C, before mixing bottom of the bed was 800 °C, top 900 °C and centre 500 °C), the across bed pressure drops suddenly by 0.3 kPa. This is a result of the sand beds density reducing with increased temperate, hence the passage of air is greater with the reduction in resistance generated by the static bed. Once these changes had been seen in the bed, then the fluidised bed was ready for solid fuel input and for the test to commence.

Each of the biomasses analysed and described in the fuel characterisation Chapter (white wood, Miscanthus, oats, straw and peanut pellets) were to be tested in the fluidised bed. Once the system and bed was pre-heated sufficiently i.e. as to enable combustion of fuel particles, the fuel was fed into the bed. With the uniform air distributor plate in place and refractory, the fuel flow was between 20-22 kg/hr depending on the fuels calorific values. The fuel flow was mediated in order to maintain an internal bed temperature range of 800-950 °C. Above the bed the temperature was higher than this ranging between 850-1000 °C with the volatile flame lifting from the bed and into the lower freeboard.

Fuel was continuously fed and operated until the onset of defluidisation occurred in each test. Each fuel was repeated at least once. If a particular fuel presented a fast agglomeration propensity, then a repeat was conducted to validate the results and to attempt to elevate the agglomeration tendency and extend fluidisation and stable operations.

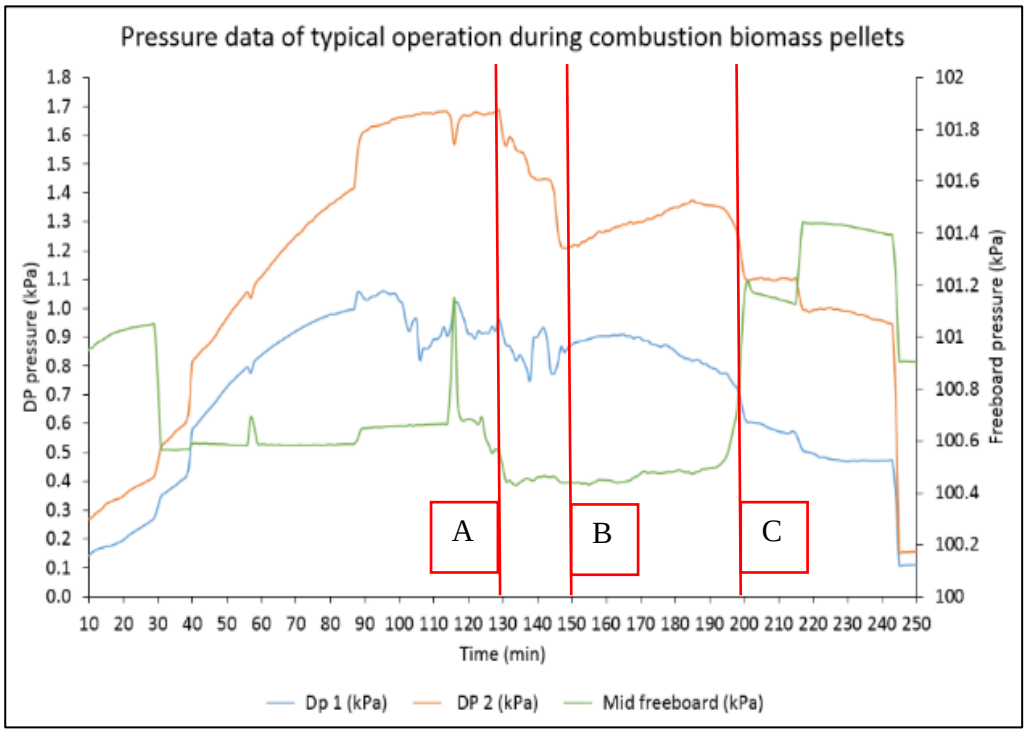

Figure 3-17 Example pressure data recorded during the combustion of biomass in a pilot scale fluidised bed combustor unit

Defluidisation and the end of the test was determined by two parameters. Figure 3-17 shows the pressure readouts recorded during the combustion of straw. The time period up to the line marked A is the pre-heat sequence. Between line A and B the gas burners are turned off and the solid fuel is screw fed into the bed. Additionally, the primary airflows are altered and redirected to continue fluidisation of the bed whilst being directed through an under-bed inlet pipe rather than through the under-bed gas burner. At line B the system and air flows are set up and the Dp measurements of 1.2 kPa is ideal and at the time the bed could be seen to be visibly bubbling through an observation window. As the bed agglomerates and the mixing of the bed decreases as a result the Dp1 (across bed) pressure decreases. The reason for the drop is a result of the air flow through the bed beginning to channel and find paths caused by the presence of agglomerated structures in the bed. As the agglomerates increase in number and volume the channelling increases and thus the Dp value continues to decrease. At the time of line C (200 minutes) the bed defluidise. The bed slumps and the air is flowing through fixed channels and primarily around the bed instead of through it. A sharp increase in the midfreeboard pressure represents an increase in suction as the air suddenly moves through the distributor plate and around the bed in a less resisting form than when the bed was fluidised and particles in the bed were mobile.

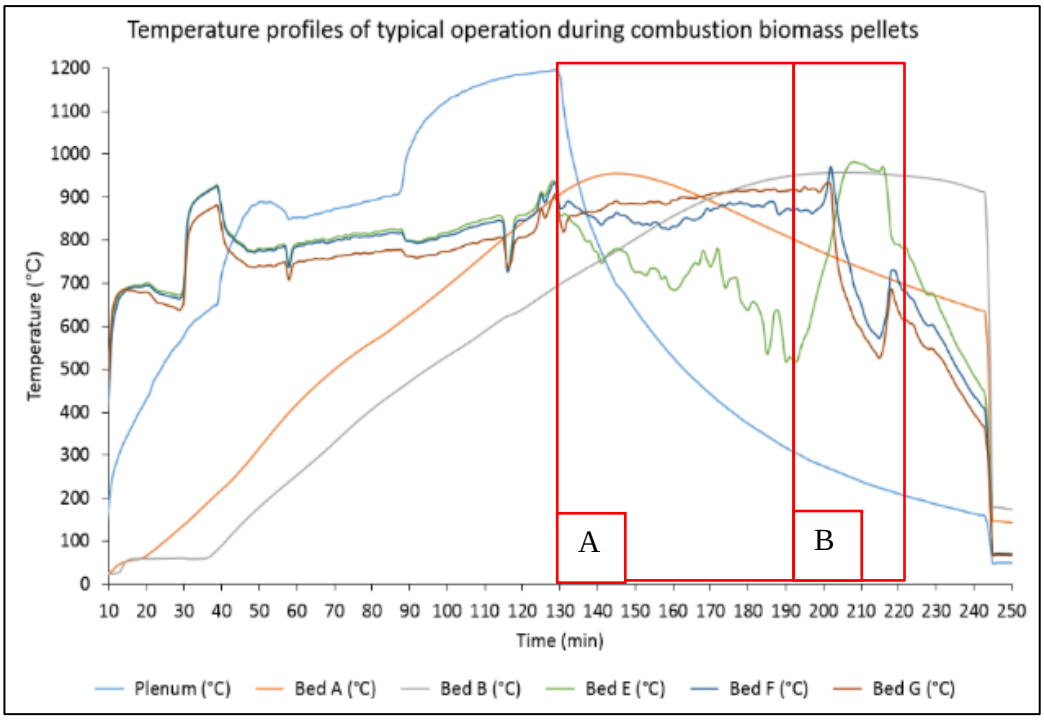

Figure 3-18 Example temperature profile data recorded during the combustion of biomass in a pilot scale fluidised bed combustor unit

The second indicator of defluidisation and the onset of agglomerates in the bed is indicated by the temperature readouts as shown in Figure 3-18. During the period in range A, the temperatures in the top of the bed remains constant (bed F and bed G). However, the temperature in the bed, (bed E), slowly reduces in temperature as the bed is mixing less and less and as a result the fuel isn't penetrating as deep. Hence the temperature in these regions decreases. As shown in range B, the temperature across the top of the bed suddenly decreases and the point which would have represented in the bed sharply increases. This is due to the bed slumping and losing depth/height. The top of the bed is now represented by bed E and as such the flame is present there giving the increased temperature reading. Following this, however, the poor air flow and poor combustion conditions result in an overall bed temperature decrease as fuel burns less efficiently.

Once the bed defluidised in each test or if the end of the work day was achieved (allowing a test period of 10 hours max), the fuel flow was stopped and the air flows were reduced to preserve the bed in its state at the time of agglomeration/test end. Samples were then taken from the bed after a cooling period of 24 hours. This included bed samples, agglomerate samples and fly ash sampling for analysis.

3.7.2.2 Non-Uniform Air Distributor

The aim of the non-uniform tests was to test the effect of the air distribution system on the bed and formation of agglomerate formation. This could be through erosion, agglomerate interference or corrosion of the bubble caps for instance. Each of the biomasses were run as in the previous uniform tests. However, before doing so the rig underwent modifications.

Figure 3-19 shows representations of the plates. The left image shows the uniform air distributor plate used for previous tests. This contained 30 evenly spaced bubble caps with diameters of 40 mm spaced 70 mm apart in each direction. The height of the caps was 100 mm from base of the plate to the top of the cap. This design was chosen to produce higher velocities (theoretical air velocities 0.74 m^3/s at 850 °C) through the bed/bubble caps over a larger area. This was to ensure even lift and bubble formation in the bed and thus more ideal fluidisation/combustion.

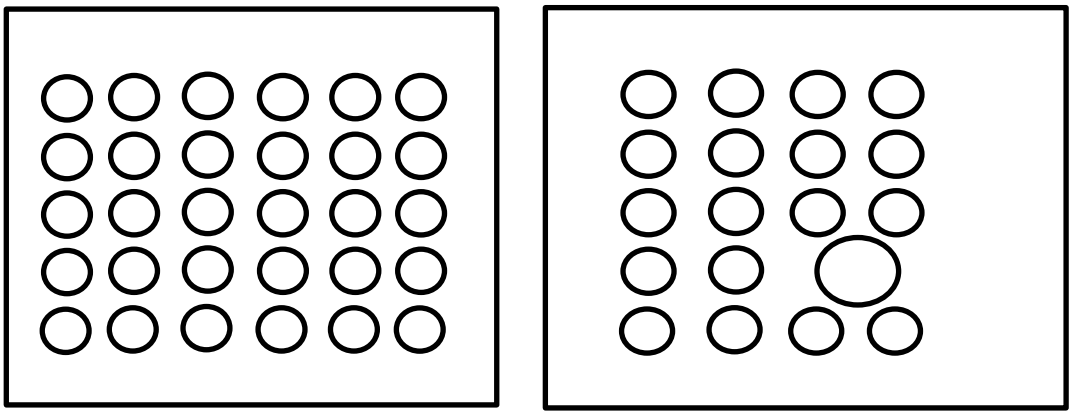

Figure 3-19 Air distribution plate layout; Left plate showing the uniform distribution layout containing 30 bubble caps, right layout using 18 caps and an ash chute

The right Image of Figure 3-19 shows the layout of the non-uniform air distributor plate. There are less bubble caps (18) with slightly larger diameters of 50 mm spaced 40 mm apart from each other in each direction. Furthermore, there is an ash chute located to one side of the plate. This was implemented to remove excess ash/bed material during testing. Around the perimeter of the ash chute is a gap of >1.5 mm giving a passage for air.

The intention of this design was three-fold; firstly, the larger lesser number of bubble caps would produce a different velocity through the bed, secondly the bubble caps and thus air flow is situated closer to the centre of the rig generating dead zones or areas of less vigorous mixing around the perimeter of the bed and corners and, thirdly the air leakage around the chute. The air flow velocity through the bed is calculated as 0.02 m^3/s because of the leakage point. These three factors would allow for the study to look at wall side agglomeration formation, the effect of a leakage point on agglomeration formation and

defluidisation time and to test the limits of this type of system in its ability to continue combustion of biomass and maintaining a good bed temperature range (800-950 °C).

Each fuel was tested individually. It was found that a flow rate closer to 35 kg/hr was required for this system layout as was found with the coal tests.

As with the uniform air tests there was a standard set of operational parameters that when exceeded, denoted the onset or occurrence of defluidisation in the bed by agglomerates. Whilst other aspects of the fuels could theoretically defluidise the bed i.e. total bed mass, all tests resulted in defluidisation before the total mass of the bed outweighed the inlet air. However, because of the difference in air flows and fluidisation in the bed caused by the non-uniform distribution a baseline data set was collected to compare the impacts of tests variables against.

Figure 3-20 shows temperature data recorded during the operation of a test in which biomass pellets were combusted with the non-uniform plate installed. Point A is the end of the pre-heat sequence, followed by a period of stable combustion and temperature recordings. At point B the temperature has fluctuated by over 400 °C. After the trough of point B there is a stable period but with slowly increasing bed temperatures until the bed temperatures fluctuates dramatically (800°C difference). This indicates the fuel is not combusting equally across the bed, only air cooling around the probe could cause such a significantly speedy temperature change. This is likely a result of slugging of the bed or

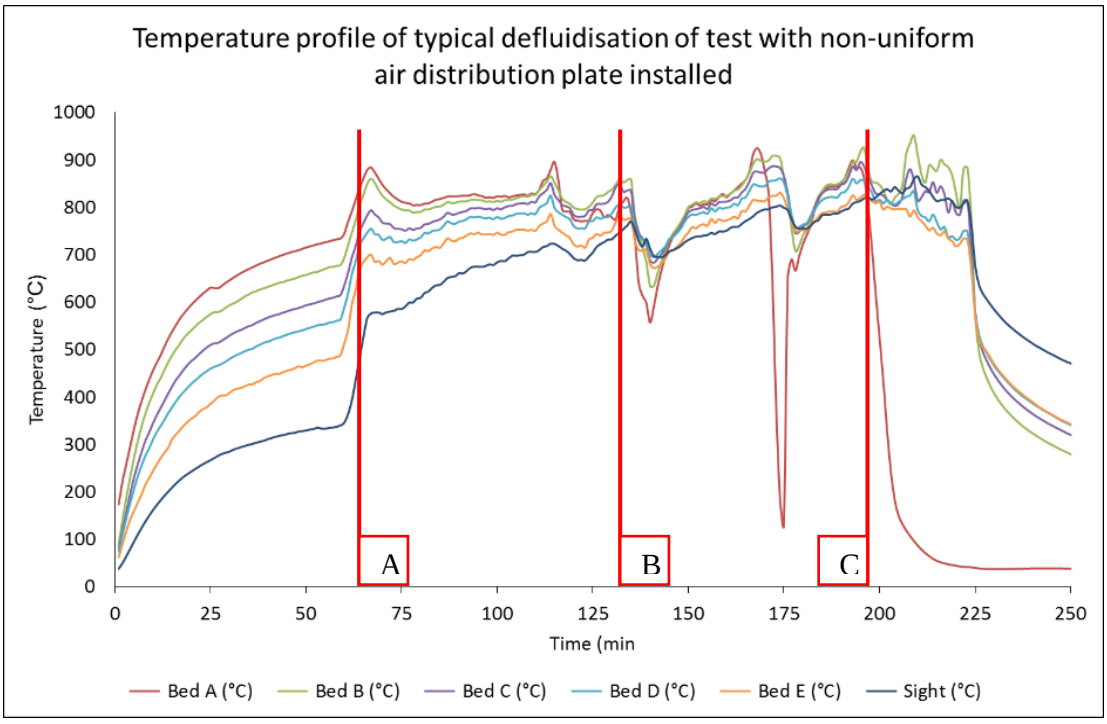

Figure 3-20 Example of a temperature profile with a defluidising system with the non-uniform air distribution plate installed

channelling. After point C the all temperatures fluctuate and the bottom thermocouple indicates bed cooling to 50 °C. This illustrates defluidisation and the lack of any bed mixing as fuel is no longer moving through the bed and combusting in isolated locations. The extreme temperature changes through this example demonstrates the effect of non-uniform air distribution. The formation of agglomerates doesn't simply result in poor mixing but, early in in the defluidisation onset, lead to the poor if any fuel mixing. Additionally, the poor air mixing results in the bed slugging and channelling faster than with the uniform air distributor.

Figure 3-21 is an example of pressure data to be expected during the defluidisation of the bed. Point A is the end of pre-heat and swap to solid fuel input. From point A to B the plenum pressure increases and midfreeboard decreases. As the bed is agglomerating and degrading, the air flow through the bed is actually becoming less resistant and air is passing with greater ease. The reason being, as the bed gradually defluidise, the air is flowing out of the larger opening, which has the least resistance for air passage. As such the air moves through the bubbles caps progressively less. Hence the plenum pressure drops and the negative pressure in the midfreeboard becomes more positive as air is bypassing the caps and simply moving through the bed unrestricted. Between point B and C, bumps in the plenum are a result of a slugging bed as the bed redistributes across the

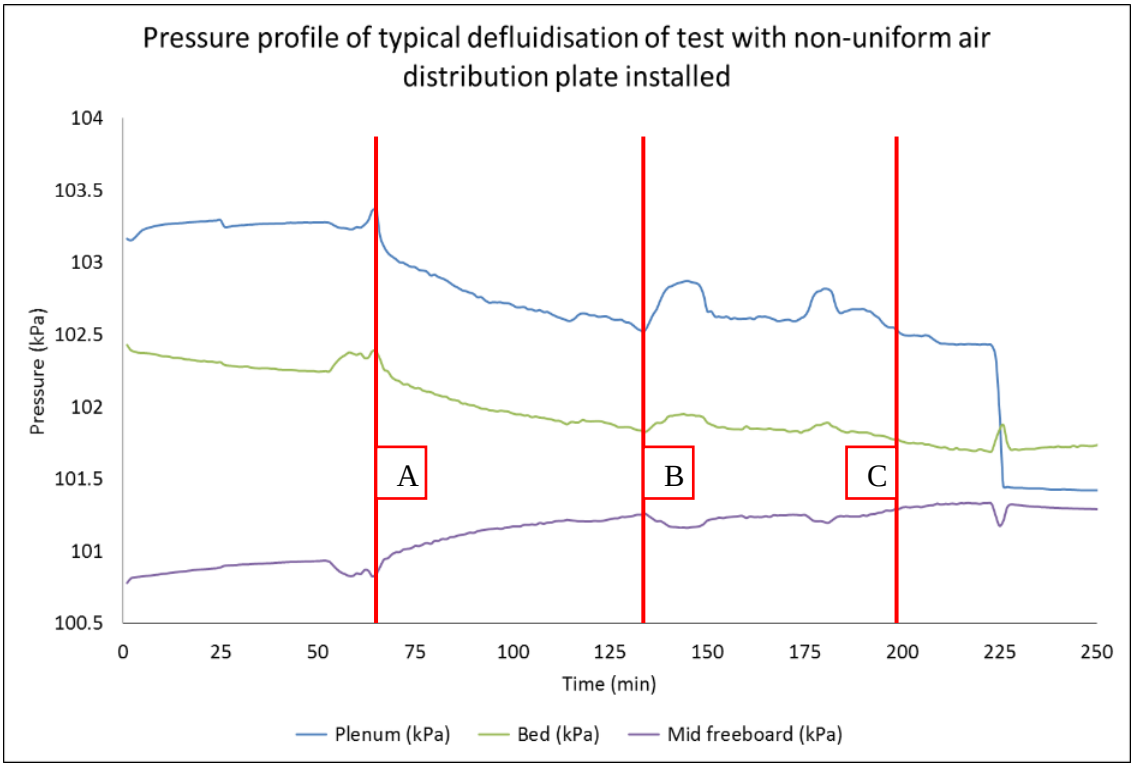

Figure 3-21 Example of pressure data with a defluidising system with the non-uniform air distribution plate installed

bed cross sectional area creating temporary resistance equally until the bed moves again unrestricting the leakage point.

During the non-uniform tests these are the traits that will identify degradation defluidisation of the bed.

4 Fuel Characterisation

Throughout this section extensive analysis was conducted on a range of coal and biomass fuels to be tested in the pilot scale rig. In order to understand the fundamental chemical and physical characteristics of the fuels it was necessary to use a wide variety of techniques which can then be used to help understand how the fuels were going to react in a combustion environment. Some of the fuels used were obtained as part of a collaborative project with Pakistan sponsored by the British Council INSPIRE programme. Other biomass fuels were obtained as representative fuels considered for use in UK power generation(Williams, 1978).

4.1 Coal

The Pakistani coals used in Chapter 6 are from an area in the northern Punjab area known as the "Salt Range". This area has a large coal field, containing approximately 8 billion tonnes of coal, which spans many kilometres. The different areas of the coal field are divided in the Western, Eastern, Central and Trans industrial Salt Range. Figure 4-1 shows the coal field and proposed power generation facility locations if the coal can be mined and utilised at an economically feasible level (Nimmo, 2016).

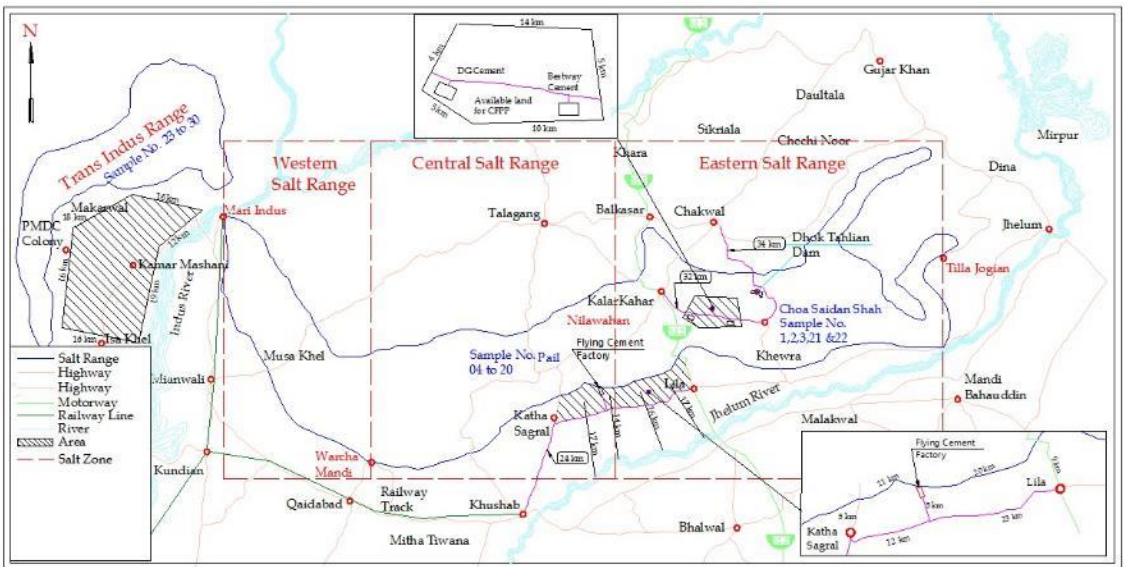

Figure 4-1 Map of coal field location and proposed power generation sites (Nimmo, 2016)

Coal has been extracted from 30 mines in the Salt Range in order to evaluate the quality of the coal and its combustion potential. The coal samples contain a mixture of sub bituminous and lignite coals which contain high concentrations of mineral matter, inorganics and organically bound sulphur. Work has been previously done by a partner Pakistani group as

part of the British Council grant (INSPIRE Grant No. 254), to identify the potential for these coals in terms of extraction. In this work the fuels were blended together into 10 batches. The batches were made up based on their geological locations and chemical compositions.

The analysis conducted on the coals within this work will use the same batches but with a focus towards the combustion potential and the agglomeration potential of those batches. Similar techniques were used on the fuels to achieve an independent perspective on the fuels chemistry. Figure 4-2 shows four examples of these coal batches and illustrates the physical differences in the batches. As the images show the coals look much more like stones or rubble than coals. This is due to their high mineral content and lower carbon content. Furthermore, the coal hasn't undergone any form of pre-treatment or cleaning and as such the fuel includes the earth debris from the mining process. This is intentional as the fuel isn't intended to be pre-treated at the time of this work and the combustion tests represent what the actual fuels in their current states would be.

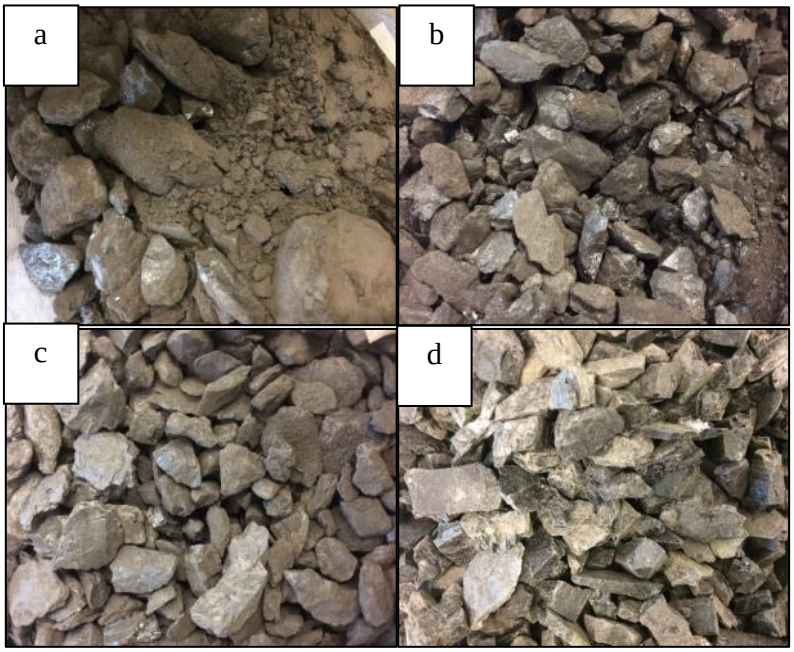

Figure 4-2 Examples of Coal batches; a) coal A, b) Coal D, c) Coal G and d) Coal J

The average particle size of the coal ranged between 10-20 mm which was sampled from a large bulk source and then refined through sieving.

4.2 Biomass

The biomass types used in Chapter 7 were selected to represents a variety of biomasses which could be utilised in a full scaled power generation facility. The variety of biomass includes white wood, oat process remnants, wheat straw, miscanthus and peanut shell pellets. These five biomasses are being investigated and/or used by a number of power generators.

Approximately 2 tonnes of each biomass pellets were sourced from a UK power plant. All analysis which has been conducted has been done as received. The biomass was then stored in large haulage satchels in a dried warehouse to maintain the pellets and limit any degradation due to weathering.

Figure 4-3 shows the different biomass pellets which have been used in a number of different tests. The average practice length is 5-15 mm with an average diameter of 4-5 mm. The pellets were formed through an extrusion process in which pneumatic pressure forced the biomass through a die, generating both heat and pressure, thus resulting in pellet formation. No binding agent has been used to form the pellets which has left some of the pellets frail and prone to collapsing however, there is enough sap and moisture in the raw fuels to give a reasonably stable short pellet.

Figure 4-3 Biomasses; a) wheat straw pellets , b) Miscanthus pellets , c) Peanut Pellets , d) Oats pellets , e) White wood pellets

4.3 Fuel Preparation

Both the coal and biomass was analysed and treated on an “as received” basis fuel i.e. moisture content was taken into consideration in calculations. The biomass and coal was received in different physical states, that being the biomass was in pellet form with a range of lengths and the coal was received partially crushed, but with varying degrees of particle size. Therefore, it was necessary to process the fuels to transform them into a state which could be analysed.

4.3.1 Homogenous Sample

Achieving a homogenous sample of solid material is, in terms of probability, impossible. No sample will ever be 100% homogenous and perfectly duplicate the result achieved by another sample from the same source material (Skoog et al., 2013). However, measures have been adopted that enable representative samples to be obtained of the original fuels and allow for comparisons with other samples of the same fuel. The biomass came in two one ton bags and each coal was received in two 100kg barrels. 10 kg of each fuel were taken from several locations from each of the fuels containers. This ensured that the 10kg sample did not simply represent one area of the fuel and thus averaged out the analytes content within the bulk fuel.

The 10 kg sample, within the lab environment, was then passed through a RT75 sample splitter. This randomly split the 10 kg sample to two 5 kg samples. This was repeated again leaving four random samples. One was then selected and it was this sample that the analysis has been performed on. By using the splitter and taking samples from numerous locations at every stage possible, the most homogenous samples obtained and the overall representation of the fuel were better achieved.

4.3.2 Size Reduction for Analysis

In order to reduce the coal to a uniform particle size it was necessary to use a mill. There was a choice between a disk mill and ball mill and it was decided while the disk mill was capable of achieving smaller particle size, the ball mills speed of processing to a particle size of approximately ≤100μm was more than satisfactory. Hence the coals were milled in a Retsch PM100 planetary ball mill. Using high centrifugal forces, a metal container spun the fuel and 10mm diameter balls occupying a third of the available volume crushed the coal particles.

Due to the physical and chemical make-up of biomass, milling the material was found to produce a sticky mat like material rather than reducing the particle size. This is due to the lignin, moisture and heat from the process combining to reshape the pellets rather than milling then. Therefore, a Retsch SM300 cutting mill was adopted to more effectively reduce the particle size. The process of using this shredded the pellets under a vacuum. The material was drawn through a grate ensuring particle sizes ≤150μm.

After the milling of the fuels, both fuels were then sieved using a series of progressively tighter woven sieves which separated the different particle size fractions. Particles collected and found to be ≤109μm were separated and saved for analysis where the other fractions were also saved but kept separate if needed for later processing.

By ensuring particle size was kept equal to the different fuels a level of "fairness" was brought to the analysis and elimination of this parameter as a variable was achieved. Therefore, any differences in fuel characteristic was due the individual fuels chemistry.

4.4 Fuel Characterisation

A number of analysis techniques were performed on the fuels in order to gauge limits of the fuel in terms of analytes type etc. which could interfere with other analysis techniques. The initial techniques performed were as followed:

- Ultimate analysis-This was in accordance with analysis standard for coal (BS ISO 17247:2013) and for biomass (ASTM D 5373).
- Proximate analysis-Testing followed British standard BI ISO 17246:2010 for coal and for biomass ash BS ISO 18122, moisture BS ISO 18134-1 and volatile matter BS ISO 18123.
- Calorific value- The standards used were; for coal BS ISO 1928:2009 and for biomass BS EN 15104:2011.
- Ash fusion- Analysis in accordance with the standard (DD CEN/TS 15370-1:2006).

4.4.1 Ultimate Analysis

Table 4-1 shows the results of the ultimate analysis performed on the fuels. The biomass has values comparable to other biomasses in the literature. That being, the sulphur content is less than the measuring tolerance of the device (<1 wt. %). The coal, as previously mentioned is a sub bituminous type, hence the sulphur content is high compared to anthracite coal and the carbon is around 50 wt. %, which is typical of lower grade coals (Wiser, 1999).

Table 4-1 Ultimate analysis results for biomass and coal samples
(Excluding ash and moisture, see Table 4-2)

Fuel	N	C	H	S	O
	(AR) (wt.%)	(AR) (wt.%)	(AR) (wt.%)	(AR) (wt.%)	(AR) (wt.%)
Coal A	0.39	22.09	1.98	3.71	26.91
Coal B	0.51	30.03	2.67	4.32	28.59
Coal C	0.44	25.09	2.22	3.40	27.15
Coal D	0.53	25.13	2.41	2.80	26.44
Coal E	0.66	31.48	3.06	3.50	29.40
Coal F	0.67	33.73	3.05	3.64	27.06
Coal G	0.66	33.65	2.84	2.65	27.45
Coal H	0.74	38.69	3.42	2.44	26.77
Coal I	0.37	20.97	1.96	2.67	26.98
Coal J	0.57	28.65	2.54	2.59	23.23
Peanut	1.25	40.36	4.49	0.09	42.06
Wheat Straw	0.72	33.02	3.94	0.08	43.84
Miscanthus	0.52	36.97	4.28	0.09	44.58
Wood	0.16	43.41	4.97	0.09	43.72
Oat	0.97	37.18	4.62	0.09	44.25

4.4.2 Proximate Analysis & Higher Heating value (HHV)

Table 4-2 shows the proximate and calorific content analysis for the biomass and coals used throughout the testing of later investigations. As with the ultimate analysis, the proximate analysis results are typical of the fuel types and reflect values available in the literature for comparable fuels.

Table 4-2 Proximate and bomb calorimetry data

fuel	Ash content (a.r) (wt.%)	moisture content (a.r) (wt.%)	Volatile matter (a.r) (wt.%)	fixed carbon (a.r) (wt.%)	HHV (a.r) (wt.%)
Peanut	4.04	7.80	80.68	18.22	19.14
Wheat Straw	8.26	10.22	75.67	5.85	15.69
Miscanthus	4.76	8.89	83.60	9.66	17.15
Wood	1.14	6.60	76.32	11.83	17.65
Oat	4.23	8.75	78.29	8.05	17.34
Coal A	39.91	5.02	32.04	23.04	17.38
Coal B	29.30	4.56	38.14	28.00	20.33
Coal C	35.44	6.26	34.04	24.25	18.93
Coal D	35.18	8.08	31.61	25.14	19.25
Coal E	27.43	4.47	37.00	31.09	20.39
Coal F	25.30	7.36	36.56	30.79	21.58
Coal G	25.14	7.82	34.94	32.09	21.40
Coal H	20.21	7.74	37.03	35.02	23.20
Coal I	39.47	7.88	33.73	18.92	16.94
Coal J	35.27	7.71	37.92	19.10	21.24

4.4.3 Ash Fusion

Table 4-3 shows the results of the analysis. It can be observed that the pellets change shape as the temperature of the furnace increases at a pre-set rate where it undergoes the four critical stages namely; initial deformation, softening, hemi sphere formation and flowing. This allows for the understanding of transformations within ash particles at temperatures experienced during combustion.

The ash fusion temperatures have been used as part of predictive and theoretical analysis of agglomeration, slagging, fouling etc. in studies such as Seggiani (1999); Niu et al. (2010); Rizvi et al. (2015a); Llorente and García (2005); Masiá et al. (2007). The ash fusion will be used in later theoretical work to evaluate the effect of biomass ashes in fluidised bed combustion and conclude as to whether this type of analysis offers prediction to fuel performance. This combined with theoretical modelling of low grade fuels is likely to offer insight and estimations to how such fuel will react in a combustion system.

Table 4-3 Ash fusion temperatures of low grade fuels

	Initial deformation	softening	Hemi-sphere formation	Flowing
Sample	**(°C)**	**(°C)**	**(°C)**	**(°C)**
Coal A	1138	1260	1365	1475
Coal B	1110	1245	1370	1485
Coal C	1070	1250	1380	1495
Coal D	1060	1290	1370	1440
Coal E	1150	1340	1365	1420
Coal F	1145	1335	1380	1460
Coal G	1065	1325	1390	1450
Coal H	985	1260	1375	1435
Coal I	1155	1305	1385	1495
Coal J	1120	1330	1380	1455
Peanut	955	975	1005	1150
Oates	905	980	995	1390
Miscanthus	965	970	1110	1260
Wheat straw	900	1115	1190	1195
White wood	1000	1105	1190	1325

4.5 X-Ray Fluorescence (XRF)

X-Ray Fluorescence (XRF) is an analytical technique that can be used to analyse the elemental content (major and minor) in fuels, ashes and other materials formed as the bi-products of combustion. However, it has been found, experimentally, that this method has a lot of inherent problems with accuracy and repeatability when samples other than coal ashes are analysed. The work in the following sections describes the reasoning and evidence of these problems and how it has been elevated in order to produce a fast and accurate method for analysing the samples produced by the tests of Chapter 6 and 7.

The following sections describe work and results from using a combination of analytical techniques to develop calibration standards and matrices required to accurately analyse biomass materials.

4.5.1 Theory

XRF is a non-destructive method for analysing solids, liquids, minerals, oils, etc. with a high level of accuracy and accurate repeatability. The speed of the technique is fast and with a fairly simple sample preparation method combined with the ability to recycle samples in further XRF analysis.

XRF utilises x-rays which are wavelengths that can be seen in the electromagnetic region of the light spectra within a range of 0.01 to 10nm (Brouwer, 2003). The x-rays within the analytical device are produced by a synchrotron or x-ray tube. The x-rays being focused towards a sample carry a specific/measurable intensity and associated energy. The x-rays can be considered both waves and photons at the same time because of their energy value. The x-ray wavelength range equates to the energies range of 0.125 to 125keV (Brouwer, 2003). The wavelengths of the x-rays are inversely proportional to the energies. The following equations determine the wavelengths of the x-rays and their associated energies (Serway et al., 2004):

$$\lambda = \frac{C}{f} \qquad \text{Equation 4-1}$$

$$E = \frac{hc}{f} \qquad \text{Equation 4-2}$$

The equations Equation 4-1 and Equation 4-2 are fundamental to the operations of the XRF and the physics applied to calculate the elemental composition of a sample (Serway et al., 2004).

The XRF analyser compromises of the following parts: x-ray source, collimator systems, analysing crystal/detector, sample and amplifier/ computer readout as shown in Figure 4-4.

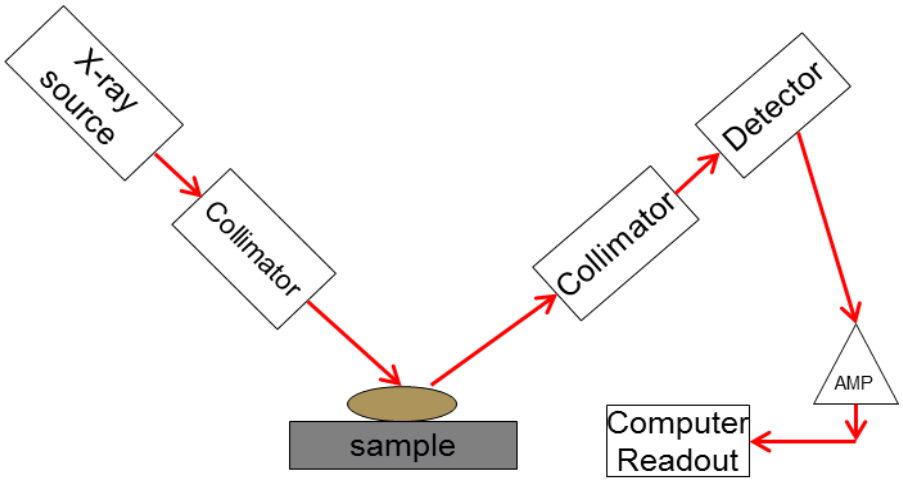

Figure 4-4 Basic XRF schematic

X-rays are produced through internal mechanisms and emitted from the source at the sample. The energy of the x-ray photons emitted are proportional to the mechanism in which they are produced, thus giving a value for later analysis calculation (Curry et al., 1990). The x-rays bombard the sample. The x-rays then interact with the matter based on the samples thickness, density and composition of sample.

The X-rays colliding with atoms with the sample result in fluorescence. Fluorescence from a sample comes from the removal of an inner orbital electron and the subsequent binding and

movement energies. When the x-rays have sufficient energies the x-ray forces an electron from the inner K or L orbital of the atom creating an initial vacancy (Shackley, 2011). The removal of this electron creates an unstable atom resulting in the atom becoming excited. The atoms internal electrical polarity forces stabilisation by moving an electron from either the L or M orbital down to the lower energy K orbital to fill the space and become stable again. However, because the electron which has filled the space has an energy higher than that for the lower orbit, energy is emitted in the form of an x-ray photon specific to the atom and the electron orbital change. This then results in a chain reaction of electrons moving to fill orbital gaps until the entire atom is stable again, and in doing so emitting X-rays which are undetected and used to identify the change (Beckhoff et al., 2007).

The energy emitted from the sample pass through a number of polarised cells which have a prearranged angle and configuration unique to the analysis and device. This results in analysis of specific analytes and in a cleaner signal in the measurement (Beckhoff et al., 2007).

The cleaned up signals from the sample are then passed through crystal's which disperse the waves into different directions based on the waves energies. The different colours and spectra of the waves are then detected by the spectrometer detector resulting in a readout on the computer analysing/logging equipment (Shackley, 2011). The intensity of the signal is a result of the concentration of each element being present in the sample. The more atoms there is of an element the higher the probability of the x-rays interacting with them, this then results in more of that wave being detected by the equipment.

4.5.2 Analysis Types

Whilst there are small variations in XRF devices between manufacturers due to design choices and cost, there are three methods of generating the analysis data, with varying levels of accuracy and repeatability (Adams et al., 1998).

Qualitative and semi quantitative analysis are methods which require no calibration standards or calibration curve. Instead they use algorithms based on "standard less fundamental parameters" (SLFP). These calculate the concentrations based on the elemental intensity by computing relationships with absorption effects. This method is typically accurate within 10-20% of actual sample values (Banks, 2014). However, because of inaccuracy found in this method it is common practice to smooth noisy data, overlap and perform matrix corrections which "fit" the algorithms to the results. This can give false readings because of the inability to measure against background peaks and other scattering wave properties.

Fully quantitative XRF analysis uses comparative data based on a database of possible photon elemental emissions to compare the data against. This method also uses calibration standards

to build calibration graphs which are used to design a matrix of the measured elements. This is then overlapped on the data being collected from the samples resulting in clearer, repeatedly accurate results. Analytes peak intensity can then be computed against concentration of the element within the sample (Banks, 2014).

The fully quantitative method is a better analytical method for determining true concentrations in a sample by XRF. However, whilst in the past standards and algorithms have been created for analysis of samples containing coal etc. fuels such as biomass have had less development. It has been shown in available literature the usefulness of this technique, examples including (JOHN K. KUHN, 1975; Kelloway et al., 2014; Evans et al., 1990; Bettinelli and Taina, 1990; Kaakinen et al., 1975; Kowalska and Urbanski, 1992; Acharya, 1992) for the determination of between 11 and 42 elements reliably in coal based samples.

However, due to the chemical and physical differences in coal and biomass (including biomass combustion products), a coal programme cannot simply be used to analyse biomass. It is therefore necessary to develop new standards and matrices to accurately measure different types of samples (inc, 2014).

4.5.3 Standards

There are a very limited number of reliable standards on the open market, which limits the accuracy which can be achieved by calibrating an XRF device. Hence a method for producing standards and comparing the data produced was necessary. Only by doing this would it be possible to analyse the samples produced in the combustion tests described later in this thesis.

It was decided that standards should be made using biomass in order to build a new XRF program. The methodology in Figure 4-5 was devised and includes analytical techniques chosen after reviewing key analytical texts such as (Svehla, 2008; Haynes and Lide, 2010) and through discussions with analytical technicians contributing to the project.

4.5.4 Differences between Devices

Whilst there are a number of different devices capable of performing XRF analysis this brings a series of inherent problems for the output of accurate and standardised results. Different devices bring a series of variations such as different operators with varying levels of expertise. Different devices and operators will also have different sample preparation, degrees of accuracy with different powered devices and with different software etc.

4.5.5 Wet Chemical Analysis

Wet chemical analysis is an analytical method in which a number of acids are used through a series of stages to digest a sample. This then allows for the sample to be totally dissolved into

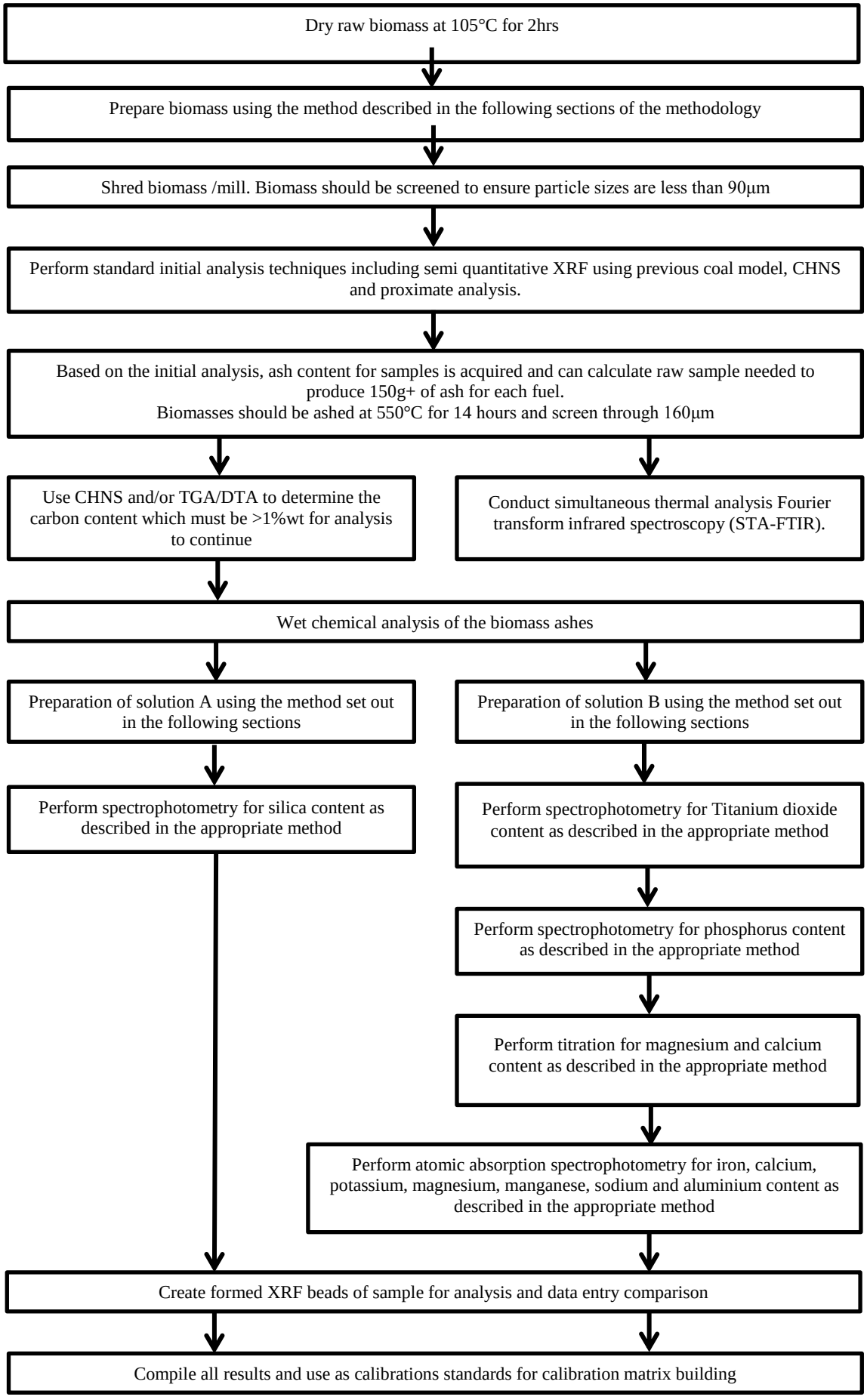

Figure 4-5 Standards development methodology

a water solution, and in a state which can then be analysed by a number of different methods in order to determine specific analytes concentrations. However, before the acid digestions could be undertaken, ashes of the biomass needed to be produced.

The work involved in the following sections is part of a larger study, in which other students were developing standards to produce a bulk of data to build a more accurate XRF program. Whilst the same methodology was used by different students, the fuels and experiences were unique in each case. Differences were found in the analysis undertaken by different student, and it is the opinion of the author and the aiding technicians that the work performed here was more accurate and encompassing. It is for this reason that the final XRF program and hence results are different to that of other students. The work is surmised in a publicised paper (Xing et al., 2016)

4.5.6 Preparation of the Samples

4.5.6.1 Ashing of Biomass Samples

The coal and biomasses have to be in a completely ashed form in order to perform the analysis and generate the standards data necessary to build a matrix. However, the method chosen to ash the fuels has to ensure that carbon content in the resulting ash equates to ≤1 wt. % of the total mass. The reason for ensuring the carbon content is; 1) any residual carbaceous compounds can retain some of the analytes and thus reduce the true concentration found in solution post acid digestion, 2) carbon physically interferes with the XRF process and, 3) the carbon content is assumed to be 0 wt. % as all carbon should be oxidised in the combustion process, therefore, if there is any carbon remaining the total of all analytes will be incorrect by a factor of the actual carbon wt. %.

For the purpose of the XRF calibration matrix study, it was suggested that the biomasses not be run in accordance with the ASTM method. This methodology subjects a sample to a heating rate of 10°C/30sec to a final temperature of 550°C and held there for a number of hours. Instead it was suggested, based on STA-FTIR results of biomass as shown in (Xing et al., 2016) that the biomass should be heated at the same rate but to a final temperature of 900°C (Paul, 1990).

The pellets were heated at 10°C/30sec to a final temperature of 900°C and held at that temperature for 14hr. However, when the crucibles were removed from the ovens (after an appropriate cooling time) it was found the ash had formed into solids.

Figure 4-6 shows the solid residues left from the ashing process. Images A and B are from two different peanut samples and c and d are the products of straw. It was found that the structures in the crucibles were hard, brittle and had large pores within the structures. These

materials are a combination of SiO_2 with other alkaline salts. The pellets were found to be burning out, causing a reduction environment as well as localised hotspots, leading to the formation of amorphous silicate glasses, alkaline salt and molten ash compounds generally found above 1100ºC. This is the reason for the high voidage and pellet like shape of the solids.

It is assumed that for all samples prepared for analysis with XRF, that the ashes are fully oxidised. This is justified with agitation, final heating rates and hold times in the preparation stages whilst using the furnaces.

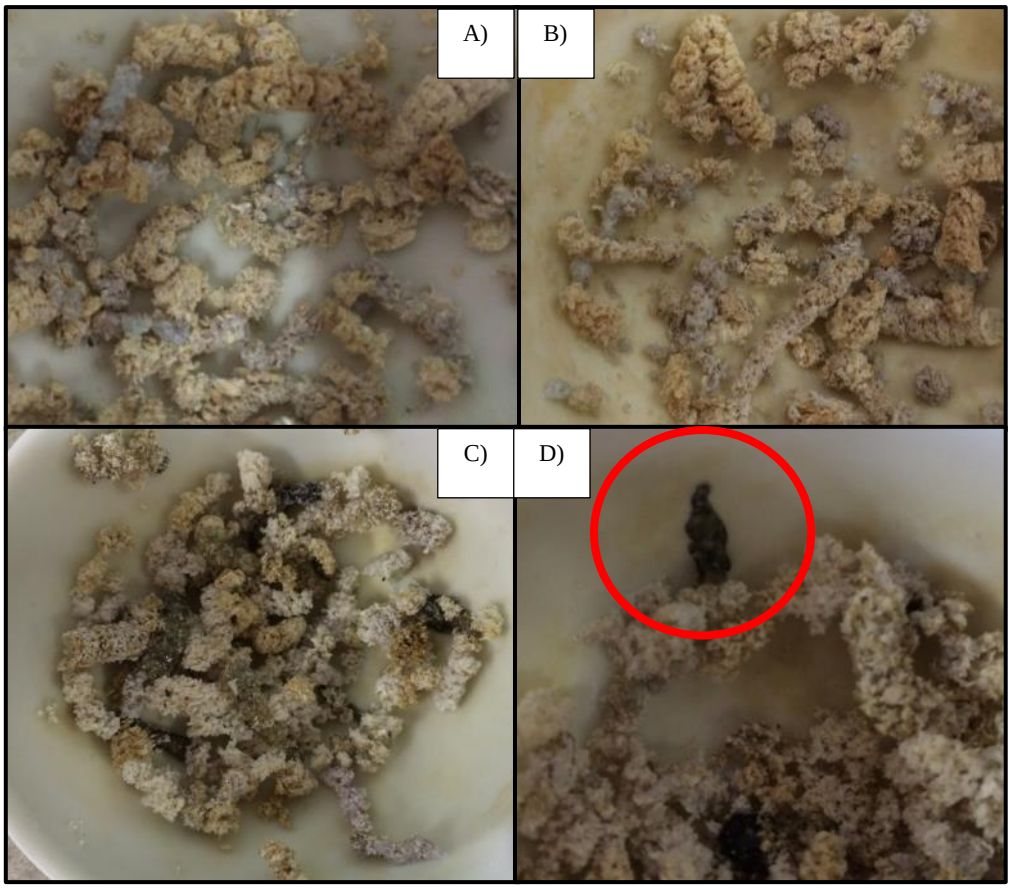

Figure 4-6 solid ash formations from combusiton of biomass at 900ºC

In the literature, a similar phenomenon has been reported in the presence of localised heating, high concentrations of compounds including Si, K, Fe and Na when heated to 800-1000ºC. The mechanisms described by Steenari and Lindqvist (1998) addresses another observation, being the hardened ash material had impregnated the surface of the quartz crucibles (red circle in Figure 4-6-D). The crucibles are designed for high temperature and acting as an inert carrier. However, because of the obvious interactions with the solids it can only be assumed that some of the analytes of interest will have been fused into the porous medium of the crucible, thus effecting the elemental content of the fuel.

The formation of the solids suggests a liquid and possible gas phase were achieved in the ash and thus some of the analytes in question could have been lost. This combined with the leeching effect seen in the crucibles renders the samples unfit for further analysis.

Further attempts to produce a good quality ash was done by following the British standard however, when removing the ash from the crucibles it was found that different reactions had occurred as shown in Figure 4-7.

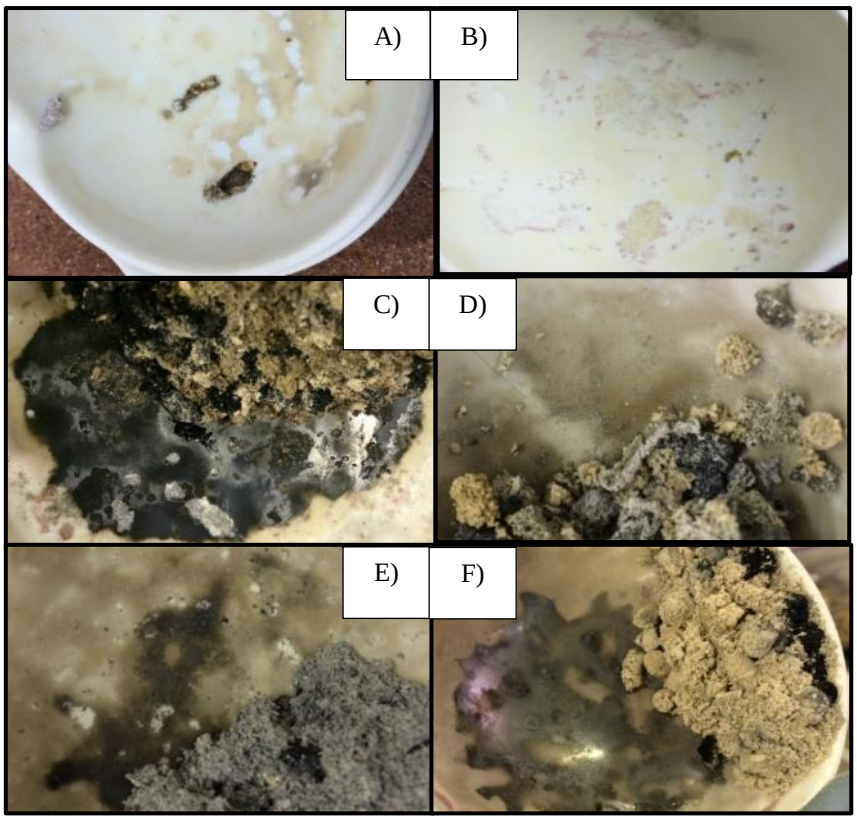

Figure 4-7 solid ash formations from combustion of biomass at 550ºC

Image A and B shows how even at the lower ashing temperature, the formation of hardened SiO_2 based amorphous compounds has formed and impregnated the surface of the crucibles. This is further evidence to the localised hotspot and combustion creating an environment in which the eutectics and slag can form. Image B has undergone hydrochloric acid cleaning, exposing the depth of the penetration.

Image C, D, E and F all show ashes which clearly contain some form of carbon. Combustion and complete burnout has not been achieved. This has resulted in the remaining carbon deposits to occur either through discolouring in the ash or a clear black layer remaining. Work done by Simoneit (2002) found that this combination of variables resulted in a pyrolysis effect, leaving the carbaceous compound, even after extended periods of heating.

Further evidence of a reducing environment, is the formation of a silvery surface as seen in image C and F. This was found to be graphitic carbon, which when heated further in an

oxidising environment would combust completely. This has been noted in work such as Kiyobayashi and Sakiyama (1993). Using their experience of Pilling (1999), the graphitic crucibles were submerged in hydrochloric acid.

This test would dissolve a non carbaceous material but was found not to giving more clarity to the compounds on the crucibles.

The carbon content of the XRF samples should be ≤1wt% of the total sample. The reasons for this have been described previously, as they adversely affect the physical analysis process and retain analytes from sample solution.

It was necessary to try a number of other temperatures and ashing variables in order to evaluate the best ash sample i.e. a sample with ≤1 wt. % carbon but without potentially releasing analytes in a gaseous slag phase. Whilst a simplified ashing program may present itself as a longer heating period, well mixed and to a higher temperature, this was found not to be the case.

Figure 4-8 shows carbon compounds separating from solution during the acid digestion process of the ashes in which the sample would be broken down and then enter solution for wet chemical analysis. In this form the carbon compounds will not enter solution. Nitric acid was added and the solution was heated to digest the carbon but even so not all analytes were guaranteed to enter solution and discrepancies were found in the analysis.

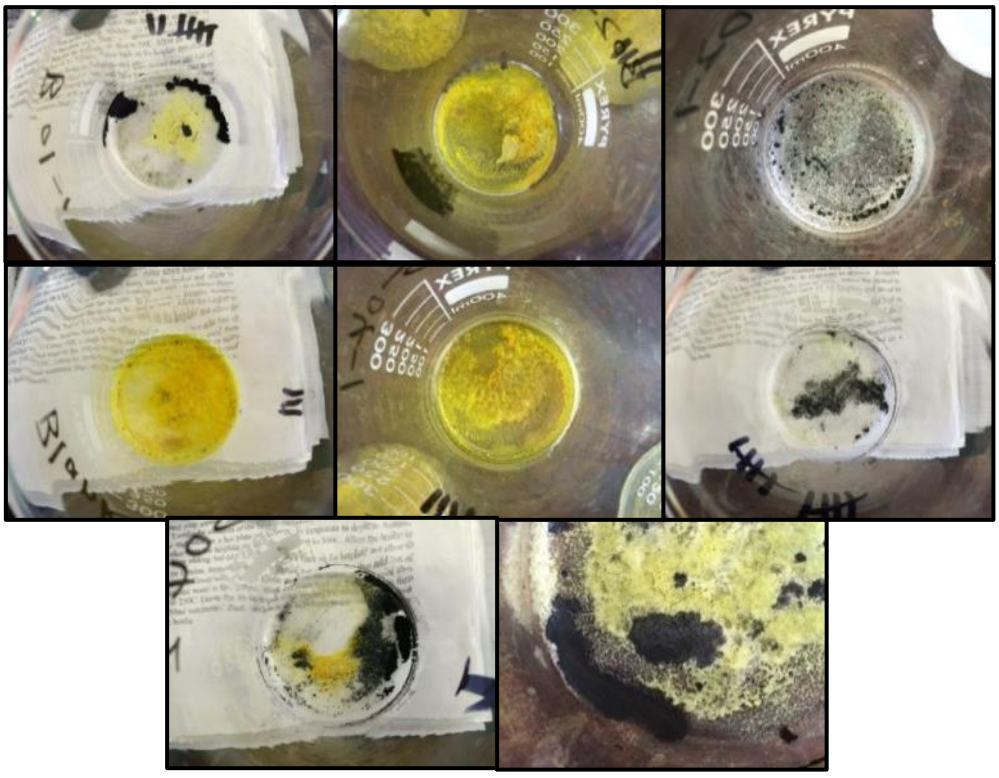

Figure 4-8 carbon separation during acid digestion of biomass ashes

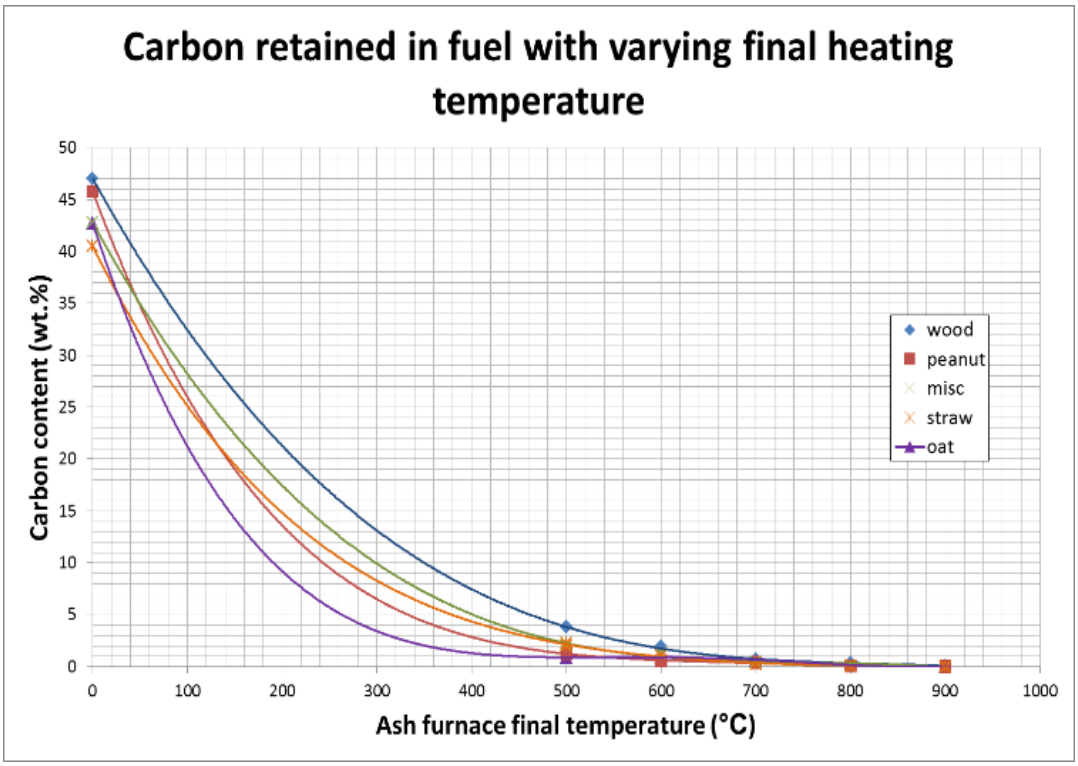

Figure 4-9 Effect of retained carbon content in fuel with increasing final heating temperature

Further attempts to form an ash which contained all of its analytes and a minimum carbon content were done at 500ºC, 600ºC, 700ºC, 800ºC, 900ºC, 850ºC and 815ºC. Ultimate analysis was performed on the ashes and compared as shown in Figure 4-9. Experience from these tests led the author to mill the pellets to a particle size of approx. 100µm in order to increase surface area and encourage O_2 penetration into the fuel and reduce hot spots forming. It was also found that stirring the sample every 2 hours for 10 hours and heating for a total of 24 hours, as the sample heated at 10ºC/30sec to 815ºC was necessary to reduce the liquid phase formation which was seen to impregnate the crucibles. A temperature of 815°C was the optimum temperature for achieving carbon burnout in the sample whilst retaining the highest concertation of lower melting temperature analytes.

4.5.6.2 SEM & SEM-EDX

In order to further understand the reasons for difference in analytical results and the way in which the ashes reacted, SEM and SEM-EDX was performed on samples. The following sections describe the findings of these analysis and possible insight to the way in which the parent fuels will react in a fluidised bed system based on the outcome of the ash. Additionally, the analysis was used to further the understanding of fuels and the retention of alkaline species which would affect the wet chemical analysis result and XRF analysis.

Throughout fuel characterisation and later analysis of ash samples etc. backscatter electron imaging is the primary method for analysing material composition and secondary emission was used to create the high definition surface topography image.

Samples were prepared using carbon paint to adhere the unusual shapes of the samples to a steel stub. The carbon paint used was applied to conduct charge around the sample as to reduce charging and light emission in the SEM analysis process. The samples were placed in a vacuum and coated in a vaporised coating of carbon.

4.5.6.2.1 Wood

Figure 4-10 shows the SEM images, (image A being a general image of the ash and image B being an enhanced image of the ash), and the SEM-EDX analysis results of areas of interest.

As image A shows the ash is made up of a variance of particle sizes which is indicated to be dominated by Ca compared to the other alkaline analytes. The result is relating to the wet chemistry and XRF results carried out on the wood ashes which indicated wood pellets to contain high Ca with Mg and Si being similarly high. Additionally, the ash visually looks quite fibrous and loosely compacted.

Image B looks at an enhanced area of the ash and as can be seen there is a distribution of ash in clumps around the image. The ash looks to still be in particulate format after the ashing process which validates the findings that a temperature of 815°C is a more appropriate temperature range to ash the biomass pellets without causing the formation of eutectic or glass like complexes.

Image B also indicates to Ca and Si being the two major components within wood ash. SEM-EDX results suggest that the distribution of the analytes around the sample isn't homogenous. This means ash samples should be milled and blended before further analysis. Further to this it shows that the biomass pellets are not equal and are likely to react differently in a combustion system, even if slightly. Finally, the ash shows that if wood pellets are combusted in FBC operating within the temperatures of 750-850°C, the ash shouldn't enter the molten phase and contribute to agglomeration.

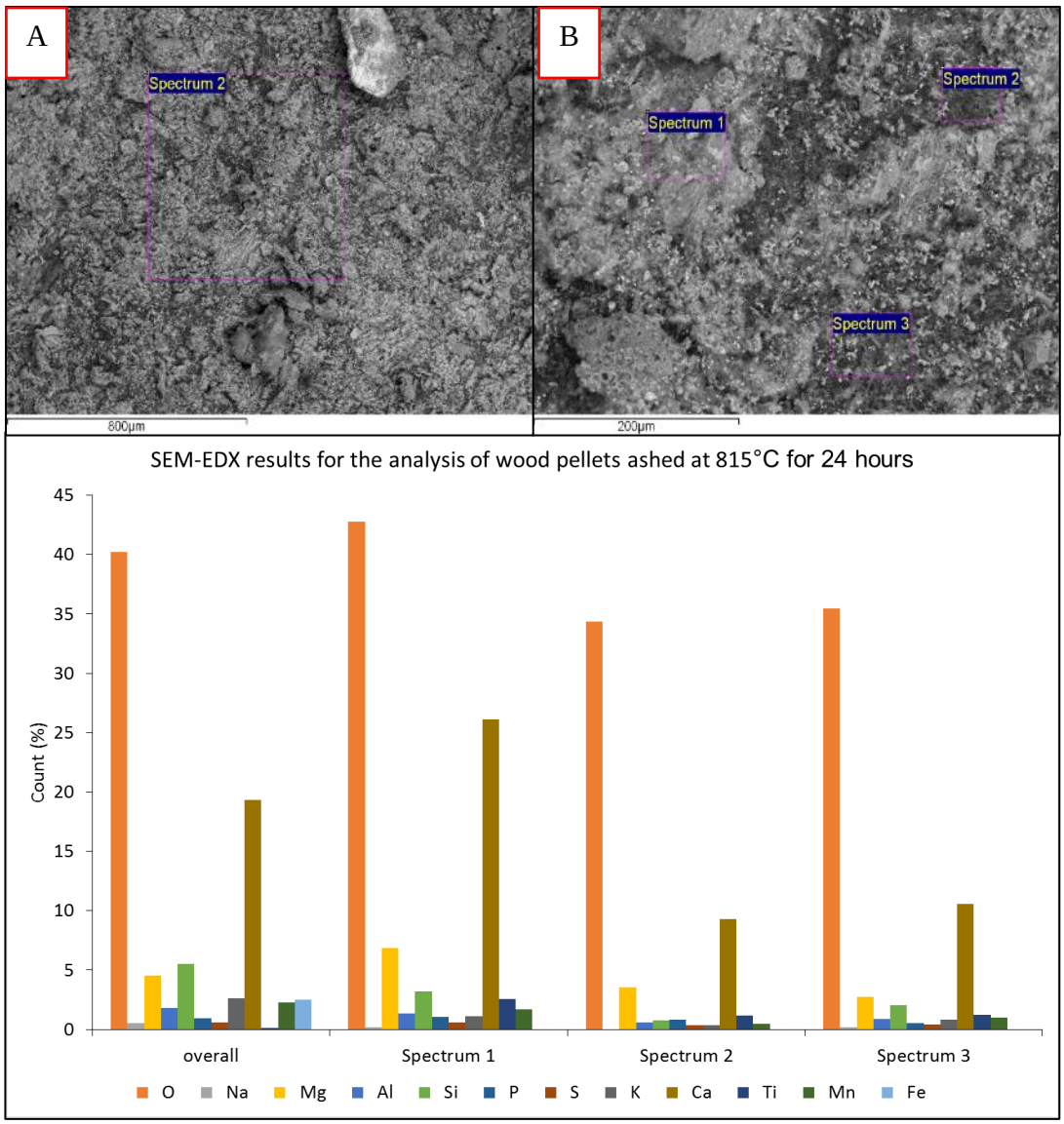

Figure 4-10 SEM images and SEM-EDX for the images shown in A and B being and overall image and enhanced area of the wood ash repectively

4.5.6.2.2 Peanut

Figure 4-11 shows the SEM images, (image A being a general image of the ash and image B being an enhanced image of the ash), and the SEM-EDX analysis results of areas of interest.

Image A gives an overview of the ash whilst B gives an enhanced view of the ash. The ash look various in particle size apart from spherical clumps distributed amongst the sample.

The areas in which the fibrous ash is present is indicated to be dominated by K_2O, CaO and SiO_2. However, the spherical anomalies are dominated by higher concentrations of Si and K. These are likely to be complexes that have formed during the high temperature oxidation process in the furnace and resulted in a liquid phase, resulting in a K-Si eutectic. However, the limitation of 815°C has reduced the propagation of the eutectic and silicate complexes throughout the ash. This validates the results seen in the ashing tests where temperatures ≥815°C were found to leave silicate glasses on the ashing crucibles.

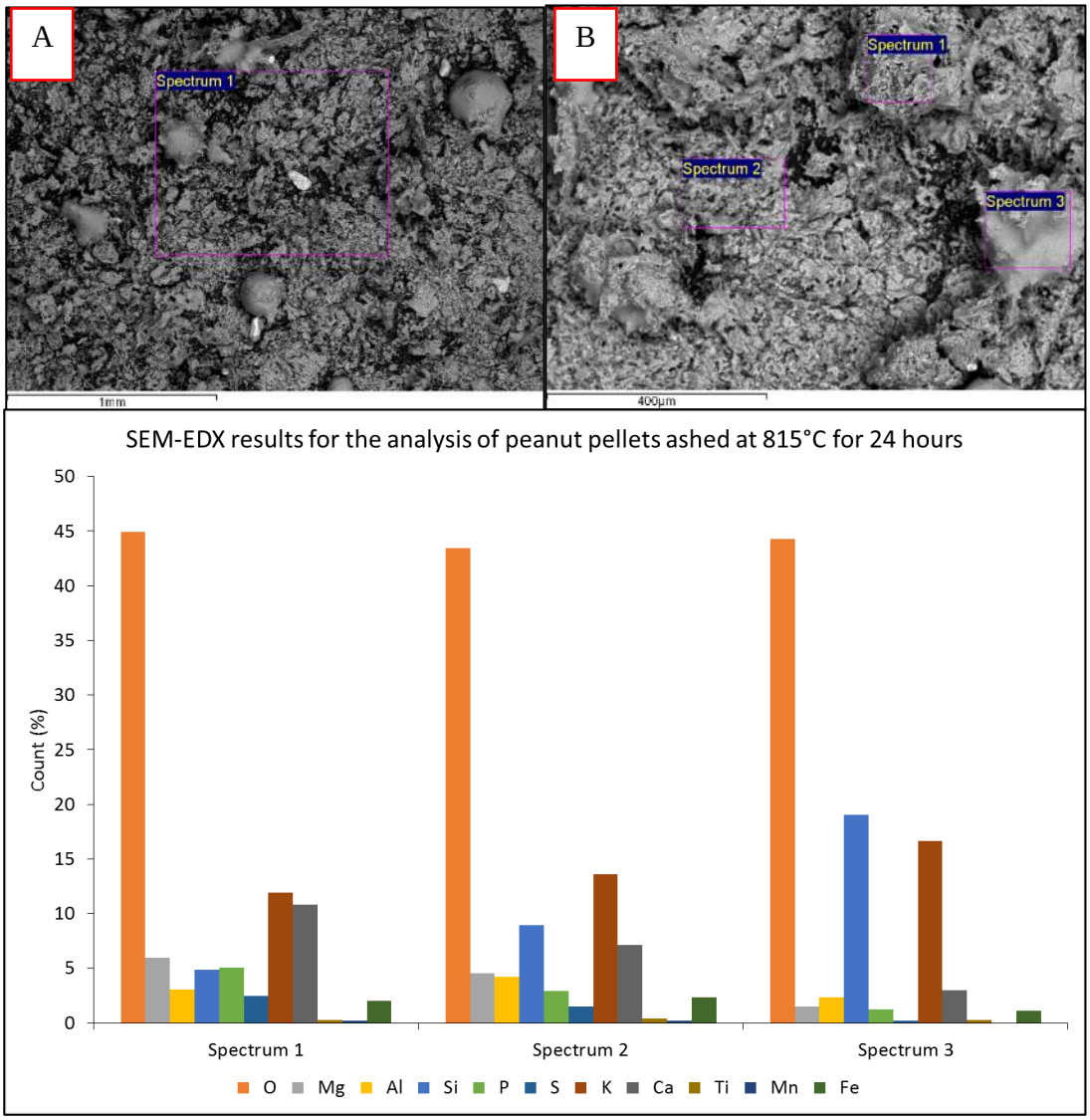

Figure 4-11 SEM images and SEM-EDX for the images shown in A and B being and overall image and enhanced area of the peanut ash repectively

Furthermore, this gives an indication that when the fuels are combusted in the fluidised bed experiments, peanut is likely to cause the onset of agglomerate formation via a low melting eutectic primarily made of Si-K groups. Localised hotspots will also further lead to the onset of eutectics and hence good mixing and bed turbulence will be necessary to keep a bed fluidised.

4.5.6.2.3 Oat

Figure 4-12 shows the SEM images, (image A being a general image of the ash and image B being an enhanced image of the ash), and the SEM-EDX analysis results of areas of interest.

As A and B both show the ash is different to that of peanut and wood pellets. This is much more flakey and flat. The shape of the ash could alter the interaction between agglomerate onset and the way in which bed particles stick together, especially with more ash being available per flake compared to the previous ashes which had smaller particles.

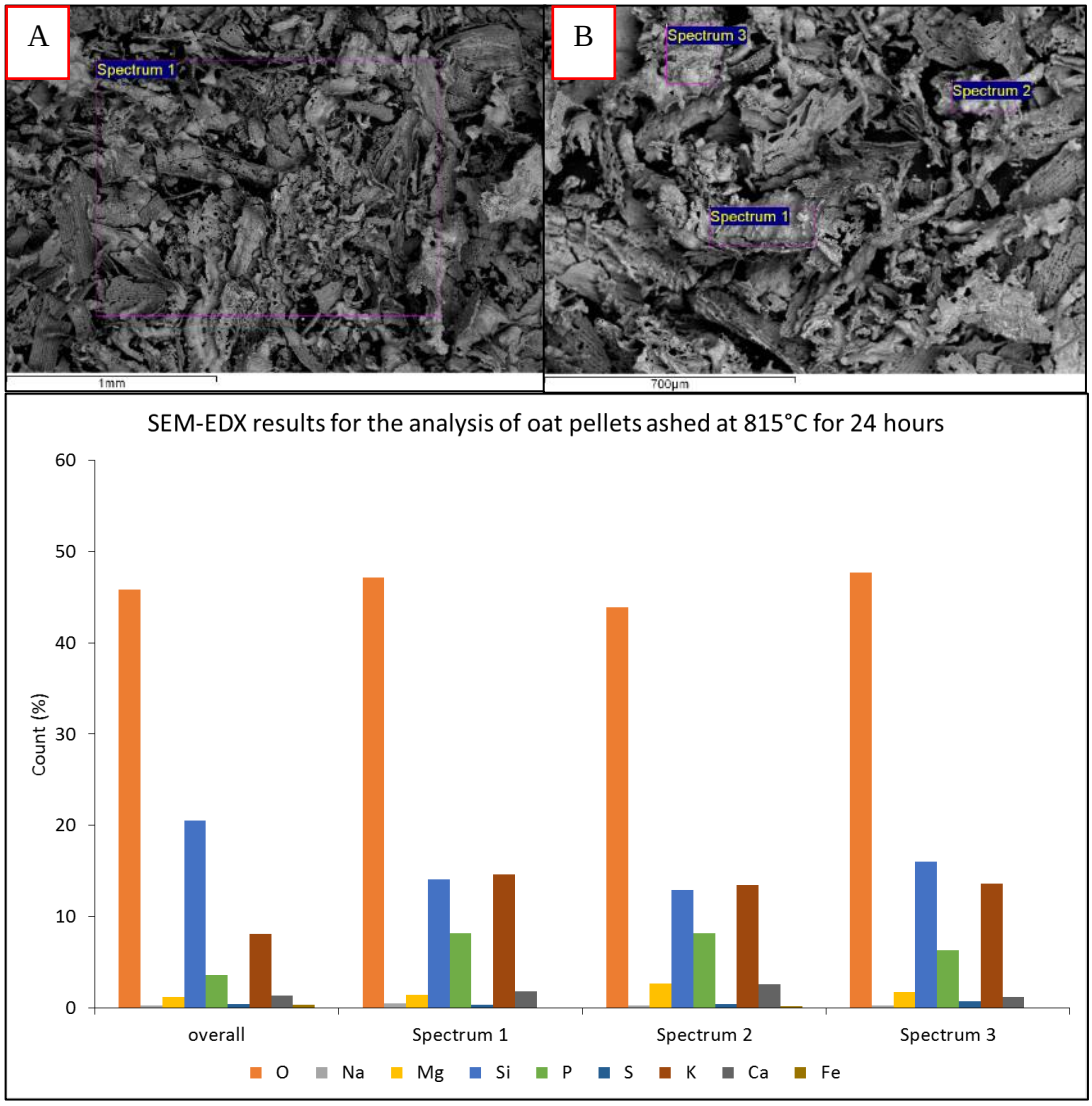

Figure 4-12 SEM images and SEM-EDX for the images shown in A and B being and overall image and enhanced area of the oat ash repectively

The SEM-EDX results suggest a high concentration of Si, K and P. These are all species associated with the onset of agglomerates and low temperature eutectics. However, they have remained in the ash, which hasn't adhered to one another so potentially this ash could perform better in a fluidised bed than peanut.

However, for further analysis in wet chemistry, XRF etc., the ash should definitely be milled to better break up the ash and produce a more homogenous sample.

4.5.6.2.4 Miscanthus

Figure 4-13 shows the SEM images, (image A being a general image of the ash and image B being an enhanced image of the ash), and the SEM-EDX analysis results of areas of interest.

As the images in A and B show, once again the ash is very different again to the ones shown previously. The miscanthus ash seems to contain if little loose ash particles, but instead seems to be made up of clumped/reacted complexes.

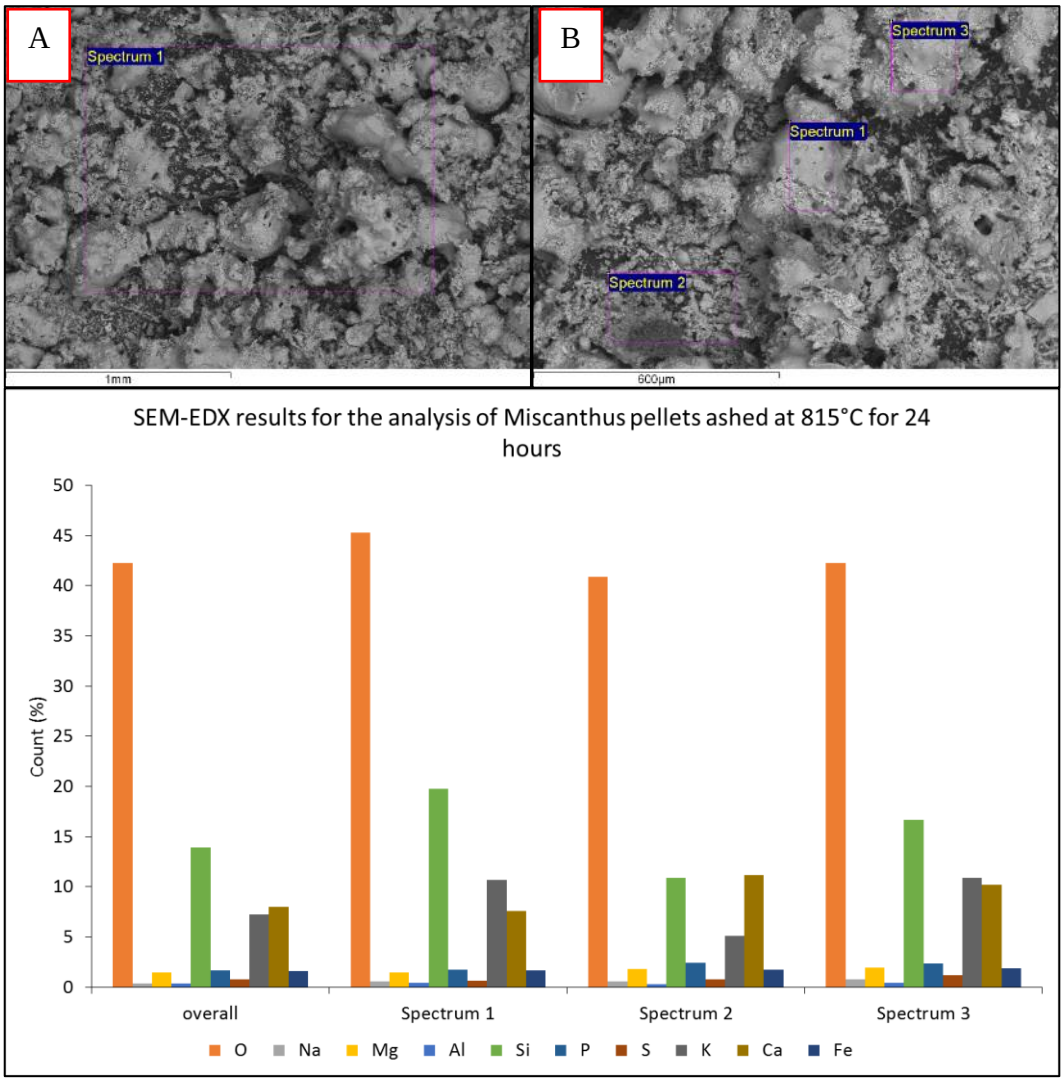

Figure 4-13 SEM images and SEM-EDX for the images shown in A and B being and overall image and enhanced area of the miscanthus ash repectively

The SEM-EDX results suggest that the clumps, whilst containing a variety of alkaline groups, is primarily made up of Si, Ca and K. As noted previously this type of clumping was seen to be made up of a Si-K complex as seen here. The high concentration of Ca isn't unexpected as Ca groups are known to react with K dominated eutectics and is a method for reducing

agglomeration formation mechanisms in fluidised beds. Hence in the ash the Ca has reacted with the Si-K in the liquid phase forming Si-K-Ca eutectics. The results here show that miscanthus will agglomerate in the bed aggressively and the liquid phase will from within normal combustion temperatures.

Furthermore, for analysis performed post ashing, the sample should be milled to ensure the liberation and mixing of all species presence as in its current state the sample will not be homogenous.

4.5.6.2.5 Straw

Figure 4-14 shows the SEM images, (image A being a general image of the ash and image B being an enhanced image of the ash), and the SEM-EDX analysis results of areas of interest.

As image A and B show there is a variety of particles present as well as larger clumped material. The finer particles of ash were indicated by SEM-EDX to have higher concentrations of Si, Ca, Fe and S. Firstly it should be noted that the fuel does contain sulphur, however, the high concertation either shows an error/limitation in the analysis or a concentrating during combustion. The result is therefore, taken as an indication not a quantitative value.

Analysis of the clumps in various stages of liquid phase formation suggests high concentrations of Fe, Si and Ca. Fe is known to react with Si and Ca in a beneficial and negative way depending on the groups it is exposed to and in what concertation. Here it seems as though it is negatively forming liquid complexes with the high concertation of Si. It is likely that this would be replicated in a fluidised bed and therefore, is likely to be an agglomerating fuel.

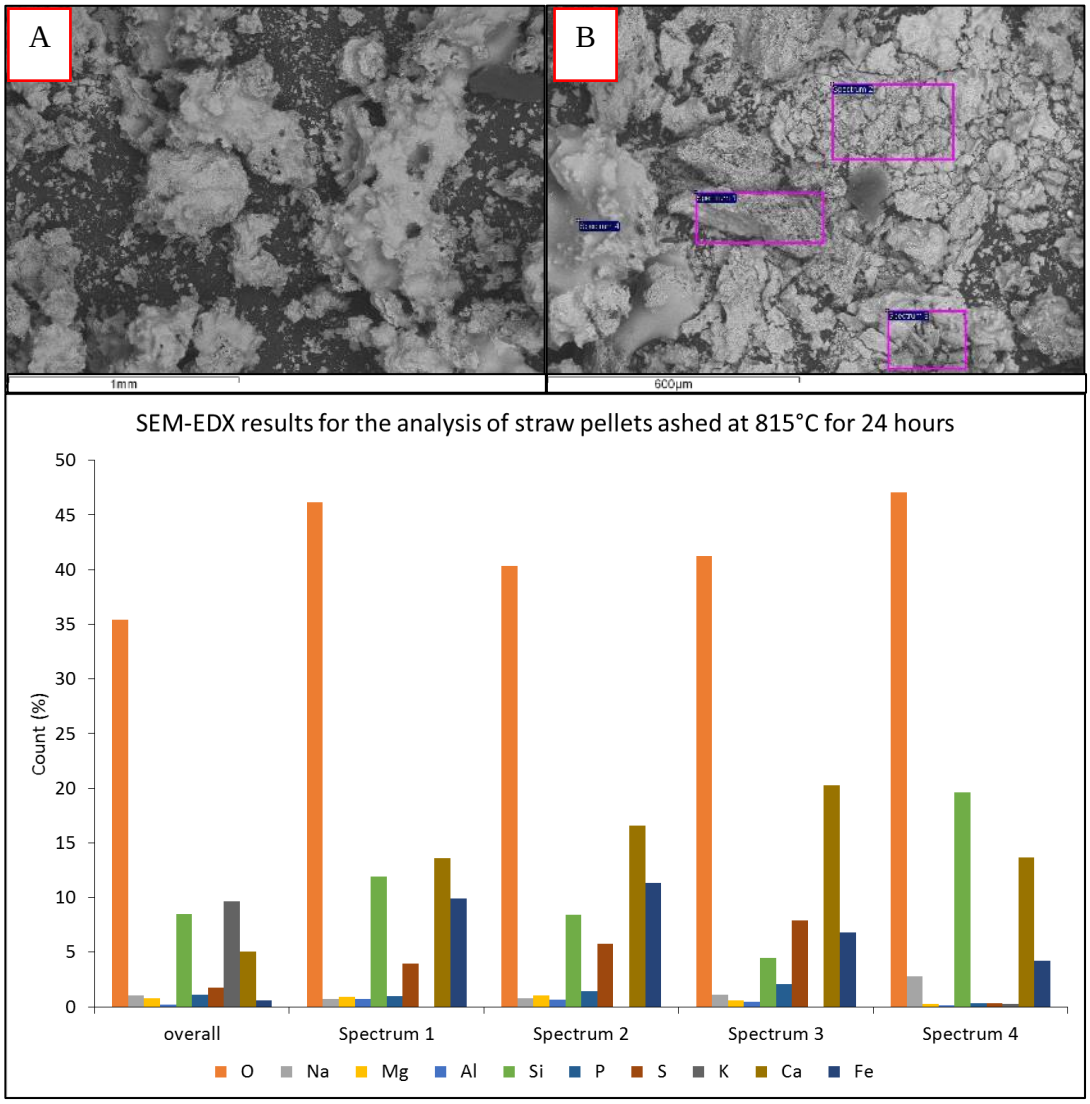

Figure 4-14 SEM images and SEM-EDX for the images shown in A and B being and overall image and enhanced area of the straw ash repectively

4.5.6.3 Ashing Notes

FBC takes place at temperatures similar to the temperatures used to ash the biomass fuel. It is therefore, likely that similar mechanisms will take place during the combustion process in the bed of the FBC unit. The liquid phase eutectic seen in these ashing tests will link to the way in which the bed reacts and shed light to any slagging or agglomeration mechanisms experienced in pilot scale testing.

4.5.7 Wet Chemical Analysis Techniques

The wet chemical analysis techniques chosen were specific in order to measure the concentration of 10 different analytes including; sodium, potassium, iron, magnesium, manganese, aluminium, calcium, phosphorus, silicon and titanium.

The techniques chosen for analysing the different analytes are as follows:

- Spectrophotometry- This method was used to measure the concentration of TiO_2, P_2O_5 and SiO_2. Reagents are added to the acid digestion solutions, which are then placed within the device and light passes through the samples at a specific wavelength. The measured absorption i.e. the photons not absorbed by the liquid due to its colour intensity is then used to calculate the concentration of the analytes in the solution.
- Atomic absorption analysis (AAS) - This method was used to measure the concentration of Na_2O, K_2O, Fe_2O_5, MgO, MnO and Al_2O_3. The acid digestion solutions were atomised in an acetylene flame. Light generated by standardised elemental bulbs then passed through the flame. Photons were absorbed by the specific analytes and thus the difference in the photons produced minus photons absorbed gives the concentration of the analytes within the solution.
- Titration- Titration was used to measure the concentration of CaO and MgO in the solutions. By the addition of a known titrant it was possible to cause a colour change. The amount of titre required for the colour change is directly proportional to the concentrate of the analytes and thus gave the concentration of the analytes in the solution.
- The wet chemical analysis was performed a number of times using slight variations on the acid digestion method. The differences included slight alterations in timings to allow analytes at different stage to be fully digested. This also involved the use of filter papers etc. to evaluate if all solids had been digested, which then required digesting into the final solution. Very little difference was found between different methodologies giving a good level of reliability in the data shown in Table 4-4.

4.5.7.1 Wet Analysis Results

Wet chemical analysis was performed on the biomass in accordance with the methodology previously stated, that being, the fuel was selected in order to maximise homogeneity. The first set of wet chemical analysis was conducted on ashes which had been ashed at a temperature of 900°C (900°C was used in the first instance to validate the use of a final temperature of 815°C in later tests. The need for this validation was due to initial variation in results, however 815°C was validated as the most appropriate temperature). This was stirred regularly, heated at a rate of 10°C/30sec etc. as previously stated.

Table 4-4 shows the results of the wet chemical analysis for ash that was produced using a final heating temperature of 900°C. As the data shows, there is little variance between the values of the repeats completed in the analysis. This shows that the analysis was conducted with a good level of accuracy and the ash was of a homogenous nature. If the values had varied greatly then this would have identified issues in both the preparation method and the skill level of the analyser.

Table 4-4 Wet chemical analysis [heating rate 10°C/30sec, max temp 900°C, 24 hour heating period, stirred every 4 hours in working hours].

Sample	Sodium %	potassium %	iron %	manganese %	aluminium %	Calcium %	Silicon %	Phosphorus %	Titanium %	magnesium % *titration	magnesium % *AAS	Silicon % *titration	Total %
Miscanthus 1	0.70	10.61	0.47	0.02	0.47	12.59	33.19	2.94	0.28	1.76	3.83	63.02	65.09
Miscanthus 2	0.67	10.54	0.46	0.02	0.56	12.78	34.31	2.56	0.17	1.75	3.94	63.83	66.01
Wood 1	2.13	7.69	1.09	0.28	2.97	20.68	49.25	1.53	0.53	3.13	5.04	89.28	91.19
Wood 2	2.11	7.16	1.13	0.27	2.81	21.00	54.52	1.33	0.03	3.18	5.33	93.54	95.69
Peanut 1	0.49	15.92	0.73	0.03	3.04	7.25	38.74	3.41	0.75	2.45	4.83	72.80	75.18
Peanut 2	0.51	15.37	0.71	0.02	3.05	7.27	39.66	3.98	1.33	2.48	4.81	74.38	76.71
Oat 1	0.50	14.01	0.13	0.01	0.42	6.44	48.89	10.83	0.50	1.94	3.12	83.68	84.87
Oat 2	0.26	12.28	0.11	0.01	0.38	6.30	49.18	9.87	1.03	1.70	2.52	81.12	81.94
Straw 1	1.72	19.01	0.17	-0.01	0.69	16.47	38.55	3.24	0.66	1.40	5.12	81.90	85.62
Straw 2	1.78	23.33	0.19	-0.02	0.73	16.61	36.75	3.10	0.72	1.41	4.42	84.61	87.62

Whilst the minimal variance is a positive outcome, it should be noted the difference in Mg concentrations, in which two different analysis techniques were attempted. The AAS method and titration method was used but produced very different values. It was found that the titrations method was very difficult to accurately identify when the colour indicator had changed as a result of the titration reaction. The colour change is unlike a standard colour change as the light is fluorescent and thus a pure black background need be applied to see the change. It is believed that the titration results are less accurate than those of the ASS method and the AAS method will be used in future analysis.

A final issue with the data seen in Table 4-5 is the total analytes concertation. When using XRF devices a total of at least 85% for total analytes is representative of the samples true concertation. As the data shows the total concentration varies between 65% and 95%. As this work was done as part of a larger investigation, it was decided that the final heating temp of 815°C would not result in a loss of analytes with lower melting points such as potassium and sodium. However, the difference in total concentrations of analytes clearly shows that there is a loss of some elements during oxidation and heating in the ashing process.

Table 4-5 Wet chemical analysis data using modified methodology

Sample	Sodium %	potassium %	iron %	manganese %	aluminium %	Calcium %	Magnesium %	Silicon %	Phosphorus %	Titanium %	Total %
Peanut	0.70	16.16	2.07	0.17	4.48	10.41	14.48	22.32	0.002	9.22	80.01
Peanut repeat	0.62	15.90	2.03	0.17	4.38	9.06	12.24	23.02	0.002	5.01	72.43
Oat	2.18	15.06	0.66	0.04	0.90	20.99	17.93	29.61	0.002	0.44	87.82
Oat repeat	2.13	14.77	0.65	0.04	0.88	20.99	18.23	29.51	0.002	0.74	87.95
Misc	0.95	8.72	1.64	0.10	0.69	14.90	12.55	30.19	0.001	1.49	71.23
Misc repeat	1.02	8.63	1.65	0.10	0.68	14.01	13.96	30.71	0.001	1.20	71.96
Wood	0.60	11.64	0.48	0.12	0.36	4.64	6.78	20.08	0.005	2.53	47.22
Wood repeat	0.59	11.42	0.46	0.12	0.38	4.92	7.99	20.65	0.005	2.67	49.19
Straw	2.13	6.48	2.63	1.14	3.82	22.39	21.25	21.07	0.001	3.99	84.91
straw repeat	2.13	6.72	2.64	1.15	3.84	22.40	21.29	21.24	0.001	4.76	86.17

The process was repeated using a lower ashing temperatures and found that a temperature of 815°C was necessary in order to reduce the of lower melting temperature elements to be lost. The results in Table 4-5 is the data from this analysis.

It was decided that the STA-FTIR results were not representative of the ashing process. During the STA-FTIR the samples are milled down to a fine uniform powder, the heating rate is uniform and the heating/combustion environment is much easier to control with reduced heat spots.

As seen previously, hot spots form when piles of the biomass are being combusted in the ashing furnace. In order to increase the surface area and burn the fuel more uniformly, the biomass was milled to less than 90 microns.

The ashing process and subsequent wet chemical analysis, as shown in Table 4-6, produced a series of data which was much more representative of the biomasses with a total analytes concertation between 98-100% for ashes ashed at 815°C.

Table 4-6 Final result for wet chemical analysis of biomass fuels

Sample Name	Sodium %	Magnesium %	potassium %	iron %	manganese %	aluminium %	Calcium %	Silicon %	Phosphorus %	Titanium %
Peanut	21.58	5.62	2.12	3.17	0.24	9.07	8.36	44.01	4.87	1.21
Wood	9.61	6.31	6.61	4.34	1.69	7.48	22.69	39.77	2.24	0.46
Oat	16.18	4.77	1.65	0.90	0.17	0.80	3.92	55.98	5.25	0.05
Miscanthus	11.65	3.24	2.95	2.60	0.14	1.42	13.52	56.54	3.85	0.07
straw	19.76	3.60	6.26	1.04	0.06	1.58	21.14	38.38	4.76	0.26
Standard	0.94	1.61	2.88	10.63	0.16	25.49	2.65	47.97	2.07	1.28

4.5.8 XRF Comparison

After completing the wet chemical analysis, and developing the preparation method data it was necessary to evaluate the performance of the XRF devices available. The reason being, after getting some preliminary data from external laboratories, and devices within the UK, it was found that the results gave varied data.

Figure 4-15 shows the results collected from different XRF devices. Each device and lab was supplied biomass ash from the same process and thus was treated in the same manner. As

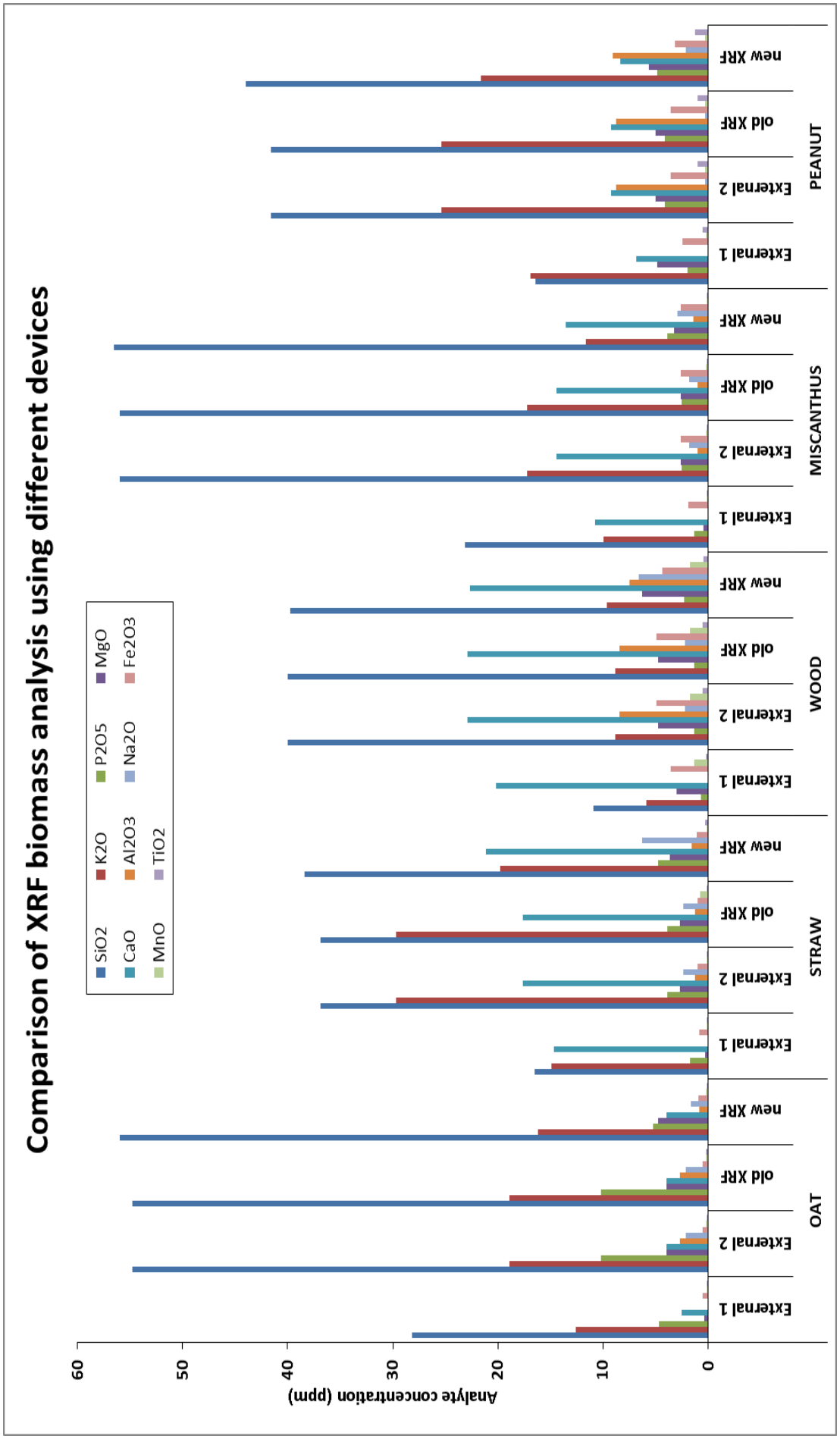

Figure 4-15 Comparison of data collected from different XRF devices using the same sampling material

Figure 4-15 shows, whilst some of the analytes measured across the different devices produced similar results, the difference between analytes is too significant to ignore.

There are a number of reasons for the difference: -

1) The experience of the user/operator is critical to the result which can be achieved in the analysis process. If the operator is unaware of how to use the device properly, unaware of the physics involved and is unaware of how the preparation can affect the result produced, then the data will vary greatly.
2) The type of analysis used. As previously stated there is more than one type of analysis. Depending on which analysis is used (qualitative, semi-quantitative and quantitative), the accuracy and the reliability of the results will vary.
3) The device used will greatly vary the result. Different devices have different detector power (kW), the type of detector, the atmosphere within the device and the complexity of the software and the algorithms used.
4) If and what type of standards are used to calibrate the XRF device will greatly alter the calibration curves and thus effect the data produced. It will also alter the way in which the normalisation program and the algorithms interoperate the raw data.

The findings shown in Figure 4-15 were discussed with technicians and the technical staff whom supplied the XRF device to be used for analytical work in this investigation at Leeds University. The previous points were highlighted as the most significant to impact the results achieved by the device. As a result, the technician running the XRF device has been given extensive training and time to become extensively familiar with all aspects of the device.

Within the limits of this investigation; the issues surrounding using XRF as a method for measuring biomass ashes and fluidised bed ash related complexes, has been addressed in terms of the effect of using different XRF devices. All such, measurements by this technique will be performed in the same manner and under the same regime, using the most modern and arguably accurate device in the Leeds University engineering labs. In doing so, comparisons can be drawn against other samples from the same device. However, caution will be taken when attempting to draw conclusions in terms of accurate quantitative data as more extensive work is needed to validate and guarantee the accuracy of the data produced by this analytical technique.

4.5.9 Pellet Preparation

Depending on the type of sample being entered into the XRF device, there is a choice of different mediums which the sample can be prepared. This includes; a fusion bead, which involves heating the sample to 1200°C in lithium borate powder, to form a glass like disk,

alternatively, the sample can be compressed into a disk with a combination of resins and waxes, or, alternatively a powder sample can be encapsulate between plastic sheets (mylar) in a capsule.

Each method has its advantages and disadvantages. The best method is creating the fusion disks, as this method can achieve more homogenous samples and present a more representative sample. However, this is a very work and time intensive method and requires a sample which will not undergo a chemical/physical change in the high temperature furnace. The pellet method is more difficult to ensure the sample is evenly dispersed but requires less time for preparation. The encapsulation method is very quick and simple, however, a large sample is needed to fill the capsule. Further to this, the plastic sheet used for encasing the sample will interfere with smaller atom elements in the sample thus distorting the results.

The three methods were run under the same conditions using a bulk ash sample. Each method of sample preparation was run using the XRF "Easyscan" method which offer less operational choices which was ideal for drawing a less convoluted comparison.

Figure 4-16 compares the data collected from each of the preparation methods against wet chemical analysis. Coals A, C, E, G and I were used as samples for the analysis as they posed the greatest contrast between the available fuels in terms of their chemical constituents and concentrations. The wet chemistry results are assumed to be the most accurate and representative based on the extensive work done prior. For each of the coals used in this part of the comparative work it is clear that no XRF method generates accurate and reliable data when compared to the wet chemistry result. Each method tends to produce data for one or more analytes which is similar to that of the wet chemical results but vary against other analytes. For instance, the Al_2O_3 value in the pushed pellet measurements and wet chemistry tend to be similar and the TiO_2 value in the fusions are similar to the wet chemical results. However, the difference in measured concentration for SiO_2 in all cases is very different to the wet chemistry results, ≥25% difference in some cases.

The preparation methods are ranked with increasing quality of results as loose powder, pellet and finally fused bead. This is due to the following reasons; firstly, the homogeneity and distribution of analytes within the sample, secondly, the homogeneity of the particles and their size fraction. The combination of varying particle sizes results in change in irregular distance between the source, sample and receiver. Combining this with radiation loss mechanisms such as Rayleigh scattering, the measured values become skewed, thirdly, the sample surface must be as flat as achievable as this will also effect the pre calibrated measured wavelength and result in smaller elements being lost in background noise and other wavelengths emitted (Van Grieken and Markowicz, 2001). The reasons stated here justify a

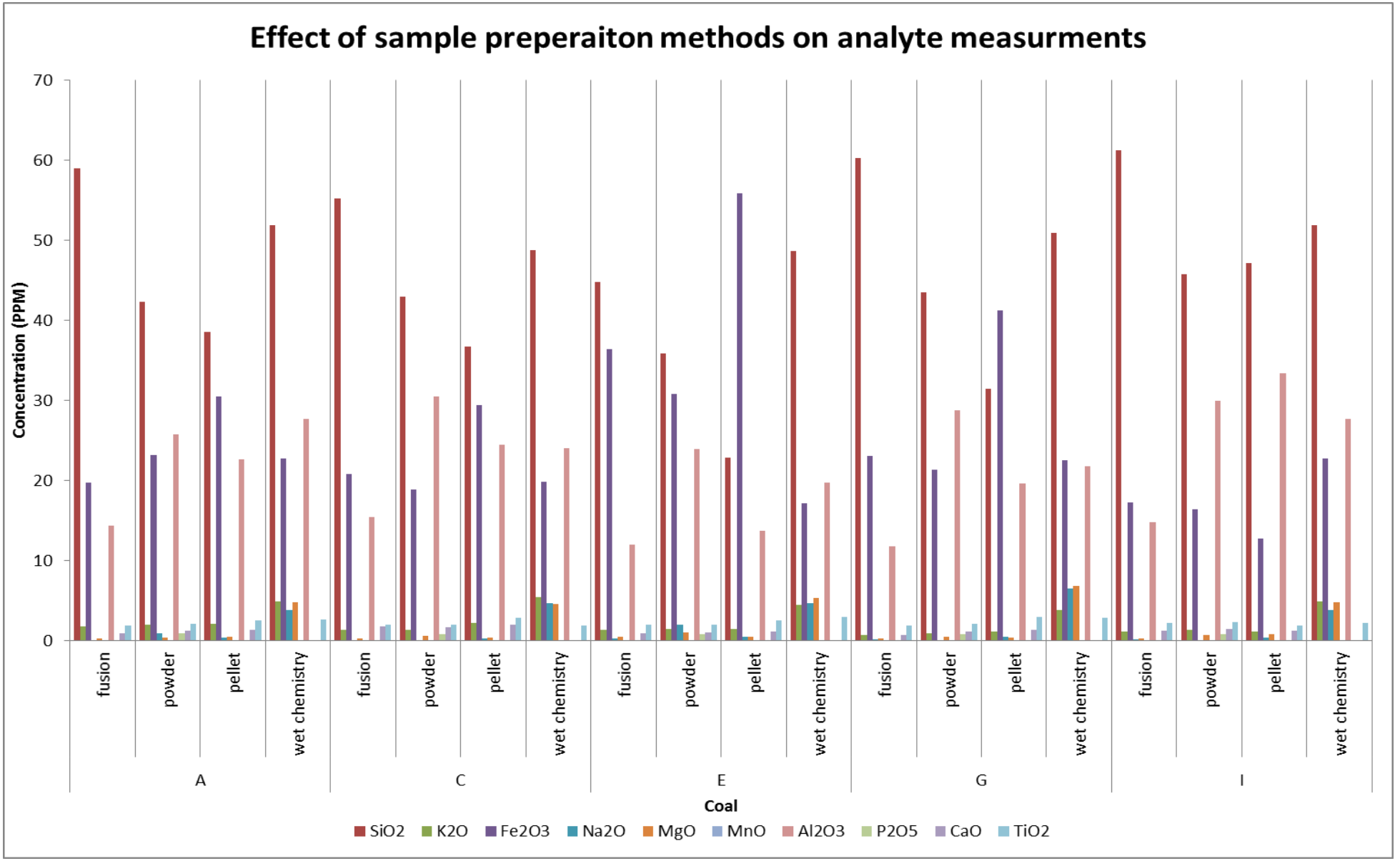

Figure 4-16 Sample preparation methods measured in a single XRF device for comparison of technique

large proportion of the differences in the samples, most notably the smaller elements which seemed to have been lost in background noise.

In the previous work the pellets were made up using a binding agent at a ratio of 1:3, sample to binder. The comparison was repeated to both validate the results collected in the previous comparison, validating repeatability, and to evaluate the effect the sample concentration in the pellets has upon measurements in analytes concentration.

The data gathered in the repeat work gave values which were similar to the original work with a variance of 2.1. It was found that the pellet with 50% sample gave measurements most similar to that of the wet chemical analysis as shown in Figure 4-17. The pellet with 90% sample was the next most closely matched. It is hypothesised that the addition of a binder and mixing caused for a better distribution of the sample within the pellets and as a result gave a more representative result. This is surprising, as the industry standard practice is to use fusion beads. This method ensures the greatest distribution of sample within the bead. However, it is the opinion of the author, based on the results seen in this work, that biomass ash, when heated to 1200°C in the fusion furnace, is likely to lose lower melting elements such as K and Na. Combine this with a normalisation program within the XRF analysis software and the values hence become less representative than that of the less accurate method i.e. pushed pellet.

The conclusion of this work suggests that for biomass and in particular biomass ash, the fusion technique may not be the most applicable route for analysis in XRF. The results presented here reinforce the need to cross validate collected data of samples with other

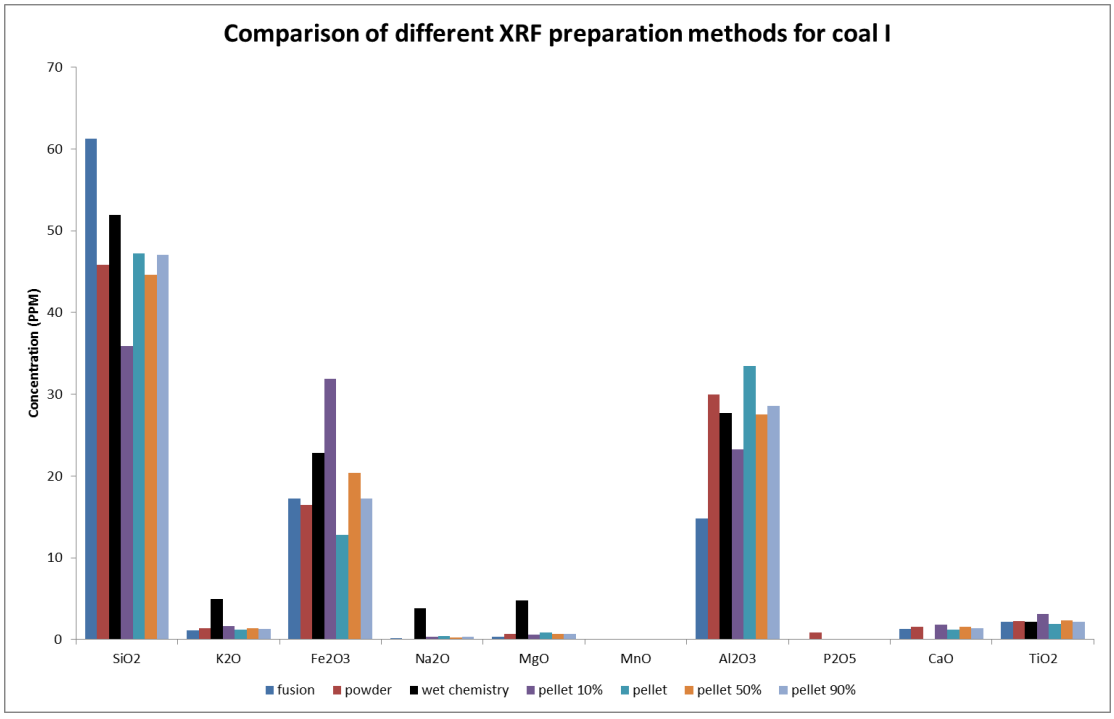

Figure 4-17 validation of XRF sample preparation methodology

analysis techniques. As such, in following results Chapters' bed samples and ash samples are to be compared against pervious analysis results to help identify any obvious variations. Secondly the application of standards is to be undertaken to better improve and background noise in the results.

4.6 Conclusion

Throughout the fuel characterisation Chapter a series of biomass and sub-bituminous coals were analysed via a number of different techniques in order to understand the chemical and physiological characteristics of each fuel.

Different techniques were employed to analyse the fuels including ultimate, proximate, SEM-EDX, ash fusion, XRF and bomb calorimetry. The analysis conducted demonstrated how the fuels would combust, how the ash would behave and identified the chemical components within the fuels. This work has illustrated the variance between the fuels and the significant differences in their fundamental makeup. This work has given information which can be used to correlate, in combustion testing, the cause of agglomerates and where species come giving an insight as to how a fuel is likely to react in fluidised bed systems.

The characterisation work has identified fundamental alkaline species within the fuels which are associated with agglomeration mechanisms. The coals high Fe, Ai and S concentrations caused by the presence of pyrite in the coal gives a strong indication to a Fe-Si dominated agglomeration mechanism likely to occur during combustion. Whereas, the biomass analysis identified high concentrations of K, Na, Si and Ca components which have been seen in the literature review Chapter to be associated with agglomeration and slagging mechanisms.

The analysis performed as well as indicating likely modes for bed slagging and agglomeration based on data in the literature has also produced a source of information required to perform predictive methods on the fuels. The data collected in this Chapter will be key to evaluating predictive methods such as indices and thermodynamic modelling techniques in Chapter 4.

A significant part of this Chapter has been the investigation of XRF application in the analysis of low grade fuels such as biomass. Throughout the Chapter and subsequent testing, XRF has been shown to produce variable results using conventional coal XRF analysis methods. However, as the work previous shows, there has been significant improvements to the analysis technique by modifying preparation sampling, ashing, validation methodology and device modifications. The XRF technique now available at the University of Leeds engineering department can better analyse low grade fuels when compared to its previous arrangement. Whilst there is likely still opportunity for improvement, as it stands at the end

of this investigation, XRF is a valuable technique for analysing low grade fuels but requires validation via other analysis techniques to ensure accuracy.

Table 4-7 is a summary of available literature which has been conducted since 2010 specifically around issues and problems and the solution being employed to tackle XRF accuracy for low grade fuels. This is an indication of the work and scope of the area in its application for such samples.

Table 4-7 literature review of research and investigations around XRF since 2010	
Sample preparation	(Loubser and Verryn, 2008; Anzelmo, 2009; Gazulla et al., 2009; Stankova et al., 2010; Wang et al., 2010; Gazulla et al., 2010; Matsunami et al., 2010; Pease, 2013; Le Roux and De Vleeschouwer, 2010; LUO et al., 2011)
XRF analysis technique(s) & methodology development	(Gazulla et al., 2010; Fernández-Ruiz et al., 2010; Robinson et al., 2009; Andersen et al., 2013; Morgan et al., 2015; Teng et al., 2013; de Jonge and Vogt, 2010; Terzano et al., 2013)
Review(s)	(Evans et al., 2014; Taylor et al., 2014; Clough et al., 2014; Gibson et al., 2014; Butler et al., 2015)

5 Modelling & Predicting Agglomeration in FBC

The testing and use of the experimental rig is a practical and empirical method which can be used to determine the outcome of combusting different fuels in a FBC unit. This data can be used and extrapolated up to more commercially scaled operations and shed light upon the likely outcomes in applying the fuels of this investigation within a commercial operation. However, the time and direct application of the results takes time and money whilst be limited by unforeseen scaling factors such as air distribution limitations known to occur in fluidised beds (Zhu, 2013).

An alternative method to a solely experimental investigation is the application of theoretical modelling to determine the likely outcome of a system or process. The results of which allow designers and operators to make informed decisions on how to proceed based on expected outcomes.

"Factsage" is a commercially available software which uses thermodynamic properties such as Gibb's energy in order to predict the chemical composition and thermodynamic changes in a defined system. This software package has a number of different applications, allowing users to enter details such as ash composition and environmental factors including temperature in order to produce data on formation of compounds typically found in slag which would form over varying temperatures in a typical combustion system. This section will show the application and crossover of the software whilst further expanding results found in the experimental work previously described in Chapter 5 and 7.

5.1 Liquid Slag Formation

Fluidised bed combustion typically has a temperature range of 800-900 °C and as such eutectic compounds forming at this temperature range are important to understanding the formation of agglomerates and slags. Agglomerates have been found to occur using the fuels described in Chapter 5 and 7. The Factsage software has an "Equilibrium "model which allows users to enter ash composition data and environmental variables which produces chemical formation data as an output. As such, the following sections will describe the application of the model in predicting and describing the formation of alkali related slag phases and in doing so relate this to the agglomerates experienced in previous Chapters.

5.2 Liquid Melt Phase Modelling

As discussed in previous sections, the liquid melt phase and the rate at which the melt phase occurs at different temperature ranges, will alter the rate of deposition and agglomeration mechanisms in fluidised beds. Experimental testing of liquid melt formations has been shown in the fuel characterisation section (Chapter 4) using the established analysis method of high temperature ash fusion. However, whilst this method gave good results as ash samples melted over increasing temperature, it was difficult to see accurate melt phases and differentiate between the different melting stages.

In order to determine, via ash fusion techniques, more accurately when melting phases are occurring, a combination of experimental and computational techniques should be adopted. For this reason, the Factsage Equilibrium model was applied to model the formation of compounds, primarily slag/liquid melt phase compounds, over variable temperature ranges, thus simulating these processes which could take place in a fluidised bed combustion system.

XRF data collected in the fuel characterisation Chapter was used as input for the biomass and coals in the FACTSAGE equilibrium model software. The analytes entered were: Ti, Si, K, Mg, Mn, Na, P, Al, Ca. The data was entered in the steps dictated in the following sections making it possible to

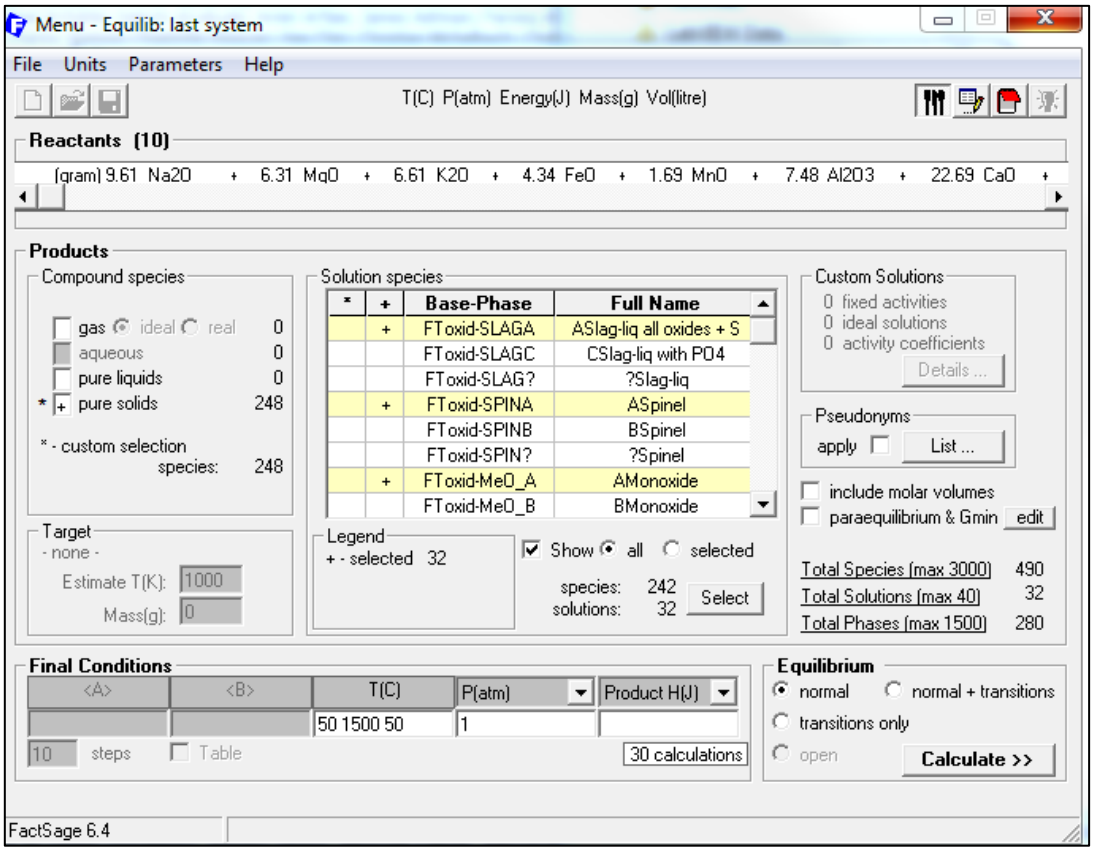

Figure 5-1 Main screen for FACTSAGE Equilibrium model software

produce theoretical predictive data which potentially represented the formation of fouling/depositing/agglomeration compounds in the experimental fluidised bed.

Table 5-1 databases and solutions included within the Factsage model for low grade fuels		
Solution species	Modelled species	description
FToxid-SLAG	MgO, Na_2O, SiO_2, K_2O, Al_2O_3, Fe_2O_3, MnO, P_4O_6 & TiO_2	slag/liquid Si rich solution K,Mg,Mn,Na,Ni,Pb,Si,Sn,Ti ,Zn,Zr, Al,As,B,Ca,Co,Cr,Cu,Fe,G; dilute S, SO_4, PO_4, H_2O/OH, CO_3, F, Cl (selection based on fuel)
FToxid-SPINA	Spinel ($MgAl_2O_4$), Magnetite (Fe_3O_4), Hercynite ($FeAl_2O_4$), Magnesioferrite ($MgFe_2O_4$), Trevorite (NiFe2O4), Pleonaste ($MgAl_2O_4$– $FeAl_2O_4$)	solid & liquid solution considered
FToxid-pPyrA & LcPy	$MSiO_3$– MAl_2SiO_6– MFe_2SiO_6, $CaMgSi_2O_6$, $CaFeSi_2O_6$ and $CaAl_2SiO_6$, $FeSiO_3$, $CaMgSi_2O_6$ – $Mg_2Si_2O_6$ & $MgSiO_3$	solid solution
FToxid-C2SaA & C2SaB	Mg_2SiO_4, Fe_2SiO_4, Mn_2SiO_4, Ca_2SiO_4	liquid solution
FToxid-Mel	$Ca_2MgSi_2O_7$, $Ca_2Al_2SiO_7$, $Ca_2MgSi_2O_7$	solid solution
FToxid-MulF	$Al_6Si_2O_{13}$,	solid solution with Fe(III) in dilute solution
FToxid-CAFS/CAF6/CAF2/CAF1/C2AF/C3AF	$CaAl_{12}O_{19}$,$CaAl_4O_7$, $CaFe_4O_7$,	$(CaO)_2(Al_2O_3)_4SiO_2$ $(CaO)_2(Fe_2O_3)_4SiO_2$ solid solution/ $CaAl_{12}O_{19}$-rich/ $Ca_2Fe_2O_5$ rich
FToxid-NAS1	$NaAlO_2$	solid solution with low-temperature $NaAlO_2$ and excess $NaAlSiO_4$
FToxid-PERO	$Ca_2Ti_2O_6$– $Ca_2Ti_2O_5$	solid solution
FToxide-AlSp	Hercynite ($FeAl_2O_4$), Spinel ($MgAl_2O_4$), Galaxite ($MnAl_2O_4$)	solid solution
FToxid-CORU	Corundum (Al_2O_3) & Hematite (Fe_2O_3)	Al_2O_3-Cr_2O_3-$Fe_2O_3^+$ (Mn_2O_3, Ti_2O_3 in dilute amounts)

The inputs were entered through the input screen shown in Figure 5-1 in the steps as followed.

Chemical species to be modelled were entered in the prompted window. For the purposes of this work the compounds were the stable oxide forms of the analytes of interest.

Selection of the correct databases was crucial. There are a variety of databases, each with pros and cons as a result of the papers and sources which the data is based on. For this work the "FToxid_SLAGA", "Fact_PS" and ELEM included the fundamental solutions of this work

however, other databases as shown in Table 5-1 were included in more comprehensive applications shown later on in the work. Using the main screen, it was possible to go through the sub categorised database and choose specific reactions to both include and exclude. This is particularly useful as some reactions have more than one database due to transition and phase boundary data which conflicts.

The core of the information is entered, now the units, variable conditions and environments for the theoretical reactions to take place within the system. Using the unit's tab, standard units were selected. Using the variables tab, the pressure, free energy, temperature range, heating rate, temperature profile spacing, phase data, type of output etc. were selected. The final inputs tweaked the system by limiting certain reactions and specifying the output objective of the software e.g. model precipitating compounds of the identification of eutectic points.

After clicking the "calculate" function, the data was produced in a number of formats including text and graphical. The software "FACTSAGE XML" is a spreadsheet program allowing for limited manipulation of the graphs and was used to produce the figures seen later in this Chapter of work.

In order to simulate the combustion environment of a fluidised bed the temperature ranges selected had to include 500-1200 °C. In most cases this range was increased to include both lower temperatures and higher temperatures (100-2500°C). This was to produce more complete data series and thus produce better graphical plots so more thorough examination of the liquid slag formation phase could be accomplished. The pressure within the system was 1 atm to simulate the atmospheric bubbling fluidised bed and the oxygen concentration was 20.95 % to simulate the air entering the combustion zone.

5.2.1 Modelling Approach

The initial modelling work, as shown in Figure 5-2 shows the evolution of a liquid phase over increasing temperature from 1 kg of ash from the fuels within this study temperature range. Image a and b contain predictive data for the coals used in the previous Pakistani coal Chapter. Whilst image c and d contain predictive data for the biomass fuels used in the biomass Chapter.

The reason for two graphs for each series of fuels is that the first image of each set i.e. a and c use a more basic modelling process, whereas image b and d uses a much more complex method.

Graph b Figure 5-2shows d the differences between the approaches. Fundamentally the FACTSAGE program uses a collection of databases which contain the thermodynamic and chemical data required for the program to calculate outputs based on the variables the user enters.

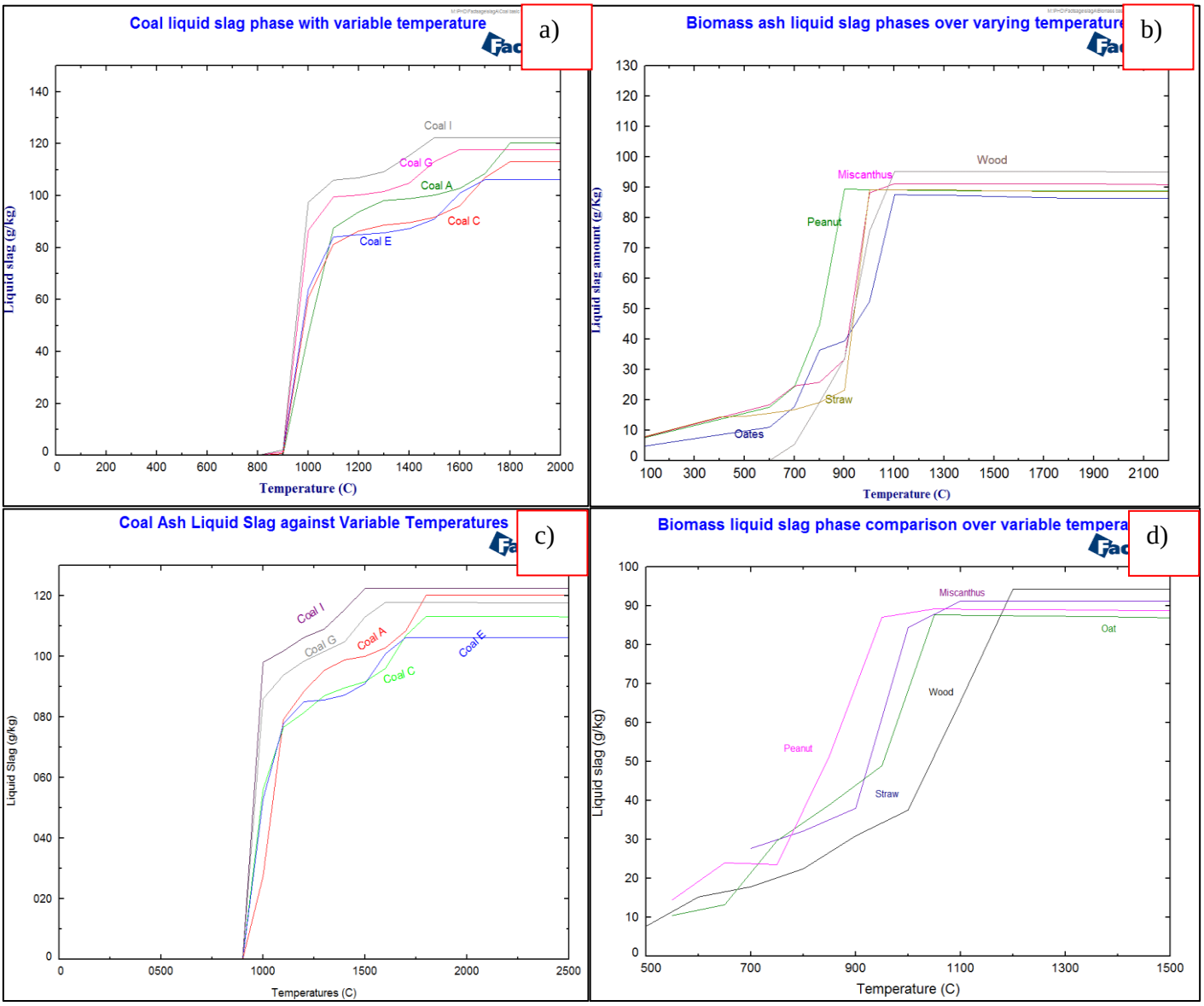

Figure 5-2 Liquid "Slag" melt phases over increasing temperature using both the basic approach and a more complex approach with FACTSAGE Equilibrium model; a) Different coals slag melt phases using the basic model, b) Different coals slag melt phases using the complex model, a) Different biomass slag melt phases using the basic model and, b) Different biomass slag melt phases using the complex model.

However, there are more than 50 databases with varying quantities of various data. The datum itself is the product of experimental research and has been reported in journals, which is referenced in the databases. For the basic model the “FT-oxid_SlagA” database was used, which holds the most complete series of data on all oxide compounds used in this work. This database is built up of validated publications and as such has been used in a number of other studies found in the literature including; (Ryś-Matejczuk et al., 2013; Reinmöller et al., 2015; Berjonneau et al., 2009).

The complex model used the same database plus an additional 47 (shown in Table 5-2) databases chosen based on their chemical content and the chemistry of the fuels demonstrated in the fuel characterisation Chapter, the paper references, experience whilst using the program and discussions with the FACTSAGE personnel.

Table 5-2 Model differences between a "basic" and more "complex" approach

Variables	Basic model	Complex model
Databases	1	48
Species	274	657
Solutions	2	48
Phases	250	296

Whilst using FACTSAGE with all the database seems advantageous, in practice the complex interactions of the chemical species doesn't always make this possible. Firstly, data between databases doesn't always agree with one another, because it has been determined experimentally and thus there is a level of variance in the result. Secondly, whilst more databases mean more available data, it also means there are more gaps between data series in the calculations, leading to errors in the calculation software and calculations reaching a state of "non-equilibrium" thus rendering the data void. Finally, the FACTSAGE software has been designed in such a way that it will attempt all calculations no matter the time period. In the authors experience, in many cases the more complex configurations left to run for 48 hours achieved little benefit if any. This will be demonstrated in the following sections and data sets.

This final point (and the others) can be seen in Figure 5-2between the two-data series of each fuel type. Both data sets show the initial slag formation phase occurring at 800°C and increasing sharply to 1300°C, followed by a curve of lesser gradient to 1800°C. In both cases this can be seen, however, the initial steep gradient and the following lesser gradient curve have slightly different bumps and angles. This is because in the complex model more compounds and phases have been evaluated giving a slight variance on the basic data. Both lines should be similar as both contain the same fundamental data in the "SlagA" database. The difference being the complex model has the potential to identify variance on this fundamental data with its more extensive data series. Because of the results seen here, i.e. the slight variance in data between basic and complex modelling approach, it was decided that both approaches should be evaluated when using FACTSAGE for modelling both poor grade coal and biomass fuels.

5.2.2 Liquid Melt Phase-Coal

The results in Figure 5-2 a and b, show that the initial liquid slag melt phase for the low-grade coals starts at 800°C. This is followed by a steep increase in liquid melt, releasing over 80% of the liquid melt by the time all the coals have achieved a temperature between 900-1000°C. For each coal, when approximately 90-95% of the total liquid melt phase has been released there is a lesser curve in the production of the melt phase until a maximum temperature of 1500-1800 C, at which point no further melt phase is produced.

The data shown in Figure 5-2 suggests that when this coal is combusted in a typical fluidised bed combustion system, the majority (up to 90 % or 100 g/kg) of the liquid slag melt phase will be released from the coal. The data produced suggests that the coals used would produce a slag melt phase when operating a fluidised bed at normal conditions. This could result in increased issues associated with the release of such melts, including agglomeration propagation. However, further analysis is required to identify the contents of the melt phase in order to establish the nature of the released compounds and thus their effect on the system.

A note should be made that there are a number of small differences between the two coal data sets but the differences are trivial and do not detach from the main trends shown in both. The complex model indicates there may be release of compounds at particular points but without further analysis these compounds at this point are not known.

5.2.3 Liquid Melt Phase-Biomass

Before analysis of the results shown in Figure 5-2, c and d, (the initial liquid slag melt phase for the biomass fuels), it should be noted that the model could not produce reliable results for any of the biomasses below 600°C. The basic model produces trend data from 0°C to 600°C however, it is highly unlikely that there will be a melt phase at the lower temperature ranges shown, especially at 0°C. When the biomass data was produced by the complex model it simply crashed until a lower temperature range of 500-600°C was entered at the input screen. This suggests there is either missing data for this combination of input species or the software was not designed for this type of fuel.

After discussion with the FACTSAGE developers it was found that the software and data used for some of the major databases referenced experimental results using coal. Because of the significant difference in thermodynamic properties of coal and biomass, when biomass type fuel data is entered in to the model there are discrepancies resulting in crashes and erroneous data. At the time of undertaking this work the author was using FACTSAGE version 6.4. Subsequent to these discussions, but outside the timescale for this work, an improved version 7.1 (October 2016) has

been released -which includes expanded databases containing more compounds and data relevant to biomass calculations.

There are significant differences between the basic and complex modelling approach for the biomass fuels. The initial slag melt phase varies between 700-900 °C in the basic model whereas the complex model has a range of 600-1000°C. In both models, there is a steep increase in the melt phase released, for 100-200°C following the initial melt. In both cases the maximum liquid melt released is approx. 100g/kg^3 at a temperature of approx. 1000°C for the basic model and 1100°C for the complex model. There are large differences between each of the biomasses in both models, but this is expected as the chemistry of each fuel is particular to each fuel. Peanut and oat show similarities as both are a seed and come from a similar part of the plant/source/growth type etc. Straw and Miscanthus also show similarities which is also to be expected as they are both grassy type biomass.

5.2.4 Liquid Melt Phase Conclusion

The data shown in Figure 5-2 indicates that the models can produce data showing trends for the melt phase of the fuels. However, the data also shows that depending on the chemical makeup of the fuel there can be large variation in the results achieved. The data produced can fluctuate dramatically with a small change in a particular chemical species such as potassium, which is an important element for fuel chemistry. This challenges the accuracy and validity of the data to real life systems that are being modelled. The coal data shows a more realistic breakdown of the expected outcome compared to the biomass. However, without further analysis of this slag break down the information is incomplete.

5.3 Liquid Slag Major Oxides

In order to understand what the "Slag" data actually represented in Figure 5-2 it was necessary to breakdown this data into its constituent parts. As the data, which was entered into the model was oxides from XRF measurements, it is these which have been chosen to calculate in Figure 5-3 to Figure 5-6.

5.3.1 Major Oxide Model Difference

Without repeating previous descriptions of the basic and complex model, there are clearly differences between the produced data in Figure 5-5 and Figure 5-6 the major oxides from the basic model and from the complex model shown in Figure 5-5 and Figure 5-6. The data for straw could not be calculated in the complex model, and the lowest calculated data for the complex model was

at 500°C whereas for the basic model data was collected at 100°C. This was due to the reasoning discussed in the previous section.

However, as can be seen between Figure 5-3, Figure 5-4, Figure 5-5 and Figure 5-6 the differences between the basic and more complex model are visible but significantly less dramatic for coal the biomass. Once again this has been previously discussed in the previous section but reinforces the statements already established, that without the biomass update to the FACTSAGE software it seems there are variances in the data produced.

5.3.2 Biomass Major Oxides

The major oxide shown for biomass within the slag of Figure 5-3 and Figure 5-4 is SiO_2. SiO_2 on its own is relatively inert and has an initial melt temperature of 1450°C (Werther et al., 2000). However, SiO_2 will react to form low melting eutectics in the presence of alkali metals and salts. The second major constituent oxide in the slag is Na_2O and K_2O. SiO_2 will form low melting eutectics with these alkali oxides to form Na_2O-SiO_2 (790-874°C) (Werther et al., 2000; Gupta et al., 2007) and K_2O-SiO_2 (764°C) (Werther et al., 2000) through the reactions shown in Reaction 5-1 and Reaction 5-2:

$$2SiO_2 + Na_2CO_3 \rightarrow Na_2O \cdot 2SiO_2 + CO_2$$ Reaction 5-1

(Werther et al., 2000)

$$4SiO_2 + K_2CO_3 \rightarrow K_2O \cdot 4SiO_2 + CO_2$$ Reaction 5-2

The melting points of these eutectics are within typical combustion conditions for a fluidised bed and thus pose a potential issue in terms of the formation of sticky particles which would lead to the onset of agglomeration. The formation of these low melting eutectics can be seen to influence the formation of the slag melt in Figure 5-2 c and d. There are sharp increases in the formation of the liquids melts at the same temperature as the formation of these eutectics. However, there is a decrease in the melt phase at around 1000°C.

This can be explained by the increase in the release of Ca, Mg, Al_2O_3 and Fe_2O_3 at around 1000°C. Ca, Mg, Al and Fe especially will compete with SiO_2 and other alkali groups to from eutectics but at higher temperatures than K and Na with SiO_2 (Duan et al., 2015). The liquid melt phase of Figure 5-2 decreases in rate after the 1000°C as the affinity of the K_2O and Na_2O complexes move away from SiO_2 structure and form high temperature eutectics (Rizvi et al., 2015b). This trend can be seen for wood especially. At 1000-1100°C CaO is released in abundance contributing to the formation of CaO-SiO_2 and K_2O-CaO-SiO_2 (Scala and Chirone, 2008).

5.3.3 Coal Major Oxides

Figure 5-3 and Figure 5-4 shows the major oxides distribution for the melt phase for the coals and indicates that similarly to the biomass results, SiO_2 is the largest constituent. However, whilst the biomass slag phase started between 600-700°C, the coal melt phases start higher at ≥900°C. There is a significant spike in the SiO_2 which decreases in gradient as well as the formation of Na_2O. Whilst in the biomass fuels this was dominant, in the case of the coal fuels the formation of FeO becomes dominant. This is indicated by the decline in SiO_2 formation and the decrease in the formation of Na_2O. The Fe complexes are dominant and have a greater affinity to form eutectics with alkali metals such as K and Na through the reactions shown in Reaction 5-3 to Reaction 5-5 (where X is Na or K), at a temperature of 1135°C (Werther et al., 2000; Olofsson et al., 2002).

$Fe_2O_3 + X_2O \rightarrow X_2Fe_2O_4$	(Werther et al., 2000)	Reaction 5-3
$Fe_2O_3 + X_2CO_3 \rightarrow X_2Fe_2O_4 + CO_2$		Reaction 5-4
$K_2O \cdot nSiO_2 + Al_2O_3 \rightarrow K_2O \cdot Al_2O_3 \cdot nSiO_2$	(Duan et al., 2015)	Reaction 5-5

Na based complexes continue to diminish for each of the coals with increased temperature as alkali metals such as this enter a vapour phase forced by preferential reactions with the Ca, Al and Mg. This is in agreement with work conducted by a number of authors, (Olofsson et al., 2002; Varol and Atimtay, 2015; Duan et al., 2015; Fryda et al., 2008), through reactions such as that in Reaction 5-3 to Reaction 5-5.

The results of the major coal oxides agree with expected reactions such as those shown in previous figures, but also agree with the experimental findings in the low-grade coal section. To summarise, the agglomerates which were found as a consequence of burning low grade fuels, contained eutectic compounds rich in Fe_2O_3-SiO_2 and Al rich complexes. These formed as a result of localised hot spots and sintering mechanisms. The temperature range correlates with the data produced here using the FACTSAGE equilibrium program. This correlation highlights two points, firstly, that the FACTSAGE software has an application in this type of combustion system and can generate trend data for the prediction and interactions a system may experience, and secondly, that the results in Chapter 5 correlate with both literature on the subject and expected outcomes in such scenarios.

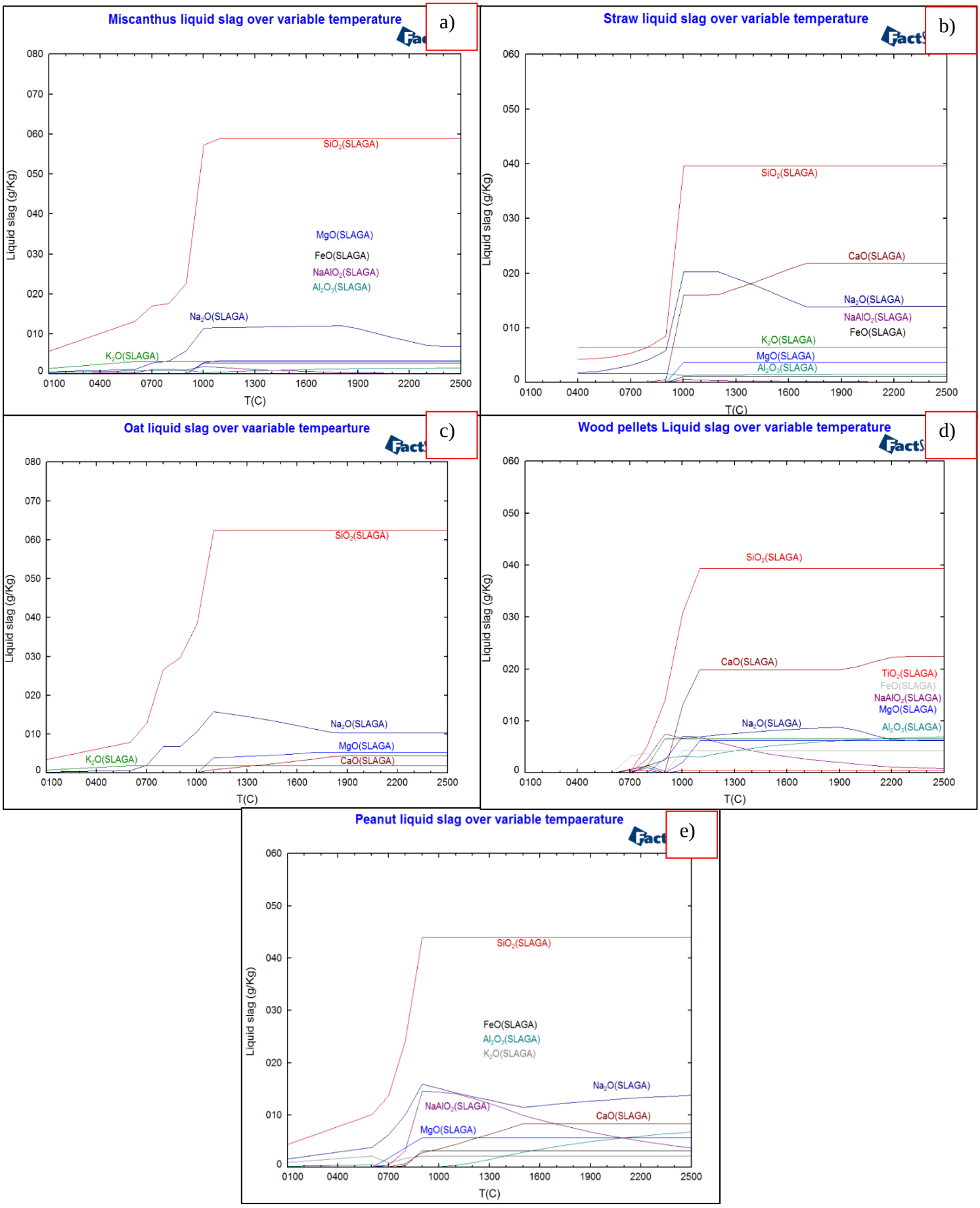

Figure 5-3 Modelled liquid slag major oxides for biomass fuels over a temperature range of 100-2500°C (basic model)

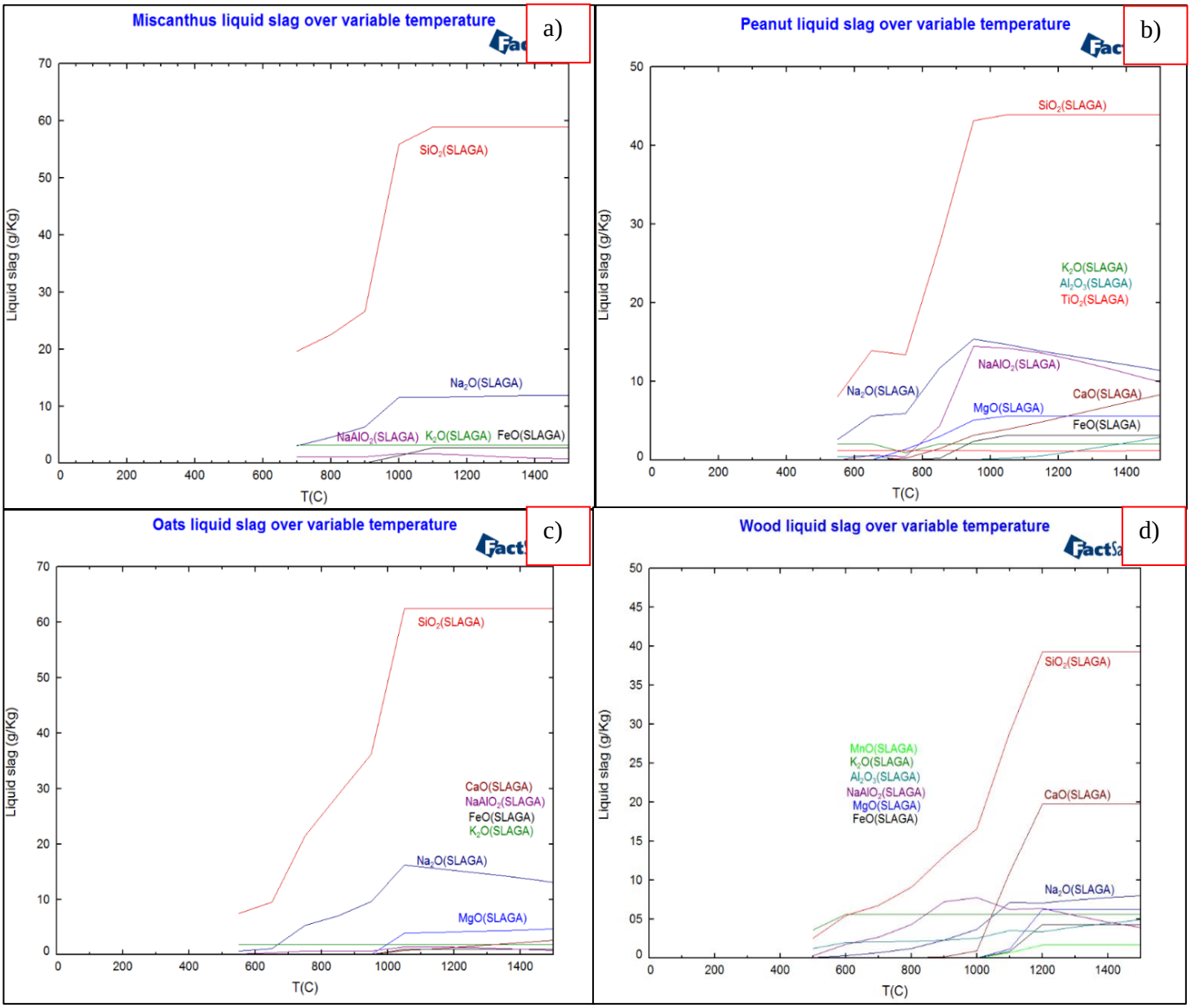

Figure 5-4 Modelled liquid slag major oxides for biomass fuels over a temperature range of 100-2500°C (complex model)

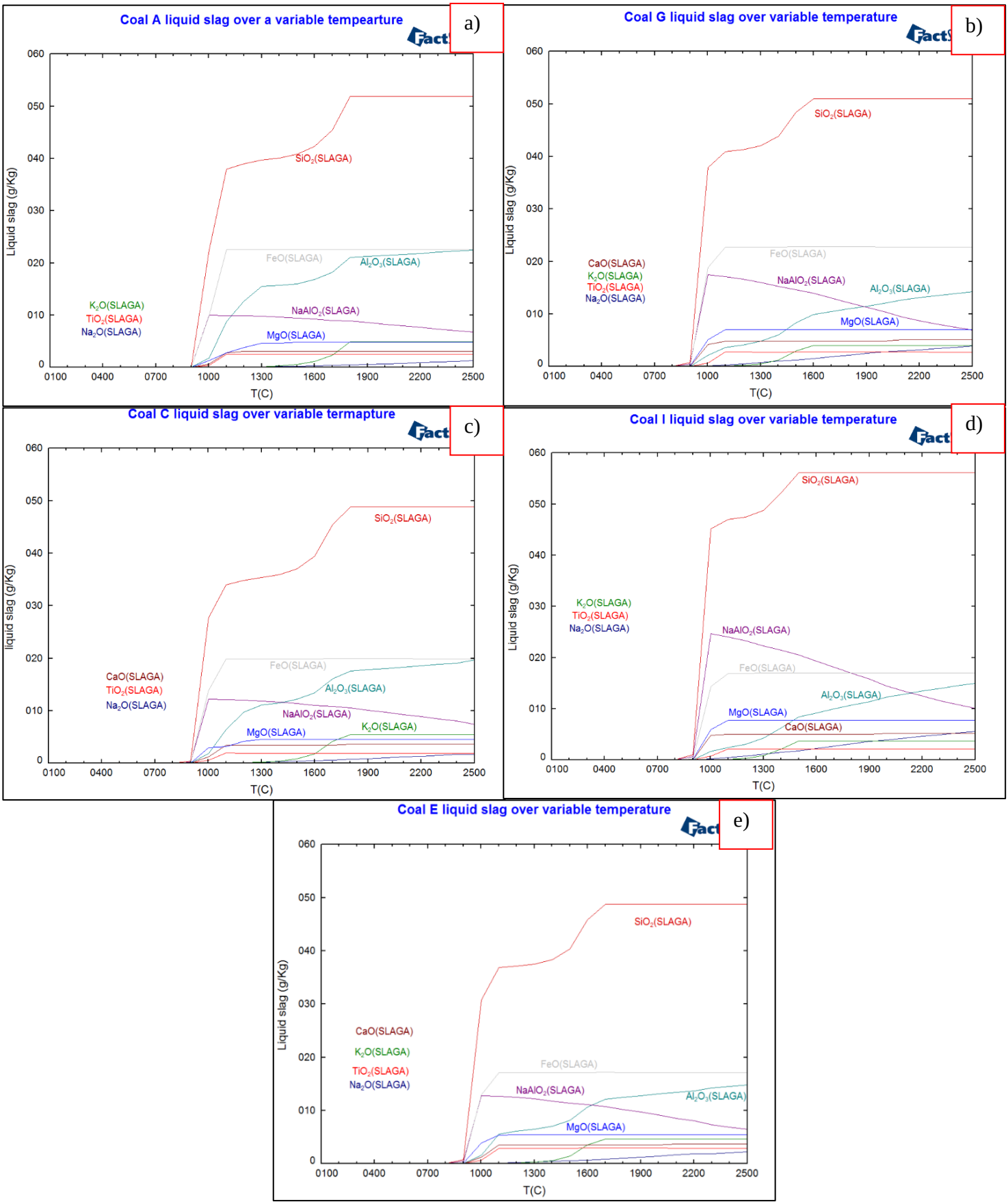

Figure 5-5 Modelled liquid slag major oxides for coal fuels over a temperature range of 500- 2500 °C (basic model)

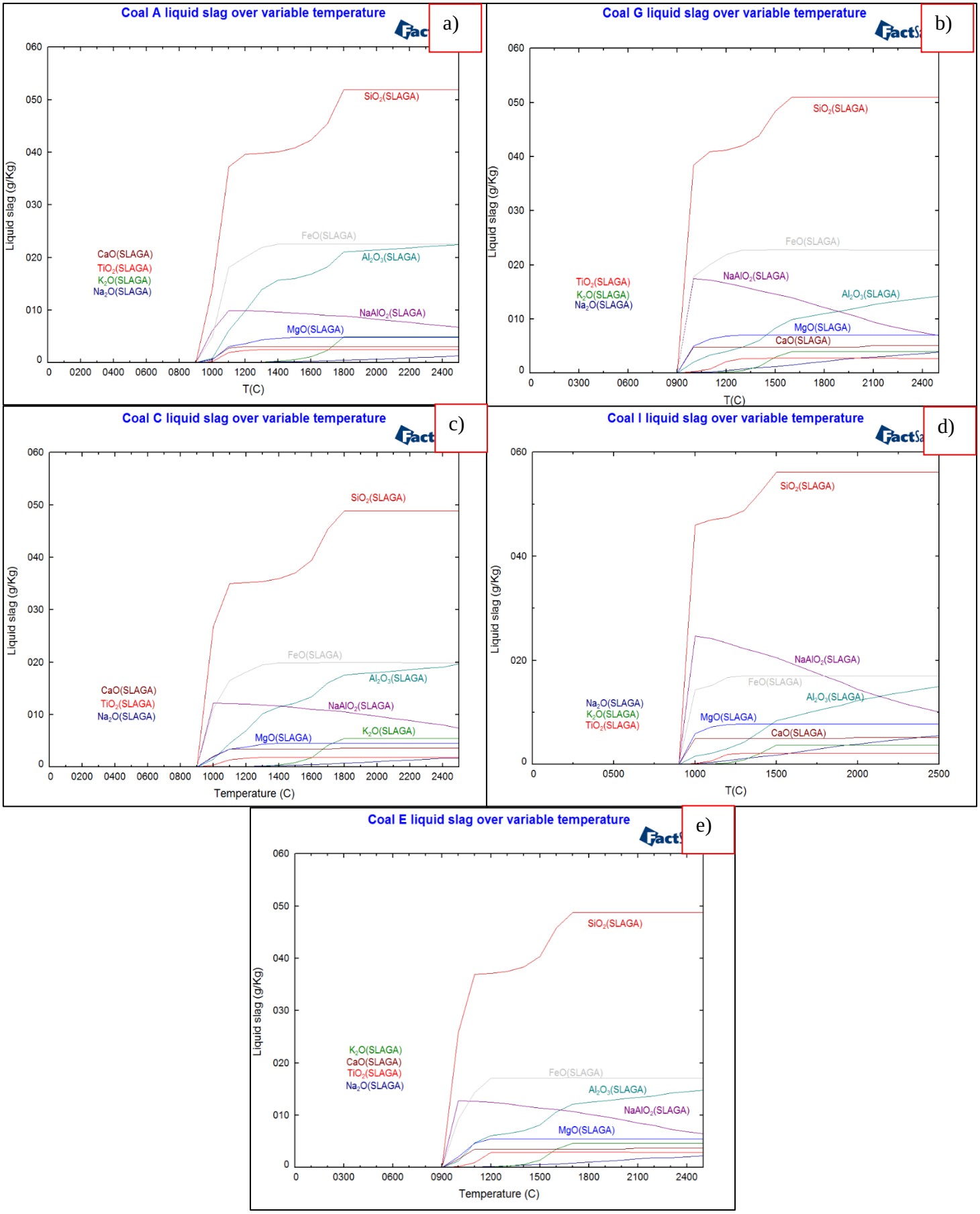

Figure 5-6 Modelled liquid slag major oxides for coal fuels over a temperature range of 500- 2500 °C (complex model)

5.3.4 Slag Major Species

Further analysis and deconstruction of the data produced in the basic and complex model was the stable solid phases which theoretically existed within the liquid melt phases. Figure 5-3 to Figure 5-6 shows the results of the stable solid phases over temperature ranges.

The data series in these plots originate from the same data series as used previously. Therefore, there are discrepancies between the complex and basic models as previously discussed and need not repeating.

However, is should be noted that the trends of all the basic vs. complex model data series are similar and represent the same outcome but with varying levels of accuracy and details for biomass fuels. The basic data has produced random data at the 0-200°C, which is then followed by a rapid increase before trends fit the correlations expected. This is the result of calculations being in a state on non-equilibrium and thus the values are incorrect and the data that is produced must be discarded as it clearly doesn't fit the rest of the data.

With reference to the coal solid phase data, the basic model contains little or no information required to calculate Fe rich complexes. As seen in the previous section FeO was a major oxide in the slag phase. However, in the basic model for stable solids the Fe rich complexes feature -. It isn't until the complex database collection is used and the addition of Fe data allows for a more realistic picture of theoretical stable solid phase data to be produced. Hence descriptions on trends etc. will refer to the complex data outputs not basic in this case.

5.3.5 Biomass Slag Major Species

As Figure 5-7 and Figure 5-8 shows, the biomass fuels produce sodium rich solid phases in the slag phase up to a maximum temperature range of 1000-1100°C. After this point the solid Na dominant phases are replaced by Ca, Mg and Na silicates and phosphates where the phosphate and silicate species are the macro networks. This system for solid phases has been experienced experimentally by (Niu et al., 2013) and through theoretical FACTSAGE analysis by (Rizvi et al., 2015b). A number of applicable high temperature complex formations of calcium and magnesium silicates were described by both as shown in Reaction 5-6 to Reaction 5-10 Whilst there are a number of complexes formed ≥1000°C, the Na rich solid phases are of more concern to typical FBC operating conditions. As described previously, these Na rich melts form at 874°C, which means agglomerates and negative effects are likely to be seen in the bed with these fuels. The data here indicates that in order to mitigate the formation of Na complexes either a different fuel, combustion temperature range or additives rich in Ca or Mg such as Kaolin ($Al_2Si_2O_5(OH)_4$, dolomite ($CaMg(CO_3)_2$,

gibbsite ($Al(OH)_3$) etc. to alter preferential reactions to less "sticky" compounds (Linjewile and Manzoori, 1999; Tangsathitkulchai and Tangsathitkulchai, 2001).

$$2CaSi_2 + 5O_2 \rightarrow 2CaSiO_3 + 2SiO_2$$ Reaction 5-6

$$2CaSiO_3 + MgO \rightarrow Ca_2MgSi_2O_7 + 3SiO_2$$ Reaction 5-7

$$2CaSi_2 + MgO + 6O_2 \rightarrow Ca_2MgSi_2O_7 + 3SiO_2$$ (Niu et al., 2013; Rizvi et al., 2015b) Reaction 5-8

$$14CaSi_2 + 2MgO + 35O_2 \rightarrow 2Ca_7Mg(SiO_4)_4 + 20SiO_2$$ Reaction 5-9

$$14CaSiO_3 + 2MgO + 21O_2 \rightarrow 2Ca_7Mg(SiO_4)_4 + 6SiO_2$$ Reaction 5-10

5.3.6 Coal Slag Major Species

Figure 5-9 and Figure 5-10 shows the data series for stable solid phases within the slag phase over increasing temperature. As the figure shows, the largest constituent parts contributing to solid phase complexes are Na, K, Ca and Mg in silicate and phosphate forms. Below 800°C, silicates are the dominant solid phases, however, between 800°C and 1000°C, with phosphate groups replacing the Si groups.

Phosphorous has been found to lower the melting temperature of eutectic complexes and thus stripping the silicates of K, Na etc. at ≥1000°C. This has been seen in a number of agglomeration/fouling studies with phosphorus rich fuels/additives/bed materials, forming sticky phosphates which adhere to the bed particles and thus creating the foundation for agglomeration mechanisms (Lindström et al., 2007; Piotrowska et al., 2010; Grimm et al., 2011; Barišić et al., 2008). An example of phosphate eutectic formation is as shown in Reaction 5-11 and Reaction 5-12:

$$Mg_3(PO_4)_2(s) + K_4P_2O_7(s) \rightarrow 3MgKPO_4(s) + KPO_3(s)$$ (Lindström et al., 2007) Reaction 5-11

$$2Mg_3(PO_4)_2(s) + 2K_4P_2O_7(s) \rightarrow 5MgKPO_4(s) + MgK_2P_2O_7(s) + KPO_3(s)$$ Reaction 5-12

As previously stated the formation of solid phase Fe complexes can be found throughout typical FBC operating temperatures. The data in Figure 5-9 and Figure 5-10 shows this. Whilst the Fe groups are effected over the temperature range i.e. also moving from silicate to phosphate groups, it should be noted that the temperatures experiments have carried out at would produce mainly Fe-Si-O2 complexes. The agglomerates found in the experimentation with these fuels produced complexes as the model theorises. This is further confirmation that the model is generating realistic experiments have occurred because of the fuels characteristics and not because of operational variables.

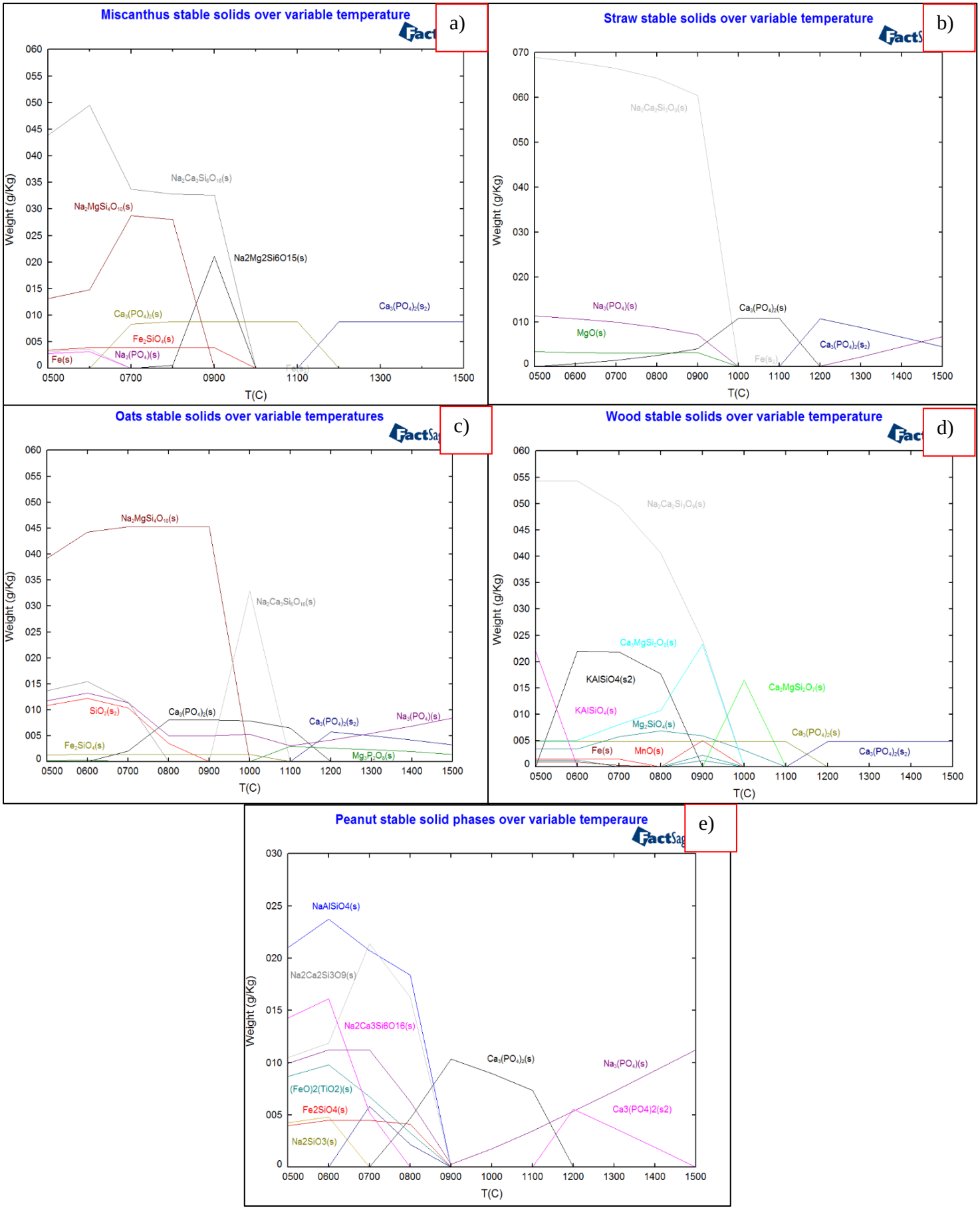

Figure 5-7 stable solid phases in biomass slags over increasing temperature (basic model)

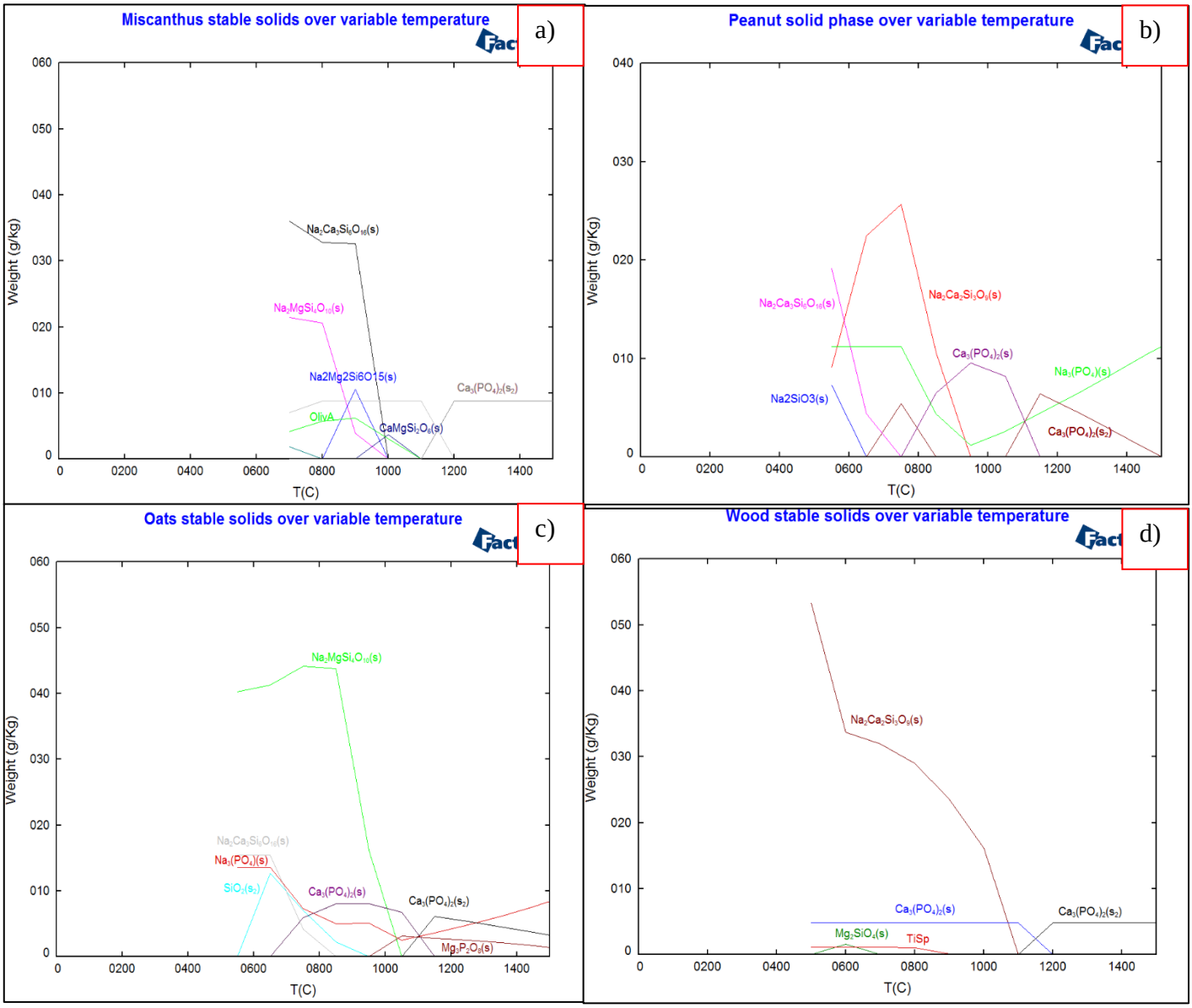

Figure 5-8 stable solid phases in biomass slags over increasing temperature (complex model)

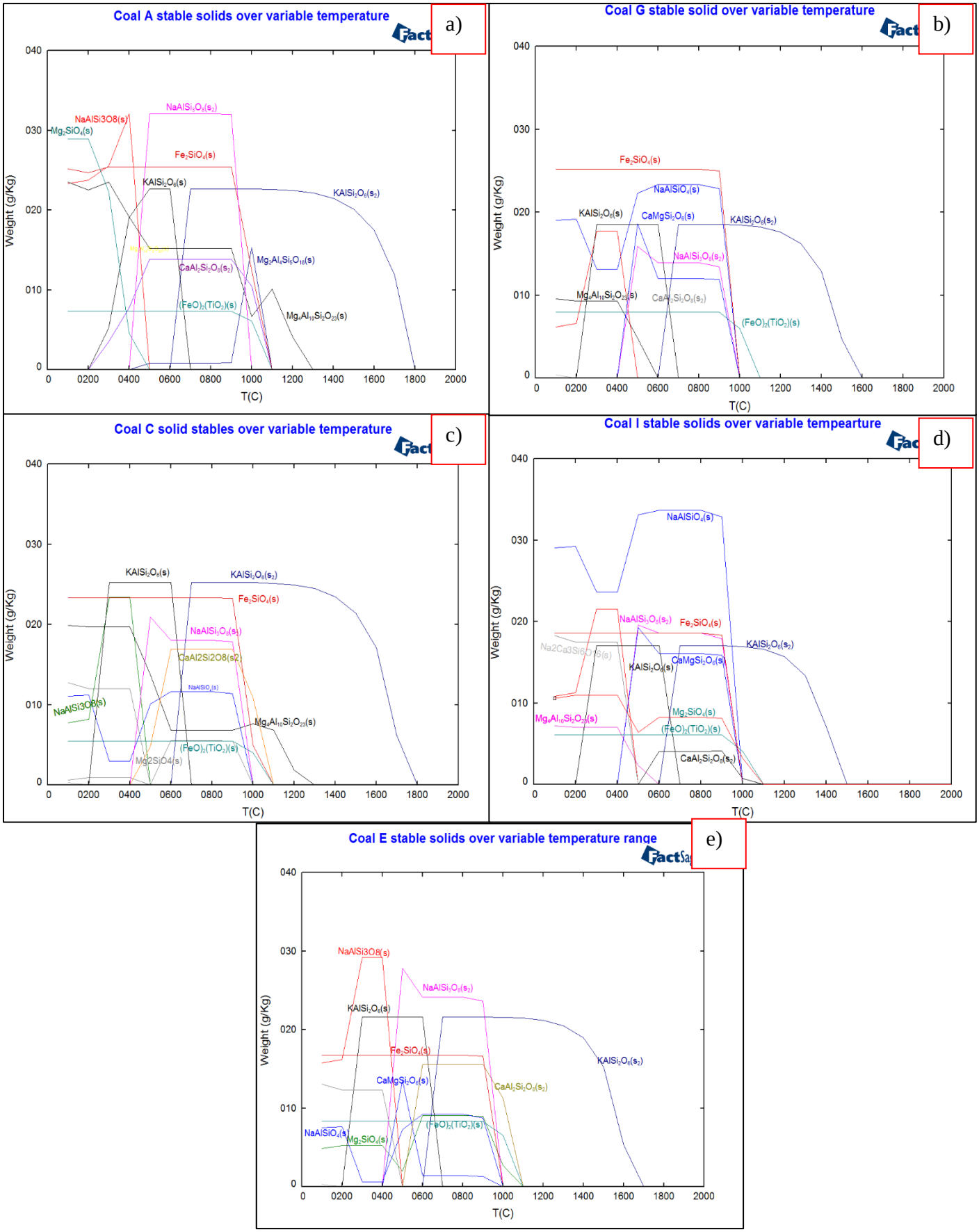

Figure 5-9 stable solid phases for low grade coals over temperature range 100-2500°C (basic model)

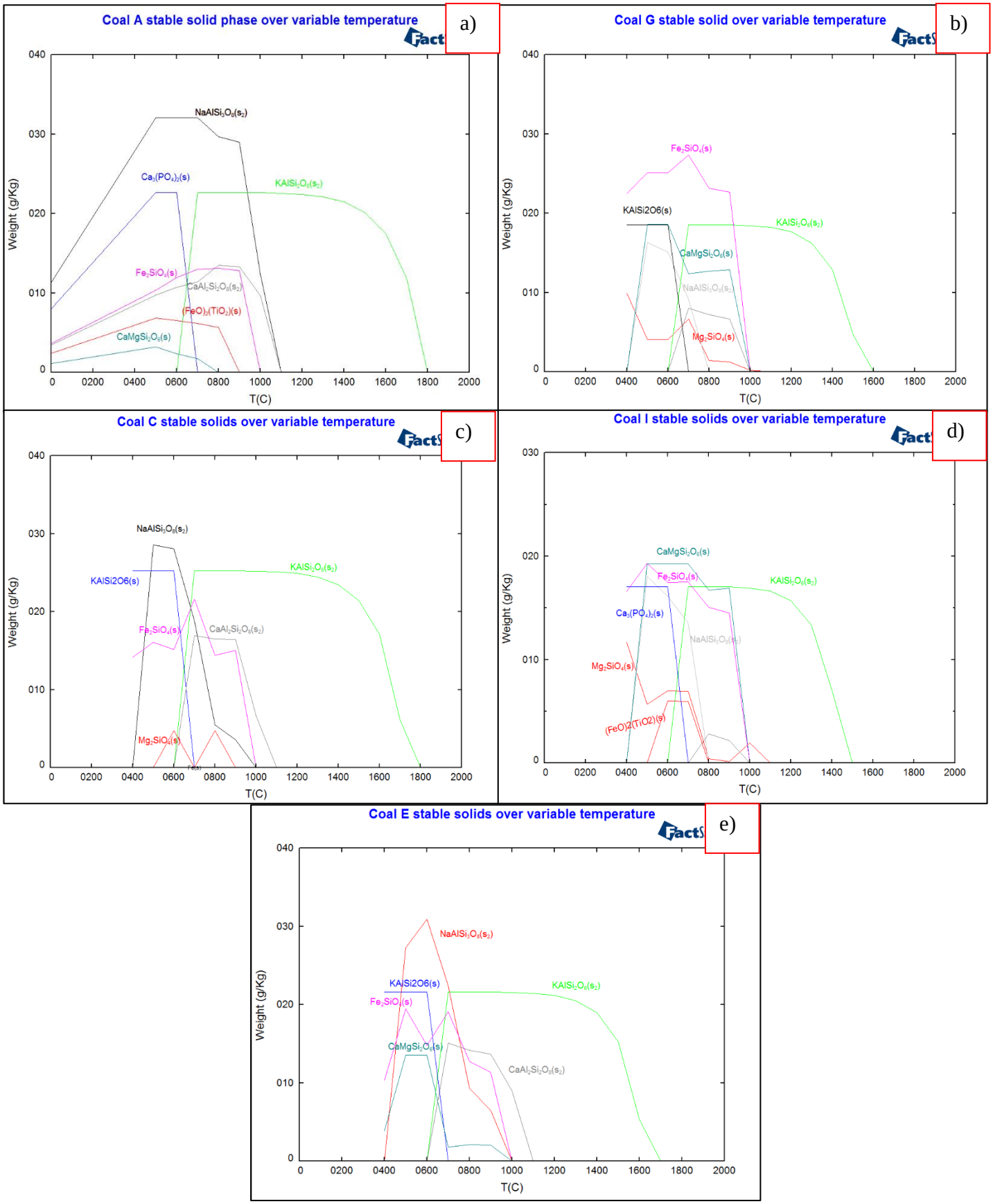

Figure 5-10 stable solid phases for low grade coals over temperature range 100-2500°C (complex model)

5.4 Ternary Diagrams

Another feature of the FACTSAGE software bundle is the phase diagram model. Phase diagrams are the graphical representation for a system in equilibrium. Within this system chemical components exist in different phases based on their composition, temperature, pressure etc. A single component system is classified as unary, two as binary and three as ternary (Campbell, 2012).

A ternary diagram is a triangular shaped diagram representing the interactions of the three components as a 2-D object. Each phase exists as its own triangle and interact on a 3-D plane but is difficult to display in this format as illustrated in Figure 5-11.

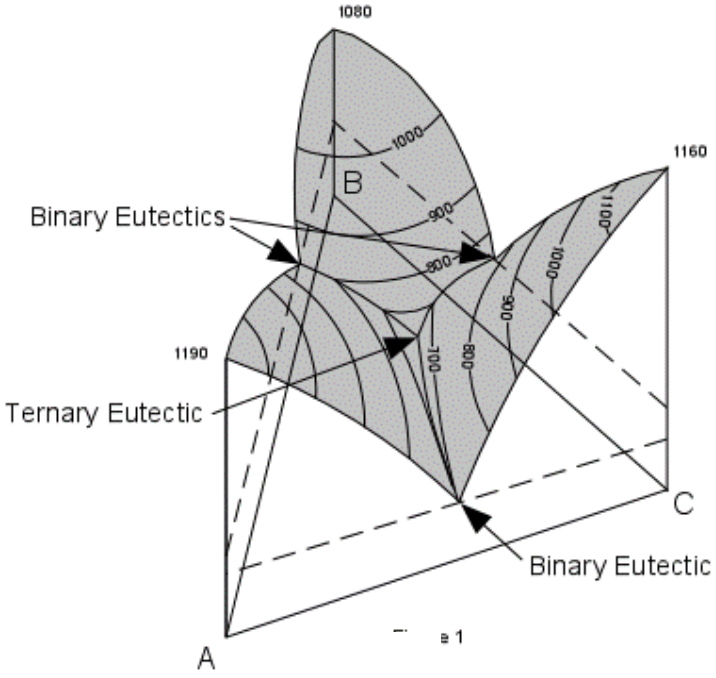

Figure 5-11 multiple phase diagram interaction to create overall 2D ternary diagram showing the liquidius surfaces of the components

Using thermodynamic data, specifically Gibbs energy, it is possible to generate phase tendencies of desired components. In doing so it is possible to model the point at which solid phases will form complexes, or primary and secondary eutectics. This is another method in which agglomerates can be predicted and relate experimentally found eutectics to modelled data. Examples of this application can be found in the literature, Teixeira et al. (2012) refers to a K_2O-SiO_2-CaO ternary diagram to explain the formations of agglomerates in FBC when co firing coal and biomass linking the fuel characteristics to results found theoretically and experimentally. Öhman and Nordin (2000) relates kaolin in the reduction of agglomerates based on its high concentration of Al_2O_3 and the effect on phase boundaries using Al_2O_3-SiO_2-K_2O plot.

The plots on the following pages (Figure 5-12), are modelled predictions as to the interaction of alkali groups of interest, based on their effect to agglomeration and sintering mechanisms in FBC. The chemical components used in the diagrams were picked based on the XRD and XRF agglomerate analysis performed in previous Chapters as they present significant interest. The key in Figure 5-13 translates what the points on the ternary diagrams represent.

Using the FACTSAGE software it was possible to plot the fuels on the ternary diagrams based on the component content which relates to the axis of the diagrams. The diagrams in Figure 5-12 show how a number of different compounds could theoretically form if the three components of each diagram were to be present over the temperature range which was specified for each diagram (100-2500°C). The coloured lines (contours) in each image are isotherms/ temperature gradients which lay between the boundary lines of ach stable phase. Therefore, the images in Figure 5-12 are in fact theoretical topographical images, representing a 3D image. By using the ternary diagrams, it is possible to eutectics points and binary eutectic points. Image A & B in Figure 5-12 hare circled points in which three boundary lines intersect with one another. This point identifies a point in which a eutectic made up of the boundary lines components. The contours around this point inform us of the temperature range the eutectics are likely to form at. Image A's eutectic will be made up of CaO-$Na_2CaSi_3O_7$-$Na_6Si_2O_7$ in this example and is indicated to form at a temperature of 846.19°C. In image B the circled point represents the formation of the nary eutectic $Ca_3Si_2O_7$-$CaSiO_3$-$K_2Si_2O_5$ at a temperature of 1019.77°C.

However, whilst it is possible to draw conclusions from the information presented in these types of diagrams, the information is only partially complete. As the interactions and data produced in each diagram can only simulate three components, other important reactions are not taken into consideration. An example being that Na and K will form low melting eutectics when in the presence of other alkali groups such as SiO_2 and FeO (Linjewile and Manzoori, 1999). Whilst each diagram suggests the formations of eutectics at specific operational limits, the information does not overlap into other ternary diagrams. For this reason, the images in Figure 5-12 show that there are a large abundance of possible eutectic/agglomerates, which could form using these types of fuel, but no single diagram can fully determine the effects of the fuels in this study. In order to do this a more complex system would be needed and is out of the capabilities of the current version of FACTSAGE and would require significant increases in both programming skills and computational power.

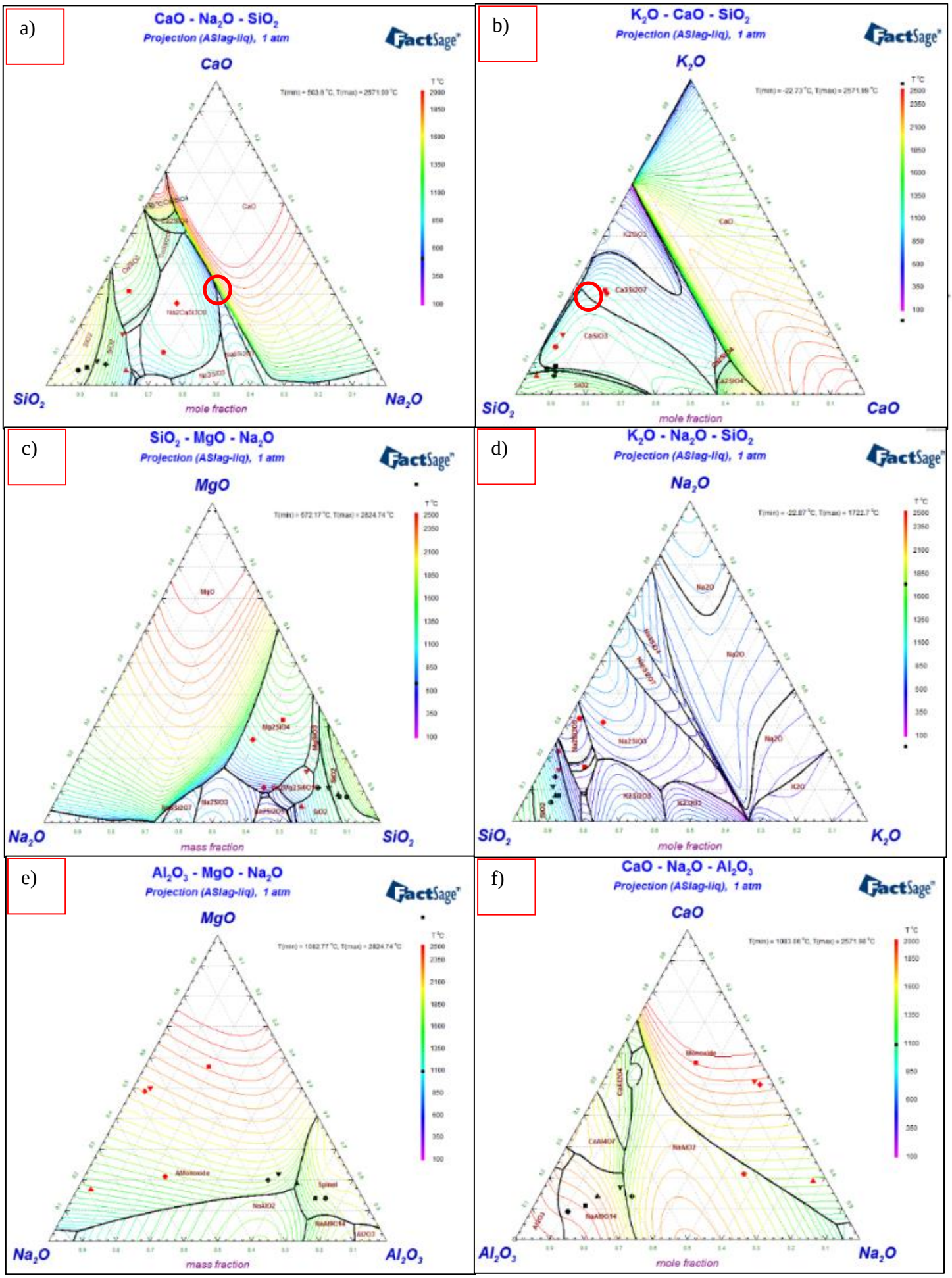

Figure 5-12 Ternary diagrams for oxides of interest; a) CaO-Na_2O-SiO_2, b) K_2O-CaO-SiO_2, c) SiO_2-MgO-Na_2O, d) K_2O-Na_2O-SiO_2, e) Al_2O_3-MgO-Na_2O & f) CaO-Na_2O-Al_2O_3

Figure 5-13 Ternary diagram fuels key

It should be also noted that throughout the process of creating the ternary diagrams in Figure 5-12, the author found that the software couldn't compute certain combinations of components. It was found that diagrams including FeO as a component would take extensive time to run (in excess of 24 hours) and once complete either crash or miss critical data such as boundary lines. After further evaluation and discussions with the software designers it was found that compounds such as the ferric components have large complexities which are inherent when combining large concentrations of reactive groups such as K or Na in the diagrams. This leads to extensive computation time and greater possibilities that the software will skip "dead end calculations" thus propagating errors in the solutions. There is a newer version of the software (version 7 as mentioned above), which addresses a number of these issues and contains further solution databases for biomass which would aid in the calculations. However, at the time of this study the software update was not available to the author and so conclusions have been drawn on the available data.

5.5 FACTSAGE Conclusions

Using the FACTSAGE Equilibrium thermodynamic software has been possible to generate predictive data for the outcomes of fuels based on their characteristics within a range of temperatures useful for FBC. However, a key finding using the approach of comparing a more basic model and a complex version of the same model has revealed software limitations:

Basic thermodynamic modelling generates data, but which questionable accuracy and reliability. Without further analysis of the data and understanding of the equilibrium calculations it is possible to mistake results and trends which may not exist in a real system.

Errors in the calculation of the model as a result of data gaps caused by inconsistencies between data sources. The inconsistencies were caused both by multiple sources of data having dissimilar values and gaps in the data leading to errors generated during iterations. It was necessary to include multiple databases in order to increase the available data for multiple reactions but it also negatively resulted in a number of fundamental errors increasing the error rate and complexity of the model.

Whilst data produced for the coals gave good repeatability and a good level of reliability based on the data produced, the same cannot be said when using biomass data (in version 6.4). The Biomass update in version 7 may remedy the issues described in previous sections but at the time when the work was carried out this was a large limitation.

However, overall the software generated data and trends which were found to agree with both work conducted in literature and with the experimental results described in later Chapters of this document. Therefore, the software could potentially be applied to FBC systems in predicting possible issues and outcomes in terms of agglomeration and fouling. However, modelling software should be used to accompany experimental work and should not be relied upon for a final definitive answer because of issues shown in this work.

In terms of both the biomass and coal results, the model has proved useful in expanding the reasoning to as what alkali groups are reacting and forming agglomerates. The results have shown that in the temperature ranges typical to FBC, Na, K, Fe and Al complexes are likely to form as silicates and metal organic groups. The structures that will form with these fuels have been found to be sticky in nature based on experience and the information in literatures and elaborate on the potential for agglomeration formation with these fuels in the FBC test of this document.

Theoretical simulations were carried out using the thermodynamic properties (Gibbs energy) associated with the fuels in the FACTSAGE software. In doing so it was possible to produce a series of data which offers explanation to the formation of agglomerates (eutectics) in tests performed described in later Chapters. The predictive data produced suggests that high concentration of potassium for biomass and high iron and sodium content in the Pakistani coals are the cause for slag and stable solid formations in the bed at temperature ranges associated with typical fluidised bed combustion.

The data produced by the FACTSAGE software complements the experimental results described in Chapters 6 and 7. For this reason, modelling studies, should be used as parallel studies to better inform experimental work and to suggest possible outcomes to the work carried out. Specifically, for fluidised bed combustion, the data highlights problematic fuels and the associated agglomerates. This could be used to address the onset of agglomerates before they interfere or defluidised a bed.

However, it was also found that there were a number of issues/limitations with the software. These are being addressed with the ongoing development of the software and need no more explanations. However, on the whole, the trends within the simulation results were in agreement with both literature and the experimental results described in later Chapters. In the future, this software will offer more insights into potential slag based agglomerate formations and will be a useful tool to accompany other methods of predicting potential issues in fluidised bed systems.

6 Low Grade Coal Combustion in FBC

The sub-bituminous coals analysed in Chapter 4 indicate a number of challenges likely to result from the combustion of the fuel particles in FBC. The following Chapter aims to combust the coals in a pilot scale rig and evaluate the emissions, pressure, temperatures, combustion performance, ease of application and effect on any agglomeration and slagging mechanisms. In doing so the applicability of the fuels in this technology will be concluded upon.

Further to developing an understanding of how the coals will react in a FBC, a number of operational variables including; bed sorbent addition, sorbent particle size, combustion temperature, sorbent to fuel ratios and co-firing with biomass will be tested to evaluate the impact on the effects seen in the previous baseline test scenarios. The results of this will give insight to the potential of the fuels via these means with the scope to the sub bituminous coals application in medium to full scale power generation facilities.

6.1 Baseline Data

The first stage of this investigation was to establish baseline results and to understand how the coals will react under steady state operation in a FBC. Each coal had different elemental makeup and as such it was assumed each coal would react slightly differently in the bed during combustion. Each baseline test aimed to establish steady state combustion whilst maintaining a thermal output of 220-230kW. The fuel flow rates and under-bed inlet air were altered in order to maintain bed temperatures, O_2 in the flue gas and a bubbling bed.

The baseline tests established the emissions levels in the flue gas, temperature profile throughout the furnace and pressures within the system such as across bed Dp. These parameters were needed in order to compare the effect of operational variables on the systems performance both in terms of fluidisation /combustion and the emissions in later tests. Comparisons against the baseline test were particularly critical when taking into consideration air requirements for fluidisation. Specifically, the air required to fluidise the bed was along the lines of 12000L/min, however, whereas previous calculations suggested airflows ≤10000 L/min. The baseline tests also gave both indicators to the onset of any agglomerate formation and the resulting defluidisation.

Figure 6-1 shows the results collected using the LabView software and program “Fluid.bed.v14.vi” described in section 3.2.1.3. This includes the emissions, temperature and pressure data recorded during an active test. Graph 1 is the temperature data recorded from thermocouples spaced at strategic locations around combustion areas and flue gas path. The period up to point A denotes the pre-heat sequence in which the bed is heated. In the order; Plenum, Bed A, Bed B and so on, the

thermocouples follow the hot gas path through the furnace and exit duct sections ending at the flue stack

The pre heat sequence lasted over a period of approx. 2 hours which was the time required to bring the bed to a point at which it would fluidise (≥650°C) and achieve a bed temperature sufficient for fuel particle ignition. At this point the solid fuel is fed via screw to the furnace at which point the fuel falls into the bed. The resulting temperature spike is noted at the point marked A. There is a transition of gas burners being extinguished and the solid fuel supplying the primary source of energy to the furnace. Following this there is a steady state period in which fluidisation and complete combustion are taking place. The plenum temperature is seen to decrease rapidly after point A. This is a result of the under-bed burner shut down and continued inlet of cool air in this region. There are small fluctuations in the temperature across the bed but any larger effects to the bed is mitigated by the thermal mass of the bed itself.

The temperature fluctuations at Point B are typical indications for the onset of agglomerates/agglomeration in the bed as a result of poor fuel mixing with an increase in larger agglomerated particles present. The sudden decrease in temperatures from 850°C and 600°C indicate an alteration in the air distribution in the bed and the channelling of regions near the thermocouple locations. At this point onwards, the mixing is reduced in the bed because of blocked flows by larger structures or the bypassing (channelling) of air through lower pressure/less resistant passages. Nevertheless, this type of result was typical for the data collected for all baseline tests and thus this type of profile was what operators looked for in normal operation in other tests. The test continues until the point marked C at which time the bed is clearly agglomerating and has reached a critical point of defluidisation. Bed temperatures grow more erratic and become difficult to maintain. At this point the test is ended. The changes in the bed and the temperature readings throughout the example of Figure 6-1 are typical to the processes that will be seen in later tests and as such will act as a gauge to the onset of agglomeration in those beds.

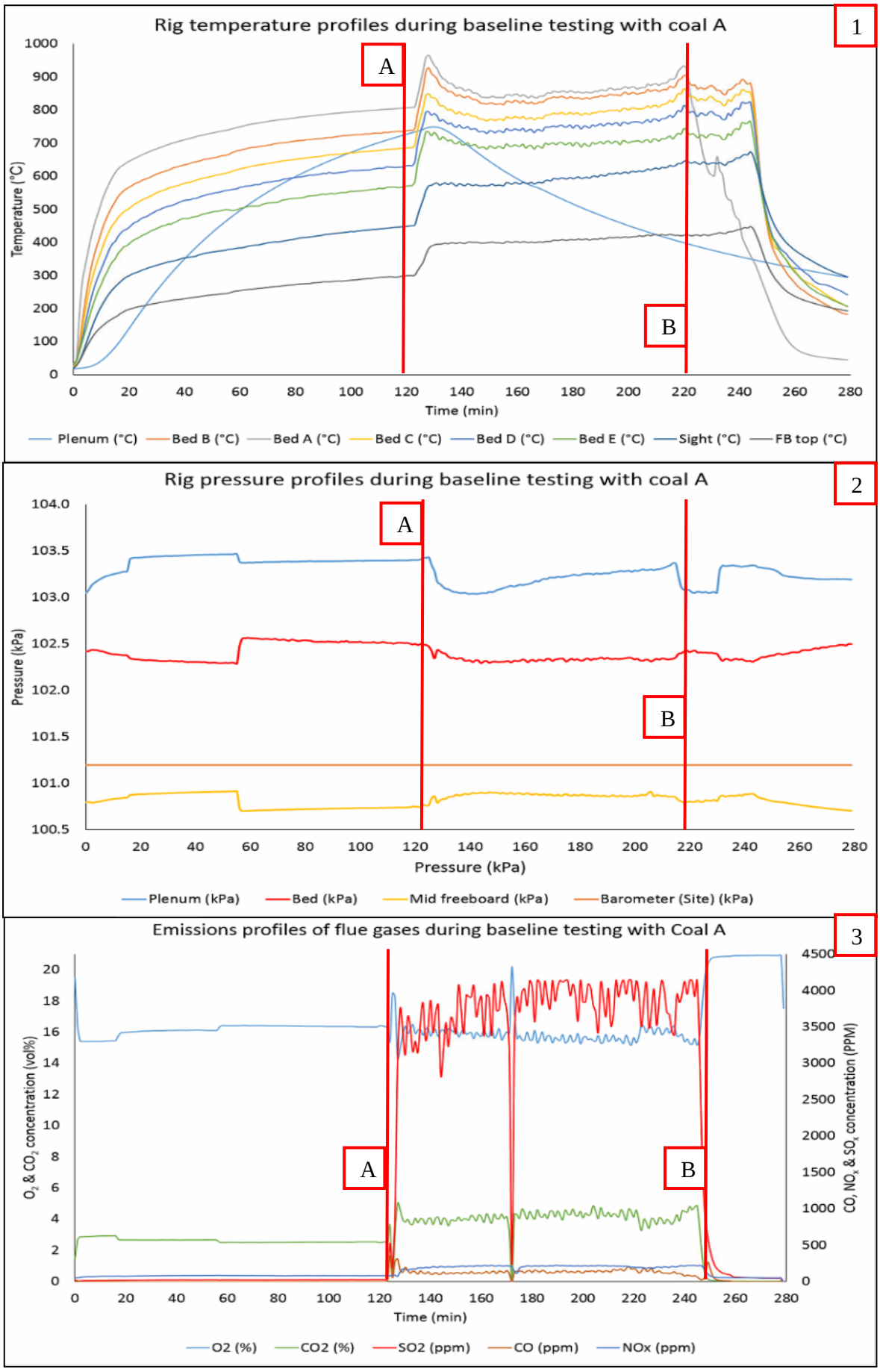

Figure 6-1 Typical data recordings for a baseline test. The example here is data from the steady state baseline test for Coal A and subsequent defluidisation. a) temperature, b) pressure and c) flue gas emission.

Graph 2 of Figure 6-1 shows the pressure readings recorded throughout the baseline test. Point A and B are marked in the same place in each of the graphs to show the key point within the baseline test needed for comparing later tests and performances for the coals.

Through the pre-heat sequence it can be seen that the under-bed pressure is positive. This is a result of the air flow at the inlet being blocked by the sand bed and thus causing resistance. The back pressure increases in the plenum with increased air flow and monitoring is to ensure the performance of the under-bed gas burner which uses stoichiometry to adjust gas flows.

The bed pressure reading is taken from within the bed. As air passage through the bed increases with the onset of fluidisation, the pressure reading increases as a result of higher airflows within the bed. This shows the change in pressure in the bed throughout the tests and thus, denotes the slow of air throughout the packed bed. The third reading and most critical is the mid-freeboard pressure. The freeboard has an induced negative pressure of $\leq 10mmH_2O$ at all times to maintain an extraction for heat and flue gases from the furnace. The negative pressure in the freeboard is varied slightly in later tests with the ongoing optimisation taking place through testing. The changes are made alongside knowledge development and in response to other operational variable changes.

At point A there is a change across the bed. The freeboard becomes more negative and the plenum less positive. This is a result of the onset of fluidisation. The resistance in air flow caused by the bed reduces, mixing begins and subsequently the onset fluidisation occurs. Initial airflows were greater than those seen in later tests which was a result of learning rig limitations. Later test reduces the rate of this change but is still seen as a breakthrough event resulting from bed density decreasing and increased mixing suddenly overcoming the forces associated with a static bed.

At point A the input of solid fuel and shut-down of the under-bed burner results in a pressure change. The under-bed pressure decreases as the burner was providing velocity to gases in the plenum. An increase in airflow occurs at this point but is masked by the decrease in pressure from the extinguished burner. The other pressures react accordingly i.e. mid freeboard becomes less negative with less resistant air movement through the bed. The readings between point A and B give early indications of the onset of agglomerates forming and as to the health of the bed.

An important measurement is the progressively increasing plenum pressure. As the bed gains weight with the increasing ash content from burnt fuel (batch process), and with the formation of agglomerates leading to changes in bed turbulence, the reduced efficiency of air passing through the bed result in an increased pressure reading. At point B, the air is poorly distributed and/or channelling through/around the bed. Consequently, at point B the bed slumps has shown as a sudden pressure drop. The freeboard fluctuates slightly with the alterations in resistance and air flow varying the level of suction in the freeboard and hence the negative pressure.

The pressures in Figure 6-1 were, representative to subsequent tests in which operational variables were changed. The changes in pressure will be used to monitor the onset of fluidisation, bed defluidisation and as a method for agglomerate formation monitoring and comparing to later tests

Graph 3 of Figure 6-1 shows the emissions data recorded in pseudo-real time to the baseline tests. The data shows that at the point of solid fuel input into the bed there is an increase in the SO_2, CO_2 etc. as a result of the combustion of coal. The emissions measured between point A and B give an indication as to the concentrations of the flue gases expected in later tests. Most importantly however, is the emissions change with the onset of agglomerates within the bed. There is a variation in the stable readings of the emissions with time approaching point B. This is a result of combustion efficiency decreasing, reduce gas-solid mixing in and above the bed, localised defluidisation and the localised depletion of O_2 influencing the flame and thus emission release. Furthermore, these changes become more extreme until bed defluidisation decreases total combustion in the bed to a point at which the test was ended. This data will be important for contrasting the combustion efficiencies and thermal performance of later tests and the influence the operational changes have upon these parameters.

It should also be noted that the baseline emissions results in Figure 6-1 are typical of the pre-heat and steady state operation and as such the SO_2 emissions will be used evaluate the effect of operational variables and Desulpheristation techniques in later experimentation it.

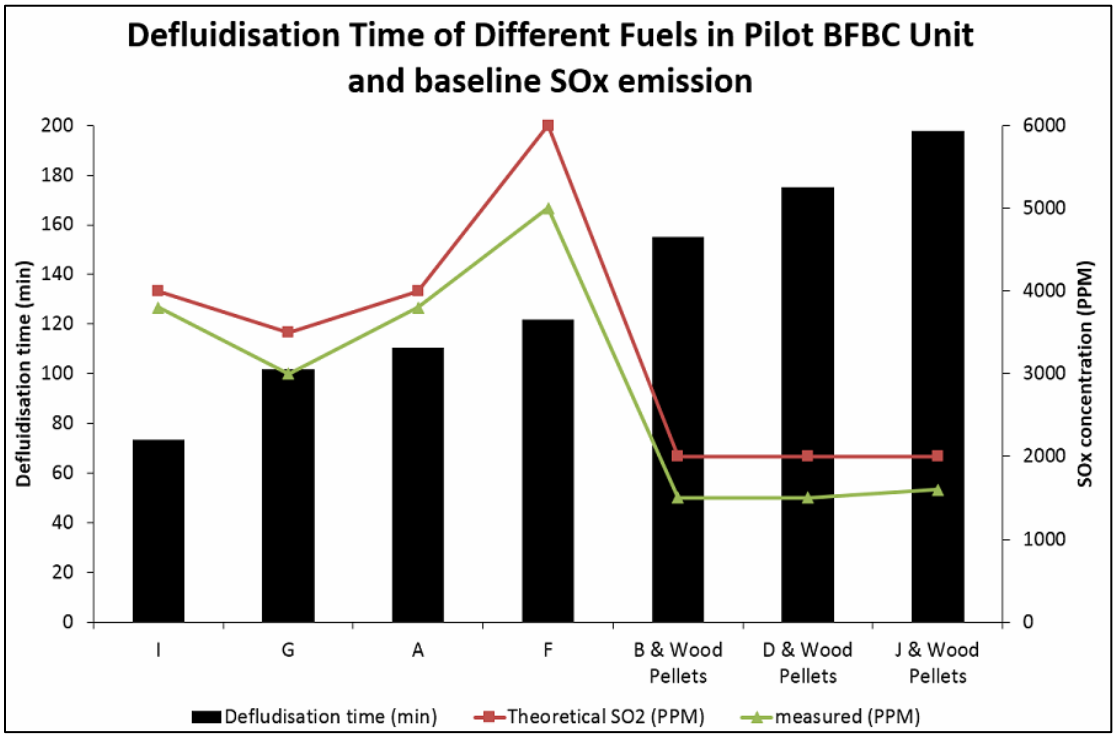

Figure 6-2 Defluidisation time and SO_2 emissions associated with normal operation in Fludised bed combustion of different low grade coals

Baseline tests were performed on each of the coal batches that were to be used in the investigation presented in this Chapter. In doing so a clear comparison could be drawn as to the effect the variables of the investigation has on emissions, combustion etc.

In each baseline test the beds eventually defluidised as a result of agglomerate build up. Defluidisation and the method chosen to determine when this had occurred for this investigation was described in the methodology Chapter 3. Figure 6-2 shows the two key parameters that will be valuated against the fuel improving techniques i.e. Defluidisation time (time between the solid fuel initial feed into the bed and characteristic bed temperature fluctuations) as a result of agglomerate formation and the SO_2 emissions. As the results show, the defluidisation time is different for each of the coals and fuel mixes. Factors influencing these results include; ash content, carbon content, mineral matter content, moisture content, pyrite content and inorganics present. Coal I which has the shortest defluidisation time, was shown in Chapter 4 to have a combination of these negative attributes. It is therefore reasonable to expect that different combination of the previously mentioned fuel variables will alter the interactions and combustion mechanisms within a FBC. Coal I contained the lowest calorific value, second highest ash content and second highest moisture content and large concentrations of alkali species such as potassium and sodium which the literature indicated would all influence (increase) the formation of agglomerates.

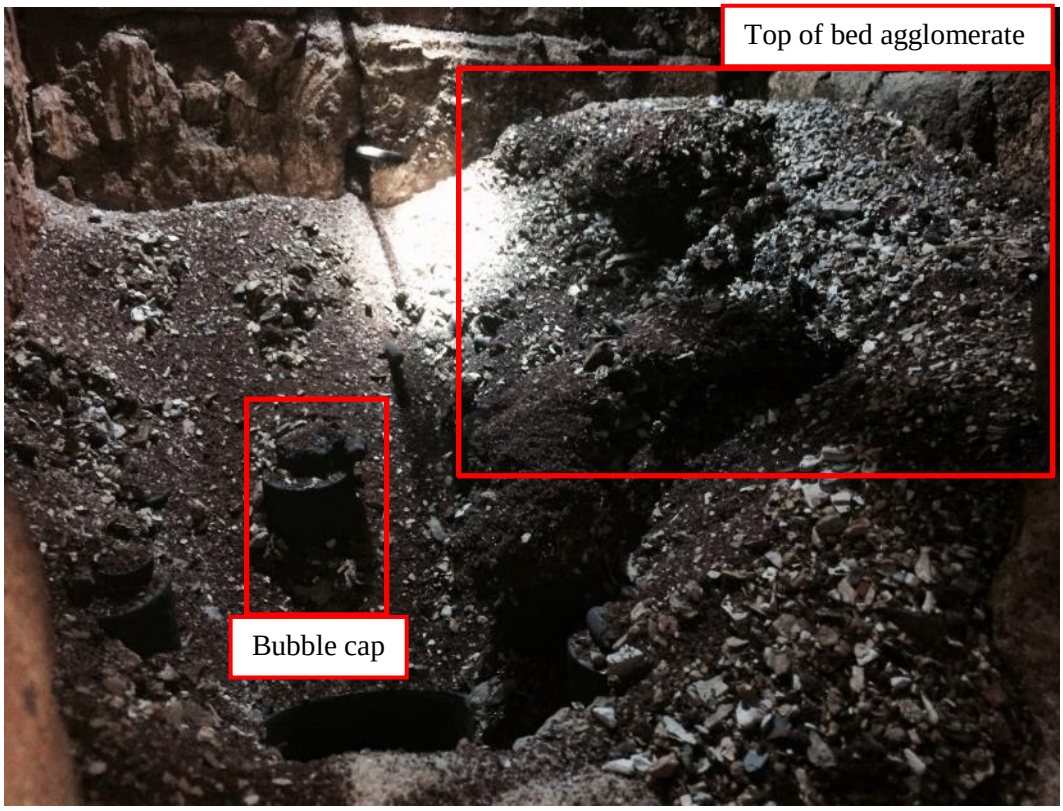

Figure 6-3 Agglomerated bed as a result of coal A combustion in the pilot scale unit

Figure 6-2 also shows the experimental and theoretically calculated SO_2 emissions associated with the combustion of each coal. The fuels which were shown to have higher organic sulphur concentrations had higher SO_2 emissions. The measured SO_2 throughout this investigation are all corrected to 6% O_2 in order to draw clear comparisons hence the value is slightly lower than that of the raw measurements. Furthermore, in each test the presence of pyrite in the fuel means a high concentration of sulphur in the fuel as well as a level of sulphur retention in the mineral matter.

As previously stated, every test resulted in the defluidisation of the bed from the formation of agglomerates. The beds agglomerated to a point in which the bed particles were no longer mixing and large areas (≥40% of the bed) were found to be fixed in alkali dominated low melting eutectics and structures. Figure 6-3 shows the bed after combustion with coal A. In this a large volume of agglomerated structure can be seen. The agglomerates were strong enough to suspend themselves against the surfaces of the refractory lining. There is also a notable amount of larger mineral particles as a result of the mineral matter in the fuel. This content increased over the test period altering the hydrodynamics of the bed and contributing to the decreased bed mixing and combustion performance throughout the test.

Figure 6-4 shows a selection of agglomerates taken from different locations around the bed following the baseline test with coal A. As can be seen the agglomerated structures are an accumulation of sand particles which have become coated in a eutectic complex. The sand particles are bonded with both mineral matter and accumulations of other foreign materials. In some cases, these were ferric compounds that accumulated in the mineral content found in the fuel. The agglomerates ranged in size; some contained large volumes of sand particles adhered to one another in 2-3mm (left image) the majority were 20-30mm (centre image) larger clumps measured between 40-250mm. The weight and density of the agglomerates fluctuated drastically as a result of the different bed and material content within the structures and the amount of melt phase which had coated the particles in those structures. The agglomerates and the mechanisms of formation are explained in the following sections

Figure 6-4 Agglomerates taken from the defluidised bed post testing of steady state combustion with Coal A

6.1.1 Agglomeration in Baseline Tests

Agglomerates were taken from each of the defluidised beds after the tests allowing time for the bed and rig to cool (24 hours). In this time a low volume of air was constantly passed through the rig to aid cooling but sufficiently small enough to ensure the structures remained intact. During testing it is assumed that some of the larger structures may have been reduced in size by the mixing and movement of bed material but after the end of the test all structures were preserved as much as possible. The following descriptions are the summarised results of the agglomerates taken from baseline testing which were analysed using SEM-EDX, XRF and XRD methods. The objective being to identify the inorganic species causing the onset of agglomeration during the combustion process and relate the mechanisms and chemical species to the analysis conducted in Chapter 4. The work here will also be applied in later modelling Chapters to relate specific alkali species seen in both the experimental and modelling tests to draw conclusions to agglomeration monitoring techniques.

6.1.2 SEM-EDX

Initial analysis of agglomerates was done using a scanning electron microscope (SEM), (Carl Zeiss EVO MA15). Secondary electron detection was a crucial detection method for the analysis giving better resolution of the samples surface morphology and topography. The secondary electron technique was used instead of backscatter because of its topological applications and the definition it achieved when looking at agglomerate samples.

Figure 6-5 shows an image from SEM analysis of a typical agglomerate found the baseline tests. Sand particles have been coated on all surfaces with a complex which has been in a gaseous or

Figure 6-5 SEM image of typical agglomerate surface. Sand particles are coated and embedded in a material which has blinded the structure of particles together

liquid phase. The image is an example of bed particles being coated in a eutectic matrix which has led to the adhesion of other colliding particles in the bed. The repeated action then leading to the growth of the agglomerated structure.

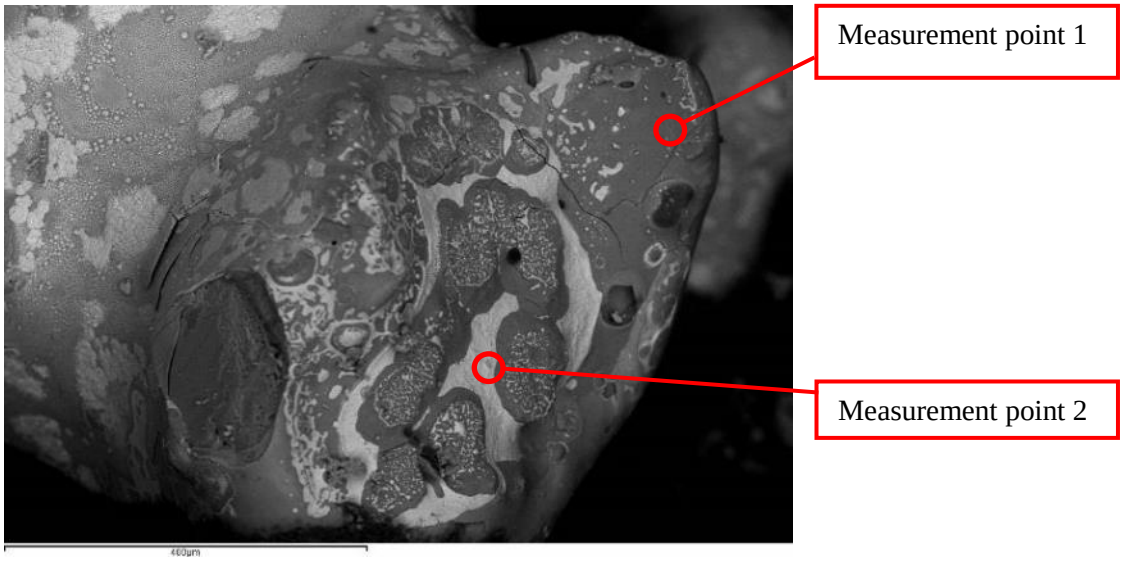

Figure 6-7 Magnification of sand agglomerated particle. The particle is coated and impregnated in an Iron/silica rich complex

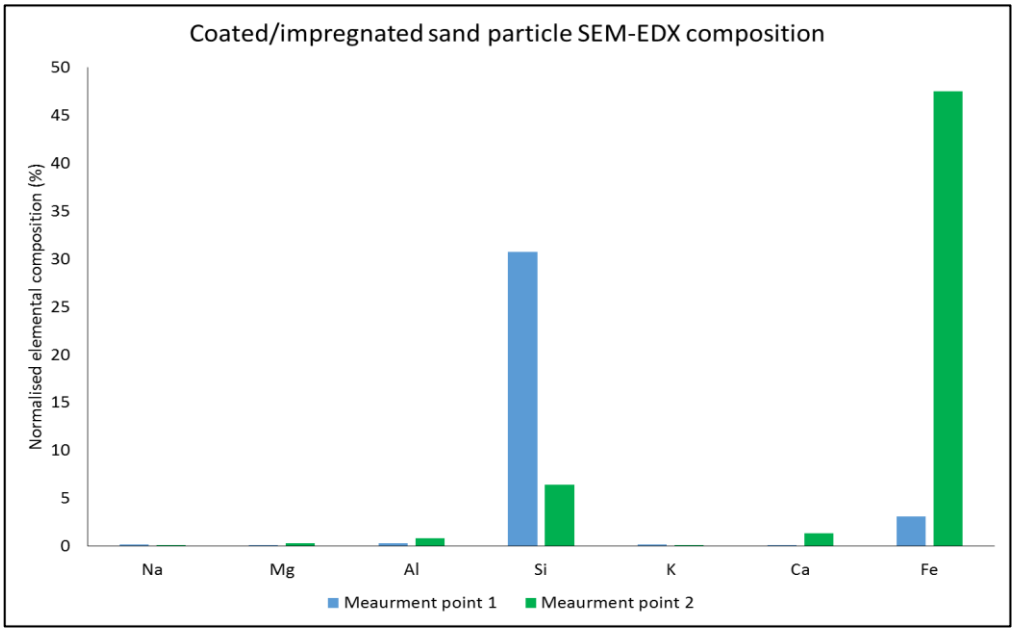

Figure 6-6 Elemental analysis by SEM-EDX of coated/impregnated sand particle found in agglomerates

Figure 6-7 shows how the particles are both coated in a melt phase and impregnated with the substance. SEM-EDX of the particle coating reveals high elemental concentrations of Si, Ca, Al and Fe as shown in Figure 6-6. These were identified in the fuel characterisation of the coals.

As described in the fuel characterisation section, the coals contained high sulphur concentrations. This was found to be in both organically bound form in the coal seams but also in the form of Pyrite

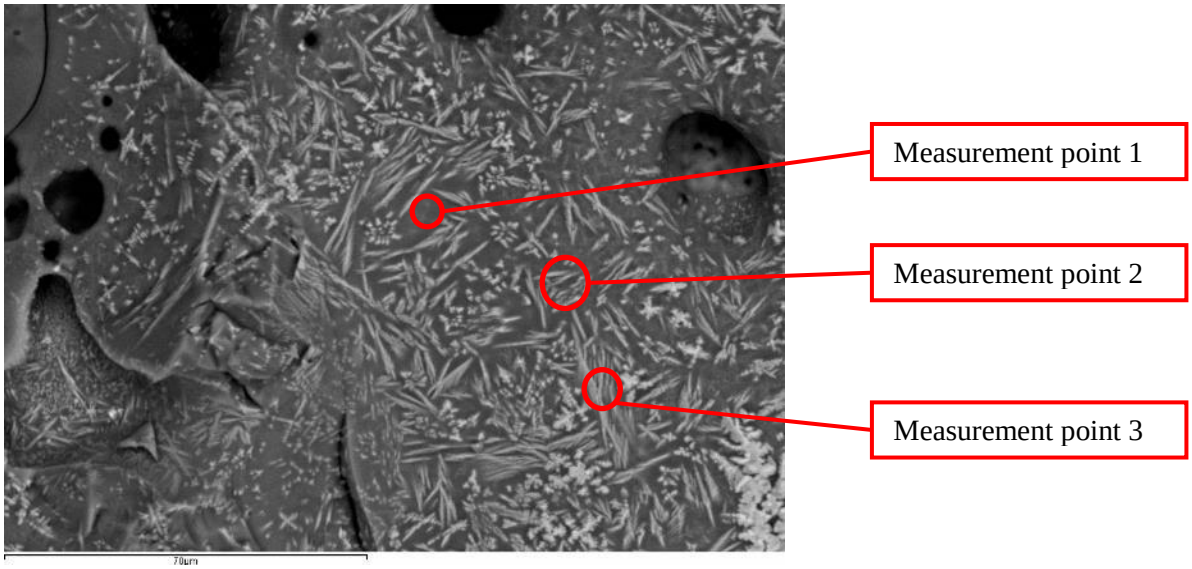

Figure 6-8 Fe-Si-Al complex crystal structure within agglomeration medium and crystal arrangment

(FeS_2). Pyrite is associated with the formation of agglomerates in FBC catalysing alkali dominated reactions and lowering melting temperatures of sticky, problematic species (Siegell, 1984b; Cebeci and Sönmez, 2002). Additional to this the presence of Aluminosilicate rich minerals in the large quantity of rubble/ash contained within the fuel as hercynicite ($Fe^{+2}Al_2O_3$) is known to react with Ca complexes extracting compounds that have been seen to reduce agglomerate growth and thus leave complexes containing alkalis link to more adhesive matrices (Brown et al., 1994).

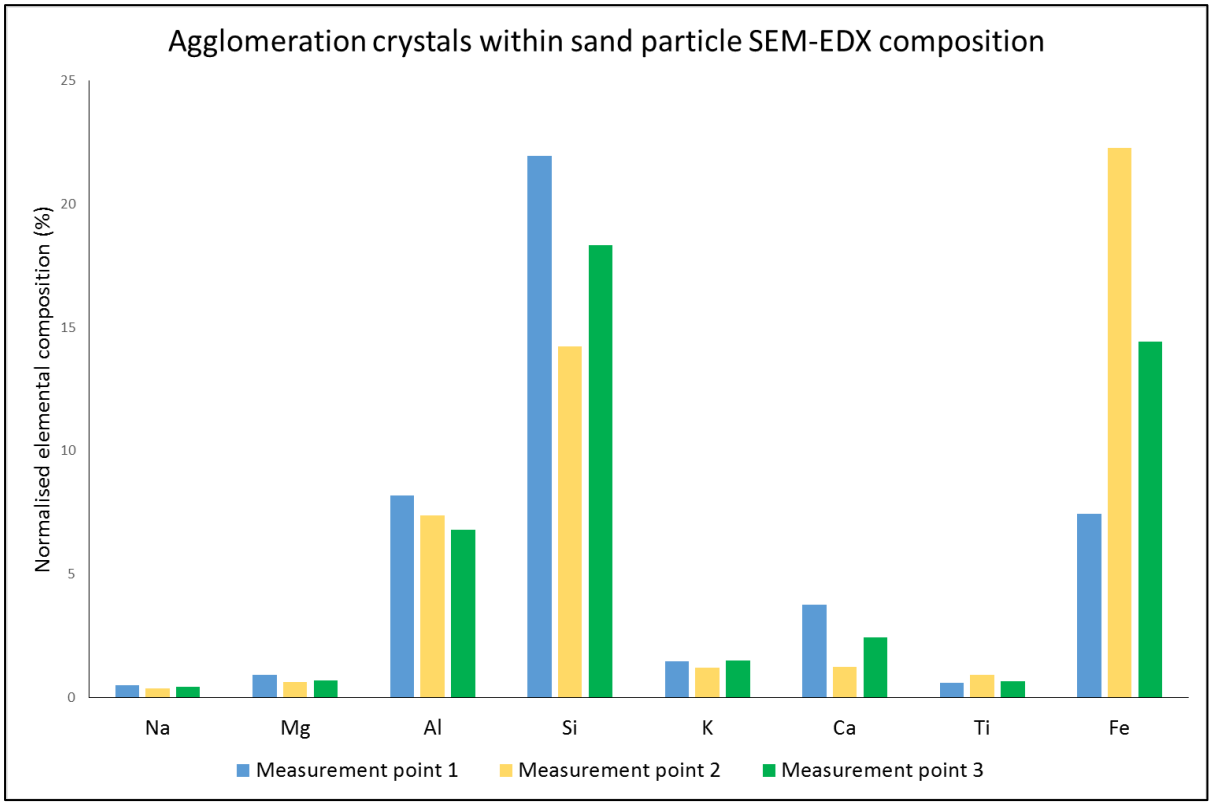

Figure 6-9 SEM-EDX elemental analysis of Fe-Si-Al crystals

The SEM-EDX gave indication that the Pyrite was a major contributor to the agglomeration mechanism. The presence of Fe rich and sulphate complexes in the analysis indicate the influence the pyrite compounds are having on the formation mechanism during combustion.

Further analysis of the melt phase on/within the bed particles is shown in Figure 6-9 and Figure 6-8. As Figure 6-9shows, there is extensive crystal formation throughout the complex . SEM-EDX of crystals and the materials between crystals indicates that the complexes are Fe-Si-Al complexes. In between these crystals the same species are also found, however, the Fe concentration is significantly less and Si is more prevalent. This indicates the crystals are forming on the surface of particles as the coating spreads around each particle bonding to the main structure. A similar formation has been noted in the work of Oliverira et al. (2011) when combusting low grade coals. This study was focused on the chemistry of Fe rich groups in coals, including pyrite and found agglomerates forming under similar oxidation processes.

To understand the agglomeration mechanism when combusting sub-bituminous coals further analysis of baseline samples was undertaken. Figure 6-10 shows the surface of an agglomerate and the initial formation of bridges occurring as bed particles coated in the liquid/solid phase interact with one another.

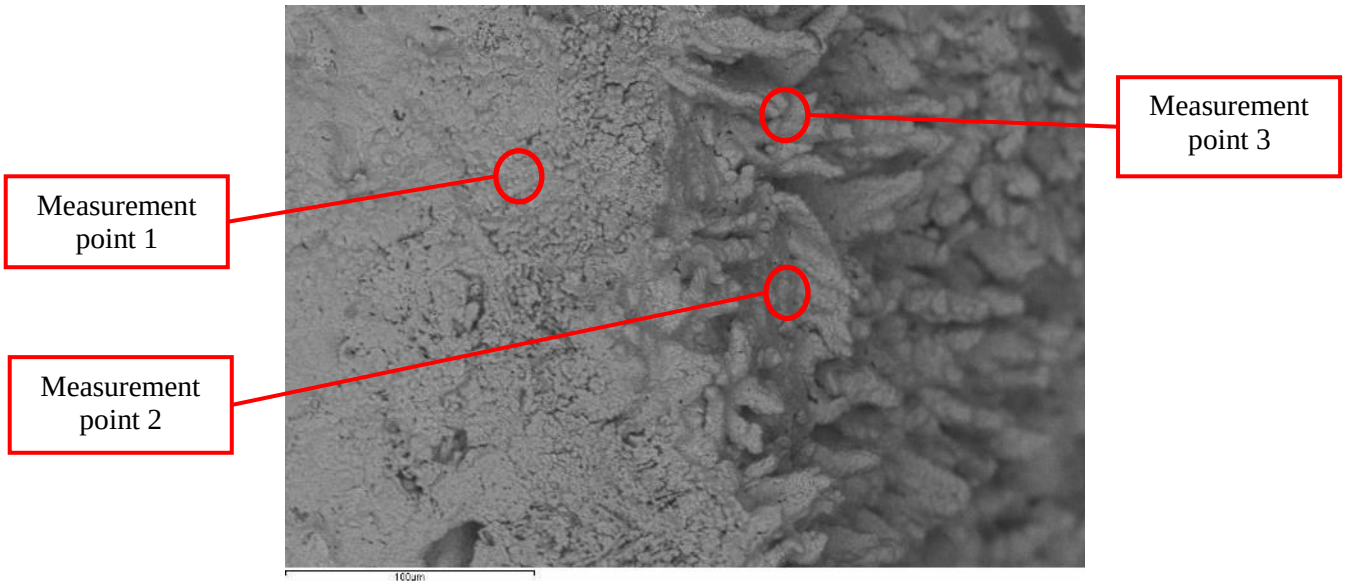

Figure 6-10 Example of bridging occurring on agglomerate surface and a stage in the propagation of agglomerate formation

There is a network of branches reaching from the surface an alkali coated particle, which during combustion will have been molten and sticky. The branching was caused by the collision of other particles and the sticky surfaces. The branches are made up of the melt phase and would have stuck temporarily to the colliding particles, forming bridges, but due to the vigorous turbulence of the bed has separated the temporarily adhering particles. This branching effect was seen within the

agglomerate samples taken in all baseline test and is a key stage in the chain growth of the agglomerates through bridging, during combustion and fluidisation of the bed material/fuel.

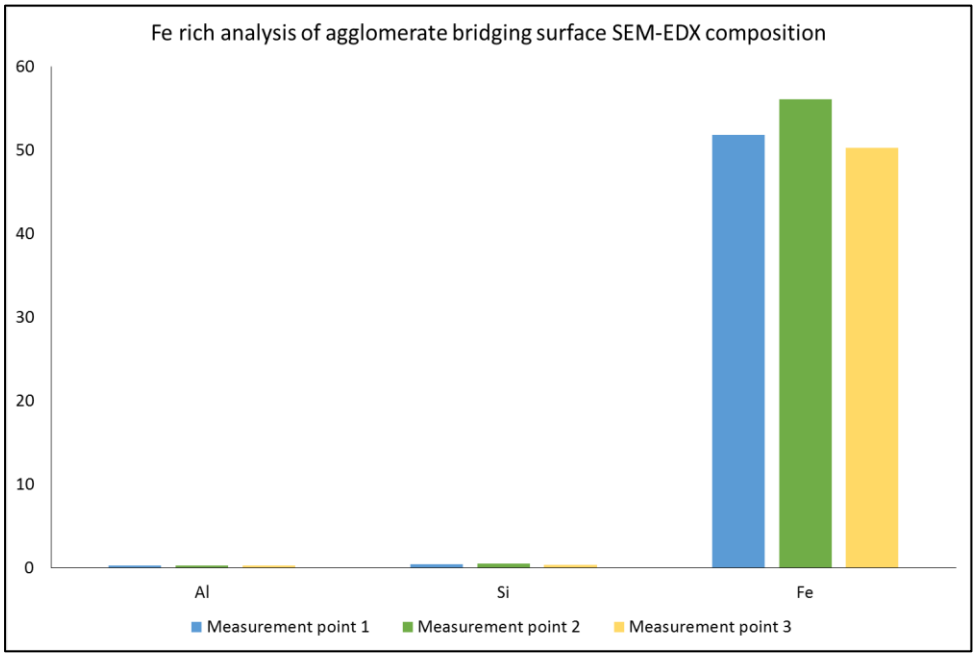

Figure 6-11 SEM-EDX elemental analysis of bridging section and emphasis of Iron rich nature

SEM-EDX analysis of the branches and the surrounding sticky surfaces was completed and is shown in Figure 6-11. As the results indicate, the branches are predominately Fe-Si based. Ferro groups are shown here to be a significant stage for the adhesion of coated bed material to one another. The results shown suggest that these ferro groups are occurring as the agglomerates causing localised hotspots. This is due to the initial stages of such complexes requiring lower melting temperature eutectics made up of K and Na for instance to create the initial structures. These are then theorised to have been lost in the gas phase with increased localised heating, thus resulting in the Fe-Si dominated structures left in the bed and presented in the results. This theory is in agreement with investigations such as Bartels et al. (2008a) which noted high alkali species in the fuel that should have been found in agglomerates but found higher melting eutectics instead.

In order to further understand and identify the complexes within the agglomerates and hence further understand the formation mechanisms of the agglomerates, it was necessary to use further analysis techniques.

6.1.3 X-ray Fluorescence (XRF)

Samples of the bed was taken and analysed using XRF. By using the modified methodology developed as described in the Chapter 4, it was possible to measure with a high level of reliability the major and minor oxide content in the sample.

The results of the XRF analysis are shown in Figure 6-12 and show that Fe, Al and Si are the major components within the bed sample. The presence of S is assumed to be due to the presence of pyrite within the samples and the retention of S within minerals containing species such as Ca bound to the agglomerate. As the coal has combusted in the bed, the agitated bed particles colliding with the fuel particles have become coated in the melt phases and localised gas phases. As a result, a concentration of Fe_2O_3, SO_3 and Al_2O_3 has built up within the bed. SiO_2 is present in the fuel and will have certainly contributed to forming silicate based matrices, however, the bed material itself is made up primarily of SiO_2 compounds and as such cannot be differentiated in this analysis. However, the higher concentration of Fe oxides clearly indicates that the bed is impregnated with alkaline species found in high concentrations within the fuel and as such has led to agglomerating bed particles via Fe-Si-Al complexes. The high concentration is particularly significant as it is assumed the majority of the SiO_2 detected in the sample originates from the sand particles and not from complexes forming from the melted ash.

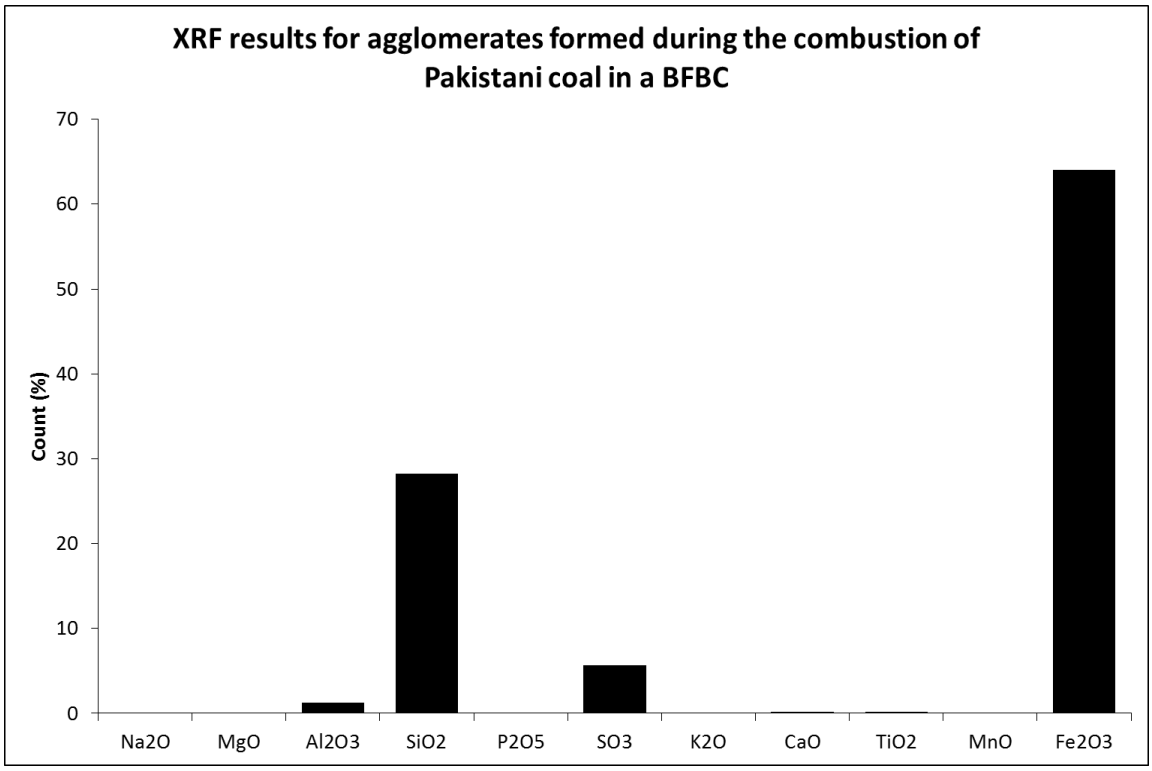

Figure 6-12 XRF analysis results of bed samples taken from the bed after the combustion of Pakistani coal G in a BFBC

The XRF analysis gives a good indication for what to expect from the analysis of bed materials from operational variable testing in terms of agglomeration mechanisms and sources of agglomerate material. The results discussed show that the bed is being populated by alkaline species released form the fuel in combustion and agglomeration of the bed material occurs as a direct result. The data here will be compared as a baseline case to the tests that are described in the following sections.

6.1.4 Agglomeration Mechanism Summary

The agglomeration mechanism for sub-bituminous coal during combustion in a FBC is dominated by the presence of pyrite in the feedstock. It is for this reason that even with the presence of other alkali species such as Ca and Mg, the results and analysis indicate that the formation process being due to Fe-Si-Al complexes and the presence of sulphates.

The proposed stages and mechanism for agglomeration in the baseline tests are as the following suggests and depicted in Figure 6-13:

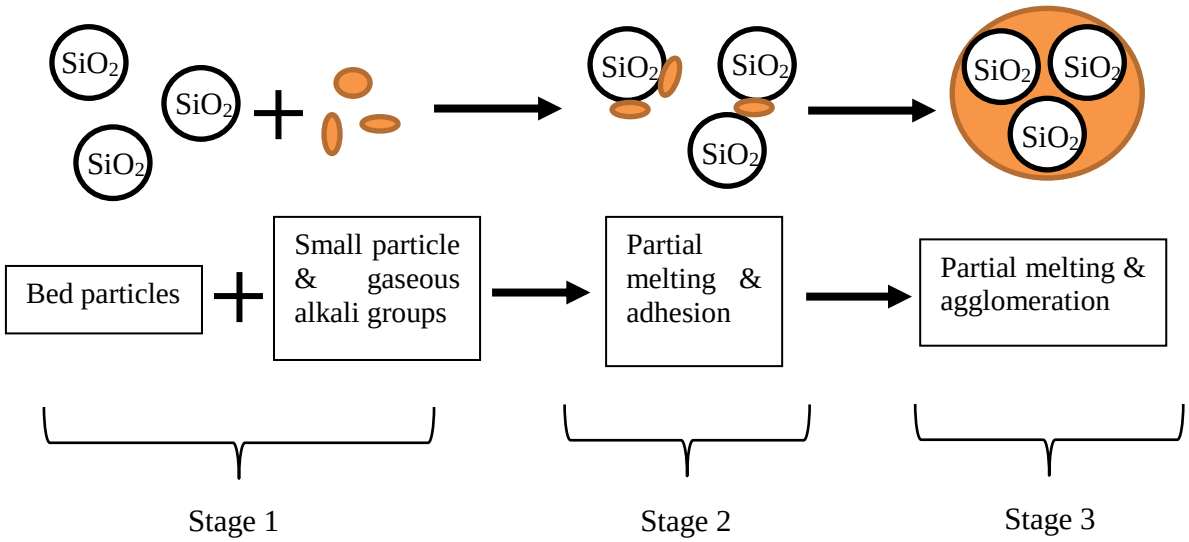

Figure 6-13 Agglomeration mechanism for low grade sub bituminous Pakistani coals in pilot scale bubbling fluidised beds

Stage 1, involves a number of routes for ash and alkali species coating the bed particles. With the highly turbulent mixing, the bed particles will be exposed and collide with alkali deposits causing the attachment of sticky species to build on the surface of the bed particles. This mechanism is more common with reactions including species such as Fe which have been shown to interact with agglomerates at temperature of ≥850 °C but has a melting temperature of 1377 °C (Fryda et al., 2008). The second method proposed is the condensing of alkali species on the surface of the bed particles. The species enter the gas phase in heated zones of the bed and, via moving bed particles. The cooler bed particles are agitated to the surface and condense the gases on the surfaces. This method is especially applicable to lower temperature melting species such as K and Na which melt between 700 and 800 °C (Pietsch, 2008b). The third method is for a chemical reaction of alkali gases to occur on the surface of the particles.

Specifically, to the formation of sticky alkali covered bed particles with concentrations in a temperature range of 800-950 °C, the first and second methods are likely to dominate the formation

of these agglomerates in the first stage. Si is known to form eutectics at 874 °C which is in the range of the operating temperatures of the tests in this work (Basu, 2006). This is likely then to have combined with the abundant FeO on the surface of the bed particles. There is the possibility that the lower melting temperature species and sulphates could catalyse the reactions of Fe and Si however it is impossible to quantify such an intricate series of reactions within this investigation.

The results of bed sample analysis via XRF in Figure 6-12 shows that the release of agglomerate species into the bed is occurring and as such a liquid/gas alkaline phase is present in increasing concertation in the bed as time/combustion progresses. The chemical content of the coals and the resulting agglomerates lend correlations with the route suggested previously.

As time continues (stage 2), the thickness of the deposits building up on the surface of the bed particles increases. Within the sticky layer, the liquid phase causes the homogenisation of the species present. In this case, Fe_2O_3-Al_2O_3-SiO_2 was found to be the main matrix present. Whilst this is the dominant species present, it is likely that other alkali species will interact and deposit with the surfaces of the matrixes however, the Fe, Si and Al are the highest in concentration in the fuel and hence highest concentration in ash and in the deposits. Localised heating is likely to cause localised sintering between particles and on the surfaces as thickness grows (Öhman et al., 2000).

With the continued build-up of a sticky surface forming matrices with the Silicate surface of bed particles, coated bed particles move and mix over one another and in colliding create extensions (seen in Figure 6-10) and sticky branches which either adhere and retain more material/particles to the first particle, or simply move on until another successful collision occurs. Eventually the build-up of particles within the matrix and eutectic creates the onset of an agglomerate.

Stage 3 is the formation and growth of the agglomerate and subsequent structures within the bed. As small agglomerates create move throughout the bed, localised heat exposure create partial melting of the eutectic complexes. This is likely where the Fe_2O_3-SiO_2 formation occurs and is embedded with lighter alkali species being lost to the gas phase. The partial meting creates liquid phases within small agglomerates and thus giving a liquid like surface in the SEM images above as well as a uniform material between bed particles.

The agglomerate will propagate in size dependant on the interactions with other particles through mechanisms described in stage 1. Additionally, the agglomerate will interact with fuel particles directly. Firstly, the sticky surface could adhere to a fuel particle and become exposed to high concentrations of alkali gases and sintering mechanisms. Furthermore, if the agglomerate is sufficient in size, localised poor mixing and localised combustion as a consequence could further increase the growth of agglomerates.

The final stages of the agglomerates within these tests involved bridge formation occurring between agglomerates which then created a growth in the overall structure. Eventually the growth and structures get to either a large enough volume or physical size to defluidise proportions of the bed in which mixing and combustion is hindered. This is defluidisation and agrees with the descriptions and experiences elaborated upon in section 6.1.1.

6.1.5 Summary

A theory to the agglomeration mechanism of the low-grade coals used in this investigation has been described in section 6.1.4, and the key constituents have been defined as Fe, Si and Al. This doesn't include the reactions occurring at lower melting points as these reactions are overwhelmed or secondary to the main complex formations dominated by Fe, Si etc. However, a key limitation of the coals (poor quality and high mineral content aside), is the high sulphur content and thus high associated SO_2 emissions potential.

As discussed in the literature review, additives containing MgO or CaO can be added to the bed in order to capture and desulphurise the flue gases of SO_2 emission. Further to this the addition of a CaO-rich sorbent to the bed has been found to react with alkali species and thus hinder the formation of agglomerates. Specifically, species such a Na, K and Fe (Chou and Lin, 2012). Therefore, it is reasonable to theorise that with the addition of limestone for the desulphurisation of the coals in the bed, benefits including reduced agglomeration potentials, extension of stable fluidisation time and operation of the rig could be experienced. The following sections investigate the effects of altering operational variables in terms of both agglomerations and desulphurisation. This will then allow for the evaluation of fuel applicability in FBC units at pilot and by extension, industrial scale. This will also allow for criticisms around the potential of the coals and any operational choices that could be employed to better combust the fuels in full scale systems.

6.2 Operational Variables & Low Grade Fuels in FBC

6.2.1 Sorbent Addition

During the sorbent addition experiments, coals: limestone were fed into the rig at ratios of 0.5, 1.0, 2.0, 3.0 and 4.0 in order to evaluate the effect on desulphurisation/sulphur retention in the bed and to look at the impact of ratio change on defluidisation and rates of agglomerate formations.

Figure 6-14 shows the data from the combustion coal: limestone blends. By altering the ratio, the literature indicated that there would be an optimum ratio between 2 and 3 where maximum sulphur would be retained in the bed by the CaO present in the limestone.

As the data shows, stable combustion of the coal with varying coal: limestone ratios were achieved. The fuel flow rate was kept at a constant 10 kg/hr which was equivalent to 56 $kW_{thermal}$. It was found in previous tests that the higher flowrates used in other tests led to agglomeration and defluidisation before the test could be completed. Hence, the flow rates were recalculated to optimise the system. This was measured against achieving bed temperatures ≥750°C whilst achieving the lowest fuel input. By decreasing the fuel flow, a cooler bed (750-850 °C instead of 800-950 °C) and lighter bed i.e. less total ash and limestone in the bed, helped extend the test beyond 30 minutes. This did not impact the findings in terms of agglomerates as they still formed but at slower rate and the Ca content was calculated on a molecular weight basis to the Sulphur in the fuel flow.

The temperature data in Figure 6-14 shows the pre-heat sequence followed by stable bed temperatures and thus demonstrates the good performance of the bed and combustion within/above the bed before the introduction of coal. Furthermore, the combustion and bed temperatures aren't altered by the addition of limestone throughout the test period and variation in coal: limestone feed ratio.

The bed pressures during the test show a different perspective of the bed and its performance. Freeboard pressure remains negative throughout with only small changes occurring as a result of air flow modification when clearing view ports. However, the pressure across the bed gradually increases over the length of the test.

The pressure increases with the increase in bed weight, increased volume and increase in varying particle sizes entering the bed as a result of constant ash and increasing limestone feed. Additionally, the presence of agglomerates forming within the bed leads to a pressure increase with alterations in the flow of air through the bed leading to less efficient air distribution throughout the bed. The Dp across the bed begins to level out near the end of the test and a maximum pressure difference is almost achieved with the onset of defluidisation of the bed, quickly followed by a decrease with the failure of the bed and spouting occurring. The is assumed, based on the theory described in (Chapter 2) that the multiple changes being made to the bed (bed weight, increased volume and increase in varying particle sizes entering the bed) altered the hydrodynamics and flow of the bed and in doing so obstructed mixing. Hence, the increase of bed Dp throughout the period in which the fuel and limestone was fed into the bed.

Coal H was a high Sulphur coal and as such the measured SO_2 emissions were in excess of 9000 ppm which while high when compared to a UK coal is comparable to the theoretical SO_2 emissions calculated previously. In Figure 6-14 the period A is the period in which the fuel stream contains only coal H.

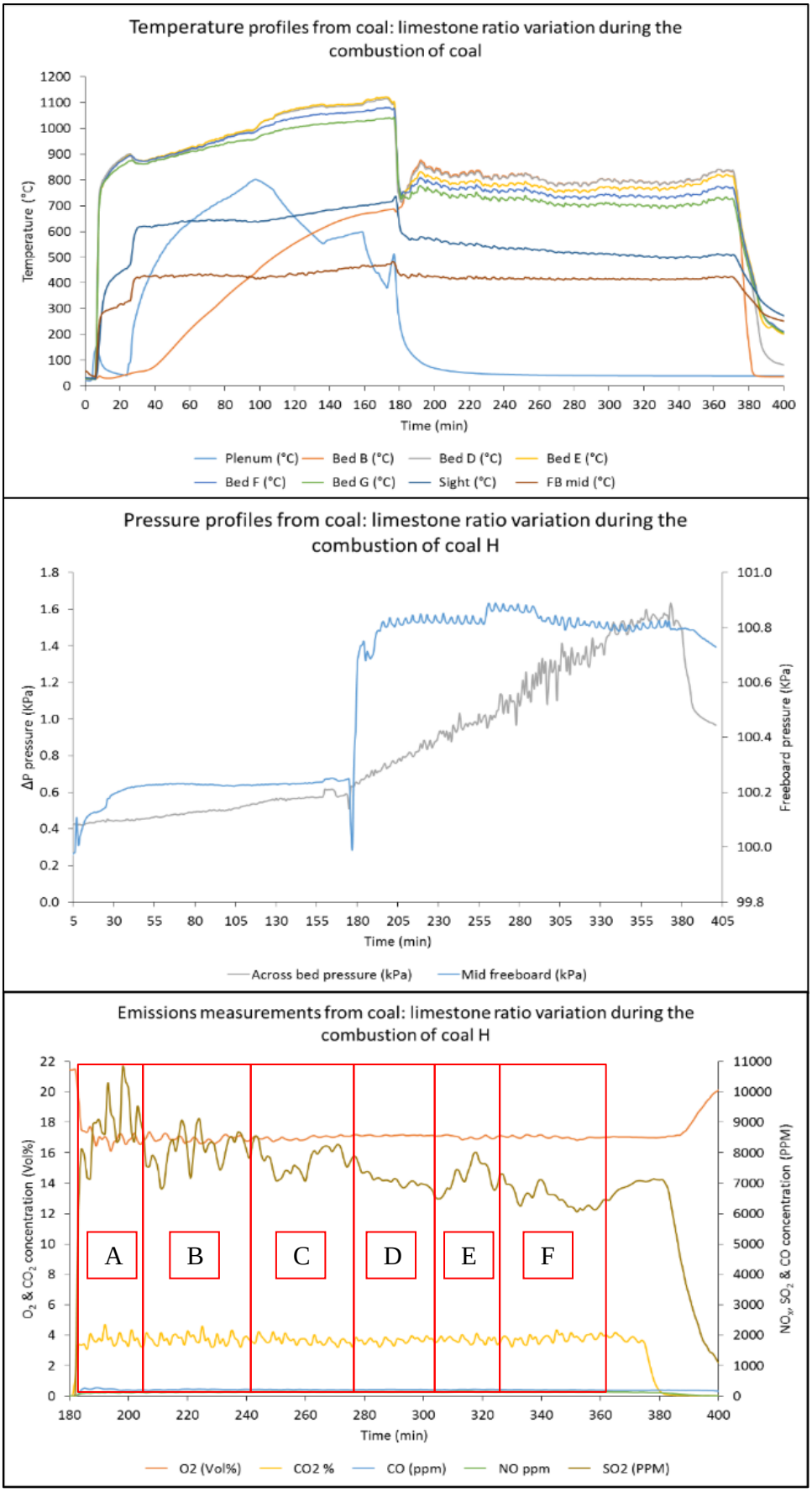

Figure 6-14 Data example from combustion of Pakistani coals with limestone sorbent [limestone and coal H]

Table 6-1 Feed rates for different Ca:S ratios on a molecular weight basis			
Ca: S	Period	Coal feed (kg/hr)	Limestone feed (kg/hr)
Coal only	A	10	0.00
0.5	B	10	0.52
1.0	C	10	0.62
2.0	D	10	1.23
3.0	E	10	1.85
4.0	F	10	2.47

The SO_2 emissions measured in the flue gas change with the changing Ca: S ratio as expected. When coal only is being combusted the SO_2 emission in the flue is measured at ≥9000 ppm. This is the baseline value which will be used to compare the ratio effect on SO_2 emission in the flue. The changes in SO_2 emission can be directly related to the Ca and sulphur retention in the bed as no other variable was altered throughout the test.

The O_2 concentration was indicated to be between 16 and 17 vol% throughout the tests. This was due to two factors. Firstly, higher air flow rates were used (≥130 kg/hr) which was a trade-off between optimising flue gas composition and ensuring high enough turbulence was sustained within the bed to perform full length test under a bubbling regime. Secondly, there was a leakage issue within the upper region of the FBC rig. The air ingress was located in a position that did not impede or alter combustion within the bed as the extraction fan ensured negative pressure throughout the freeboard. Hence, combustion operated at near ideal levels. However, the leak effected the downstream measurements made in the flue gas analysis and as such the SO_2 emissions were normalised to a standard O_2 concentration of 9 vol. %, (normalised values for O_2 was calculated to be 9% vol. as this is a representative value for FBC combustion emission). By normalising the data the dilution factor in the SO_2 measurements has been minimised. The effect of SO_2 retention will be further discussed in the discussion section later in the Chapter.

As previously indicated, the combustion of coals with the addition of limestone in the pilot scale tests presented problems due to the high agglomeration propensity experienced. Samples were taken from the bed using the same method as for the baseline tests for further analysis.

6.2.1.1 SEM-EDX

Figure 6-15 and Figure 6-16 are point of interest from the SEM-EDX analysis of samples taken from the bed after coal: limestone blends had been combusted to investigate the desulphurising method on agglomeration and SO_2 retention.

Figure 6-15, image 1 shows the agglomeration of bed particles and the matrix binding the structures together in both bridging and fusing mechanisms. In all points of measurement, the surfaces were found to be made up of Si-Fe-Al complexes which is in agreement with the ash analysis conducted

in Chapter 4 and baseline results. Image 1 shows several stages in the agglomeration growth process. The small clustered like particles between the bed particles are ash particles and matrices of alkali species sticking the bed particles together. The bridge point between entrapped bed particles is dominated by Si-Fe complexes with less lower melting temperature alkali species than the surface of the agglomerates. This illustrates further the theory that residence time and localised heating caused by the onset of agglomeration is driving away lower melting temperature species such as K in a gas phase.

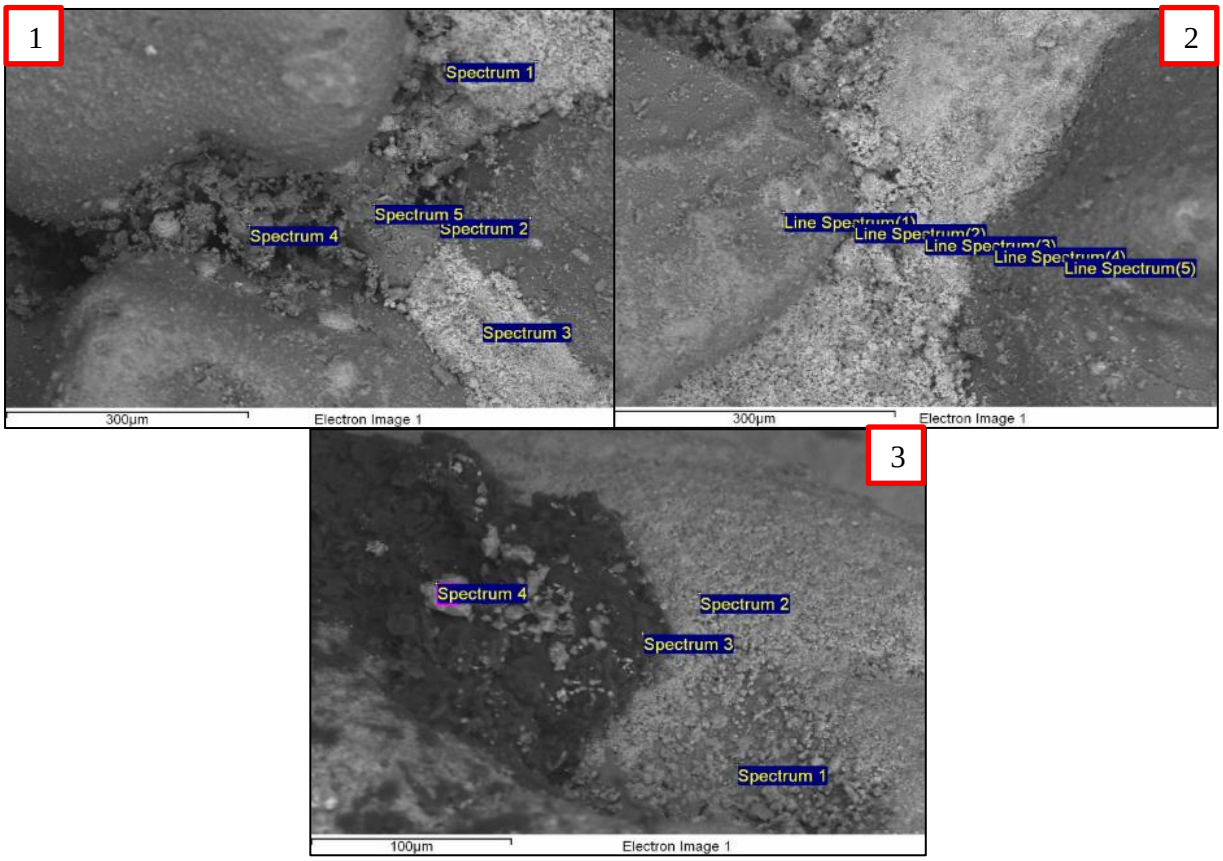

Figure 6-15 SEM images and the locations of SEM-EDX from wood combustion. Images are as followed; 1) agglomerated bed particles, 2) fusion point between bed particles, and, 3) surface of agglomeration

Image 2 further reinforces the previous point that the surface of the bed particles is coated in a Si-Fe-Al dominated complex with small concentrations of other alkali species. However, the strong bond between the sand particles is dominated by Si-Fe complexes.

Image 3 shows further evidence of the mechanisms above. However, there is also indication of limestone embedded within the agglomerate. The limestone particle is bound in the agglomerate but is found to have a low sulphur content. This indicates that limestone particles are being coated by the alkali melt phase present in the bed and adhering them to the forming agglomerates. In doing so limiting the sulphur retention of the limestone. This mechanism could be due to a lack of mixing caused by binding with the agglomerate. This coating and incorporation into the agglomerates is

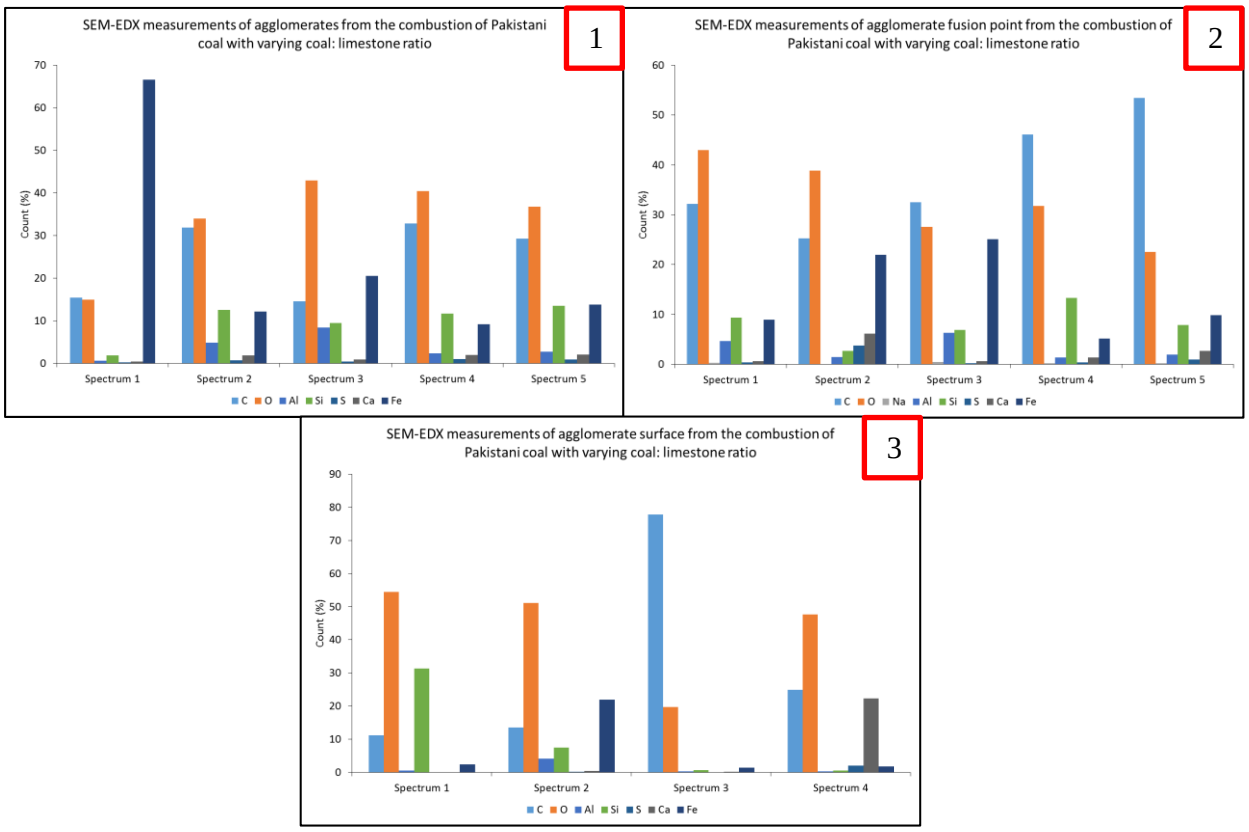

Figure 6-16 SEM-EDX results for the selected samples shown in Figure 6-15

assumed to be limiting the effective surface area of the limestone to the passing gases and thus reducing retention into such limestone particles. Finally, the limestone had low concentrations of Fe and Al on its surface. It is likely that the matrix coating the sand particles is also to some extent coating the limestone. This would inhibit the active surface and thus reduce desulphurisation and sulphur retention potential.

The results here show that the mechanism for agglomerate formation to be in agreement with that found in baseline tests. This is then followed by a Si-Fe matrix with low concentrations of low melting temperature alkali species which is likely a result of localised heating from poor mixing caused by the agglomerate presence and increasing size. Furthermore, the results show that the agglomeration potential of the coal is inhibiting the sulphur retention and thus desulphurisation potential of the limestone by coating the pores, reducing mixing and reducing active surface area of the limestone. With more extensive agglomeration and extended operation time the desulphurisation potential of limestone will decrease with these coals.

6.2.1.2 XRF

Bed samples were taken after the test and analysed as described in the baseline bed samples analysis.

Samples of the bed were taken after two different tests in which coal A was combusted with the addition of limestone sorbent. The Ca:S ratio was varied throughout test but the total limestone in the bed increased throughout the period. It was assumed therefore that the Ca inventory of the bed would be high and this would be seen in the CaO concertation measured using XRF. As the results in Figure 6-17 show, the bed content was dominated, as with the baseline tests, with Fe, Al and Si oxides.

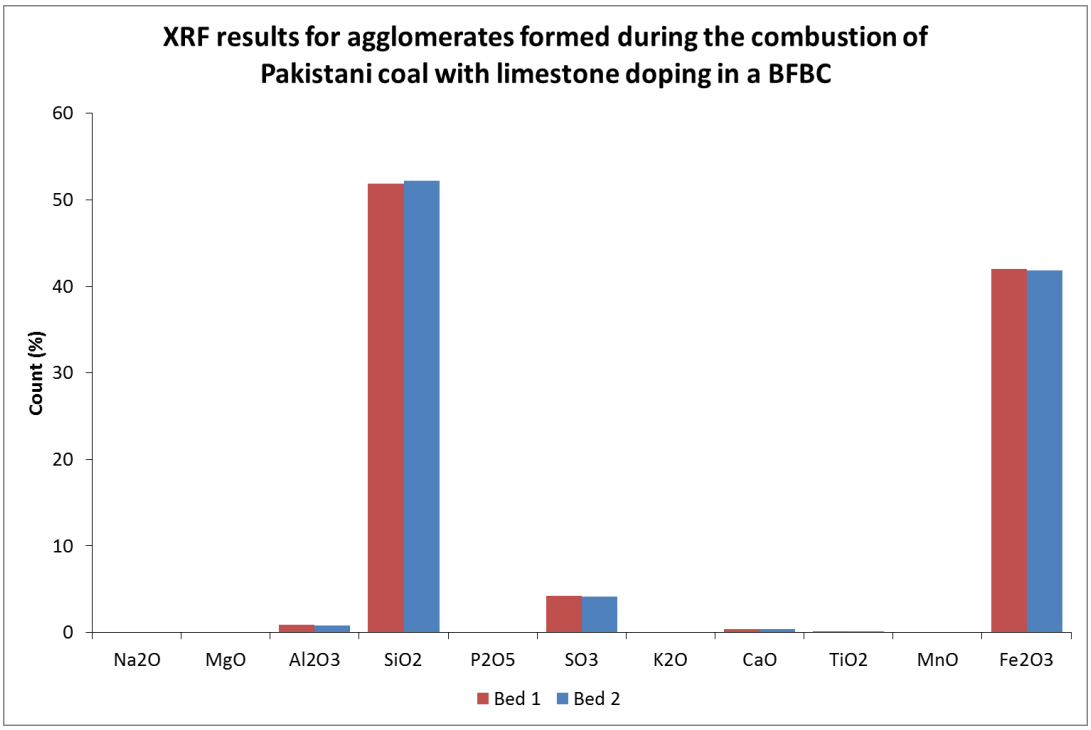

Figure 6-17 XRF analysis results of bed samples taken from the bed after the combustion of Pakistani coal A with limestone at variable Ca:S ratios in a BFBC

XRF results only measured trace amounts of CaO in the agglomerates even though there was a significant Sulphur concentration present. The data suggests that the limestone was reacting with the sulphur during combustion and hence the presence of Si to be expected. The low CaO measurement from XRF is likely an indication to the high reactivity of the calcium and reinforcing the highly efficient retention of S oxides in limestone. The samples used for XRF analysis are therefore assumed to contain only a small percentage of limestone.

The XRF results highlights the effect of agglomeration on desulphurisation and the addition of limestone sorbents to FBC. As seen in results, the sticky surfaces of the complexes have a high infinity to adhere to the porous surfaces of the limestone particles. This has been seen to impact the limestone in two ways, 1) the limestone contributes to the agglomeration growth mechanism by creating a porous medium for eutectics to bond to, and, 2) the limestones desulphurisation potential become less as the blocked pores of the limestone react with less sulphur oxides.

6.2.2 Sorbent Particle Size

During the sorbent particle tests the aim of the experiments was to alter the average size of the limestone being blended with the coal feed. The coal fuel flow rate was kept constant (32kg/hr) and the ratio of limestone to coal was also kept fixed (1:3). As discussed in the literature review, authors such as (Khan and Gibbs, 1995; Basu, 2013b; Kunii et al., 2013; Dam-Johansen and Østergaard, 1991; Leckner, 1998) have previously investigated the effect of sorbent particle size on desulphurisation in FBC during the combustion of coal. It was seen that the available surface area and hence sulphur retention reactions were impacted by particle size. Muenzer and Bonn (1980) found that the optimum particle size ranges for sulphur retention were 10-20 μm and 200-400 μm. These different ranges are due to the impact the particle ranges have on packing in the bed and associated movement of particles and gases. Additionally, the particle sizes were suggested to have an impact on the fluidity of the bed as the average particle size altered with the increase in sorbent particle size. The following section describes the results of varying the limestone particle size and discusses the implication of agglomerate formation and impact of a Ca rich additives with varying particle sizes.

Figure 6-18 shows the data recorded when coal I was combusted with limestone with a varying particle size. This includes the temperatures, pressures and emissions resulting from the combustion of the coal and limestone blends. The three ranges of particle size used were 0-2 mm, 2.8-4 mm and 4-5.6 mm with a ratio of coal to limestone of 3.0 to replicate realistic desulphurisation parameters (Hlincik and Buryan, 2013; Tarelho et al., 2005).

Graph 1 shows the temperatures in which period A, B and C are marked. These represent the different particle size ranges; 0-2 mm, 2.8-4 mm and 4-5.6 mm respectively. As the temperature data shows the temperature decreased with the introduction of the different sized limestone: coal mix. The fuel flow was kept at a constant flow of 35 kg/hr. Whilst the pressures varied very little throughout the test, the changes in the temperatures suggest an impact on combustion. The different limestone particle sizes could have impacted the way in which the bed, fuel and sorbent were mixing. Therefore, a particle range such as 2.8-4 mm, which is within normal FBC specification, was evidently going to mix better and thus combust more efficiently in the bed.

The emissions data (graph 3) marked A, B and C show the effect of limestone particle size on the emissions of SO_2 with a constant fuel supply. Range A with range 0-2 mm reduced the emission of SO_2 from 4500 to 3000 ppm. Range B shows the sulphur retention decreased as the flue gas measurement increased from 3000 to ≥4500 ppm. Range C resulted in the sulphur retention altering again with SO_2 in the flue gas decreasing to approx. 4000 ppm. With the variation of limestone

particle size there was clearly and impact on the sulphur retention in the bed with 0-2 mm particles reducing the SO_2 concentration in the flue gas $\geq$ 3000 ppm.

Whilst the smallest limestone particle range (A) resulted in the greatest reduction of SO_2 concentration in the flue gas it also impeded on combustion the most. As the implication of particle size in the bed Geldart graph states (Figure 2-5), small particle ranges are known to interfere with fluidisation, mixing and thus the performance of combusting fuel particles. The work by Geldart and Rhodes (1986) is further justified by the middle particle range producing the optimum combustion environment and mixing regime as evident by the highest bed temperatures for the same fuel feed rate

Throughout these tests the formation of agglomerates led to the defluidisation of the bed and thus defluidisation. The formation of agglomerates was not attributed to the variance in the particle size but instead the inherent quantity of Fe and Al groups in the fuel stock. Whilst limestone was found in all of the agglomerates, no preference was found for a particular particle size or range. Instead a mixture of all particles was coated and entrained in the eutectic complexes as found within the Ca: S tests.

.

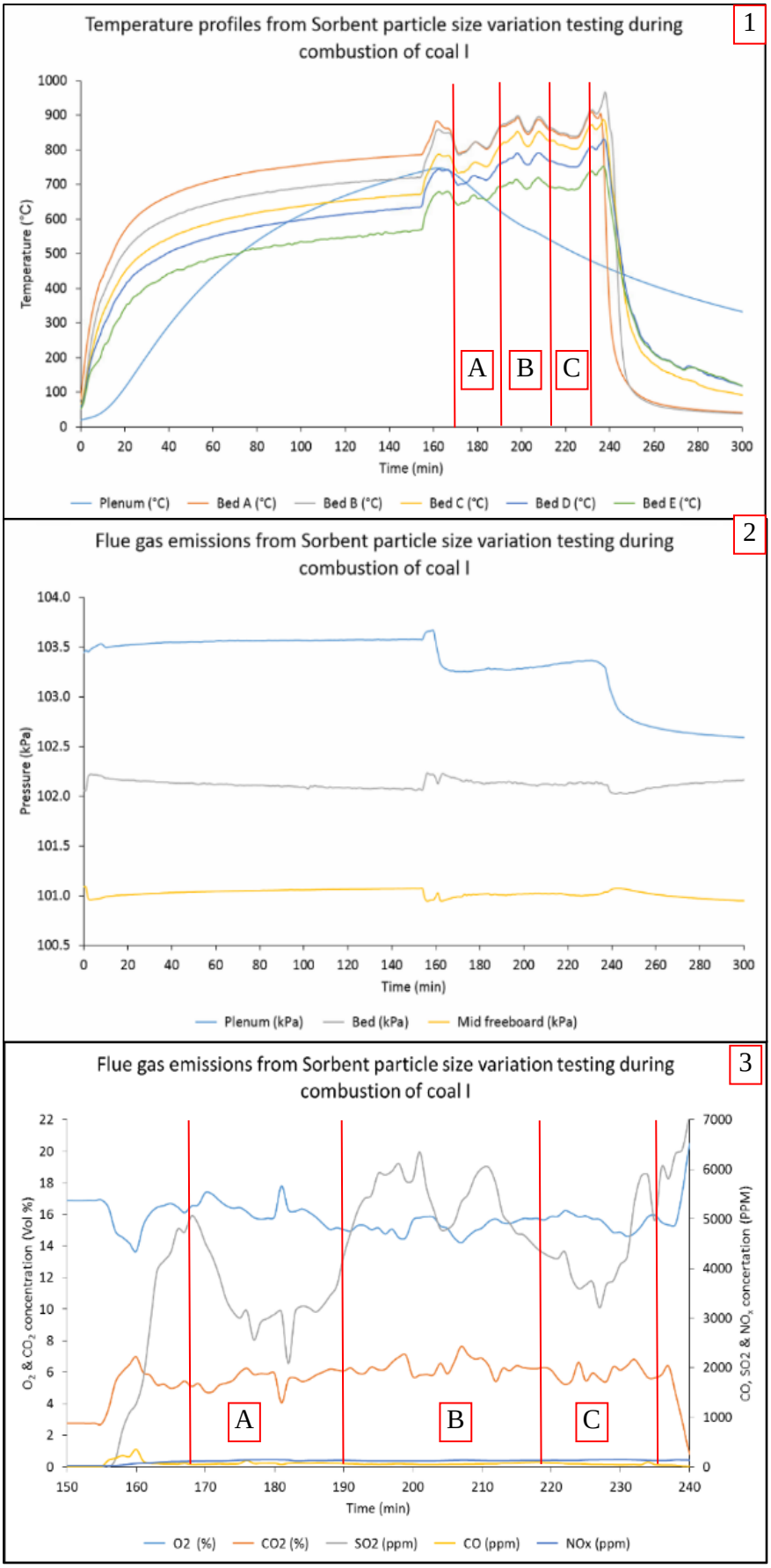

Figure 6-18 Graphs from the combustion of coal I with limestone whilst varying sorbent average particle size; 1) temperatures, 2) pressures and, 3) emissions

6.2.2.1 SEM-EDX

SEM-EDX analysis found little difference in the agglomerates compared to the baseline data and thus the baseline agglomeration mechanisms is applicable in these results.

The images in Figure 6-19 and SEM-EDX results in Figure 6-20 are point of interest from the analysis of materials taken from the bed after the previously described tests.

Image 1 shows the surface of limestone taken from within the bed after the test. The EDX data shows that there are high levels of sulphur present. The SEM image shows that the pores of the limestone are also sealed, however, there are still large cracks and troughs within the limestone that visually don't seem to have undergone desulphation reactions. The limestone particle was taken from an agglomerate and it seems as though the desulphurisation has once again been inhibited to some extent by the coating of a liquid phases.

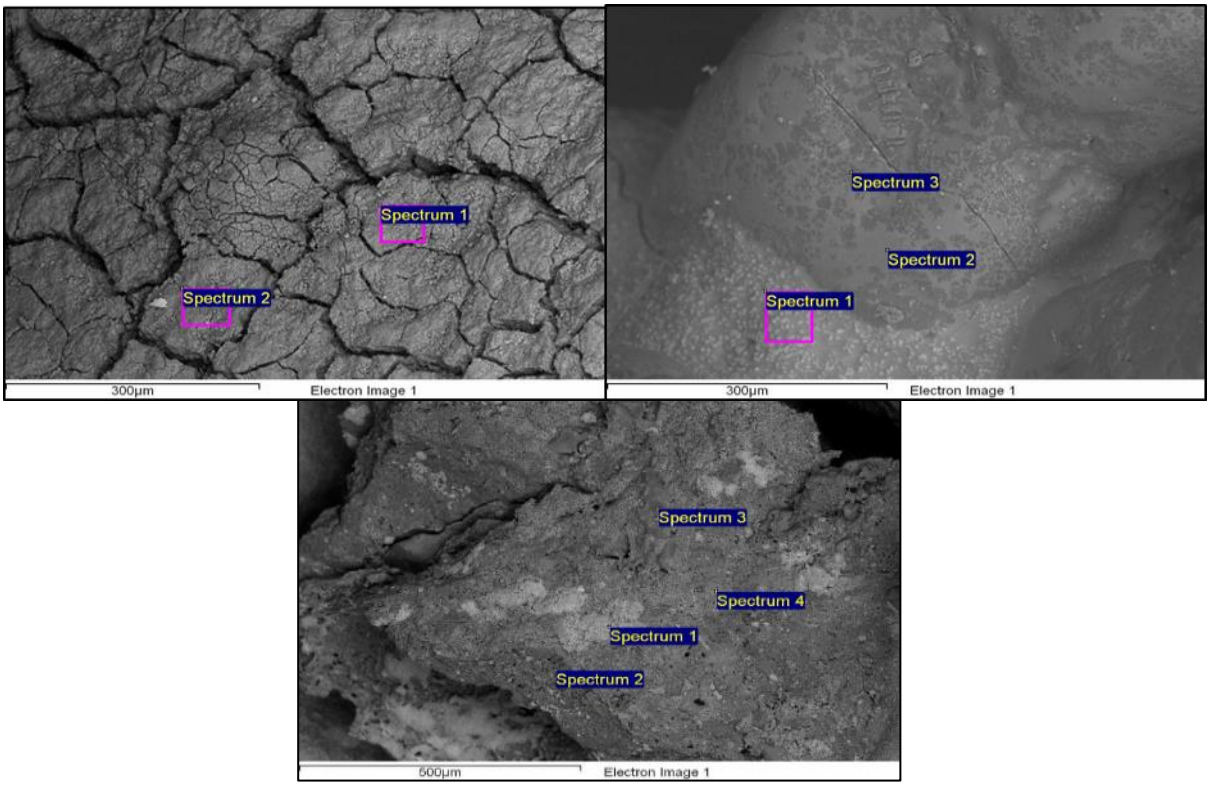

Figure 6-19 SEM images and the locations of SEM-EDX from wood combustion. Images are as followed; 1) Surface of limestone, 2) surface of agglomerate, and, 3) Agglomerated area with ash surface

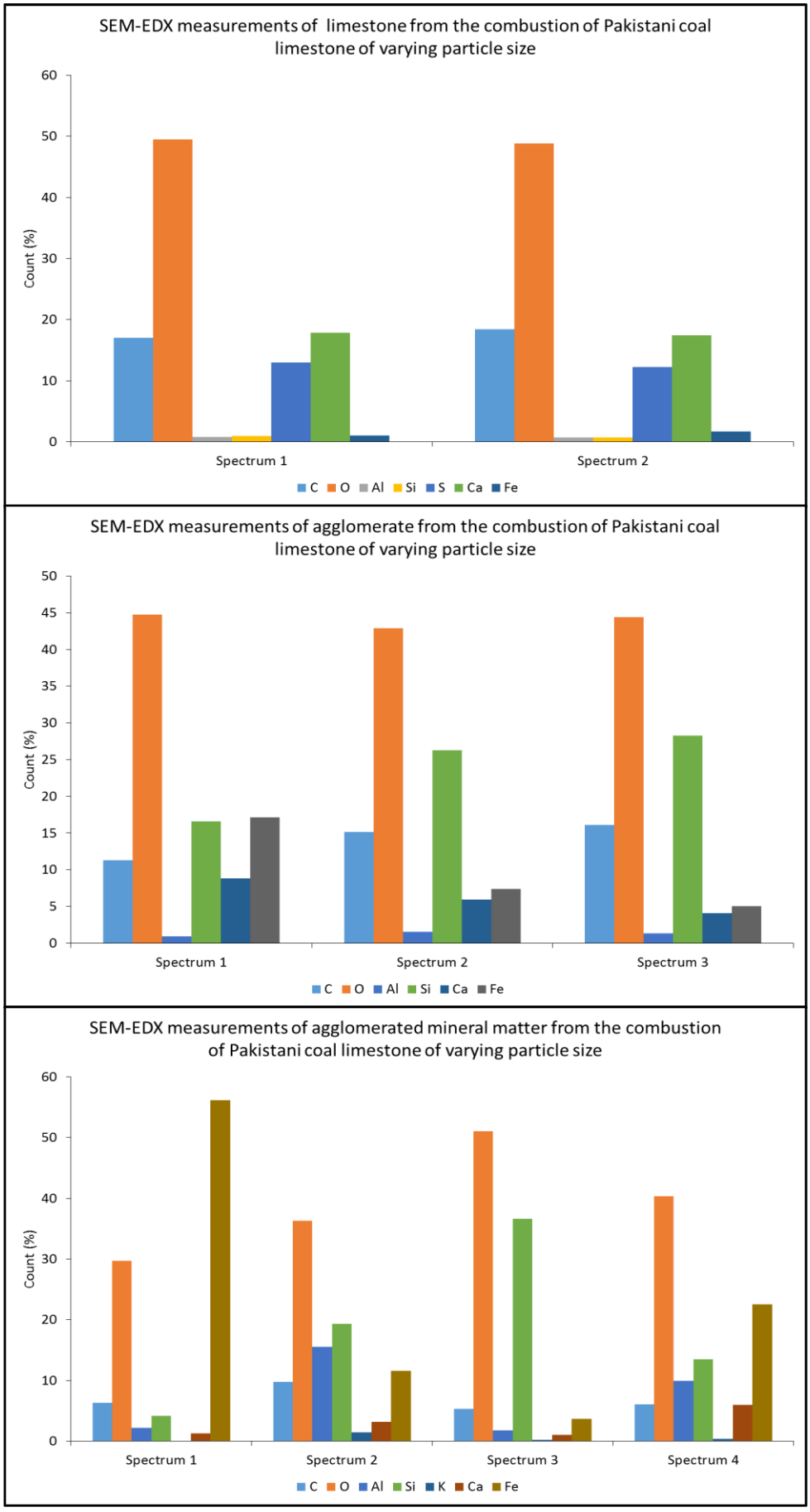

Figure 6-20 SEM-EDX results for the selected samples shown in Figure 6-19

Image 2 shows agglomerated bed material similar to that seen in the baseline and Ca: S ratio tests. The bed particles embedded within the agglomerate have lower concentrations of agglomerate species on the surface of the particles. It would seem as though the surface of the structures are coated in very little eutectic matrix. Perhaps with the change in particle size, the change in mixing or limitation of particles mixing in the bed, there has been a resulting limitation of particles exposed to the eutectic matrix.

Image 3 shows an ash particle and bed particle which was contained within the core of an agglomerate. This was indicated to have a mixture of species including Al, Si, K, Ca and Fe. The presence of a complete ash particle indicates combustion of the fuel but also a limitation in the localised temperatures. The ash didn't melt which suggests poor mixing and entrainment into the bed or cooler zones forming on the bed.

The results from the SEM-EDX data show that the agglomeration mechanism and alkali species responsible for the propagation of the agglomerates are as seen in previous sections. However, the influence of changing the limestone particle size doesn't seem to be limited to the effect on desulphurisation. The different particle sizes will alter the mixing within the bed and thus alter the way in which bed particles both interact with one another and become exposed to the sticky alkali species and bed ash.

Therefore, the changing in particle size is likely to lead to both positive and negative effects with respect to the formation of agglomerates. However, because of the inherent poor quality of the coal, the build-up of alkali species in the bed continued and agglomerates inevitably formed and led to the defluidisation of the bed.

6.2.2.2 XRF

The XRF results for bed samples taken from the combustion of coal I with varying average limestone particle size are shown in Figure 6-21. The results of this bed sample analysis show very clear similarities with previous tests and baseline results. Whilst the particle sizes varied in size, the mechanism for the onset of agglomeration did not.

It should be noted that the Fe_2O_3 concentration in the bed sample from this test was approximately 5% less than seen in the Ca:S ratio tests. It is assumed that the mixing of the bed slowly decreased with an increase in total bed mass with a fixed inlet air flow as well as the particle sizes impacting the particle entrainment into the bed.

The dispersion of the alkali species in the agglomerates and the bed seems to have been stifled by the poor mixing brought on with different average particle sizes. Hence the concentration of alkali

species has fluctuated slightly compared to the baseline agglomerates that the results have been compared to.

The different particle size range of the sorbents retained different concentrations of sulphur as the literature review suggested. However, the impact on mixing was unexpected and will be discussed further in later sections.

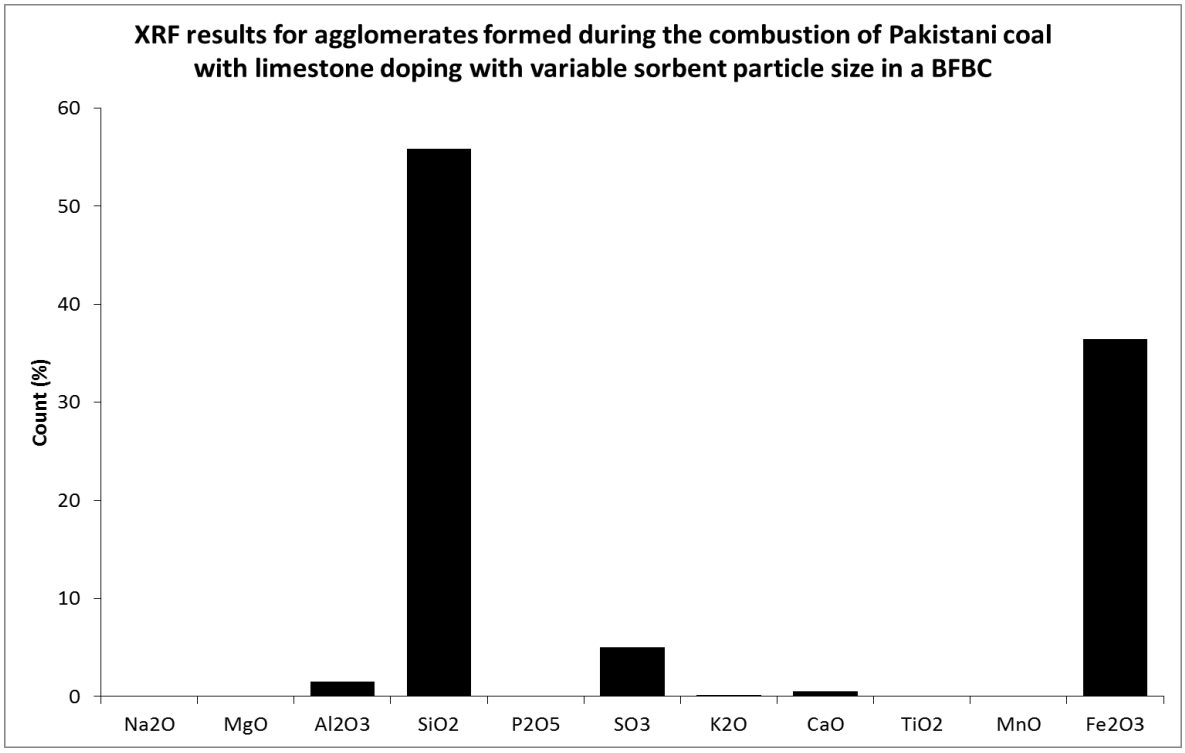

Figure 6-21 XRF analysis results of bed samples taken from the bed after the combustion of Pakistani coal I with limestone with varying average sorbent particle size in a FBC

6.2.3 Combustion Temperature

The objective of these tests was to investigate the effects of the flame temperature on the retention and hence desulphurisation potential during combustion of coal I. During these tests the coal was blended with limestone at a ratio of 1:3 (molar ratio of Ca:S). Literature and industry practice, as well as results from previous sections show that a Ca:S ratio of 3-2.5 is the most effective ratio for desulphurisation (Kunii et al., 2013; Tarelho et al., 2005; Tarelho et al., 2006). Therefore, in order to increase the temperature of the bed the fuel/limestone feed rate was increased/decreased accordingly. The base fuel flow rate to achieve ≥700-750 °C was determined to be at 34-35 kg/hr. The fuel flow was increased in steps (+1 kg/hr) to 38-40 kg/hr to achieve a maximum temperature of ≥950°C.This was mediated as necessary to combat system changes to maintain stable combustion and a bubbling fluidised bed.

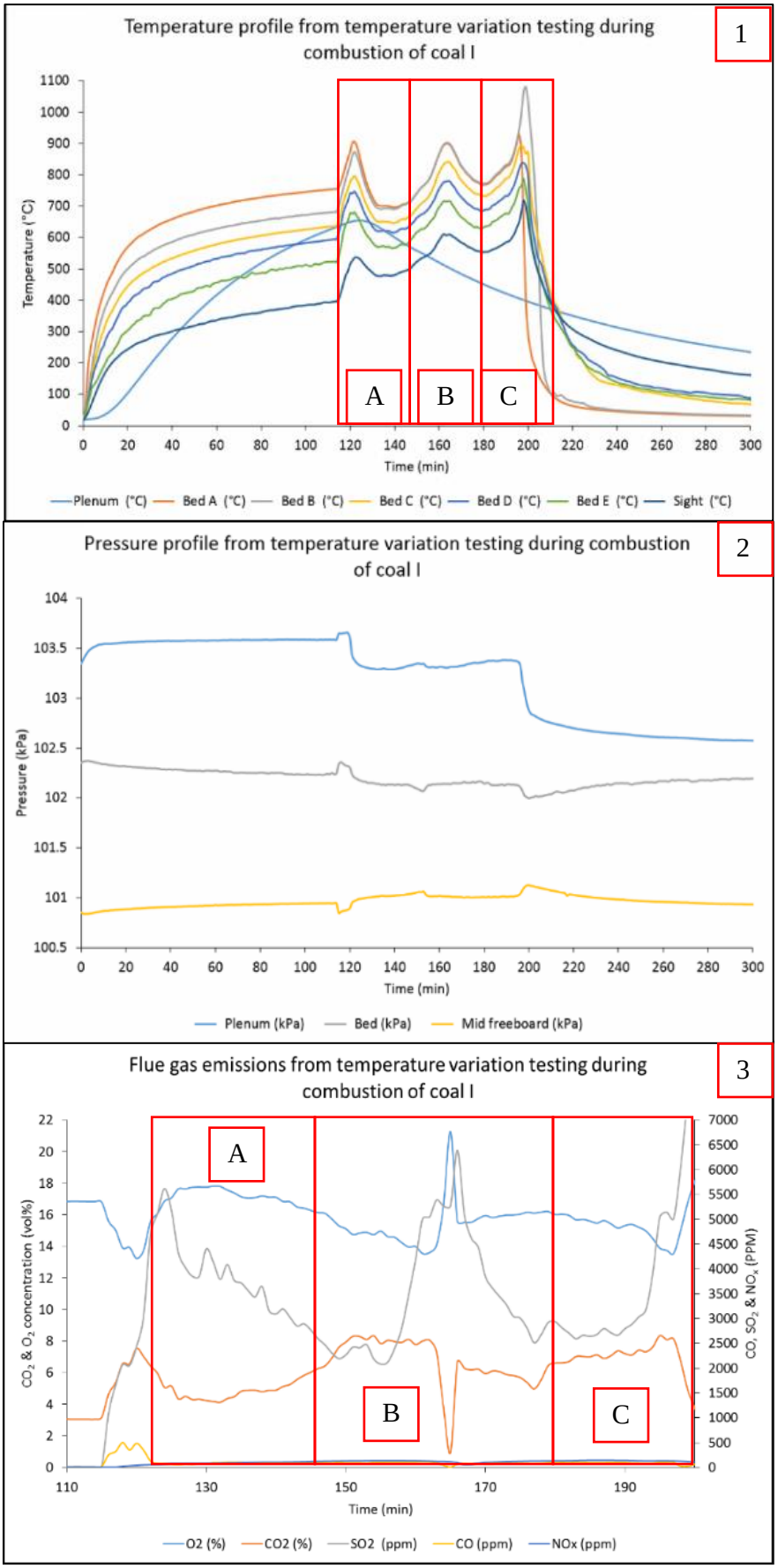

Figure 6-22 Data from combustion of coal I over varying system combustion temperatures; 1) temperatures, 2) pressures, and, 3) emissions

Figure 6-22 shows the data collected when the bed temperatures was altered in stable operation. Once again pressure data from these measurements shows little change other than what had been seen in previous test with the loading of material in the bed over time. Graph 1 and 3, temperature and emissions respectively have range A, B and C highlighted. The ranges indicate the period in which the modified fuel flows took place. Small changes to the fuel flow (0.5 kg/hr steps) were found to have drastic effects in the performance of the bed. It was found that these changes took significantly longer to occur in the results and the bed, ≥20mins. This was due to screw feeder loading and mixing regime into the bed. Small changes to the fuel flow were found to make extreme changes in both the temperatures and SO_2 emission. These tests were repeated using smaller fuel flow increments 0.1kg/hr to better control the experiments.

As the data shows from range A to B, an increase in the bed temperature exceeded the desirable increase of 50 °C and instead increased by ≥100 °C. This is followed by a dip in the temperatures as the bed re-stabilises. The periods A, B and C are the resulting increments of a more controlled test in which the target temperature ranges were achieved and held.

The retention of SO_2 was impacted by the temperature of the bed and furnace area. With increasing temperature, the literature discussed previously noted a decrease in the limestones reaction efficiency as a consequence of the calcination reactions of the limestone being impeded. The data shows there was a limiting temperature for efficient sulphur retention of ≥750-≤820°C. Furthermore, different combustion temperatures were shown in Chapter 2.10.1 to impact the propagation and rate of formation of agglomerates. The peak temperature for SO_2 retention is also normal combustion temperatures for FBC systems and for large concentrations release of alkali species in the gas phase.

It was evident that elevated temperatures in the bed beyond normal operational limits (>900°C) resulted in more amorphous glass materials in agglomerate samples, more extensive agglomerates and agglomerates with a much harder structure. Figure 6-23 shows an image of the bed and the extent of the agglomeration that occurred as a repercussion of excessive heating.

There was a large amount of material containing the mineral matter and limestone which can be seen to be protruding from the agglomerated structures throughout Figure 6-23. Image A shows the typical agglomerate which was found in the bed and repeats tests. Image B has blackened areas made up of hardened glass like areas (circle) throughout the top surface of the agglomerates which were located near the surface of the bed. As the mechanism for agglomeration in Figure 6-13 suggested, there is an impact of sintering in homogenising the eutectic matrix on the surface of the

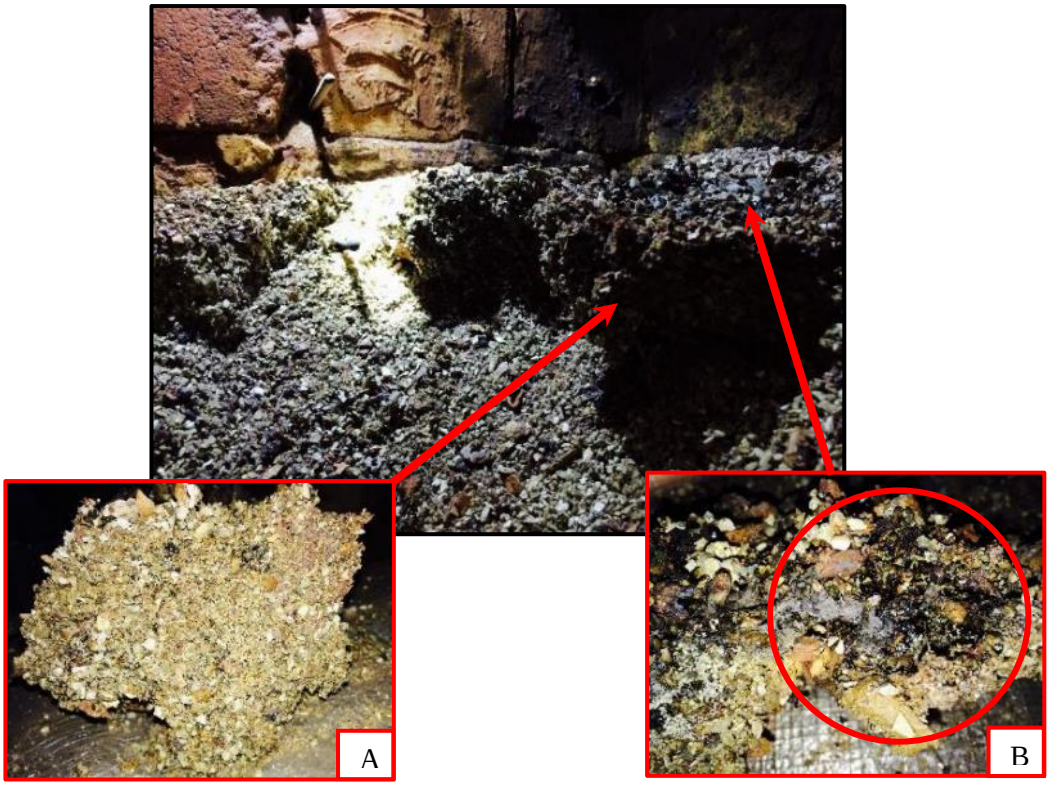

Figure 6-23 Agglomerated bed of temperature variable tests combusting coal I and Limestone (ratio 3.0). Bottom of the bed found to be standard agglomerate as in other tests, top of bed found to contain sintered material

agglomerating particles as well as a separate sintering impact on the formation of higher temperature dependant complexes. Whilst the sintered material and agglomerates consistently contained Fe-Si-Al the samples indicate that localised hotspots on the surface of the bed have resulted in silicate glass formation which has been further accelerated by poor mixing brought on by the decreased mixing resulting from higher temperature agglomerate formation.

6.2.3.1 SEM-EDX

The images in Figure 6-25 and SEM-EDX images in Figure 6-24 are point of interest from the analysis of materials taken from the bed after the previously described tests.

Image 1 shows the typical type of agglomerate found within the bed. SEM-EDX indicates high Si-Fe-Al matrixes as with the previous tests. Where in previous tests the high concentrations of Fe were found more in the fusion points within the agglomerate, those Fe rich complexes were found to coat more of the bed particles here. The higher temperatures which the agglomerates were exposed to will have liberated high volumes of liquid and gaseous inorganic species. The result of this is that more bed particles surfaces were coated in more of the Fe-Si rich complexes seen to be very strong in previous tests.

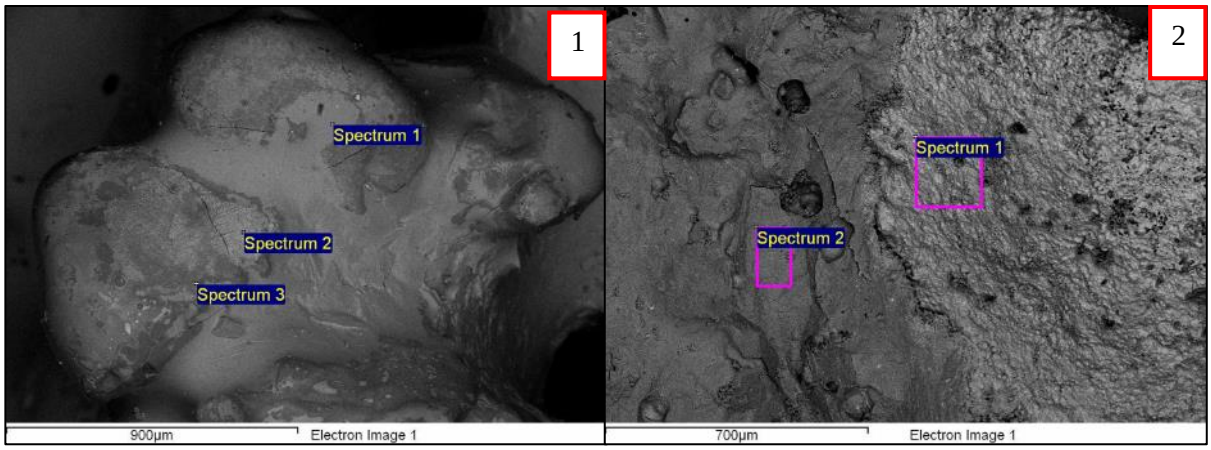

Figure 6-25 SEM images and the locations of SEM-EDX from wood combustion. Images are as follows; 1) agglomerated bed particles, and, 2) fusion point between limestone and bed particle

Further to the sintering process, image 2 shows the point at which a limestone particle has fussed with a bed particle. This has not been seen in previous tests. Rather than the limestone adhering with a particle surface there would be a eutectic surface adhering them together. In image 2 the sand particle is clearly fussed to the limestone particle. The EDX data suggests the presence of Fe, Si and K. Limestone or materials rich in CaO and MgO are known to react with alkali species and reduce agglomeration potential. It would seem here as though the limestone particle has reacted with these species, but in doing so, due to elevated temperatures, has created a eutectic surface which is sticky enough and attractive enough to bond with bed particles. This has propagated the growth of agglomerates which have then encapsulated this particle.

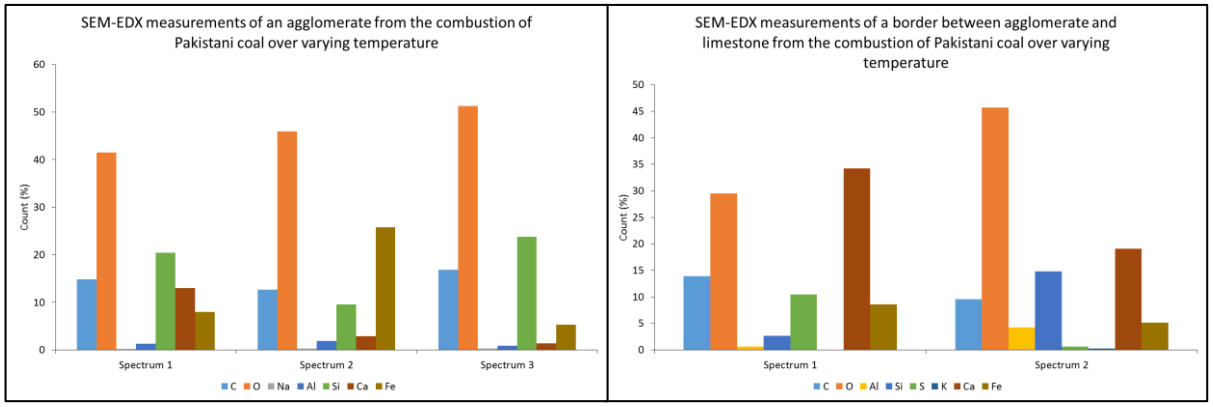

Figure 6-24 SEM-EDX results for the selected samples shown in Figure 6-25

The results here show that the agglomeration mechanism is the same as previously described. However, the change in bed temperatures and combustion temperatures seems to have influenced the bonding of limestone particles to bed particles without independent eutectic formation. The CaO rich limestone should have positively reduced the agglomeration potential but is shown here to likely have contributed to the formation of agglomerates within the bed.

6.2.3.2 XRF

Samples from the bed were taken from the bed in a similar fashion to previous tests and analysed using XRF. The results of the agglomerates show similarities to the baseline study however the bed samples as seen in Figure 6-26 show a slight difference in the alkaline species present.

The major species in the bed are Si, Fe, Al and S as was the case in the previous bed samples. The XRF results indicate that the Fe concentration in the agglomerates increase with increased average bed temperature when compared to baseline results from previous testing. This is due to higher temperature calcination of limestone reducing the reactions on the active surface with Fe as seen in previous tests. As the variable changing in this test was the temperature, it is assumed that the higher temperatures (≥900°C) led to the Fe components being in a more fluid melt phase or alternatively more so in the gas phase. The higher temperatures would likely allow for a less viscous Fe complex which has coated the bed particles and thus the concentration in the agglomerates is slightly elevated. The higher XRF result can also be attributed to the normalisation algorithms in the device. With higher temperatures, the lower melting temperature species will have been lost in the flue gas. Therefore, the total remaining material in the eutectic will be dominated by the higher melting temperature species such as Fe-Si.

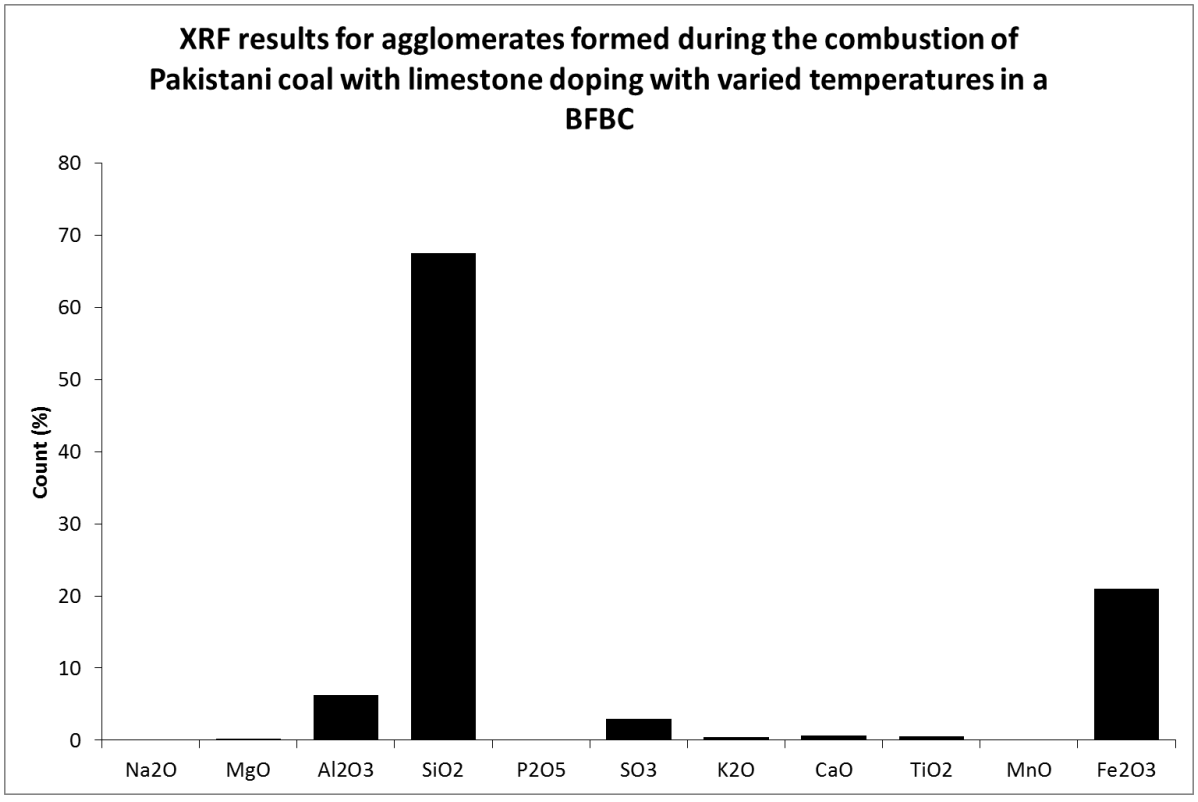

Figure 6-26 XRF analysis results of bed samples taken from the bed after the combustion of Pakistani coal I with limestone at variable temperatures in a BFBC

6.2.4 Co-firing with Biomass

The objective of these tests was to evaluate the desulphurisation potential of biomass and coal blends whilst looking at bed performance with respect to stable combustion and the effect on agglomeration. During these tests wood pellets were mixed with different coals with similar calorific value in batches creating fuel blends containing 100%, 80%, 70%, 60%, 50%, 40% and 0% coal content (on wt.% basis). In doing so, it was possible to analyse the change in SO_2 emission as a result of biomass in the fuel and to evaluate the combustion behaviour within the rig.

Figure 6-27 shows the measurements recorded during the test of Co-firing wood pellets with coal J. Graph 1 shows the temperatures within and above the bed remained fairly constant with the changes in fuel batches. The objective fuel flow was 39 kg/hr to achieve a thermal output of 200-205 kW. Period A-F represent the different batches within the bed from 100% coal to 0%. The average bed temperature throughout the test moved from 750 to 810 °C. This is a result of the degradation of the bed and onset of agglomeration along with the volatile flame becoming the dominant form of combustion whereas the char combustion was the primary source of combustion with higher coal ratios.

Graph 2 shows that pressures throughout the period in which solid fuel was the primary method for combustion and very little changed. However, over the 280 minute solid fuel combustion time, the midfreeboard pressure slowly increased whilst the bed pressures slowly decreased. This is a result, again, of agglomeration build up in the bed and total volume of ash/mineral matter loading the bed.

Most significantly, the emission data shown in graph 3, shows the changing SO_2 emissions with the change in the fuel blends. The other measured emissions remain fairly constant throughout the test, once again indicating ideal stable combustion.

Figure 6-28 shows the measured SO_2 emissions as a result of biomass: coal ratio change. Additionally, the theoretical SO_2 emission based on the fuel input is also plotted to compare the theoretical against the experimental. It was found that as the percentage of coal in the fuel decreases as the percentage of biomass increases, the SO_2 emission decreases. At 100% coal content, the SO_2 emission for coal B and D was 5800 and 5600ppm. With an increase in biomass in the fuel ratio of 50:50, the SO_2 emissions dropped to 5500 ppm and 4500 ppm for coal B and D respectively. For coal B this is a 5% reduction in the SO_2 emission and for coal D a 19% reduction in SO_2 emission for a 50% reduction in the primary sulphur source.

The results show a decrease in the SO_2 emission as a result of the fuel blend change. However, the data indicates that instead of the sulphur being retained within the bed as a result of the presence of biomass, instead the reduction in total sulphur seems to influence the SO_2 emission. The presence

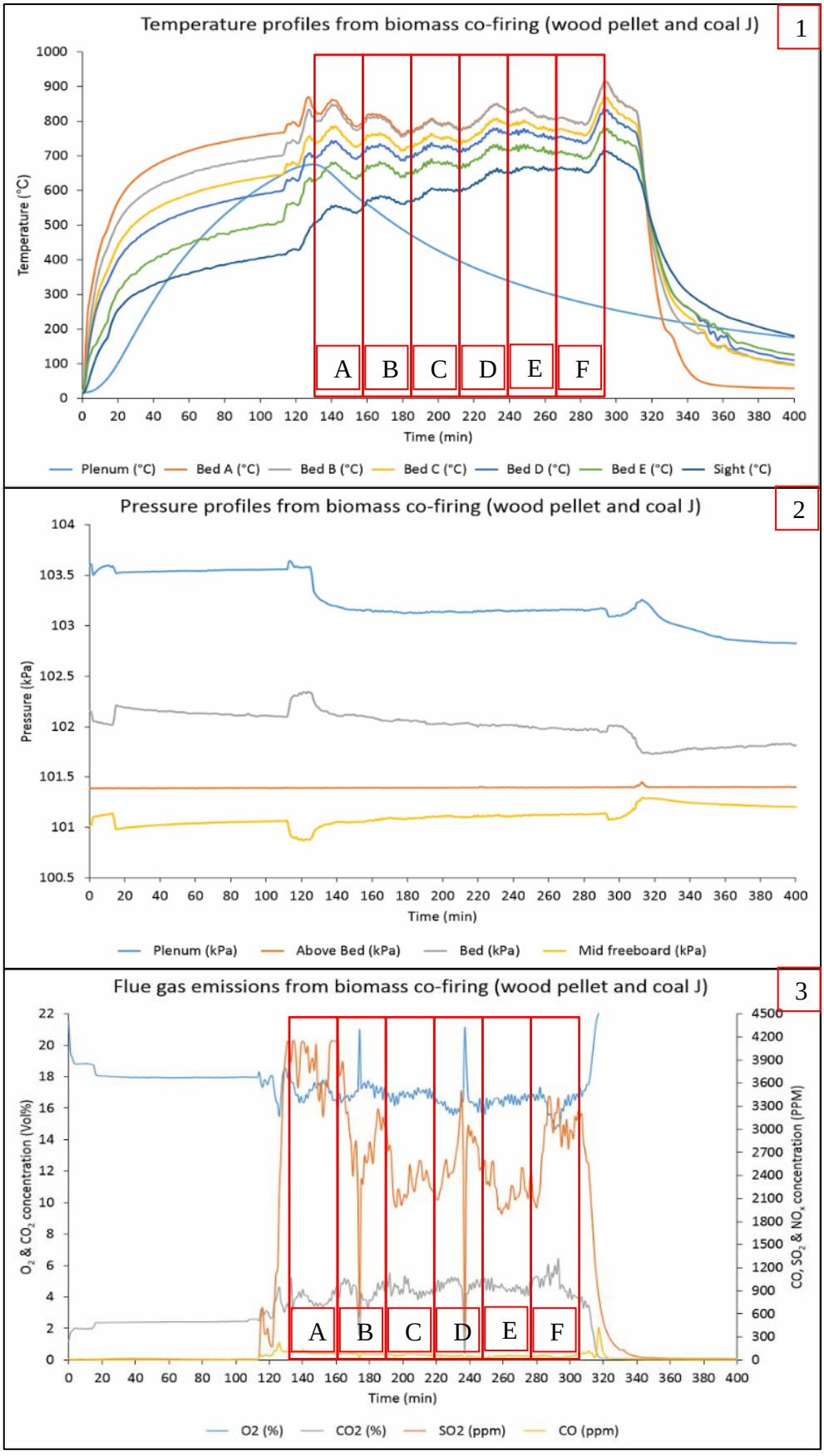

Figure 6-27 Data for the co-firing of Pakistani coals and white wood pellets; 1) temperatures, 2) pressures, and, 3) emissions

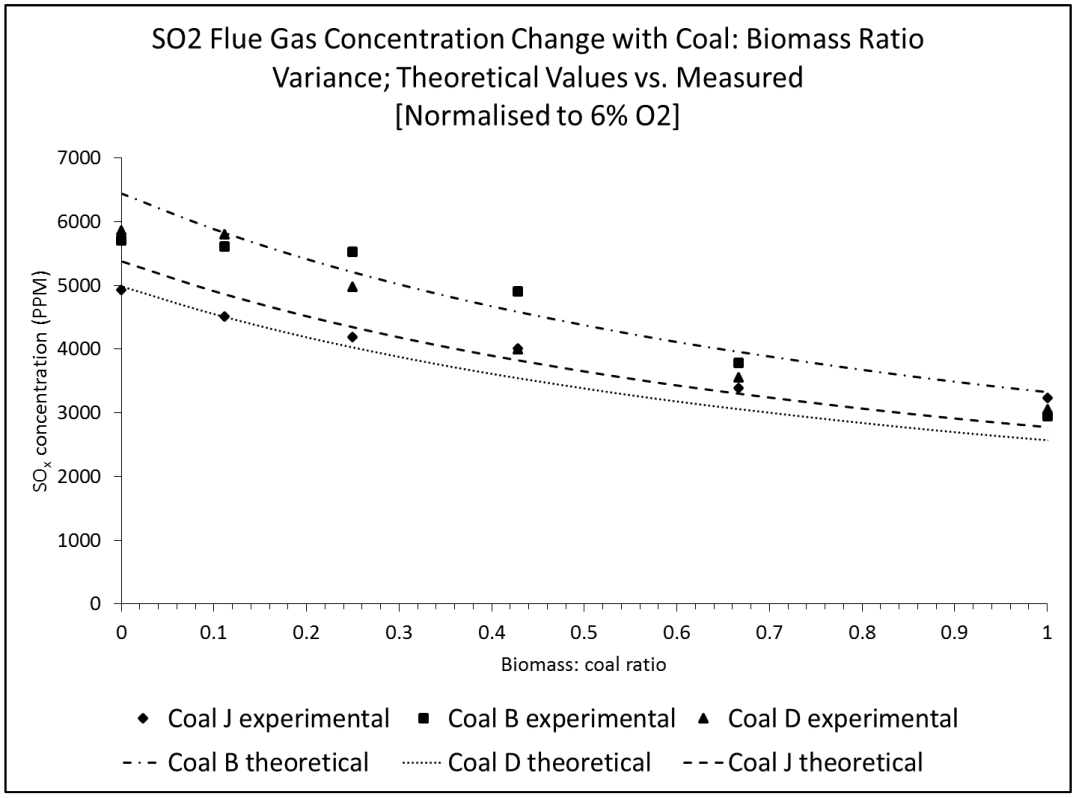

Figure 6-28 Experimental and theoretical SO_2 emissions with varying biomass: coal feed ratio

of biomass in the fuel seems to have improved the stability of combustion, giving more ideal flame shape through the furnace and thus better temperature spread.

Instead an increase in the biomass content in the fuel feed reduces the input of total sulphur in the system and therefore less oxidised to SO_2 in the flue gases.

The effect of blending the coal with a clean biomass like wood resulted in benefits such as an extended period of fluidisation and operation before agglomeration led to defluidisation of the bed. The bed did eventually defluidise but whereas, combusting the coals on their own in the case of coal I running for 74 minutes, coal G 102 minutes and coal A 109 minutes, by co-firing biomass the tests extended to 155, 175 and 198 minutes for coal B, D and J respectively.

The bed was found to be in a different state to the previous tests. Figure 6-29 shows the surface of the agglomerated bed after the co-firing of wood pellets and Pakistani coal D. The circled area draws attention to the protruding structures which were found throughout the bed. These are similar to those seen in the combustion temperature tests in which higher temperatures resulted in sintered areas and more extensive agglomerated structures. However, in other tests the agglomerates were dominated by the mineral matter and other impurities of the coal. In the agglomerates here less mineral matter etc. can be identified and instead more sand particles make up the structure of the agglomerates. The different densities, weights, shape etc. seem to have separated the biomass

Figure 6-29 agglomerated structures and ashed pellets from the Co-firing of wood pellets and coal

pellets to the surface of the bed as mixing and defluidisation set in whereas, the coal particles still combusted in lower regions of the bed or alternatively combusted on the surface but with little if any material left behind for analysis. There will have been an impact in the distribution of heat and combustion and this can be seen by the spike at the end of the test in the graph 1 of Figure 6-27. The volatile matter is burning above the bed creating the raised temperatures measured and the coal is burning in the bed thus maintaining the bed temperature.

6.2.4.1 SEM-EDX

The images in Figure 6-30 and SEM-EDX images in Figure 6-31 are point of interest from the analysis of samples taken from the bed after the previously described tests.

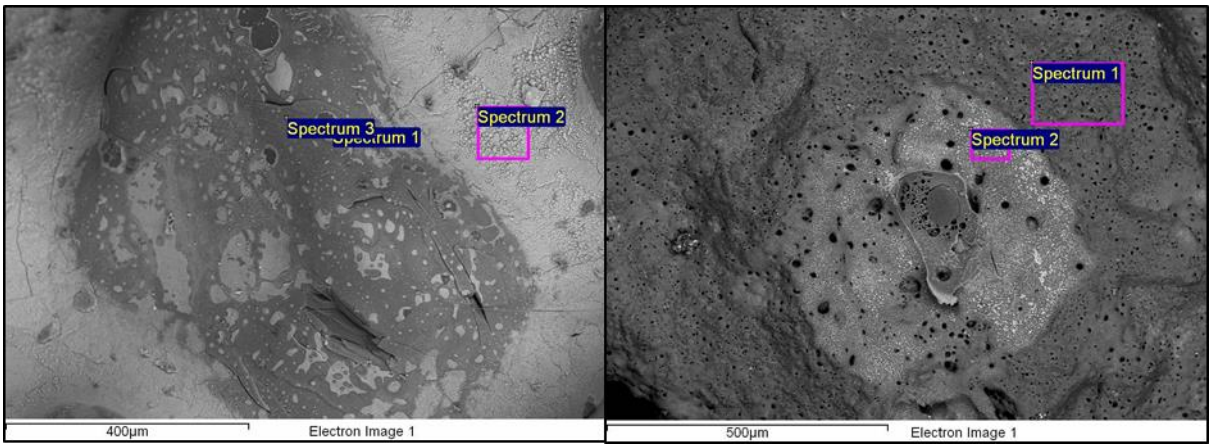

Figure 6-30 SEM SEM images and the locations of SEM-EDX from wood combustion. Images are as followed; 1) Surface of agglomerates taken from the co-firing test bed, and, 2) embedded particles in agglomerated mineral matter

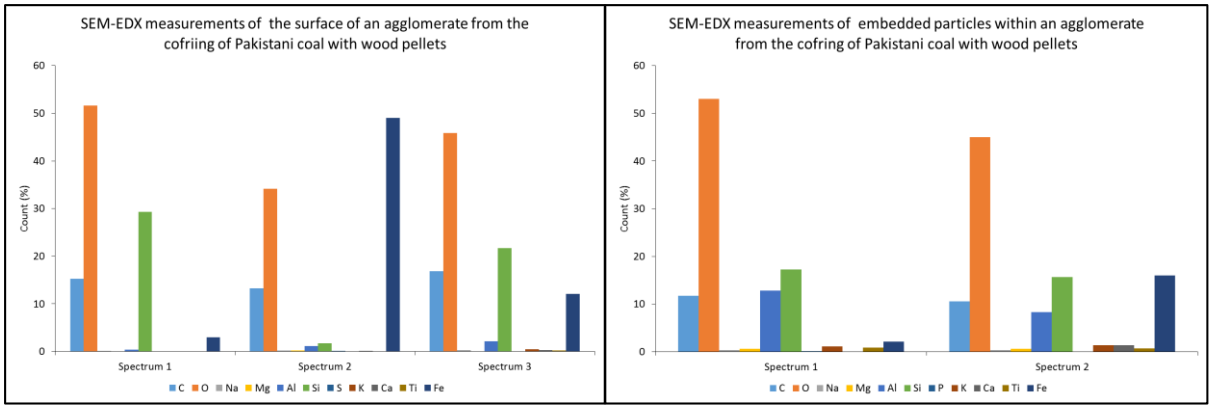

Figure 6-31 SEM-EDX results for the selected samples shown in Figure 6-30

Image 1 shows an agglomerate from the bed during the co-firing of wood pellets and coal D. In this image, sand particles are embedded in a matrix of Fe-Si rich material. The agglomerated surface was found to contain traces of the alkali species identified in the XRF ash analysis. Across the surface of the agglomerate, as with previous samples, the agglomerates were dominated by Fe-Si-Al complexes.

Image 2 shows the other types of surfaces found within the agglomerates. These were areas which were found close to ashed pellets which had pores/openings. However, the EDX measurements still indicate that these areas are mainly Si-Fe complexes. However, around the area in which the particle is embedded, the traces of alkali species is slightly higher than in the rest of the agglomerates. This suggests that perhaps pellets combusting near the surface of the agglomerates are interacting with agglomerates. Additionally, localised heat could explain the holes/pores in the surface. With heating, some species will move to the gas phase, increasing small areas of pressure and leaving the liquid phase of the agglomerate surface, hence leaving the pitted surface as show in image 2.

The results here show similar results to previous agglomerations and SEM data. The wood contained an ash content ≤1.5% therefore the total ash present interacting with the bed compared to the high ash content of the coal is negligible. The coal ash and mineral matter dominated the formation of the agglomerate and the defluidisation of the bed. The wood pellet seems to have simply reduced the total amount of these components entering the bed and in doing so extending the operation of the rig.

6.2.4.2 XRF

Bed sample analysis completed using XRF is shown in Figure 6-32. Again, the main oxide constituents within the bed are Fe, Si, Al and S. However, because of the biomass and its alkali

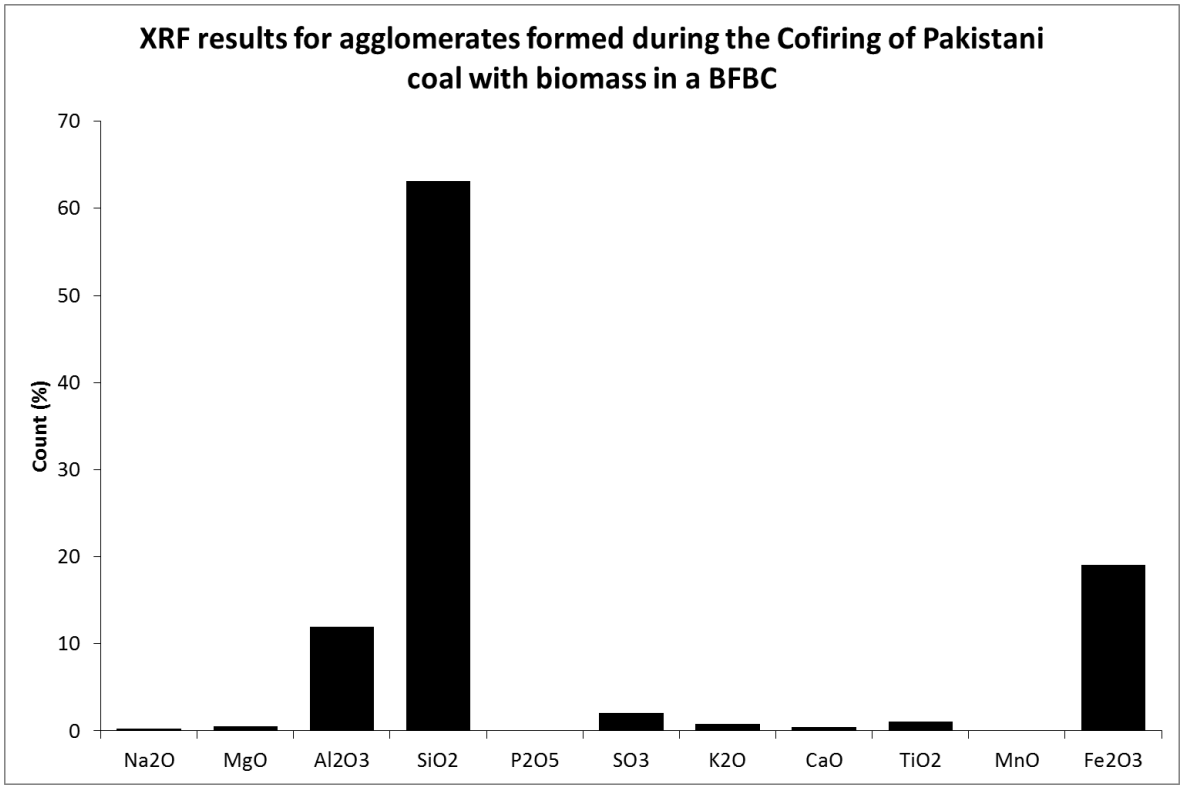

Figure 6-32 XRF analysis results of bed samples taken from the bed after the co-firing of Pakistani coal B with wood pellets in a BFBC

content within the fuel, there are trace amounts of alkaline species not seen in the previous XRF bed analysis, this includes; Na, K, Mg, K, Ti and Mn oxides between 0.5 and 2%.

Increased concentrations of other species including Fe, Si and Al were seen in the agglomerate samples analysed and described previous. However, a small volume of components associated with the stickiness of agglomeration and ash have remained within the bed as shown by Figure 6-32. The low concertation of alkaline species in the bed is due to a large majority of the coated bed particles become engulfed in the agglomeration mechanism and in large bodies of material. The trace amounts of species such as Na and K in the bed sample are likely the result of fuel particles burning out on the surface of the bed at the end of the tests when the bed is defluidised and air flow reduced. Thus, there is a small amount remaining on some of the sand particles which were likely located to final combustion of biomass particles.

6.3 Discussion

The following section discusses the results in more details and disseminates the findings with terms to the performance of the fuels in FBC respective to agglomeration and flue gas emissions.

6.3.1 Baseline Tests

The baseline tests were conducted in order to understand the effect of different sub bituminous coals in a FBC system. This included analysis of operational data, samples from beds and in-depth measurements of agglomerates and similar materials caused as a consequence of combusting such fuels. The baseline tests were also performed in order to generate a level of understanding with data that could then be compared against others tests in which different operational variables could be applied and assessed. The following sections are the discussions surrounding different aspects that could be used to assess the impact and thus applicability of the coals in a full-scale system.

6.3.1.1 Performance of Coals

The combustion of sub-bituminous coals presented a number of issues with respect to stable flame formation. The fuels were very difficult to combust in a steady fashion with a constant thermal output. This is due to the variability in the fuel composition i.e. high mineral matter, ash content and calorific content within the fuel particles. This resulted in a fluctuation in the combustible material entering the bed per unit time. The fluctuation was then seen as a flame favouring one side of the bed which can be correlated to hot and cold spots forming in the bed with inconsistent combustion. These factors contributed to the formation of agglomerates which were seen in all coal tests. The variability in volatile content constantly altered the flame position from an in-bed flame to above bed flame. Both have very different properties in terms of heating the bed, igniting other fuel particles and the loss of heat to the flue gases. This generated further variability in the bed temperatures as well as difficulty in changing and optimising operational variables. Small changes in the fuel flow were often found to make little difference to the bed temperatures, followed by a spike in heat as slug of high calorific content particles entered the bed respectively. This increased the range of the combustion temperatures and increased the formation rate of agglomerates.

6.3.1.2 High Sulphur

The coals contained high volume of pyrite (FeS) which presented a high volume of inorganically bound sulphur to the fuel. The sulphur content of the coals is significantly higher than that of coals burnt in power generation sites throughout Europe and thus requires desulphurisation to be commercially viable.

The baseline tests and subsequent tests all showed a release of high SO_2 emissions of ≥4500 ppm (corrected to 6%O_2) without the modification of operational parameters or the addition of sorbents in the bed. This gave a bench mark values for subsequent tests. Subsequent operational variables will compare the SO_2 to evaluate the fuel application potential of the coals via these means in different scale utilities.

6.3.1.3 Agglomeration

The baseline tests produced large quantities of agglomerated structures consisting of mineral matter from the coal, coal ash, bed particles and alkali concentrations in low temperature melting eutectics. The liquid phases forming the eutectic complexes were dominated by Fe-Si-Al matrices. It was found that the high concentration of Fe species, from the pyrite in the coal, led to agglomerates forming liquid phases with the combustion temperature range for fluidised bed combustion (750-950°C). Whilst Fe has a melting temperature above the constituents in the agglomerates, the presence of high concentrations of S in the fuel is likely to have catalysed the formation of Fe-Si-Al dominated compounds.

The analysis previously shown is a baseline case for the agglomerates and associated mechanism for the combustion of the coals in this investigation. As all the coals contained similar levels of alkali species, especially high concentrations of sticky species such as K and Na as well as the presence of Fe and Al it was expected that these would dominate the agglomerates forming in subsequent tests.

The agglomerates were found to propagate in size and lead to the eventual defluidisation of the bed in all baseline tests. This was induced by either large structures impeding mixing, fluidisation and combustion, or for the structures to be of a size that trapped incoming fuel into a localised area creating large cool spots and a combustion zone dominated by sintering under the fuel feeder port. The data recorded throughout the baseline tests and the subsequent chemical and physical analysis performed on bed samples allowed for comparisons in other tests to evaluate the impact of the variable in that test.

6.3.1.4 Performance of Rig

The most significant unforeseen issue with the rig was the leakage issues and the ingress of air in the upper freeboard regions. This resulted in the measured O_2 concentration in the baseline tests being between 16 and 17 vol%. Hence the values that have been reported are corrected to 6%O_2 which is standard for this type of combustion environment and excess air level. The air was found to be leaking downstream before the sampling point and away from the bed and combustion zone thus, wasn't seen to interfere with the combustion of the fuels. The freeboard region was kept under negative pressure at all times (between 10-15 mmH_2O) and thus the air didn't move in the direction of the main flame.

Overall the rig showed a good capability to combust the fuels and was fully commissioned before the baseline tests. The data collected with the baseline tests was evidence to the performance of the rig and gave confidence and experience to conduct the rest of the investigation successfully. The

values were used to compare against other subsequent tests and gauge the impact of operational variables.

6.3.2 Ca:S Ratio Tests

The use of sorbents as additives in FBC is a common practice for addressing agglomeration, slagging, fouling and as a method for emission control. As the literature review, has shown in Chapter 2, limestones and dolomites have been evaluated for their SO_2 capturing capabilities in numerous combustion technologies.

Limestone was added at different ratios to validate the findings seen in the literature and demonstrate that SO_2 could be controlled and reduced in the flue gas through its application. Sulphur retention in the bed was achieved and the ratios used illustrates that the most efficient ratio for sulphur retention with a limestone additive is between 2-2.5:1. The results of the experimental work shown in section 6.2.1 are in agreement with the results demonstrated in the literature (Barišić et al., 2008; Hlincik and Buryan, 2013; Khan and Gibbs, 2000; Tarelho et al., 2005; Tarelho et al., 2006). The results show that the quality of the fuels combustion can be improved with the addition of limestone. The following sections will elaborate on varying additive parameters to optimise and improve FBC applications for sub bituminous coals.

The SO_2 concentration against Ca:S ratio is shown in Figure 6-33. There was a decrease in SO_2 concentration in the flue gas as a result of the calcium in the limestone reacting with SO_2 and retaining it as calcium sulphates in the bed. The data suggests that a ratio between 3 and 4 retained the most SO_2 and thus had the largest impact on desulphurising the system. However, the calcium utilisation efficiency ($Ca_{\eta\%}$) has also been plotted in Figure 6-33 using Equation 6-1.

$$Ca_{\eta\%} = 100 \times \left(\frac{Coal\ only\ SO_2 - \Delta SO_2}{\Delta SO_2 \times Ca{:}S\ ratio}\right) \qquad \text{Equation 6-1} \qquad \text{(Nimmo et al., 2004)}$$

Whereas the lowest SO_2 emission was measured between a Ca: S ratio of 3 and 4, the calcium utilisation efficiency is shown to be highest at a Ca: S of 0.5. The $Ca_{\eta\%}$ is highest at 0.5 because it is the lowest volume of limestone and thus Ca in the fuel mix but is achieving a higher proportion reduction in SO_2 concentration in the flue compared to the higher limestone flows.

Whilst the desulphurisation potential of the limestone is clearly demonstrated in the results and literture alike, it was found there were implications as to the opeartion of the bed as a result of the increased mineral matter content in the tests. Figure 6-14 shows the pressure measurements made during testing with varying Ca:S ration and that as time progressed the bed Dp increased with the increased weight of the bed and the formation of agglomerates.

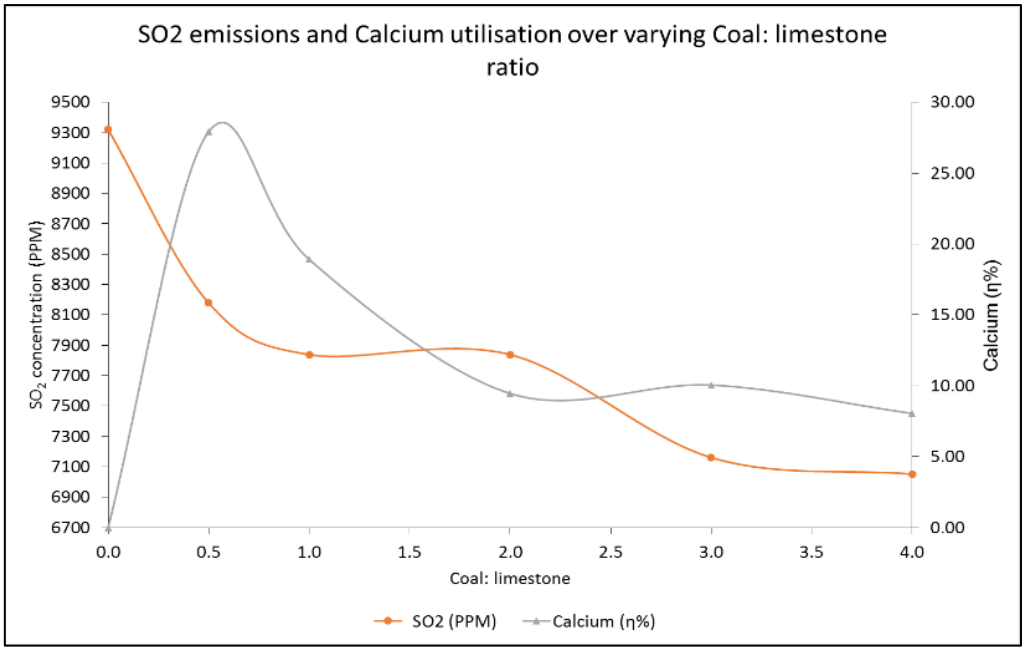

Figure 6-33 SO_2 concentration in the flue as a result of combusting varying ratios of coal H and limestone against the calcium utilisation efficiency

Figure 6-34 shows how as the test progressed and the Ca: S was changed the total limestone in the bed increased and thus the Ca inventory within the bed increased. The loading of the bed increases with the increase in limestone feed rates required for the respective ratios.

As the test is progressing and limestone is loading the bed, the available Ca surface area is being used up in the desulphurisation mechanism. However, the efficiency of this reaction in ideal scenarios is 97% and thus there is an increasing value of unreacted Ca which can act to retain SO_2

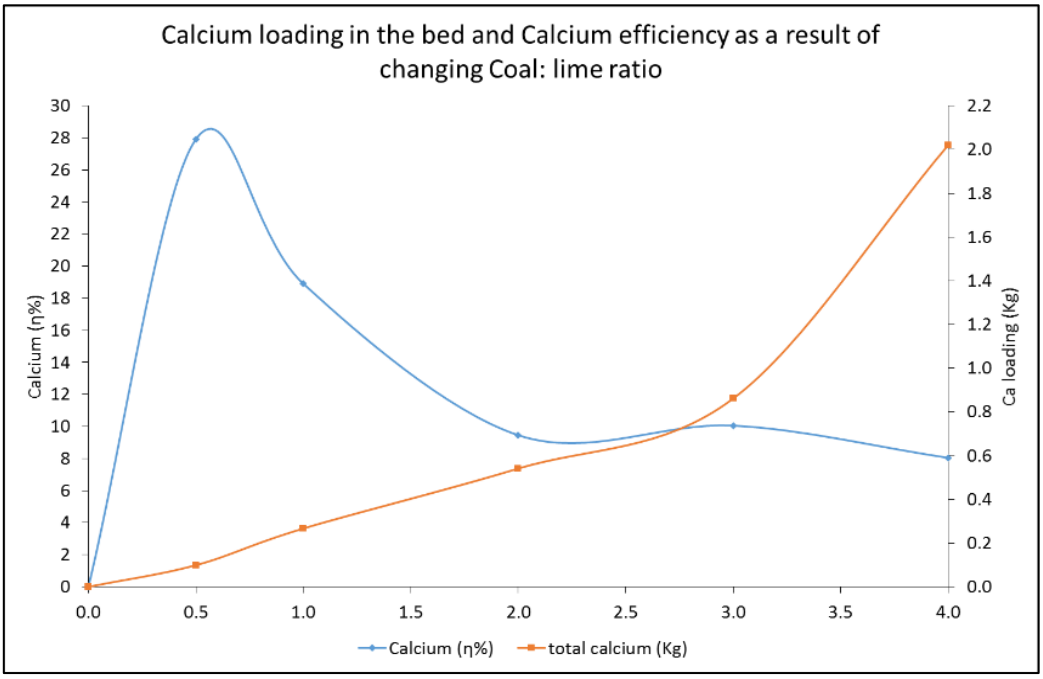

Figure 6-34 Calcium utilisation efficiency and calcium loading in the bed over varying coal and limestone ratios

during the test as the Ca:S is being altered However with this in mind the calcium utilisation efficiency decreases with increasing calcium availability, both in terms of total bed loading and limestone feed rate.

Three factors were limiting the effective desulphurisation reactions in these tests; 1) the increasing total volume of bed is reducing the turbulence of mixing and thus impeding the gas-solid reactions on the limestone surfaces, 2) the increasing volume of inert mineral matter from the fuel is altering the flows within the bed. Increasing mineral matter volume from the fuel altered the average bed particle size thus altering mixing, and 3) the onset and propagation of agglomerates is binding with limestone limiting its desulphurising potential whilst also coating limestone particles with eutectic complexes. The complexes block the Ca reactive pores and thus limit the SO_2 retention. Therefore, whilst the increased ratio of Ca:S in the literature and results shows a peak of efficiency, there is a limitation in this efficiency capped by overdosing and unreacted material. The most efficient desulphurisation ratio is still 2-2.5 in the results presented here however the overdosing and residual Ca is covered less as a potential factor in the literature and the results of this investigation indicate it has a potential that needs to be considered when applying a limestone to desulphurise this type of coal.

During tests in which the Ca:S ratio was varied it was found that the bed would agglomerate and defluidise. Figure 6-35 shows an example of the agglomerates which were found in all tests for which the Ca:S was altered. As the images show, the agglomerate is made up of bed particles, fuel particles, ash and limestone. Due to the poor quality of the coal and its high alkali species concentration and mineral matter, it was found that the agglomerates consisted of large quantities of larger inert particles, stuck together with eutectic complexes on the surfaces of the large particles.

Figure 6-35 Images of agglomerates from the combustion of Pakistani coal with varying coal: limestone ratios. Left image showing the embedding of limestone in agglomerate, right image showing larger particles trapped in bed agglomerate with sintered top layer

Surrounding the mineral matter was large volumes of sand, coated in the eutectic, with limestone particles embedded between. Further to this, on the surface of the agglomerates were areas of liquid phase silicates which were likely the result of sintering from localised hotpots induced by the poor mixing caused by the formation of the agglomerate structure. The agglomerates found were made up of several layers with weak and strong structures throughout. This illustrates the formation of separate agglomerate mechanisms which have propagated in size and bound to one another. This has led to the propagation of the agglomerate structure and the eventual defluidisation of the bed. There was found to be little literature on the effect of limestone on sub bituminous coals which have been seen to have a high rate of aggressive agglomeration.

The limestone is CaO dominated and as such it was expected that the active sites would react with alkali species such as K and Na. The results in Figure 6-20 and Figure 6-21 show that the limestone retained an amount of sulphur and in doing so reduced the SO_2 measured in the flue. However, the high concentration of the Fe-Si-Al eutectic was found on the surfaces of the lime embedded within the agglomerates. This indicates that the limestone was impeded in sulphur retention as its active sites and pores became enriched with the low melting temperature eutectic. Furthermore, the high volume of limestone in the agglomerates would suggest that the limestone actively adhered to the eutectics and in doing so significantly contributed to the agglomeration mechanism. The extent of this mechanism is not understood but as shown in the literature review limestone can be used to react with eutectics and reduce agglomeration. In this case however, it would seem the high alkali content of the coal has overwhelmed the positive effects of the limestones in the bed.

The results of the agglomerate analysis show clear similarities with the baseline results and the samples taken from these series of tests. This is a clear indication that whilst the CaO from the limestone may react with the melt phase and gas phases during the agglomerate formation mechanism, the volume is high enough to overpower the benefits. Furthermore, the eutectics complexes were seen to impede the limestone by blocking active sites. In conclusions to this, limestone was successful in reducing the SO_2 emissions but the efficiency measured wasn't as high as initially projected based on indications from the literature. As a standalone technique for desulphuring the fuel it has validity but is limited by its potential efficiency due to the alkali content of the coals.

6.3.3 Temperature Tests

Varying the temperature of the fluidised bed was found to alter the effective sulphur retention within the bed. By increasing the bed temperature beyond 830 °C there was a direct effect on SO_2 retained in the bed. Figure 6-36 shows the temperature and the resulting effect on sulphur emissions. As the temperature is increased beyond normal FBC temperatures (750-850°C), the

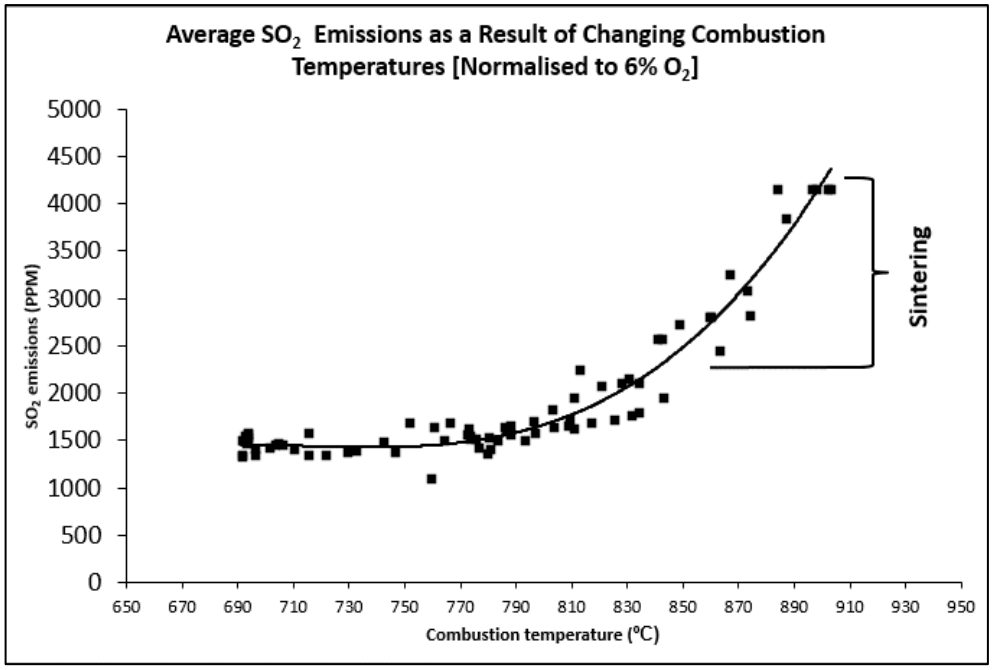

Figure 6-36 Temperature variance effect of desulphurisation during fluidised bed combustion of Pakistani coal I

concentration of SO_2 measured in the flue gas increases. This agrees with findings in the literature (Kunii et al., 2013; Tarelho et al., 2005; Tarelho et al., 2006). Furthermore, the literature suggests that above 870°C, sintering mechanisms can occur, especially as a result of localised hotspots exceeding these temperature ranges. This is a result of the localised reduction in mixing and localised hotspots contributing to the presence of liquid phases with increasing overall bed temperatures.

The results correlate with the literature, such as Wu [21] who reported an optimum temperature range of being between 800°C and 900°C. However, the consequence of these temperatures on the formation of agglomerates is not considered in the same experiments. The results of this investigation emphasise the need to keep combustion temperatures low as to achieve high sulphur retention in the bed but minimising known agglomeration temperature ranges. The results in Figure 6-36 showed that a SO_2 emission level of 1500 ppm was achieved at 750°C compared to ≥4000 ppm at 900 °C . This is due to the calcination and $CaSO_4$ reactions occurring with the limestone and SO_2 at these temperatures. When combusting the sub-bituminous coals with their variability as described in the baseline section, there was seen to be a limitation to the combustion stability. As such, trying to maintain a specific/small range of combustion temperatures which achieves an optimum retention in S is less feasible than with a higher-grade coal.

Further to the SO_2 retention difference, whilst trying to alter the bed temperature through fuel flow alterations, temperature variations and unexpected changes in combustion occurred. The test showed that whilst trying to alter this variable the variability and inconsistency in the fuel and the

sheer volume of mineral matter increased with the addition of limestone impeded stable operations. If this fuel was to be used in an industrial operation which required ramping up and down the fuel could present variation in the combustor and lead to other issues such as accelerated agglomeration, sintering, fouling etc.

The agglomerates found within the bed were comparable to the other tests within this investigation. However, higher temperature ranges resulted in the increased rate of agglomerate formation with signs of sintering on the surface of the bed. Ash fusion tests performed in the fuel characterisation of the coals found that initial deformation/melting of the coal ash didn't occur until 1100°C. The ash in these tests soften ≥1350 °C. Therefore, three possibilities for the sintered material exist; 1) the agglomerates are occurring because of low temperature melting eutectics as previously discussed and this, with the elevated temperatures, is leading to further eutectics or, 2) With the increased agglomerate formation, the bed has defluidised locally. As can be seen in Figure 6-23, the agglomerates/sintered material occur on one side of the bed. This is where the fuel fee falls into the bed. With localised defluidisation the fuel would amass and in doing so create a localised hotspot in which elevated temperatures could exceed 1350 °C (section 4.4.3) and hence the formation of a SI-Al-Fe rich glassy material forms (sinters), 3) Whilst the ash fusion temperatures indicated that the ash of the fuels in this investigation would melt ≥1350°C there were under oxidising conditions. Oxidising conditions were used to simulate the environments in a FBC i.e. Large volume of excess air and O_2. However, the fluctuations observed in temperatures, pressures, bubble formations and flame shape indicate that both oxidising and reducing zones could have occurred in the bed at the same time. Reducing conditions have lower melting temperatures than oxidising and thus, sintered liquid melt phases could have occurred in O_2 deficient zones of the bed leading to the onset of large sintered zones throughout the bed. Reducing conditions are highly probable under the fuel entrance point with a larger volume of O_2 being consumed in this zone with the high abundance of fuel stripping the localised atmosphere of O_2 hence reducing environments occurring.

The results show that there was a clear temperature range in which the limestone fed with the fuel retained the highest percentage of SO_2 in the bed. However, the peak efficiency at >870°C is above the melting temperatures of K, Na etc. as described in the baseline section. Hence, whilst optimising this operational variable has the potential to reduce SO_2 emissions, the impact on agglomerate formation remain constant. In order to reduce the agglomerate formation, the efficiency would be reduced with the lower temperature range of the bed. The temperature of 870°C poses issues on the formation of agglomerates and potential increase the rates of formation. However, as tests required an exceedance of these temperatures the rate effect cannot be quantified. The higher temperatures

resulted in harder agglomerates forming with melt phase but this was to be expected. This again is a consequence that is not included when considering the formation rates of agglomerates when identifying efficient SO_2 removal whilst combusting low grade coals.

6.3.4 Particle Size Tests

Figure 6-37 illustrates the effect of varying sorbent particle size on the retention of SO_2 emissions in a FBC. The data shows that when limestone particles of 0-2 mm are fed with the fuel the least amount of SO_2 is emitted in the flue gas and is therefore retained in the bed. This is can be related to the diffusion and dispersion of the limestone particles that alters with each range of the sorbent alongside the active surface area of the particles available. The range 0-2mm has the largest potential surface area for active Ca reactions and is small/light enough to have the highest dispersion potential of all the ranges. Hence, the particles are more agitated moving around in reactive combustion zones compared to the other ranges.

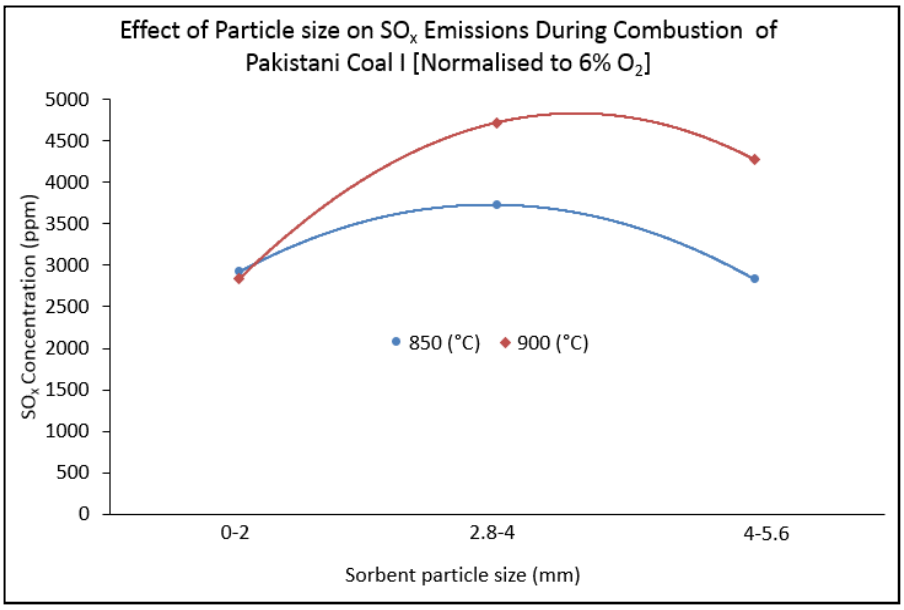

Figure 6-37 SO_2 emissions measured at flue gas sampling point with varying temperature and particle size

Temperature ranges of the bed were altered to evaluate the impact average bed temperature on the retention capacity of the sorbent. As shown there is little different with the smallest particle range. However, with the other two ranges the increase in temperature of 50 °C results in 992 ppm and 1444 ppm increase in SO_2 emission for particle ranges 2.8-4 and 4.5-6 respectively. Further to this, the results indicated that the middle range retained the least concentration of SO_2 and the largest particles fell between the two ranges in terms of retention potential. This is in agreement with the work demonstrated by Muenzer and Bonn (1980). The literature surveyed in Chapter 2 doesn't take into account the impact that particle sizes and optimised specifications have on the hydrodynamics

of the bed. Whilst the desulphurisation propensity was noted to very high with smaller particle sizes it was also found that the state of combustion was also most beneficially affected in the same range.

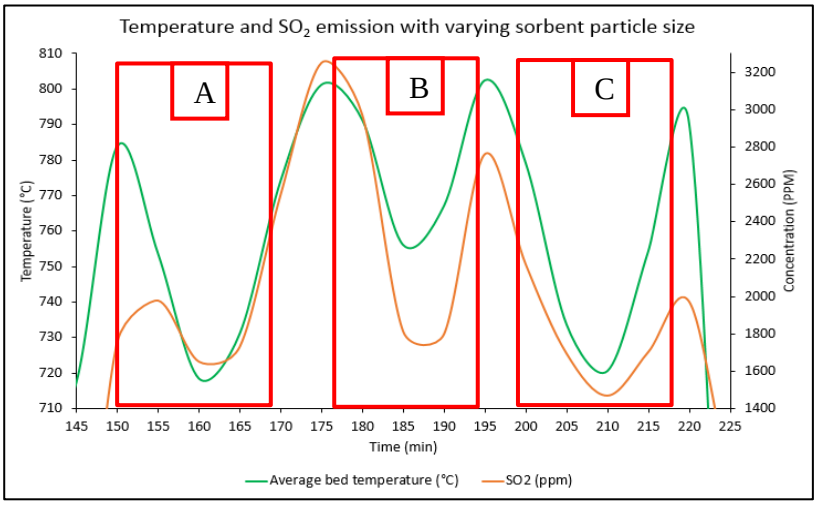

Figure 6-38 Temperature variance across the bed as a result of variable combustion conditions with the alteration in sorbent average particle size range; A-0-2mm, B- 2.8-4mm and C-4.5-6mm.

Figure 6-38 shows the average bed temperature, (Bed A through to Bed B), the subsequent SO_2 emission from the bed and the different limestone particle size ranges. Input of limestone decreases the bed temperature in each case. This is due to the limestone requiring heating to bring it to the same temperature as the bed and endothermic calcination reactions occurring, thus there is a delay in the desulphurisation effect. However, the temperature decrease for each range is different with range B, 2.8-4mm having least heat loss for the same volume of material. This is due to the range being most similarly sized to the particles in the bed and thus impacting mixing into the bed the least. Range A as described in Geldart (1973), will act more as a powder type and be extremely difficult to fluidise and particles lift as a small plugs rather than bubble thus interfering with bed fluidity and consequently fuel mixing and combustion. Range C has a comparable heat loss effect to group A, which coincides with the work by Geldart (1973), who found larger group particles such as ≥4.5 mm to create larger bubbles bursting at the surface of the bed, creating temporary voids. This is filled by larger particles settling near the distributor plate and thus redirecting/altering bed air flow. Therefore, in terms of optimising the desulphurisation process whilst maximising mixing and bed hydrodynamics and thus the combustion process range B was also the best particle size range in these tests.

The beds agglomerated because of a combination of the total bed weight, impurities in the fuel and the average bed particle size increasing over the length of the tests. The average particle size increased because of fuel mineral matter not necessarily the limestone presence (limestone made up less than 5% of the beds total). However, there was no clear indication to one fuel having a more significant impact on the agglomeration rate compared to the others. The limestone particles found

in the agglomerates included a mixture of all particle ranges injected into the bed. Whilst each range will have impacted fluidisation and the mixing slightly differently it was the limitation of bed weight that defluidised these systems with the addition of agglomerates forming.

6.3.5 Co-firing Biomass Tests

Co-firing of biomass and sub bituminous coal is a feasible method for fuel blending in Pakistan because of the large abundance of indigenous forests across Pakistan. In terms of availability and feasibility the abundance of wood is an attractive proposition for combustion improvements in FBC.

When co-firing wood pellets with the low-grade coals, it was found that the defluidisation time extended, as shown in Figure 6-2. The time till defluidisation can be seen to almost double for similar coals when wood pellets are substituted for the coal in the blend. The addition benefitted the bed in two ways; firstly, the addition of wood pellets meant a reduction in the coal. The reduction meant there was less mineral matter in the bed which had been seen in pervious tests to both react with eutectic formation and to impact fluidisation by alternating the average particle size in the bed, thus interfering with ideal fluid dynamics. The second benefit was the reduction in FeS (pyrite) and thus a reduction in the agglomerate mechanism seen previously. The wood pellets increased the K and Na concentration in the fuel which was shown in the Chapter 2 to react with components such as Fe. The eutectic formation of Si-K-Fe and Si-Na-Fe is linked with agglomeration, however, the rate of formation was seen to be less than the mechanism dominated by the high concentration of FeS. A combination of these two factors can be linked to the extended defluidisation time.

The temperature and pressure data in Figure 6-27 is a reflection of the more ideal combustion taking place when using a blend of wood pellets and Pakistani coal. The results in section 7.4.1 will later demonstrate the combustion profile of biomasses in FBC and the results previous in this Chapter demonstrate the temperature profiles etc. associated with coal combustion. By co-firing coal and biomass, the bed was loaded with carbon which was primarily sourced in the coal, whilst the above bed and freeboard region experienced a more prominent volatile flame as a result of the high volatile concertation sourced in the biomass pellets. The result of combining the fuels resulted in a more even spread of temperatures, a more manageable thermal mass (bed) and greater flexibility/ability to absorb fuel variability. The results of the co-firing made the continued operation of the bed easier to operate than when combusting just coal.

Co-firing the fuels reduced the SO_2 emissions measured in the flue gases. As Figure 6-28 shows, there was a downward trend with the increase in biomass in the fuel blend. The correlation in SO_2

reduction and increased biomass ratio can be related to two parameters. Firstly, biomass in general contains very little sulphur (wood < 0.1wt%). Therefore, by increasing the biomass volume in the blend and decreasing the coal volume, the total organic bound sulphur entering the furnace decreases. As such, a percentage difference in SO_2 emissions can be calculated based on the sulphur entering the furnace compared to that measured. This was shown in Figure 6-28 where the SO_2 emissions measured correlated to those calculated. There was a slight variance in the theoretical and measured results. The difference between measured and theoretical results can be attributed to the retention of sulphur in the bottom ash. Wood pellets were chosen because they contained the highest concentration of alkali species known to react and retain sulphur (Ca and Mg). As the SEM-EDX and XRF results indicated, there was some retention of S in the ash and agglomerates. The retention was much less than predicted before testing, and was found to make little improvement in terms of SO_2 reduction. However, the reduction in SO_2 emission is attributed to reduced total sulphur input to the furnace.

Agglomerates formed in all of the co-firing tests. The image shown in Figure 6-29, shows how when agglomeration was occurring and the biomass pellets would combust on the upper surface of the bed whereas the presence of coal burnout was not to be seen. The biomass contained less ash so if a crust had formed on the bed with the onset of agglomerates then localised ashes for coal particles should have been seen. It is assumed that the higher density coal particles which were also bigger, larger in weight (approx. 10-15g for biomass pellet and >20g for coal) sank into the bed with the fluid movement of the bed. Some small areas of the bed were found to have coal burnout pile but not to the extent of the biomass pellets. The onset of localised defluidisation as a consequence of eutectic formation is likely to have caused this phenomenon of separation.

The separation of particles as agglomeration occurred will have influenced the distribution of inorganics throughout the bed as coal inorganics were locked into the bed whereas biomass based inorganics reacted on the upper surface creating variations of the eutectics. It is assumed for this reason that glassier K dominated silicates were experienced on top of the bed without sintering temperature being achieved, and the agglomerates seen in previous tests were seen more prevalent in the lower regions of the agglomerates. This separation mechanism is interesting but the initial agglomeration mechanism is linked to the Fe-Si dominating eutectic seen in previous tests as there was too little a volume of the inorganic ash in the biomass ash to significantly impact the formation mechanism.

The elemental analysis of agglomerate samples taken from the Cofiring tests showed that whilst the agglomerate formation mechanism was dominated by the presence of Fe-Si-Al, the presence of the lower temperature melting components such as K and P were interacting with the eutectic

complexes. Because of the lower carbon content in the bed as a consequence of the reduced coal volume in the blends the bed temperatures were lower than in coal only fuel flows. However, the same eutectic complexes can be found in co-firing and coal only tests with different bed temperatures. It was found that the increased alkali content of the biomass with respect to P and K could have impacted the agglomeration mechanism. complexes containing P, K and sulphates have been seen in the literature (Barišić et al., 2008; Lindström et al., 2007; Piotrowska et al., 2010) to lower the temperatures of melt phases for complexes interacting with Al and Fe. The role which P plays in these systems and reactions is disputed because of the wide range of reactions links P can follow in such reactions. However, the SEM-XRD results in Figure 6-31 indicates that the presence of P and similarly catalytic compounds in the presence of the eutectic results in an increase in the Al concertation and reducing in Si. This would suggest that the sample taken from an area dominated by melt phases has an agglomerate mechanism sharing the route shown in the previous sections as well as a catalytic route specifically due to the presence of biomass in the fuel blend.

6.4 Conclusions

Throughout this Chapter a series of Pakistani sub-bituminous coals were combusted in a pilot scale fluidised bed to evaluate the effect of the coals in an FBC environment. The results of these tests allowed for the evaluation of emissions, combustion stability and agglomeration propensity. By using these parameters (and others) the potential for improving the fuels in terms of combustion stability, agglomeration severity and SO_2 emission reduction by altering operational variables, co-firing with biomass and blending a limestone sorbent in the fuel was possible.

6.4.1 Combustion of Sub-Bituminous Coals

Each of the coals used in combustion experiments throughout this Chapter underwent a baseline test in which the coal was used to achieve stable operation. In these tests the operational variables were the same for each coal in order to compare the effects later operational changes had on the performance of the rig and to create a platform of information that would indicate any improvement seen in the use of the coals via system optimisation.

The baseline test gave clear indication as to the high emission of SO_2 and other flue gases as a result of combusting the coals in FBC and indicated that if these coals were to be used in full scale operation, these are parameters which would require control and mediation to allow for compliance of the coals with emissions legislation etc. The range of the SO_2 emissions was between 3000-$\geq$5000ppm which was found that the high volume of pyrite in the coals led to the high concentration of SO_2 in the flue gas.

It was found that the coals would combust with a level of stability at the beginning of the experimental tests. However, the varying calorific content, inorganics content and moisture content led to the combustion and subsequent temperatures fluctuating. In some cases, the fluctuations were seen to be ≥380°C which makes the stable and continued operation of the coals difficult and unpredictable. Furthermore, as the tests progressed the high volume of inert mineral material in the coals would lead to the average particle size in the bed increasing, the total weight of the bed increasing, the fluidisation decreasing and the rate of mixing to decrease. All these factors led to fluctuating combustion both in and above the bed which in turn was a result and cause of localised hotspots. These were all contributing factors to the onset of agglomerates and sintered material in the bed.

In every baseline tests in which the sub-bituminous coals were combusted, the bed eventually defluidised as a result of the formation of agglomerates and the decrease of fluidisation because of the previously stated points. The agglomerates were found to be dominated by eutectics containing Fe-Si-Al and in a number of cases S as a result of the high pyrite mineral matter getting bound into the agglomerated structures. The temperatures at which eutectics contacting Fe-Si etc. are higher than the average combustion temperature recorded in during testing. It could be seen by areas of different agglomerates that the impact of localised defluidisation and localised hotspots had contributed to the formation of melt phases containing these species. Further to this, the presence of S, P and lower melting temperature alkali species seen in higher concentrations in the coal, is assumed to have influenced the formation of the eutectic complexes via an unquantified catalytic mechanism. Evidence of the catalysis occurring was seen in the varying concentration of such species in agglomerates which contained varying levels of silicate melts, i.e. more melt resulted in less catalytic species. Thus, the higher temperatures the agglomerates caused via localised hotspots as a repercussion of the catalytic reactions, released the lower melting temperature species in the gas phase leaving a Fe and Al dominated silicate material behind.

The results of the baseline tests highlighted the difficulty in combusting the coals in FBC technologies because of its propensity to form agglomerates in typical operating conditions and demonstrating the need to modify the fuel, technology or process in order to accommodate its high levels of emissions and ash/mineral content.

6.4.2 Effect of Operational Changes

Using literature of Chapter 2 a number of operational variables were chosen to evaluate the application potential of coals in FBC systems with regards to their control of combustion, impact of SO_2 emissions and rates of agglomeration.

1) Ca:S tests

Limestone was added to the fuel feed at different ratios calculated on the Ca and sulphur content of the limestone and coal. In doing so the limestone acted as a sorbent which underwent calcination reaction sin the bed and thus reacted in the presence of SO_2 compounds and retained the sulphur in calcium sulphates, hence the SO_2 emissions in the flue stack were measurably less. It was found that a Ca:S ratio of 2-2.5 was the most effective when desulpurising sub-bituminous coals. It was also shown that there the Ca utilisation efficacy was higher when at a Ca:S ratio of 2 because of the available Ca in the bed and the increasing Ca inventory in the bed caused by the test being a batch process. The results were in agreement with literature and studies that were cited in the literature review and as such were compared to the results of similar experimentation.

The focus of limestone addition was to evaluate the sorbent effect and reduction in SO_2 emissions. However, previous literature hadn't shown the effect on combustion and the formation of agglomerates which resulted from the introduction of the limestone to the bed.

Whilst the Ca and Mg content of the limestone was predicted to reduce agglomeration tendencies during combustion, it was found the formation rate of agglomerates was similar to that of the baseline tests. The high inorganic and alkali content in the coals resulted in the liberation of eutectic complexes, which whilst absorbed by limestone, was in high enough volume to overpower any positive effects caused by the presence of the limestone. As such, the agglomerates were found to contain limestone particles which were seen to have been coated in the eutectic melt in which the pores of the limestone had become blocked by liquid phases. The formation of eutectics, dominated by Fe-Si-Al, meant a reduction in the active retention of SO_2 emissions which is the justification behind the decrease in SO_2 emissions being less than prior calculations suggested.

The formation of the agglomerates and the presence of an increased volume of sorbent material in the fuel feed (limestone) resulted in less ideal combustion. The bed was much cooler than in baseline tests and in higher Ca:S ratio tests the volume of carbon per unit of fuel feed resulted in cold spots and areas of incomplete combustion.

The use of limestone held potential for desulphurising the high sulphur coals in FBC however, the implications of agglomerate formation and loss of efficiency raises concerns over the need to overdose a system to meet emissions targets. Furthermore, the limestone was an ineffective method in these tests for the reduction of agglomerates resulting from the chemical constituents of the coals.

2) Temperature tests

Studies in the literature indicated that there was an optimum temperature in which the desulphurising potential of the limestone could be maximised. This was due to the calcination

reactions and the formation of calcium sulphates. It was found that a temperature of 830-880°C retained the highest concentration of S during testing with the coals which was in agreement with the literature.

Two issues arouse as a direct consequence of varying the combustion temperatures; firstly, the fuels variability as previously described, generated temperature fluctuations which made maintaining strict temperature ranges difficult. Secondly, the average temperature was shown to be in the ranges being controlled for the test, but investigation of the bed after the tests showed localised areas of eutectic and melt phase formation. This was due to localised hotspots and the combustion of coal particles with varying intestines because of individual particles content, resulted in the fluctuations seen in the flame. This was not seen in any other tests and is assumed to have occurred because of air changes needed to maintain temperatures and fluidisation causing poor localised mixing and thus an agglomerate/sinter mechanism occurring.

Tests in which the temperature range was varied were found to contain more sintered or more extensively dominated by liquid phase's eutectic complexes within and above the bed in post-test investigations. An increase in combustion temperatures and bed temperatures impacted the SO_2 retention of the limestone whilst causing the formation or more stable and extensive agglomerate structures in the bed made up of Fe-Si and Fe-Si-Al rich compounds.

3) Particle size tests

The average particle size of the limestone feed was varied and in doing so demonstrated the effect on combustion, S retention and formation of agglomerates.

It was found that the rate of agglomeration didn't vary significantly between the rages as any impact that the particle size could have had on the mechanism was over powered by the high content of alkali components in the fuel and the high mineral matter contributing to the alteration in bed mixing.

The different particle sizes did result in a variation in combustion as a result of particle entrainment in the turbulent bed and the distribution of the particles. The literature review had clearly shown different particles influenced mixing differently, however whilst larger particles were assumed to mix less readily, it was the dispersion of smaller particles that caused the largest problem to combustion stability. With the larger limestone particles in the fuel blend a more uniform mixture entered the bed and dispersed better. This was compiled by the increase in average particle size caused by the mineral matter building up in the bed throughout the test. Whilst this test demonstrated the influence of particle size on combustion and mixing, it emphasised the need for

constant removal of bottom ash, not simply because of total bed weight, but because of its implications to mixing regimes and particle dispersion.

The results of the investigation showed that surface area and available reactive surfaces increased the rate of S retention and that smaller particles maximised this. However, there is a trade-off and a peak in efficient S retention and bed mixing that needs consideration when altering this operational variable.

4) Co-firing biomass tests

Limestone was replaced with wood pellets and different ratios of a coal: biomass blend was investigated. In this series of tests the wood contained Ca and Mg which was theorised to retain S in the bed similar to limestone, as well as reduce the total S content entering the bed. It was found that the SO_2 emission reduced with an increase of wood in the fuel blend but this was almost proportional to the reduction in S in the fuel feed. A small variation was seen between experimental and theoretical SO_2 emissions which was linked to retention in the bed. However, the concertation achieved by this method indicated that very little coal would be a in a fuel blend to achieve SO_2 emissions desirable for extended combustion.

The incorporation of biomass increased the stability of the flame seen during testing which was a result of the increased volatile matter in the fuel. A mixture of carbon form the coal in the bed and volatile matter in the biomass combusting above the bed resulted in better temperature distribution throughout the system and a more even distribution of combusting gases in and above the bed. The flame was seen to flicker less and there was a more stable output in terms of pressures, temperatures and emissions demonstrating the increase in fuel performance a multi staged burn and blend option poses on FBC technologies.

The bed did agglomerate but the rate and thus time for agglomeration to occur and defluidise the bed increased when compared to a coal only system. The biomass contained little ash compared to the coal and therefore the content of ash that could melt and contribute to the formation of eutectics was less than a coal only system. However, the presences of increased alkali species K. Na and P in the biomass compared to the coal resulted in agglomerates including higher concentrations of these species. The backbone of the agglomerates was Fe-Si-Al but the presences of the lower temperature melting species is likely to have contributed to these mechanisms via catalytic mechanisms and alternative agglomeration routes. This was evident by the presence of the alkali components in the samples taken from the bed.

Biomass co-firing offered a realistic means of potentially remedy the negative impacts of using a sub-bituminous coal but the best results were seen when using higher percentages of biomass than

coal. Therefore, if a country such as Pakistan were to use such a coal in FBC this investigation has shown that the operational variables previous could improve combustion of the coals before co-firing techniques need to be employed to give ideal operation.

6.4.3 Remedies for Coal Problems

The operational variables and addition of sorbents to the coal blend shown in this investigation illustrate the ability to optimise the combustion of sub-bituminous coals in FBC. It has been shown that through Sorbent addition such as limestone the emission of SO_2 can be reduced and controlled through retention in the bed. Alternative sorbents containing similar retentive species can be found in dolomites, kaolin and biomasses and as such offer an alternative method for controlling high emissions of SO_2 gases.

Similarly the investigation illustrated the impact of controlling temperature, sorbent particle size and the ratio of Ca:S in the fuel blend. By following a program of optimisation, a full-scale system could adopt these parameters as a cheap and accessible method for improving the fuels applicability in FBC utilities.

Other potential remedies for improving the combustion, agglomeration propensity and flue gas emissions includes;1) increasing the bed depth to increase the thermal mass to absorb fluctuations in fuel variability and thus ensuring a more stable flame, heat output and ensure a constant operation, 2) replacing the bed material with a sorbent or alkali rich material such as olivine which contains high Mg concentrations which react with species such as K, Fe etc. and in doing so remove them through bottom ash systems, 3) fuel washing in which the coal is left to soak in water or a chemical which leaches out specific components and in doing so improves the previously desired qualities and allows for easy handling of the fuel component which is undesired, and 4) using a multi-staged firing system in which higher grade and lower grade coals are fed into the bed strategically to balance the combustion whilst moderating any negative effects one fuel may have over another.

A number of potential remedies could be employed for the improvement of operation when using the coals in this investigation. Each poses a cost and complexity of operation but as the results showed each coal had individual characteristics that could be addressed by one or more technique unique to that coal.

6.4.4 Application to Full Scale FBC

The sub-bituminous coals used through this investigation posed issues in terms of agglomerate formation, high concentrations of controlled emissions and difficult with respect to combustion and flame shape. Whilst the pilot scale rig is $1m^3$, a full-scale system would be multiple times larger

with a much deeper and broader bed. A key limitation for the pilot scale units was the effect of fluctuations in the coals ash, mineral, GCV and inorganic content. The smaller bed therefore reacted quicker and was effected by smaller changes, whereas a larger system would absorb the fluctuations better and produce a much more stable heat and combustion output.

If this were combined with emission reduction techniques and agglomeration prediction and monitoring techniques outlined in Chapter 2 and 7, then the formation of agglomerates and the impact that have could be managed and mitigated. Therefore, the Pakistani sub-bituminous coals illustrate potential to alleviate economic fuel supply concerns in a developing country which has indigenous fuel stocks available.

7 Biomass Combustion in FBC

7.1 Summary

The focus of this Chapter is to evaluate a number of aspects surrounding the application of biomasses in FBC. By analysing the fuels physiology, chemistry, combustibility and ease of use in a FBC system, conclusions will be drawn as to the fuels applicability in pilot scale and industrial systems.

The first series of tests used a pilot scale FBC rig which simulated ideal combustion and aimed to sustain good fluidisation and combustion. The results of the tests included emissions data, ash samples, bed samples and agglomerates. By measuring these type of samples, the issues and problems found with combusting biomass in FBC will be compared against fuel characterisation data and modelling data and in doing so evaluate predictions of agglomeration formation in beds and conclude on the fuels ease of use.

The second series of tests will incorporate a non-uniform air distribution plate within the fluidised bed. In these tests the plate will be changed to alter the air flows through the bed and to create an uneven distribution of air throughout the bed. Samples and performance will be evaluated to compare how the fuel would perform in pilot scale FBC. The aim of this work is to asses problems which can occur in industrial scale operations dud to non-uniform air flows and suggest predictive methods and operational remedies that could reduce the defluidisation time/effect seen in the beds.

The focus of these tests was to understand agglomeration propensity of the fuels and as such the defluidisation time of the beds when operating the fuels in both ideal and non-ideal beds. By comparing results and evaluating agglomerate formation mechanisms, this Chapter will conclude on methods to avoid agglomeration and further the use of these fuels in fluidised bed combustor units.

The following section includes the emissions, pressure and temperature results of the tests performed with the uniform air distributor plate installed for the combustion of biomass fuels. The post analysis includes SEM and XRF analysis.

7.2 Uniform Air Distribution

With the uniform air distribution plate installed, sustained operation of biomass was attempted. It was found that the different fuels with their varying physical and chemical compositions would react in the bed very differently. The following descriptions are the results from those tests.

7.2.1 Wood Pellets

Figure 7-1 shows the temperature, pressure and emissions data from the combustion of wood pellets in the fluidised bed rig. Wood pellets was the easiest to operate with in terms of most stable flame, least interference with the bed (agglomerates) and the only test to sustain operation without defluidisation as a result of agglomerate formation.

At point A (Figure 7-1), the gas burners are extinguished, solid fuel is fed into the bed and then the air flows are altered to prioritise under-bed flow and restrict the burner's air flows. Between Point A and B the system is tested. Visual inspections of the bed via a side port allows the operators to physically see the bed bubbling, (example in Figure 7-2), this is related to the inlet air flow. It was found that a measured airflow of 135 kg/hr was required to produce a stable level of bubbling.

Stable combustion was continued in this way for 150 minutes at a fuel flow rate of 21 kg/hr. As the test progressed the temperatures and pressures began to fluctuate, with an increase in both temperature and pressure the fluctuations as time continued. This is also shown in the emissions data before point D. Fairly consistent emissions become less constant with CO levels increasing. This culminates to the assumption that the bed is fluidised but mixing is less efficient. As the rig and fuel had demonstrated a stable period it was decided to proceed with inlet air changes to evaluate combustion and rig performance.

The data between points B and C on all graphs in Figure 7-1 is the period in which air flow rates were altered. Figure 7-3 compares the measured inlet air to the rig against the temperatures across the rig and freeboard section of the rig. As the graphs shows, the air was increased to approx. 200 kg/hr, and then decreased in increments after a period of sustained combustion and fluidisation

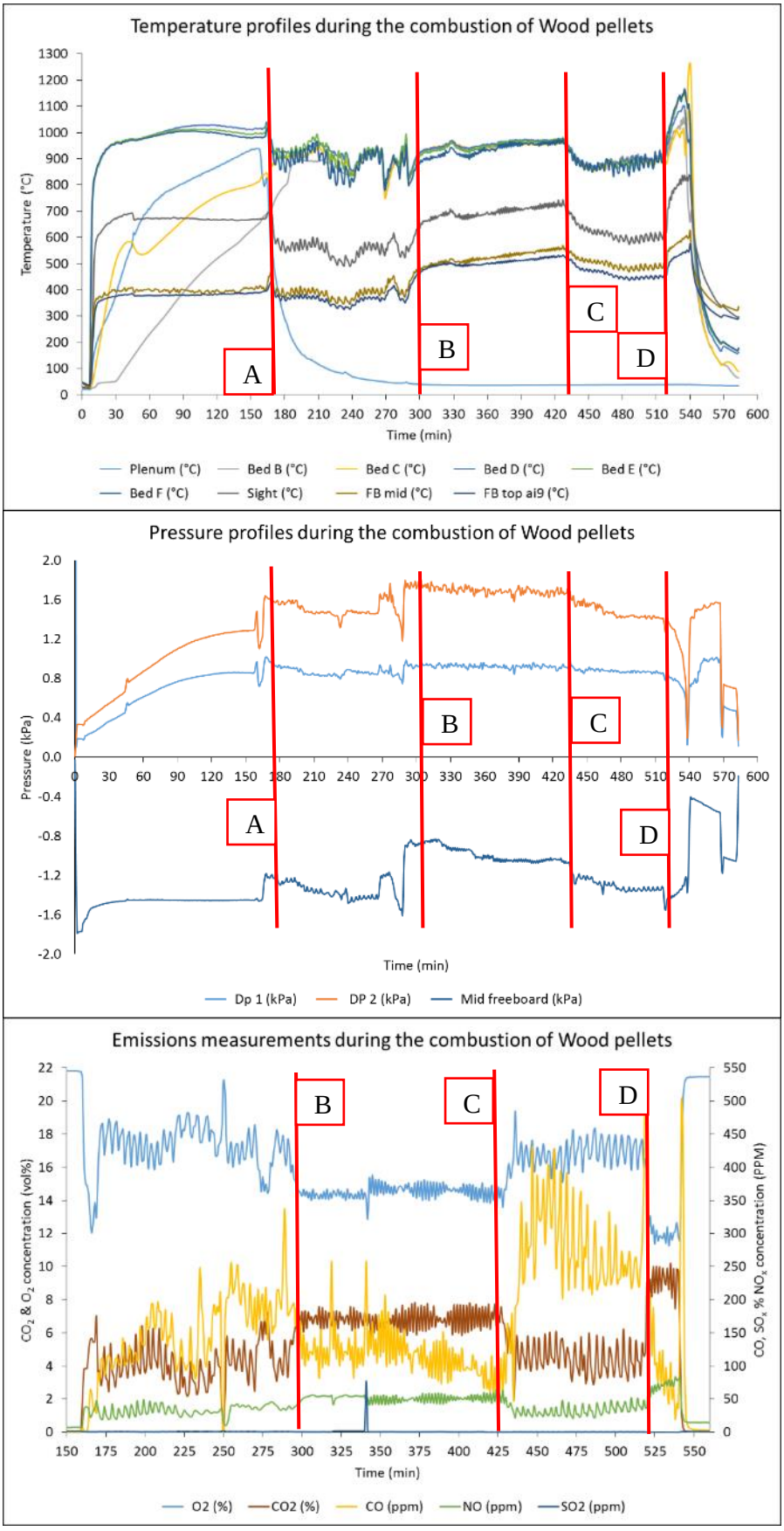

Figure 7-1 Temperature, pressure and emissions data collected during the combustion of wood pellets with a uniform air distribution plate installed

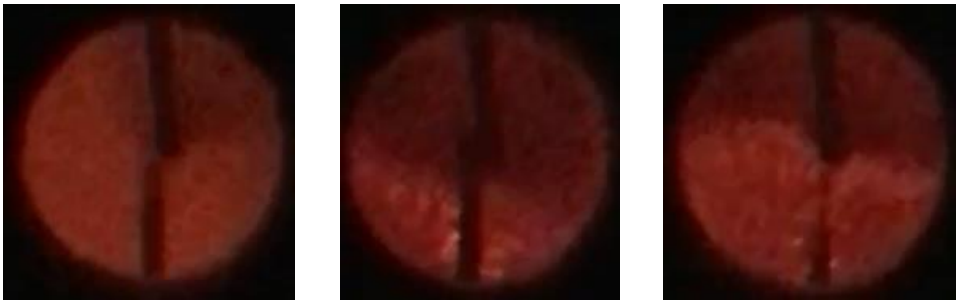

Figure 7-2 Images of the side view port looking down on top of the bubbling bed. These images show the protruding thermocouples in the bed with bubbles of sand bursting around them

and been seen in the recorded data of Figure 7-1. As Figure 7-3 shows, when the air flow was reduced to 180, 170 and 160 kg/hr the temperatures remain reasonably stable. Ranges B to C in Figure 7-1 confirm that the conditions in the rig remained stable. Combustion was both visibly seen to be as stable with validation in the consistent emissions and temperature recordings. However, after the airflow had been reduced to 145 kg/hr and less, the temperatures across the rig were seen to decreases (Figure 7-3). Region C to D in the temperature and emissions data of Figure 7-1, show instability in operation. The temperatures decrease uniformly across the rig by a minimum of 100°C, whilst the O_2 and CO concentrations measured in the flue increase dramatically. This indicates the combustion of the wood pellets is less efficient and the onset of incomplete combustion is present. The pressure readouts indicate that the bed is still fluidised. Therefore, the

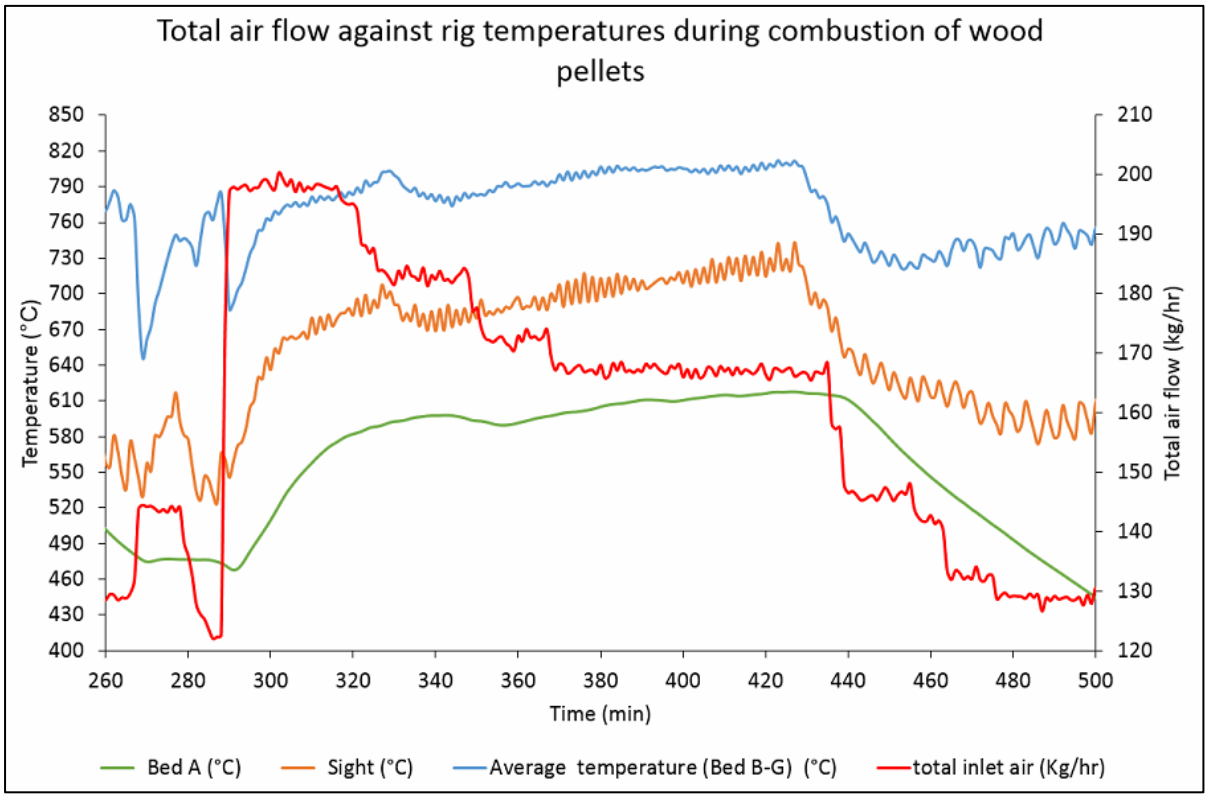

Figure 7-3 total inlet air flow rates against rig tempeartures during the combustion of wood pellets

reduction in air has reduced the fluidisation to a state of bubbling but consequently the bubbling is not violent or agitated enough to mix the fuel into the bed or distribute the air across the bed uniformly. Hence, with the air reduced back to original air flow rates (130 kg/hr), the temperature and emissions continue to suggest poor combustion. Inevitably the reduction in airflow caused the defluidisation of the bed. This was the end of the pre-determined test period and agglomeration was not the cause for the end of the test/defluidisation.

Defluidisation was determined as a series of parameters as described in the experimental methodology.

7.2.1.1 SEM-EDX

Samples from the bed post-test found there were very little if any agglomerates. Small cylindrical clusters measuring 3mm in diameter were the only signs of agglomeration. The agglomerates and any clump/clustered sample seen in the bed were prepared as with previous samples for SEM i.e. affixed to stubs with carbon paint and coated using carbon plasma.

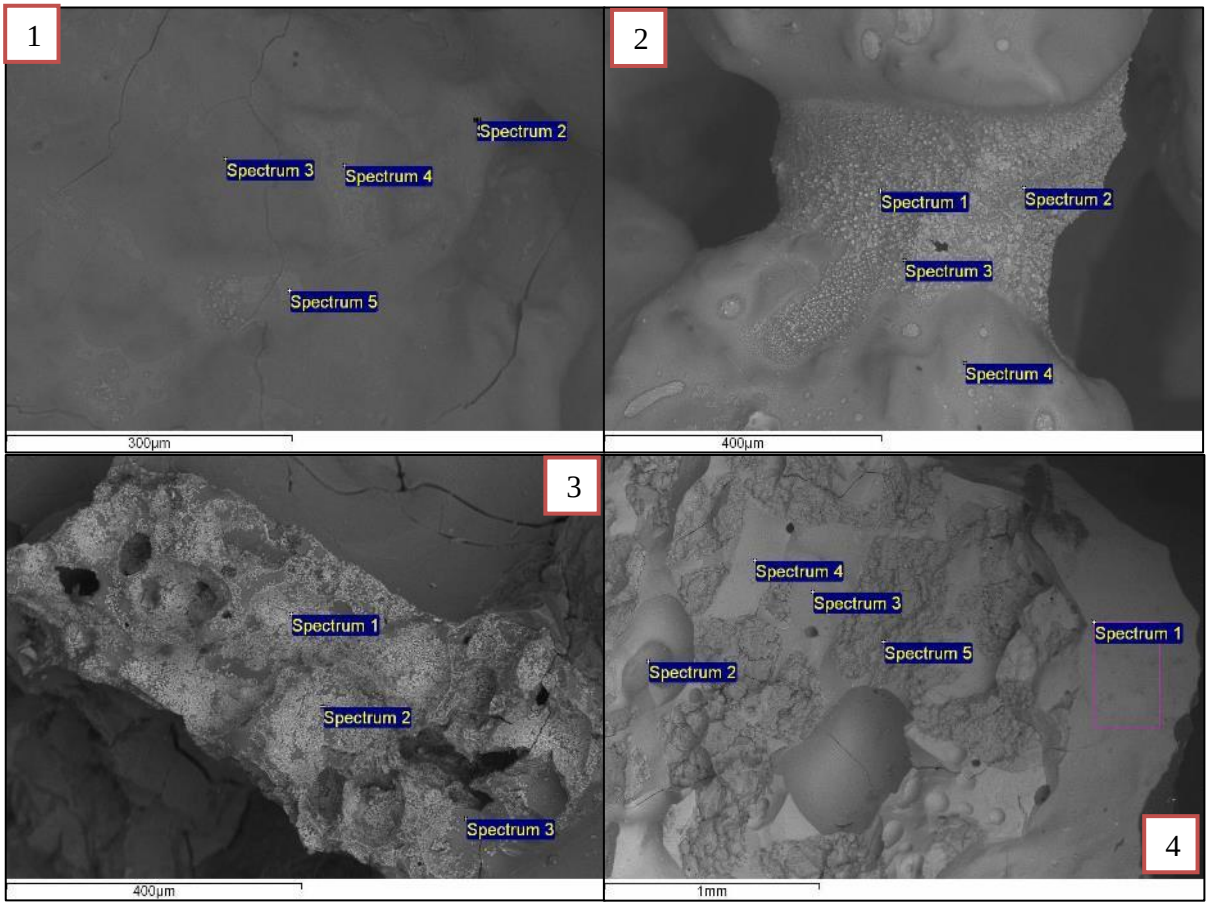

Figure 7-4 A collection of SEM images and the locations of SEM-EDX from wood combustion. Images are as followed; 1) Surface of agglomerate, 2) enhanced image of bridging between agglomerates, 3) combustion point of wood pellet, and, 4) cross section of agglomerate

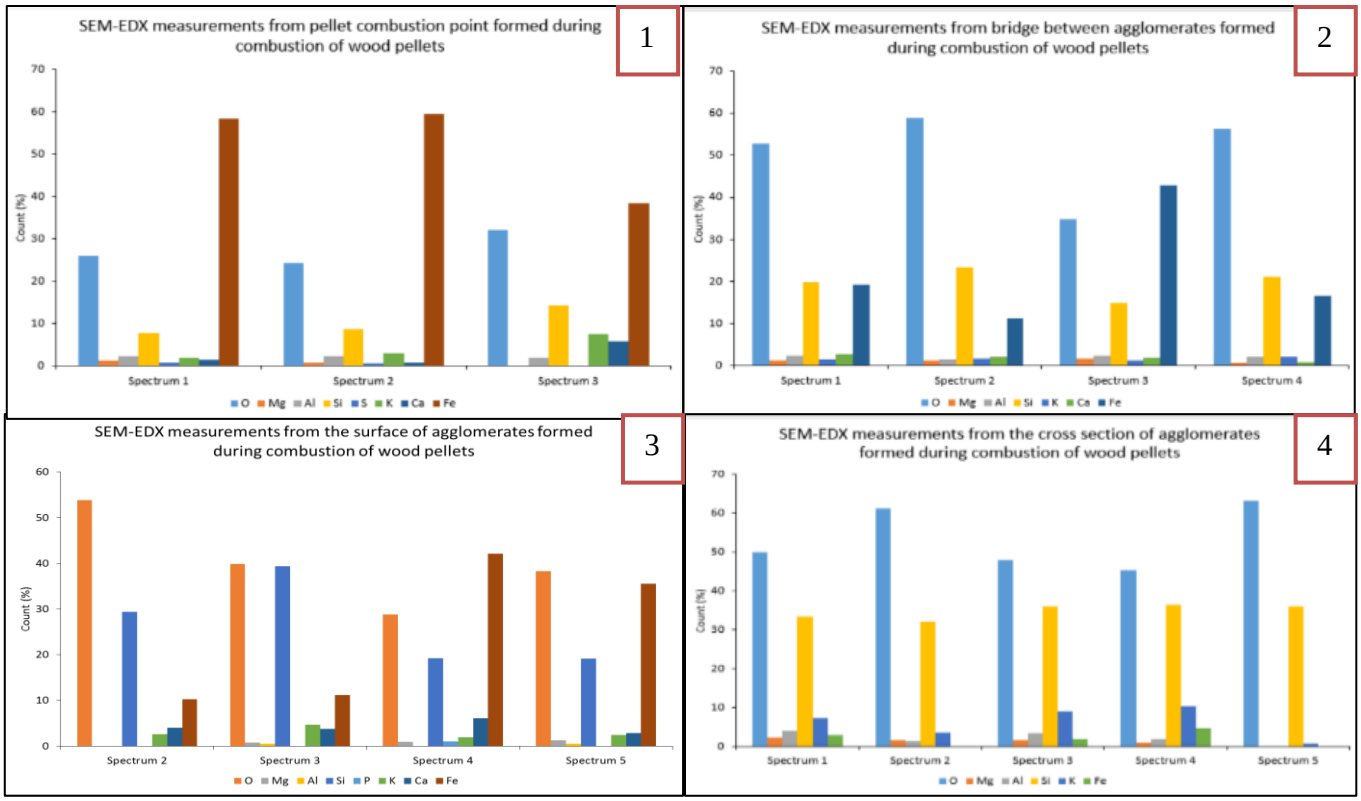

Figure 7-5 shows the SEM-EDX results for the selected samples shown in Figure 7-4

Figure 7-4 shows four SEM images of significant findings found during SEM analysis and Figure 7-5 shows SEM-EDX analysis conducted on samples taken from the bed after combustion of wood pellets with the uniform air distribution plate installed. Image 1 shows the surface of a typical agglomerate found in the bed. SEM-EDX analysis indicates that Si, Fe and K are the three major components within the agglomerate, with traces of Al and Mg around the surface. The Si will have been sourced from the sand particle embedded in the agglomerate with Si-Fe-K complexes adhering the materials together. Image 2 shows the bridging between two agglomerates. SEM-EDX indicates Fe and Si to be dominant in the fused bridge area with K more concentrated on the surface of the agglomerates rather than in the bridge. Image 3 shows the location in which a pellet combusted and consequently created a localised area of heat. In doing so SEM-EDX result shows concentrations of Fe to be higher than in the surrounding area where the agglomeration is present. Image 4 shows the cross section of a bed agglomerate. The SEM-EDX results indicate that Fe is present in-between the sand particles which have formed within the agglomerate structure.

The SEM and SEM-EDX analysis were found to indicate that the agglomerates which were taken from the bed post combustion of wood pellets were highly concentrated in problematic species including Fe, Si and K. This falls in line with results from XRF analysis and SEM-EDX work conducted in the fuel characterisation Chapter on the ashes.

The results here give insight into the agglomeration mechanism within the bed. The results from the pellet combustion location in Image 3 shows that with high localised temperatures resulting in Fe being the major constituent in forming agglomerates. The higher temperature is likely to have caused lower temperature alkaline species into a gaseous phase and thus producing a lower concentration in the agglomerates.

Additionally, the results from images 2 and 4 suggest that once agglomerates have started to form the main complex of lower melting eutectics is made up of Si-K-Fe. However, the bonding and bridging between these agglomerates is dominated by Fe-Si eutectics. The initial agglomerates containing K will have produced a sticky surface in which sand particles etc. will have adhered and propagated the formation of agglomerates. With localised reduction of turbulence and mixing, the combustion of pellets is combusting and generating localised hotspots. In doing so a Fe-Si eutectic is liberated and becomes the main mechanism for adhering agglomerates together and thus further propagating the agglomerated structure.

7.2.1.2 XRF

XRF analysis was performed on bed samples taken after the completion of tests combusting biomass pellets. The XRF analysis used the methodology described in the fuel characterisation Chapter 4.

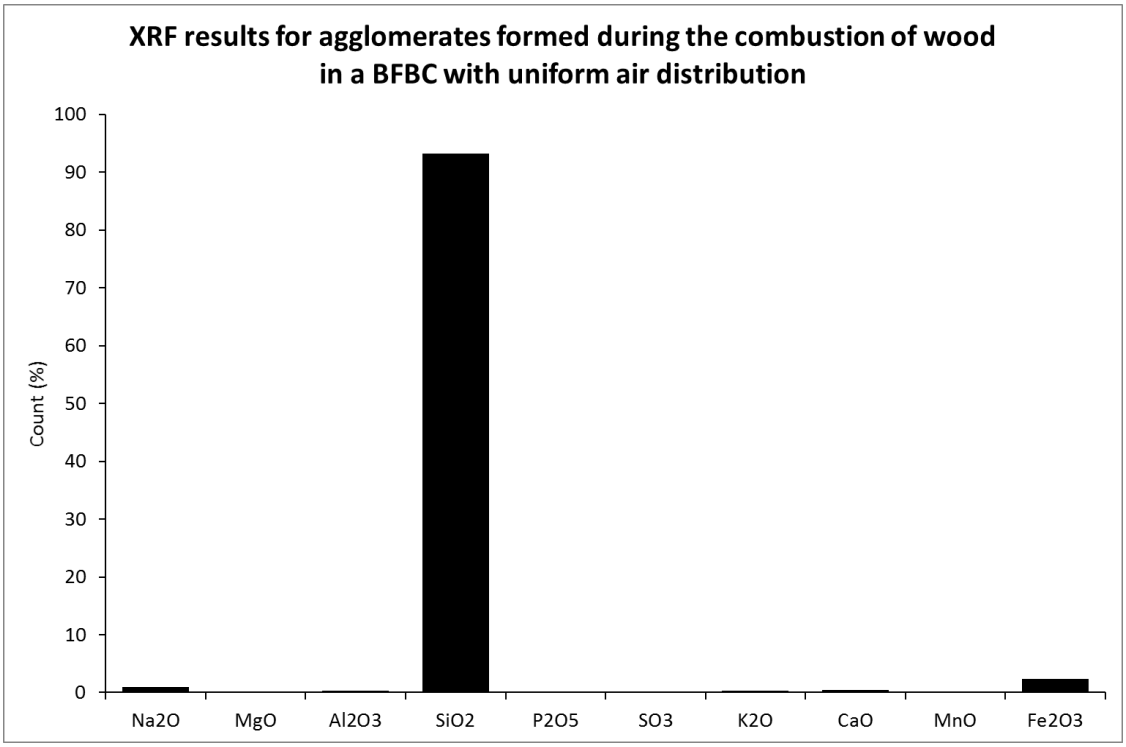

Figure 7-6 XRF analysis of bed samples taken after testing from the combustion of wood pellets in a BFBC with uniform air distribution

As Figure 7-6 shows, the bed contained mainly Si, Na, Ca and Fe. The wood pellets were shown to have the lowest fraction of ash and as such the bed content, excluding concentrations of ash in agglomerates, were very low. As such the high SiO_2 concentration in the bed is accounted for as bed material. The low concentration of other alkali species is an indication that the majority of bed particles coated in alkali species had clustered in larger agglomerated structures.

7.2.2 Peanut Pellets

Figure 7-7 shows the temperature, pressure and emissions data recorded during the combustion of peanut pellets with the uniform air distribution plate installed. The data from this test shows the difficulty associated with the combustion of biomass fuels with higher concentrations of less desirable species including Na, K and Fe groups. Subsequently this test ended with the defluidisation of the bed as a result of agglomerates forming.

The Pre-heat time of this test was 2 hours, which was longer than required to achieve a bed temperature of ≥600 °C. The justification for this was that if the bed were to defluidise, as it did, that this would be the result of low temperature eutectics forming in a single mechanism. To elaborate, if the bed was cooler than ≥600°C it was feared that in the time it took for the solid fuel to achieve a bed temperature of ≥750°C, there would be a window of opportunity in which species with lower melting temperatures than fluidised bed combustion could form agglomerates that would not be found in an industrial scenario where the pre-heating would have achieved higher temperatures associated with normal operating conditions. This assumption and concern comes from ternary diagram data shown in Chapter 5.

After the pre-heat sequence, had achieved an average temperature of 700 °C (point A Figure 7-7), then the gas burners were replaced with peanut pellets. As a side note, the CO emission up to point A is due to lower gas velocity produced by the under-bed burner during the test. On site, other gas fired units were operating and reduced the overall gas availability. In order to reduce pre-heat time whilst achieving the before mentioned conditions, lower air velocities were used in the under-bed burner. This resulted in a good level of heating but the over bed burner burnt in less desirable conditions hence the higher CO concentration. This value decreased as the bed heated, decreased in density and eventually fluidised. The CO decreased as a result of air passing through the bed with less resistance and the over bed burner having a better stoichiometric ratio of O_2.

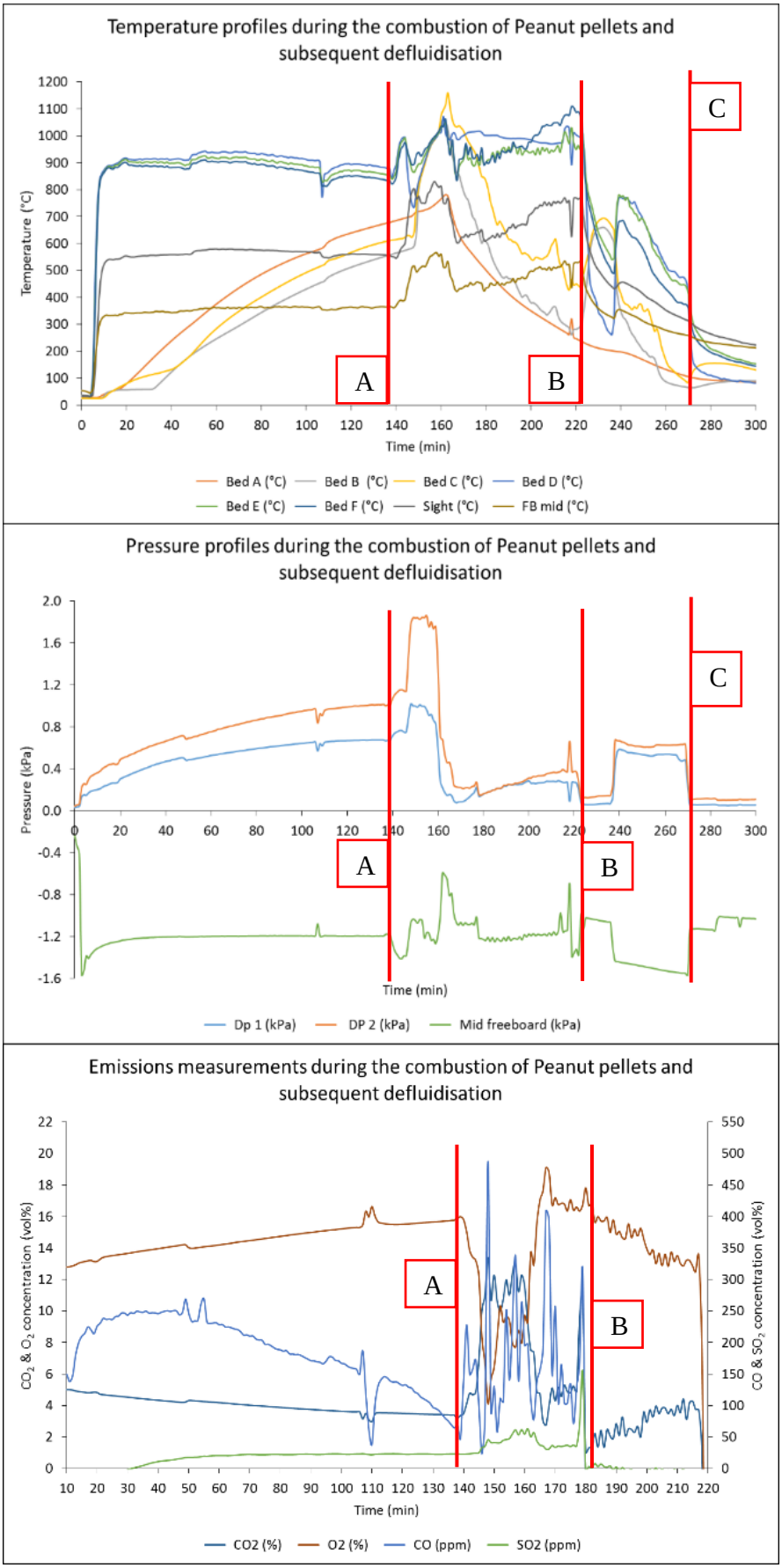

Figure 7-7 Temperature, pressure and emissions data collected during the combustion Peanut pellets and defluidisation of the bed with a uniform air distribution plate installed

After the introduction of biomass, the bed soon experienced problems. As the pressure chart shows, a higher air flow was used creating an across bed ΔP of 2kPa, but this created higher bed temperatures with higher excess air. The airflow was reduced to normal flow rates with a measured total air flow of 150 kg/hr. However, the Dp decreased to levels less than in normal operations. During period A to B, Bed B and C both exceeded 1000°C and all other bed temperatures were uncontrollable. Fuel flow was reduced from 21 kg/hr to 19kg/hr to evaluate the effect of less fuel. The results were a constant temperature. This is seen as the stable period to point B.

The emissions through period A to B was erratic. O_2 decreased to normal concentrations for combustion initially but returned to ≥16 vol.% as the test continues CO throughout this period varies between ranges of 50-500 ppm. Additionally, CO_2 spikes and drops with the availability and depletion of O_2. The emissions show that the combustion in the bed was incomplete and poor. This coincides with the bed temperature changes and low pressure Dp. Summarising period A to B, the bed is agglomerating rapidly as soon as solid fuel enters the bed. This generates temperature spikes which are addressed immediately. However, throughout the period rapid agglomeration was occurring. The emissions indicate non-uniform combustion. Therefore, it is safe to assume that there are localised hotpots of fuel burning producing excessive CO concentrations. It is likely that sintering occurred as a result of non-uniform combustion and the initial temperature spike.

With the onset of agglomeration through the bed (point B spikes in pressure and temperature). Bursts of higher flow rate air were put through the bed in an attempt to break up agglomerated structures and extend the test. This, in this case, actually worsened the situation. Bed temperatures after point B plummeted and the across bed Dp also decreased. It is thought that the bursts of air blew the loose un-agglomerated bed material away from the unobstructed bubble caps. This resulted in very little fuel mixing and thus combustion on top of agglomerated material and complete failure of the bed. Point C shows the end of the tests after the agglomeration and defluidisation had taken over. The peanut pellets led to speedy and total agglomeration.

7.2.2.1 SEM-EDX

Figure 7-8 shows the four SEM images of interest picked from SEM and Figure 7-9 shows SEM-EDX analysis conducted on samples taken from the bed after combustion of peanut pellets with the uniform air distribution plate installed. Image 1 shows the surface of an agglomerate taken from the bed post combustion of peanut pellets. SEM-EDX indicates that the major components within the sample are K and Si. Image 1 was typical for most agglomerates found within the bed, however, the branching seen in image 2, was found on a number of samples around the bed. This branching effect is the result of agglomerates and material moving against one another in the turbulent bed. The SEM-EDX results indicate that within these branched areas upon the surface of the

agglomerates the alkaline content is made up of a number of species including K, Si, Al, Mg, Ca and P. Only within these types of branches was this clustering of species seen. Image 3 shows the cross section of an agglomerate with sand particles embedded with the agglomerate complex. However, SEM-EDX indicates that the agglomerate is made up primarily of Si and Fe. Only nearer the surface of the agglomerate are the species named in image 2 found. Within the core of the agglomerate a eutectic made up almost entirely of Fe-Si is present. It is assumed that whilst a majority of the Fe comes from the ash a proportion must be reacting with the sand which was found to contain a proportion of Fe. In the coal tests this was overshadowed by the Fe content of the Coal but as biomass contains less ash than coal the bed Fe content must be considered.

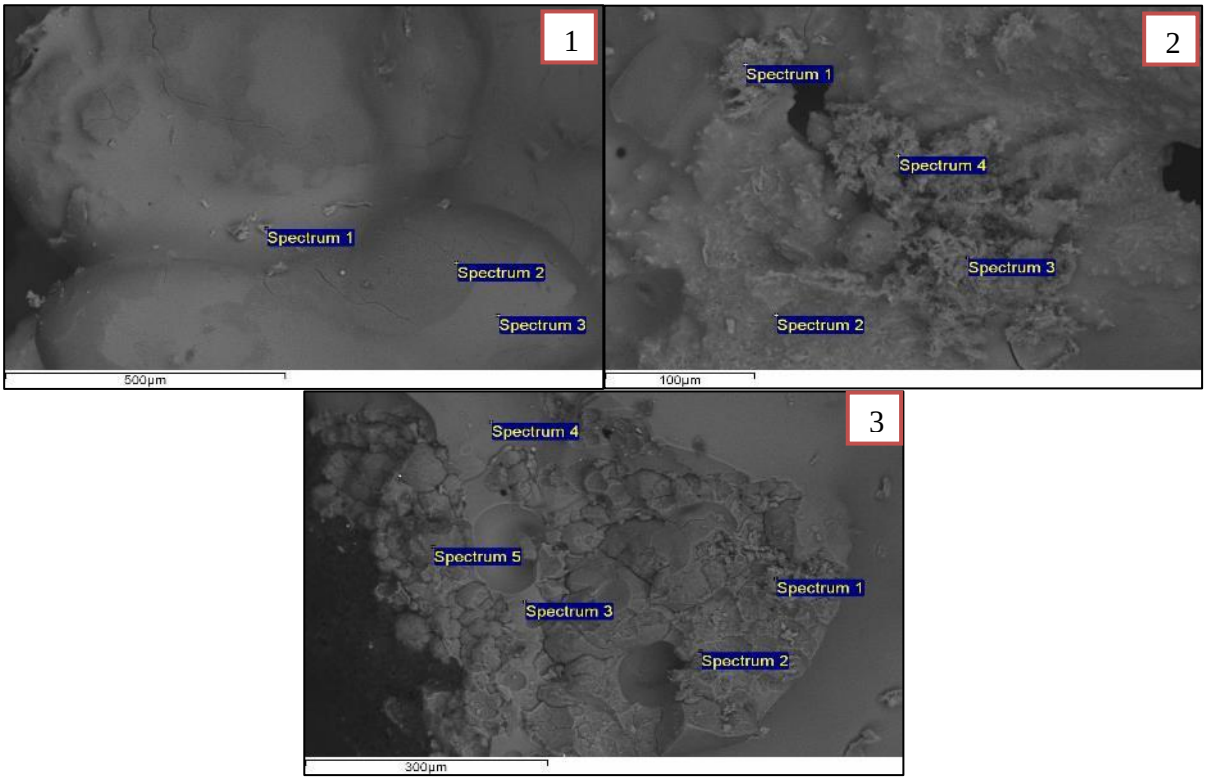

Figure 7-8 A collection of SEM images and locations of SEM-EDX from peanut combustion. Images show the following; 1) surface of agglomerate, 2) enhanced image of branching and alkaline complex, and, 3) cross section of agglomerate

The data from analysis of image 1 and 2 shows that in the early stages of the agglomeration process, the dominant eutectic is comprised of Si-K. However, the branching and propagation of the agglomerate seem to be linked to the branching of occurring on the surface of the agglomerates containing a cluster of alkaline species (image 2). The eutectic/complex would be very sticky due to the presence of such a mixture of alkaline species and hence leads to the adhesion of agglomerates and sand particles to one another. The data from image 3 shows that once an agglomerate grows in size, the internal eutectic is made up primarily of Si-Fe with only a thin layer of surface material containing other alkaline species. Once an agglomerate has formed is likely that

constant exposure to heat and mixing to sand particles results in the sticky surface wither being lost as in the gaseous state or sticking to other particles in the liquid phase. If there are a low concentration of these surface species, then it is likely they are distributed throughout the bed but with lower concertation. This theory is validated by ash analysis work shown in the fuel characterisation Chapter 4.

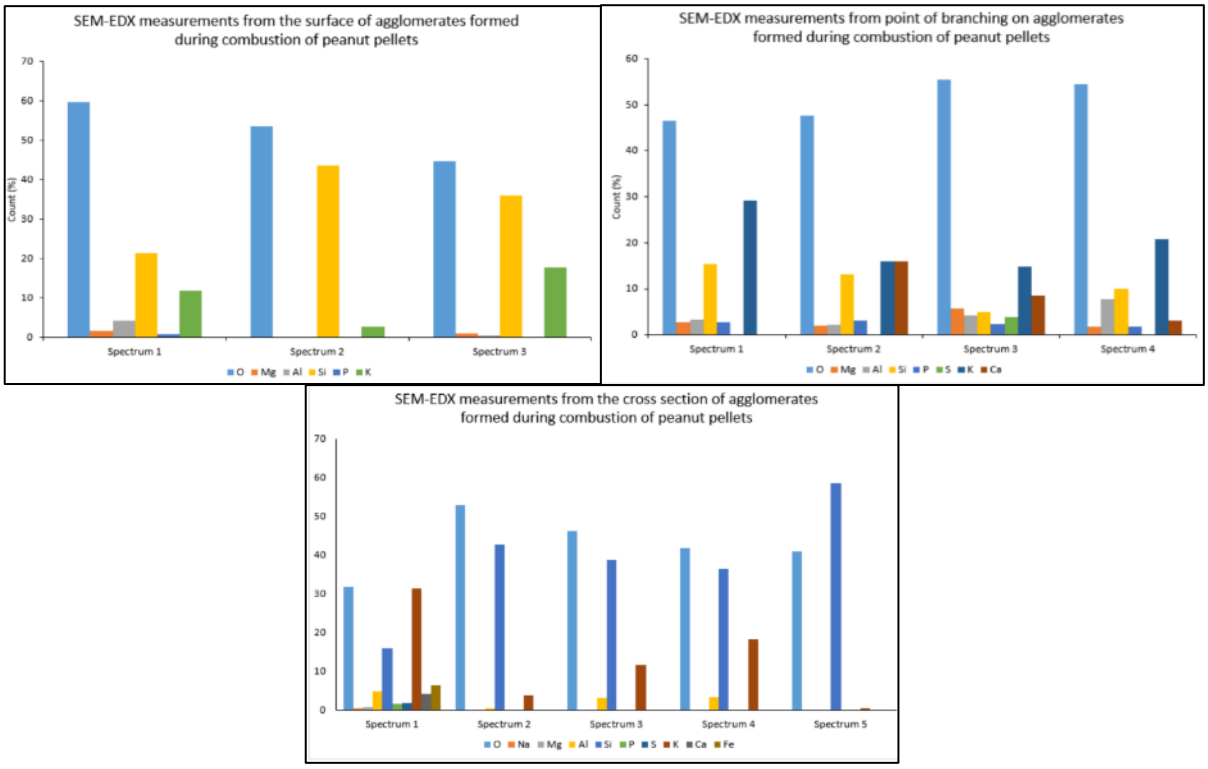

Figure 7-9 shows the SEM-EDX results for the selected samples of Figure 7-8

7.2.2.2 XRF

The XRF analysis of bed samples taken after the combustion of peanut pellets is shown in Figure 7-10. The figure show that the samples taken from the bed after combustion were made up of Si based compounds. This is assumed to be because of the silica sand bed material. The next main component is K, Fe and Ca oxides. The K concentration has contributed to the formation of the agglomerates. Furthermore, the higher concentration of K in the pellets is likely the key component for the fast agglomeration and defluidisation time of the bed. The Fe concentration, as seen in the coal test and literature, will have also contributed to the formation of low melting eutectics in the bed during combustion.

The results in Figure 7-10 correlates to the analysis of Figure 7-9 SEM-EDX results. The combination of data give a good foundation and indication to the significance of Si-K, K-Fe and Si-K-Fe complexes in the onset of agglomeration during the combustion of peanut pellets.

7.2.3 Oats Pellets

After the difficulty seen in maintaining stable operation with peanut pellets, it was decided that a similar approach with the pre-heat would be used for oats pellets. The concern is based on the fuel characterisation analysis performed in Chapter 4. Oat and Peanut pellets had similar chemical characteristics and performed similarly in ash fusion testing and thus share similar melt phases.

Figure 7-11 shows the temperature, pressure and emissions data recorded during the test. Pre-heat was performed in the same manner as with peanut pellets, until with an average bed temperature of ≥700°C was achieved. Fuel was then switched from gas to oats pellets at point A.

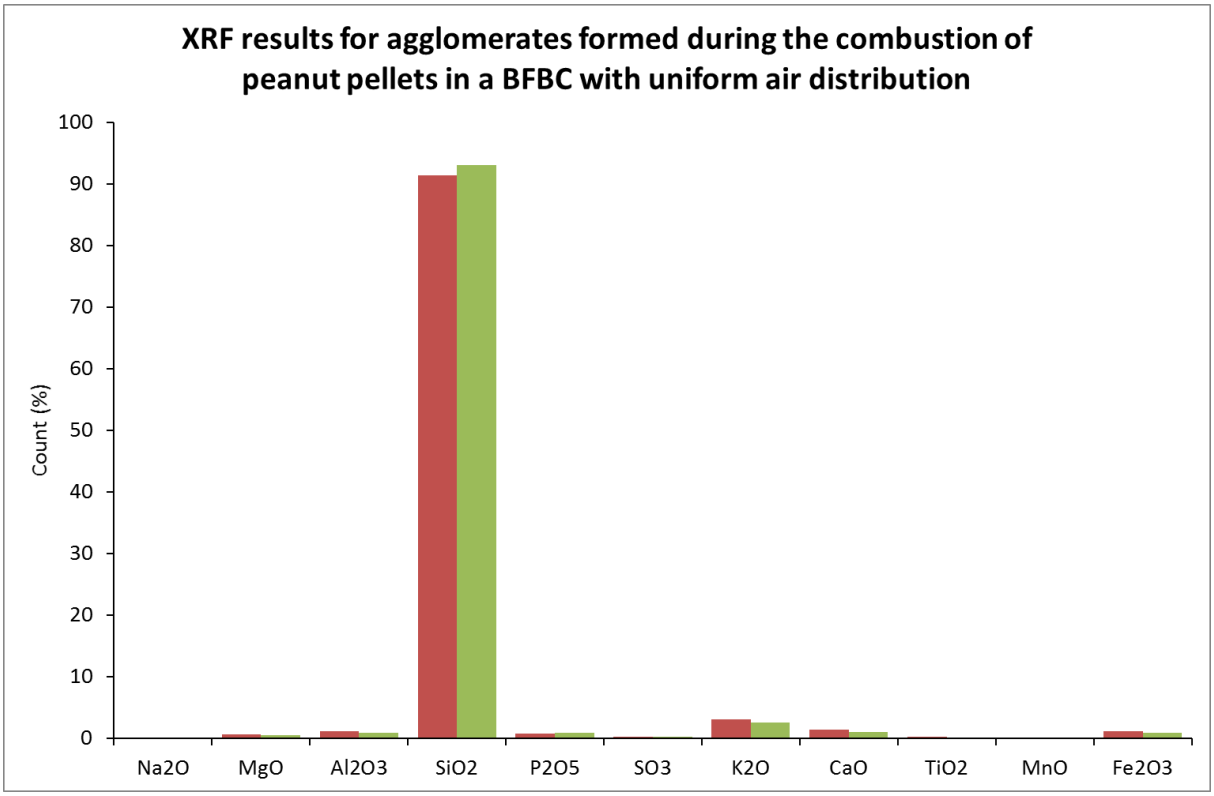

Figure 7-10 XRF analysis of bed samples taken after testing from the combustion of peanut pellets in a BFBC with uniform air distribution

Immediately after biomass was introduced into the bed there were problems controlling the bed temperatures. An initial fuel flow rate of 19 kg/hr had been chosen as this was less than required to achieve a bed temperature of 900°C on a theoretical basis. Fluctuating, but within the range of expected temperatures, continued for 19 minutes to point B. As the pressure data shows the across bed Dp remained at 1.8 kPa throughout this period. The air flow rate was 160 kg/hr. This was slightly higher than the peanuts test to ensure that agglomerates or poor mixing wasn't a result of insufficient air but instead due to agglomerate formation. Between point A and B the O_2 concentration averaged approx. 8 vol% which was desirable and indicated combustion at 60 %

excess air, which was once again close to operational targets. The CO and CO_2 emissions through this period fluctuates dramatically, however, this indicates that while the bed was fluidised and combustion was relatively stable, there was localised variation in the bed and air channelling occurring.

The effects of the channelling can be seen by the sudden system change at and after point B to point C. Bed temperature D shoots to ≥1350°C as Bed B and C temperatures decreased sharply to 550 and 500 °C respectively. Across bed pressure decreases to 0.5 kPa and the O_2 concentration increases to ≥12 vol%. The period between point B and C shows a sudden change in the bed which was later found to be due to sintering. The fuel contains high concentrations of Fe, Na and Si species associated with liquid phases and agglomeration. After point B the bed degrades with poor mixing occurring, the onset of agglomerated and sintered bed material occurred leading to the channelling of air flows and slumping of bed. This idea is reinforced by the gradual and step increases in mid freeboard pressure. With the onset of agglomeration and channelling in the bed, the air is no longer uniformly passing through the bed material and instead moving through less resistant and less covered bubble caps. Hence the freeboard negative pressure slowly equalises to ambient pressure.

Before point C and at point C there are further extreme spike in bed temperature and emissions. The fuel is stopped due to the fear of damaging internal equipment. However, it is already clear by point C that the bed had agglomerated, defluidised and was no longer operating in a condition in which would be suitable for the combustion of fuel for steam generation.

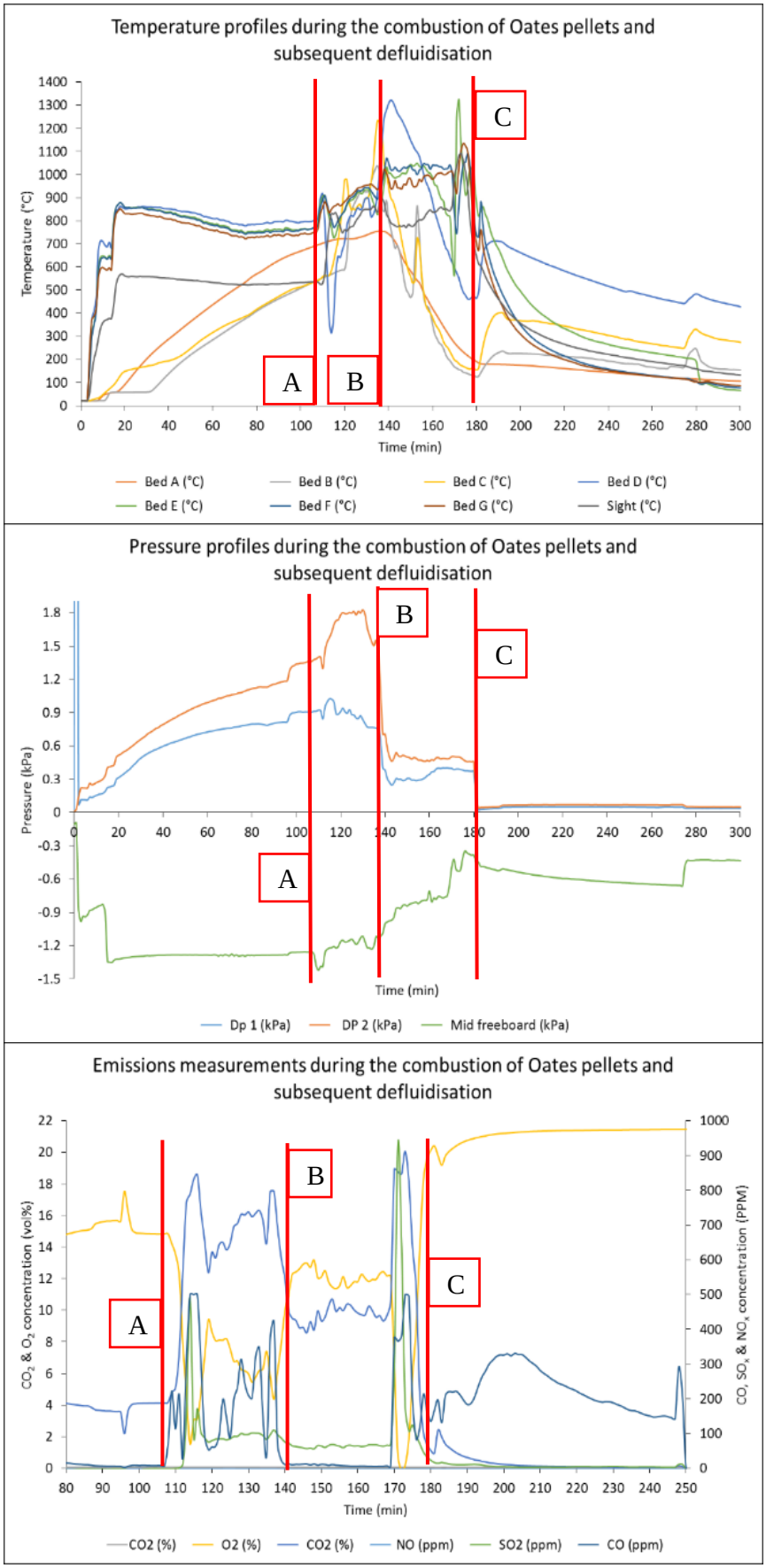

Figure 7-11 Temperature, pressure and emissions data collected during the combustion Oats pellets and defluidisation of the bed with a uniform air distribution plate installed

7.2.3.1 SEM-EDX

Figure 7-12 shows four SEM images and Figure 7-5 shows SEM-EDX analysis conducted on the samples taken from the bed after combustion of oats pellets with the uniform air distribution plate installed.

The results found that agglomerates from the combustion of oat pellets were very similar to that of peanut. The only significant difference being the concentration of alkaline species, primarily K, to be less than in peanut sample and found only in surfaces of agglomerates. Image 1 shows a cross section of an agglomerate and how sand particles are squashed together with a thick outer layer of a previously liquid phase. Image 2 shows a cross section of a thinner piece of agglomerate and how the sand particle is still similarly sized but the outer agglomerated layer is thinner. Additionally, the agglomerate can be seen to be impregnating and penetrating the sand particles within the main structure of the mass. The data suggests a slightly different mechanism for agglomeration with oat pellets. With the onset of agglomeration in the bed the increased temperature of localised combustion could have liberated alkaline species into the gas phase and thus left the agglomerates with lower concentrations of alkaline species. However, the SEM and SEM-EDX data does conform to visual results of the bed. There was large volume of smaller masses built up into large loose structures. The structures are shown in image 1. Therefore, a different agglomeration path is being taken, or the mixing, temperatures or alkaline species are limiting agglomeration sizes but not the propagation of overall structures throughout the bed.

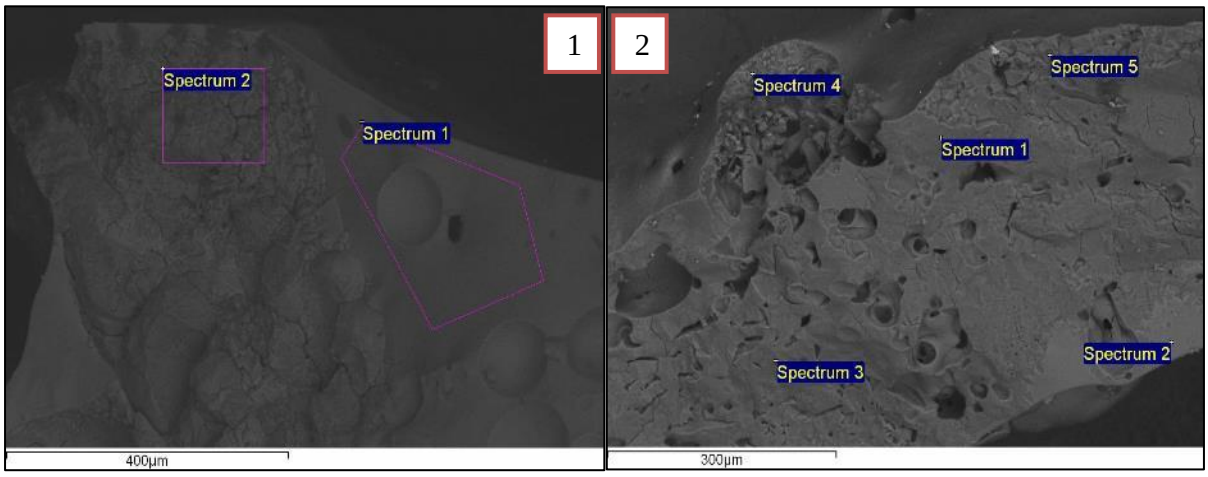

Figure 7-12 SEM images and location of SEM-EDX measurements from oats combustion. The images show the following; 1) cross section of agglomerate, and, 2) cross section of liquid agglomerate/sintered area

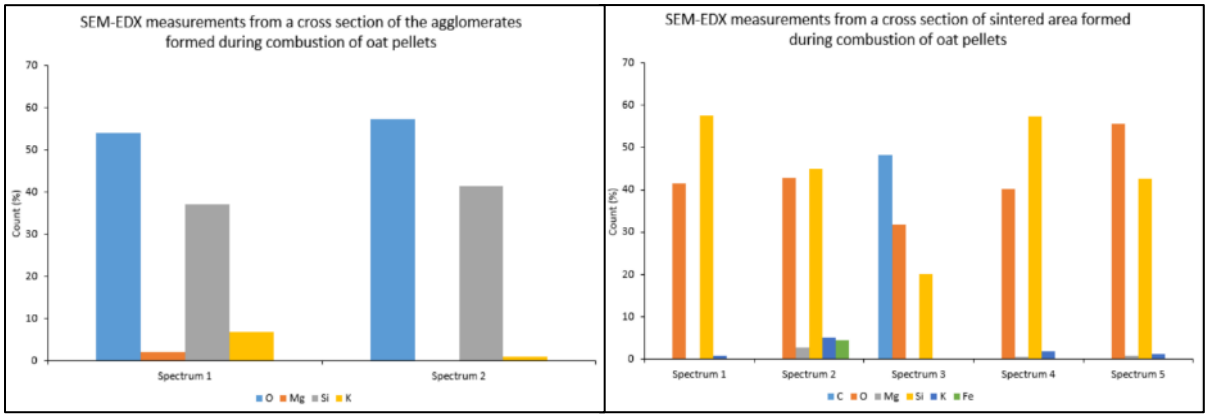

Figure 7-13 shows SEM-EDX results for the selected samples of Figure 7-12

7.2.3.2 XRF

Figure 7-14 shows the results for XRF analysis of samples taken from the bed after the combustion of oat pellets. The XRF results shows, as with previous analysis, that the majority of measured species are Si based, whilst K and P are the next most significant components in the agglomerates. K, Si and P have all been seen in the literature and in previous tests to contribute to the formation of agglomerates at accelerated rates.

The results, coupled with the results of Figure 7-13, indicate the significance of Si-K, Si-P and Si-K-P in the formation of agglomerates when combusting oat pellets.

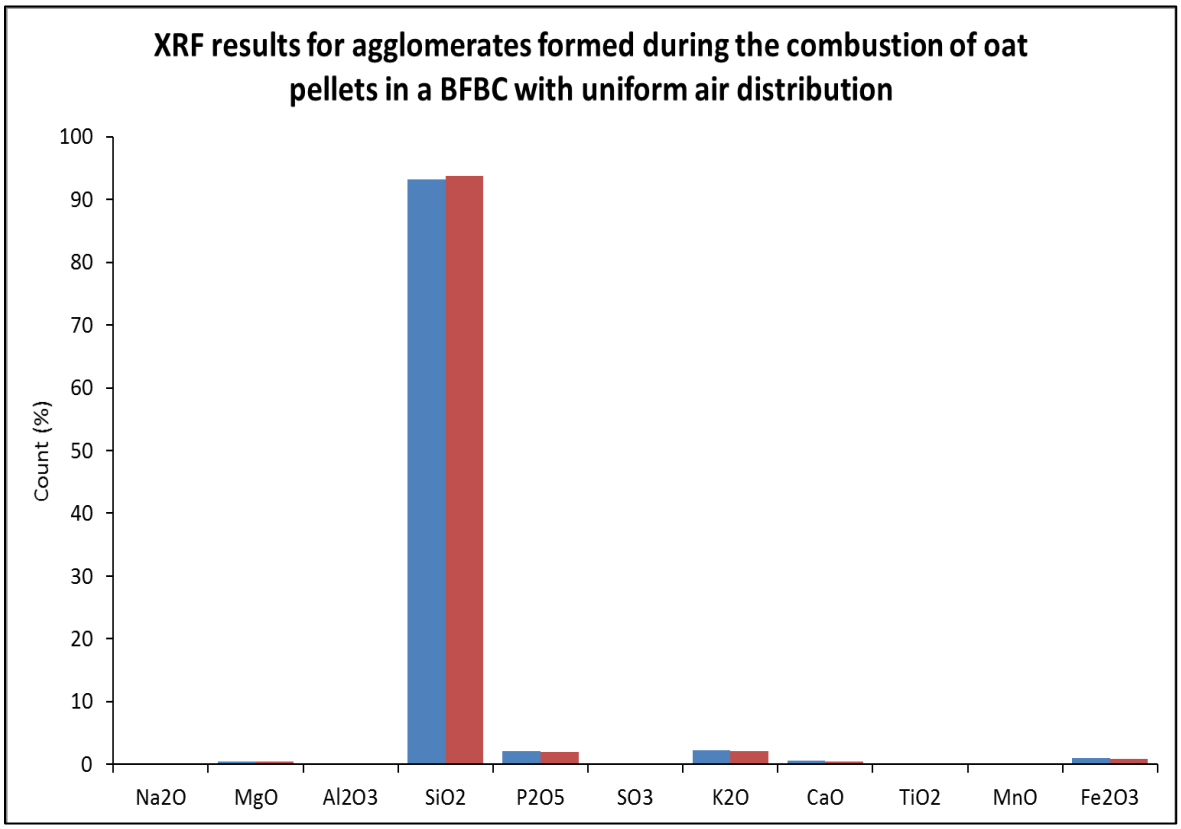

Figure 7-14 XRF analysis of bed samples taken after testing from the combustion of oat pellets in a BFBC with uniform air distribution

7.2.4 Straw Pellets

The combustion of straw pellets was repeated as it was found that the defluidisation time as a direct result of agglomerates forming in the bed was less than 35 minutes. Whilst this is similar to other discussed earlier, the fuel was almost impossible to control in a manner resembling stable combustion. The repeat test was performed in order to validate the difficulty associated with combusting this fuel in a FBC unit.

Figure 7-15 shows the temperature pressure and emissions data measured during the test. Once the pre-heating had finished at point A, the fuel was switched from gas to straw pellets. Stable combustion only lasted for 5 minutes. The O_2 concentration was measured at 9 vol. % which was the intended value for the experiment. The fuel flow was fixed at 20 kg/hr, with an air flow of 120 kg/hr. However, as time progressed the CO emission measured increased from approx. 50 ppm to ≥150 ppm.

When the bed temperatures suddenly decreased 23 minutes into the test the air was increased to 135 kg/hr. It was visually observed that at this flow the bed was still bubbling but beyond was creating a violent bed with an undesirable flow of materials was being violently ejected. As a result of the flow rate increase, the bed mixes and fluidises better. However, as the emissions show the bed was degrading and combustion was suffering, even with the increased mixing viewed from the side port.

The CO emissions increase to ≥500 ppm whilst the O_2 also increased to ≥14 vol. %. This is an indication of poor combustion occurring above and within the bed. Furthermore, at point B the bed temperatures fall sharply, the across bed Dp falls and the emissions slump. The agglomerates forming in the bed have defluidised the bed completely and fuel is combusting on top of the bed rather than in it. At this point the test has ended.

The emissions data and temperature data show that the bed was degrading as soon as solid fuel was combusting in the bed. The bed temperatures were more desirable than previous repeats with an average bed temperature of 775°C. Even so the bed material agglomerated with impurities within the fuel immediately.

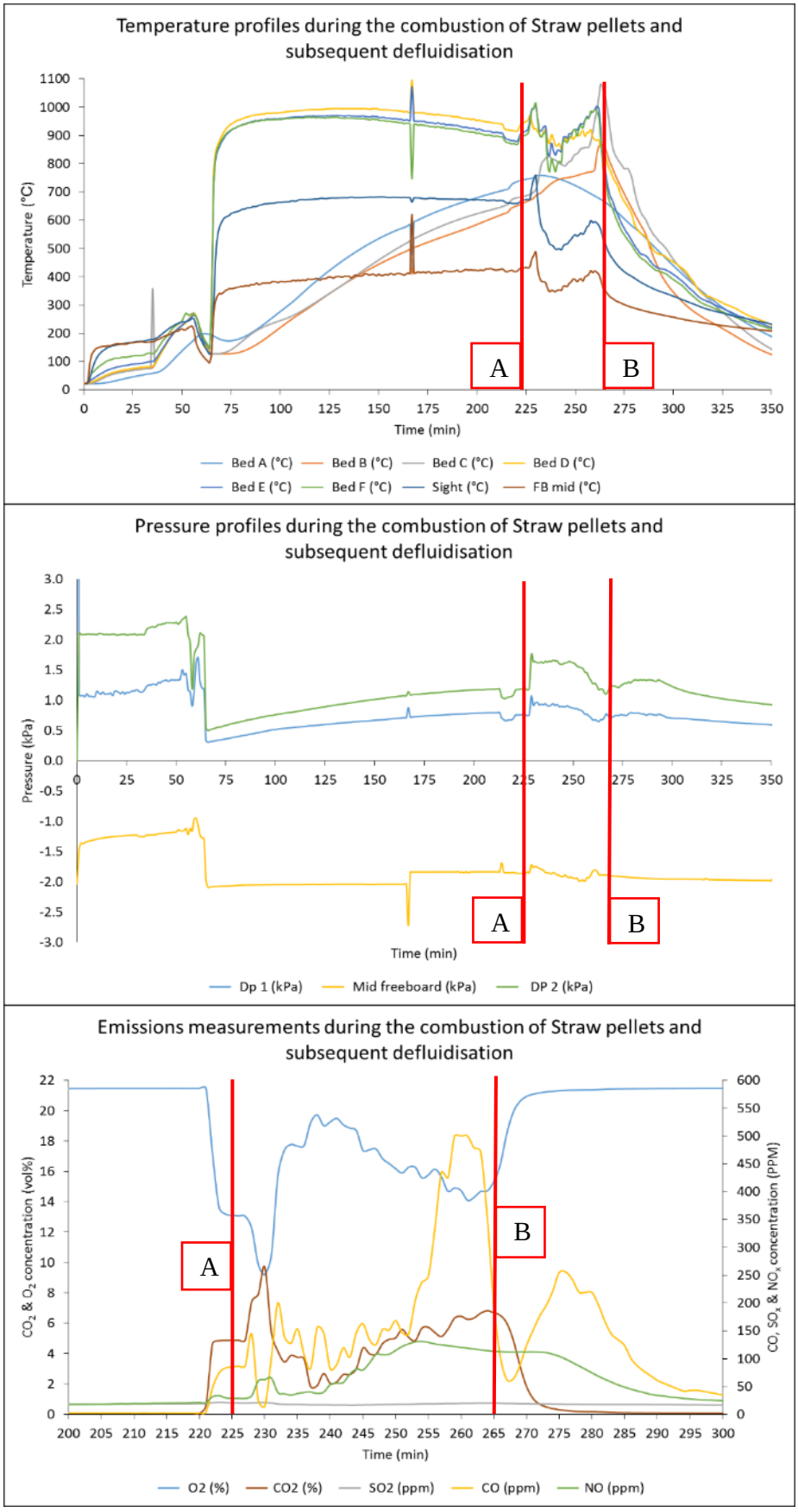

Figure 7-15 Temperature, pressure and emissions data collected during the combustion Straw pellets and defluidisation of the bed with a uniform air distribution plate installed

7.2.4.1 SEM-EDX

Figure 7-16 shows four SEM images and Figure 7-17 shows SEM-EDX analysis conducted on the samples taken from the bed after combustion of straw pellets with the uniform air distribution plate installed.

The agglomerates found in the bed after the combustion of straw pellets were very different to those found in previous tests. Image 1 and 2 show a bubble-like effect found around the bed particles both on the surface and embedded within agglomerated structures. Within these bubbled structures high concentrations of alkaline species including Si, K, P and Fe were found to make up the majority present.

Image 3 and 4 are examples of the surface of agglomerates in the bed. Image 3 shows a crystalline structure made up predominately of Si and K. The crystals are likely the product of a eutectic formation where Si-K is cause of the surface crystals. Whereas, in other areas around agglomerates the branching effect seen in image 4 is more common. Within these branches clusters of agglomeration species are found (K, Ca, P and Si), similarly to those in the peanut agglomerates. The SEM-EDX indicates there is also S present within the branches. This increase in localised concertation with increases in localised Ca concertation is assumed to be the results of a Sulphation reaction.

Image 5 shows the cross section of agglomerates found within the bed and SEM-EDX indicates that the agglomerate complex between sand particles are made up of complexes containing K-Si-Ca-Fe. Whilst this is the case for the internal structure of the agglomerate, image 6 shows the bond point between bed particles, and SEM-EDX indicates that on the surface in these locations Fe-Si-K complexes are dominant.

The results displayed here suggest an agglomeration mechanism similar to peanut, wood and oat pellet agglomeration. However, it doesn't follow the same exact process but instead share similarities with each. The bubble effect (image 1 and 2) can be linked to that found in the wood data but instead of depositing Fe concentrates, a liquid phase is formed with K concentrated within. This K liquid phase would create a sticky liquid capable to stick particles together. This is potentially the initial stages of this mechanism.

The branching effect is similar to that of peanut and has the same cluster effect of alkaline species in these branches. Similarly, the complexes in the branches would be very sticky and are likely to have formed in shape as a result of particle moving against and moving away from the branch source location. This is the next stage in the propagation of the agglomerate.

The difference in internal and external structure of the eutectics bounding the sand particles together in image 5 and 6 is likely the final stage of the agglomerate formation. The internal structure is a matrix containing Si-Fe-K and because of the high concentration of K this structure builds in size more quickly than previous agglomerates. In doing so retaining K and other lighter components. However, the exposed surface which underwent continued heating and oxidation, the Fe-Si complex is dominant, with a loss of K and lighter alkaline species. It is expected that, based on what was seen in other tests, Fe-Si eutectics would merge these smaller agglomerates together into larger more load bearing agglomerated structures.

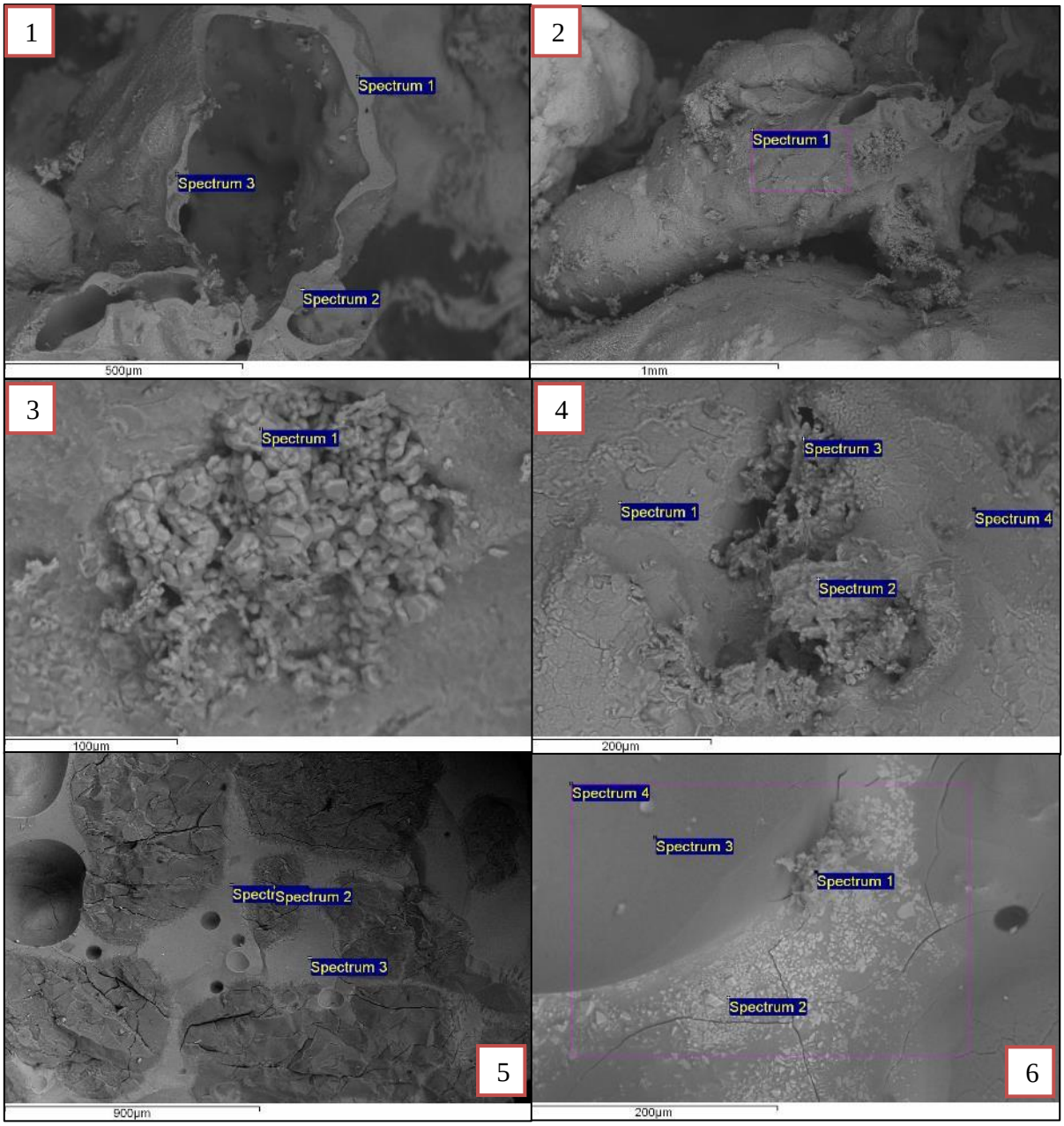

Figure 7-16 A collection of SEM images and SEM-EDX locations from straw combustion. The images are; 1) bubble agglomerate formed around combusting pellet, 2) Structure remaining from pellet combusting internally, 3) enhanced area of agglomerate surface, 4) enhanced area of surface with branching, 5) cross section of agglomerate, and, 6) surface of sintered material

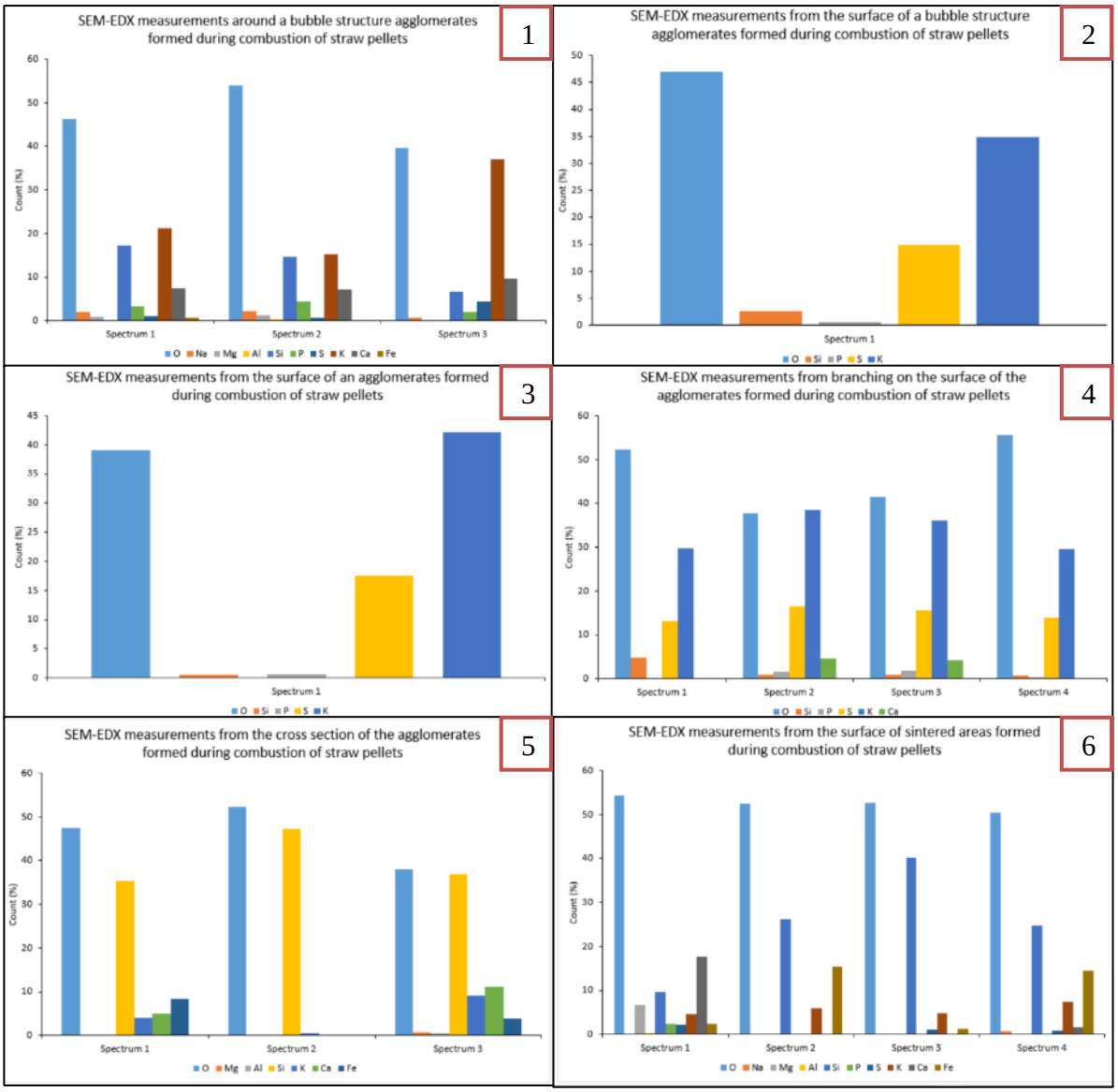

Figure 7-17 shows the SEM-EDX results for the selected samples in Figure 7-16

7.2.4.2 XRF

Figure 7-18 shows the results from the XRF analysis of bed samples taken from the rig after the test was complete. As the figure shows the main component is Si with K, Ca, Na and Fe making up the majority of the other alkaline species in the agglomerates. This is similar to previous tests but shows a correlation between the alkaline species in Chapter 4 and those in the agglomerates.

Na, K and Fe have been noted to contribute to the agglomeration in the bed and this is further shown by the results in Figure 7-17 and Figure 7-18.

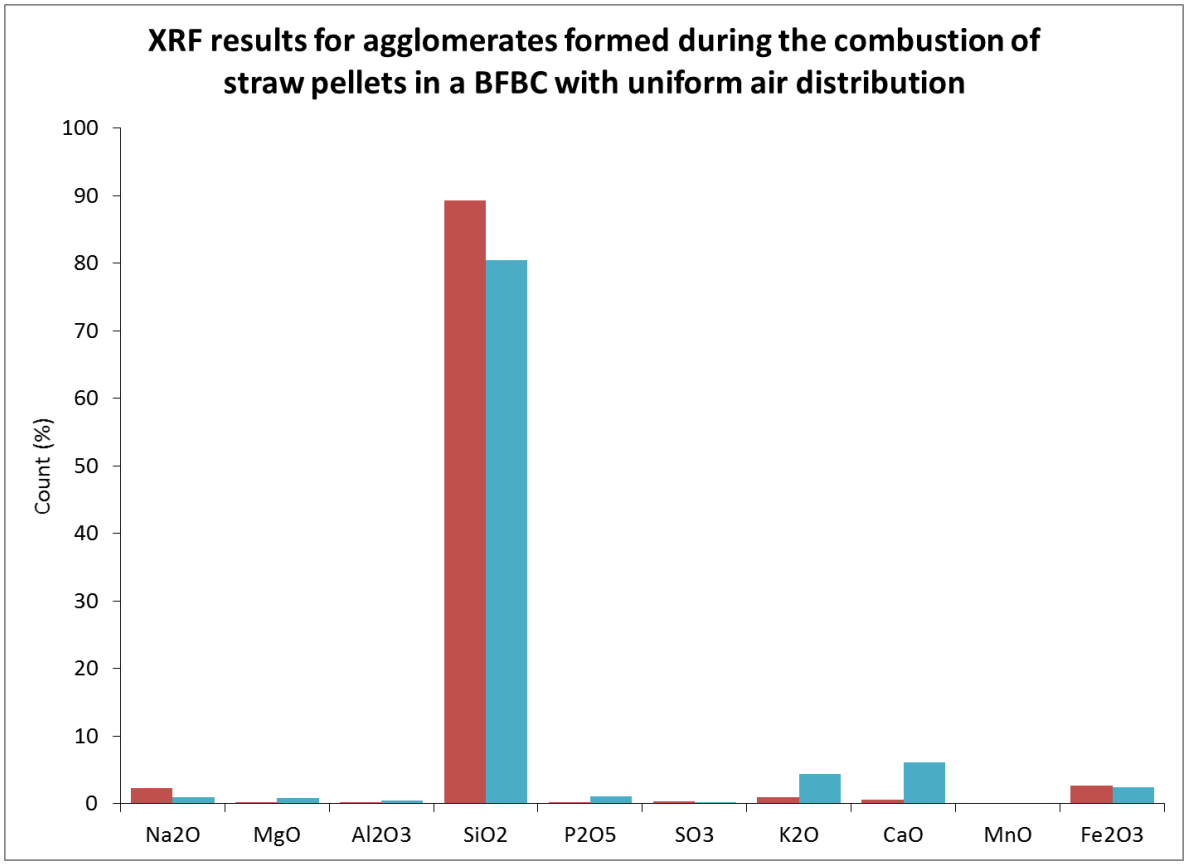

Figure 7-18 XRF analysis of agglomerated bed samples taken after testing from the combustion of wood pellets in a BFBC with uniform air distribution

7.2.5 Miscanthus Pellets

Miscanthus shares similarities with straw. They are both grassy type fuels and their plant physiology lends to similar distributions of alkaline species on specific regions of the plant and thus concentrations of specific groups such as K and Na. This reasoning assumes that the combustion of Miscanthus would be similar to the performance of straw pellets.

Figure 7-19 shows the temperature, pressure and emissions data measured during the combustion of Miscanthus pellets. The Miscanthus test is another example of how a biomass fuel will combust in a fluidised bed and immediately degrade a bed. It was found that Miscanthus is very difficult to control in terms of combustion and in terms of sustaining a fluidised bed.

The total measured air flow rate was set at 130 kg/hr at point A when gas was switched to Miscanthus pellets. As the previous test had shown an increase in the under-bed air didn't result in improved combustion or fluidisation of the bed. Within 8 minutes of the fuel entering the bed, temperatures decrease sharply as the bed slumps. This is a result of the bed agglomerating aggressively. The across pressure Dp rapidly increases with the onset of agglomeration. At point B the bed has agglomerated and the system fails to operate in a stable manner. The increase in

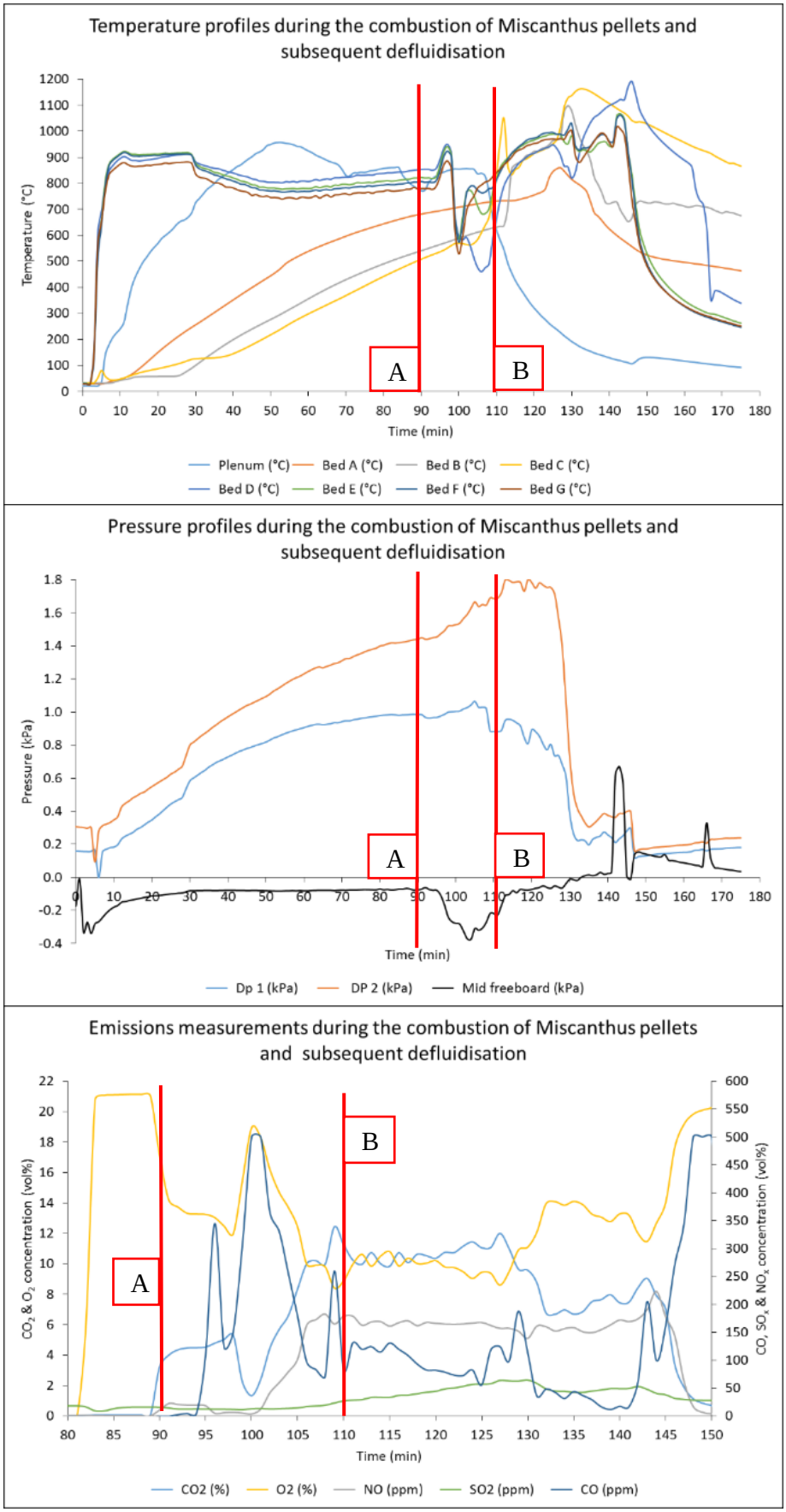

Figure 7-19 Temperature, pressure and emissions data collected during the combustion Miscanthus pellets and defluidisation of the bed with a uniform air distribution plate installed

midfreeboard pressure is evidence of agglomeration as the air moving through the bed is unimpeded by bed material.

Throughout the period of A to B, the CO and O_2 emissions fluctuate in a manner displaying combustion fluctuations. With the slumping and channelling of the bed, the combustion is consuming and change the availability of O_2 and the incomplete combustion is varying in intensity. This continues until the bed defluidise completely and inevitable air channelling and re directing of air around the agglomerated bed results in relatively normal emission concentrations.

The distribution of heat throughout the bed wasn't uniform. After point B the fuel is combusting on top of the bed rather than in it. The temperatures recorded above the bed reach ≥1050 °C. The onset of sintering is likely to have occurred with material at the top of the bed because of this. Furthermore, the bottom of the bed cools with the restriction of fuel to the lower regions of the bed. Once the bed has agglomerated, the rig is acting more like a grate incinerator rather than a fluidised bed and suspending the fuel upon the surface of the bed rather than in it.

7.2.5.1 SEM-EDX

Figure 7-20 shows four SEM images and Figure 7-5 shows SEM-EDX analysis conducted on samples taken from the bed after combustion of straw pellets with the uniform air distribution plate installed.

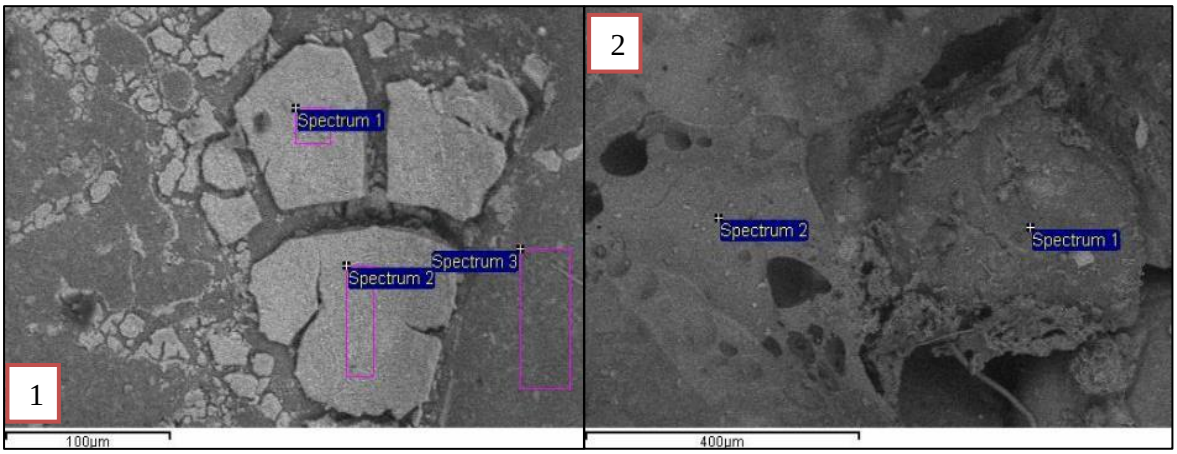

Figure 7-20 SEM images and SEM-EDX measurement location from miscanthus combustion. The images are as followed; 1) surface of agglomerate, and, 2) agglomerate bridging between sand particles

The agglomerates within the bed from the combustion of miscanthus pellets were very similar to the structures and shapes found within the bed after straw pellet combustion. That being there were bubbled areas and high concentrations of K which had formed liquid phases in the agglomerate. This is evident from image 2 which shows bed particles stuck within the agglomerate with a series

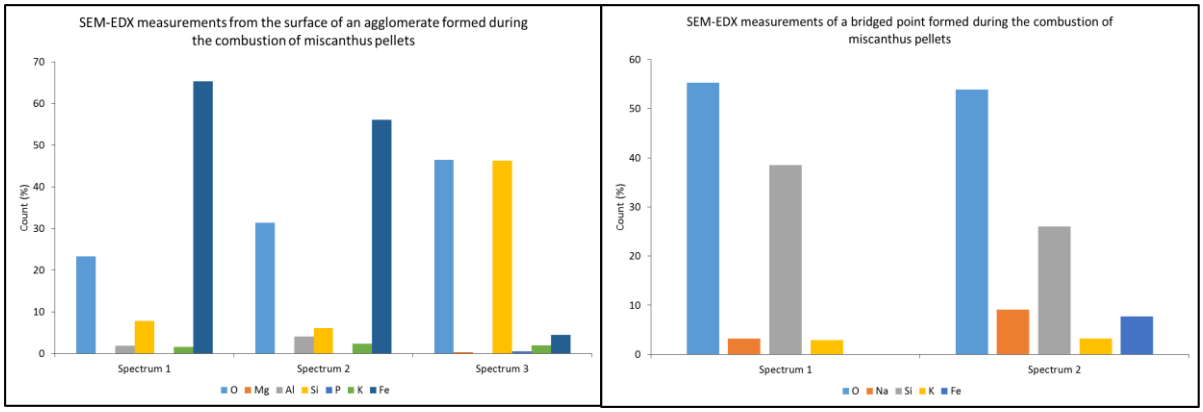

Figure 7-21 SEM-EDX results for the points of interest samples analysed and described in Figure 7-20

of bridges being formed from the main body of the agglomerate to the new particles. The complexes adhering the particles together was indicated to be Si-K rich.

However, there were some differences found when the agglomerates propagated in size to larger structures. Image 1 shows the surface of an agglomerate. Here there are plate like masses. These were found to be primarily made up of Fe with very little Si etc. The plate like structures were seen to follow the contours of areas in which two or more large agglomerates had adhered to one another. The fused point between the structures which would become more structurally sturdy over time then built up the Fe rich plates on the surface. The high Fe source is assumed again to be a combination of the Fe in the biomass ash and Fe reacting from the bed material. The extent of the Fe in the structures indicates that a reaction is occurring and making any Fe a significant part of the agglomerate formation mechanism. Quantifying the role the Fe in bed and the ash however is difficult.

The agglomeration mechanism seems to be very similar to that of the straw tests, however, as to the cause of the Fe plates in the fusion point, there is still question. Possibly with veins of different alkaline species in the fuel/ash there were Fe rich seems which then present themselves in a liquid phase as a result of localised heating as a result of the larger agglomerate forming.

7.2.5.2 XRF

Figure 7-22 shows the results of XRF analysis for bed samples taken from the combustion of Miscanthus pellets. As the data shows, the high concentration of Si, due to silica sand, is the main component in the samples. However, Fe is the next significant component, which was seen to be high in concentration in the pellets and in the SEM-EDX analysis of Figure 7-21.

The data of this section shows the significance of Fe in the formation of agglomerate's. Additionally, the rate of agglomeration when combusting Miscanthus pellets had the second highest rate of formation.

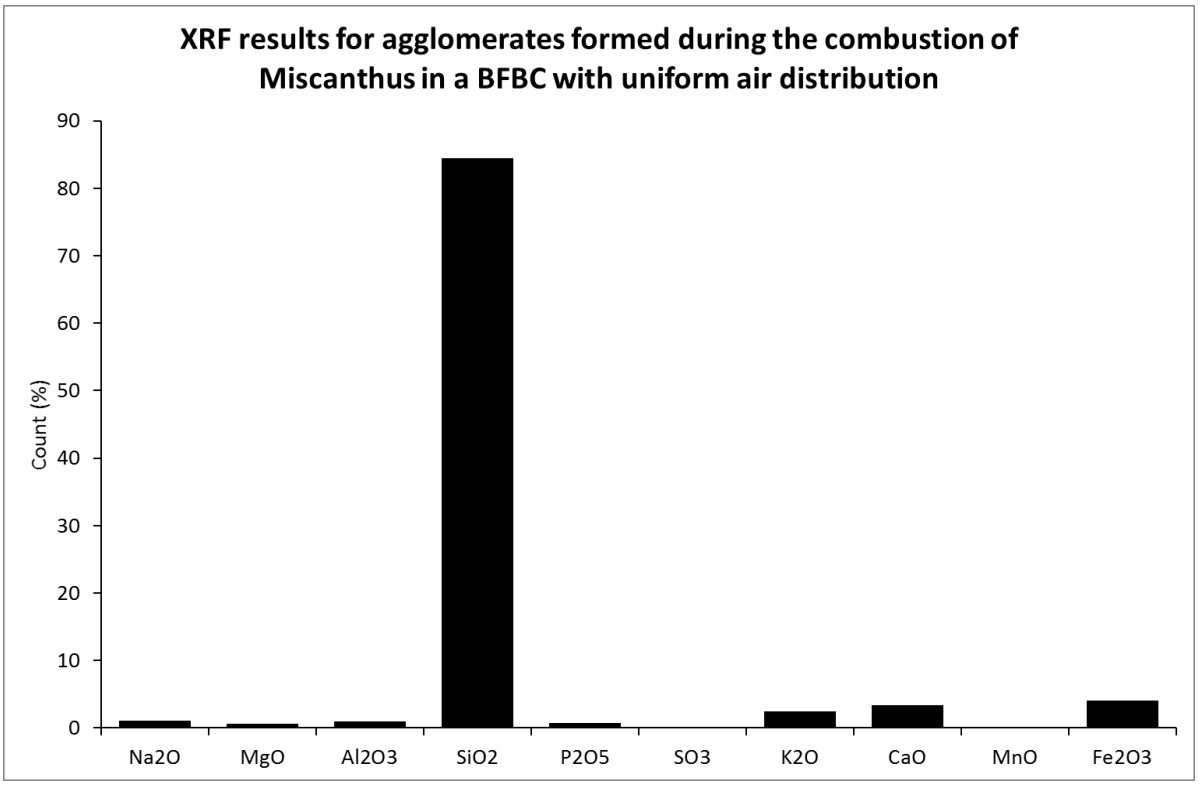

Figure 7-22 XRF analysis of bed samples taken after testing from the combustion of miscanthus pellets in a BFBC with uniform air distribution

7.3 Non-Uniform Air Distribution

The findings of the previous section have shown the performance of biomass fuels under typical operational conditions, and the effect biomass has upon a bed in a bubbling fluidised bed unit. This section will now evaluate the effect of biomass in the same type of operation.

As described in the experimental methodology Chapter 3, the non-uniform plate was designed so the air flow would impact the bed in a number of ways. There is an area in which the air flow will experience less resistance (the leakage point) around a material emptying chute. The bubble caps are also located nearer the centre of the rig leaving dead zones around the edge of the bed. Further to this the height of the bubble caps is 50 mm taller leaving a larger dead space below the bubble caps. Finally, the reduction in bubble cap number will alter the velocity of the air flow from the bubble caps to that seen in the uniform air distribution plate. The differences are as shown in

At the time of the non-uniform plate installation and operation of the rig the burners and pressure transducers were set up in a slightly different layout to that of the uniform plate test. For these

reasons, the heating capacity of the under-bed burner is less than that of the previous system. Additionally, the difference in pressure readouts is a result of the rig alterations. This has not impeded in the accuracy and validity of the data in any way, instead the base case for comparison is slightly different.

7.3.1 Wood Pellets

Wood pellets were combusted in a similar manner to the uniform plate test. However, because of the changes in the rig air flows, fuel flows and subsequent pressures, temperatures etc. were different.

Figure 7-23 shows the temperature, pressure and emissions measurements made during the combustion of wood pellets with the leakage plate installed. Point A indicates the point at which the preheat sequence finished and gas was replaced with wood pellet combustion. There is a continued increase in temperatures across the bed and freeboard area to point B.

Whilst the temperatures are stable throughout the full extent of the test, the pressure measurements offer an alternate perspective. At point A the switch in fuels and redirecting of under-bed air can be seen. However, between point A and B there is a progressive decrease in bed and plenum pressure and increase in freeboard pressure. This continues after point B but with less severity. The increase in freeboard pressure with the increase in freeboard pressure indicates a change in air movement and bed resistance. From point A, air is finding less resistance and moving through the bed unabated which increases freeboard pressure and decreasing the back pressure in the plenum. This is a result of the air moving from an even distribution through the bubble caps and instead moving through the leakage point with increasing volume as the test continues. The bed material and fuel must still be moving to the leakage point as the bed temperature remains constant. There was no agglomerate found in the bed post-test bed. Therefore, the leakage in this scenario never defluidised the bed but instead impeded ideal fluidisation.

This is further emphasised by the emission measured throughout the test. At point A in the emissions data the fuel changeover can be seen. Over the test period the emissions are fairly steady state, apart from point A to B where the CO emission declines in line with the pressure change across the rig/bed. As the temperature continue to increase to point B and further the CO emissions are being converted to CO_2 with the continuously heated freeboard region until it drops to approx. 10ppm. Whilst this test was able to continuously operate with the leakage point in place for an extended period of time, it should be noted that wood was comparatively easier to combust as found with previous tests. There were no agglomerates found in this test was only a coating similar to that of the previous wood tests on bed particles. on the operation of the rig it was seen that the O_2

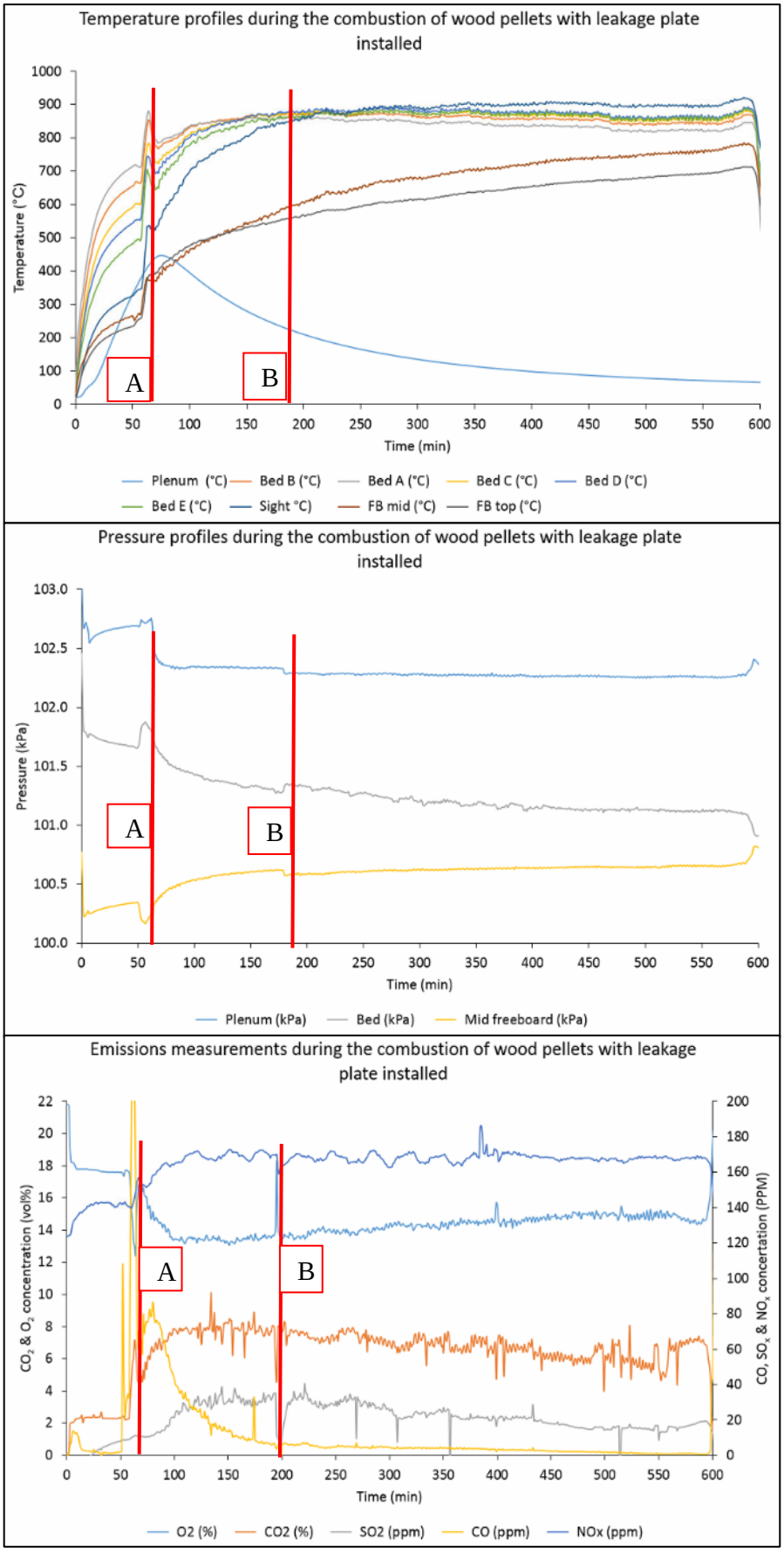

Figure 7-23 Temperature, pressure and emissions data collected during the combustion wood pellets and defluidisation of the bed with a non-uniform air distribution plate installed

concentration never dropped below 13 vol. % over the test. In the previous test an airflow of 9000 L/min was found to be a maximum required to run but with the leakage an airflow of ≥12000L/min was required to keep the bed bubbling or in a state near to bubbling. This test was a baseline test and expected to perform well because of the low agglomeration potential. It was theorised even a small volume of agglomeration would propagate fast in these poorly mixing beds and thus defluidise and impede operation more quickly than that of the uniform air plate.

7.3.1.1 SEM-EDX

Figure 7-24 shows SEM images and Figure 7-25 shows SEM-EDX analysis conducted on samples taken from the bed after combustion of wood pellets with the non-uniform air distribution plate installed. Image 1 shows a sand particle which has been coated in a liquid phase indicated to be made up of Si, Ca and Fe. On the surface of particles such as this and upon larger agglomerate surfaces there were found embedded crystal structures such as those shown in image 2 and 3. The crystals of image 2 were indicated to be largely made up of K-Ca complexes. The structure in image 2 is an example of a bridge which has formed between sand particles and is indicated to be a eutectic containing Si-K-Ca. The crystal structures of image 3 were commonly found on the surface of areas in which a number of bridges had formed between bed particles. The SEM-EDX data indicates that these were made up of Si-K-P complexes. Additionally, the crystals in image 3 were found to be moving into a liquid phase, looking as if they had begun or undergone some form of melting.

Image 4 is a typical amalgamation of processes found embedded within larger structures. There would be a combination of clustered alkaline species within a branched structure, with a bubbled/localised combustion point adjacent. The clusters were indicated to be made up of Si-Fe-K complexes whereas the bubble adjacent to these areas were found to contain more species but in lower concentration.

Images 5 and 6 were typical of surfaces of larger agglomerates which were large in size and difficult to break apart. The area between agglomerates and bed particles were indicated to be high in Fe. The enhanced image 6 shows that there were in fact clusters of agglomerate species but Fe-Si was still dominant. On the surface of the fusion/bridged point balls of alkaline species have formed as a result of a liquid phase moving in the bed. It should also be noted that Ca was also highly concentrated in these clusters.

The mechanism for agglomeration, based on the results found are slightly different to those of the uniform air plate test. In the mechanism for wood pellets here the sand particles are initially coated with a liquid phase on the surface containing Si-Fe-Ca complexes. The bridging and building up of

agglomerate surfaces and structure was found to be related to the formation of crystals on the surface which contained a sticky K-Ca. These melted under constant heat to create a sticky surface.

The surface in areas in which Fe was present led to the clustering of alkaline species and thus a sticky surface to adhere to bed material. In image 4 a pellet has been caught and combusted locally creating the bubble and low concertation in a localised area of alkaline species which were reminiscent in concertation to XRF data in previous wood ash analysis. The sticky K rich and Fe

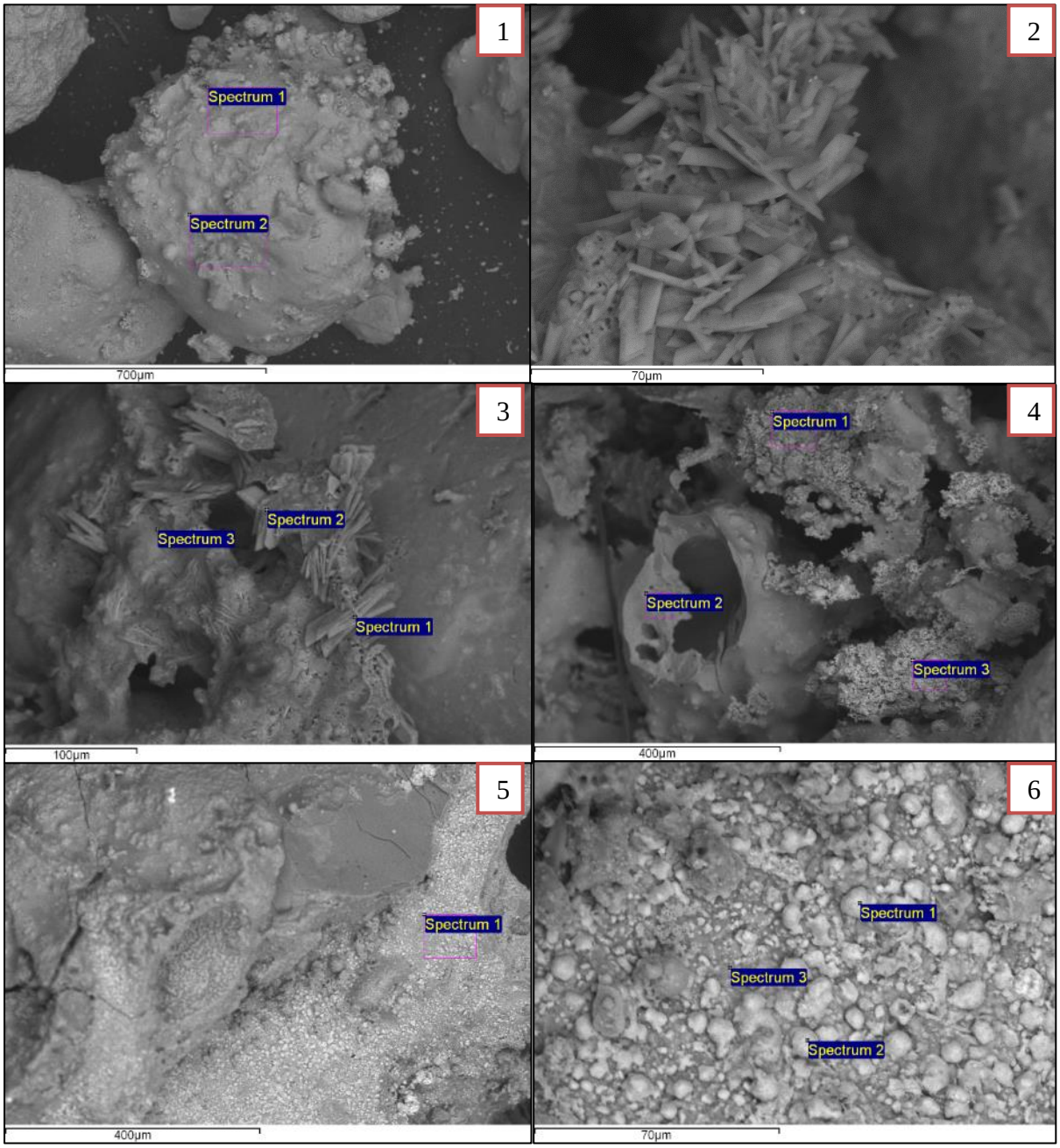

Figure 7-24 shows a series of SEM images and SEM-EDX measurement locations from point of interest for samples collected form the combustion of wood pellets. The images are follows; 1) Sand particle coated in agglomerate complex, 2) crystal formation bridged between sand particles, 3) crystal formations upon the surface of agglomerates, 4) branching on the surface of agglomerates, 5) fusion point between agglomerate structures, and, 6) enhanced images of fusion point between agglomerates.

rich surface seem to be the primary methods for building of agglomerates and forming strong bonds between agglomerates and eutectic surfaces. The Fe-Si concentrations found on the particle surfaces are linked to higher combustion temperatures melting lower melting temperature alkane groups into the gas phase.

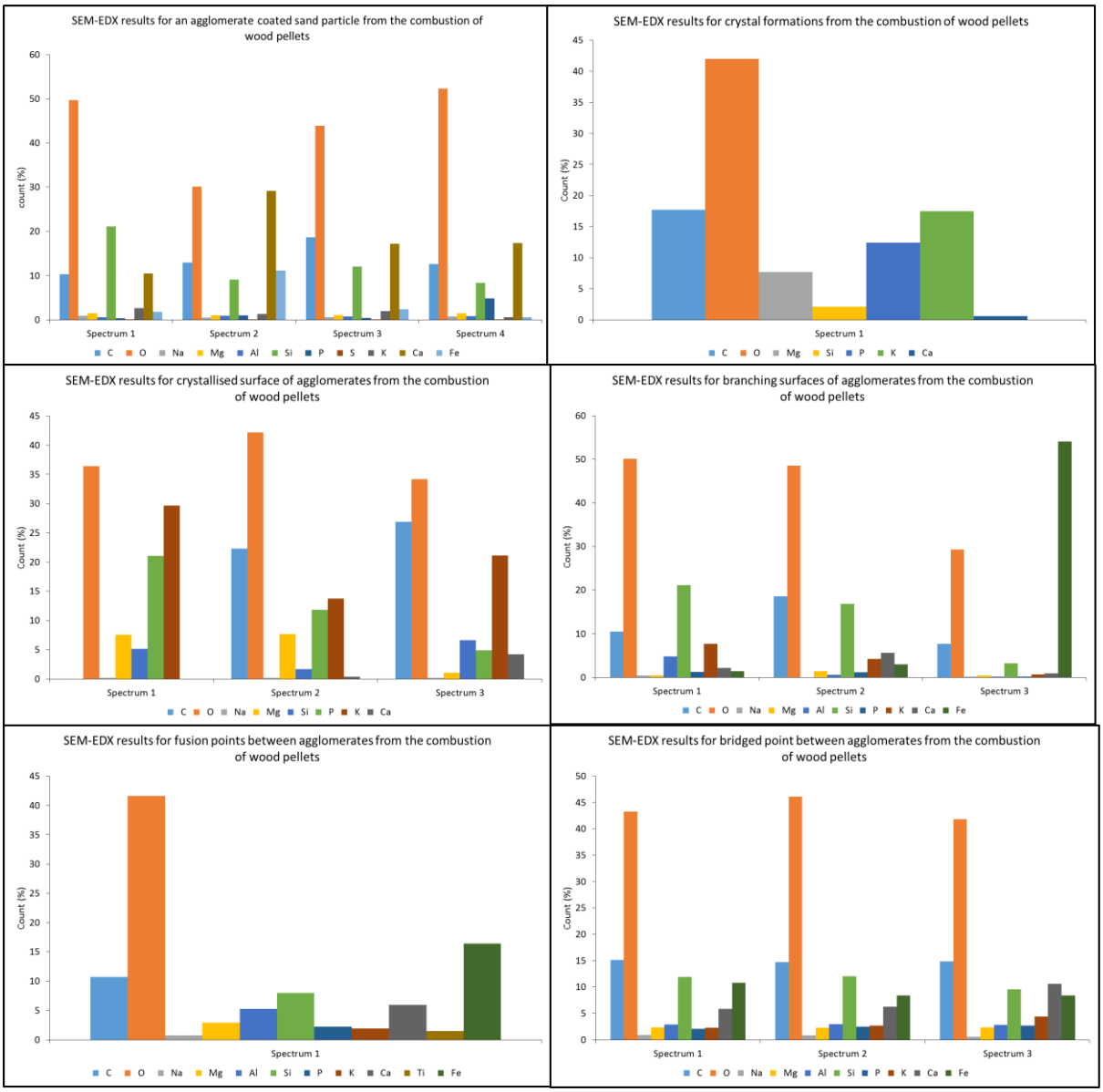

Figure 7-25 SEM-EDX results for the points of interest samples analysed and described in Figure 7-24

7.3.1.2 XRF

Figure 7-26 shows the XRF results for bed samples taken from the bed after the combustion of wood pellets with a non-uniform air distribution plate installed. The looser agglomerated material with less significant bridging components resulted in a higher proportion of sand particles making up the agglomerates with less complexes between or on the surfaces on the particles. As a result,

the XRF analysis had a high concentration of Si with lower concentrations of alkaline species such as K and Fe.

However, the alkaline species and matrices leading to the formation of the agglomerates were similar to the examples seen in previous tests. The XRF results both relate back to the fuel analysis and the data in Figure 7-24 and Figure 7-25 .

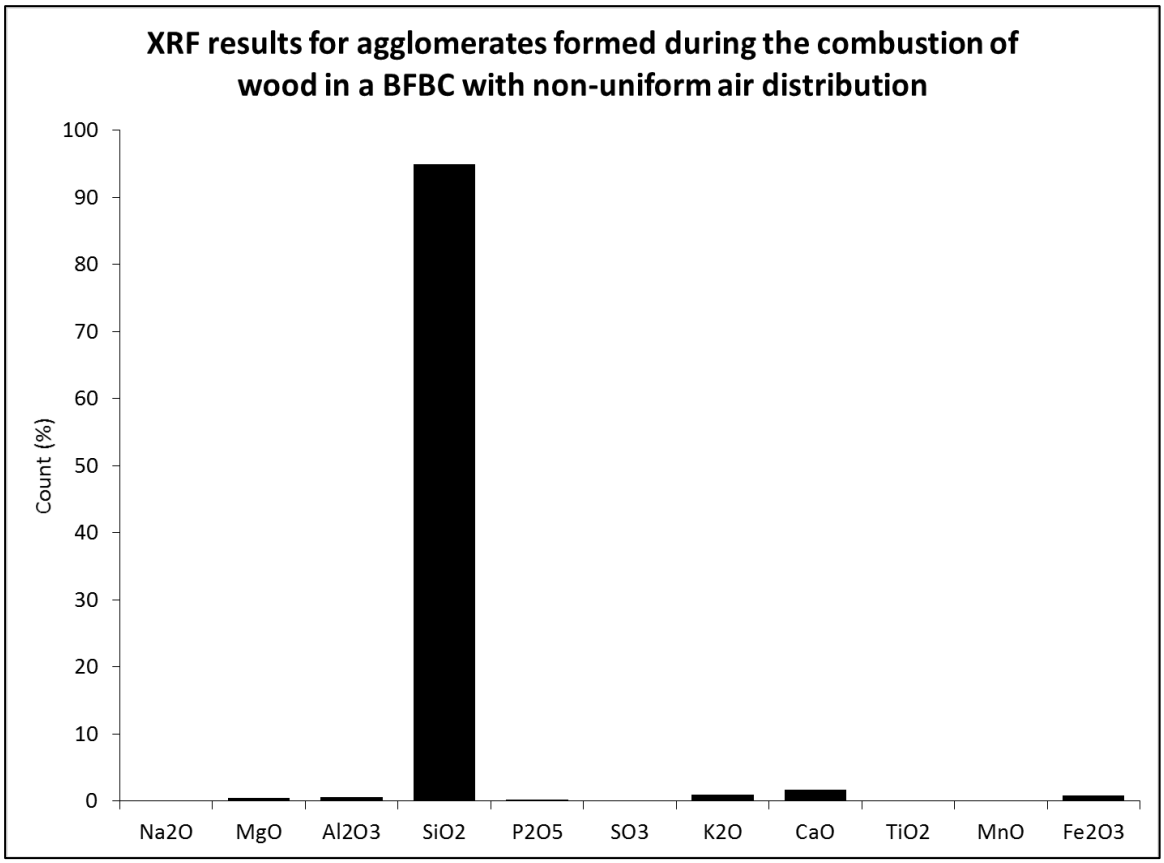

Figure 7-26 XRF analysis of bed samples taken after testing from the combustion of wood pellets in a BFBC with non-uniform air distribution

7.3.2 Peanut Pellets

Figure 7-27 shows the temperature, pressure and emissions data measured during the combustion of peanut pellets with the leakage plate installed. Point A shows the crossover of gas to solid fuel after the completion of the preheat sequence.

Immediately after point A the temperatures across the bed fluctuate, followed by a sudden decrease in bed temperatures at point B. The temperatures regain normal ranges between point B and C but with Bed A increasing to ≥950°C and then progressively decrease. At point C the bed temperature remains fairly constant at 750-850 °C but with Bed A dropping and erratically shooting up temporarily throughout the test post point C. The data shows that the combustion initially is good with stable temperatures and thus combustion of material. After point B the dip in the decrease suggests that the fuel either isn't mixing in the bed or isn't combusting. The decrease in bed A after

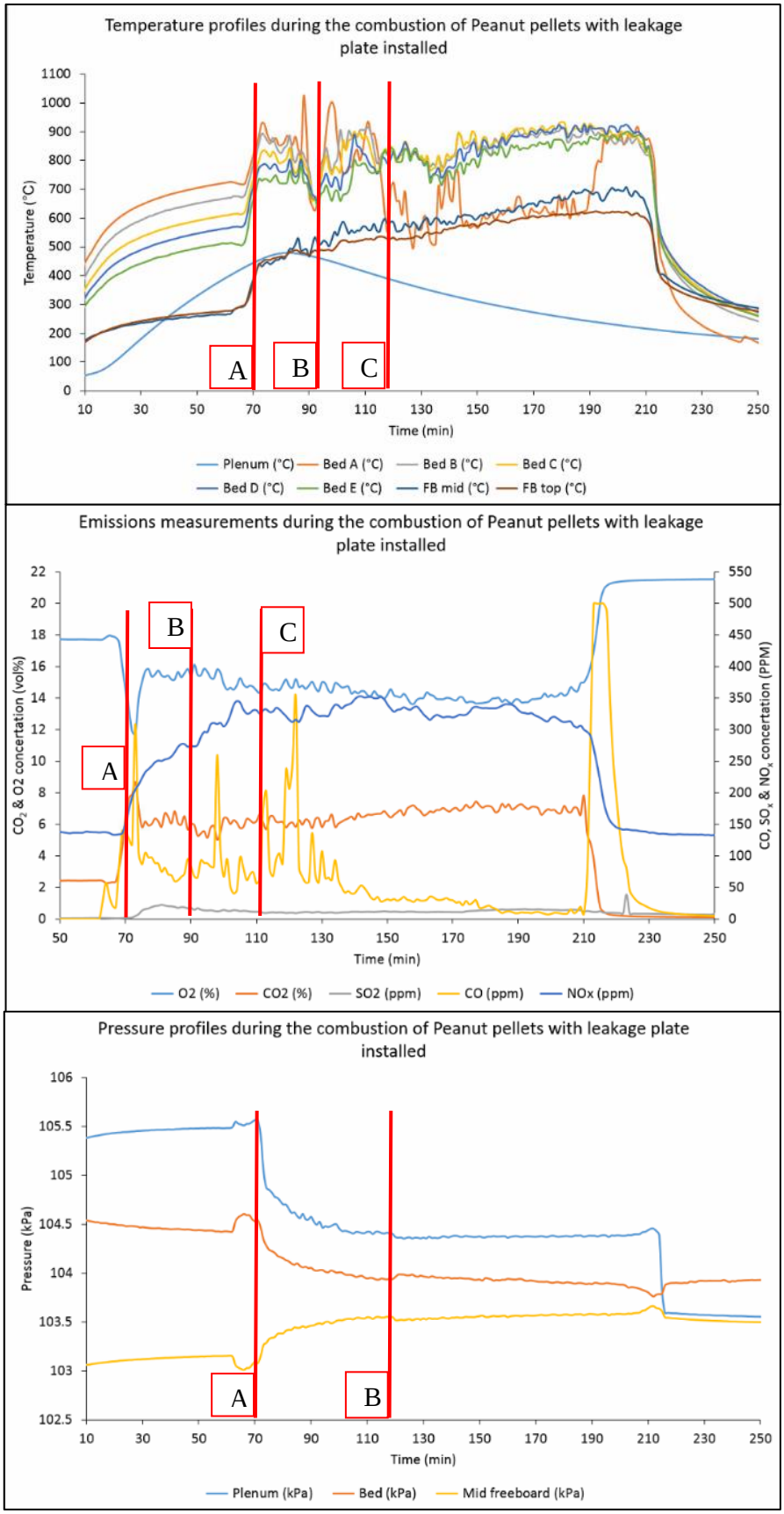

Figure 7-27 Temperature, pressure and emissions data collected during the combustion peanut pellets and defluidisation of the bed with a non-uniform air distribution plate installed

point B indicates that combustion is affected by the condition of the bed. Furthermore, after point C the fluctuations and cooling indicate poor mixing in the bed.

It was noted after this test the Bed A thermocouple lies in a position in which a channel seems to form with the onset of agglomeration in the bed. This particular point of the air flow of the leakage point and bubble caps surrounding seem to converge. Combine this with a bed decreasing in height/voidage/reduced through put of uniform air, the thermocouple measures the cooling effect seen in a defluidising bed. Therefore, this is a good indication of the onset of agglomeration.

In the emissions data, the CO spikes and drop sharply and repeatedly. This is with the bed slumping and partially defluidising and refludising temporarily. The O_2 concentration drops to a more desirable 12 vol. % however, this immediately increases to ≥15 vol. %. Air is bypassing combustion zones and hence the O_2 in the flue is higher. The increased air flow rate increases the O_2 concentration but the airflow should achieve an excess air of appx 150% whereas the measurements are closer to an excess air of 250%, in excess of normal operation. However, a reduction of airflow would result in defluidisation of the partly or completely fluidised bed. This was a serious limitation with the leakage in place.

The emissions actually move to more ideal operating conditions when agglomeration has set in, past point C. Once again, channelling and diverted air around the slumped bed and through the leakage point creates localised combustion areas. In these points high velocity air is combusted with fuel which is why the CO_2 concertation remains steady throughout. The NO emission increases with the onset of agglomerates and defluidisation, point B and beyond. The localised hotspot combustion could be forming localised environments for the formation of NO from organically bound nitrogen.

The pressure changes in the pressure graph correlate with previous findings. An increase in midfreeboard as a result of reduced bed resistance on air passage. Plenum pressure decreases as back pressure reduced. Bed pressure reduces with reduction of air in bed voids. The air is moving through the leakage point thus reducing the pressure of air at the bubble caps. This increases resistance at the bubble caps, redirecting air further to the leak. Agglomerates allow for channelling and limit the ability for the bed to fluidise again. The leakage accelerates defluidisation. The addition of dead space and limited mixing will allow for faster agglomerate formation also.

7.3.2.1 SEM-EDX

Figure 7-28 shows SEM images and Figure 7-29 shows SEM-EDX analysis conducted on samples taken from the bed after combustion of peanut pellets with the non-uniform air distribution plate

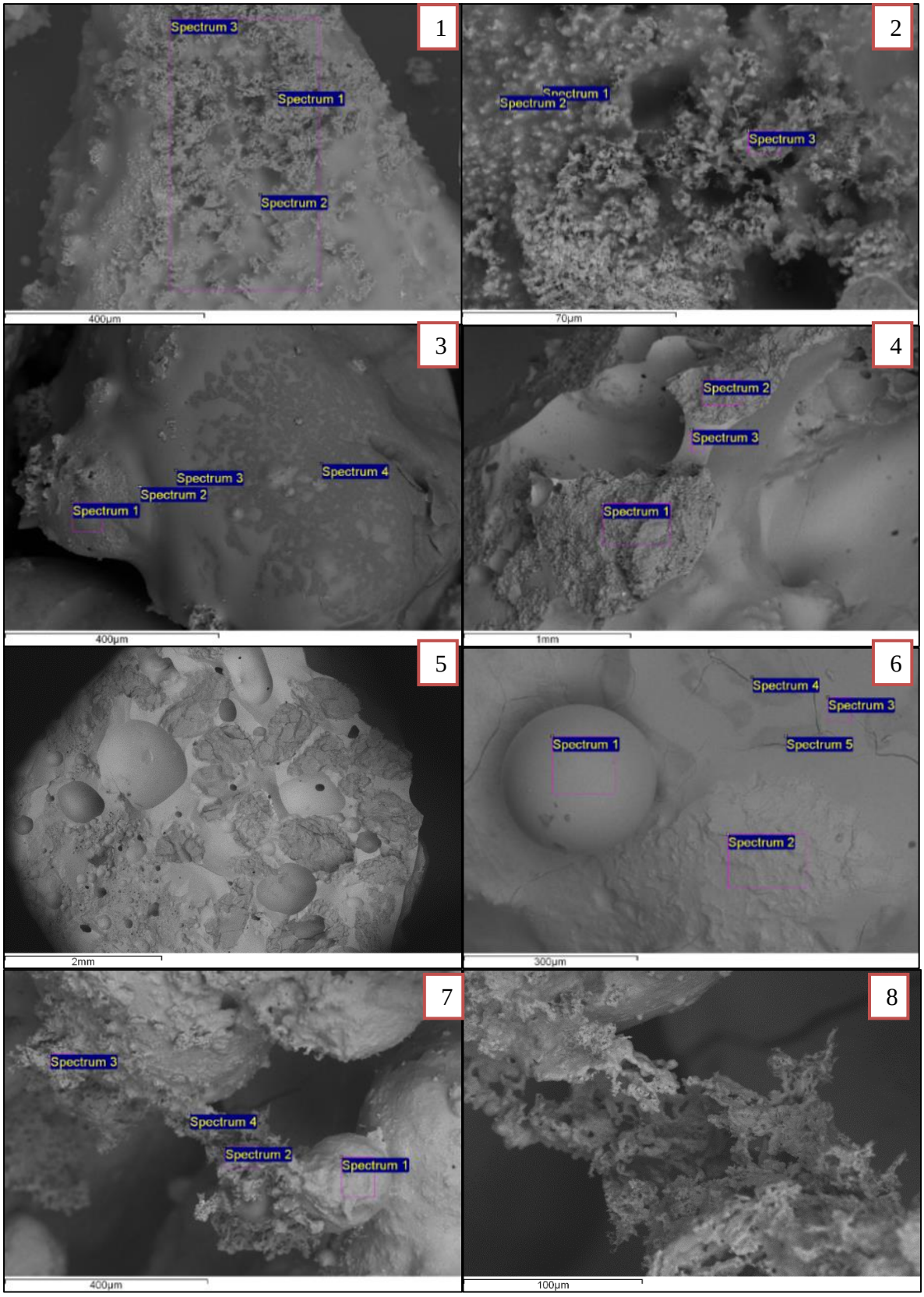

Figure 7-28 shows a series of SEM images and SEM-EDX measurement locations from point of interest for samples collected form the combustion of peanut pellets. The images are follows; 1) branching on the surface of agglomerated bed particle, 2) enhanced image of branching, 3) surface of agglomerated bed particle, 4) cross section of bridged agglomerate, 5) cross section of agglomerate, 6) surface of liquid phase agglomerate, 7) agglomerate branching, and ,8) enhanced image of branched bridging.

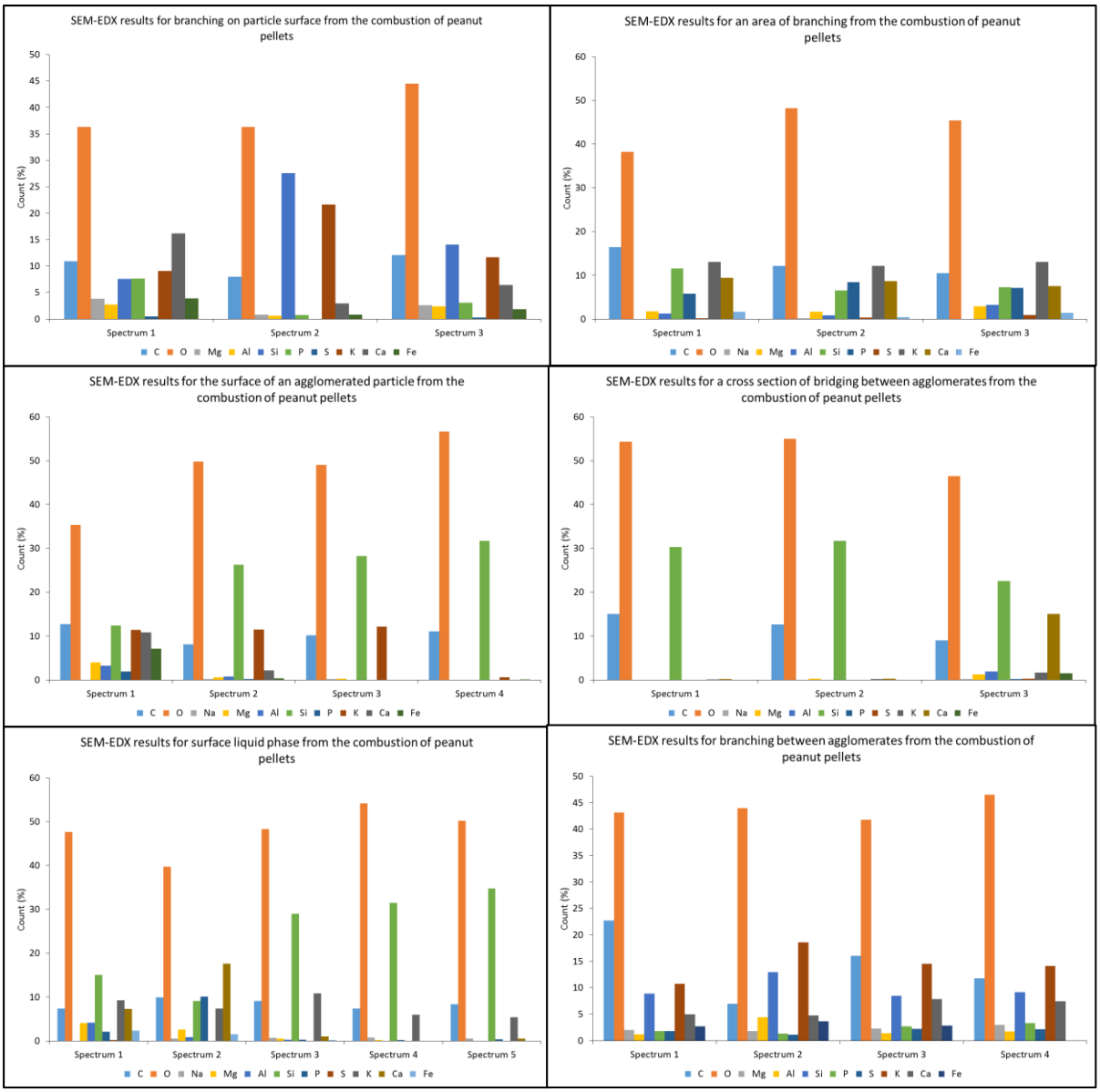

Figure 7-29 SEM-EDX results for the points of interest samples analysed and described in Figure 7-28

installed. Image 1 and image 2 show the branching found on the surface of agglomerates with image 2 focusing on particularly compact areas of agglomeration. SEM-EDX data indicates that the branching once again contains concertation of alkaline species with Fe, Si, Ca, K and P making up a majority of the material. The analysis show that there is an even distribution of Ca, K, Si and P in the different branches. The branches would once again be creating a very stable and sticky surface to adhere to other bed particles.

Image 3 shows the surface of a bed particle which has been coated in a complex which was in liquid phase and as such, left a liquid like pattern on the particle. The surface area which has the largest cover of the complex has other materials embedded in it displaying the process of adhesion the bed parties undergoes during agglomeration. The liquid phase was indicated to be primarily Si-K. When

looking at the cross section of an agglomerate (image 4), the surface data agrees with the results of image 3 but the internal bridging of the agglomerate contains high concentrations of Ca with trace amounts of K and Fe.

An abnormality found in the agglomerates of these tests were the voids within the agglomerates. This suggests the presence of gas and/or internal pressure acting upon the agglomerate. Analysis of the perimeter of such voids gave no indication of high concentrations of alkaline species compared to the surrounding eutectic complex. It was hypothesised that combustion occurring within the agglomerate cause the voids but the lack of carbonates etc. disproves this. It is more likely that the agglomerate, mixing/rolling within the bed captures gases/air, and being in a molten semi solid state simply encapsulates gases which then trapped during cooling.

Image 6 shows the surface of an agglomerate and reinforces the theory of liquid phases and the transaction to a gas phase. The bubble-like sphere in the agglomerate matrix is made up of a cluster of alkaline species; Si, Mg, Al, P, K, Ca and Fe. The heating of this particle has led to the expansion of gases within the agglomerate and hence the creating of this shape. This would account for the loss of such species in these sand previous agglomerates.

Image 7 and 8 show the branching and bridging found within the agglomerates from these tests with K and Ca indicated as to the backbone of the eutectic. These types of bridges were not found in the tests with uniform air. The agglomerates here contained a greater number of weaker structures which were preserved as a result of low velocity flows caused by the non-uniform air flow through the bed.

The agglomerate mechanism was found to be similar to that of the uniform air test, however, most significantly, weaker agglomerates and eutectic structures were able to form as a result of the poorer mixing within the non-uniform bed.

7.3.2.2 XRF

Figure 7-30 shows the results for XRF analysis of bed samples taken from the bed after the combustion of peanut pellets. As the results shows K, Fe and Al make up a majority of the species associated with agglomeration (other than Si sourced in the bed material).

This once again correlates to the analysis previously performed on the fuels and samples. Furthermore, the trends for more brittle agglomerates to form relates back to the combustion of wood pellets with a non-uniform air distributor in place.

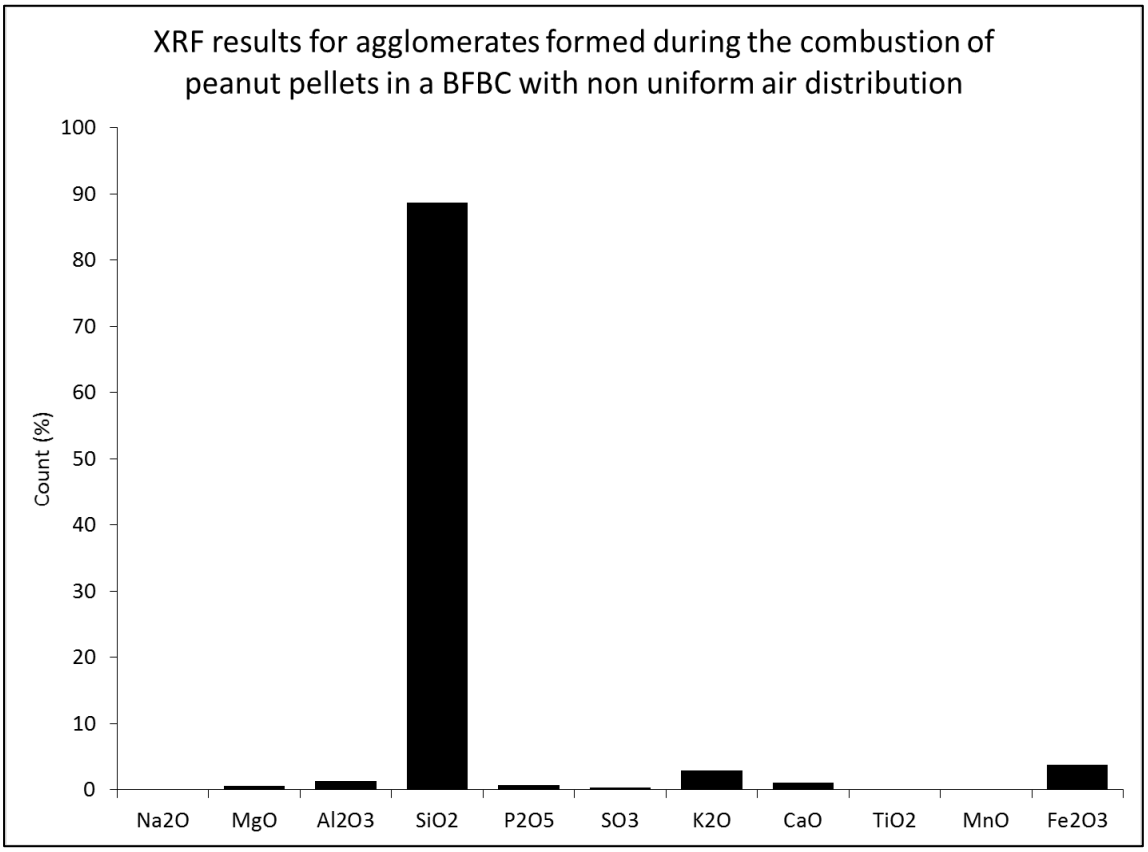

Figure 7-30 XRF analysis of agglomerated bed samples taken after testing from the combustion of peanut pellets in a BFBC with non-uniform air distribution

7.3.3 Oats Pellets

Figure 7-31 shows the temperature, pressure and emission data the combustion of oat pellets with the leakage plate installed.

The results seen here were reminiscent of the peanut tests. After pre-heat, has finished, point A, oat pellets are being combusted. Stable combustion seems to be occurring to point B by the results of the temperatures throughout the bed. However, again the pressure changes across the bed indicate degradation of the bed and reduction in mixing/fluidisation.

At point B measurements were of a similar value which in the peanut tests the bed had defluidised as the result of the formation of agglomerates. Once there was a temperature slump, point B to C, and the pressures had declined enough that it was decided that the bed was going to defluidise. A pulse of high flow air entered the bed in an attempt to both break up weak agglomerate structures and to redistribute material around the bed and into potential depleted bed areas around the leak point. This resulted in a short increase in plenum pressure, a slight increase in flue gas O_2 and a drop-in bed temperatures.

The results of this effort were bed temperatures returning to a more typical operational range and the pressure to remain steady. They didn't improve however, simply ceased degrading. Within 4-5

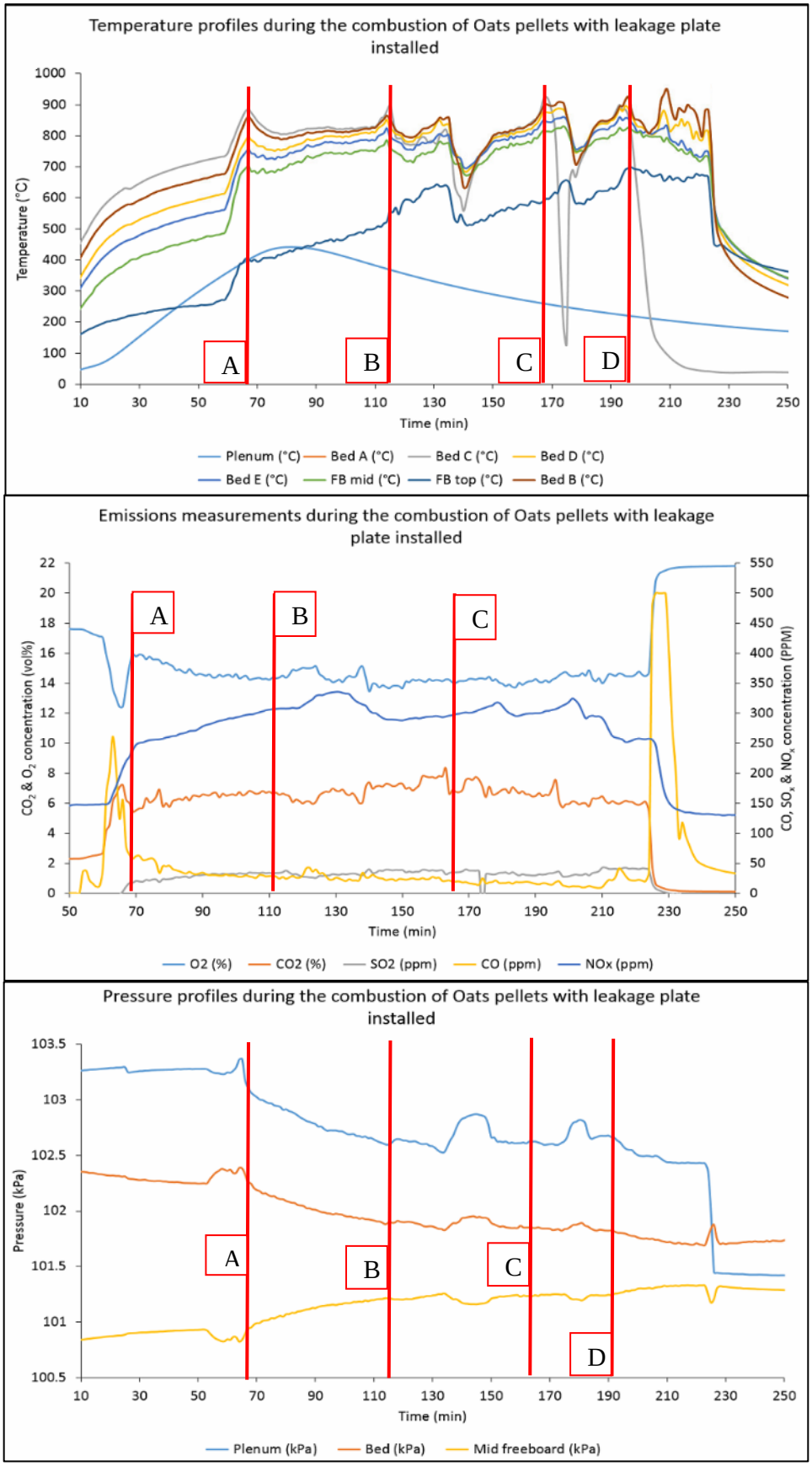

Figure 7-31 Temperature, pressure and emissions data collected during the combustion oats pellets and defluidisation of the bed with a non-uniform air distribution plate installed

minutes the bed temperatures began to spike and pressures started to decrease again. Between point C and D another pulse was attempted resulting in a temporary improvement of the bed again.

After point D temperatures, pressures and emissions indicate agglomerates are present and controlling the mixing of the bed and the combustion process. The test is therefore, ended.

The pulsing in this test was found to improve the fluidisation temporarily. However, it is more likely that redistribution of material redirected air through the bubble caps mitigating channelling air temporarily. This is why the degradation after the pulses was similar in length as it represents the time to redistribute materials and airflows across the cross section of the bed.

7.3.3.1 SEM-EDX

Figure 7-32 shows SEM images and Figure 7-33 shows SEM-EDX analysis conducted on samples taken from the bed after combustion of oat pellets with the non-uniform air distribution plate was installed.

The way in which agglomerates formed as a result of oat pellets combusting in these tests compared to the uniform test is very different to that of the miscanthus and peanut tests. Image 1 and 2 show bed particles which have been coated in an agglomerate complex. The shape and structure of the agglomerates resembles the ash analysed in the fuel characterisation Chapter. It is possible here to see the ash, which hasn't melted, but instead formed low melting eutectics within the ash, which has then adhered to the surface of the bed particles. SEM-EDX suggests that the complex is made up of Si-P-K. The measured concentrations show relevance to the concentrations measured in the initial ashes. This further suggests that the ashes haven't melted entirely but instead have a partial liquid phase in which alkali species haven't distributed.

Image 3 emphasises the type of structure and the fibrous ash nature of the agglomerate. The particles are being held together by ash particles in a semi liquid phase and the depth of the agglomerate within and on the surface of the bed particles is minimal.

Image 4 shows the surface of the coated ash particle. Here the partially meted agglomerate can be seen and the onset of small branching regions. As the test was very short it is likely that the period of combustion wasn't extensive enough to melt the ash and thus the agglomerate formation didn't occur as previously seen. Instead a loosely packed cluster of material has adhered together with ash particles. It is wrong to call these clusters of materials agglomerate in the conventional sense. The results here instead suggest the early stages of agglomeration for oat pellets.

Further to this point, image 5 shows a bridge forming between particles. The outline of the ash particles can be seen and is partially consumed with a liquid phase. The SEM-EDX results for image 5 show lower concentrations of lighter alkaline species than the flakey ashed area. This

coincides with the theory that there was a partial liquid phase as a result of increased temperature. Hence the lighter Na and P concertation's are less in the bridge after being lost to a gas phase.

The loose/weak type of structures that led to the defluidisation of the bed didn't occur with the uniform bed as the mixing/air flow broke up the structures. However, with the air flow altered as it was, these types of structures were able to propagate significantly enough to impede the bed and fluidisation.

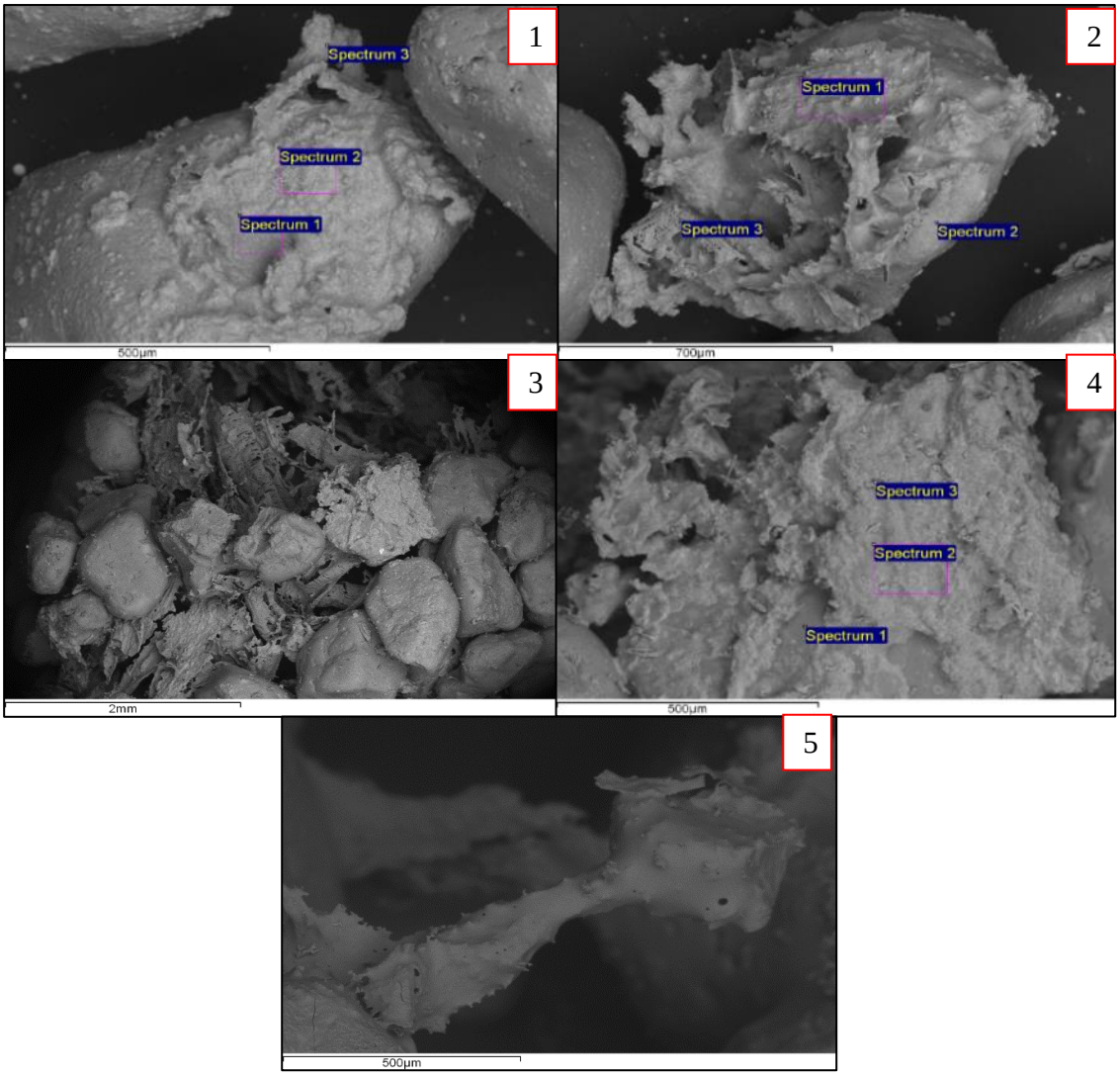

Figure 7-32 shows a series of SEM images and SEM-EDX measurement locations from point of interest for samples collected form the combustion of oat pellets. The images are follows; 1) bed particles coated in agglomerate complex, 2) bed particle bonded to ash, 3) fibrous agglomerate structure, 4) surface of agglomerate, and, agglomerate bridging point.

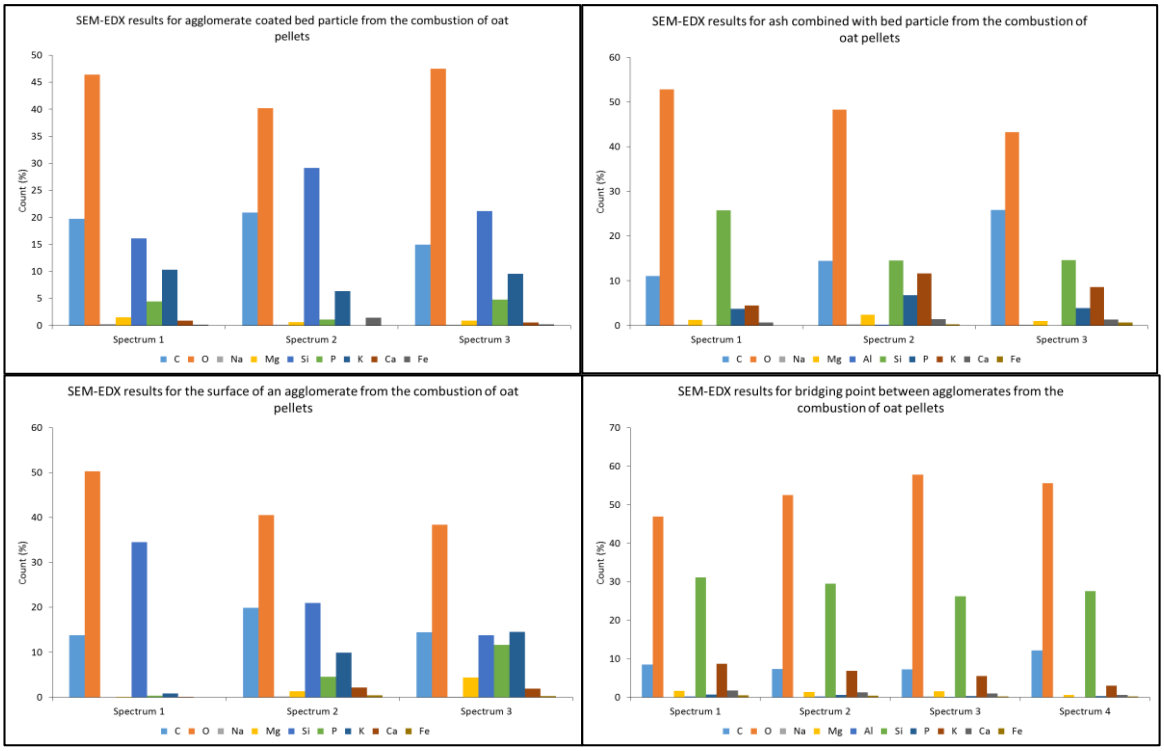

Figure 7-33 SEM-EDX results for the points of interest samples analysed and described in Figure 7-32

7.3.3.2 XRF

Figure 7-34 shows the XRF results of a bed sample taken after the combustion of oat pellets. The XRF results correlate with the species identified by the SEM-EDX analysis in the previous descriptions.

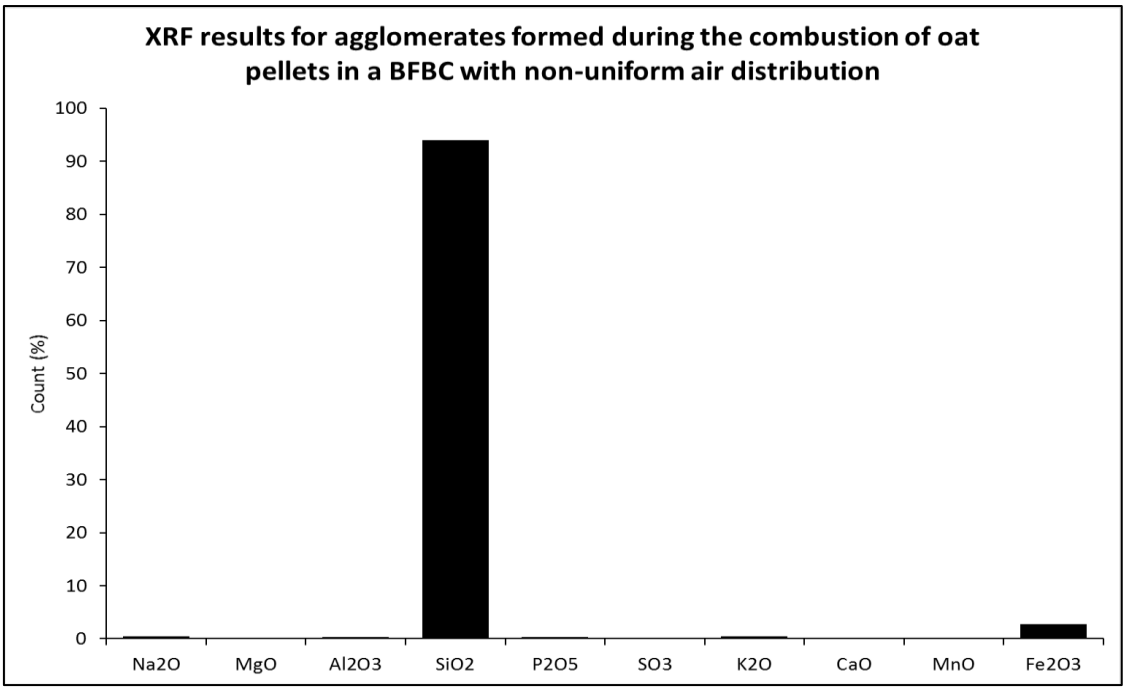

Figure 7-34 XRF analysis of agglomerated bed samples taken after testing from the combustion of oat pellets in a BFBC with non-uniform air distribution

The results show that during the combustion of oat pellets with a non-uniform bed the onset of agglomerate formation was dominated by Fe and Si alkaline groups. Furthermore, Na and K were lost in the gas phase indicating elevated temperatures as well as their potential initial impact on the formation of agglomerates. This was influenced partially by the air flow and was seen in the uniform tests to occur in a slightly different mechanism.

7.3.4 Straw Pellets

Figure 7-35 shows the temperature, pressure and emission measurements made during the combustion of straw pellets with the non-uniform plate installed.

The defluidisation time while combusting straw pellets was the shortest biomass test (10 minutes max) and thus was repeated to check validity of the results. The same result was found in the repeat.

At point A in Figure 7-35, the pre-heat sequence finished and gas was switched off for straw pellets as the primary method of combustion. The bed temperatures immediately reach 750-850°C as intended and rig pressure initially indicate stable conditions in the bed and flame. However, within 8-10 minutes the bed temperatures sharply decrease to a range of 500-700°C. Additionally, the bed pressures reduce to values indicating no resistance by the bed. Throughout this period A to B, the CO and CO_2 emissions fluctuate. At point A to B there were significant problems in the bed.

Point B to C shows on all graphs, sudden and catastrophic failure of the bed. The bed temperatures spike and with bed A reaching ≥1180°C, which would allow for sintering. Bed pressure remain at levels indicating little bed fluidisation/mixing. CO emissions fluctuated and fell between 100-500 ppm with O_2 fluctuating from 14 to 21 vol.%.

The bed agglomerated within minutes of the fuel entering the bed. As the emissions indicate, combustion wasn't steady and the presence of variable CO indicate localised combustion with the presence of reducing environments. When CO fluctuates in the extreme and O_2 reaches atmospheric concertation's, it is assumed air is passing through the bed without interacting with fuel in the combustion zones. This can only happen through the designed leakage point.

With air bypassing combustion zones the fuel built up under the feeder point with poor mixing within the bed. This is the reason for the temperature spike. It is likely that directly under the feeder was ≥1200 °C as the thermocouples were centred to the bed and thus the fuel would have spilled over in a pile to generate the measured temperatures.

The early and significant onset of agglomeration is evident by the pressure measurements. As soon as the temperatures slump there is and excessive pressure measurement to accompany them. This shows that the air isn't fluidising the bed and is likely moving primarily through the leak point. The

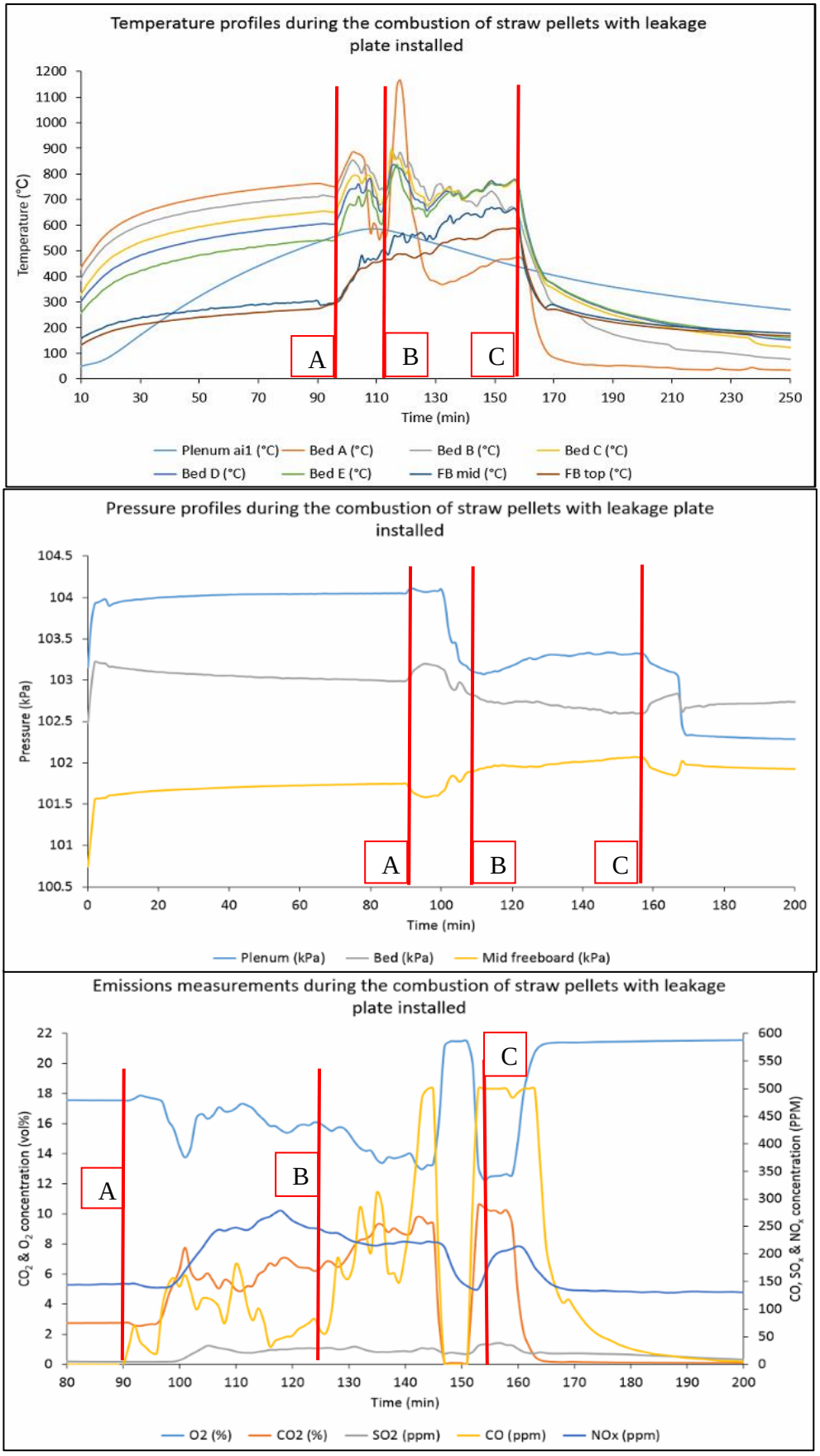

Figure 7-35 Temperature, pressure and emissions data collected during the combustion straw pellets and defluidisation of the bed with a non-uniform air distribution plate installed

fuel is known to agglomerate fast and aggressively as seen in the uniform plate tests and fuel characterisation. The fast formation of agglomerates, even if weak initially in the test, was enough to interfere with mixing the bed material and hence allow the leak point to reduce in bed height. This then resulted in air reduction in bubble caps and for the agglomeration to accelerate whilst temperatures increased which will have created the onset of further structures within the bed.

This all culminated to the failure of the bed speedily and aggressively. The agglomerates found in the bed were large, hardened and present throughout the bed apart from around the leak point.

7.3.4.1 SEM-EDX

Figure 7-36 shows SEM images and Figure 7-37 shows SEM-EDX analysis conducted on samples taken from the bed after combustion of straw pellets with the non-uniform air distribution plate installed.

The agglomerates found from these tests were much more relatable to those in the uniform air test with straw pellets. Image 1 and 2 show the surface of the agglomerates and the coating of sand particles with thick alkaline eutectic layers dominated by Si and K.

Furthermore, to the similarities found, image 3 shows the embedding of sand particles with agglomerates which have been made up of a liquid phase impregnating sand particle pores. K and Si are the major constituents of the structures. Image 4 shows the surface of a bridging point between agglomerates in which large concertation's of Fe were found. This is similar to the mechanisms found in the uniform air test bridging.

Whilst the branching seen in image 5 is reminiscent of the results previously discussed, with SEM-EDX showing clumping of alkaline species, the formations shown in image 6 also occurred. Branching occurs from particles moving of the sticky surfaces of the agglomerate. However, the structures in image 6 contains clustering/branching points alongside molten liquid, bubbled phases which are in many cases hollow. The strength of these structures is weak and brittle. As a result of the immobilised bed/ poor mixing as a consequence of the non-uniform plate, these areas seem to have melted/entered a liquid phase instead of adhering to a bed particle and thus propagating the agglomerates. Instead a weaker structure is formed with more spaces between particles and more solid, smaller concentrated agglomerates (such as image 3).

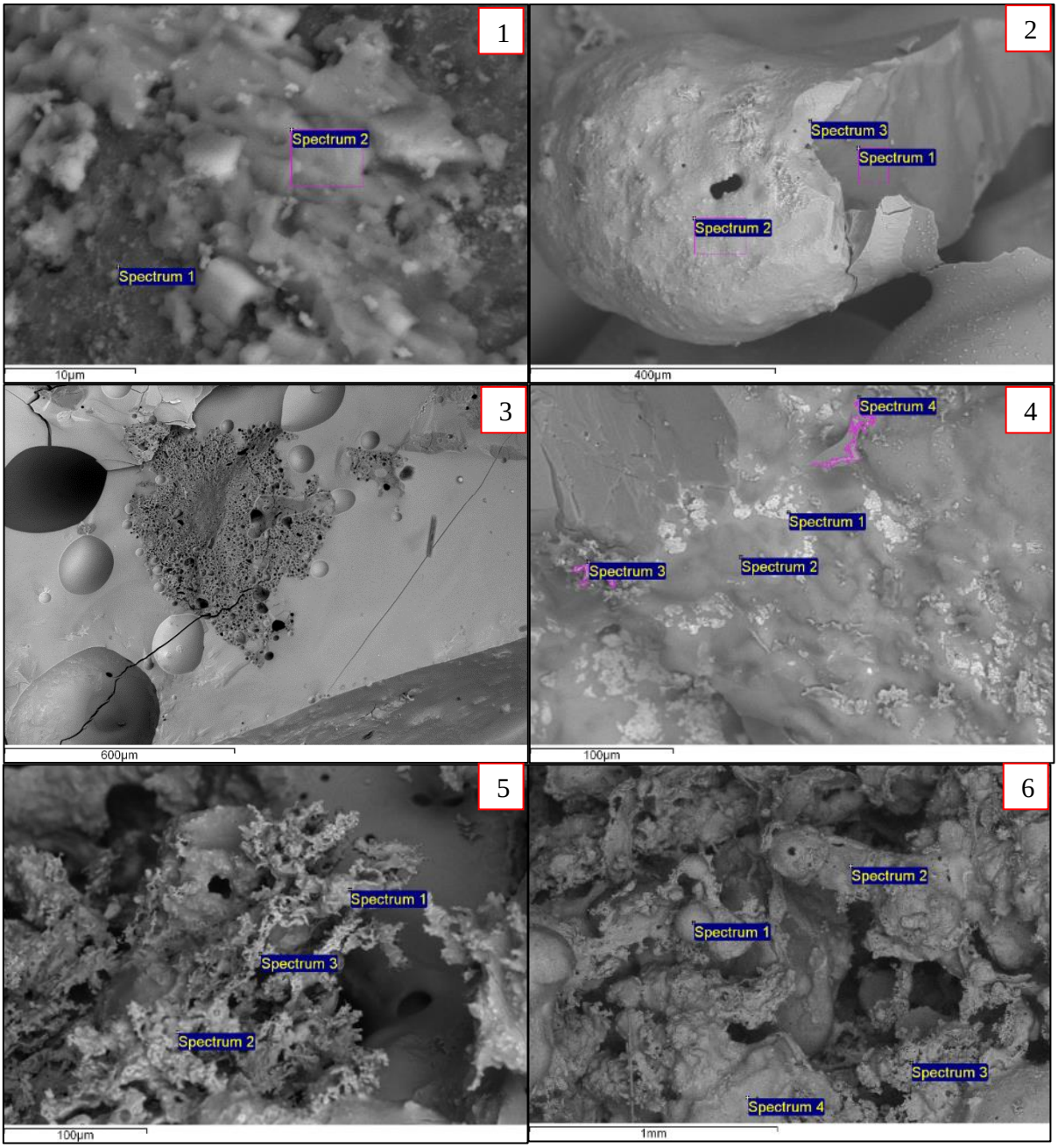

Figure 7-36 shows a series of SEM images and SEM-EDX measurement locations from point of interest for samples collected form the combustion of straw pellets. The images are follows; 1) enhanced area of agglomerated surface, 2) break away section of agglomerated bed particle, 3) cross section of agglomerate, 4) surface of fused area between agglomerates, 5) branching on surface of agglomerate, and, 6) complex structures between agglomerates.

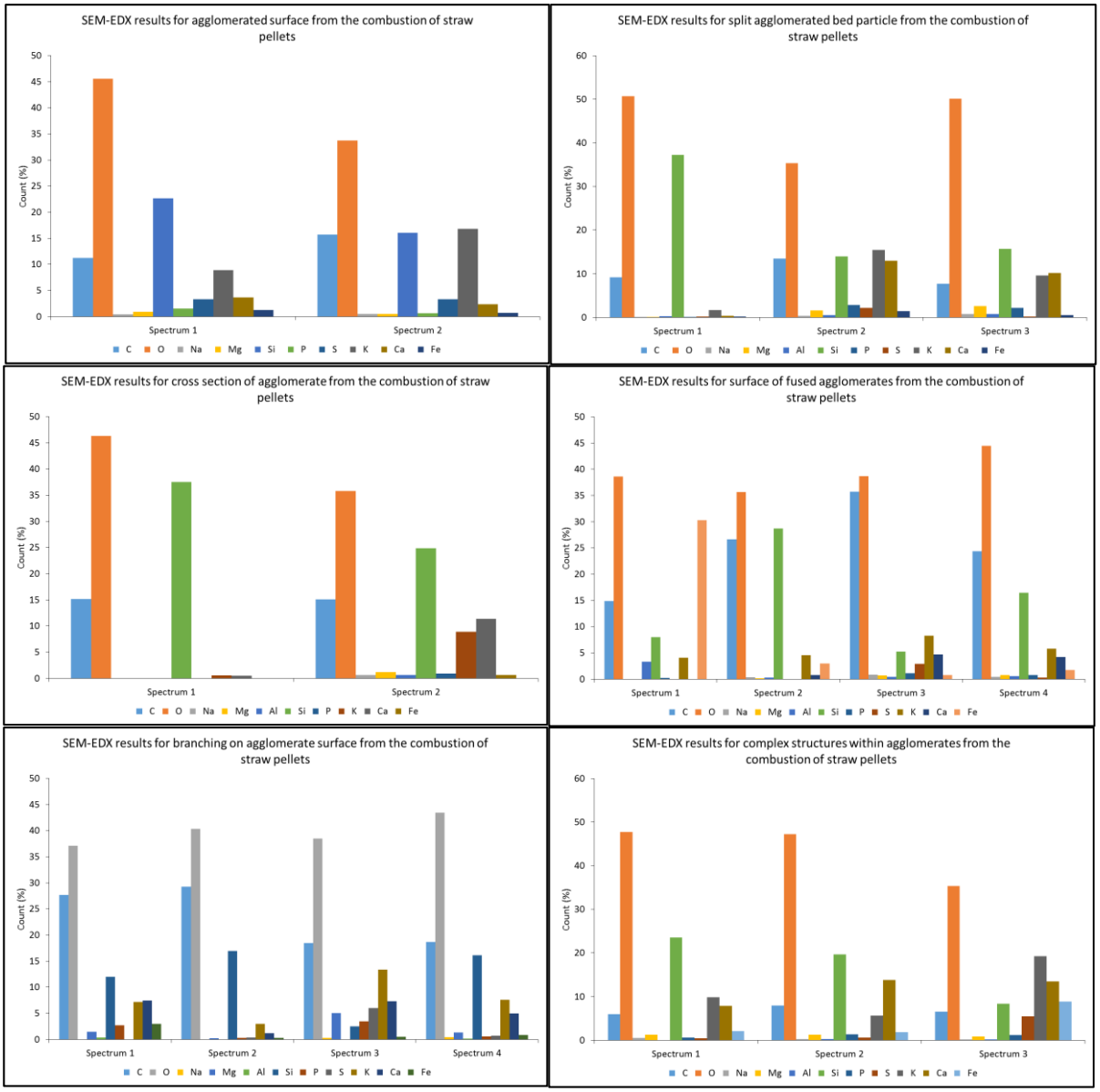

Figure 7-37 SEM-EDX results for the points of interest samples analysed and described in Figure 7-36

7.3.4.2 XRF

Figure 7-38 shows the XRF results of bed samples taken after the combustion of straw pellets in a non-uniform air distributed system. The data correlates with the results of the SEM-EDX data.

Straw pellets were shown in Chapter 4 to have high levels of K (6-26%), Ca (4-76%) and P (21-44%) which relates to the higher concentrations measured in XRF analysis of bed samples. The data for straw pellet samples further adds evidence to the importance of K, Fe, Ca and in some cases P to the formation of agglomerates in fluidised beds.

The XRF analysis shows fluctuation in the analytes found within the samples taken from the bed. The samples were taken from different regions in the bed but indicates that areas experienced different localised fluidisation and localised combustion and as such different concentrations of agglomerate formed. Alternatively, this could be an indication of the variability in chemical and physical makeup of the pellets and its impact on agglomerate formation.

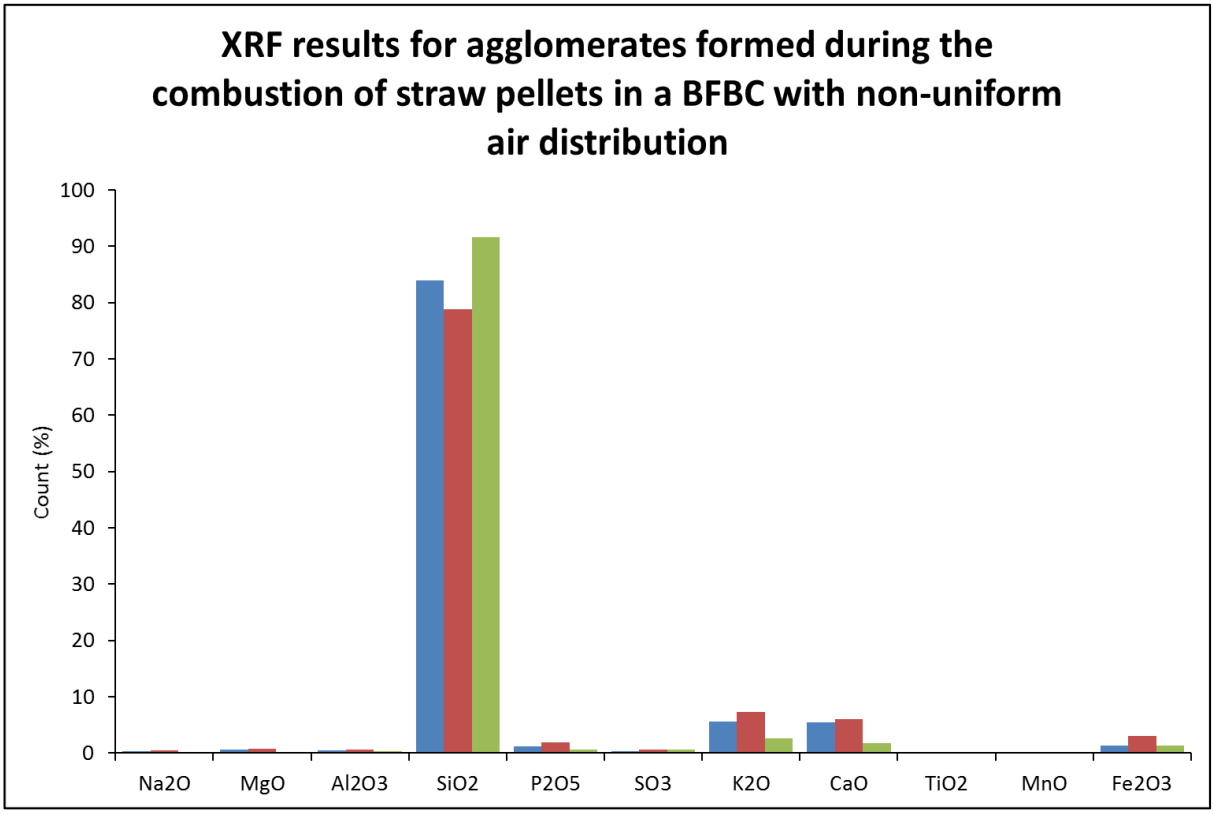

Figure 7-38 XRF analysis of agglomerated bed samples taken after testing from the combustion of straw pellets in a FBC with non-uniform air distribution

7.3.5 Miscanthus Pellets

Figure 7-39 shows the temperature, pressure and emission measurements made during the combustion of Miscanthus pellets with the non-uniform plate installed.

Miscanthus is similar to straw as previously described and for this reason it was assumed that it would react similarly in the rig as straw pellets. It was found that the Miscanthus pellets defluidised the bed slower than straw pellets (10 minutes difference).

Once the pre-heat period had finished and gas was replaced by miscanthus pellets the bed temperatures started to fluctuate, as shown by period A to B. At point B Bed A temperatures spikes to ≥1100°C and then fall to approx. 550°C. Between point B and C bed temperatures A fluctuates by approx. 250°C. These sudden changes are the result of the bed slumping and bed material movement stalling. The bed wasn't completely defluidised in this period and so it is likely that low air moment broke through the bed and caused localised mixing. However, at point C Bed A

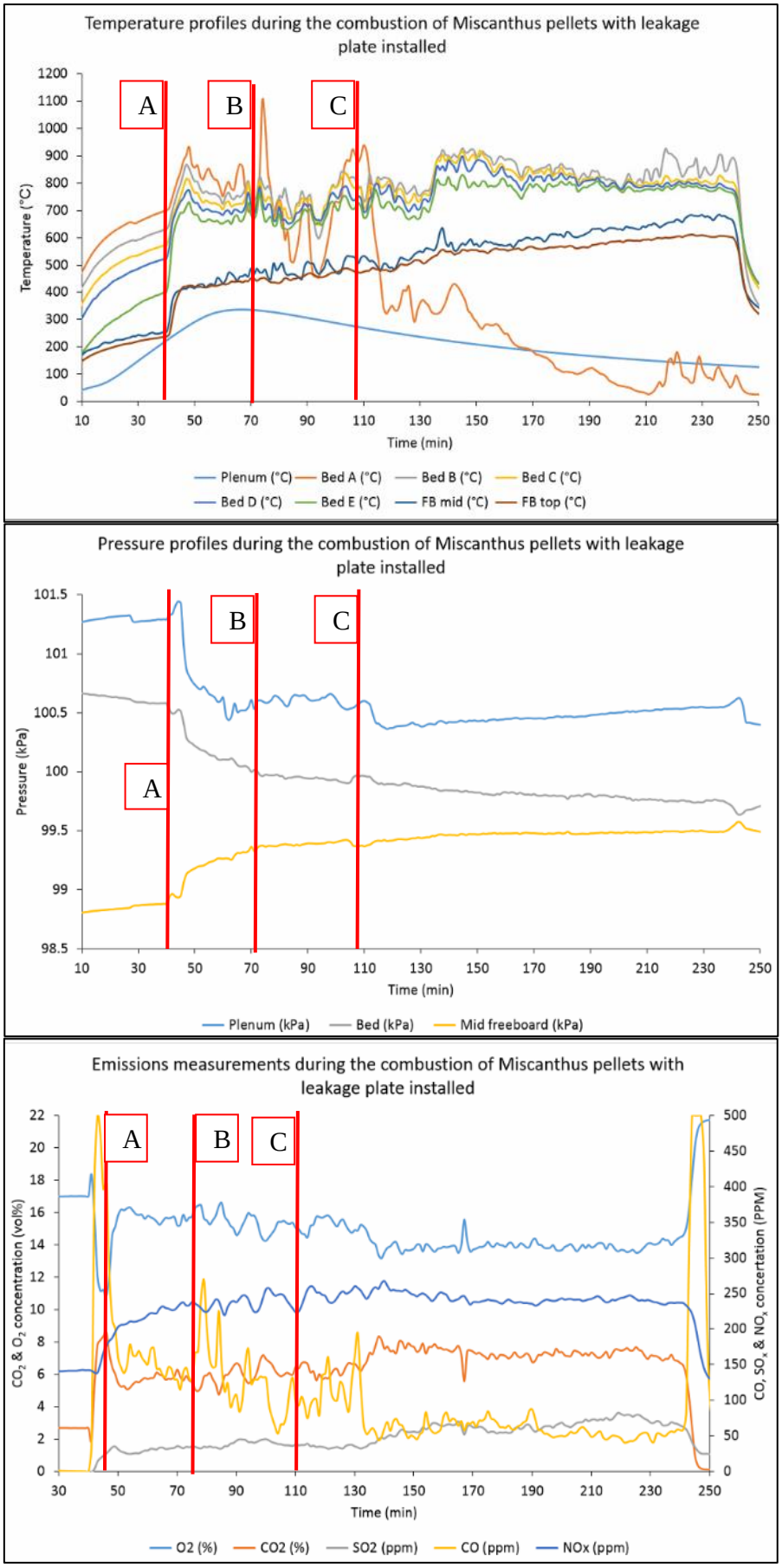

Figure 7-39 Temperature, pressure and emissions data collected during the combustion Miscanthus pellets and defluidisation of the bed with a non-uniform air distribution plate installed

temperatures plummets to ≤300°C and remains there. The other bed temperatures remain at ≥700 °C. The fuel is falling into the void created by the leak at this time and combusting fuel at a constant rate which is the reason for the constant temperature. The bed isn't uniformly heated and the fuel isn't mixing in. Instead the fuel is combusting near the thermocouple locations, and thus non-representative temperatures of the bed as a whole.

The pressure reading from this test are very similar to that of previous tests in which the bed has agglomerated and defluidised with the leak in place. Point A shows the end of the pre-heat and the immediate collapse in ideal pressures. The pressures changes at point B to C coincide with the temperature changes seen in the bed. This suggests a change in the mixing in the bed. When the bed mixing fluctuates, the temperature fluctuate dramatically. It is with these fluctuations in pressure that the air is changed in flow through the leak and bubble caps. As the leak point fills with falling material the pressure returns to more stable conditions (not ideal) and as a result the returned air flow in the bubble caps causes better mixing, increasing distribution and thus temperatures return to more normal operational ranges. Once the leak loses material and air flow through the bubble caps have less flow and hence poor mixing etc. resulting in temperature drops. When the bed completely defluidises with the presence of extensive agglomeration at point C the Bed A temperature fell and the pressures indicate little if any flow resistance across the bed.

The emissions data also coincide with the sudden onset of poor mixing and formation of agglomerates in the bed. After preheat (point A), the emission concentrations begin to settle to stable combustion ranges. However, at point B, when the bed is clearly destabilised and flow/mixing is impeded the CO emissions reflect the changes in the bed with fluctuations and increased in concentration to ≥250ppm. All other emissions fluctuate with the changes seen in the pressure and temperature measurements. They become stable when defluidisation and agglomeration have set in due to channelling

7.3.5.1 SEM-EDX

Figure 7-40 shows four SEM images and Figure 7-41 shows SEM-EDX analysis conducted on samples taken from the bed after combustion of miscanthus pellets with the non-uniform air distribution plate installed.

Agglomerates from the Miscanthus tests presented a collection of individual agglomerating phenomena which has been seen in variations in other tests.

Image 1 shows an agglomerated bed particle and the subsequent attachments of smaller particles and materials to the sticky surface. The SEM-EDX data indicates that the complex is primarily Si-K and thus the surface is expected to be sticky and adhesive.

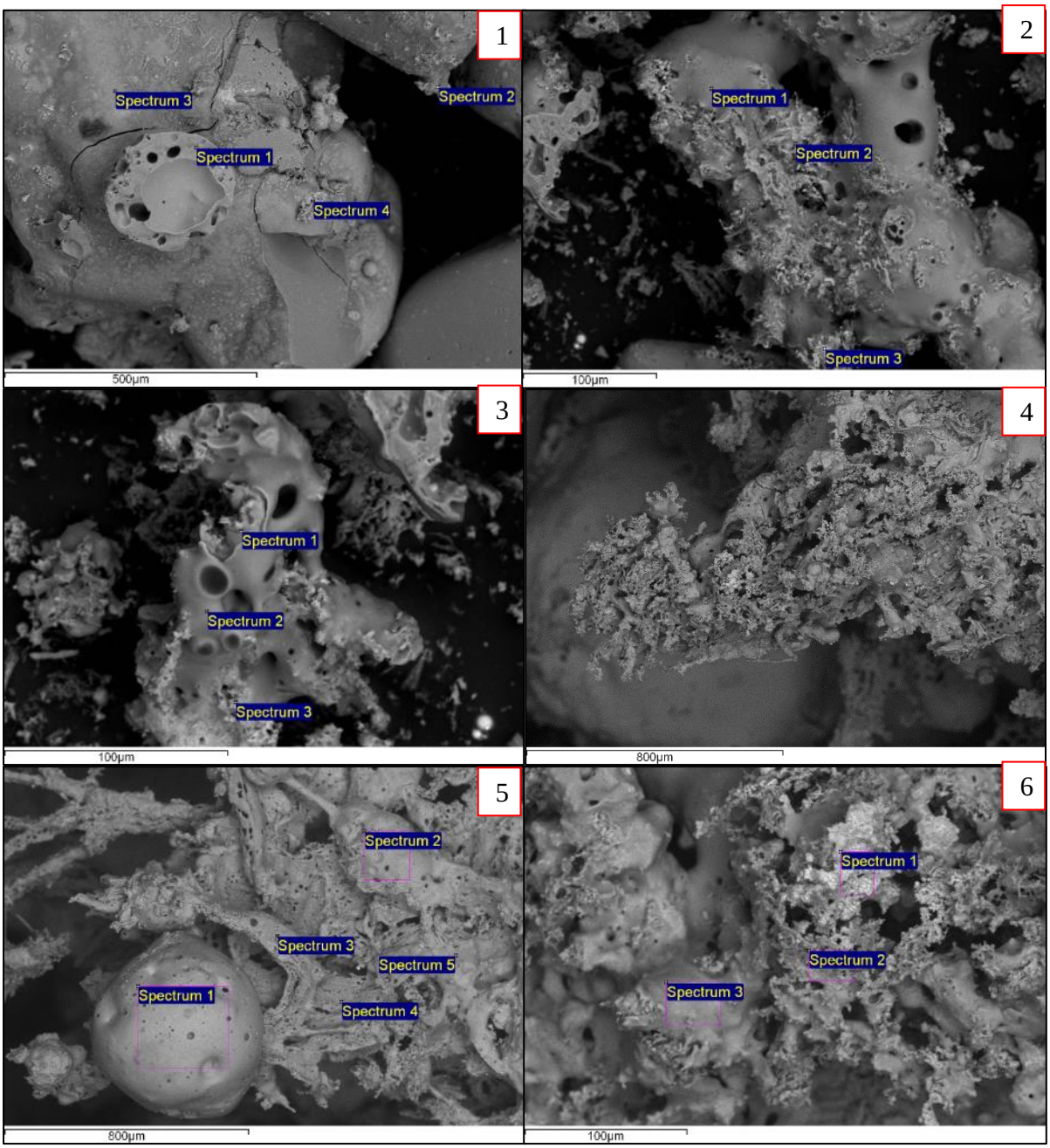

Figure 7-40 shows a series of SEM images and SEM-EDX measurement locations from point of interest for samples collected form the combustion of straw pellets. The images are follows; 1) agglomerate and cross section, 2) branching on molten agglomerate area, 3) surface of agglomerate, 4) branching to bridging mechanism, 5) liquid agglomerate branch like complex, and, 6) branching on agglomerate surface

Image 2 shows branching embedded on a series of bridges made up of an ash molten phase. The results here correlate with the findings of previous analysis. The molten regions analysed have low concentrations of species except Si-K. Whereas, the branched areas contain clusters of species. It is reasonable to assume that when the eutectic is heated sufficiently to enter the liquid phase, which lower temperatures species are lost to the gas phase.

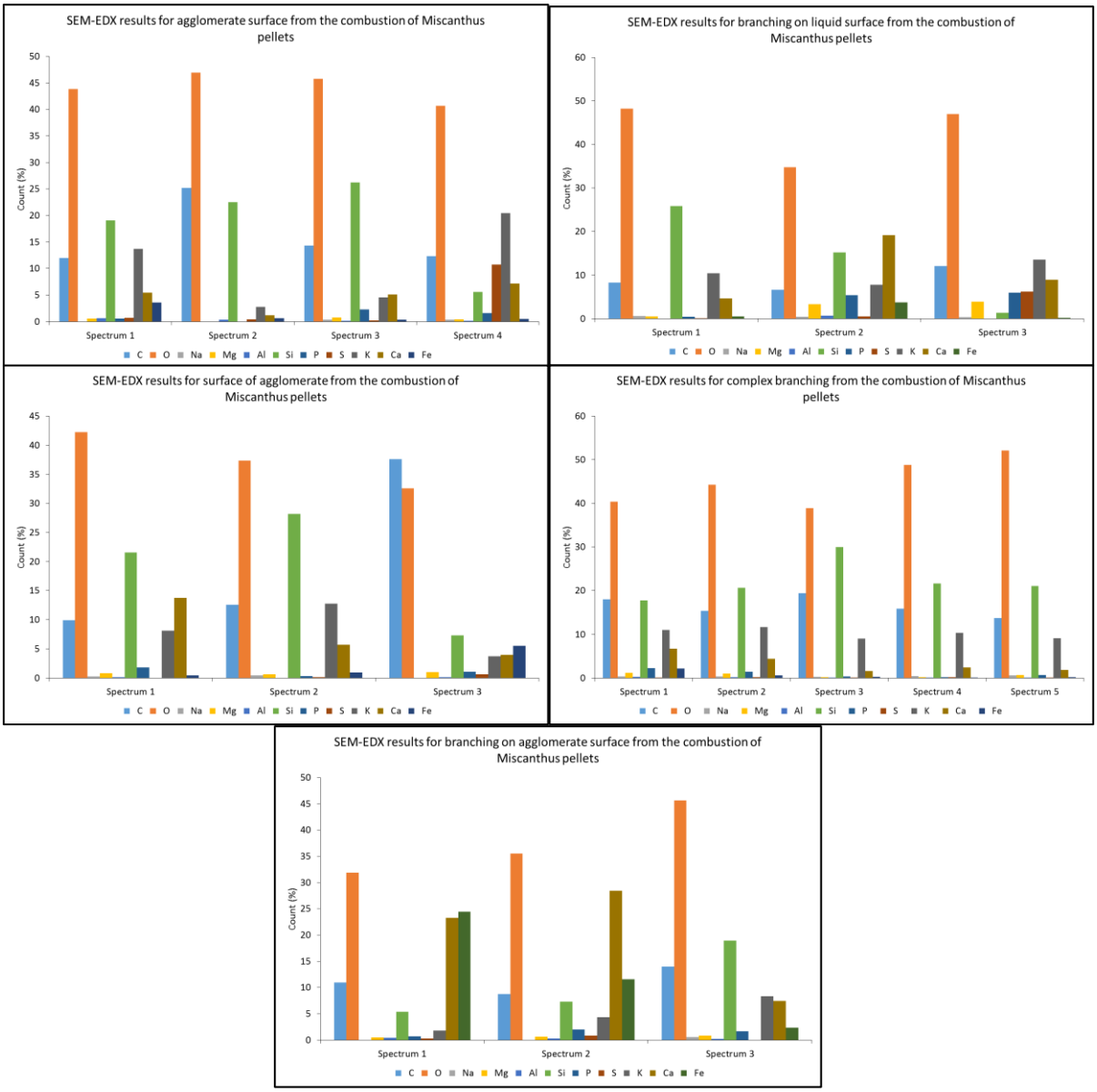

Figure 7-41 SEM-EDX results for the points of interest samples analysed and described in Figure 7-40

Image 3 shows the surface of a bed particle being engulfed by a liquid phase eutectic made up primarily of Si, Ca and K. The particles have an ash particle adhered to it and has thus become immobilised. Localised heating or poor mixing within the agglomerated region has led to a temperature increases and thus the eutectic has formed a liquid phase.

Image 4 shows extensive branching coming from a bed particle. The structure is seen to make up of a series of extending branches. Within the core of the extension can be seen a molten region, yet the surface is made up of non-liquid phase eutectics. The branching has formed when a liquid phase has adhered to branched regions and ash within the bed and thus the structure has grown. This was not found in the uniform bed tests because the lower air flow rates here allow for the structure to

exist. Any vigorous mixing would likely break up these structures. Therefore, there is an effect here of the propagation of agglomerates as a result of poor air flow/mixing.

Image 5 and 6 show another example of branching and extensive web like structure within the agglomerated masses which didn't exists with the uniform plate. The structures in image 5 contain concentrations of Si-K-Ca. The branched effect seen in image 6 also contains Si-K-Ca but with the addition of other alkaline species. It is theorised that the web structure is a result of branches extended as particles moving against the branches adhere and then break free, but in doing so extend the branches in a direction. By repeating this mechanism, the formation of the weak web structure builds up. Once again however, this type of structure wasn't found in the uniform tests. The structure didn't exist with good mixing and thus emphasises the effect of poor mixing on agglomeration propagation.

7.3.5.2 XRF

Figure 7-42 shows the XRF results of agglomerated bed sample taken after the combustion of miscanthus pellets. Whereas with previous XRF analysis of bed samples taken after the combustion of biomass with a non-uniform air distributor in place, the concentration of species other than Si are higher.

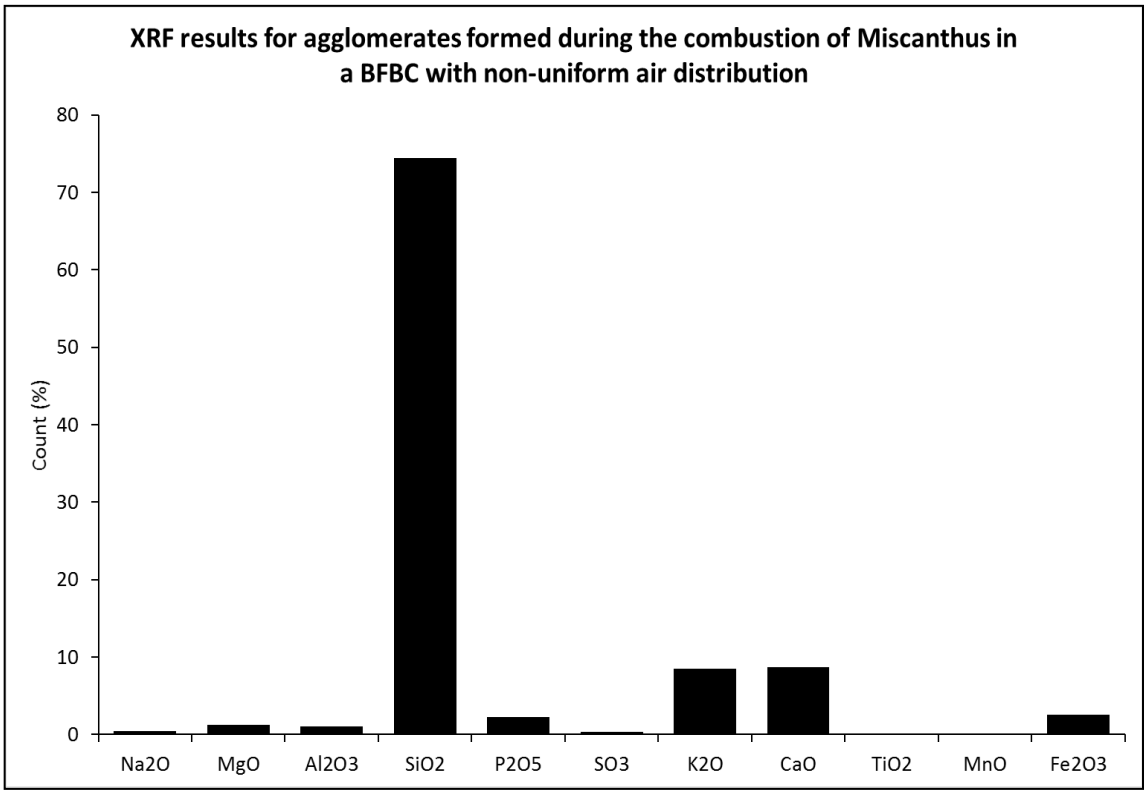

Figure 7-42 XRF analysis of bed samples taken after testing from the combustion of miscanthus pellets in a BFBC with non-uniform air distribution

Alkaline species K, Ca and Fe were again seen to be a majority contributor to the formation of agglomerates. This agrees with previous fuel characterisation and SEM-EDX analysis. Furthermore, the XRF analysis shows how the reduced fluidisation in the bed leads to the increased formation of more brittle agglomerates made up of species seen less in more strengthened agglomerates.

7.4 Discussion

The following section will discuss the performance of the two plates, the performance of the biomasses in these systems by evaluating agglomeration mechanisms and tests performance and finally conclude on findings to solutions to problems found during the previously described tests.

7.4.1 Fuel Performance

A key objective of this investigation was the applicability of biomass fuels as a combustion fuel in fluidised bed combustors at industrial scale and thus their implication and full scale. A large number of tests have been shown in previous sections with variable success in sustained operation. The following data in Table 7-1is a summary of the outcomes produced during stable operation of each biomass.

The data summarised in Table 7-1 illustrates the differences in combustion characteristics between the fuels, the effect of the distribution plates on the combustion environment and demonstrates the variability of operation when combusting biomass fuels.

As the data illustrates, there was variability between the temperatures achieved in the bed, above the bed and at the furnace exit. This was a direct result of the combustibility of each biomass and the respective combustion zones associated with each biomass. Wood pellets were found to be the most stable in terms of combustion which is seen in equal distribution of temperatures through the furnace and the smallest range of emissions. However, when compared to a problematic fuel such as Miscanthus which had large emissions ranges and larger fluctuations in temperature. The data gives an indication to the applicability of each biomass and the potential difficulty for employing each fuel in FBC at pilot scale and full scale facilities.

The data in Table 7-1 also shows the differences associated with a uniform air distribution system and a non-uniform air distribution system. Wood as an example, has a different, more erratic temperature spread for the non-uniform air system when compared to the uniform air system. The difference comes as a result of poor fuel distribution caused by the lower mixing and turbulence of the bed due to the non-uniform air plate. Consequently, the combustion of fuel is less uniform and as such the temperatures within the furnace fluctuate causing the wider temperature ranges and

Table 7-1 Summary data for the combustion of biomass fuels in a fluidised bed combustion unit						
Fuel		Wood	Peanut	Oats	Straw	Miscanthus
Temperatures (°C)						
Uniform air	bed	700-750	698-875	690-899	550-690	560-920
	freeboard	750-780	580-790	520-810	310-380	540-715
	boiler exit	300-340	420-518	200-301	370-410	200-250
Non-uniform air	bed	870-880	775-885	790-860	650-800	655-812
	freeboard	730-860	610-815	650-770	540-760	582-781
	boiler exit	300-585	460-650	500-630	242-340	416-632
Emissions						
Uniform air	CO_2 (vol.%)	7-8	3-8	4-10	1-6	4-10
	CO (ppm)	53-60	140-250	8-420	86-240	4-250
	NO (ppm)	1-15	1-30	0-16	33-120	11-160
	SO_2 (ppm)	1-8	0-150	0-159	20-30	15-62
Non-uniform air	CO_2 (vol.%)	5-7	6-7	6-8	3-9	5-8
	CO (ppm)	1-78	7-127	21-57	21-311	48-178
	NO (ppm)	150-169	250-348	250-331	140-278	176-260
	SO_2 (ppm)	16-38	9-20	17-37	7-33	13-80
Defluidisation time (min)						
Uniform air		N/A	83	48	55.5	43
Non-uniform air		N/A	76	135	33.5	74
SEM-EDX1						
Uniform air	1	Fe	K	K	K	Fe
	2	Ca	Ca	Fe	Ca	K
	3	K	P	Mg	Fe	Na
Non-uniform air	1	K	K	K	K	K
	2	Ca	Ca	P	Ca	Fe
	3	Fe	Na	Ca	Fe	Fe
XRF2						
Uniform air	1	Fe	K	K	K	Fe
	2	Na	Ca	P	Ca	Ca
	3	Ca	Fe	Fe	Fe	K
Non-uniform air	1	Ca	Fe	Fe	K	Ca
	2	K	K	K	Ca	K
	3	Fe	Ca	Na	Fe	Fe

1. Ranking of analytes concentrations based on SEM-EDX analysis.
2. Ranking of analytes concentrations based on XRF analysis.

emissions variations. With respect to each fuel, a larger difference in the temperature ranges and emissions as a result of the air plate change is an indication of how flexible each fuel is within a damaged or variable system. The difference between wood pellets and straw pellets for instance would indicate that if a system were likely to experience and air flow changes then wood pellets would be more beneficial to that system.

The results of differences in temperatures, emissions and the effect of the plate changes are further emphasised in the defluidisation times. This will be described further in subsequent sections, however, the differences in defluidisation times do not imply one plate is better than another. The effect of the combustion characteristics of each fuel directly influences the applicability of each fuel in a particular combustion environment. Oat pellets were seen to defluidise quicker in a uniform system than in a non-uniform system. This is due to the poor mixing and the in ability of ash particles to coat sufficient bed particles to agglomerate and cause local defluidisation required to propagate eutectic structures. However, the volatile mass was sufficient in the combustion zones in which air was passing to sustain temperatures and emissions associated with relatively good combustion.

Table 7-1 also includes the three highest concentrations of alkaline species in bed samples taken after each test. Si was ignored for the purpose of this summary as the majority of silicon can be assumed to be from the bed material. Whilst the fuels contained variable concentrations of Si and was seen to form silicate glasses etc. it is the other components and their interactions with Si which are most significant to the formation of eutectics and agglomerates.

The effect the fuels had on agglomerates and air flow will be described in subsequent sections however, the ranking of concentrations shown in Table 7-1 illustrates the similarities and differences in agglomerate and slagging mechanisms between each fuel. The fuel characterisation results of Chapter 4 correlates to the build-up in concertation of alkaline species such as K, Fe and Ca in the bed samples, however, the combination of high concentration alkaline species for each fuel indicates which fuel is likely to have the highest agglomerate forming potential. Furthermore, with a change in air distribution plate, fuels such as peanut has a change in the three analytes. This indicates that there is likely more than one mechanism for agglomeration and slagging associated with that fuel and thus could be more problematic than another.

The results show that the wood pellets were easiest to sustain stable operation with, which can be associated with its primary alkaline species in the bed samples as well as showing least variability between plates. The lower ash content in the wood pellets and the contents pf that ash being made up of less problematic elements with regards to agglomeration resulted in the reduced agglomeration rates and stability of bed fluidisation throughout tests. This combination of

information when compared to another biomass such as Miscanthus which was the opposite is each regard, demonstrates the applicability of each fuel in FBC systems. Furthermore, it demonstrates how the different fuels will achieve different combustion dynamics and offer different challenges in pilot and full scale operations.

7.4.2 Operational Performance

There was a difference in both the ease of which the rig could be operated with the different plates installed as well as the overall performance of combusting biomass pellets with two different plates installed. Figure 7-43 will be used to highlight and describe the differences found in the operational performance with the two different plates installed.

When operating the rig with the uniform plate installed it was found that the sustained and stable operation was much easier to both alter and control. With uniform air being distributed throughout the bed, less air was required to fluidise the bed material. This resulted in reduced O_2 concentrations in the flue gas and combustion and operations were conducted at excess O_2 levels closer to desired concentrations (10 vol. %, excess air 120%). For this reason when adjustments were made to the bed in terms of air flow, fuel flow etc. the bed and system would react as expected. This was due to the system always being in steady state and changes such as air flow being an even change to the system. Whereas when the non-uniform plate was installed an air change wouldn't necessarily

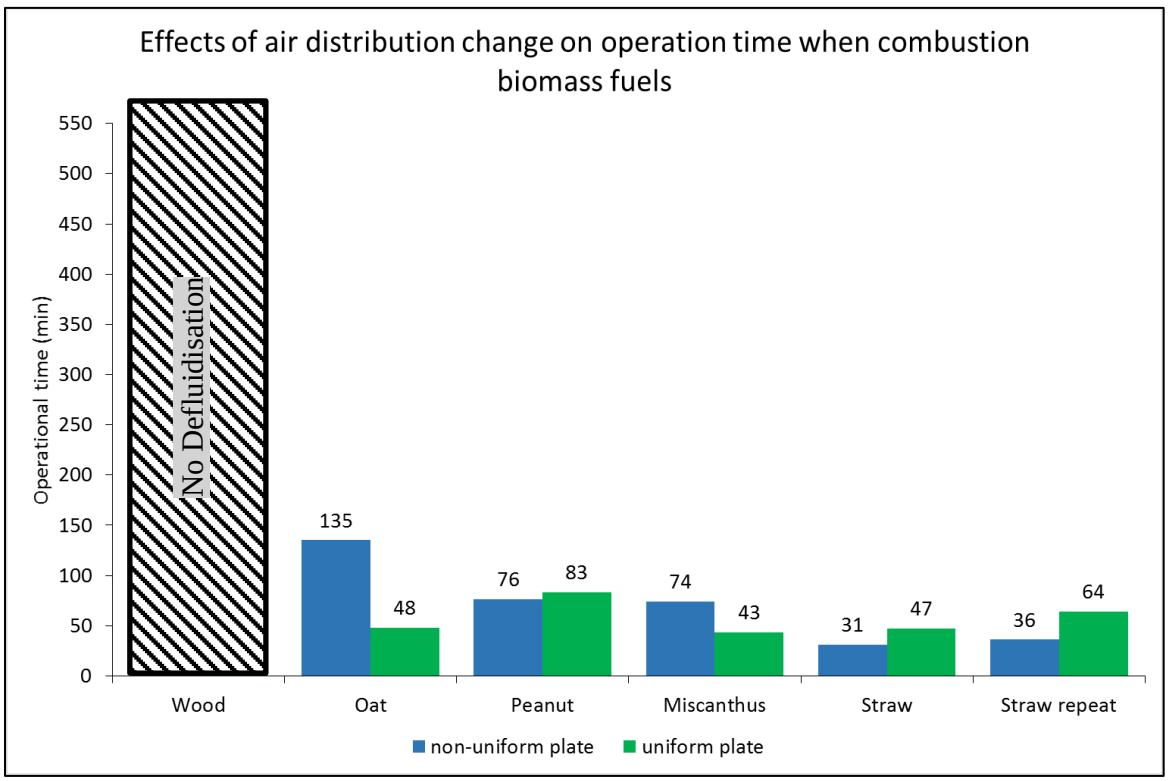

Figure 7-43 Defluidisation time of different biomasses with a uniform and non-uniform distribution plate installed

affect the whole bed but present a higher flow through the leak and lead to chain reactions that reduced the performance of the bed.

It was found that when the non-uniform plate was installed the bubbling of the bed and fluidisation was both more difficult to control and predict. The leakage point required a higher air flow (≥10000 L/min) to fluidise. The leakage allowed a high throughput of air and without a high airflow it was found would move through the leak rather than the bubble caps because of the resistance caused by the weight of the bed surrounding the bubble caps. Further to this, if air flow and fuel flow were altered, it was assumed that a proportion of the flow change was effecting most of the bed but an unquantifiable effect was being caused by the leakage point. For this reason system change had to be in larger value than with the uniform plate and caused more extreme variation in the operation of the bed. Overall the performance of the bed and rig was hindered and made much more complex with the leakage present than with the uniform plate installed.

There was a difference in the rate of defluidisation between the two plates. As Figure 7-43 shows, different fuels had different defluidisation times and more over the plate installed in those tests seemed to influence the defluidisation time further.

Wood pellets did not lead to the defluidisation of the bed but instead the period in which the test could run limited running time and thus the tests were ended. Each of the other fuels with both plates installed led to defluidisation by the formation of agglomerates. The difference in defluidisation time between the two plates for a fuel such as oat comes down to operational changes caused by the presence or lack of an air leak. With the uniform plate installed the pre-heat time was almost double the length of the leakage plate test. With the uniform air plate the air was distributed evenly throughout the bed during pre-heat and in doing so acted as a cooling factor to the bed. Further to this heat absorbed by the air in the plenum and bed led to an increased temperature in the midfreeboard and top freeboard region (regardless of over bed burner presence). Whilst the uniform plate led to better heating of the rig overall, it also limited the heat rate of the bed which was the limiting factor before fuel could be fed into the bed and thus limited the operational time achieved with biomass pellets being the primary form of combustion. With the leakage plate a significant proportion of the air passed through the leak rather than the bubble caps. In doing so, the area around the leak was cooled but the bubble caps and surrounding bed were heated much faster. As soon as the average bed temperature was ≥400 °C, the bed density reduces significantly and mixing increases around the bubble cap and eventually bed. This mechanism leads to a much quicker heating of the bed but at a consequence of the upper freeboard regions being cooler than with the uniform plate installed. This has implications to CO conversion and oxidation reactions, especially if tests were run for 24 hours for instance. The increasing temperature in the upper

freeboard would alter flue gas composition over time. However, because of the relatively short period in which these tests were run, changes in the flue gas composition were found to be due to operational changes rather than by freeboard temperatures in this capacity.

The time between the end of the pre-heat period and the defluidisation of the bed/end of the test are represented by the values shown in Figure 7-43. The results show that when the uniform plate is installed the Peanut and straw tests take longer to defluidise. Whereas with the leakage plate installed oats and Miscanthus take longer to defluidise. This is due to the alkali species found to be within the agglomerates and is further discussed in following discussion. However, alkali species aside, the leakage plate was predicted to limit defluidisation time across all fuels. It was found that the leakage point created a region in the bed of high mixing and high turbulence therefore, increasing the number of localised collisions and the force of those collisions. This acted to break up weaker agglomerated structures and thus extend the time before agglomerate size led to defluidisation. As later discussions show, the presence of Mg-P-Si eutectic dominated agglomerates would back up this theory as this type of eutectic and stricture are known to be weaker than eutectics found in the uniform tests which were made up primarily of Si-Fe complexes. Hence the uniform tests lasted longer in fuels in which these species were in lower concentrations in the fuel ash and the opposite with fuels with higher concentrations of the species.

There were clear differences in the performance of the rig and bed when the two plates were installed. With the uniform plate installed the bed was easier to control but because of the experimental design changes the fuel flow required to achieve the desired bed temperatures was 22 kg/hr rather than 35 kg/hr when combusting wood pellets. This is due to the increase of thermal mass around the bed area and the increase in both insulation, reflection of heat back in to the combustion chamber and most importantly ideal combustion and ideal fluidisation /mixing in the bed.

7.4.3 Impact on Fluidisation

The uniform plate resulted in good mixing throughout the bed, less dead zone regions, fewer hotspots and all inlet air being exposed to the bed around the bubble caps. The impact on fluidisation was that the bed was fluidised uniformly and mixing was seen across the bed rather than in specific zones. The uniform plate created an across bed ΔP of approx. 1.8 KPa which was higher than that of the non-uniform plate. The result was the leak which bypassed the bed and thus the pressure within the plenum was less than with the uniform plate and the negative pressure in the freeboard for the uniform tests was more negative because of the bed obstruction compared to the non-uniform plate bypassing the bed which induced a less negative freeboard pressure. Furthermore, small changes in air flows and fuel feeding were seen to make an equal change to the

bed and combustion zone. This was a direct result of good combustion. Whereas with the non-uniform plate installed larger changes were required to see changes in the data readouts as more significant air flows for instance were required to alter the bubbling bed.

The non-uniform plates leak meant that the bed fluidised bit for very short periods of operational time. With the high velocity exit at the leak the bed material would be displaced and a chain reaction of higher velocity and less resistance by bed material would occur. This directly impacted the air flow through the bubble caps. With more air leaking through the bed leak, the resistance caused by med material around the bubble caps overpowered the decreasing pressure of air moving through the bubble caps. This chain reactions slowly but eventually led to the air moving though the bubble caps becoming negligible and thus mixing, fluidisation and combustion all decreased in operational performance and condition.

7.4.4 Impact on Combustion

The air distribution plate impacted the way in which the air interacted with the fuel whilst combusting. The superficial velocity increased with the installation of the leakage plate as the inlet air flow was increased from 4000 L/min to 10000 L/min. As a result the heat from combustion in the bed was absorbed by the cooler inlet air. This led to the distribution of heat throughout the rig moving from the rig into the freeboard.

Figure 7-44 shows the combustion profiles from biomass tests when the uniform air distribution plate and non-uniform distribution plate was installed. With the non-uniform distribution plate installed the bed temperatures within the bed (between 0 and 0.7m), were ≥800 and <850 °C. Furthermore, the lower freeboard (1.5 m) and mid freeboard (2.0 m) were found to be approximately ≥800°C and ≤700°C respectively. Whereas with the uniform plate installed the average bed temperature was ≥950 °C with the lower free board and mid freeboard averaging ≤700 °C and ≤550 °C respectively.

The explanation for the difference between the plates comes down to a number of factors; 1) the air though put of the plates, as previously described, was higher for the non-uniform/leakage plate. The air moving through the leak point was significant and because of the localised poor mixing etc. will have bypassed most of the combustion and instead acted to cool the bed and localised area. Whereas the uniform plate has all air coming through into combustion zones and being heated so less cooling affect was seen in the bed region, 2) mixing was less turbulent in the non-uniform test as a result of air passing through the leak and less through the bubble caps. The poor mixing meant fuel was found nearer the surface of the bed and the volatile flame associated with biomass combustion was combusting above the bed and in the lower freeboard regions, hence the bed

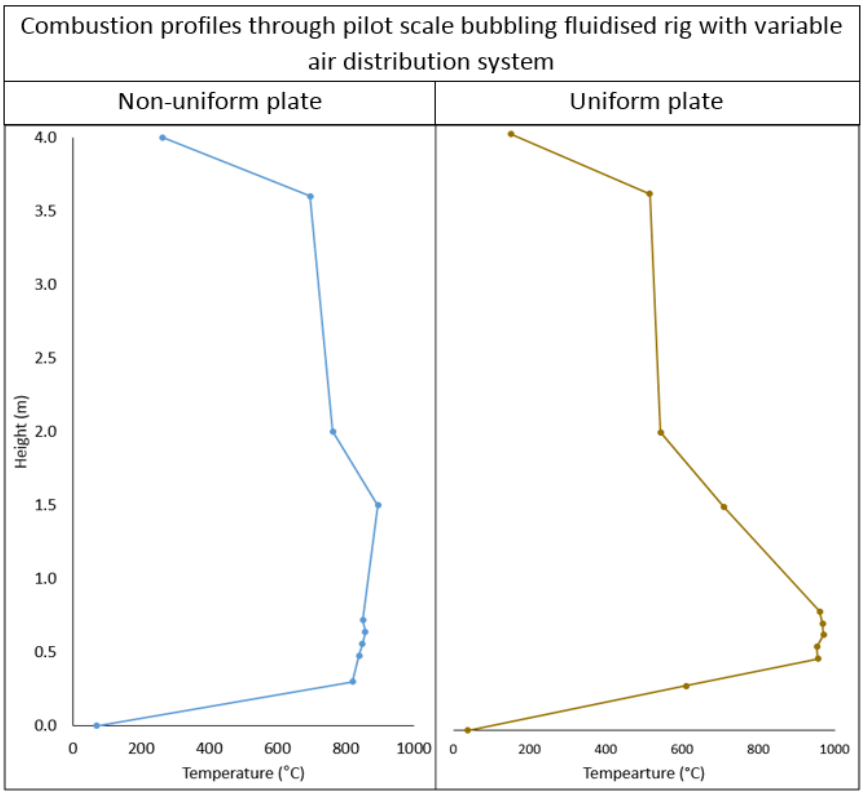

Figure 7-44 combustion profiles using wood pellets from across the rig with different air distribution plates installed

temperature is less than the uniform plate and has higher freeboard temperatures in the lower freeboard than the uniform plate. Furthermore, the turbulent mixing of the uniform bed mixed the pellets thoroughly and hence combustion was primarily within the bed and the volatile flame combusted within the bed rather than in the freeboard regions, and, 3) uniform combustion as a result of turbulent mixing and uniform air distribution was seen with the uniform air distribution plate but with the leakage plate was seen to either combust in specific regions or on the side nearest to the screw feeder inlet. With the uniform plate the ideal operation of the bed meant fuel combusted evenly within the bed, however, with the leakage plate, all the negative implications meant that combustion wasn't uniform across the bed. This limited the combustion and thus the energy release form the biomass plate and is represented as a lower peak temperature compared with the uniform plate. If the fuel wasn't mixing into the bed, good combustion would be seen as higher temperatures at the top or in the lower freeboard. However, the temperatures here never match the peak temperatures of the uniform plate's bed temperatures. Hence combustion was operating much more ideally with the uniform plate installed.

The implications to combustion between the two plates are evident within the results of the tests and the combustion profiles. With the uniform plate installed the mixing was more turbulent and uniform and thus fuel was combusting within the bed under more ideal conditions. Whereas with

leakage plate the opposite was the case where good mixing and distribution of both air and fuel led to the combustion of fuel being more ideal and contained within the bed as desired and thus temperatures represent the ideal combustion in the desired bed area.

Implications to agglomeration with the two different plates is significant. With the leakage plate installed, mixing was hindered and the formation of hotspots occurred. As a result of this agglomeration through a mechanism dominated by Fe-Si-P-Ca eutectics was found to form at increasing rates. Further to this, the localised hotspots caused by the poor mixing with the leak plate will result in sintering mechanisms propagating agglomerate growth and strength.

The poor mixing caused by the leakage plate was found to cause poor distribution of the pellets throughout the bed and in a number of tests for the pellets to be combusting on the surface of the bed and not within. Therefore, there is a higher concentration of liquid/melt phase's alkali species in these heated fuel rich zones. This causes significant agglomeration rate due to the high concentration and availability of eutectic in these zones which will develop agglomerates of significant strength and size more quickly than in other regions of the bed.

The leakage led to a smaller amount of bed material being exposed to the biomass pellets. Therefore, as the initial eutectics were forming, smaller volumes of bed material were exposed to the sticky complexes. Thus, a more significant volume of eutectic was present in the small volume of bed material but resulting in agglomerated structures forming in significant quantities and total size, much faster than if an even distribution of the eutectic was distributed throughout all bed particles.

The poor mixing and onset of agglomeration are evident by the structures and distribution of the agglomerated structures as shown in Figure 7-45.

A significant result of the poor mixing and regions of low if any mixing was the finding of eutectics and agglomerated structures which were not present in the uniform distribution tests. Crystallised structures with concentrations of Mg-K-P were found to be present but not in the uniform test samples. It is believed that these weaker structures were able to contribute to the formation of larger agglomerated structures and thus increase the rate and size of agglomerates forming in the leakage tests. Furthermore, areas in which stationary pellets had combusted with no bed movement, caused bubble like features (examples in Figure 7-24), in which a bubble shape made up of liquid phase alkali species were able to form. The result being the localised area was made up of a sticky melt which would propagate the agglomerate growth further.

However, when the uniform distribution plate was installed and the tests were repeated and compared, it was found that the previously described phenomena couldn't exist. The even air

Figure 7-45 Agglomerated bed as a result of combusting straw pellets

distribution and constant turbulent mixing of bed particles throughout meant that localised hotspots were reduced in number, fuel was mixed throughout and less localised concentrations of alkali species were able to form, weaker structures were broken up by the moving particle collisions and the primary eutectic was made up of Fe-Si-K complexes.

Agglomerates still formed with the uniform plate installed, however, the increased overall average bed temperature is likely to have contributed to the onset of agglomeration. Biomass fuels have higher agglomeration potential due to their high alkali and alkaline species concentrations. However, the addition of increased bed temperatures acts to create a liquid phase in the bed and thus provide the environment necessary to form agglomerates. The uniform plate altered the way in which the agglomerated structures propagated in size once the initial eutectics had formed whilst offering greater operational stability and control.

7.4.5 Biomass and Fluidised Bed Combustion

Biomass combusted in a bubbling fluidised bed was found to cause both benefits and repercussions to the system in a number of aspects. Most significantly and foremost is the agglomeration caused by the presence of alkali and alkaline species in high concentration in the fuel. The presence of Si, K, Fe and P was found to be the main components within the agglomeration mechanism evident by the measurements made in the agglomerates taken from the bed. The presence of the alkali species led to the formation of complexes/ low temperature eutectics which coated the particles within the bed. As such the bed particles became sticky, adhered to one another in the bed and thus the agglomerates formed. Through hotspots and localised poor mixing the alkali species in the biomass pellets led to sintering and structures representing those mechanisms to form. Whilst alkali

species are present in other fuels such as coal, it is clearly evident that in these test the high concentrations of K, Na etc. components led to increased rates of agglomerate formation and the onset of defluidisation as a result. Furthermore, the XRF data in the fuel characterisation and the XRF data of the agglomerates and bed material show that the high concentrations of specific alkali species can be related to the higher rates of agglomerate formation. It is for this reason that such significant differences in defluidisation time can be seen between fuels in Figure 7-43.

Another unforeseen consequence of using different biomass pellets was the effect on the flame and combustion environment within and above the bed. As data in both the uniform and non-uniform sections described previously show different fuels combusted in different manners regardless of similar operating conditions. This is due to the physical makeup of the pellets in terms of what part of the plants were used to make up the pellets and the way in which the pellets broke up during combustion. White wood pellets generated very stable combustion environments with particles breaking up and burning at a fairly even rate throughout the bed. This can be seen by stable temperatures when a steady state fuel feed was applied. Whereas when you compare the wood pellet combustion to the peanut pellets combustion results, where the temperature profiles were fluctuating by >400 °C with operations running in steady state. The bed, inlet air, pressure difference etc. were all similar between these tests, therefore, the pellets themselves and the way in which they combusted is the only explanation for the difference.

The biggest benefit in stable operations was that the emissions from the combustion of the pellets were low with respect to NO, SO_2 and CO. The fuels combusted completely until the onset of agglomeration was found to alter mixing etc. and thus alter the combustion environments between oxidising and reducing atmospheres. Slight variations in emissions were noted between biomass fuels, however, the values recorded were negligible with respect to the total emission. This is especially true for NO concentrations measured and shows the tests again ran well as the low NO emissions are typical of the cooler flame in a fluidised bed combustor.

7.4.6 Implications to Full Scale Plant

With the combustion of white wood, the tests demonstrated that sustained operation of BFBC while combusting biomass is possible and generates emissions desirable by full scale operations in the energy industry, especially when considering the decreasing emissions limits being implemented throughout Europe and the UK. However, all biomasses demonstrated some form of agglomeration with wood having the least potential and straw having the highest potential for agglomeration. If these fuels were to be utilised in full scale operations the beds would be larger but the higher fuel flows would balance out this factor. Special attention would be needed to combust these fuels in full scale BFBC. However, the concept has been proven in the work of this study.

The consequence of a leak of damaged plate was shown to alter agglomeration and in most cases, increase the rate of eutectic formation. If a leak were found in a full-scale operation the size of the leak could be the leading factor to determine the extent of the issue. In the pilot scale tests the leak represented 2 broken bubble caps because of the area the hole occupied. In full scale operations hundreds of bubble caps would be used and the interference of a couple of bubble caps would only create small issues in the bed. However, it could lead to localised poor mixing and hotspots and thus initiate the first stages in agglomerate formation. Therefore, the work here shows that a large leak would cause combustion, mixing and temperature distribution problems. However, for this to occur in a full-scale operation, pressures and temperatures throughout the bed would have been seen to alter and this could be addressed at the next planned outage without major influence on the performance of the combustor.

7.4.7 Potential Remedies

The results of the previously described investigation have shown that K, Si, Fe and Ca are chemical components fundamental to the formation of agglomerates in the bed. There are a number of process and techniques that could be employed to reduce the likelihood of agglomeration related mechanisms causing bed defluidisation and/or an unexpected outage of the furnace:

7.4.7.1 Bed Cleaning

A widely-adopted method for the maintenance and reduction of agglomeration related mechanisms is online cleaning of the bed. This is done by bleeding of the bed at a constant rate or removing partitioned sections of the bed. This is then sieved to remove bed material and particles which have clumped together. The “clean” material which isn’t removed is then returned to the bed. By doing this the build-up of agglomerates is reduced or controlled and hence a FBC unit can be kept online. There is an associated cost with this process but it often outweighs the cost of an outage and boiler clean (Basu, 2013a; Oka, 2003).

7.4.7.2 Bed Material

As the results of this investigation demonstrated, silicates containing and varying concentration of potassium, sodium, calcium and iron were the primary cause for agglomerate and slag mechanisms in the bed. Therefore, a potential method for addressing these specific alkaline species would be through the use of alternative bed materials. The sand used in the experimental testing was silicon based and thus aided the propagation of agglomerates. However, if an alternative mineral such as olivine were to replace the silica sand then the agglomeration mechanisms could potentially be mitigated.

Olivine is a mineral made up of magnesium iron silicates which falls under nesosilicates. The high concentrations of Mg^{2+} and Fe^{2+} leads to a number of reactions with alkaline groups such as K and Na forming a surface on the olivine bed particles with a higher melting temperature than with a silica sand. This results in bed material being coated but with very few bridging interactions occurring between particles and thus there is little if any agglomeration related propagation and structure build up in the bed (Grimm et al., 2012). A number of studies have been conducted to the application of olivine in fluidised beds for their tar removal uses as well as agglomeration mitigation properties (Grimm et al., 2012; Fryda et al., 2008; Virginie et al., 2012; Koppatz et al., 2011). The data in the literature has shown that with high alkaline concentrations in fuels for fluidised bed combustion, olivine can have positive impacts on bed fluidity. However, consequences of olivine are focused to fouling effects seen in economiser regions due to KCl release and particle size elutriated in the flue gases due to olivine's high attrition rates. However, the severity of the agglomeration mechanism seen in the fuels of this study require some form of system modification to ensure sustained stable operation.

7.4.7.3 Additives

An alternative means to address specific chemical components within the bed which are attributed to agglomeration is the addition of additives. Kaolin for instance is a mineral dominated by aluminium silicates. Aluminium silicates have been seen in a number of studies (Davidsson et al., 2008; Vamvuka et al., 2008; Steenari and Lindqvist, 1998; Davidsson et al., 2007; Öhman and Nordin, 2000) to increase the melting temperature of bed material and bottom ash particles. By injecting a mineral such as kaolin either directly into a furnace or mixing it in with the fuel there is a simplistic method available to mitigate specific chemical components within the bed and thus improve the fuel. Alternative additives are available including pot ash, coal ash and steel industry residues, however, considering the data produced during this investigation, kaolin and aluminium silicate based additives are appropriate for the fuels concerned.

The previously mentioned remedies for agglomeration of the biomass fuels were chosen for their impact regardless of a system in which the air is being uniformly distributed or in a situation in which it is not. Whilst there would be an impact on the efficiencies of additives, due to the reduction in mixing, there would still be benefits seen as a result of their addition. The remedies mentioned would prolong a bed even in the air distribution system was failing. Of course, there is a limitation to that statement but the options could be applied to prolong a bed to its next planned outage.

7.5 Conclusions

Throughout this Chapter a number of biomass pellets were combusted in a pilot scale bubbling fluidised bed combustor. The objective of this investigation was to look at the effect of biomass as a fuel feedstock for FBC unit and the impact a uniform and non-uniform or damaged air distribution system would have whilst combusting biomass.

Different biomass pellets were combusted in the pilot scale rig with varying success. Whilst stable operation was achieved with each fuel, the length of time before the onset of defluidisation was quite varied. All fuels other than wood pellets led to the formation of agglomerates which directly impacted fluidisation and consequently led to defluidisation of the bed. With this in mind, the biomass could be utilised in a FBC unit, however, the result suggests that different fuels would produce different challenges and degrees of success in sustained operation.

The cause of the agglomerates in this investigation was a collection of alkaline species forming eutectics. The eutectics were found to be dominated by silicates containing varying concentrations of K, Ca, Fe and P. These alkaline species were coved in the literature review and have been reviewed for their connection to agglomerate formation. Bed particles were found to be coated in a sticky layer made up of the aforementioned alkaline species. When the particles collided with one another in the turbulent bed, the particles would stick together if conditions were correct. Localised mixing and temperatures led to the hardening of bridges between particles and the propagation of agglomerated structures within the bed. Larger structures were also found to have sintered regions. This was a result of localised defluidisation causing fuel particle sot combust in a stationary position and hence local temperatures increased to conditions in which sintering occurred.

The air distribution plate was modified throughout the testing period to evaluate the effect of combusting the biomass fuels when there was a uniform air flow through the bed and when the air flow was non-uniform. The results showed that whilst a non-uniform bed created areas of good and poor mixing, this did not necessarily increase the formation of agglomerates. With fuels, such as Oat pellets, weaker agglomerates containing larger crystals made up of K and P were able to form in a uniform bed. However, in a non-uniform bed the high turbulent region acted to break up the weaker larger structures building up. Therefore, extending the lifespan of the bed. However, overall the impact of a non-uniform air distributor was on the furnace temperatures and subsequent emissions. Whilst a bed was flexible enough to continue combustion, the quality of the combustion and concentration of emissions was less desirable. The non-uniform plate led to combustion variation and flame fluctuations leading to hot and cold zones which directly impacted the formation of NO and CO. In a full scale unit, a small change in the air distribution plate would be

seen as a slow degradation of emission and temperature spread throughout the boiler. However, the plate used in these tests was large enough to air bypassing and non-uniform flow which wouldn't be allowed to occur in a full scale unit. Therefore, the results show the extreme effect of the air change but give important information as to the changes to be expected and measured in a furnace to measure its health and efficiency.

The fuels in this investigation were seen to pose serious agglomeration risk and problems if applied in full scale units. However, the investigation has shown that the fuels can be combusted and achieve temperatures and emissions which are desirable in power generation facilities. Therefore, with online bed management and the application of additives, different bed materials and online bed cleaning technologies, the fuels could be applied for full scale operations. The results of this investigation have identified the most probable route for agglomerate and eutectic formation in the bed and as such gives important information which could be applied to mitigate and manage the formation of these structures in a full-scale bed.

8 Conclusions

The investigations presented in this thesis evaluated and analysed five biomasses in pellet form and a range of low grade sub bituminous coals from a single northern Pakistan coal seam. The fuels were characterised and analysed in such a way as to evaluate their applicability in pilot to full scale FBC power generation operations and to evaluate the potential for agglomeration during combustion as a result of the chemical and physiological make-up of the fuel. Furthermore, a number of operational variables were altered to evaluate the effects associated and translate them to combustion of the fuels in full scale operations.

The literature review showed the extensive work that has been carried out with fluidised bed combustion and identified current theories and highlight areas which haven't been investigated. It also highlighted the need for investigations in low grade coals and biomass combustion and the respective issues associated with combusting those fuels in FBC technologies. The literature review created a foundation which allowed for the development of methodology and focus this investigation towards specific operational variables as well as helping build up a knowledge for the application of the fuels in full scale industrial operations.

The methodology chapter evaluated operational variables that could be utilised for the study of low grade coals and effect of operational variables when combusting a biomass fuel in FBC. This also included the commissioning, design and modifications of the pilot scale rig. The work in this Chapter allowed for the author to develop the rig whilst implementing a design which allowed for operational variables to be altered with a uniform and non-uniform air distribution system to be tested.

The fuel characterisation chapter included analysis of the coals and biomasses. This data was fundamental for theoretical modelling and predictive methods were evaluated for applicability. The fuel characterisation also identified key alkaline species which were attributed to agglomeration and slagging mechanisms seen in experimental work.

A significant side project resulting from the fuel characterisation work was the validation and development of XRF analysis with respect to low grade coals but most significantly biomass ash. A number of shortfalls were identified in the sampling, ashing and processing methods for XRF. These were tested and compared to wet chemistry methods

and in doing so improved the accuracy and reliability of XRF analysis with respect to the fuels in this thesis.

Thermodynamic modelling and predictive methods were applied and validated for its application to FBC and with the fuels in this thesis. Predictive indices, fuel characterisation techniques and thermodynamic model FACTSAGE were all used to predict the likelihood of agglomerate formation in FBC using the fuels previously described. The fuel characterisation work gave an insight to which fuels would create a liquid melt phase but didn't simulate FBC conditions in a way that could result in direct conclusions. The theoretical modelling gave extensive and insightful information to the slag formation, temperature ranges and chemical constituents likely to be released during the combustion of the fuels. The model gave indication to particular agglomerate and slag formation mechanisms. However, limitations and issues were demonstrated through the testing of the model as to the models application in FBC environments. The modelling was a useful tool and gave strong indications as to the outcome of using the fuels of this study but required experimental validation.

Combustion of low grade sub bituminous coals in fluidised beds allowed for the investigation to the coals ability to combust in a stable manner in a FBC pilot scale rig. A number of fundamental operational variables were altered to identify methods for improving combustion and operational length by minimising agglomeration propensity whilst controlling the emission of SO_2 in the flue gas. The investigation identified Fe, S and Si as the key constituents of eutectics within the bed leading to the formation of agglomerates and thus the onset of bed defluidisation. By altering operational variables, it was possible to improve certain aspects such as SO_2 retention, combustion temperatures and emissions whilst mediating agglomerate formation. The results included the applicability of the coals in full scaled operations, issues likely to occur as a result of combusting the fuels and the best method of operating with the fuels.

The final investigated the application of biomass fuels in FBC and the associated issues found to occur as a consequence. Results correlated the results seen in the fuel characterisation. Analysis of the bed samples and agglomerates taken after the combustion of the different biomasses. It was found that Si, K, Na and P were key alkaline species in the formation of low temperature melting eutectics. As well as combusting each fuel, the rig was modified as described in the experimental methodology, to evaluate the effect of a uniform air distribution system and a non-uniform air distribution system. Parallel tests were run and found that the change in air flow uniformity effected different fuels agglomeration mechanisms in different ways. Both positive and negative effects

were seen to occur and consequently the defluidisation time with each fuel were seen to alter in different ways. The results of this investigation allowed for speculation to the applicability of the fuels in full scale operations and offered remedies which could be employed in all cases to better the combustion and sustain a bed for longer before potential defluidisation occurring due to agglomerated structures forming.

8.1 Application to Industry

As described in the introduction of this thesis, biomass and low grade fuels stand to play a significant role in the global energy market as populations continue to increase, countries look to use cheaper indigenous fuel supplies and standards of life rely more on electrification. Low grade fuels such as sub bituminous coals present an alternative to expensive imports in countries such as Pakistan, Japan and India. Furthermore, with the global political and social scene moving towards more stringent emissions targets and reductions, the need for development and implementation of low emissions technologies and research is becoming more and more common place. As such, the work and results within the experimental and theoretical Chapters of this thesis have the following industrial applications:

1) Theoretical investigation- The results of theoretical investigation have shown how indices, thermodynamic models and fuel data can be used to predict the slagging tendencies of low grade fuels. The results give clear indication as to temperature ranges and operational parameters that are likely to have a higher or lower risk with slagging and agglomeration. This type of investigation gives industrial boiler designers and decision makers with regards to fuel specification, another tool and method of indication when applying low grade fuels to fluidised bed combustors.
2) Experimental biomass testing- The results of biomass testing in Chapter 7 indicates a mechanism of agglomeration while combusting five biomass fuels. The results are directly relevant to industrial applications as a number of the different biomasses are used in industrial applications globally. The results of these fuels give performance engineers and reliability engineers insight into potential causes for slag/agglomeration, boiler outages and allow for the identification of counter measures to be applied based on these results to improve the system.

   The testing of two different air flows is another series of information and knowledge which could be applied to industrial units when air flows are an issue in a bed. The results showed how different fuels react differently with the different air regimes.

This is significant when engineers are considering impacts of boiler efficiencies and degradation of air systems.

3) Experimental coal testing- The results, similarly to the biomass results, give the trends of slagging and agglomeration mechanism required to implement counter measures to issues related to combusting low grade coals. With a number of fluidised bed combustors being installed to burn low grade coals in countries such as Pakistan, the information of this thesis has direct application as to the performance and considerations needed when combusting the coals. Furthermore, it highlights the challenges and poses potential remedies that should be considered in the design phase for successful and continued running of industrial power generation facilities.
4) Fuel characterisation-The results are significant to both the analytical and power generation applications. The proper analysis of these fuels and fuels like them are required to understand the fuels chemistry and physiology and ensuring limits and specifications are adhered to. If analytical designers and companies are to apply their equipment in the developing industry then continued research and development is needed as demonstrated within this thesis. The results give clear indication to areas that require resources and as such has significant industrial application.

8.2 Future Work

As a result of the work conducted throughout the previously described investigations, there are a number of areas in which further research and expansion of current work would yield data and information into the use of low grade fuels in fluidised bed combustors.

8.2.1 Fuel Characterisation

The fuel characterisation work was fundamental to understanding the way in which the low-grade coals and biomasses would react in a combustion environment. Furthermore, the results indicated a large variation in the chemical and physical contents of the fuels. The work lends itself to an extension of work using a wider range of these types of fuels to understand the variability of the fuels. A larger range of fuels would allow investigators to better understand variability and then to look at the impact of the fuel variability of combustion systems. Considering that fluidised bed is able to generate constant thermal output with variable fuel input, comparing the fuel characterisation and variability against experimental trialling would generate useful trends to industrial impact and application.

A significant component of the fuel characterisation Chapter was the improvement and validation of XRF analysis techniques for low grade coals and biomass ashes. The areas

of sampling preparation, ashing and sample medium were investigated with improvements produced in the current work. Continued work with XRF applications is needed to further develop algorithms, validate and improve normalisation software and build a matrix up of different lithium tetra borate mixtures for better setting alkaline rich ashes. This work would allow to improve repeatability, accuracy and the range of application the XRF analysis could have with biomass related samples. A significant problem area was setting samples in glass mediums but this method could offer the best level of accuracy in the analysis. Therefore, efforts should be driven towards fine tuning this technique.

Further development of fuel characterisation techniques such as XRF gives another tool which can potentially achieve high accuracy, high reliability and a wide range of application to different types of samples. Continued work in these areas would allow for a quicker more reliable technique applicable in the biomass and low grade combustion sector.

8.2.2 Experimental work

The findings from the experimental results yielded from the combustion of low grade coals and biomasses gave strong indication to the potential for such fuels in pilot to industrial scale power generation applications. Consequently, there are a number of other areas which should now be investigated to continually develop the understanding of how the fuels will react under other operational variables, the effect of extended operations and the impact of system modifications.

The experimental results demonstrated they impact of combustion the fuels of this thesis in terms of emissions, temperature profiles, agglomeration and slagging mechanisms and the impact of altering specific operational variables. The result of this work gave positive outcomes and as such potential remedies could be provided to address issues seen in testing. However, due to the time and scope limitation of the work conducted certain operational variables weren't trialled. Altering the bed height would be the next variable to test. Bed depth can be used to moderate mixing, reduce the impact of agglomerates and slag in the bed and alter thermal loading in a furnace. Investigating this would allow for potential emissions improvements, extended defluidisation times with high alkaline fuels and potential for bed degradation development i.e. the effect of different sand volumes on alkaline propagation throughout a bed.

Other external variables could also be trialled to evaluate the potential for bed improvement and continued operation including bed additives such as kaolin and other

aluminium silicate based minerals and altering the bed material from silica to mineral such as olivine. Testing these system changes would help evaluate the impact of higher melting temperatures caused by specific desirable alkaline groups (Ca, Mg and Al). Furthermore, there is a direct impact to the industrial power generation sector as to which option offers the easiest, cheapest and most effective counter measure to agglomeration and slagging seen as a consequence of combusting low grade fuels.

An important consideration for future work is the length to which previous tests were conducted for. Whilst most of the coals and biomass fuels had defluidisation times within the 8-10 hour operation window allowed when using the pilot scale rig, it would have been useful to continue the tests when comparing cleaner fuels such as wood. By extending future testing, the application to industry becomes more significant as extended testing would develop slagging and fouling build ups within the rig. As industrial facilities, can operate for up to 6 months continuously, future investigations should consider combustion times an important variable for pilot to industrial comparisons. This modification would also allow for better validation of results against those seen in industrial boilers.

An important area which was outside the scope of this thesis is the impact of the fuels on corrosion in boilers/furnaces. If extended tests were available and achievable through operational variable changes, then corrosion probes and testing could be performed using the pilot scale rig. Corrosion type events accounts for 39-67% of plant forced shutdowns (Payer et al., 1978; Shibli, 2014)(variance due to technology types) and thus has significant application and interest to the industrial sector and the implementation of the type of fuels investigated in this thesis. Therefore, a valuable area of research in the future would be corrosion studies when possible in pilot scale testing.

The pilot scale rig was modified during the course of experimental work as shown in Chapter 7. This demonstrated the importance of changing the technology to evaluate the impact alternative designs and technological choices have upon the same fuels. Whilst there are a number of bubbling fluidised bed installations in the UK (Stevens croft, Blackburn meadows and Wilton 10), international projects are more focused to circulating fluidised bed combustion units. As described in the literature review (Chapter 2), efficiencies and scale limitation of bubbling fluidised units makes circulating system in a majority of cases more desirable. Therefore, a significant modification to the experimental rig would be the installation of a secondary combustion chamber and secondary cyclone. This type of rig would have a wider audience in terms of interest of the results and as such find more industrial partners and installations the work could be

compared to. As such the impact of the results would be larger and offer significant developments and engineering improvements when combusting low grade fuels.

8.2.3 Modelling

The work performed yielded good results with respect to slagging causing components and temperatures. However, there was a difference between the two approaches in which a simple model was compared to a more comprehensive model. The simple model gave more extensive ranges it could work in but the comprehensive model produced data with more specificity to changes over temperatures ranges.

In the most recent updates of FACTSAGE version 7 and above, there has been developments in chemical databases and thermodynamic properties for biomass fuels and ashes. An investigation could now be performed, using future updates and more data becomes available, and against the coal based model and its applicability when using biomass type input properties. This type of validation study is needed to compare the previous results, the new series of results achievable and again compare them to the experimental work conducted on those fuels. This work has the potential to yield more accurate and complete data series to the slag potential of biomass fuels. It would also give a level of reliability to FACTSAGE's application in industrial applications and fluidised bed based power generation operations.

The low-grade coal application of the work conducted gave a good level of reliability and correlation to the results coming from analysing bed samples post combustion testing. However, to check the extent of FACTSAGE's use with low grade coals, a wider variety of fuel properties should be tested in the model. Additionally, the parameters which FACTSAGE uses to calculate slagging propensity etc. are quite generic. For application in fluidised bed further work is needed to consider high air flow, high turbulence and the impact that almost isothermal systems have on localised combustion and alkaline component interaction.

A combination of the previous future work would allow for FACTSAGE's application in the power generation to be extended from conventional systems such as PF coal to the increasing number of alternate power generation methods including grate fired furnaces, fluidised beds and further afield oxygen based carbon capture developments. Currently the model shows a strong potential for power generation and as a predictive tool for low grade fuels however, with continued development and validation could offer more definitive results for decision making in combustion systems.

8.3 Research Dissemination

The research in this thesis has been included in a number of papers, presentations both visual and oral and has been presented in a series of in seminars, meetings and forums during the course of the PhD. Table 8-1 summarises the forums in which the research has been reviewed.

Table 8-1

Format	Description	
Papers	Chilton. S, Daood. S, Nimmo. W, Rehman.S & Williams.G. (2017) The effects of low grade coals in pilot scale fluidised bed combustion with respect to agglomeration and fuel upgrading.	Under review
	Chilton. S, Daood. S, Nimmo. W, Rehman.S & Williamss.G. (2016/7) Prediction of agglomeration from the Combustion of biomass in a 350kW Pilot Scale Bubbling Fluidised Bed Combustion (BFBC) Unit.	Under review
	Asad Naeem Shah, Nasir Hayat, Fiaz Hussain Shah, Muhammad Javed, Muhammad Akram, Stephen Chilton, William Nimmo. (2016) Optimization of fluidized bed combustion (FBC) to control emissions with emphasis on desulfurization of high sulphur coals during combustion using limestone and biomass. Fuel Processing Journal	Under review
	Xing, P., Mason, P. E., Chilton, S., Lloyd, S., Jones, J. M., Williams, A. & Pourkashanian, M. (2016). A comparative assessment of biomass ash preparation methods using X-ray fluorescence and wet chemical analysis. Fuel, 182, 161-165.	Published
	Rehman S, Shah AN, Mughal HU, Javed MT, Akram M, Chilton S & Nimmo W (2016) Geology and combustion perspectives of Pakistani coals from Salt Range and Trans Indus Range. International Journal of Coal Geology, 168, 202-213.	Published
	Belhadj E, Chilton S, Nimmo W, Roth H & Pourkashanian M (2016) Numerical simulation and experimental validation of the hydrodynamics in a 350 kW bubbling fluidized bed combustor. International Journal of Energy and Environmental Engineering. 7.1 (2016): 27-35.	Published
	Ullah, A., Hong, K., Chilton, S., & Nimmo, W. (2015). Bubble-based EMMS mixture model applied to turbulent fluidization. Powder Technology, 281, 129-137.	Published
Conferences	11th ECCRIA 2016	Oral
	EUBCE Netherlands 2016	Oral
	EUBCE Austria 2015	Visual
	Leeds Emissions 2015	Oral
	Combustion Symposium 2014	Visual
	Bioenergy 2014	Visual
	OXY3 Spain 2013	Visual
Meetings & Seminars	CRF Enviro and characterisation Annual meeting 2016	Oral
	CRIEPI Japan 2015	Oral

	Bioenergy hub Leeds 2014	Visual
	14th APGTF 2014	
	CRF Warick 2014	
	13th APGTF 2013	
	Cambridge biomass forum 2013	

9 **Bibliography**

Abanades, J.C. et al. 2005. Fluidized Bed Combustion Systems Integrating CO2 Capture with CaO. *Environmental Science & Technology.* 39(8), pp.2861-2866.

Abelha, P.G., I; Boavida, D; Seabra Barros, J; Cabrita, I; Leahy, J; Kelleher, B; Leahy, M. 2003. Combustion of poultry litter in a fluidised bed combustor☆. *Fuel.* 82(6), pp.687-692.

Acharya, B. 1992. Quantitative determination of minerals in Indian coal by X-ray diffraction. *Fuel.* 71(3), pp.346-348.

Adams, F. et al. 1998. Microscopic X-ray fluorescence analysis and related methods with laboratory and synchrotron radiation sources. *Journal of Analytical Atomic Spectrometry.* 13(5), pp.319-331.

Administration, E.I. 2016. *Total Energy.* USA.

Agarwal P, K. and La Nauze R, D. 1989. Transfer processes local to the coal particle: a review of drying, devolatilization and mass transfer in fluidized bed combustion. *Chemical engineering research & design.* 67(5), pp.457-480.

Agarwal, P.K. et al. 1986. Coupled drying and devolatilization of wet coal in fluidized beds. *Chemical Engineering Science.* 41(9), pp.2373-2383.

Álvarez-Ayuso, E. et al. 2006. Environmental impact of a coal combustion-desulphurisation plant: Abatement capacity of desulphurisation process and environmental characterisation of combustion by-products. *Chemosphere.* 65(11), pp.2009-2017.

Andersen, L.K. et al. 2013. Quantitative X-ray fluorescence analysis of biomass: Objective evaluation of a typical commercial multi-element method on a WD-XRF spectrometer. *Energy & Fuels.* 27(12), pp.7439-7454.

Annamalai, K. et al. 1987. Experimental Studies on Combustion of Cattle Manure in a Fluidized Bed Combustor. *Journal of Energy Resources Technology.* 109(2), pp.49-57.

Anthony, E. and Preto, F. 1995. Pressurized combustion in FBC systems. In: Cuenca, M.A. and Anthony, E.J. eds. *Pressurized Fluidized Bed Combustion.* Springer, pp.80-120.

Anthony, E.J. et al. 2003. Agglomeration Behavior of Dolomitic Sorbents during Long-Term Sulfation. *Energy & Fuels.* 17(2), pp.348-353.

Anzelmo, J. 2009. The Role of XRF, Inter-Element Corrections, and Sample Preparation Effects in the 100-Year Evolution of ASTM Standard Test Method C114.

Armesto, L. et al. 2003a. Co-combustion of coal and olive oil industry residues in fluidised bed. *Fuel.* 82(8), pp.993-1000.

Armesto, L. et al. 2002. Combustion behaviour of rice husk in a bubbling fluidised bed. *Biomass and Bioenergy.* 23(3), pp.171-179.

Armesto, L. et al. 2003b. N2O emissions from fluidised bed combustion. The effect of fuel characteristics and operating conditions. *Fuel.* 82(15), pp.1845-1850.

Arromdee, P. et al. 2010. Experimental Study on Combustion of Sunflower Shells in a Pilot Swirling Fluidized-Bed Combustor. *Energy & Fuels.* 24(7), pp.3850-3859.

Banks, S. 2014. *XRF Analysis – Choosing a Quantitative or Qualitative Analysis.* [Online]. [Accessed 23/05/2017]. Available from: http://www.uis-as.co.za/index.php/2-news/9-xrf-analysis-choosing-a-quantitative-or-qualitative-analysis.

Barišić, V. et al. 2008. The role of limestone in preventing agglomeration and slagging during CFB combustion of high phosphorus fuels. *World Bioenergy, Jönköping (Sweden)*. [Online]. Available from: https://www.researchgate.net/profile/Vesna_Barisic/publication/228802853_The_role_of_limestone_in_preventing_agglomeration_and_slagging_during_CFB_combustion_of_high-phosphorous_fuels/links/55b616bf08aec0e5f436daa3.pdf.

Barnes, I. 2010. Ash utilisation–impact of recent changes in power generation practices. *IEACC Centre*. 1.

Barnes, I. 2015. Operating experience of low grade fuels in circulating fluidised bed combustion (CFBC) boilers.

Barroso, J. et al. 2006. Study of coal ash deposition in an entrained flow reactor: Influence of coal type, blend composition and operating conditions. *Fuel processing technology*. 87(8), pp.737-752.

Bartels, M. et al. 2008a. Agglomeration in fluidized beds at high temperatures: Mechanisms, detection and prevention. *Progress in Energy and Combustion Science*. 34(5), pp.633-666.

Bartels, M. et al. 2008b. Detecting and counteracting agglomeration in fluidized bed biomass combustion. *Energy & Fuels*. 23(1), pp.157-169.

Barton, C. et al. 1993. Latrobe Valley, Victoria, Australia: a world class brown coal deposit. *International journal of coal geology*. 23(1), pp.193-213.

Basu, P. 1990. Heat transfer in high temperature fast fluidized beds. *Chemical Engineering Science*. 45(10), pp.3123-3136.

Basu, P. 1999. Combustion of coal in circulating fluidized-bed boilers: a review. *Chemical Engineering Science*. 54(22), pp.5547-5557.

Basu, P. 2006. *Combustion and Gasification in Fluidized Beds*. Taylor & Francis.

Basu, P. 2013a. *Circulating Fluidized Bed Boilers: Design and Operations*. Elsevier Science.

Basu, P. 2013b. *Fluidized Bed Boilers: Design and Application*. Elsevier Science.

Basu, P. and Sarka, A. 1983. Agglomeration of coal ash in fluidized beds. *Fuel*. 62(8), pp.924-926.

Baxter, L. et al. 1995. *Application of advanced technologies to ash-related problems in boilers*. Sandia National Labs., Albuquerque, NM (United States).

Baxter, L.L. 1993. Ash deposition during biomass and coal combustion: A mechanistic approach. *Biomass and Bioenergy*. 4(2), pp.85-102.

Beckhoff, B. et al. 2007. *Handbook of Practical X-Ray Fluorescence Analysis*. Springer.

Beér, J.M. 1977. The fluidised combustion of coal. *Symposium (International) on Combustion*. 16(1), pp.439-460.

Berjonneau, J. et al. 2009. Determination of the liquidus temperatures of ashes from the biomass gazification for fuel production by thermodynamical and experimental approaches. *Energy & Fuels*. 23(12), pp.6231-6241.

Berndes, G. et al. 2003. The contribution of biomass in the future global energy supply: a review of 17 studies. *Biomass and Bioenergy*. 25(1), pp.1-28.

Bettinelli, M. and Taina, P. 1990. Rapid analysis of coal fly ash by x-ray fluorescence spectrometry. *X-Ray Spectrometry*. 19(5), pp.227-232.

Biagini, E. et al. 2002. Devolatilization rate of biomasses and coal–biomass blends: an experimental investigation. *Fuel*. 81(8), pp.1041-1050.

Birol, F. 2010. World energy outlook 2010. *International Energy Agency*. [Online]. 1. Available from: http://www.oecd.org/berlin/46389140.pdf.

Boavida, D. et al. 1997. 'The Relative Importance of the Contribution of Volatile to the Formation of NO and N2O During the Combustion of Coal in a FBC. In: *Proc., 14th International Conference on Fluidized Bed Combustion*, pp.977-982.

Bolea, I. et al. 2014. Heat transfer in the external heat exchanger of oxy-fuel fluidized bed boilers. *Applied Thermal Engineering.* 66(1–2), pp.75-83.
Bonn, B. and Richter, E. 1990. Aspects of coal combustion in atmospheric and pressurised fluidised beds. *Fuel Processing Technology.* 24(0), pp.319-353.
Borah, R.C. et al. 2011. A review on devolatilization of coal in fluidized bed. *International Journal of Energy Research.* 35(11), pp.929-963.
Borghi, G. et al. 1985. A model of coal devolatilization and combustion in fluidized beds. *Combustion and Flame.* 61(1), pp.1-16.
Breeze, P. 2014. coalfired power plants. *Power Generation Technologies.* Elsevier Science.
Brouwer, P. 2003. *Theory of XRF : getting acquainted with the principles.* Almelo: PANalytical.
Brown, R.C. et al. 1994. *Bed material agglomeration during fluidized bed combustion. Technical progress report, 1 April 1994--30 June 1994.* Iowa State Univ. of Science and Technology, Ames, IA (United States).
BRUKER. 2014. XRF Data Differences: Quantitative, Semi-Quantitative, and Qualitative Data. [Online]. Available from: http://www.bruker.com/products/x-ray-diffraction-and-elemental-analysis/handheld-xrf/xrf-data-primer-quantitative-semi-quantitative-qualitative.html.
Brus, E. et al. 2005. Mechanisms of bed agglomeration during fluidized-bed combustion of biomass fuels. *Energy & Fuels.* 19(3), pp.825-832.
Butler, O.T. et al. 2015. 2014 atomic spectrometry update - a review of advances in environmental analysis. *Journal of Analytical Atomic Spectrometry.* 30(1), pp.21-63.
Campbell, F.C. 2012. Thermodynamics and phase diagrams. *Phase Diagrams: Understanding the Basics.* ASM International, pp.41-64.
Cebeci, Y. and Sönmez, İ. 2002. The investigation of coal–pyrite/lignite concentration and their separation in the artificial mixture by oil agglomeration. *Fuel.* 81(9), pp.1139-1146.
Chaivatamaset, P. et al. 2013. A prediction of defluidization time in biomass fired fluidized bed combustion. *Applied Thermal Engineering.* 50(1), pp.722-731.
Chen, G. et al. 2004. Biomass gasification integrated with pyrolysis in a circulating fluidised bed. *Solar Energy.* 76(1–3), pp.345-349.
CHEN, X.-l. et al. 2005. Analyzing energy consumption of wood pelletizing. *Liaoning Forestry Science and Technology.* 5.
Cheng, H. and Hu, Y. 2010. Municipal solid waste (MSW) as a renewable source of energy: Current and future practices in China. *Bioresource Technology.* 101(11), pp.3816-3824.
Cheng, J. et al. 2003. Sulfur removal at high temperature during coal combustion in furnaces: a review. *Progress in Energy and Combustion Science.* 29(5), pp.381-405.
Chern, J.-S. and Hayhurst, A.N. 2012. Fluidised bed studies of: (i) Reaction-fronts inside a coal particle during its pyrolysis or devolatilisation, (ii) the combustion of carbon in various coal chars. *Combustion and Flame.* 159(1), pp.367-375.
Chirone, R. et al. 2006. Mechanism and prediction of bed agglomeration during fluidized bed combustion of a biomass fuel: effect of the reactor scale. *Chemical engineering journal.* 123(3), pp.71-80.
Chou, J.-D. and Lin, C.-L. 2012. Inhibition of agglomeration/defluidization by different calcium species during fluidized bed incineration under different operating conditions. *Powder technology.* 219, pp.165-172.
Cliffe, K.R. and Patumsawad, S. 2001. Co-combustion of waste from olive oil production with coal in a fluidised bed. *Waste Management.* 21(1), pp.49-53.

Clough, R. et al. 2014. Atomic spectrometry updates. Review of advances in elemental speciation. *Journal of Analytical Atomic Spectrometry.* 29(7), pp.1158-1196.
Cohen, J.E. 2001. World population in 2050: assessing the projections. In: *Conference Series-Federal Reserve Bank of Boston*: Federal Reserve Bank of Boston; 1998, pp.83-113.
Cohen, J.E. 2003. Human Population: The Next Half Century. *Science.* 302(5648), pp.1172-1175.
Cotton, A. et al. 2013. Hydrodynamic characteristics of a pilot-scale cold model of a CO2 capture fluidised bed reactor. *Powder Technology.* 235(0), pp.1060-1069.
Cranfield, R.R. and Geldart, D. 1974. Large particle fluidisation. *Chemical Engineering Science.* 29(4), pp.935-947.
Cuenca, M.A. and Anthony, E.J. 2012. *Pressurized Fluidized Bed Combustion.* Springer Netherlands.
Curry, T.S. et al. 1990. *Christensen's Physics of Diagnostic Radiology.* Lea & Febiger.
Czakiert, T. et al. 2010. Oxy-fuel circulating fluidized bed combustion in a small pilot-scale test rig. *Fuel Processing Technology.* 91(11), pp.1617-1623.
D'Apote, S.L. 1998. IEA biomass energy analysis and projections. In: *Proceedings of biomass energy conference: Data, analysis and Trends, Paris: OECD,* pp.23-24.
Dam-Johansen, K. and Østergaard, K. 1991. High-temperature reaction between sulphur dioxide and limestone—I. Comparison of limestones in two laboratory reactors and a pilot plant. *Chemical Engineering Science.* 46(3), pp.827-837.
Davidson, J.F. 2000. Circulating fluidised bed hydrodynamics. *Powder Technology.* 113(3), pp.249-260.
Davidson, J.F. and Harrison, D. 1987. Mobile particulate systems. *Fluidised Particles.* UMI, pp.173-196.
Davidsson, K.O. et al. 2008. Countermeasures against alkali-related problems during combustion of biomass in a circulating fluidized bed boiler. *Chemical Engineering Science.* 63(21), pp.5314-5329.
Davidsson, K.O. et al. 2007. Kaolin Addition during Biomass Combustion in a 35 MW Circulating Fluidized-Bed Boiler. *Energy & Fuels.* 21(4), pp.1959-1966.
Davies, C.E. and Fenton, K. 1997. Pressure fluctuations in a fluidized bed: A potential route to the continuous estimation of particle size. *Transactions of the Institution of Professional Engineers New Zealand: Electrical/Mechanical/Chemical Engineering Section.* 24(1), p12.
Davis, S. et al. 2014. Biomass in the energy industry: an introduction. [Online].
de Diego, L.F. et al. 2013. Optimum temperature for sulphur retention in fluidised beds working under oxy-fuel combustion conditions. *Fuel.* 114(0), pp.106-113.
de Jonge, M.D. and Vogt, S. 2010. Hard X-ray fluorescence tomography—an emerging tool for structural visualization. *Current opinion in structural biology.* 20(5), pp.606-614.
De Wit, M. and Faaij, A. 2010. European biomass resource potential and costs. *Biomass and bioenergy.* 34(2), pp.188-202.
DECC. 2012. UK energy in brief 2012. *Department for business, energy and industrial stratergy.* [Online]. Available from: https://www.gov.uk/government/uploads/system/uploads/attachment_data/file/540135/UK_Energy_in_Brief_2016_FINAL.pdf.
Desroches-Ducarne, E. et al. 1998. Modelling of gaseous pollutants emissions in circulating fluidized bed combustion of municipal refuse. *Fuel.* 77(13), pp.1399-1410.
Duan, F. et al. 2015. Bed agglomeration characteristics of rice straw combustion in a vortexing fluidized-bed combustor. *Bioresource Technology.* 183, pp.195-202.
Dudley, B. 2015. *BP Statistical Review of World Energy 2015.* Petroleum, British.

Dunne, D. and Agnew, J. 1992. Thermal upgrading of low-grade, low-rank South Australia coal. *Energy Sources.* 14(2), pp.169-181.
Durães, L. et al. 2007. Fe2O3/aluminum thermite reaction intermediate and final products characterization. *Materials Science and Engineering: A.* 465(1), pp.199-210.
Eggleston H.S., B.L., Miwa K., Ngara T. and Tanabe K. (eds). 2006. 2006 IPCC Guidelines for National Greenhouse Gas Inventories, . *IPCC 2006.* [Online]. Available from: http://www.ipcc-nggip.iges.or.jp/public/2006gl/pdf/0_Overview/V0_0_Cover.pdf.
Ekşioğlu, S.D. et al. 2009. Analyzing the design and management of biomass-to-biorefinery supply chain. *Computers & Industrial Engineering.* 57(4), pp.1342-1352.
Elled, A.L. et al. 2013. Composition of agglomerates in fluidized bed reactors for thermochemical conversion of biomass and waste fuels: Experimental data in comparison with predictions by a thermodynamic equilibrium model. *Fuel.* 111, pp.696-708.
Ergun, S. and Orning, A.A. 1949. Fluid Flow through Randomly Packed Columns and Fluidized Beds. *Industrial & Engineering Chemistry.* 41(6), pp.1179-1184.
Escudero, D. and Heindel, T.J. 2011. Bed height and material density effects on fluidized bed hydrodynamics. *Chemical Engineering Science.* 66(16), pp.3648-3655.
Eslami, A. et al. 2012. Sequential Modeling of Coal Volatile Combustion in Fluidized Bed Reactors. *Energy & Fuels.* 26(8), pp.5199-5209.
Evans, E.H. et al. 2014. Atomic spectrometry updates: Review of advances in atomic spectrometry and related techniques. *Journal of Analytical Atomic Spectrometry.* 29(5), pp.773-794.
Evans, J.R. et al. 1990. Analysis of eight Argonne premium coal samples by X-ray fluorescence spectrometry. *Energy & Fuels.* 4(5), pp.440-442.
Evans, S. 2016. UK emissions lowest since the 1920's as renewables overtake coal. *carbon brief.*
Fang, W. et al. 2008. Distribution of electrostatic potential in a gas− solid fluidized bed and measurement of bed level. *Industrial & Engineering Chemistry Research.* 47(23), pp.9517-9526.
Fernández-Ruiz, R. et al. 2010. Optimization of the quantitative direct solid total-reflection X-ray fluorescence analysis of glass microspheres functionalized with Zr organometallic compounds. *Spectrochimica Acta Part B: Atomic Spectroscopy.* 65(6), pp.450-456.
Fernando, R. 2007. *Cofiring of Coal with Waste Fuels.* International Energy Agency Coal Research.
Fernando, R. 2012. Cofiring high ratios of biomass with coal. *IEA clean coal centre 2012.* january 2012.
Frei, C. et al. 2013. *World energy scenarios: Composing energy futures to 2050.* Conseil Francais de l'energie, 12 rue de Saint-Quentin, 75010 Paris (France).
Freme, F. 2009. US Coal supply and demand: 2009 review. *Retrieved September.* 25, p2010.
Fryda, L.E. et al. 2008. Agglomeration in fluidised bed gasification of biomass. *Powder Technology.* 181(3), pp.307-320.
Fu, W. et al. 1989. A general model of pulverized coal devolatilization. *Fuel.* 68(4), pp.505-510.
Fueyo, N. and Dopazo, C. 1995. Fluidization fundamentals. In: Cuenca, M.A. and Anthony, E.J. eds. *Pressurized Fluidized Bed Combustion.* Springer Netherlands, pp.38-79.

Fujino, M. et al. 1985. The electric potential distribution profile in a naturally charged fluidized bed and its effects. *Int. Chem. Eng.;(United States).* 25(1).
Gajewski, A. 1985. Investigation of the electrification of polypropylene particles during the fluidization process. *Journal of electrostatics.* 17(3), pp.289-298.
García-Labiano, F. et al. 2011. Calcium-based sorbents behaviour during sulphation at oxy-fuel fluidised bed combustion conditions. *Fuel.* 90(10), pp.3100-3108.
Gardnerbrown, J. 2005. *The Combustion Systems Ltd., (CSL), Fluidised Combustion Process Design Manual.* Combustion Systems Ltd

Casella CRE Energy Ltd.
Gatternig, B. 2015. *Predicting Agglomeration in Biomass Fired Fluidized Beds*. PhD thesis, Erlangen-Nuremberg.
Gayan, P. et al. 2004. Circulating fluidised bed co-combustion of coal and biomass. *Fuel.* 83(3), pp.277-286.
Gazulla, M. et al. 2010. Methodology for the determination of minor and trace elements in petroleum cokes by wavelength-dispersive X-ray fluorescence (WD-XRF). *X-Ray Spectrometry.* 39(5), pp.321-327.
Gazulla, M.F. et al. 2009. New methodology for sulfur analysis in geological samples by WD-XRF spectrometry. *X-Ray Spectrometry.* 38(1), pp.3-8.
Geldart, D. 1968. The expansion of bubbling fluidised beds. *Powder Technology.* 1(6), pp.355-368.
Geldart, D. 1973. Types of gas fluidization. *Powder Technology.* 7(5), pp.285-292.
Geldart, D. and Rhodes, M. 1986. From minimum fluidization to pneumatic transport—a critical review of the hydrodynamics. *Circulating fluidized bed technology.* 1, pp.21-31.
Ghani, W. et al. 2009. Co-combustion of agricultural residues with coal in a fluidised bed combustor. *Waste Management.* 29(2), pp.767-773.
Gialan, D. 2012. *biomass for power generation.* IRENA international renewable energy agency.
Gibson, B. et al. 2014. Atomic spectrometry update. Review of advances in the analysis of metals, chemicals and functional materials. *Journal of Analytical Atomic Spectrometry.* 29(11), pp.1969-2021.
Gogolek, P. and Grace, J. 1995. Fundamental hydrodynamics related to pressurized fluidized bed combustion. *Progress in Energy and Combustion Science.* 21(5), pp.419-451.
Grimm, A. et al. 2012. Bed Agglomeration Characteristics in Fluidized-Bed Combustion of Biomass Fuels Using Olivine as Bed Material. *Energy & Fuels.* 26(7), pp.4550-4559.
Grimm, A. et al. 2011. Bed agglomeration characteristics in fluidized quartz bed combustion of phosphorus-rich biomass fuels. *Energy & Fuels.* 25(3), pp.937-947.
Grubor, B. et al. 1995. *Biomass FBC combustion--Bed agglomeration problems.* New York, NY (United States): American Society of Mechanical Engineers,.
Guenther, C. et al. 2002. A numerical investigation of an industrial scale gas–solids CFB. *Circulating Fluidized Bed Technology VII.* pp.483-488.
Gulyurtlu, I. et al. 2013. 9 - Pollutant emissions and their control in fluidised bed combustion and gasification. In: Scala, F. ed. *Fluidized Bed Technologies for Near-Zero Emission Combustion and Gasification.* Woodhead Publishing, pp.435-480.
Gupta, C.K. and Sathiyamoorthy, D. 1998. *Fluid Bed Technology in Materials Processing.* Taylor & Francis.
Gupta, R. et al. 2007. *Impact of Mineral Impurities in Solid Fuel Combustion.* Springer US.

Harrison, R.M. 2001. Air pollution: sources, concentrations and measurments. *Pollution: Causes, Effects and Control.* Royal Society of Chemistry.
Hassan, M.R., D. 2014. Electricity regulation in the UK: overview. *Practical law.* [Online]. Available from: http://uk.practicallaw.com/1-523-9996#a578279.
Haynes, W.M. and Lide, D.R. 2010. *CRC Handbook of Chemistry and Physics: A Ready-reference Book of Chemical and Physical Data.* CRC Press.
Hecking, H. 2016. Twenty-first century, the century of coal? CO2 prices to curb coal demand. *Oxford Review of Economic Policy.* 32(2), pp.260-281.
Hendrickson, G. 2006. Electrostatics and gas phase fluidized bed polymerization reactor wall sheeting. *Chemical Engineering Science.* 61(4), pp.1041-1064.
Hetsroni, G. 1982. *Handbook of multiphase systems.* Hemisphere Pub. Corp.
Hlincik, T. and Buryan, P. 2013. Evaluation of limestones for the purposes of desulphurisation during the fluid combustion of brown coal. *Fuel.* 104(0), pp.208-215.
Hoffmann, B.S. et al. 2012. An evaluation of the techno-economic potential of co-firing coal with woody biomass in thermal power plants in the south of Brazil. *Biomass and Bioenergy.* 45, pp.295-302.
Hoogwijk, M.M. 2004. *On the global and regional potential of renewable energy sources*. PhD thesis, Utrecht University.
Howard, J.B. 1987. The Chemistry of Coal By N. Berkowitz, Elsevier, 1985, 513 pp. *AIChE Journal.* 33(1), pp.171-171.
Howard, J.R. 1989. *Fluidized Bed Technology: Principles and Applications.* Adam Hilger.
Howard, J.R. and Elliott, D. 1983. Fluidized Bed Industrial Boilers and Furnaces. *Fluidized beds: combustion and applications.* Applied Science Publishers.
Husain, T. 2010. Pakistan's energy sector issues: energy efficiency and energy environmental links. *The Lahore Journal of Economics.* 15, p33.
ISHIDA, M. and TANAKA, H. 1982. An optical probe to detect both bubbles and suspended particles in a three-phase fluidized bed. *Journal of Chemical Engineering of Japan.* 15(5), pp.389-391.
Ishiguro, M. and Akiyama, T. 1995. Recent developments in energy supply and demand in asian developing countries. *Energy Demand in Five Major Asian Developing Countries: Structure and Prospects.* World Bank.
Jiang, Y. et al. 2014. Acoustic emission detection of particle movement in a cross-flow moving bed. *Industrial & Engineering Chemistry Research.* 53(10), pp.4075-4083.
Johnsson, J.E. 1994. Formation and reduction of nitrogen oxides in fluidized-bed combustion. *Fuel.* 73(9), pp.1398-1415.
Jones, M.G. and Williams, K.C. 2008. Predicting the mode of flow in pneumatic conveying systems—A review. *Particuology.* 6(5), pp.289-300.
Kaakinen, J.W. et al. 1975. Trace element behavior in coal-fired power plant. *Environmental Science & Technology.* 9(9), pp.862-869.
Kabe, T. 2004. *Coal and Coal-related Compounds: Structures, Reactivity and Catalytic Reactions.* Elsevier.
Kai, T. and Furusaki, S. 1987. Methanation of carbon dioxide and fluidization quality in a fluid bed reactor—the influence of a decrease in gas volume. *Chemical engineering science.* 42(2), pp.335-339.
Karthikeyan, M. et al. 2009. Low-rank coal drying technologies—current status and new developments. *Drying Technology.* 27(3), pp.403-415.
Kaygusuz, K. 2012. Energy for sustainable development: A case of developing countries. *Renewable and Sustainable Energy Reviews.* 16(2), pp.1116-1126.

Kelloway, S.J. et al. 2014. Quantitative chemical profiling of coal using core-scanning X-ray fluorescence techniques. *International Journal of Coal Geology.* 128–129(0), pp.55-67.
Khan, A.A. et al. 2009. Biomass combustion in fluidized bed boilers: Potential problems and remedies. *Fuel Processing Technology.* 90(1), pp.21-50.
Khan, T. and Turton, R. 1992. The measurement of instantaneous heat transfer coefficients around the circumference of a tube immersed in a high temperature fluidized bed. *International Journal of Heat and Mass Transfer.* 35(12), pp.3397-3406.
Khan, W.Z. and Gibbs, B.M. 1995. The influence of air staging in the reduction of SO 2 by limestone in a fluidized bed combustor. *Fuel.* 74(6), pp.800-805.
Khan, W.Z. and Gibbs, B.M. 2000. High temperature desulphurization by fine limestone during staged fluidized-bed combustion. *The Canadian Journal of Chemical Engineering.* 78(6), pp.1102-1110.
Kim, Y. et al. 2013. Effect of the Fukushima nuclear disaster on global public acceptance of nuclear energy. *Energy Policy.* 61, pp.822-828.
Kiyobayashi, T. and Sakiyama, M. 1993. Combustion calorimetric studies on C60 and C70. *Fullerenes, Nanotubes, and Carbon Nanostructures.* 1(3), pp.269-273.
Knutsson, P. et al. 2014. Effect of bed materials mixing on the observed bed sintering. In: *11th International Conference on Fluidized Bed Technology, CFB 2014; Beijing; China; 14 May 2014 through 17 May 2014*, pp.655-660.
Koornneef, J. et al. 2007. Development of fluidized bed combustion—An overview of trends, performance and cost. *Progress in Energy and Combustion Science.* 33(1), pp.19-55.
Koppatz, S. et al. 2011. Comparison of the performance behaviour of silica sand and olivine in a dual fluidised bed reactor system for steam gasification of biomass at pilot plant scale. *Chemical Engineering Journal.* 175, pp.468-483.
Koppejan, J. and van Loo, S. 2012. Biomass Fuel Properties and Basic Principles of Biomass Combustion. *The Handbook of Biomass Combustion and Co-firing.* Taylor & Francis, pp.7-54.
Koukouzas, N. et al. 2009. Quantitative evaluation of minerals in fly ashes of biomass, coal and biomass–coal mixture derived from circulating fluidised bed combustion technology. *Journal of Hazardous Materials.* 169(1–3), pp.100-107.
Kowalska, E. and Urbanski, P. 1992. Advantages and limitations of XRF method for rapid sulphur determination in coal samples. *Nukleonika.* 37(3), pp.77-83.
KUHN, J.H., W; SHIMP,N. 1975. Trace Elements in Fuel. *Advances in Chemistry.* 141(141), p236.
Kulasekaran, S. et al. 1999. Mathematical modeling of fluidized bed combustion 3. Simultaneous combustion of char and combustible gases. *Fuel.* 78(4), pp.403-417.
Kunii, D. et al. 2013. *Fluidization Engineering.* Elsevier Science.
Kuo, J.T. et al. 1997. Effect of air distribution on solid fuel bed combustion. *Journal of energy resources technology.* 119(2), pp.120-128.
Lan, J. et al. 2001. Study on control of NOx and N 2 O in a coal-fired fluidized bed test rig. In: *16 th International Conference on Fluidized Bed Combustion*, p.2001.
Latva-Somppi, J. 1998. Experimental studies on pulp and paper mill sludge ash behavior in fluidized bed combustors.
Le Roux, G. and De Vleeschouwer, F. 2010. Preparation of peat samples for inorganic geochemistry used as palaeoenvironmental proxies. *Mires and Peat.* 7, pp.pp. 1-9.
Leckner, B. 1998. Fluidized bed combustion: Mixing and pollutant limitation. *Progress in Energy and Combustion Science.* 24(1), pp.31-61.

Leckner, B. and Lyngfelt, A. 2002. Optimization of emissions from fluidized bed combustion of coal, biofuel and waste. *International Journal of Energy Research.* 26(13), pp.1191-1202.
Lewandowski, I. and Heinz, A. 2003. Delayed harvest of miscanthus—influences on biomass quantity and quality and environmental impacts of energy production. *European Journal of Agronomy.* 19(1), pp.45-63.
Li, C.Z. 2004. *Advances in the Science of Victorian Brown Coal.* Elsevier Science.
Li, S. et al. 2010. A model for agglomeration in bio-fuel fired fluidized bed. *Journal of Thermal Science.* 19(5), pp.451-458.
Lin, B.-q. and Liu, J.-h. 2010. Estimating coal production peak and trends of coal imports in China. *Energy Policy.* 38(1), pp.512-519.
Lin, C.-L. et al. 2011. Effect of particle size distribution on agglomeration/defluidization during fluidized bed combustion. *Powder Technology.* 207(1–3), pp.290-295.
Lin, W. and Dam-Johansen, K. 1999. *Agglomeration in fluidized bed combustion of biomass--Mechanisms and co-firing with coal.* Technical Univ. of Denmark, Lyngby (DK).
Lin, W. et al. 2003. Agglomeration in bio-fuel fired fluidized bed combustors. *Chemical Engineering Journal.* 96(1), pp.171-185.
Lindström, E. et al. 2007. Slagging Characteristics during Combustion of Cereal Grains Rich in Phosphorus. *Energy & Fuels.* 21(2), pp.710-717.
Linjewile, T.M. and Manzoori, A.R. 1999. Role of Additives in Controlling Agglomeration and Defluidization During Fluidized Bed Combustion of High-Sodium, High-Sulphur Low-Rank Coal. *Impact of Mineral Impurities in Solid Fuel Combustion.* Boston, MA: Springer US, pp.319-331.
Link, J. et al. 2004. Validation of a discrete particle model in a 2D spout-fluid bed using non-intrusive optical measuring techniques. *Canadian Journal of Chemical Engineering.* 82(1), pp.30-36.
Liu, H. and Gibbs, B. 2002. Modeling of NO and N 2 O emissions from biomass circulating fluidized bed combustors. In: *Proceedings of the 7. international conference on circulating fluidized bed technology. 7. vol. ed*.
Liu, Z. et al. 2010. Electrostatic charging behaviour of dielectric particles in a pressurized gas–solid fluidized bed. *Journal of Electrostatics.* 68(4), pp.321-327.
Llorente, M.F. and García, J.C. 2005. Comparing methods for predicting the sintering of biomass ash in combustion. *Fuel.* 84(14), pp.1893-1900.
Löffler, G. et al. 2001. NOx and N2O formation mechanisms—a detailed chemical kinetic modeling study on a single fuel particle in a laboratory-scale fluidized bed. *Journal of energy resources technology.* 123(3), pp.228-235.
Loubser, M. and Verryn, S. 2008. Combining XRF and XRD analyses and sample preparation to solve mineralogical problems. *South African Journal of Geology.* 111(2-3), pp.229-238.
LUO, X. et al. 2011. Progress on Determination of TFe and Other Elements in Iron Ores by Fused Glass-Wavelength Dispersive X-ray Fluorescence Spectrometry. *Chinese Journal of Inorganic Analytical Chemistry.* 3, pp.00-07.
Lutz, W. et al. 2001. The end of world population growth. *Nature.* 412(6846), pp.543-545.
Lyngfelt, A. and Leckner, B. 1992. Residence time distribution of sorbent particles in a circulating fluidised bed boiler. *Powder Technology.* 70(3), pp.285-292.
Makansi, J. 2005. PFBC presents its clean coal credentials. *Power (New York).* 149(9).
Marinov, V. et al. 1992. Ash agglomeration during fluidized bed gasification of high sulphur content lignites. *Fuel Processing Technology.* 31(3), pp.181-191.

Masiá, A.T. et al. 2007. Characterising ash of biomass and waste. *Fuel Processing Technology.* 88(11), pp.1071-1081.
Mathews, J.A. 2008. Carbon-negative biofuels. *Energy policy.* 36(3), pp.940-945.
Matsunami, H. et al. 2010. Rapid simultaneous multi-element determination of soils and environmental samples with polarizing energy dispersive X-ray fluorescence (EDXRF) spectrometry using pressed powder pellets. *Soil Science & Plant Nutrition.* 56(4), pp.530-540.
McIlveen-Wright, D. et al. 1999. Options for small and medium scale power generation from biomass. *Developments in Chemical Engineering and Mineral Processing.* 7(1-2), pp.85-114.
McKendry, P. 2002. Energy production from biomass (part 1): overview of biomass. *Bioresource technology.* 83(1), pp.37-46.
Mehrani, P.H., T; Grace, J. 2005. Electrostatic charge generation in gas–solid fluidized beds. *Journal of electrostatics.* 63(2), pp.165-173.
Mellish, M. 2013. Annual energy outlook 2013. *US Energy Information Administration, Washington, DC.* [Online]. pp.60-62. Available from: https://www.eia.gov/outlooks/aeo/pdf/0383(2013).pdf.
Merrick, D. 1984. Fluidised bed combustion. *Coal combustion and conversion technology.* Macmillan.
Minchener, A. 2003. Fluidized bed combustion systems for power generation and other industrial applications. *Proceedings of the Institution of Mechanical Engineers, Part A: Journal of Power and Energy.* 217(1), pp.9-18.
Morgan, T.J. et al. 2015. Quantitative X-ray Fluorescence Analysis of Biomass (Switchgrass, Corn Stover, Eucalyptus, Beech, and Pine Wood) with a Typical Commercial Multi-Element Method on a WD-XRF Spectrometer. *Energy & Fuels.* 29(3), pp.1669-1685.
Muenzer, H. and Bonn, B. 1980. SULFUR CAPTURING EFFECTIVITY OF LIMESTONES AND DOLOMITES IN FLUIDIZED BED COMBUSTION. *Proceedings of the International Conference on Fluidized Bed Combustion.* 3, pp.997-1003.
Nagle, M. et al. 2011. Fruit processing residues as an alternative fuel for drying in Northern Thailand. *Fuel.* 90(2), pp.818-823.
Natarajan, E. et al. 1998. Experimental determination of bed agglomeration tendencies of some common agricultural residues in fluidized bed combustion and gasification. *Biomass and Bioenergy.* 15(2), pp.163-169.
Nimmo, W. et al. 2004. Calcium magnesium acetate and urea advanced reburning for NO control with simultaneous SO2 reduction. *Fuel.* 83(9), pp.1143-1150.
Niu, Y. et al. 2013. Further study on biomass ash characteristics at elevated ashing temperatures: The evolution of K, Cl, S and the ash fusion characteristics. *Bioresource Technology.* 129, pp.642-645.
Niu, Y. et al. 2010. Study on fusion characteristics of biomass ash. *Bioresource Technology.* 101(23), pp.9373-9381.
Nunes, L. et al. 2016. Biomass combustion systems: A review on the physical and chemical properties of the ashes. *Renewable and Sustainable Energy Reviews.* 53, pp.235-242.
Öhman, M. et al. 2004. Slagging tendencies of wood pellet ash during combustion in residential pellet burners. *Biomass and Bioenergy.* 27(6), pp.585-596.
Öhman, M. and Nordin, A. 2000. The role of kaolin in prevention of bed agglomeration during fluidized bed combustion of biomass fuels. *Energy & fuels.* 14(3), pp.618-624.
Öhman, M. et al. 2000. Bed Agglomeration Characteristics during Fluidized Bed Combustion of Biomass Fuels. *Energy & Fuels.* 14(1), pp.169-178.

Oka, S. 2003. Fundemental processes in fludized bed combustion boiler furnaces. *Fluidized Bed Combustion.* Taylor & Francis, pp.37-136.
Okumura, Y. et al. 2002. Evolution prediction of coal-nitrogen in high pressure pyrolysis processes. *Fuel.* 81(18), pp.2317-2324.
Oliverira, M. et al. 2011. A multi-analytical approach to understand the chemistry of Fe-minerals in feed coals and ashes. *Coal Comb Gasif Prod.* 3, pp.51-62.
Olofsson, G. et al. 2002. Bed agglomeration problems in fluidized-bed biomass combustion. *Industrial & engineering chemistry research.* 41(12), pp.2888-2894.
Pahari, A.K. and Chauhan, B.S. 2006. *Engineering Chemistry.* Laxmi Publications.
Papo, G.T. 2015. *Assessment of South African coals in a bubbling fluidised bed combustion testing facility*. PhD thesis, University of

the Witwatersrand.
Paul, A. 1990. *Chemistry of Glasses.* Springer.
Paulrud, S. et al. 2001. Reed canary-grass ash composition and its melting behaviour during combustion. *Fuel.* 80(10), pp.1391-1398.
Payer, J.H. 1978. A report to NBS by Battelle Columbus Laboratories. *Economic effects of metallic corrosion in the United States*-. Battelle Memorial Institute. Columbus Laboratories

United States. National Bureau of Standards: U.S. Dept. of Commerce, National Bureau of Standards.
Pease, P. 2013. Fused glass sample preparation for quantitative laser-induced breakdown spectroscopy of geologic materials. *Spectrochimica Acta Part B: Atomic Spectroscopy*. 83, pp.37-49.
Perlack, R.D. et al. 2005. *Biomass as feedstock for a bioenergy and bioproducts industry: the technical feasibility of a billion-ton annual supply*. U.S Department of Energy. TN: DTIC Document.
Pietsch, W. 2008. Agglomeration processes: phenomena, technologies, equipment. *Agglomeration Processes.* Wiley, pp.29-132.
Pilling, G. 1999. *Salters Higher Chemistry.* Pearson Education.
Piotrowska, P. et al. 2010. Fate of alkali metals and phosphorus of rapeseed cake in circulating fluidized bed boiler Part 2: Cocombustion with coal. *Energy & Fuels.* 24(8), pp.4193-4205.
Podolski, W.F. et al. 1995. Air emissions from pressurized fluidized bed combustors. In: Cuenca, M.A. and Anthony, E.J. eds. *Pressurized Fluidized Bed Combustion.* Springer Netherlands, pp.257-317.
Ponnusami.Gounder. 1995. *Supercritical steam pressurised circulating fluidised bed boiler*.
Qing-tao, Z. 2009. Cause and Countermeasure of CFB Boiler Heating Surface Abrasion.
Quaak, P. et al. 1999. *Energy from Biomass: A Review of Combustion and Gasification Technologies.* World Bank.
Ramos Caicedo, G. et al. 2002. Minimum fluidization velocities for gas–solid 2D beds. *Chemical Engineering and Processing: Process Intensification.* 41(9), pp.761-764.
Razzak, S. et al. 2009. Phase holdup measurement in a gas–liquid–solid circulating fluidized bed (GLSCFB) riser using electrical resistance tomography and optical fibre probe. *Chemical Engineering Journal.* 147(2), pp.210-218.
Rehman, S.u. et al. 2016. Geology and combustion perspectives of Pakistani coals from Salt Range and Trans Indus Range. *International Journal of Coal Geology.* 168, Part 2, pp.202-213.
Reinmöller, M. et al. 2015. Relationship between ash fusion temperatures of ashes from hard coal, brown coal, and biomass and mineral phases under different

atmospheres: A combined FactSage™ computational and network theoretical approach. *Fuel.* 151, pp.118-123.
Rizvi, T. et al. 2015. Prediction of biomass ash fusion behaviour by the use of detailed characterisation methods coupled with thermodynamic analysis. *Fuel.* 141, pp.275-284.
Robinson, J.M. et al. 2009. Energy dispersive X-ray fluorescence analysis of sulfur in biomass. *Energy & Fuels.* 23(4), pp.2235-2241.
Rogner, H.-H. 1997. An assessment of world hydrocarbon resources. *Annual review of energy and the environment.* 22(1), pp.217-262.
Romero, J.B., and L. N. Johanson. 1962. Factors affecting fluidized bed quality. *Chemical Engineering Progress, Symposium Series* 58(38), pp.28-37.
Ross, D.P. et al. 2000. Devolatilisation times of coal particles in a fluidised-bed. *Fuel.* 79(8), pp.873-883.
Ryś-Matejczuk, M. et al. 2013. Investigation of Coal Slags and Related Oxide Systems by KEMS. *ECS Transactions.* 46(1), pp.271-279.
Sano, Y. et al. 1983. Mutual Diffusion CoeMcient of PAN-DMF System. *KAGAKU KOGAKU RONBUNSHU.* 9(1), pp.1-7.
Sau, D.C. et al. 2007. Minimum fluidization velocities and maximum bed pressure drops for gas–solid tapered fluidized beds. *Chemical Engineering Journal.* 132(1–3), pp.151-157.
Scala, F. and Chirone, R. 2006. Characterization and early detection of bed agglomeration during the fluidized bed combustion of olive husk. *Energy & fuels.* 20(1), pp.120-132.
Scala, F. and Chirone, R. 2008. An SEM/EDX study of bed agglomerates formed during fluidized bed combustion of three biomass fuels. *Biomass and Bioenergy.* 32(3), pp.252-266.
Schweitzer, J. et al. 2001. Local gas hold-up measurements in fluidized bed and slurry bubble column. *Chemical Engineering Science.* 56(3), pp.1103-1110.
Seddighi K, S. et al. 2013. Progress of Combustion in an Oxy-fuel Circulating Fluidized-Bed Furnace: Measurements and Modeling in a 4 MWth Boiler. *Energy & Fuels.* 27(10), pp.6222-6230.
Seggiani, M. 1999. Empirical correlations of the ash fusion temperatures and temperature of critical viscosity for coal and biomass ashes. *Fuel.* 78(9), pp.1121-1125.
Serway, R. et al. 2004. *Modern Physics.* Cengage Learning.
Seville, J. and Clift, R. 1984. The effect of thin liquid layers on fluidisation characteristics. *Powder Technology.* 37(1), pp.117-129.
Shackley, M.S. 2011. An introduction to X-ray fluorescence (XRF) analysis in archaeology. *X-ray fluorescence spectrometry (XRF) in geoarchaeology.* Springer, pp.7-44.
Shafie, S.M. et al. 2012. A review on electricity generation based on biomass residue in Malaysia. *Renewable and Sustainable Energy Reviews.* 16(8), pp.5879-5889.
Shah, M.R. et al. 1994. Characterization of Lakhra coal by TG/DTG. *Fuel science & technology international.* 12(1), pp.85-95.
Sheahan, T. and Briens, L. 2015. Passive acoustic emission monitoring of pellet coat thickness in a fluidized bed. *Powder Technology.* 286, pp.172-180.
Shibli, A. 2014. *Coal Power Plant Materials and Life Assessment: Developments and Applications.* Elsevier Science.
Siegell, J.H. 1984. High-temperature de fluidization. *Powder Technology.* 38(1), pp.13-22.
Sieminski, A. 2014. International Energy Outlook. [Online]. 2014. Available from: https://www.eia.gov/pressroom/presentations/sieminski_11182014.pdf.

Simeonn, N.O., S; Anthony, E. 2003. Fluidized Bed Combustion. *Fluidized Bed Combustion.* CRC Press, pp.xi-xvii.
Simoneit, B.R.T. 2002. Biomass burning — a review of organic tracers for smoke from incomplete combustion. *Applied Geochemistry.* 17(3), pp.129-162.
Skoog, D. et al. 2013. *Fundamentals of Analytical Chemistry*. Cengage Learning.
Skrifvars, B.-J. et al. 1994. Sintering mechanisms of FBC ashes. *Fuel.* 73(2), pp.171-176.
Skrifvars, B.-J. et al. 1999. Predicting bed agglomeration tendencies for biomass fuels fired in FBC boilers: a comparison of three different prediction methods. *Energy & Fuels.* 13(2), pp.359-363.
Skrifvars, B.J. et al. 1992. Sintering of ash during fluidized bed combustion. *Industrial & Engineering Chemistry Research.* 31(4), pp.1026-1030.
Slade, R. et al. 2011. *Energy from biomass: the size of the global resource.* Imperial College Centre for Energy Policy and Technology and UK Energy Research Centre, London.
Sloss, L. 2010. emissions from co firing coal, biomass and sewage sludge *IEA clean coal centre 2010.* October 2010.
Smil, V. 2006. Plows, plagues, and petroleum: How humans took control of climate. *International History Review.* 28(4), pp.931-932.
Sokhansanj, S. et al. 2009. Large-scale production, harvest and logistics of switchgrass (Panicum virgatum L.)–current technology and envisioning a mature technology. *Biofuels, Bioproducts and Biorefining.* 3(2), pp.124-141.
Solomon, P.R. and Colket, M.B. 1979. Coal devolatilization. *Symposium (International) on Combustion.* 17(1), pp.131-143.
Sowinski, A. et al. 2010. Investigation of electrostatic charge distribution in gas–solid fluidized beds. *Chemical Engineering Science.* 65(9), pp.2771-2781.
Speight, J.G. 2012. *The Chemistry and Technology of Coal.* 3 ed. Taylor & Francis.
Spinelli, R. et al. 2005. Harvesting and transport of root biomass from fast-growing poplar plantations. *Silva Fennica.* 39(4), p539.
Srinivasan, R.A. et al. 1998. Mathematical modeling of fluidized bed combustion — 2: combustion of gases. *Fuel.* 77(9–10), pp.1033-1049.
Stallmann, J.J. and Neavel, R.C. 1980. Technique to measure the temperature of agglomeration of coal ash. *Fuel.* 59(8), pp.584-586.
Stankova, A. et al. 2010. A simple LIBS method for fast quantitative analysis of fly ashes. *Fuel.* 89(11), pp.3468-3474.
Steenari, B.M. and Lindqvist, O. 1998. High-temperature reactions of straw ash and the anti-sintering additives kaolin and dolomite. *Biomass and Bioenergy.* 14(1), pp.67-76.
Stein, M. et al. 2000. Solids motion in bubbling gas fluidised beds. *Chemical Engineering Science.* 55(22), pp.5291-5300.
Stone, C.L. 2004. *The Basics of Biology.* Greenwood Press.
Strezov, V. et al. 2000. Quantifying the heats of coal devolatilization. *Metallurgical and Materials Transactions B.* 31(5), pp.1125-1131.
Subramanian, R.S. 2004. *Flow through Packed Beds and Fluidized Beds.* Clarkson University: Engineering.
SUI, L.-m. et al. 2012. Design Improvement of Biomass Flat-die Briquetting Machine *Agricultural Equipment & Vehicle Engineering.* 5, p007.
Suyadal, Y. 2006. Gas temperature profiles at different flow rates and heating rates suffice to estimate kinetic parameters for fluidised bed combustion. *Experimental Thermal and Fluid Science.* 30(7), pp.613-620.
Svehla, G. 2008. *Vogel's Qualitative Inorganic Analysis.* 7 ed. Pearson Education.

Tangsathitkulchai, C. and Tangsathitkulchai, M. 2001. Effect of bed materials and additives on the sintering of coal ashes relevant to agglomeration in fluidized bed combustion. *Fuel processing technology.* 72(3), pp.163-183.
Tarelho, L. et al. 2005. The influence of operational parameters on SO2 removal by limestone during fluidised bed coal combustion. *Fuel Processing Technology.* 86(12–13), pp.1385-1401.
Tarelho, L.A.C. et al. 2006. Influence of limestone addition on the behaviour of NO and N2O during fluidised bed coal combustion. *Fuel.* 85(7–8), pp.967-977.
Taylor, A. et al. 2014. Atomic spectrometry update: Review of advances in the analysis of clinical and biological materials, foods and beverages. *Journal of Analytical Atomic Spectrometry.* 29(3), pp.386-426.
Teixeira, P. et al. 2012. Evaluation of slagging and fouling tendency during biomass co-firing with coal in a fluidized bed. *Biomass and Bioenergy.* 39, pp.192-203.
Teng, H.P. et al. 2013. The Phase Transformations during Fluidized-Bed Combustion of Biomass. In: *Applied Mechanics and Materials*: Trans Tech Publ, pp.366-369.
Terzano, R. et al. 2013. Spatially resolved (semi) quantitative determination of iron (Fe) in plants by means of synchrotron micro X-ray fluorescence. *Analytical and bioanalytical chemistry.* 405(10), pp.3341-3350.
Thorsell, S. et al. 2004. Economics of a coordinated biorefinery feedstock harvest system: lignocellulosic biomass harvest cost. *Biomass and Bioenergy.* 27(4), pp.327-337.
Thy, P. et al. 2010. Bed agglomeration in fluidized combustor fueled by wood and rice straw blends. *Fuel Processing Technology.* 91(11), pp.1464-1485.
Topal, H. et al. 2003. Olive cake combustion in a circulating fluidized bed. *Fuel.* 82(9), pp.1049-1056.
Tsuji, H. et al. 2002. *High Temperature Air Combustion: From Energy Conservation to Pollution Reduction.* Taylor & Francis.
Urkan, M.K. and Arikol, M. 1994. Burning times of volatiles from Turkish coals during fluidized bed combustion. *Fuel.* 73(5), pp.768-772.
Vamvuka, D. et al. 2008. Control methods for mitigating biomass ash-related problems in fluidized beds. *Bioresource Technology.* 99(9), pp.3534-3544.
Van de Velden, M. et al. 2008. The solids flow in the riser of a Circulating Fluidised Bed (CFB) viewed by Positron Emission Particle Tracking (PEPT). *Powder Technology.* 183(2), pp.290-296.
Van der Pligt, J. 1992. *Nuclear energy and the public.* Blackwell Publishing.
Van Dyk, J. et al. 2009. Viscosity predictions of the slag composition of gasified coal, utilizing FactSage equilibrium modelling. *Fuel.* 88(1), pp.67-74.
Van Grieken, R. and Markowicz, A. 2001. *Handbook of X-ray Spectrometry.* 2 ed. CRC Press.
van Heek, K.H. and Hodek, W. 1994. Structure and pyrolysis behaviour of different coals and relevant model substances. *Fuel.* 73(6), pp.886-896.
van Ommen, J.R. et al. 2000. Early warning of agglomeration in fluidized beds by attractor comparison. *AIChE Journal.* 46(11), pp.2183-2197.
Varol, M. and Atimtay, A.T. 2015. Effect of biomass-sulfur interaction on ash composition and agglomeration for the co-combustion of high-sulfur lignite coals and olive cake in a circulating fluidized bed combustor. *Bioresource Technology.* 198, pp.325-331.
Verrastro, F. and Ladislaw, S. 2007. Providing energy security in an interdependent world. *Washington Quarterly.* 30(4), pp.95-104.
Virginie, M. et al. 2012. Effect of Fe–olivine on the tar content during biomass gasification in a dual fluidized bed. *Applied Catalysis B: Environmental.* 121–122, pp.214-222.

Visser, H.J. et al. 2008. Biomass Ash-Bed Material Interactions Leading to Agglomeration in FBC. *Journal of Energy Resources Technology.* 130(1), pp.011801-011806.
Volborth, A. 1987. *Coal science and chemistry.* Elsevier.
Vuthaluru, H.B. et al. 2000. Behaviour of inorganic constituents and ash characteristics during fluidised-bed combustion of several Australian low-rank coals. *Fuel Processing Technology.* 67(3), pp.165-176.
Wang, J. et al. 2009. Agglomeration detection by acoustic emission (AE) sensors in fluidized beds. *Industrial & Engineering Chemistry Research.* 48(7), pp.3466-3473.
Wang, L.K. et al. 2007. *Advanced Air and Noise Pollution Control: Volume 2.* Humana Press.
Wang, Y.-L.Q., Yue-Hua; Deng, Jun-Hua. 2010. Discussion and application of sample preparation by fusion in X-ray fluorescence spectrometry. *Metallurgical Analysis.* 12, p005.
Ward, C.R. and Christie, P. 1994. Clays and other minerals in coal seams of the Moura-Baralaba area, Bowen Basin, Australia. *International Journal of Coal Geology.* 25(3), pp.287-309.
Weiguo, L. et al. 2015. Feature extraction and early warning of agglomeration in fluidized bed reactors based on an acoustic approach. *Powder Technology.* 279, pp.185-195.
Werther, J. 1999. Measurement techniques in fluidized beds. *Powder Technology.* 102(1), pp.15-36.
Werther, J. et al. 2000. Combustion of agricultural residues. *Progress in Energy and Combustion Science.* 26(1), pp.1-27.
Wilhelm, R.H. and Kwauk, M. 1948. Fluidization of solid particles. *Chemical Engineering Progress.* 44(3), pp.201-218.
Williams, G. 1978. Imperialism and development: A critique. *World Development.* 6(7), pp.925-936.
Wilson, W.E. 1972. A Critical Review of the Gas-Phase Reaction Kinetics of the Hydroxyl Radical. *Journal of Physical and Chemical Reference Data.* 1(2), pp.535-573.
Wiser, W.H. 1999. *Energy Resources: Occurrence, Production, Conversion, Use.* Springer New York.
Wu, Z. 2003. Understanding fluidised bed combustion.
Xing, P. et al. 2016. A comparative assessment of biomass ash preparation methods using X-ray fluorescence and wet chemical analysis. *Fuel.* 182, pp.161-165.
Xutao, W. and Bailiang, Z. 2008. Application and problems of Biomass Briquetting Densification Fuel (BBDF) technology in China. In: *Proceedings of ISES World Congress 2007 (Vol. I–Vol. V)*: Springer, pp.2458-2461.
Yang, W.C. 2003. *Handbook of Fluidization and Fluid-Particle Systems.* 2 ed. Taylor & Francis.
Yang, Y. et al. 2016. Effects of agglomerates on electrostatic behaviors in gas–solid fluidized beds. *Powder Technology.* 287, pp.139-151.
Yonglong, W. and HouShulin, Z.L. 2013. Development and prospect of straw conveyor technology and equipment. *Journal of Agricultural Mechanization Research.* 9, pp.11-16.
Youssef, M.A. et al. 2009. Experimental study on Egyptian biomass combustion in circulating fluidized bed. *Applied Energy.* 86(12), pp.2644-2650.
Zanchi, G. et al. 2012. Is woody bioenergy carbon neutral? A comparative assessment of emissions from consumption of woody bioenergy and fossil fuel. *GCB Bioenergy.* 4(6), pp.761-772.

Zheng, J. et al. 1982. A model for desulphurisation with limestone in a fluidised coal combustor. *Chemical Engineering Science.* 37(2), pp.167-174.
Zhong, W. et al. 2006. Hydrodynamic characteristics of spout-fluid bed: Pressure drop and minimum spouting/spout-fluidizing velocity. *Chemical Engineering Journal.* 118(1–2), pp.37-46.
Zhong, W. et al. 2008. Fluidization of biomass particles in a gas− solid fluidized bed. *Energy & Fuels.* 22(6), pp.4170-4176.
Zhou, W. et al. 2011. Two-dimensional computational fluid dynamics simulation of nitrogen and sulfur oxides emissions in a circulating fluidized bed combustor. *Chemical Engineering Journal.* 173(2), pp.564-573.
Zhu, Q. 2013. Developments in circulating fluidised bed combustion. In: IEA.